PROMOTING RESILIENCE OF VULNERABLE THROUGH ACCESS TO INFRASTRUCTURE, IMPROVED SKILLS, AND INFORMATION (PROVATI^3)

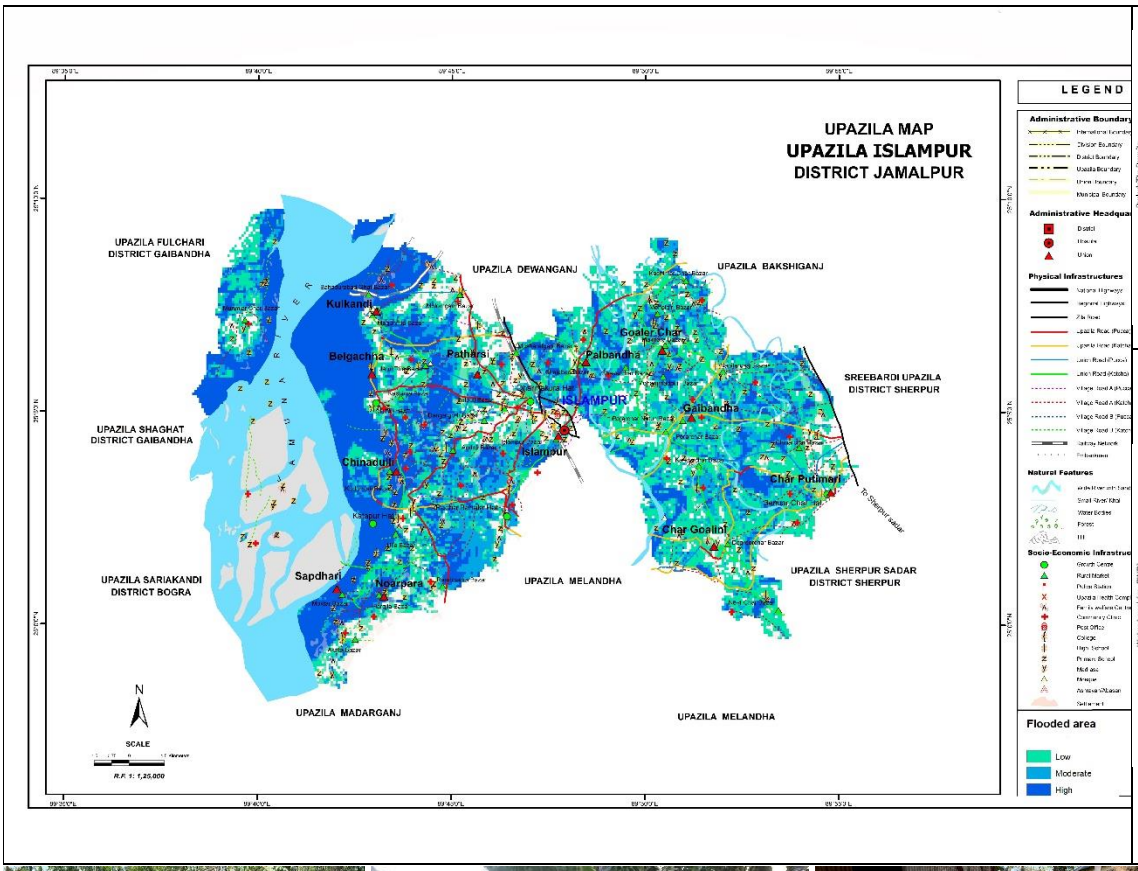

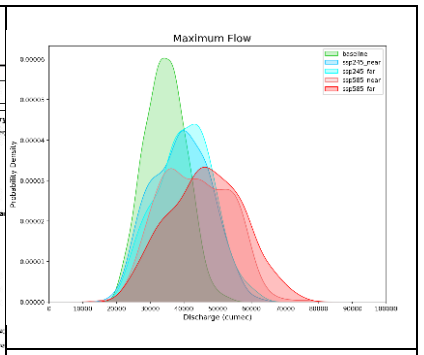

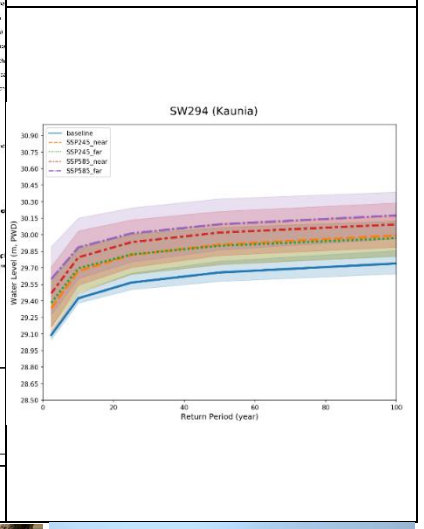

FINAL REPORT

CLIMATE CHANGE AND FLOOD PREPAREDNESS RESEARCH FOR BUILDING CLIMATE RESILIENT INFRASTRUCTURE

Submitted by

Institute of Water and Flood Management
Bangladesh University of Engineering and Technology

June 2022

RESEARCH TEAM

Sl. No.	Discipline	Name of Professional
1.	Principal Investigator (Hydrology and Climate Change)	Dr. A.K.M. Saiful Islam
2.	Co-Investigator (Senior Hydrologist)	Dr. G.M. Tarekul Islam
3.	Co-investigator (Flood Risks Assessment)	Dr. Sujit Kumar Bala
4.	Climate Modeler (Post-doc)	Dr. Mohan Kumar Das
5.	Research Assistant (Data analysis & hydrological modeling)	Wasif Bin Mamoon Anik Chandra Banik
6.	Research Assistant (Data analysis & hydrological modeling)	Faruque Abdullah
7.	Research Assistant (Data analysis & hydrological modeling)	Maruf Billah

TABLE OF CONTENTS

Page No.

RESEARCH TEAM ii
TABLE OF CONTENTS iii
LIST OF TABLES viii
LIST OF FIGURES xii
LIST OF PHOTOGRAPHS xix
ABBREVIATIONS AND ACRONYMS xxi
EXECUTIVE SUMMARY xxiii
CHAPTER ONE INTRODUCTION 1
1.1 Background 1
1.2 Rationale of the study 1
1.3 Objectives of the study 2
1.4 Scope of Work 3
1.5 Limitations of the work 3
CHAPTER TWO STUDY AREA 4
2.1 Project Area 4
2.1.1 Jamalpur District 6
2.1.2 Rangpur District 6
2.1.3 Gaibandha District 6
2.1.4 Kurigram District 7
2.1.5 Lalmonirhat District 7
2.1.6 Nilphamari District 8
2.2 River Network 9
2.3 Climate System 12
2.4 Geology and Seismology 15
2.5 Agroecological systems 19
CHAPTER THREE BRAHMPUTRA-TEESTA BASIN MODELING 21
3.1 Introduction 21
3.2 Conceptual basis of SWAT Modeling 26
3.2.1 Water Balance 27
3.2.2 Snow 28
3.2.3 Canopy Storage 29
3.2.4 Infiltration 29
3.2.5 Evapotranspiration 29
3.2.6 Lateral Subsurface Flow 30
3.2.7 Surface Runoff 30

3.2.8 Return Flow....30
3.3 Routing Phase of the Hydrologic Cycle....31
3.4 Hydrology....31
3.4.1 Rainfall Intensity....31
3.4.2 Percolation....32
3.4.3 Lateral Flow....32
3.4.4 Shallow Aquifer....32
3.4.5 Deep Aquifer....33
3.4.6 Transmission Loss....33
3.4.7 Evaporation Loss....33
3.4.8 Bank Storage....34
3.4.9 Channel Water Balance....34
3.5 Steps of SWAT Modeling....34
3.5.1 Data Collection....35
3.5.2 Digital Elevation Model, Land use, and Soil Data....35
3.5.3 Weather and Discharge data....38
3.6 Climate Model Data....38
3.6.1 CMIP6 Global Climate Models....38
3.7 Bias Correction of climate data....41
3.8 Steps of Model Setup....42
3.8.1 Watershed Delineation....43
3.8.2 Weather Data Definition....44
3.8.3 Simulation Method Selection....45
3.8.4 Model Calibration and Validation....45
3.8.4.1 SWAT-CUP....45
3.8.4.2 Performance Evaluation of the Model using Statistical Indicators....47
3.8.4.3 Sensitive Parameter Selection for Calibration....48
3.8.4.4 Calibration and Validation Using SWAT-cup....50
3.8.4.5 Performance of the Model....53
3.9 SWAT Model Simulation and Outputs....53
CHAPTER FOUR HYDRODYNAMIC MODELING FOR FLOODING....61
4.1 Introduction....61
CHAPTER FOUR HYDRODYNAMIC MODELING FOR FLOODING....62
4.1 Introduction....62
4.2 HEC-RAS Model....62
4.3 HEC-GeoRAS....63

4.4 Methodology 64
4.4.1 Data collection 64
4.5 Setting up HEC-GeoRAS 66
4.5.1 Pre-processing the DEM 66
4.5.2 Creating RAS layers for geometric data using HEC-GeoRAS 66
4.6 HEC-RAS 1D Model Setup 69
4.6.1 Exporting and Modifying Geometry Data 69
4.6.2 Boundary Condition and Model Simulation 69
4.7 Calibration and Validation of HEC-RAS 1D Model 70
4.8 Performance Evaluation of HEC-RAS 1D Model during Major Flood Years 74
4.9 Summary and Discussions 78
CHAPTER FIVE RAPID FLOOD MAPPING USING SENTINEL-1 SAR IMAGES 79
5.1 Introduction 79
5.2 Methodology for flood inundation mapping 81
5.2.1 Data acquisition 83
5.2.3 Pre-processing of SAR image 84
5.2.4 Processing of SAR image 84
5.2.5. Cloud-based platform for flood mapping 88
5.3 Flood inundation mapping for 2004, 2007, 2016, 2017 and 2019 and 2020 90
5.3.1 Floods in 2004 90
5.3.2 Floods in 2007 90
5.3.3 Floods in 2016 91
5.3.4 Floods in 2017 93
5.3.5. Floods in 2019 94
5.3.6. Floods in 2020 95
5.4 Accuracy assessment of Flood Maps using ground truthing 102
5.4 Flood Vulnerability Mapping 112
5.5 Planform Analysis for estimation of erosion and accretion of river 132
5.5.1 Modified Normalized Difference Water Index (MNDWI) 132
5.5.2 Satellite Image Processing for Planform Analysis 134
5.5.3 Planform Analysis of different Flood Shelters and Markets 136
5.5.4 Combined flood and erosion risk of the infrastructure 136
5.5.5 Combined Flood and Bank Erosion Risks for School cum Flood Shelters 138
5.5.6 Combined Flood and Bank Erosion Risks for Markets 176
CHAPTER SIX FLOOD FREQUENCY ANALYSIS 277
6.1 Introduction 277

6.2 Flood Frequency Analysis....278
6.2.1 Selected Stations for Frequency Analysis....278
6.2.2 Methods of Frequency Analysis....279
6.2.3 Selection of Suitable Method....280
6.3 Design Flood Frequency....281
6.3.1 Flood Frequency analysis for Jamuna River....282
6.3.2 Flood Frequency analysis for Dudhkumar River....284
6.3.3 Flood Frequency analysis for Dharala River....285
6.3.4 Flood Frequency analysis for Teesta River....286
6.3.5 Flood Frequency analysis for Ghaghat River....287
6.3.6 Flood Frequency analysis for Old Brahmaputra....288
6.3.7 Flood Frequency analysis for Jhenai River....289
6.3.8 Flood Frequency analysis for Bangali River....290
6.4 Design Water-level for Various Return Periods....291
6.5 Changes in Flood Frequency Considering Climate Change....301
6.6 Increase of crest height of Village, Union and Upazila Roads, markets and school cum flood shelters....310
CHAPTER SEVEN CLIMATE-RESILIENT INFRASTRUCTURES DESIGN....312
7.1 Review of the existing guidelines....312
7.2 Design of Climate Resilient Growth Centers/Markets....319
7.3 Design of Climate-Resilient Roads and Culverts....320
7.4 Design of Climate-Resilient Flood Shelters....329
7.5 Monitoring and maintenance of roads and other infrastructures....329
7.6 Socializing and Engendering Design of Infrastructures of PROVATi^3 Project....330
7.6.1 Socializing and PROVATi^3 Project....330
7.6.2 Socializing Approaches in PROVATi^3 Project....331
7.6.3 Experiences of Bangladesh in Socializing Infrastructures....335
7.6.4 Suggestions for socializing infrastructure....337
CHAPTER EIGHT OBSERVATIONS FROM FIELD VISITS....339
8.1 Field visit to the Jamalpur flood vulnerable Area....339
CHAPTER NINE CONCLUSIONS AND RECOMMENDATIONS....345
9.1 Conclusions....345
9.2 Recommendations....346
REFERENCES....348
Appendix A: Hydrological and Morphological Data Collected from BWDB....354
Appendix A1: Daily time-series water level data to be collected from BWDB....355

Appendix A2: Discharge data to be collected from BWDB. 356
Appendix A3: River x-section data to be collected from BWDB. 356
Appendix B: Cross-sectional Profiles of Brahmaputra-Teesta River Systems 357
Appendix B1. X-section of the Dudhkumar River 358
Appendix B2. X-section of the Teesta River 363
Appendix B3. X-section of the Brahmaputra-Jamuna River 369
Appendix B4. X-section of the Old Brahmaputra River 373
Appendix B5. X-section of the Ghaghat River 378
Appendix B6. X-section of the Bangali River 381
Appendix B7. X-section of the Jhenai River 388

LIST OF TABLES

Page No.

Table 2.1: Summary of the projected area. 5

Table 2.2: Summary of different districts within the study area. 8

Table 2.3: Seismic zones of Bangladesh (BNBC, 2012). 17

Table 3.1: List of Regional Climate Models used in HELIX. 25

Table 3.2: Description of the Global Circulation Models (GCMs) used in the HELIX project. 26

Table 3.3: List of CMIP6 Climate Models used in the study. 40

Table 3.4: Model performance rating. 48

Table 3.5: Parameters used for calibration of the SWAT model. 49

Table 3.6: List of most sensitive parameters according to their P-values and t-stats. 51

Table 3.7: Model performance analysis. 53

Table 4.1: Summary of data sets that are available to be used for hydrodynamic modeling. 65

Table 4.2: Summary of Model calibration and validation. 71

Table 4.3: Performance rating of different evaluation parameters. 74

Table 4.4: A summary of the Performance Evaluation of the model. 75

Table 5.1: Detailed data information on acquired data. 84

Table 5.2: Damage information at a glance for flood 2017. 93

Table 5.3. Area affected during the 2017 and 2019 floods in 6 districts of our study area. 95

Table-5.4: Framework of the confusion matrix 102

Table 5.5: Location of ground truthing of flood inundation. 103

Table 5.6: Accuracy assessment of Flood map of 2019. 107

Table 5.7: Accuracy assessment of Flood map of 2020 107

Table 5.8: Criteria for assessing flood risks based on flood inundation mapping. 137

Table 5.9: Criteria for assessing river bank erosion risk based on planform analysis. 137

Table 5.10: Shifting of the river banks and flood vulnerability of the Abdul Gani Govt. Primary school (North direction). 140

Table 5.11: Shifting of the river banks and flood vulnerability of the Chinarchar Uttarpara Govt. Primary school (Southeast direction). 142

Table 5.12: Shifting of the river banks and flood vulnerability of the Shapdhori Govt. Primary school (East direction).....144

Table 5.13: Shifting of the river banks and flood vulnerability of the Shuknagori Govt. Primary school (West direction). 146

Table 5.14: Shifting of the river banks and flood vulnerability of the All Haz Gohor Uddin Junior school (West direction). 148

Table 5.15: Shifting of the river banks and flood vulnerability of the Ajam Kha Government Primary school (West direction). 150

Table 5.16: Shifting of the river banks and flood vulnerability of the Dalia Baishpukure Tistarchar Government Primary school (West direction). 152

Table 5.17: Shifting of the river banks and flood vulnerability of the Dalia Baishpukure Tistar char Government Primary school (West direction). 154

Table 5.18: Shifting of the river banks and flood vulnerability of Jongra 3 No Battala Government Primary school (West direction). 156

Table 5.19: Shifting of the river banks and flood vulnerability of Pollimari Government Primary school (West direction). 158

Table 5.20: Shifting of the river banks and flood vulnerability of Shoulmari Charvorot Government Primary school (West direction). 160

Table 5.21: Shifting of the river banks and flood vulnerability of Tapakharibari 1 No Government Primary school (North East direction). 162

Table 5.22: Shifting of the river banks and flood vulnerability of Jotindra Naraya Government Primary School, Kurigram District (East direction) 164

Table 5.23: Shifting of the river banks and flood vulnerability of Kochabari Bhurongamari Government Primary School (East direction). 166

Table 5.24: Shifting of the river banks and flood vulnerability of Sayadpur Government Primary School (East direction).....168

Table 5.25: Shifting of the river banks and flood vulnerability of Bashir Nagar Government Primary School (East direction).....170

Table 5.26: Shifting of the river banks and flood vulnerability of Bekrir Char Government Primary School (East direction).....172

Table 5.27: Shifting of the river banks and flood vulnerability of Chinirpatol Government Primary School (East direction).....174

Table 5.28: Combined flood and bank erosion risks of the proposed school cum flood shelters in the selected locations. 175

Table 5.29: Combined flood and bank erosion risks of the proposed markets in the selected locations. 176

Table 6.1: Brief descriptions of Frequency analysis 279

Table 6.2: Statistical parameters used for goodness of fit of the PDFs. 281

Table 6.3: Fitted PDFs and the corresponding values of PPCC, RMSD, and Chi-square for the maximum water level of Jamuna River at Noonkhawa. 282

Table 6.4: Fitted PDFs and the corresponding values of PPCC, RMSD, and Chi-square for the maximum water level of Jamuna River at Chilmari. 282

Table 6.5: Fitted PDFs and the corresponding values of PPCC, RMSD, and Chi-square for the maximum water level of Jamuna River at Bahadurabad. 283

Table 6.6: Fitted PDFs and the corresponding values of PPCC, RMSD, and Chi-square for the maximum water level of Jamuna River at Sirajganj. 283

Table 6.7: Fitted PDFs and the corresponding values of PPCC, RMSD, and Chi-square for the maximum water level of Dudhkumar River at Pateswari. 284

Table 6.8: Fitted PDFs and the corresponding values of PPCC, RMSD, and Chi-square for the maximum water level of the Dharala River at Taluk-Simulbari. 285

Table 6.9: Fitted PDFs and the corresponding values of PPCC, RMSD, and Chi-square for the maximum water level of the Dharala River at Kurigram. 285

Table 6.10: Fitted PDFs and the corresponding values of PPCC, RMSD, and Chi-square for the maximum water level of Teesta River at Kaliganj 286

Table 6.11: Fitted PDFs and the corresponding values of PPCC, RMSD, and Chi-square for the maximum water level of Teesta River at Kaunia. 286

Table 6.12: Fitted PDFs and the corresponding values of PPCC, RMSD, and Chi-square for the maximum water level of Teesta River at Haripur. 286

Table 6.13: Fitted PDFs and the corresponding values of PPCC, RMSD, and Chi-square for the maximum water level of Ghaghat River at Jafarganj 287

Table 6.14: Fitted PDFs and the corresponding values of PPCC, RMSD, and Chi-square for the maximum water level of the Ghaghat River at Gaibandha. 287

Table 6.15: Fitted PDFs and the corresponding values of PPCC, RMSD, and Chi-square for the maximum water level of the Old Brahmaputra River at Jamalpur. 288

Table 6.16: Fitted PDFs and the corresponding values of PPCC, RMSD, and Chi-square for the maximum water level of Jhenai River at Baushi Bridge. 289

Table 6.17: Fitted PDFs and the corresponding values of PPCC, RMSD, and Chi-square for the maximum water level of Jhenai River at Offtake Jhenai. 289

Table 6.18: Fitted PDFs and the corresponding values of PPCC, RMSD, and Chi-square for the maximum water level of the Bangali River at Mohimganj. 290

Table 6.19: Fitted PDFs and the corresponding values of PPCC, RMSD, and Chi-square for the maximum water level of Bangali River at Simulbari 291

Table 6.20: Design Water-level for 2. 33, 10, 20, 50, 100-year Return Period. 292

Table 6.21: Frequency analysis of Dharala River at Kurigram (SW77) using mean ensemble climate projections for the near and far future. 301

Table 6.22: Frequency analysis of Dudhkumar River at Pateswari (SW81) using mean ensemble climate projections for the near and far future. 303

Table 6.23: Frequency analysis of Brahmputra River at Chilmari (SW45.5) using mean ensemble climate projections for the near and far future. 304

Table 6.24: Frequency analysis of Jamuna River at Bahadurabad (SW46.9L) using mean ensemble climate projections for the near and far future. 305

Table 6.25: Frequency analysis of Teesta River at Dalia (SW291.5R) using mean ensemble climate projections for the near and far future. 306

Table 6.26: Frequency analysis of Teesta River at Kaunia (SW294) using mean ensemble climate projections for the near and far future. 308

Table 6.27: Frequency analysis of Old Brahmaputra River at Jamalpur (SW225) using mean ensemble climate projections for the near and far future. 309

Table 6.28: Increase of crest height of village, union and Upazila roads of LGED for 10-year return period design flood considering climate change. 311

Table 6.29: Increase of crest height of market and flood shelters of LGED for 100-year return period design flood considering climate change. 311

Table 7.1: Dimension of road embankment, bridges, and culvers (Planning Commission, 2004). 313

Table 7.2: Typical gaps by type of road, meters per kilometer 315

Table 7.3: Specification of filter fabrics used as revetment filter layer (non-woven needle-punched geotextile). 328

Table 7.4: Specification of geotextile material for manufacturing of geo-sand containers. 329

Table 8.1: A summary of the major observations from field visits. 339

Table 9.1: Recommendations for Climate Resilient Infrastructures under this PROVATi^3 project. ...346

LIST OF FIGURES

Page No.

Figure 2.1: Study Area of the project. 4

Figure 2.2: River systems of the study area. 9

Figure 2.3: Major river network of the study area. 12

Figure 2.4: Climatic sub-regions of Bangladesh. 13

Figure 2.5. Rainfall distribution of Bangladesh. 14

Figure 2.6: Natural hazards are expected to change due to climate change. 15

Figure 2.7: Earthquake zones of Bangladesh (Source: BNBC, 2012). 16

Figure 2.8: Earthquake zones of Bangladesh (Source: BNBC, 2012). 18

Figure 2.9: Agroecological zones of Bangladesh (Source: BARC Edaphic Maps). 20

Figure 3.1: Brahmaputra-Teesta River Basin. 22

Figure 3.2: Hydrologic process in SWAT. 28

Figure 3.3: The routing phase of the hydrological cycle is used in the SWAT model. 31

Figure 3.4: (a) DEM, (b) land use map, and (c) soil map of Brahmaputra River Basin. 37

Figure 3.5: Comparing CMIP5 and CMIP6 scenarios from 1880-1900 and 2090-2100 for currently available runs. (Source: Carbon Brief). 39

Figure 3.6: Comparison of the multi-model model ensemble (blue) mean seasonal cycle of bias-corrected (a) precipitation, (b) maximum temperature, and (c) minimum temperature against the observations for the 1985–2014 period. The shaded area represents the uncertainty of all the used CMIP6 Global Circulation Models (Mishra et al., 2020). 42

Figure 3.7: A brief framework of the SWAT model (Aqnouy, 2019). 43

Figure 3.8: Sub-basins and delineated stream network of Brahmaputra River Basin. 44

Figure 3.9: A conceptual illustration of the relationship between parameter uncertainty and prediction uncertainty (Abbaspour, 2007). 47

Figure 3.10: Comparison of the simulated flow with the observed for calibration (1985-1999). 52

Figure 3.11: Comparison of the simulated flow with the observed for validation (2000-2014). 52

Figure 3.12: Simulated maximum annual discharge (cumec) for the baseline (1985-2014), near-future period (2025-2054), and far-future period (1971-2014) under SSP245 54

Figure 3.13: Simulated maximum annual discharge (cumec) for the baseline (1985-2014), near-future period (2025-2054), and far-future period (1971-2014) under SSP245 54

Figure 3.14: Multi-model ensemble mean monthly percentage increase of flow at Bahadurabad (SW 46.9L) in the Brahmaputra-Jamuna river in the near (2025-2054) and far future (2071-

2100) with respect to the baseline period (1985-2014) under SSP2-45 and SSP5-85 scenarios.....55

Figure 3.15: Simulated maximum monthly discharge (cumec) for the near future period (2025-2054) compared to baseline (1985-2014).....56

Figure 3.16: Percentage change in mean monthly discharge (cumec) for the far future period (2071-2100) compared to baseline (1985-2014). 57

Figure 3.17: Variability in multi-model maximum monthly discharge (cumec) for the near future period (2025-2054) compared to baseline (1985-2014).....58

Figure 3.18: Variability in multi-model maximum monthly discharge (cumec) for the far future period (2071-2100) compared to baseline (1985-2014).....58

Figure 3.19: Probability density functions (PDF) of maximum monthly discharge (cumec) for the near (2025-2054) and far future period (2071-2100) compared to baseline (1985-2014).....59

Figure 3.20: Probability density functions (PDF) of mean monthly discharge (cumec) for the near (2025-2054) and far future period (2071-2100) compared to baseline (1985-2014).....59

Figure 3.21: Probability density functions (PDF) of minimum monthly discharge (cumec) for the near (2025-2054) and far future period (2071-2100) compared to baseline (1985-2014).....60

Figure 4.1: DEM of the Study Area is used for HEC-RAS modeling. 66

Figure 4.2: Pre-processing with HEC-GeoRAS.....67

Figure 4.3: Generating RAS layers with HEC-GeoRAS. 68

Figure 4.4: Discharge and Water-level stations of the study area.....70

Figure 4.5: Comparison of R^2 during calibration and validation period in the Jamuna, Ghaghat, and Bangali rivers.....72

Figure 4.6: Comparison of R^2 during calibration and validation period in the Teesta, Dharala, and Dudhkumar rivers. 73

Figure 4.7. Comparison of Simulated Hydrograph and Observed Water-level on 2017 Flood event. ..76

Figure 4.8. Comparison of Simulated Hydrograph and Observed Water-level on 2019 Flood event. ..77

Figure 5.1: Study area map used for satellite image analysis.....81

Figure 5.2: Methodology for flood inundation mapping.....83

Figure 5.3: Pre-processing of the image, orbit files, image filtering (a), radiometric calibration (b), and terrain correction (c). 84

Figure5.4: Backscatter value has been converted from a linear scale to a nonlinear logarithm scale, before conversion (a) and after the conversion (b). 85

Figure 5.5: Histogram of pixel values in a nonlinear logarithm scale.....85

Figure 5.6: Preprocessed archive or pre-flood image (a), preprocessed crisis or during flood image (b), RGB visual flood map (c), final flood map (d).....87

Figure 5.7: A working window of Google Earth Engine (GEE) using python API using Jupiter notebook.....88

Figure 5.8: The flood map of (a) 2004, (b) 2007 developed using the MODIS images and (c) 2016, (d) 2017, (e) 2019, (f) 2020 developed using Sentinel-1 image.....101

Figure 5.9: Update flood map of 2016 developed using Sentinel-1 image.....108

Figure 5.10: Update flood map of 2017 developed using Sentinel-1 image.....109

Figure 5.11: Update flood map of 2019 developed using Sentinel-1 image.....110

Figure 5.12: Update flood map of 2020 developed using Sentinel-1 image.....111

Figure 5.13: Flood vulnerability mapping based on inundation frequency.....112

Figure 5.14: Flood vulnerability mapping for Bhurungamari Upazila of Kurigram district.....113

Figure 5.15: Flood vulnerability mapping for Sadar Upazila of Kurigram district.....113

Figure 5.16: Flood vulnerability mapping for Nageswari Upazila of Kurigram district.....114

Figure 5.17: Flood vulnerability mapping for Rajarhat Upazila of Kurigram district. 114

Figure 5.18: Flood vulnerability mapping for Rajibpur Upazila of Kurgram district.....115

Figure 5.19: Flood vulnerability mapping for Phulbari Upazila of Kurigram district. 115

Figure 5.20: Flood vulnerability mapping for Chilmari Upazila of Kurigram district.....116

Figure 5.21: Flood vulnerability mapping for Rowmari Upazila of Kurigram district.....117

Figure 5.22: Flood vulnerability mapping for Ulipur Upazila of Kurigram district. 118

Figure 5.23: Flood vulnerability mapping for Melandah Upazila of Jamalpur district.....119

Figure 5.24: Flood vulnerability mapping for Dewanganj Upazila of Jamalpur district. 120

Figure 5.25: Flood vulnerability mapping for Bakshiganj Upazila of Jamalpur district.....121

Figure 5.26: Flood vulnerability mapping for Madarganj Upazila of Jamalpur district. 122

Figure 5.27: Flood vulnerability mapping for Islampur Upazila of Jamalpur district. 123

Figure 5.28: Flood vulnerability mapping for Sadar Upazila of Jamalpur district. 123

Figure 5.29: Flood vulnerability mapping for Fulchari Upazila of Gaibandha district.....124

Figure 5.30: Flood vulnerability mapping for Sadullahpur Upazila of Gaibandha district.....125

Figure 5.31: Flood vulnerability mapping for Shaghata Upazila of Gaibandha district. 126

Figure 5.32: Flood vulnerability mapping for Sundarganj Upazila of Gaibandha district.....127

Figure 5.33: Flood vulnerability mapping for Sadar Upazila of Gaibandha district.....127

Figure 5.34: Flood vulnerability mapping for Gangachra Upazila of Rangpur district. 128

Figure 5.35: Flood vulnerability mapping for Kaunia Upazila of Rangpur district. 129

Figure 5.36: Flood vulnerability mapping for Patgram Upazila of Lalmonirhat district. 130

Figure 5.37: Flood vulnerability mapping for Dimla Upazila of Nilphamari district. 130

Figure 5.38: Flood vulnerability mapping for Hatibandha Upazila of Lalmonirhat district. 131

Figure 5.39: Satellite image processing for planform analysis of different rivers for the year 2020, (a) Dudhkumar, (b) Dharala, (c) Teesta, (c) Jamuna, (d) Old Brahmaputra. 135

Figure 5.40: River planform analysis near Abdul Gani Govt. Primary school from the year 1989 to 2020 using satellite data. Here river bank line for years (a)1989, (b) 2000, (c) 2010 and (d) 2020, (e) bank line shifting from the year 1989 to 2020 and (f) on google earth image. ..140

Figure 5.41: River planform analysis near Chinarchar Uttarpara Govt. Primary school from the year 1989 to 2020 using satellite data. Here is the river bank line of years (a)1989, (b) 2000, (c) 2010 and (d) 2020, and (e) bank line shifting from the year 1989 to 2020 and (f) on google earth image.....142

Figure 5.42: River planform analysis near Shapdhori Govt. Primary school from the year 1989 to 2020 using satellite data. Here is the river bank line of years (a)1989, (b) 2000, (c) 2010 and (d) 2020, and (e) bank line shifting from 1989 to 2020 and (f) on google earth image. 144

Figure 5.43: River planform analysis near Shuknagori Govt. Primary school from the year 1989 to 2020 using satellite data. Here is the river bank line of years (a)1989, (b) 2000, (c) 2010 and (d) 2020, and (e) bank line shifting from the year 1989 to 2020 and (f) on google earth image.....146

Figure 5.44: River planform analysis near All Haz Gohor Uddin Junior school from the year 1989 to 2020 using satellite data. Here is the river bank line of years (a)1989, (b) 2000, (c) 2010 and (d) 2020, and (e) bank line shifting from the year 1989 to 2020 and (f) on google earth image.....148

Figure 5.45: River planform analysis near Ajam Kha Government Primary school from the year 1989 to 2020 using satellite data. Here is the river bank line of years (a)1989, (b) 2000, (c) 2010 and (d) 2020, and (e) bank line shifting from the year 1989 to 2020 and (f) on google earth image.....150

Figure 5.46: River planform analysis near Dalia Baishpukure Tistarchar Government Primary school from the year 1989 to 2020 using satellite data. Here is the river bank line of years (a)1989, (b) 2000, (c) 2010 and (d) 2020, and (e) bank line shifting from the year 1989 to 2020 and (f) on google earth image.....152

Figure 5.47: River planform analysis near Dalia Baishpukure Tistar char Government Primary school from the year 1989 to 2020 using satellite data. Here is the river bank line of years (a)1989, (b) 2000, (c) 2010 and (d) 2020, and (e) bank line shifting from the year 1989 to 2020 and (f) on google earth image.....154

Figure 5.48: River planform analysis near Jongra 3 No Battala Government Primary school from the year 1989 to 2020 using satellite data. Here is the river bank line of years (a)1989, (b) 2000, (c) 2010 and (d) 2020, and (e) bank line shifting from the year 1989 to 2020 and (f) on google earth image.....156

Figure 5.49: River planform analysis near Pollimari Government Primary school from the year 1989 to 2020 using satellite data. Here is the river bank line of years (a)1989, (b) 2000, (c) 2010 and (d) 2020, and (e) bank line shifting from the year 1989 to 2020 and (f) on google earth image.....158

Figure 5.50: River planform analysis near Shoulmari Charvorot Government Primary school from the year 1989 to 2020 using satellite data. Here is the river bank line of years (a)1989, (b) 2000, (c) 2010 and (d) 2020, and (e) bank line shifting from the year 1989 to 2020 and (f) on google earth image.....160

Figure 5.51: River planform analysis near Tapakharibari 1 No Government Primary school from the year 1989 to 2020 using satellite data. Here is the river bank line of years (a)1989, (b) 2000, (c) 2010 and (d) 2020, and (e) bank line shifting from the year 1989 to 2020 and (f) on google earth image.....162

Figure 5.52: River planform analysis near Jotindra Naraya Government Primary School, Kurigram District, from the year 1989 to 2020 using satellite data. Here river bank line of years (a)1989, (b) 2000, (c) 2010 and (d) 2020, and (e) bank line shifting from the year 1989 to 2020 and (f) on Google Earth image.....164

Figure 5.53: River planform analysis near Kochabari Bhurongamari Government Primary School, Kurigram District, from the year 1989 to 2020 using satellite data. Here river bank line of years (a)1989, (b) 2000, (c) 2010 and (d) 2020, and (e) bank line shifting from the year 1989 to 2020 and (f) on Google Earth image.....166

Figure 5.54: River planform analysis near Sayadpur Government Primary School from the year 1989 to 2020 using satellite data. Here river bank line of years (a)1989, (b) 2000, (c) 2010 and (d) 2020, and (e) bank line shifting from the year 1989 to 2020 and (f) on Google Earth image.....168

Figure 5.55: River planform analysis near Bashir Nagar Government Primary School from the year 1989 to 2020 using satellite data. Here river bank line of years (a)1989, (b) 2000, (c) 2010 and (d) 2020, and (e) bank line shifting from the year 1989 to 2020 and (f) on Google Earth image.....170

Figure 5.56: River planform analysis near Bekrir Char Government Primary School from the year 1989 to 2020 using satellite data. Here river bank line of years (a)1989, (b) 2000, (c) 2010 and (d) 2020, and (e) bank line shifting from the year 1989 to 2020 and (f) on Google Earth image.....172

Figure 5.57: River planform analysis near Chinirpatol Government Primary School from the year 1989 to 2020 using satellite data. Here river bank line of years (a)1989, (b) 2000, (c) 2010 and (d) 2020, and (e) bank line shifting from the year 1989 to 2020 and (f) on Google Earth image.....174

Figure 6.1: Selected stations for Frequency analysis. 278

Figure 6.2. Probability plot along with 90% confidence interval of the P3, Gumbel, LP3, and P3 distribution fitted to the annual maximum water level data of the Jamuna River at Noonkhawa, Chilmari, Bahadurabad, and Sirajganj.....283

Figure 6.3: Probability plot along with 90% confidence interval of the LP3 distribution fitted to the annual maximum water level data of the Dudhkumar River at Pateswari. 284

Figure 6.4: Probability plot along with 90% confidence interval of the P3, LN3 distribution fitted to the annual maximum water level data of the Dharala River at Taluk-Simulbari and Kurigram. 285

Figure 6.5: Probability plot along with 90% confidence interval of the P3, LN3 distribution fitted to the annual maximum water level data of the Teesta River at Kaliganj and Kaunia. 287

Figure 6.6: Probability plot along with 90% confidence interval of the LN3, P3 distribution fitted to the annual maximum water level data of the Ghaghat River at Jafarganj and Gaibandha.288

Figure 6.7: Probability plot along with 90% confidence interval of the LN3 distribution fitted to the annual maximum water level data of the Old Brahmaputra River at Jamalpur. 289

Figure 6.8: Probability plot along with 90% confidence interval of the P3 distribution fitted to the annual maximum water level data of the Jhenai River at Baushi Bridge and Offtake Jhenai. 290

Figure 6.9: Probability plot along with 90% confidence interval of the P3 distribution fitted to the annual maximum water level data of the Bangali River at Mohimganj and Simulbari. 291

Figure 6.10: Design Water-level for a corresponding return period of the Jamuna River at a) Noonkhawa, b) Chilmari, c) Bahadurabad, d) Sirajganj. 294

Figure 6.11: Design Water-level for a corresponding return period of the Dudhkumar River at Pateswari. 295

Figure 6.12: Design Water-level for the corresponding return period of the Old Brahmaputra at Jamalpur. 295

Figure 6.13: Design Water-level for the corresponding return period of the Dharala River at a) Taluk-Simulbari, b) Kurigram. 296

Figure 6.14: Design Water-level for the corresponding return period of the Teesta River at a) Kaliganj, b) Kaunia.....297

Figure 6.15: Design Water-level for the corresponding return period of the Ghaghat River at a) Jafarganj, b) Gaibandha. 298

Figure 6.16: Design Water-level for the corresponding return period of the Jhenai River at a) Baushi Bridge, b) Offtake Jhenai. 299

Figure 6.17: Design Water-level for the corresponding return period of the Bangali River at (a) Mohimganj, (b) Simulbari. 300

Figure 6.18: Frequency of maximum water level (m, PWD) of Dharala River at Kurigram (SW77) using climate projections for the near future (2025-2054) and far future (2071-2100) with respect to the baseline period (1985-2014). 302

Figure 6.19: Frequency of maximum water level (m, PWD) of Dudhkumar River at Pateswari (SW81) using climate projections for the near future (2025-2054) and far future (2071-2100) with respect to the baseline period (1985-2014). 303

Figure 6.20: Frequency of maximum water level (m, PWD) of Brahmputra River at Chilmari (SW45.5) using climate projections for the near future (2025-2054) and far future (2071-2100) with respect to the baseline period (1985-2014).....304

Figure 6.21: Frequency of maximum water level (m, PWD) of Jamuna River at Bahadurabad (SW46.9L) using climate projections for the near future (2025-2054) and far future (2071-2100) with respect to the baseline period (1985-2014).....306

Figure 6.22: Frequency of maximum water level (m, PWD) of Teesta River at Dalia (SW291.5R) using climate projections for the near future (2025-2054) and far future (2071-2100) with respect to the baseline period (1985-2014). 307

Figure 6.23: Frequency of maximum water level (m, PWD) of Teesta River at Kaunia (SW294) using climate projections for the near future (2025-2054) and far future (2071-2100) with respect to the baseline period (1985-2014). 308

Figure 6.24: Frequency of maximum water level (m, PWD) of Old Brahmaputra River at Jamalpur (SW255) using climate projections for the near future (2025-2054) and far future (2071-2100) with respect to the baseline period (1985-2014).....310

Figure 7.1: Slope protection work with gunny bagged Rip-Rap and Geotextile. 315

Figure 7.2: Slope protection work with CC block and geotextile. 316

Figure 7.3: Slope protection work with brick block and geotextile. 316

Figure 7.4: Slope protection work with brickbat mattressing and geotextile. 316

Figure 7.5: A typical cross-section of an embankment as per the guideline of BWDB. 317

Figure 7.6: Typical village road section. 317

Figure 7.7: Village road section (HBB). 318

Figure 7.8: Typical union road section. 318

Figure 7.9: Change in the magnitude of the flood level for a particular return period in the Brahmaputra River at Bahadurabad. 322

Figure 7.10: Change in the magnitude of the flood level (1949-1998 and 1999-2020) for a particular return period in the Brahmaputra River at Bahadurabad. 322

Figure 7.11: Typical multi-layer revetment system. 324

LIST OF PHOTOGRAPHS

Page No.

Photo 7.1: Failure of abutment of a bridge constructed by constricting the width of the Darbhanga River in Islampur Upazila of Jamalpur. 313

Photo 7.2: Failure of a culvert built in the floodplain of the Jamuna River in Jamalpur. 314

Photo 7.3: Failure of a culvert built in the floodplain of the Jamuna River in Jamalpur. 314

Photo 7.4: A submersible road in Islampur Upazila of Jamalpur.....321

Photo 7.5: A causeway in Islampur Upazila of Jamalpur. 321

Photo 8.1: There is no slope protection on this newly constructed village road. The slope of the road is highly vulnerable during floods. CC-block type of protection should be used as the road extends right from the abutment of a bridge in Kamalbarti Bazar, Bakshiganj, Jamalpur. But it was learned during the field visit that the slope of the road would be protected by vetiver grass which may not be suitable along the bank of a river during flood flows.....340

Photo 8.2: Damage of a bridge in Bakshiganj Upazila in Jamalpur. The damage appears to be due to the inadequate opening of the one-span bridge. As the area is located in the floodplain of the mighty Jamuna and the Dashani rivers, the waterway width of the river/canal should never be reduced while constructing a bridge.....340

Photo 8.3: Damage to the approach road of a bridge is probably due to seepage pressure developed during flood flow from the other side of the road. The slope should have been constructed with adequate filter material so that the seepage pressure can no longer develop and undermine the slope as well as the road itself.....341

Photo 8.4: Damage of a road due to slope failure in Bankishang Upazila, Jamalpur. 341

Photo 8.5: Damage of a village road due to overflowing. This road would connect a flood shelter in Chinar Char in Bakshiganj, Jamalpur. While renovating the road, the sufficient opening should be ensured by providing a culver of adequate size so that the flood flow can safely pass beneath the culvert without damaging the curve itself and the road. 342

Photo 8.6: Chinar Char Uttarpara Primary School. A new flood shelter-cum-primary school would be constructed on these premises. The corrugated sheet of the school clearly marks the flood of 2019 and 2020. The plinth level of the flood shelter should be set above the highest flood level or the 100-year flood level with an appropriate freeboard.....342

Photo 8.7: A flood-proofing straw pile in the Shapdhori Union of Islampur Upazila of Jamalpur district. The straw piles will not be inundated even during the flood. 343

Photo 8.8: A village road constructed with rigid pavement (RCC) in Madarganj Upazila, Jamalpur. This type of road is more climate-resilient, especially during floods. The village roads in areas vulnerable due to floods should be constructed with RCC with appropriate side slopes so that the damage is minimum even during overtopping during extreme flood events. 343

Photo 8.9: The side slope of the road, located in Madarganj Upazila, is almost vertical, thus making it utterly vulnerable during flood flow. 344

Photo 8.10: A poorly designed primary school in Shukh Nagari village of Madarganj Upazila. The two buildings have two different plinth levels. The plinth of the school gets inundated even during the moderate flood. A new flood shelter would be constructed on these premises. The plinth should be set at a 100-year flood level with an appropriate freeboard. 344

ABBREVIATIONS AND ACRONYMS

AEZ	Agro-Ecological Zone
BMD	Bangladesh Meteorological Department
BNBC	Bangladesh National Building Code
BUET	Bangladesh University of Engineering and Technology
BWDB	Bangladesh Water Development Board
DEM	Digital Elevation Model
DTM	Digital Terrain Model
GBM	Ganges Brahmaputra Meghna
GIS	Geographical Information System
GISM	Geographic Information System Model
GOB	Government of Bangladesh
GRD	Ground Range Detected
HEC-RAS	Hydrologic Engineering Centers River Analysis System
HRU	Hydrologic Response Unit
IFAD	International Fund for Agricultural Development
IGA	Income Generation Activities
IWFM	Institute of Water and Flood Management
LGED	Local Government Engineering Department
MNDWI	Modified Normalized Difference Water Index
MoDMR	Ministry of Disaster Management and Relief
MSL	Mean Sea Level
NDRCC	National Disaster Response Coordination Centre
NSE	Nash-Sutcliffe Efficiency
PET	Potential evapotranspiration
PROVATI^3	Promoting Resilience of Vulnerable through Access to Infrastructure, Improved, Skills, and Information
PWD	Public Works Department
RMSE	Root Mean Square Error
SNAP	Sentinel's Application Platform
SRTM	Shuttle Rudder Topography Mission
SWAT	Soil Water Assessment Tool
SWAT-CUP	SWAT Calibration and Uncertainty Program

TIN	Triangular Irregular Network
USGS	United State Geological Survey
UTM	Universal Transverse Mercator
VST	Vocational Skills- Training
WGS84	World Geodetic System
WXGEN	Weather Generator Tools

EXECUTIVE SUMMARY

Since 2016, Bangladesh has been observing major floods almost every year in the Teesta-Brahmaputra basins, which have caused severe damage to many rural infrastructures. Bangladesh is one of the most vulnerable countries to climate variability and change because of its geographic location, low deltaic floodplain, and hydro-meteorological influence of erratic monsoon rainfall and other extreme climate events. The central- north of Bangladesh is affected by seasonal flooding, river erosions, and low density and quality of rural infrastructure (low percentage of paved roads). Considering the environmental stress and socio-economic conditions, districts in north-central Bangladesh are some of the poorest and most vulnerable districts in the country. The situation is aggravated due to the adverse impacts of climate variability and change. To improve the resilience of the people living in flood-vulnerable areas of north-central Bangladesh, a new project entitled 'PROVATi^3 (Promoting Resilience of Vulnerable through Access to Infrastructure, Improved Skills, and Information)' has been designed. The goal of the project is to promote sustainable livelihoods for poor households and smallholders in selected 25 Upazilas of the Brahmaputra-Teesta flood plain area of six North-central districts of Bangladesh.

Under the PROVATi^3 project, IWFM-BUET will carry out a research study to build climate-resilient infrastructures. The overall objective of the study is to carry out a detailed hydrological, hydraulic, and morphological analysis of the watersheds to determine suitable design criteria for the proposed flood-vulnerable areas in order to build climate-resilient infrastructures. The results should indicate the necessary modifications in design on roads, culverts/bridges, markets, slope protection, etc., and might lead to up-dates in design standards at LGED. To achieve this goal, this study has been designed to assess the impact of climate change on the Teesta-Brahmaputra river system; assess erosion and accretion of land/char due to meandering of rivers; determine flood risk zones by combining both model results with ground-based and satellite image analysis of historic floods and potential impact of climate change on river flows of each project Upazila, and prepare a guideline for designing the climate-resilient infrastructures.

To carry out this study, baseline data, including socio-economic setting, climate, land use characteristics, river system and morphology, hydrological characteristics, and the infrastructures and communication network, have been collected. Details of this data collection

procedure and the types of collected are described in Chapter Two. Chapter Three presents the concept of the hydrological modeling of the Brahmaputra-Teesta river basins considering climate change scenarios. Chapter Four provides the methodology used in this study to determine future floodwater levels using 1-D hydraulic modeling. In Chapter Five, the process of flood inundation mapping using high-resolution satellite images has been described. This Chapter also presents the methodology of the assessment of the change of the river planform using historical images and locating the erosion and accretion areas. Chapter Six presents the flood frequency analysis at the gauge stations of the rivers nearby the study area. This Chapter also presents the design water level for the various return period for the present and future, considering climate change projections. Chapter Seven provides guidelines for designing climate-resilient roads, markets, and flood shelters. This Chapter also highlights the concept of the socializing and engendering Design of Infrastructures. Chapter Eight presents the key issues of the failure or damage, or resilience of different infrastructures that are observed during the field visits in the study area. Chapter Nine presents the conclusion of the study, including a summary of the key findings and recommendations of the study.

Hydrological modeling of the Brahmaputra-Teesta River basins has been conducted using SWAT modeling. The model showed a very good agreement between the observed and simulated discharges. The NSE values are found at 0.90 and 0.86, coefficient of determination values (R^2) values are found at 0.91 and 0.90, and the PBIAS values are 3.5 and 3.1 for the calibration and validation stage. The well-calibrated hydrological model is simulated forced with CMIP6 climate projections over the basin under balanced SSP2-4.5 and high-end SSP5-85 scenarios. Changes in future peak water level height are determined by simulating a 1-D hydraulic model, HEC-RAS, for the major rivers of the study area. Most of the stations provided very good results in terms of R^2 (>0.8) except Simulbari (SW 10) station in the Bangali river and Gaibandha (SW 97) station in the Ghaghat river.

Flood risks are assessed using historical satellite image analysis of major floods in 2004, 2007, 2016, 2017, 2019, and 2020. The accuracy of flood inundation maps is validated using 159 observed points data. The result of the accuracy assessment of the 2019 and 2020 flood maps was found satisfactory.

Table E1: Accuracy assessment of Flood map of 2019.

Parameters	Flood	Non-flood
Precision	0.98	0.33
Recall	0.75	0.89
F-1 score	0.85	0.49
Overall accuracy	0.76	

Table E2: Accuracy assessment of Flood map of 2020.

Parameters	Flood	Non-flood
Precision	0.92	0.63
Recall	0.76	0.86
F-1 score	0.83	0.73
Overall accuracy	0.79	

Based on planform analysis using historical satellite images, bank erosion risks are also identified for the proposed markets and flood shelters. Finally, combined flood and bank erosion risks on the infrastructures in the most vulnerable locations are assessed as presented in the table below. All of these composite flood vulnerability maps are prepared in an open source-based Google KML format which can be easily visualized and shared across many applications.

Table E3: Criteria for assessing flood risks based on flood inundation mapping.

Flood Risk Criteria
High Risk: • If a major flood occurs at least five times out of 6 major floods in the last two decades within 100m peripheries. Moderate Risk: • If a major flood occurs at least three times out of 6 major floods in the last two decades within 100m peripheries. Low Risk: • If a major flood occurs at most two times out of 6 major floods in the last two decades within 100m peripheries.

It is noteworthy to mention that major floods in the last two decades (2000-2020) occurred in 2004, 2007, 2016, 2017, 2019, and 2020.

Table E4: Criteria for assessing river bank erosion risk based on planform analysis.

River Bank Erosion Risk Criteria
High Risk: • Major Rivers: Historically, bank lines were within 1000m of the market or shelter. • Moderate Rivers: Historically, bank lines were within 300m of the market or shelter. • Minor Rivers: Historically, bank lines were within 50m of the market or shelter. Moderate Risk: • Major Rivers: Historically, bank lines were within 2000m of the market or shelter. • Moderate Rivers: Historically, bank lines were within 1000m of the market or shelter. • Minor Rivers: Historically, bank lines were within 100m of the market or shelter. Low Risk: • Major Rivers: Historically, bank lines were more than 3000m from the market or shelter. • Moderate Rivers: Historically, bank lines were within 1500m of the market or shelter. • Minor Rivers: Historically, bank lines were more than 200m from the market or shelter. However, if any interventions in the river, such as the construction of a dam, barrage, bridge, bank protection, or unplanned sand mining or dredging in the river, the risk may be changed, any record-breaking extreme events occur, and the morphology of the river may abruptly change, which would change the degree of vulnerability criteria. Here, the major rivers in the study area as Brahmaputra, Jamuna, and Teesta. Moderate rivers are Dharla, Dudhkumar, Old Brahmaputra, Ghagat, and Bangali, while minor rivers are their distributaries and tributaries.

Table E5: Combined flood and bank erosion risks of the proposed school cum flood shelters in the selected locations.

No	Shelter name	Upazila	District	River name	Distance from River (m)	Flood Risk	Bank Erosion Risk
1	Abdul Gani GPS	Bakshigonj	Jamalpur	Dasani	360	Low	Low
2	Chinarchar Uttar para GPS	Bakshigonj	Jamalpur	Dasani	420	Low	Low
3	Shapdhori Govt. Primary school	Jamalpur	High	Brahmaputra	159	High	High
4	Shukhnogory GPS	Madargonj	Jamalpur	Jamuna	2007	Moderate	Low
5	All Haz Gohor Junior School	Hatibandha	Nilphamari	Teesta	670	Low	Moderate
6	Ajam Kha GPS	Kaunia	Rangpur	Teesta	2880	Low	Low
7	Dalia Baishpukure Tistarchar GPS	Dimla	Nilphamari	Minor River	830	Moderate	Low
8	Char Holdibari GPS	Jaldhaka	Nilphamari	Teesta	1040	Moderate	Moderate
9	Jongra 3 No Battala GPS	Patgram	Lalmonirhat	Dharala	720	Moderate	Moderate
10	Pollimari GPS	Kaunia	Rangpur	Teesta	4860	Low	moderate
11	Shoulmari Charvorot GPS	Jaldhaka	Nilphamari	Teesta	290	Low	High
12	Tapakharibari 1 No GPS	Dimla	Nilphamari	Teesta	130	Low	High
13	Jotindra Naraya Government Primary School	Kurigram	Phulbari	Teesta	350	Low	High
14	Kochabari GPS	Bhurongamari	Kurigram	DudKumur	1960	Low	Low
15	Saiyadpur GPS cum Shelter	Gaibandha Sadar	Gaibandha	Teesta	190	Low	High
16	Bashir Nagor GPS	Shadullahpur	Gaibandha	Karotoya	2020	Low	Low
17	Bekrir Chaer GPS	Sundorgonj	Gaibandha	Teesta	2810	Low	High
18	Chinirpatol Government Primary School	Shaghata	Gaibandha	Brahmaputra	410	Low	High

Table E6: Combined flood and bank erosion risks of the proposed markets in the selected locations.

Sl.	District	Upazila	Market Name	Rivers	Distance from River (m)	Flood Risk	Bank Erosion Risk
1	Gaibandha	Sadullapur	Boxigonj Bazar	Minor river	105	Low	Low
2	Gaibandha	Sundarganj	Charokerhat Bazar	Minor river	2250	Low	Low
3	Gaibandha	Sundarganj	Jamaler Hat	Minor river	2350	Low	Low
4	Gaibandha	Saghatta	Dakhin Dighalkandi	Brahmaputra	10	Moderate	High
5	Gaibandha	Saghatta	Falia Bottala	Minor river	380	Low	Low
6	Gaibandha	Saghatta	Futani Bazar			Low	N/A***
7	Gaibandha	Saghatta	Ullah Bazar	Brahmaputra	400	Low	High*
8	Gaibandha	Saghatta	Nayabondar Bazar	Minor river	290	Low	Low
9	Gaibandha	Saghatta	Ullah Sonatala	Minor river	10	Low	High*
10	Gaibandha	Sadullapur	Kantanagar Bazar	Minor river	420	Low	Low
11	Gaibandha	Gaibandha Sadar	Lenga Bazar	Minor river	730	Low	Low
12	Gaibandha	Gaibandha Sadar	Puratan Badiakhali Hat	Minor river	30	Low	High
13	Gaibandha	Gaibandha Sadar	Balua Hat	Minor river	5800	Moderate	Low
14	Gaibandha	Fulchhari	Purbo Fulchori Bazar	Brahmaputra	1545	Low	Moderate
15	Rangpur	Gangachara	Bagerhat	Teesta	760	Low	High
16	Rangpur	Gangachara	Abuliarhat	Teesta	1170	Moderate	Moderate
17	Rangpur	Gangachara	Ichli Bazar (SKS Bazar)	Teesta	430	Low	High
18	Rangpur	Kaunia	Ekotarhat	Minor rivers	810	Low	Low
19	Rangpur	Kaunia	Haqueer Hat	Teesta	1100	Low	Moderate
20	Rangpur	Kaunia	Bhaier Hat	Minor river	65	Low	Moderate
21	Rangpur	Kaunia	Bhutsora (Mirbag) Hat	Minor river	200	Moderate	Moderate
22	Jamalpur	Islampur	Bulakip (ara Bazar)	Minor river	10	Low	High
23	Jamalpur	Islampur	Mondalpara Bazar	Brahmaputra	185	Low	High**
24	Jamalpur	Islampur	Napiterchar Bazar	Minor river	600	Low	Low
25	Jamalpur	Islampur	Shirajabad Bazar	Old Brahmaputra	760	Low	Moderate
26	Jamalpur	Islampur	Akota Bazar	Jamuna	835	Low	High
27	Jamalpur	Dewanganj	Amkhowa Bazar	Jinjiram	2100	Low	Low
28	Jamalpur	Dewanganj	Molla Para Bazar(Tilokpur)	Old Brahmaputra	500	Low	High
29	Jamalpur	Dewanganj	Sanandabari	Minor river	240	Low	Low
30	Jamalpur	Dewanganj	Khorma bazar	Minor river	420	Low	Low
31	Jamalpur	Melandaha	Bhabki Bazar	Minor river	1375	Low	Low
32	Jamalpur	Melandaha	Bhaluka(Tarankandi Bazar)	Old Brahmaputra	1450	Low	Low
33	Jamalpur	Melandaha	Char Gobindi Bazar	Jamuna	1200	Low	Moderate
34	Jamalpur	Melandaha	Gazipur Bazar	Minor river	75	Low	Moderate

Sl.	District	Upazila	Market Name	Rivers	Distance from River (m)	Flood Risk	Bank Erosion Risk
35	Jamalpur	Melandaha	Gobindoganj Bazar	Minor river	20	Low	High*
36	Jamalpur	Melandaha	Mahmudpur	Minor river	1850	Low	Low
37	Jamalpur	Melandaha	Jhawgora Bazar	Minor river	2430	Low	Low
38	Jamalpur	Melandaha	Kahetpara bazar	Minor river	35	Low	High
39	Jamalpur	Madarganj	Koali Kandi Bazar	Minor river	60	Low	Moderate
40	Jamalpur	Madarganj	Millon Bazar	Minor river	1550	Low	Low
41	Jamalpur	Madarganj	Nabbo Char Bazar	Minor river	500	Low	Low
42	Jamalpur	Madarganj	Rayerchara Bazar	Minor river	1250	Low	Low
43	Jamalpur	Madarganj	Tegharaia Bazar	Minor river		Low	N/A***
44	Jamalpur	Madarganj	Nalsia bazar	Minor river	550	Moderate	Low
45	Jamalpur	Melandaha	Talukpara Bazar	Minor river	70	Moderate	Moderate
46	Jamalpur	Melandaha	Tegharia Bazar	Minor river	775	Low	Low
47	Jamalpur	Bakshiganj	Duttapara Ananda Bazar	Minor river	205	Low	Low
48	Jamalpur	Bakshiganj	Parchim kamalerbatti Bazar	Jinjiram	1070	Low	Low
49	Jamalpur	Melandaha	Saguna Bazar	Minor river	1280	Low	Low
50	Lalmonirhat	Hatibandha	Dighir Hat	Teesta	2581	Low	Low
51	Lalmonirhat	Hatibandha	Chander Hat	Minor rivers	780	Low	Low
52	Lalmonirhat	Hatibandha	Muktijoddha Hat	Teesta	2400	Low	Low
53	Lalmonirhat	Hatibandha	Nowdabash Hat			Low	N/A***
54	Lalmonirhat	Patgram	Burimari Hat	Dharala	300	Low	Moderate
55	Lalmonirhat	Patgram	Kamarar Hat	Dharala	3000	No	Low
56	Lalmonirhat	Patgram	Kashirdangga Hat	Dharala	2650	Low	Low
57	Lalmonirhat	Patgram	Nayer Hat	Teesta	463	Moderate	High*
58	Lalmonirhat	Patgram	Shofinagar Hat	Minor river	1420	Low	Low
59	Lalmonirhat	Patgram	Sharkaar Hat	Dharala	1610	Low	Low
60	Lalmonirhat	Patgram	Loliter Hat	Dharala	2287	Low	Low
61	Kurigram	Bhurungamari	Baldia Bazar	Dudkumur	1350	Low	Low
62	Kurigram	Bhurungamari	Muktijodha Hat Bhurungamari	Minor river		Low	N/A***
63	Kurigram	Bhurungamari	Chowdhurir hat	Dudkumur	400	Low	Moderate
64	Kurigram	Nageshwari	Schooler Hat	Minor river		Moderate	N/A***
65	Kurigram	Nageshwari	Chilakhana Hat	Minor river	800	Moderate	Low
66	Kurigram	Nageshwari	Maniganj Bazar	Minor river	450	Low	Low
67	Kurigram	Nageshwari	Berubari Hat	Minor river	190	Low	Low
68	Kurigram	Phulbari	Bokultala Bazar	Dharala	770	Low	Moderate
69	Kurigram	Phulbari	Ghogurhat Bazar	Minor river		Low	N/A***
70	Kurigram	Phulbari	Shiber Bazar	Minor river	410	Low	Low
71	Kurigram	Phulbari	Boroloi Bazar	Dharala	1770	Low	Low
72	Kurigram	Rajarhat	Chandamari Hat	Teesta	2750	Low	Low
73	Kurigram	Rajarhat	Panga	Minor river		Low	N/A***
74	Kurigram	Rajarhat	Sharishabari Hat	Teesta	1000	Low	High
75	Kurigram	Rajarhat	Chowrahat	Dharala	2470	Low	Low
76	Kurigram	Chilmari	Jorgach Hat	Brahmaputra	740	Low	High*
77	Kurigram	Chilmari	Karai Barisal	Brahmaputra	700	Low	High**

Sl.	District	Upazila	Market Name	Rivers	Distance from River (m)	Flood Risk	Bank Erosion Risk
78	Kurigram	Chilmari	Thana Hat	Brahmaputra	2050	Low	Low
79	Kurigram	Chilmari	Fakirar Hat	Brahmaputra	350	Low	High*
80	Kurigram	Ulipur	Hatia Vobesh	Brahmaputra	590	Moderate	High*
81	Kurigram	Ulipur	Mollar Hat	Brahmaputra	330	Low	High
82	Kurigram	Ulipur	Jatiner Hat	Minor river	580	Low	Low
83	Kurigram	Kurigram Sadar	Panchgachi Bazar	Brahmaputra Dharala	2770	Low	Low
84	Kurigram	Kurigram Sadar	Rajmallir Hat	Dharala	50	Moderate	High
85	Kurigram	Kurigram Sadar	Rajarhat Bazar	Brahmaputra	2750	Moderate	Low
86	Kurigram	Kurigram Sadar	Masterer Hat	Dharala	1030	Low	Low
87	Kurigram	Raumari	Baraikandhi Hat	Jinjiram	1700	Low	Low
88	Kurigram	Raumari	Saydabad Bazar	Jinjiram	900	Moderate	Moderate
89	Kurigram	Char Rajibpur	Rajibpur GC	Brahmaputra	790	Low	High
90	Nilphamari	Jaldhaka	Balagram Bazar	Minor river	2000	Low	Low
91	Nilphamari	Jaldhaka	Bhabonchur Bazar	Minor river	68	Low	Moderate
92	Nilphamari	Jaldhaka	Dakligonj Hat	Teesta	830	Low	High
93	Nilphamari	Jaldhaka	Golmunda Bazar	Teesta	170	Low	High
94	Nilphamari	Jaldhaka	Kaligonj Bangha Bandhu Bazar	Minor rivers	2058	Low	Low
95	Nilphamari	Jaldhaka	Kathali Nayer Hat	Minor river	830	Low	Low
96	Nilphamari	Jaldhaka	Pathanpara Hat	Minor river	1930	Low	Low
97	Nilphamari	Jaldhaka	Shibur Hat	Minor river	2750	Low	Low
98	Nilphamari	Dimla	Tunirhat	Minor river	840	Low	Low

Notes:
** Protected by Embankment, which can be considered under "low" risk;*
*** Located on the island (char);*
****N/A (Not Applicable): Image resolution is not adequate to identify bank lines*

Changes in the future discharge in the Brahmaputra-Teesta basin are assessed using SWAT hydrological models under SSP2-4.5 and SSP5-8.5 climate change scenarios. Probability density functions (PDF) of maximum monthly discharge for the near (2025-2054) and far future period (2071-2100) compared to baseline (1985-2014) at Bahadurabad (SW46.9L) in Brahmaputra river are presented in the figure below.

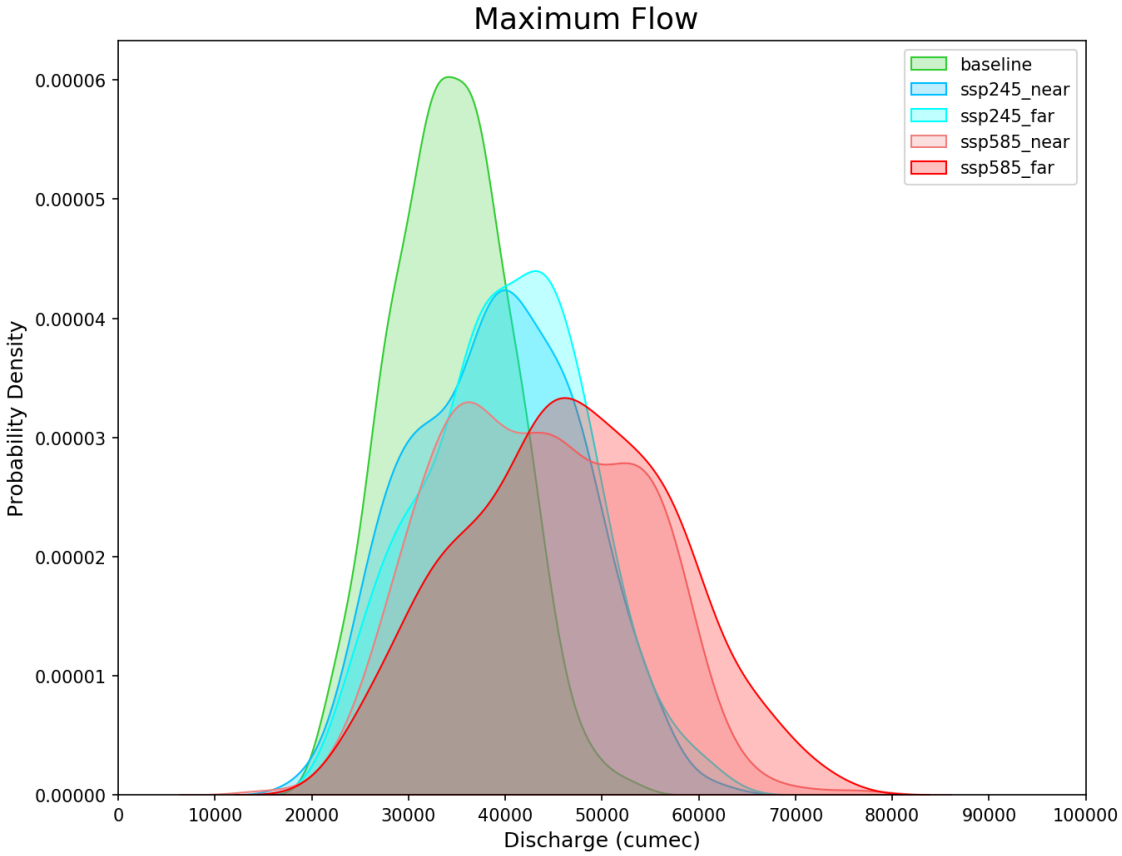

Figure E1: Probability density functions (PDF) of maximum monthly discharge for the near (2025-2054) and far future period (2071-2100) compared to baseline (1985-2014) at Bahadurabad (SW46.9L) in Brahmaputra river.

In order to plan and design climate-resilient infrastructures, it is vital to assess how much the flood level will increase in the future due to climate change. Accordingly, the crest level of the roads and plinth level of the commercial center (Bazar), flood shelter, and other infrastructures need to be raised. The flood level for various return periods would be estimated for the projected climate change scenarios. The frequency of the maximum water level of Brahmaputra-Jamuna River at Bahadurabad (SW46.9L) using climate projections for the near future (2025-2054) and far future (2071-2100) with respect to the baseline period (1985-2014) are shown in the figure below. Frequency analysis of other stations is provided in detail in Chapter Six. Due to the uncertainty of future changes in water levels (varies from 11 cm to 38 cm), an increase of 30 cm (0.3 meter) of the crest level of the roads is recommended, while an increase of 50 cm (0.5 meter) of the crest level of the markets and flood shelters are recommended for the study area.

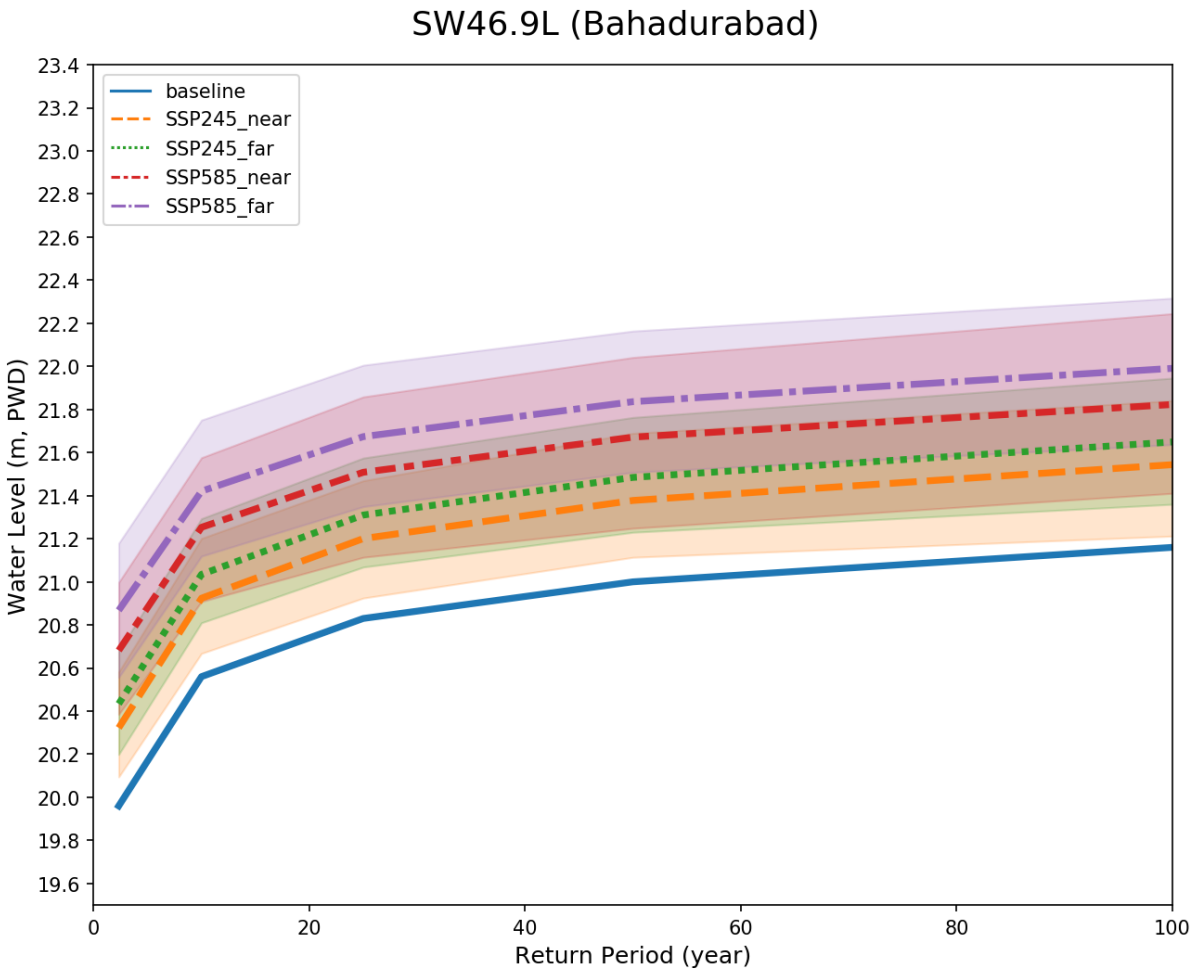

Figure E2: Frequency of maximum water level (m, PWD) of Brahmaputra-Jamuna River at Bahadurabad (SW46.9L) using climate projections for the near future (2025-2054) and far future (2071-2100) with respect to the baseline period (1985-2014).

The design flood level for the infrastructures depends on the condition of the soil, proximity to the river, flood inundation frequency, and the importance of the infrastructures. In this context, a recent field visit after the 2020 floods was made by BUET and LGED Project Design Team to vulnerable flood-vulnerable sites of the Jamalpur district during 17-19 March 2021. Based on the analysis and experience from the field observations, a few recommendations have been made, as presented in the table below.

Table E5: Recommendations for Climate Resilient Infrastructures under this PROVATi[3] project.

Infrastructure	Parameters	Recommendations	References
Village/Union Road	Design Crest Level	10-year return period and freeboard of 0.3m	Table 6.20
		Additional increment of 0.3 m considering climate change	Table 6.28
	Side Slope	• The minimum slope is 1:1.5 • The minimum slope is 1:2.0 (Sandy Soil) • The actual side slope should be determined by slope stability analysis	Figures 7.1-7.3
	Slope protection	• vetiver grass (*Chrysopogon zizanioides*) • Clay Blanket and vetiver grass (Sandy Soil) • CC Block (Riverside)	
	Road Surface	• BC (Not Frequently Inundated Areas) • RCC (Frequently Inundated Areas)	Figure 5.9-5.12
	Culverts	Hydraulic Analysis is recommended for designing the size and number of culverts	Table 7.1
	Bridges	Waterway opening should be adequate to pass the flow of the river	
	O&M	Periodic monitoring and maintenance are essential to make the road climate resilient	
Flood Shelter	Design Plinth Level	100-year return period and freeboard of 0.5m	Table 6.20
		Additional increment of 0.5 m considering climate change	Table 6.29
	Erosion vulnerability	Planform analysis of nearby river banks should be carried out	Figure 5.18-5.21 Table 5.10-5.13
	O&M	Periodic monitoring and maintenance are essential to make the flood shelter climate resilient	
Markets	Design Plinth Level	100-year return period and freeboard of 0.5m	Table 6.20
		Additional increment of 0.5 m considering climate change	Table 6.29
	Erosion vulnerability	Planform analysis of nearby riverbanks should be carried out	Figure 5.14-5.17 Table 5.4-5.9
	O&M	Periodic monitoring and maintenance are essential to make the market climate resilient	

A few new initiatives which can be included in the infrastructures project for achieving better socialization and engendering design of infrastructures are also recommended, such as-

- Provision and Marking of historical flood events in important structures, locations, GCMs, etc.
- Making infrastructures community-friendly
- Removing gender biases

- Poverty analysis for influence zone of rural road infrastructures for conforming poverty incidence and ranking
- Poverty analysis and its distribution and poverty profile of a project area
- Social/ Gender Analyses along the influence zone of a project
- Comprehensive poverty, social, and gender Analyses
- Connection of rural areas with community-based initiatives
- Employing good practices in addressing social and gender at home and abroad; and
- Provision and Providing Innovative Options.

This study has suggested taking Bangladesh Delta Plan 2020 into consideration. The Bangladesh Delta Plan (BDP) 2100 is a long-term, integrated, and holistic vision of water and land management throughout Bangladesh. Investment planning to implement this long-term vision will be done under the principles of adaptive delta management (ADM). This adaptive approach to delta planning selects investment programs with the long-term goal of sustained development based on climate-sensitive management. The purpose of the current study is to conduct climate change and flood preparedness research for building climate-resilient infrastructure. As such, the study is well aligned with the long-term goal of sustained development based on climate-sensitive management, as outlined in BDP.

CHAPTER ONE
INTRODUCTION

1.1 Background

Although Bangladesh is now considered at the lower end of a middle-income country (MIC), mass poverty persists, and extreme poverty is pervasive in various parts of the country. The central- north of Bangladesh is affected by seasonal flooding, river erosions, and low density and quality of rural infrastructure (low percentage of paved roads). The area lacks access to input and output markets, given bad connectivity. In addition, the population tends to have only one secured agricultural season. Remoteness causes low levels of investment and few off-farm businesses. The increasing population growth and overall gradual increase in income in Bangladesh (partly due to remittances and an increase in export earnings from Ready-made Garment Sector) have created a demand for off-farm services (construction, small businesses, etc.). The situation is aggravated due to the adverse impacts of climate variability and change. Considering the environmental stress and socio-economic conditions, districts in north-central Bangladesh are some of the poorest and most vulnerable districts in the country. The rural population of that area, especially char dwellers, the poor, and the small producers, face several constraints: a) poor transport and market infrastructure that limits access to larger markets, increase the cost of production through higher input and transportation costs, and lowers farm-gate prices due to remoteness; b) over-dependence on agriculture and daily agricultural labor with very limited opportunities for off-farm sources of income; and c) vulnerability to the effects of climate change, such as increased frequency of extreme weather events, which in consequence damage standing crops, livestock and other assets.

1.2 Rationale of the study

In order to improve the resilience of the people living in flood-vulnerable areas of north-central Bangladesh, a new project entitled 'PROVATi[3] (Promoting Resilience of Vulnerable through Access to Infrastructure, Improved Skills, and Information)' has been designed. The project is grounded on the strong justification of reduction of extreme poverty, enhancing preparedness against annual floods and adverse impacts of climate change, mitigating measures against loss due to climate change, promoting diversification into off-farm income, and creating a platform for further economic and social development by catalyzing new investments in agriculture, non-farm businesses and improving access to social services including locally-relevant people-

centric flood early warnings. The concept of the PROVATi^3 Project was endorsed by the Government of Bangladesh (GoB) in December 2016 and by the International Fund for Agricultural Development (IFAD) in February 2017. The PROVATi^3 project reflects a deep commitment of GoB and IFAD to reduce extreme poverty.

The project concept and design-build on several innovative features in the area of climate-proofing infrastructure, economic empowerment of ultra-poor people working on construction and maintenance through continued guidance towards income generation activities (IGA), improved maintenance of structures for long-term sustainability, vocational skills training (VST) for on- and off-farm employment, local flood information and dissemination at the village level, project management and monitoring, and knowledge management for wider mainstreaming of good practices. Improved resilience of the population in flood-vulnerable and extremely poor areas is the central theme of the project.

The goal of the project is to promote sustainable livelihoods for poor households and smallholders in selected 25 Upazilas of the Brahmaputra-Teesta flood plain area of six North-central districts of Bangladesh. The project has avoided "spreading thin" its resources over too many Upazilas but followed a strategy to rather have a significant impact and reduced management costs in a few selected Upazilas. Under this project, IWFM-BUET has carried out a research study to build climate-resilient infrastructures. The results should indicate the necessary modifications in design on roads, culverts/bridges, markets, ghats, slope protection, etc., and might lead to up-dates in design standards at LGED (2005).

1.3 Objectives of the study

The overall objective of the study is to carry out a detailed hydrological, hydraulic, and morphological analysis of the watersheds to determine suitable design criteria for the proposed flood-vulnerable areas to build climate-resilient infrastructures. Specific objectives include the following-

1. To assess the impact of climate change on the Teesta-Brahmaputra river system;
2. To assess erosion and accretion of land/char due to meandering of rivers;
3. To determine flood risk zones by combining both model results with ground-based and satellite image analysis of historic floods and the potential impact of climate change on river flows of each project Upazila;
4. To assess damage from flooding.

1.4 Scope of Work

The scope of work of this study is limited to the following:

- Collection of meteorological, hydrological (water level, discharge at river gauges), and morphological data (x-section of rivers).
- Review of existing peer-reviewed literature, a compilation of reports, maps, books, etc.
- Direct observation through a field visit to the study area.
- Analysis of Multi-Model Ensemble Regional Climate Projections for the Brahmaputra-Teesta basin.
- Setup, calibration, and validation of a hydrological model for the Brahmaputra and Teesta river basin.
- Assessment of the impact of climate change on the Teesta-Brahmaputra river system.
- Downloading of time series high-resolution satellite images.
- Assessment of erosion and accretion of land/char due to the meandering of rivers
- Determination of flood risk zones by applying satellite information, past flood history, and the potential impact of climate change on river flows of each project, Upazila.
- Providing guidelines for the design of climate-resilient infrastructures.
- Interaction with LGED and other partners of the project.
- National Level disseminating workshop on climate resilient Infrastructures.
- Reporting on the study.

1.5 Limitations of the work

The two-dimensional flood inundation modeling needs high-resolution accurate topographic information. It was expected that a high-resolution digital elevation model (DEM) would be purchased from the Survey of Bangladesh (SOB). Unfortunately, it was not possible for them to process and provide us high a resolution DEM over the study area during the project period. To overcome this limitation, we carried out a flood frequency analysis based on one-dimensional model output, which was later applied to the nearest market or flood shelter locations.

CHAPTER TWO
STUDY AREA

2.1 Project Area

The project will be implemented in six districts (Gaibandha, Kurigram, Rangpur, Nilphamari, Lalmonirhat, and Jamalpur) with a main focus on the worst poverty has stricken districts – Jamalpur, Kurigram, and Gaibandha - of Bangladesh. Major parts of these districts are flood-prone due to the convergences of the Brahmaputra (the Jamuna river) and Teesta rivers. The project will cover selected districts (see Figure 2.1) to reduce the high incidence of poverty in the North-central region of Bangladesh.

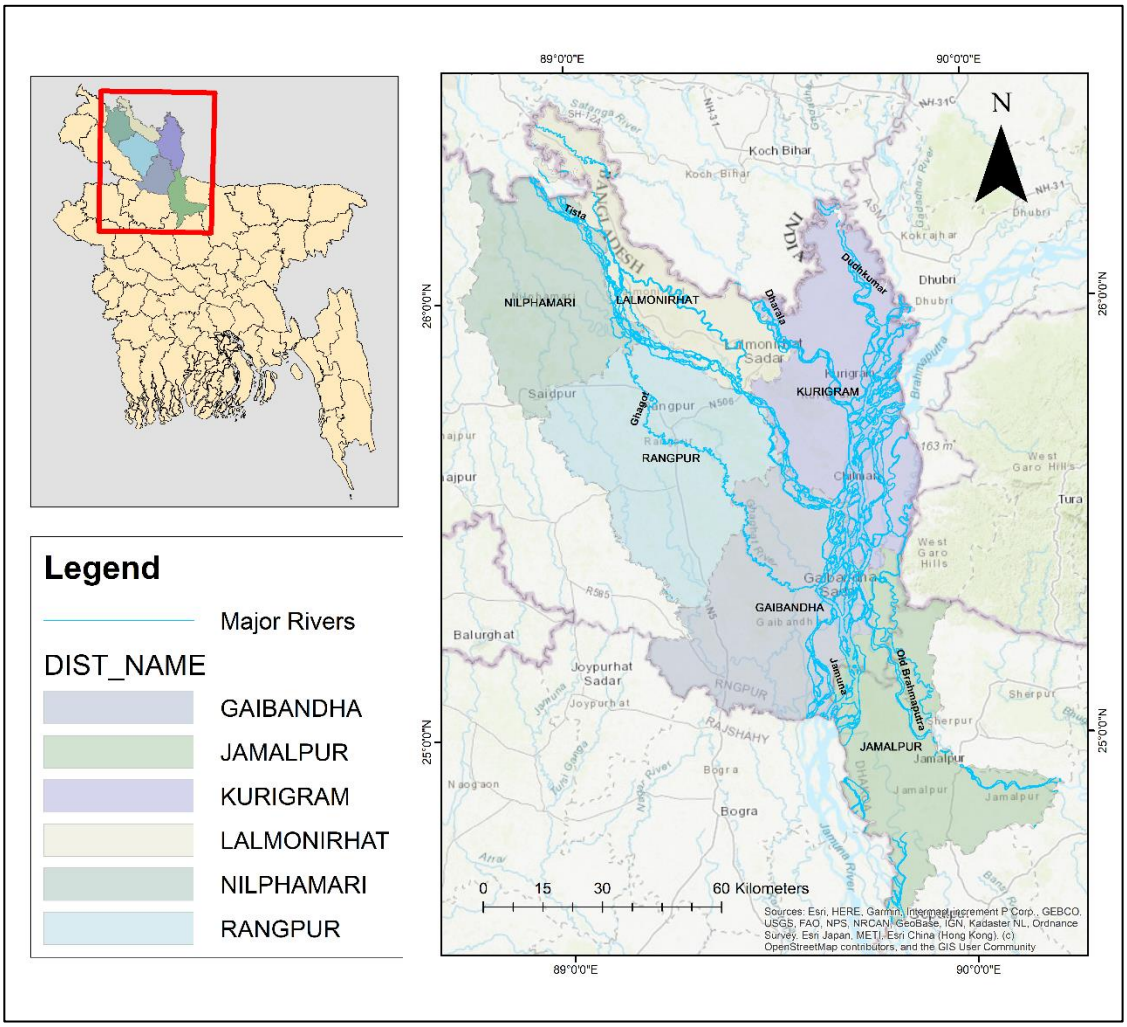

Figure 2.1: Study Area of the project.

Within the six districts, the project will implement development activities in 25 poorer and vulnerable Upazilas. The project infrastructure will be primarily built-in 90 unions, which are

mostly char and low-lying and worst poverty-stricken areas within the 25 Upazilas. The project covers some 303,000 households (approximately 45% of the total population) from 90 Unions within the 25 target Upazilas. Target beneficiaries include poor women and men, marginal and small farmers, traders and shop owners in the markets, micro-entrepreneurs, and other local private and government institutions. The infrastructure and flood information system will benefit the overall population of the project areas. A summary of the project area, along with the flood-affected river, is provided in Table 2.1. District-wise, population density, area, number of unions, and literacy rates are provided in Table 2.2.

Table 2.1: Summary of the projected area.

District	**No. of Upazila**	**Projected Upazila**	**Name of the Projected Upazila**	**Flood-affecting River**
Jamalpur	6	5	Madarganj, Melandaha, Islampur, Dewanganj, Bakshiganj	Old Brahmaputra
Gaibandha	7	5	Shaghata, Fulchari, Gaibandha Sadar, Sadullahpur, Sundarganj	Teesta, Ghaghat
Kurigram	5	9	Char Rajibpur, Chilmari, Raumari, Ulipur, Rajarhat, Kurigram Sadar, Phulbari, Nageshwari, and Bhurungamari	Teesta, Dharla, Dudhkumar
Rangpur	8	2	Gangachara, Kaunia	Ghaghat, Teesta
Nilphamari	7	2	Dimla, Jaldhaka	Teesta
Lalmonirhat	9	2	Hatibandha, Patgram	Teesta

2.1.1 Jamalpur District

Jamalpur district has 7 Upazilas, of which Jamalpur Sadar is the largest (489.56 sq km, it occupies 24.09% of the total area of the district), and Bakshiganj is the smallest (204.30 sq km). Jamalpur District (Mymensingh Division) area 2031.98 sq km, located between 24°34' and 25°26' north latitudes and between 89°40' and 90°12' east longitudes. It is bounded by Meghalaya state of India, Kurigram, and Sherpur districts on the north, Tangail district on the south, Mymensingh and Sherpur districts on the east, Jamuna river, Bogra, Sirajganj, and Gaibandha districts on the west. Of the 17 districts of the Dhaka Division, Jamalpur district occupies the 6th position, and it occupies the 33rd position among the 64 districts of Bangladesh.

The main rivers in this district are Jamuna, Old Brahmaputra, Banar, Jhenai, Kharka Beel, Kaiyer Beel, Chiradhuni Beel, Chilmari Beel, Kaludaga Lake, Ranipukur Dighi, and Harishchander Dighi are notable. Main sources of income are from Agriculture 65.50%, non-agricultural labourer 3.30%, industry 0.81%, commerce 11.88%, transport and communication 2.94%, service 5.76%, construction 1.22%, religious service 0.19%, rent and remittance 0.30%' and others 8.10%.

2.1.2 Rangpur District

Rangpur district has an area of 2370.45 sq. km., located between 25°18' and 25°57' north latitudes and between 88°56' and 89°32' east longitudes. It is bounded by Nilphamari and Lalmonirhat districts on the north, Gaibandha district on the south, Kurigram district on the east, and Dinajpur district on the west. The main rivers in this district are Teesta, Jamuneshwari, Ghaghat, Karatoya, Chikali, and Akhira. Main sources of income*:* Agriculture 62.99%, non-agricultural labourer 4.66%, industry 1.11%, commerce 13.28%, transport and communication 3.90%, service 6.32%, construction 1.18%, religious service 0.20%, rent and remittance 0.20% and others 6.16%.

2.1.3 Gaibandha District

The former name of Gaibandha was Bhabaniganj. Bhabaniganj Sub Division was established on 27 August 1858. The headquarter of the Sub Division was transferred to Gaibandha in 1875 when Bhabaniganj was submerged into a river bed due to erosion. Once this region was included in the Baharbandh Pargana, Gaibandha Town was turned into a municipality in 1923. The municipality was abolished in 1960, and it was turned into a Town Committee. In 1973,

the Town was again turned into a Paurasabha. Gaibandha district was formed in 1984. Of the seven Upazilas of the district, Gobindaganj is the largest (481.66 sq km, it occupies 22.10% of the total area of the district), and Palashbari is the smallest Upazila (190.67 sq km). Gaibandha District (Rangpur Division) area 2179.27 sq km, located between 25°02' and 25°39' north latitudes and between 89°11' and 89°46' east longitudes. It is bounded by Kurigram and Rangpur districts on the north, Bogra district on the south, Jamalpur and Kurigram districts, and Brahmaputra river on the east, Joypurhat, Dinajpur, and Rangpur districts on the west. The main rivers in this district are Brahmaputra, Jamuna, Testa, Karatoya, Bangali, and Ghaghat. Main sources of income: Agriculture 65.08%, non-agricultural labourer 2.48%, industry 0.77%, commerce 11.85%, transport and communication 4.22%, service 5.37%, construction 1.19%, religious service 0.19%, rent and remittance 0.22% and others 8.63%.

2.1.4 Kurigram District

Kurigram Sub Division has 9 Upazilas in Ulipur is the largest (504.19 sq km, it occupies 22% of the total area of the district), and Char Rajibpur is the smallest (111.03 sq km). Kurigram District (Rangpur Division) area 2296.10 sq km, located between 25°23' and 26°14' north latitudes and between 89°27' and 89°54' east longitudes. It is bounded by the West Bengal state of India on the north, Gaibandha and Jamalpur districts on the south, the Assam state of India on the east, and West Bengal of India Rangpur and Lalmonirhat districts on the west. The main rivers in this district are Jamuna, Old Brahmaputra, Dharala, Dudhkumar, Teesta, and Zinzira; Chakir Posar Beel is notable. Main sources of income: Agriculture 70.41%, non-agricultural labourer 4.74%, industry 0.51%, commerce 9.45%, transport and communication 2.02%, service 4.98%, construction 0.77%, religious service 0.15%, rent and remittance 0.21% and others 6.76%.

2.1.5 Lalmonirhat District

Lalmonirhat district has 5 Upazilas, of which Hatibandha is the largest (288.42 sq km) and Aditmari is the smallest (195.03 sq km). Lalmonirhat District (Rangpur Division) area is 1241.46 sq km, located between 25°46' and 26°33' north latitudes and between 89°01' and 89'36' East longitudes. It is bounded by the West Bengal state of India on the north, Rangpur district on the south, Kurigram district and West Bengal of India on the east, and Nilphamari and Rangpur districts on the west. Lalmonirhat may be called a district of enclaves; it has 33 enclaves. The two biggest enclaves of the district are Dahagram and Angarpota, which are connected with the mainland by Tin Bigha Corridor. The main rivers in this district are Dharala

and Teesta. Main sources of income: Agriculture 72.78%, non-agricultural labourer 3.46%, industry 0.5%, commerce 10.49%, transport and communication 2.38%, service 4.45%, construction 0.69%, religious service 0.19%, rent and remittance 0.2% and others 4.86%.

2.1.6 Nilphamari District

Nilphamari Sub-division has six Upazilas, of which Nilphamari Sadar is the largest (373.09 sq km), and Saidpur is the smallest (121.68 sq km). Nilphamari District (Rangpur Division) area 1580.85 sq. Km, located between 25°44' and 26°19' north latitudes and between 88°44' and 89°12' east longitudes. It is bounded by the West Bengal state of India on the north, Rangpur district on the south, Lalmonirhat district on the east, and Panchagarh and Dinajpur districts on the west. The main rivers in this district are Teesta, Jamuneshwari, Buri Teesta, and Ghagat. Main sources of income: Agriculture 68.51%, non-agricultural labourer 3.93%, industry 0.66%, commerce 11.77%, transport and communication 3.06%, service 5.93%, construction 0.89%, religious service 0.23%, rent and remittance 0.17% and others 4.85%.

Table 2.2: Summary of different districts within the study area.

District	**Area (sq.km)**	**Upazila**	**Union**	**Village**	**Population**		**Density (per sq. km)**	**Literacy rate (%)**
					Urban	Rural		
Nilphamari	1580.85	6	61	370	235839	1335851	994	98.8
Jamalpur	2031.98	7	68	1346	331264	1775945	1037	31.8
Lalmonirhat	1241.46	5	42	476	141361	367982	894	42.3
Rangpur	2370.45	8	83	1435	457234	2085207	1101	41.91
Gaibandha	2179.27	7	82	1243	195107	1943074	981	35.7
Kurigram	2296.1	9	73	1903	278071	1514002	720	33.45

2.2 River Network

Bangladesh is mainly occupied by the recent alluvial and floodplain sediments. The project study area is mainly comprised of the Teesta-Brahmaputra floodplain. The major rivers in this projected area are the Jamuna, Old Brahmaputra, Teesta, Ghaghat, Jamuneswari, Dharala, Dudhkumar, Bangali, and Buri Teesta (Figure 2.2).

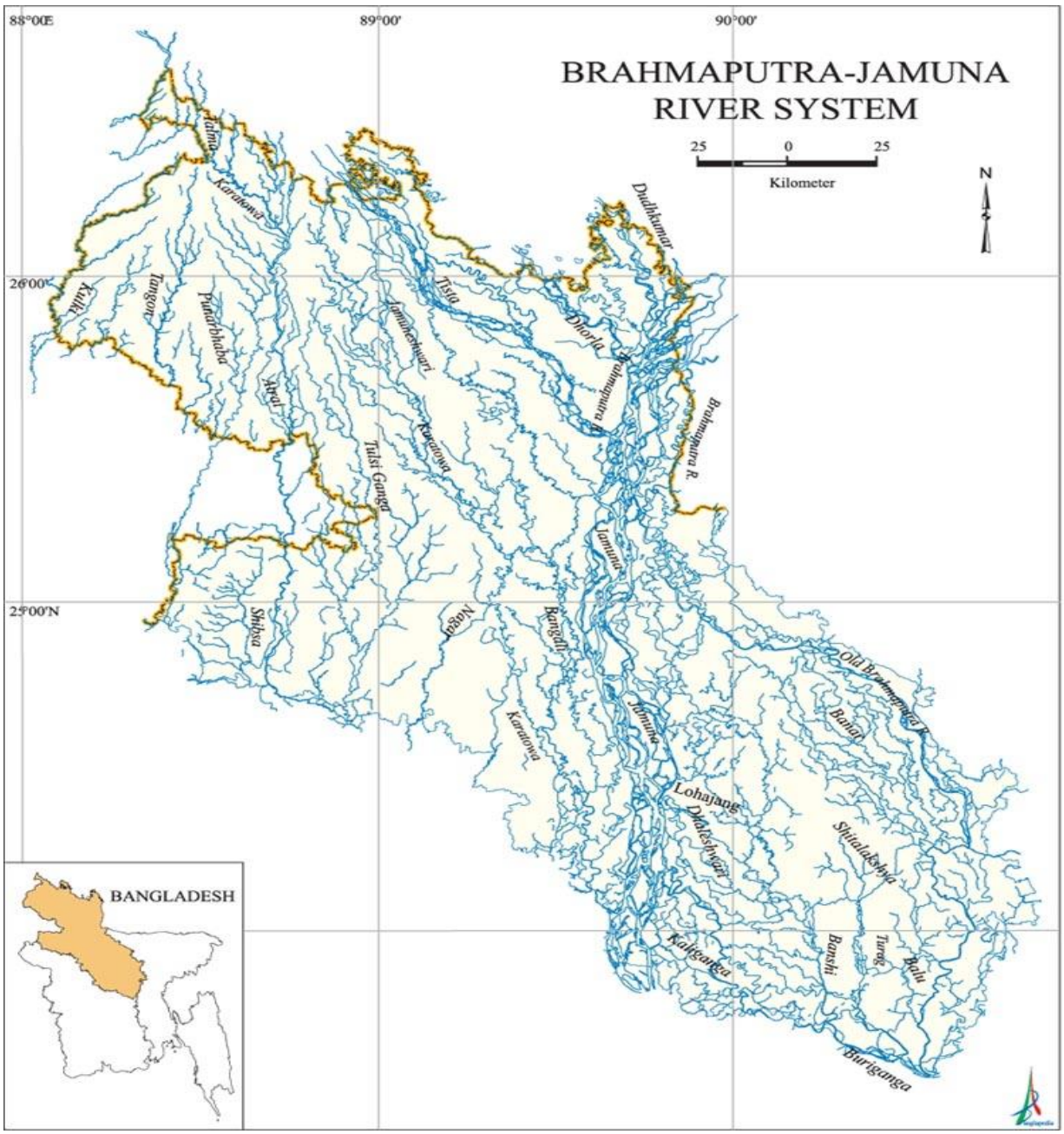

Figure 2.2: River systems of the study area.

Brahmaputra-Jamuna River System is one of the three major river systems of Bangladesh. Brahmaputra-Jamuna and Old Brahmaputra, with their main tributary Teesta and a good

number of small tributaries and distributaries, constitute the largest floodplain of Bangladesh. Except for a small portion in the north, the entire floodplain lies within the Pleistocene Terrace regions.

Again**, Teesta Floodplain** covers most of Rangpur and adjoining regions that actually lie in the younger part of the Teesta alluvial fan that covers several different landscapes. Physically, the floodplain stretches between the Himalayan Piedmont Plain in the west and the right bank of the north-south flowing Brahmaputra in the east. The diversity results from the fact that the Teesta has occupied and abandoned several different channels during the past few thousand years, including the valleys now occupied by Mahananda, Punarbhaba, Atrai, Little Jamuna, Karatoya, and Ghagaht rivers. The small floodplains of the Dudhkumar and Gangadhar rivers are also included in this unit. The main geomorphic agent of this unit is the river Teesta. This river, along with the others, brings sediments of different sizes to the floodplain at different times.

Teesta River originates in Chitamu Lake in the Sikkim Himalayas at an altitude of about 7,200 m and comes down first to the Darjeeling plain and then to the Duar plain of West Bengal (India). It enters Bangladesh at the Kharibari border of the Nilphamari district. Up to the close of the 18th century, it flowed directly into the Ganges. The excessive rains of 1787 created a vast and choked the original Atrai channel. This resulted in the Teesta bursting into the Ghagat, which at that time was a very small river. After passing through Lalmonirhat, Rangpur, Kurigram, and Gaibandha districts, this deluge falls into the Jamuna south of Chilmari river port. The total length of the river is about 315 km, of which nearly 115 km lies within Bangladesh.

Old Brahmaputra River is a river that originates from the left bank of the Brahmaputra to the north of Bahadurabad. Flowing more or less to the southeast, it passes by Jamalpur and Mymensingh towns and falls into the Meghna at Bhairab Bazar. River shifting has been a characteristic feature of the Bengal basin, affecting small sections or even the entire river. The most dramatic was the shifting of the courses of the Teesta, Brahmaputra, and lower Ganges river channels, as evident from maps prepared hundreds of years ago. James Renell produced the most accurate map back in 1760. According to this map, the Brahmaputra at that time was flowing a course east of the Madhupur tract, presently known as the Old Brahmaputra. The lower part of the Brahmaputra channel between Dhaka and Mymensingh

subsequently was silted up, diverting the Old Brahmaputra flow to the Shitalakhsya river and then to the Dhaleswari and Meghna rivers southeast of Dhaka.

Ghaghat River is a distributary of the Teesta river originating in the Nilphamari district. It takes a meandering course from north to southeast and, after passing through Gaibandha town, joins the Brahmaputra a few kilometers north of Fulchhari Ghat. The Ghaghat has a distributary named the Bangali that flows from the east of Gaibandha town, moves south, and meets the Karatoya south of Sherpur Upazila of the Sherpur district. It is a sluggish stream for most of its course and choked with weeds. In ancient times, the Ghaghat was an important distributary of the Teesta, but at present, it is separated from the Teesta and has become a small channel. The total length of the Ghaghat is 236 km. Its flow varies from 50 to 2,500 cusec, whereas the Bangali has a flow varying from 400 to 21,000 cusec.

Dharla River is one of the transboundary rivers of Bangladesh. It enters the country at Lalmonirhat through Changra Bandha of Patgram. In its upper course, it is known as the Jaldhaka or Singimari. Near Patgram Upazila, it again flows back to India and continues an easterly course. Suddenly it turns south and enters Bangladesh for the second time through Kurigram and then follows a meandering course. Dharla is a tributary of the Brahmaputra river. The main channel of this river originates in Kuch Bihar (India). It flows into the Brahmaputra a few kilometers southeast of Kurigram town. The length of the river within Bangladesh is about 75 km.

Dudhkumar River, the Raidak or the Sankosh river of West Bengal (India), enters Bangladesh near Pateshwary and is renamed the Dudhkumar. The river receives the Gadadhar and the Gangadhar as tributaries at Pateshwary and travels along a 52 km long meander course, and joins the Brahmaputra at Kurigram Sadar Upazila.

Major river networks in the study area are shown in Figure 2.3.

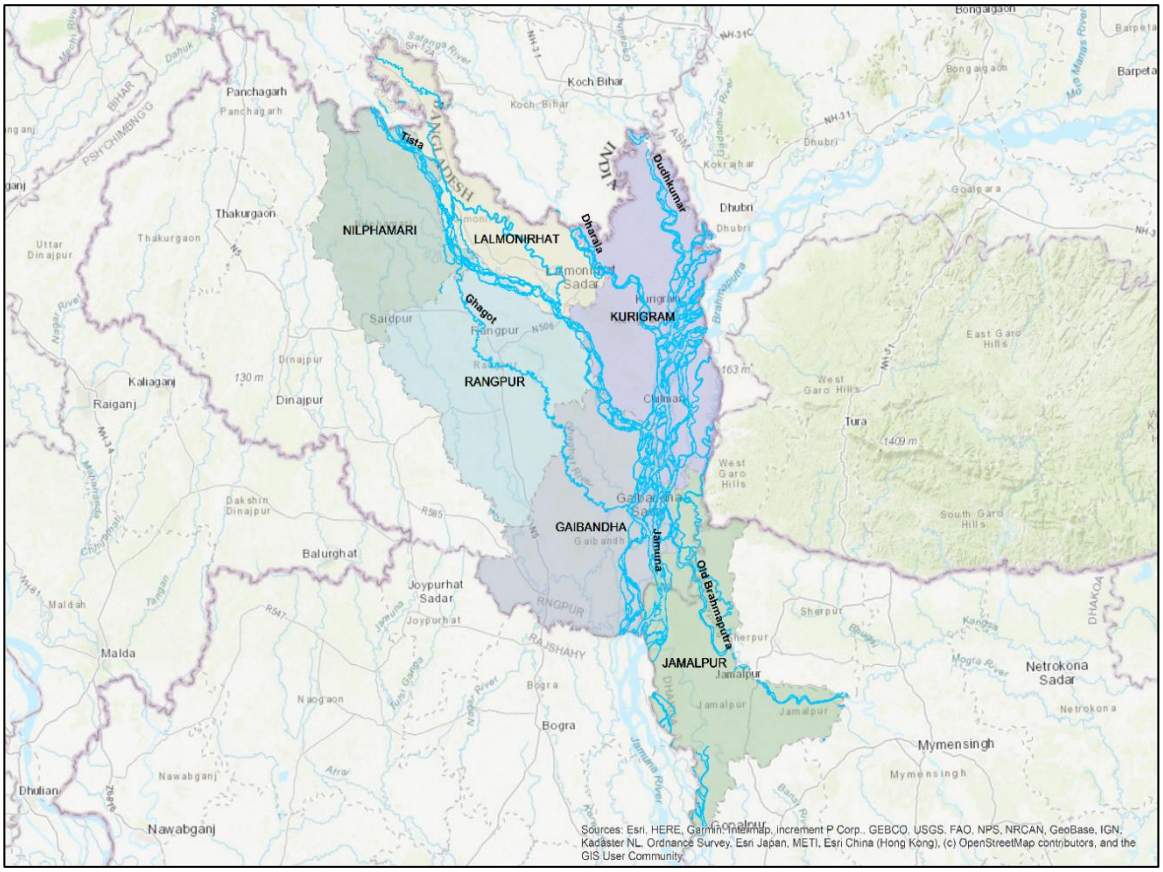

Figure 2.3: Major river network of the study area.

2.3 Climate System

Monsoon climate dominates this region, where rainfall is abundant. The average annual rainfall in this region is a little over 1,900 mm. Climatic sub-regions of Bangladesh and mean annual rainfall are shown in Figure 2.4 and Figure 2.5, respectively. Teesta is the prominent river of this region, which has a mean monthly discharge of about 2,430 cumecs. Teesta rises in Chitamu Lake in Tibet that joins the Brahmaputra in the Rangpur district of the country. It flows through a magnificent gorge known as the Sivok Gola in the Darjeeling district. It is a wild river in the Darjeeling Hills, where its valley is clothed with dense forest, but its drainage area in the mountain is only 12,500 sq km. Up to the close of the 18th century, it flowed into the Ghaghat, but after the destructive floods of 1787, in which a large part of the Rangpur district was laid waste, it suddenly turned east and joined the Brahmaputra. The monthly mean discharge of the Dharla that borders the western boundary of the floodplain is about 1,440 cumec. There are many old channels that used to be occupied by this river. Karatoya, through which it joined the Ganges, is still known as the Buri Teesta or Old Teesta.

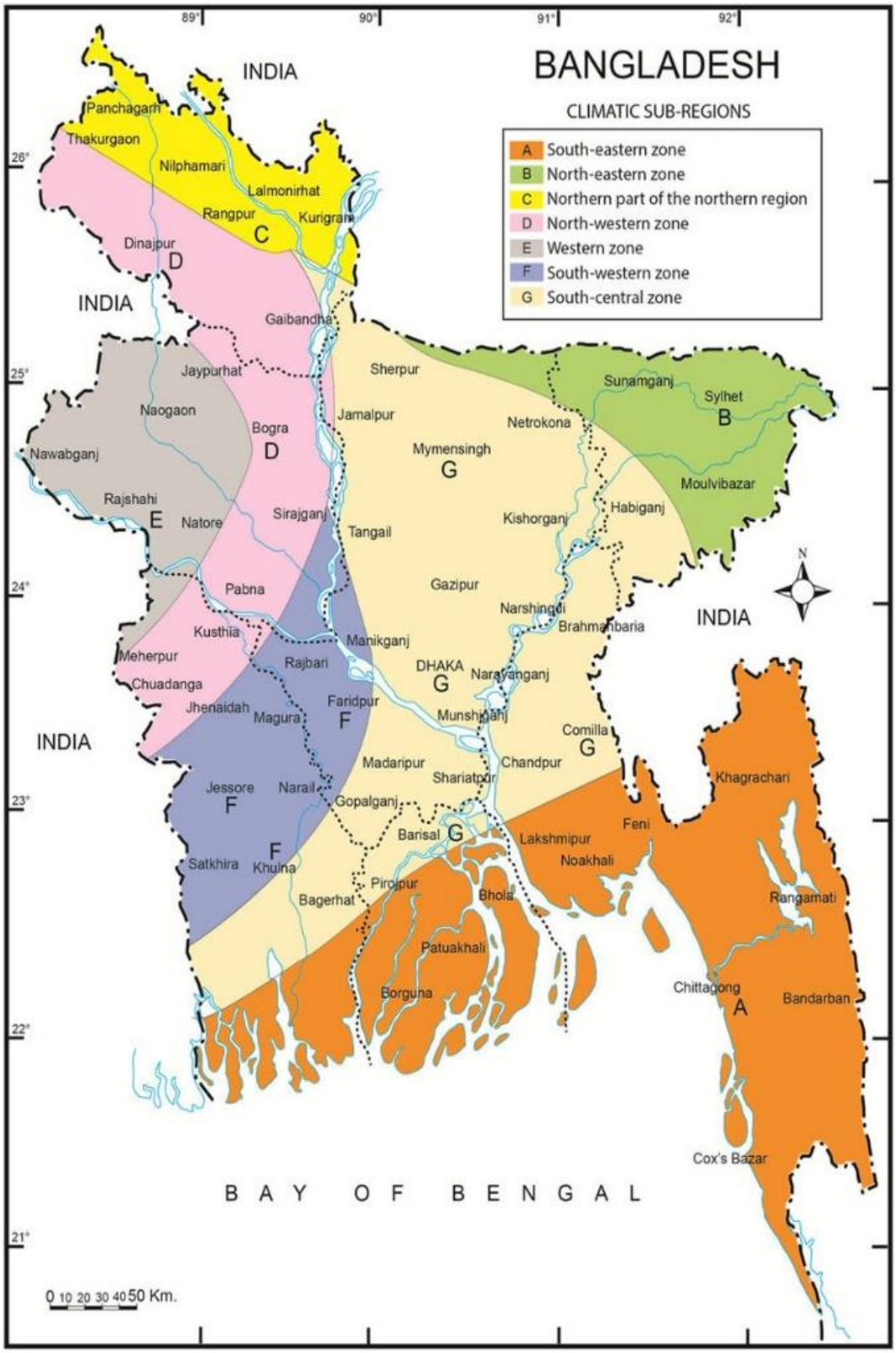

Figure 2.4: Climatic sub-regions of Bangladesh.

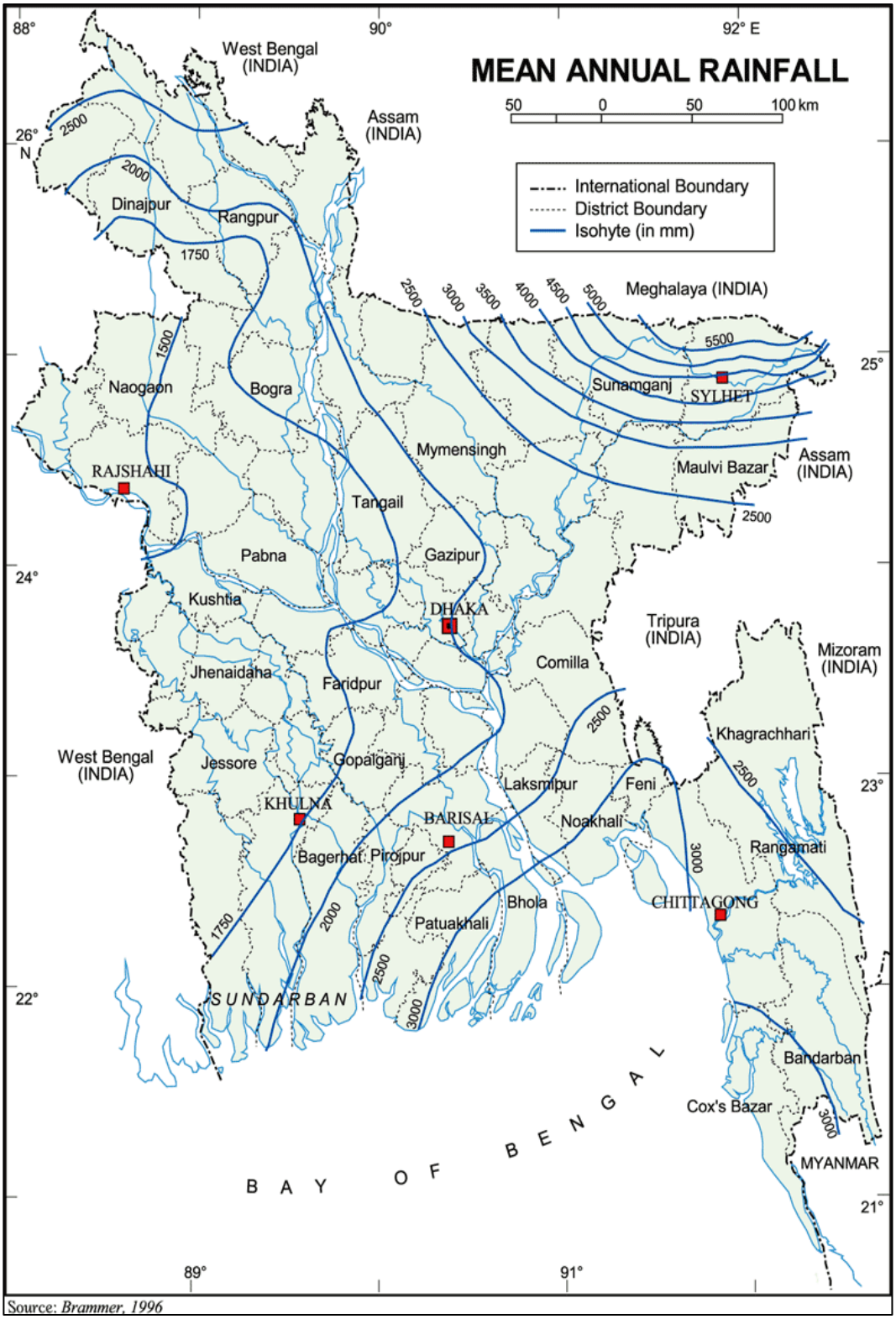

Figure 2.5. Rainfall distribution of Bangladesh.

The project area is in the six north-central districts of Bangladesh, which is characterized by high exposure to annual monsoon floods, reducing the potential for agricultural production and limiting accessibility. Infrastructure maintenance and design are challenged by increased water flows and floods, and riverbank erosion. Climate change will pose additional threats by enhancing extreme hazards such as floods, droughts, or riverbank erosion. Figure 2.6 shows the expected changes in natural hazards due to climate change.

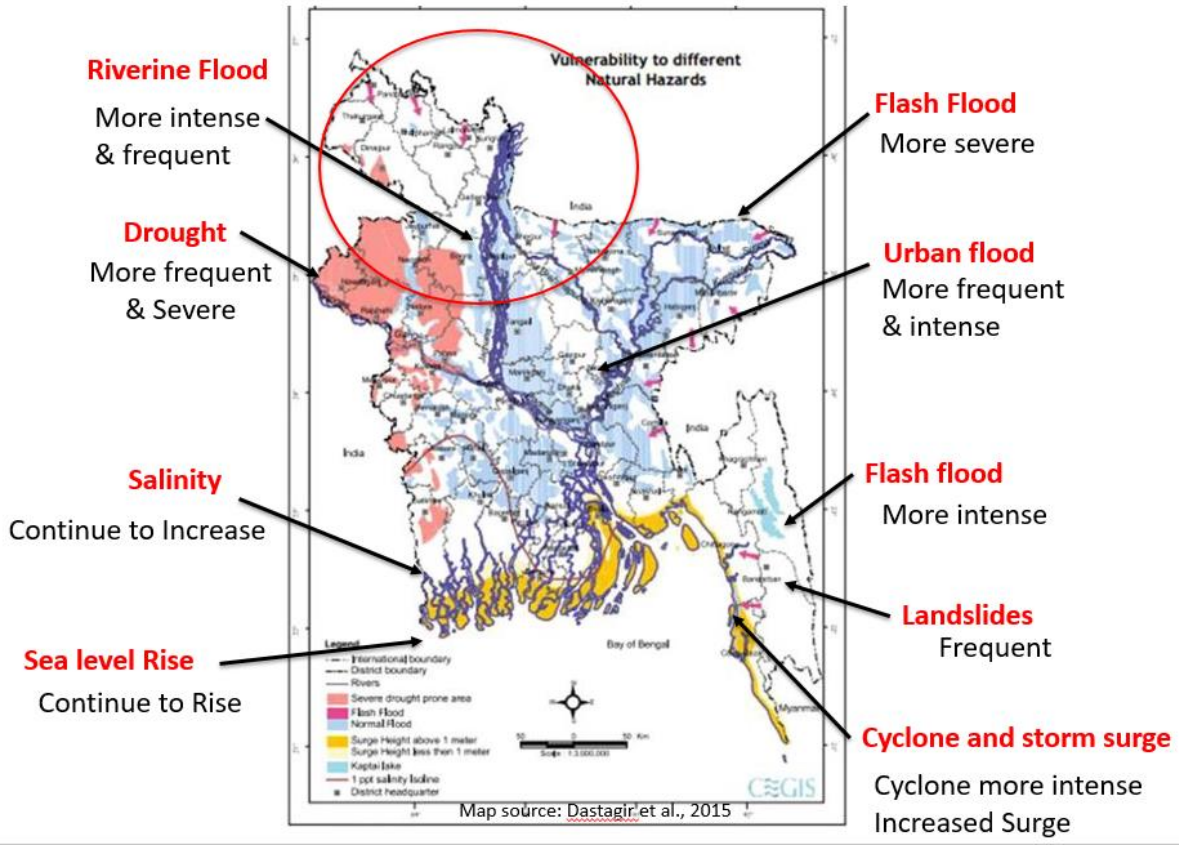

Figure 2.6: Natural hazards are expected to change due to climate change.

2.4 Geology and Seismology

The soil types of the project area are Grey floodplain soil, Grey floodplain & non-calcareous brown floodplain soil, Mixed grey, dark grey & brown floodplain soil, and Non-calcareous brown floodplain & grey floodplain soil (Figure 2.7).

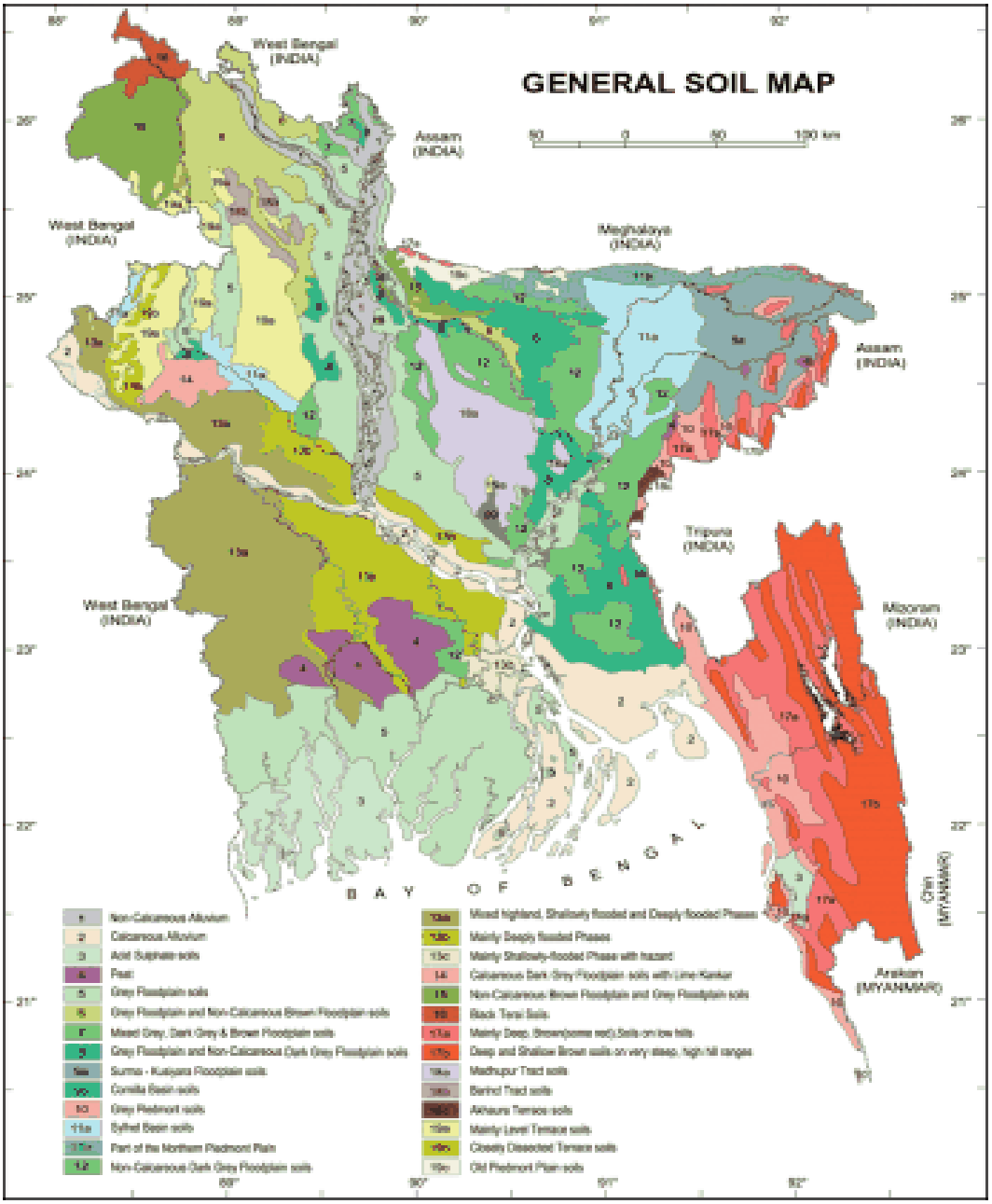

Figure 2.7: Earthquake zones of Bangladesh (Source: BNBC, 2012).

Based on earthquake epicenters and morphotechtonic characteristics under Bangladesh National Building Code, Bangladesh is divided into four seismic zones, namely Zone-1, Zone-2, Zone-3, and Zone-4 (Table 2.3).

Table 2.3: Seismic zones of Bangladesh (BNBC, 2012).

Seismic Zone	**Location**	**Seismic Intensity**	**Seismic Zone Coefficient, Z**
1	Southwestern part, including Barisal, Rangamati, Jessore, Rajshahi	Low	0.12
2	Lower Central and Northwestern parts, including Noakhali, Rangamati, Pabna, and Dinajpur, as well as the Southwestern corner, including Sundarbans	Moderate	0.20
3	Upper Central and Northwestern parts, including Brahmanbaria, Sirajganj, Rangpur	Severe	0.28
4	Northeastern part, including Sylhet, Mymensingh, Kurigrtam	Very Severe	0.36

The project area is located in Zone-3 & Zone-4 of earthquake zones which is a zone of very moderate seismic intensity with a basic seismic co-efficient of 0.28 & 0.36 (Figure 2.8). Thus, special care should be given in design and construction, considering alluvial formations and seismic activities. During seismic or earthquake delineation, ground condition (firm or soft) has not been taken into consideration in Bangladesh. Hence special precaution is needed in considering the risk of earthquakes to any water structure in floodplain formations.

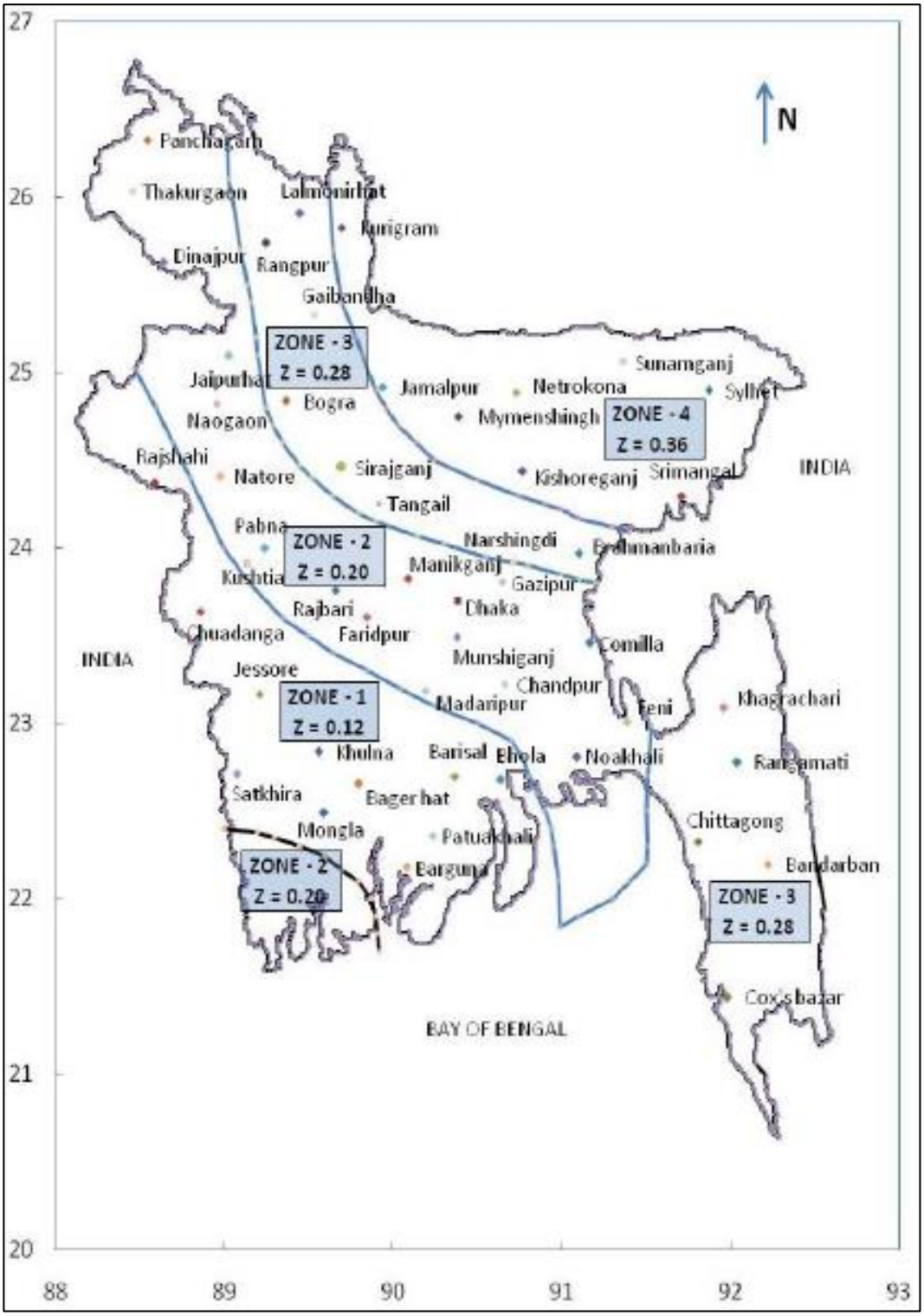

Figure 2.8: Earthquake zones of Bangladesh (Source: BNBC, 2012).

2.5 Agroecological systems

The present project site is located in the Agro-ecological Zone (AEZ)-9: 'Old Brahmaputra Floodplain,' and part of Rupganj is occupied by AEZ-2: 'Active Teesta Floodplain (Figure 2.9). Agroecological Zone land areas are recognized on the basis of hydrology, physiography, soil types, tidal activity, cropping patterns, and seasons. In fact, an agroecological zone indicates an area characterized by homogeneous agricultural and ecological characteristics. This homogeneity is more prominent in the sub-region and unit levels. The agroecological zones of Bangladesh have been identified on the basis of four elements such as physiography, soils, land levels in relation to flooding, and agroclimatology. Bangladesh has been tentatively divided into 30 agroecological zones. These 30 zones have been subdivided into 88 agroecological sub-regions, which have been further subdivided into 535 agroecological units.

*The AEZ-2 region**, Active Teesta Floodplain*** (9,468 sq. km) this region occupies the major part of the Teesta floodplain as well as the floodplain of the Atrai, Little Jamuna, Karatoya, Dharla, and Dudhkumar rivers. Most areas have broad floodplain ridges and almost level basins. There is an overall pattern of olive-brown, rapidly permeable, loamy soils on the floodplain ridges, and grey or dark grey, slowly permeable, heavy silt loam or silty clay loam soils on the lower land and parent materials medium in weatherable K minerals. Eight general soil types occur in the region, moderately acidic throughout, low in organic matter content on the higher land, but moderate in the lower parts. The fertility level is low to medium. Soils, in general, have a good moisture-holding capacity.

The AEZ-9 region ***Old Brahmaputra Floodplain*** (7,230 sq km) this region occupied a large area of Brahmaputra sediments before the river shifted to its present Jamuna channel about 200 years ago. The region has broad ridges and basins. Relief is irregular, especially near the old and present river channels. Soils of the area are predominantly silt loams to silty clay loams on the ridges and clay in the basins. Organic matter content is low on the ridges and moderates in the basins. Topsoils are moderately acidic, but subsoils are neutral in reaction. The general fertility level is low.

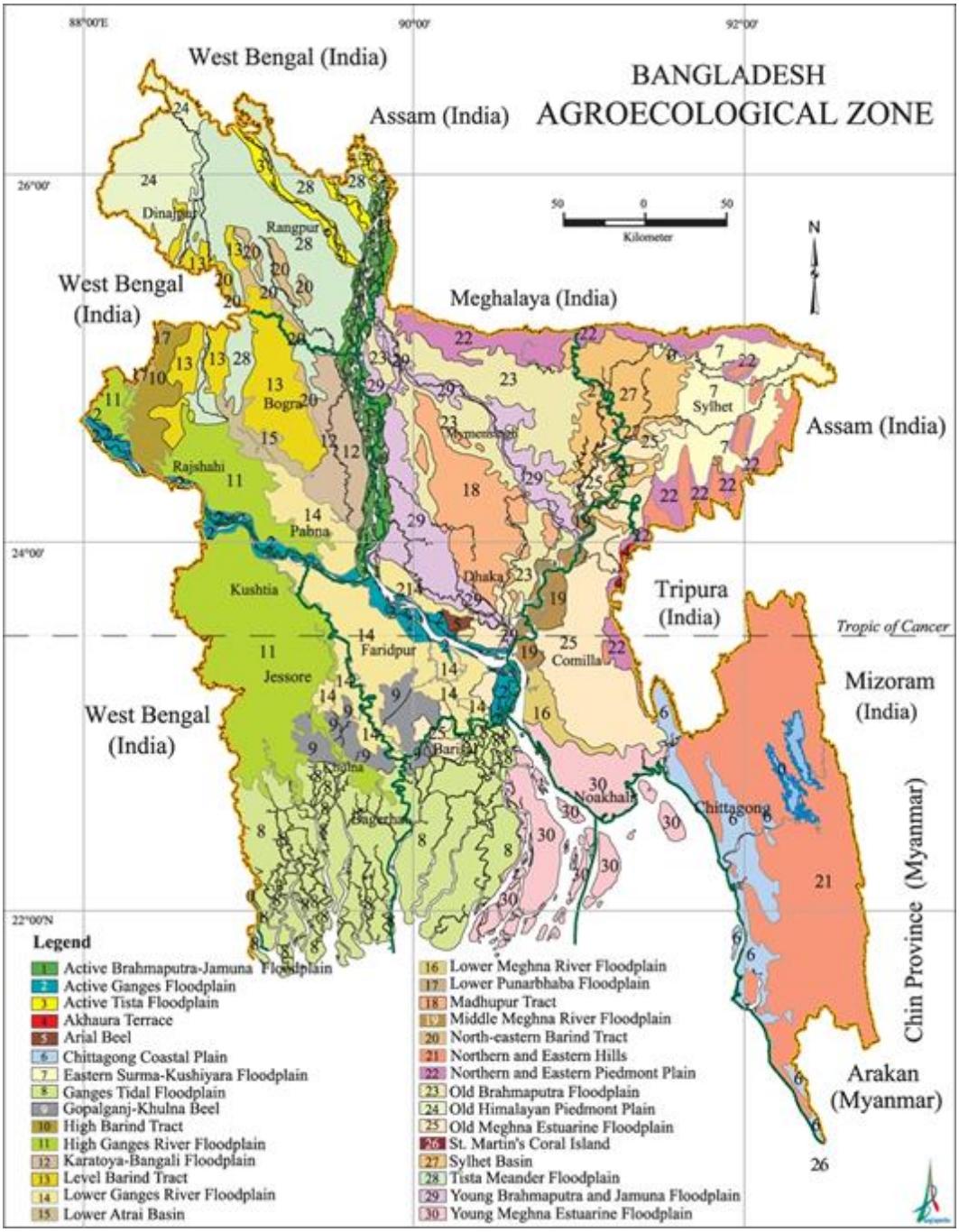

Figure 2.9: Agroecological zones of Bangladesh (Source: BARC Edaphic Maps).

CHAPTER THREE
BRAHMPUTRA-TEESTA BASIN MODELING

3.1 Introduction

An increase in global average temperature due to climate change is likely to intensify the global hydrological cycle, which in turn will impact regional water resources (Oki and Kanae, 2006; Arnell, 1999). For instance, any change either in the frequency or the total amount of precipitation over a river basin can cause a change in the magnitude and timing of the river's discharge, thereby changing the mean discharges along with the intensity of floods and droughts (Immerzeel, 2008). The impacts of climate change on regional water resources are still uncertain and under investigation, especially the impacts of extreme events such as floods and droughts (Andersen and Shepherd, 2013). Although estimating the changes in future mean discharges is necessary for overall water resources management, quantifying the future extreme discharges is of greater urgency because future changes in hydrological extremes are thought to be greater than mean hydrological conditions (Huang et al., 2015; Uhe, 2019). Increased floods and droughts have the obvious potential to cause massive damage to society and the environment in many ways, including the decline of crop yields, thus increasing the risk of poverty and hunger (Abbaspour et al., 2009). Therefore, several countries have set the quantification of the impacts of climate change on regional water resources as a priority, using meaningful spatial and temporal resolutions over long-term strategic planning (Uniyal et al., 2015). Recent studies have shown that floods and other extreme meteorological disasters are likely to be exacerbated in Europe due to climate change (Forzieri et al., 2016, Alfieri et al., 2015).

Bangladesh, as a part of the greatest Ganges-Brahmaputra-Meghna deltaic plain, is highly vulnerable to climate change. The quantity of water flowing through this basin is affected due to natural variability in hydrological conditions, as well as changes in land use, water use, and climate (Chalov et al., 2015). Nowadays, global warming causes a change in the frequency of rainfall and temperatures. According to IPCC 5^{th} Assessment Report, 2014, the average temperature of the world will increase by about 1.5ºC from 2030-to 2052. With this change in the Earth's climate system, the global hydrologic cycle is apprehended to be perturbed at alarming scales, and the existing level of water scarcity in the South Asian region is likely to

face more stress and uncertainty in the coming years. Historically, water-related issues in this basin have resulted from both high and low flows. Flood is a common phenomenon in this region, and a severe flood occurs almost every year (Kumar, 2017). Low flows are caused by scarcity of rainfall outside the summer monsoon and sometimes by the failure of this monsoon season to develop within its natural extent.

The Brahmaputra River Basin consists of the Ganges and Brahmaputra, which originate in Tibet, and the Barak River starting in India. These rivers all converge in Bangladesh as the Meghna River and flow out to the Bay of Bengal. The river basin is a wide land area made up of parts of India, Tibet, Bhutan, Nepal, and Bangladesh. The Brahmaputra River flows for 1,800 miles through Tibet, India, and Bangladesh. Starting in the Himalayas in Tibet as the Tsangpo River, the river flows eastward for 704 miles. At the Shuomatan Point, the river bends and enters India crossing the Assam Valley. It then flows south through Bangladesh, exiting the Ganges-Brahmaputra Delta into the Bay of Bengal. About 625 million people live in the basin, 80% of which are farmers and need water for their crops and animals.

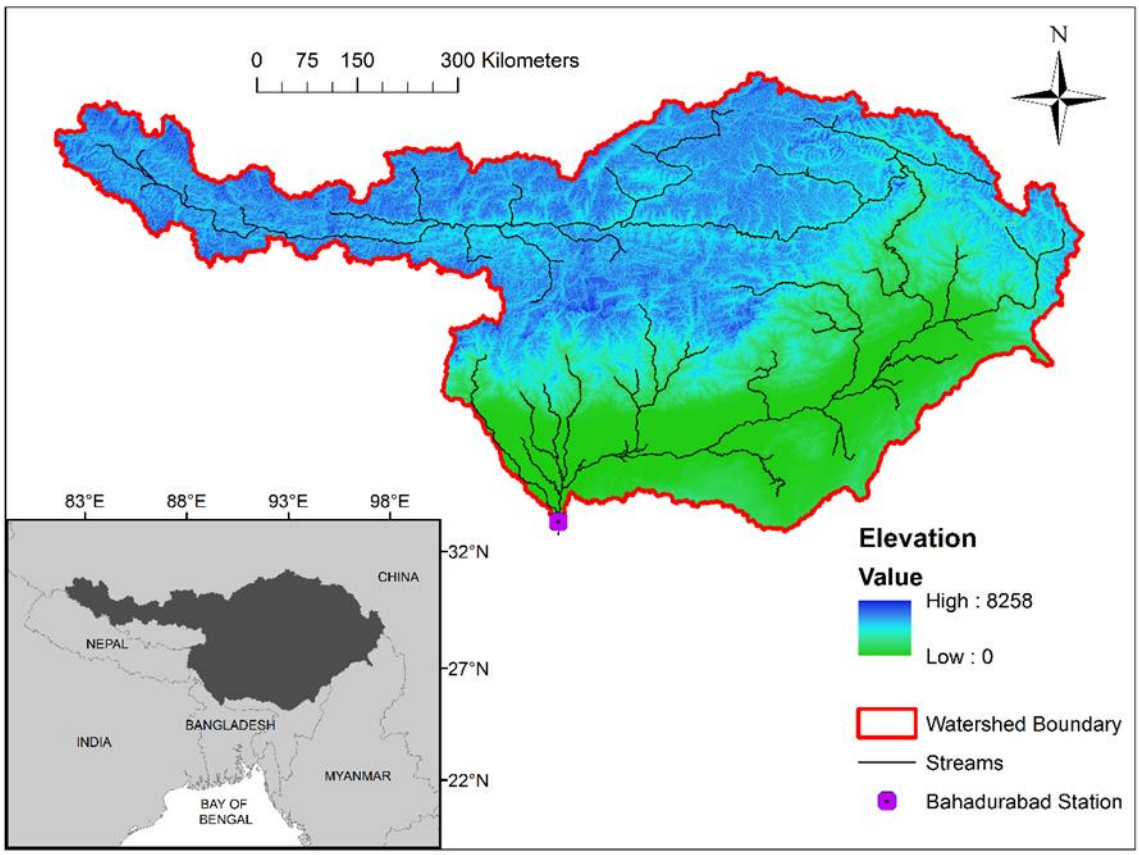

Figure 3.1: Brahmaputra-Teesta River Basin.

Bangladesh gets 94% of its water from rivers flowing into the country, equating to 2.9 billion metric tons from the basin. The high use of the water source is clearly reflected in the largely agricultural-based economies of all the countries the river flows through. The monthly average flow rate varies from 3,244 m3/s in March to 44,752 m3/s in July. The average annual flow rate is 19,160 m3/s, the fourth highest in the world. So this basin plays a vital role in the overall agricultural, economic, and climatic conditions and monsoon flood situations of Bangladesh. So it is really important to develop a hydrological model to analyze the impact of land-use changes in the major portion of the upstream basin area on the monsoon flow and also to assess the impact of changes in rainfall and temperature on the Brahmaputra River Basin. Previously, several studies on water flow in Ganges-Brahmaputra-Meghna River Basin have been conducted using different modeling approaches. However, only a few studies have been conducted to assess the water flow of the Brahmaputra river basin. In most cases, empirical or regression models were developed relating the climate parameters to the streamflow. Due to the non-linearity of the hydrologic processes, it is not sufficient to use conceptual, empirical, or regression models to predict streamflow. At the same time, some calibrated model parameters of these models may not be accurate when the hydrologic regime of the river basin changes because of anthropogenic impacts. However, the model set-up can be challenging due to the large amounts of data requirement on both static states (soils, vegetation, topography, drainage network, etc.) and dynamic variables (rainfall, streamflow, soil moisture, evapotranspiration, etc.) over the basin from multiple nations and data collection agencies. These factors, along with future climate change impacts, have made this whole process more complicated and challenging. Various surface hydrology models have been developed to quantify water flow in hydrological components. SWAT is among the very few models that have the capacity to incorporate predicted changes in temperature, precipitation, and land cover simultaneously while simulating the hydrological components. Numerous studies have been conducted implementing the SWAT model to assess climate, land use, and agricultural impacts.

Mirza (1997) used an empirical model to test the sensitivity of runoff of the Ganges-Brahmaputra-Meghna basin to the change in temperature and precipitation from -1°C to +5°C and -10% to +20%, respectively. At the Gauhati station on the Brahmaputra river, runoff changes for +2°C temperature and +10%, precipitation changes were found +13%, which is lower than the Ganges. Salehin (2011) used a grid-based model over the Ganges-Brahmaputra-Meghna for both conditions as a coarser and fine model. The coarse grid model has a snowmelt runoff module, which calculates snowmelt and glacial melt runoff in the Ganges and

Brahmaputra basins following the temperature index method. The coarse grid model is verified against observed daily discharge at important locations, Bahadurabad on the Brahmaputra and Hardinge Bridge on the Ganges, and against available monthly discharge data in the Nepalese part of the Ganges basin. The author used CRU (climate Research units) data as a precipitation source for their model and also recommended the use of meteorological satellite data (Tropical Rainfall Measuring Mission or TRMM data) for this kind of hydrological model. Masood (2014) assessed the impact of climate change on the GBM basin in three-time slices- present-day (1979–2003), near-future (2015–2039), and far-future (2075–2099) periods. He used MRI AGCM3.2S data as input in a macro scale hydrologic model H08. It was found that by the end of the 21st century, +14, +15, and +18 % changes in runoff will occur in the Brahmaputra, Ganges, and Meghna basin due to the mean change in precipitation of +14.0, +10.4, and +15.2 % (entire GBM is projected to be warmed 3ºC). Imran (2018) assessed the potential changes to the water balance of the Teesta River basin due to climate change using SWAT. After assessing the results from GCM solutions for the 2080s, four scenarios, i.e., Wettest, Driest, Warmest, and Coolest, have been selected for detailed analysis. During the wettest period, the precipitation was found to be increased by 11.71%, while it decreased by 1.76% for the dry period. The increase in temperature for the coolest and the warmest scenario was found to be 2.24°C and 5.34°C. Again, the general trend emerging from the flow analysis is that the Dalia point will experience a more severe shortage of water during the lean season, whereas much as a 25% decrease in flow has been found even without any upstream controls. Mohammed (2018) assessed the possible changes in floods in the Bangladesh part of the densely populated Ganges–Brahmaputra–Meghna (GBM) delta at 1.5°C, 2°C, and 4°C global warming levels using SWAT. This study was undertaken with the aim of joining the efforts of the global scientific community to assist in the preparation of the upcoming Special Report on 1.5 Degrees by the Intergovernmental Panel on Climate Change. Results indicate that the flood peaks of the GBM Rivers are more likely to synchronize in the future. Results also indicate that the flood magnitudes may become more severe in the future. At global warming levels of 1.5°C, 2°C, and 4°C, flood flows with a 100-year return period are projected to increase by about 27%, 29%, and 54% for the Ganges; 8%, 24%, and 63% for the Brahmaputra; and 15%, 38%, and 81% for the Meghna, respectively, compared with a baseline of 1986–2005. Again, Farzana (2019) used the Soil and Water Assessment Tool (SWAT) to predict stream runoff in Halda Basin in Bangladesh. While the calibrated performance of the model was satisfactory (R^2 = 0.80, NSE = 0.71), the model was unable to track the extremely low flow peaks due to the temporal and spatial variability of rainfall which may not be fully captured by using data from

one rainfall gauging station. Groundwater delay time, baseflow alpha-factor, and curve number were the most sensitive parameters influencing model performance. This study improves understanding of the key processes of a catchment in a data-poor, monsoon-driven, and small river basin and could serve as a baseline for scenario modeling for future water management and policy framework.

At IWFM, BUET in HELIX research project, a semi-distributed hydrological model, Soil and Water Assessment Tool (SWAT) (Arnold et al. 1998), has been applied to assess the impact of climate change on the major river flow. SWAT has been simulated for future discharges derived from the 11 different regional climate model data, as shown in Table 3.1. A Description of the Global Circulation Models (GCMs) used in that study is presented in Table 3.2. SWAT has recently become one of the most commonly used hydrological models around the world for investigating climate change impacts on regional water resources because of its flexibility and robustness (Jha et al., 2006; Gosain et al., 2011; Narsimlu et al., 2015, Bharati et al., 2016). In this current project, the SWAT output on two major rivers at the entry points of Bangladesh, namely, Bahdurabad at the Brahmaputra River and Dalia at the Teesta River, will be applied.

Table 3.1: List of Regional Climate Models used in HELIX.

	Institute	**GCM**	**RCM**	**Res.**	**RCP**
1	CSIRO	ACCESS1.0	CCAM-1391M	0.5°	8.5
2	CSIRO	CCSM4.0	CCAM-1391M	0.5°	8.5
3	SMHI	CNRM-CERFACS-CNRM-CM5	RCA4	0.5°	8.5
4	CSIRO	CNRM-CM5	CCAM-1391M	0.5°	8.5
5	SMHI	ICHEC-EC-EARTH	RCA4	0.5°	8.5
6	CSIRO	MPI-ESM-LR	CCAM-1391M	0.5°	8.5
7	MPI-CSC	MPI-M-MPI-ESM-LR	REMO2009	0.5°	8.5
8	SMHI	MPI-M-MPI-ESM-LR	RCA4	0.5°	8.5
9	SMHI	NOAA-GFDL-GFDL-ESM2M	RCA4	0.5°	8.5
10	SMHI	IPSL-CM5A-MR	RCA4	0.5°	8.5
11	SMHI	MIROC-MIROC5	RCA4	0.5°	8.5

Figure 3.1 shows the schematic representation of the SWAT basin model for the Brahmaputra River. The simulated discharges to estimate the future change in frequency, magnitude, and timing of both annual maximum and minimum discharges have been analyzed. Moreover, we also quantified the uncertainty to estimate the future change in mean monthly discharges.

Table 3.2: Description of the Global Circulation Models (GCMs) used in the HELIX project.

GCMS Name	**Institution**
ACCESS1-0	Commonwealth Scientific and Industrial Research Organization (CSIRO) and Bureau of Meteorology (BOM), Australia.
CSIRO-Mk3-6-0	Australian Commonwealth Scientific and Industrial Research Organization (CSIRO) Marine and Atmospheric Research (Melbourne, Australia) in collaboration with the Queensland Climate Change Centre of Excellence (QCCCE) (Brisbane, Australia).
EC-EARTH	European Earth System Model
GFDL-CM3	Geophysical Fluid Dynamics Laboratory (GFDL) of the National Oceanic and Atmospheric Administration (NOAA).
HadGEM2-AO	National Institute of Meteorological Research, Seoul, South Korea
MIROC-ESM	Japan Agency for Marine-Earth Science and Technology, Kanagawa, Japan (JAMSTEC); Atmosphere and Ocean Research Institute, The University of Tokyo, Chiba, Japan (AORI); and National Institute for Environmental Studies, Ibaraki, Japan (NIES).
MPI-ESM-LR	Max Planck Institute for Meteorology.
MPI-ESM-MR	Max Planck Institute for Meteorology.
MRI-CGCM3	Meteorological Research Institute, Tsukuba, Japan.
NorESM1-M	Norwegian Climate Centre.

The Intergovernmental Panel on Climate Change (IPCC) recently published the WG1 report in August 2021. The latest CMIP6 Climate models for this IPCC Sixth Assessment Report (AR6) (https://www.wcrp-climate.org/wgcm-cmip/wgcm-cmip6) have been included in the current study.

3.2 Conceptual basis of SWAT Modeling

The SWAT model is physically based and computationally efficient and uses readily available inputs and users to study long-term. SWAT is a spatially distributed, continuous-time scale watershed scale model (Arnold et al., 1998). It was developed to predict the impact of land management practices on water, sediment, and agricultural chemical yields in large complex

watersheds with varying soils, land use, and management conditions over long periods of time. SWAT divides a watershed into sub-watersheds. Each sub-watershed is connected through a stream channel and further divided into Hydrologic Response Units (HRU). HRU is a unique combination of soil and vegetation type in a sub-watershed, and SWAT simulates hydrology, vegetation growth, and management practices at the HRU level. Weather, soil properties, topography, vegetation, and land management practices are the most important inputs for SWAT to model hydrologic and water quality in a watershed (Neitsch, 2002). SWAT allows a basin to be subdivided into sub-basins to evaluate hydrology, weather, sediment yield, nutrients and pesticides, soil temperature, crop growth, tillage, and agricultural management practices. The model accounts for spatial details and is a better predictor of long-term yields rather than a single flood event (Arnold et al., 1998).

3.2.1 Water Balance

To accurately predict the movement of pesticides, sediments, or nutrients, the hydrologic cycle, as simulated by the model, must conform to what is happening in the watershed. The simulation of the hydrologic cycle can be separated into the land phase and the water or routing phase. A schematic of pathways available for water movement in SWAT is shown in Figure 3.2. It involves various elements such as Snow, canopy storage, infiltration, evapotranspiration, lateral subsurface flow, surface runoff, transmission losses, return flow, etc. The hydrologic cycle simulated by swat is based on the water balance equation:

$$SW_t = SW_0 + \sum_{i=1}^{t}(R_{day} - Q_{surf} - E_a - W_{seep} - Q_{gw}) \quad \ldots\ldots\ldots\ldots\ldots \quad (3.1)$$

Where SW_t is the final soil water content (mm H2O), SW_0 is the initial soil water content on the day i (mm H2O), R_{day} is the amount of precipitation on the day I (mm H2O), Q_{surf} is the amount of surface runoff on the day i (mm H2O), E_a is the amount of evapotranspiration on the day i (mm H2O), W_{seep} is the amount of water entering the vadose zone from the soil profile on the day i (mm H2O), and Q_{gw} is the amount of return flow on the day i (mm H2O).

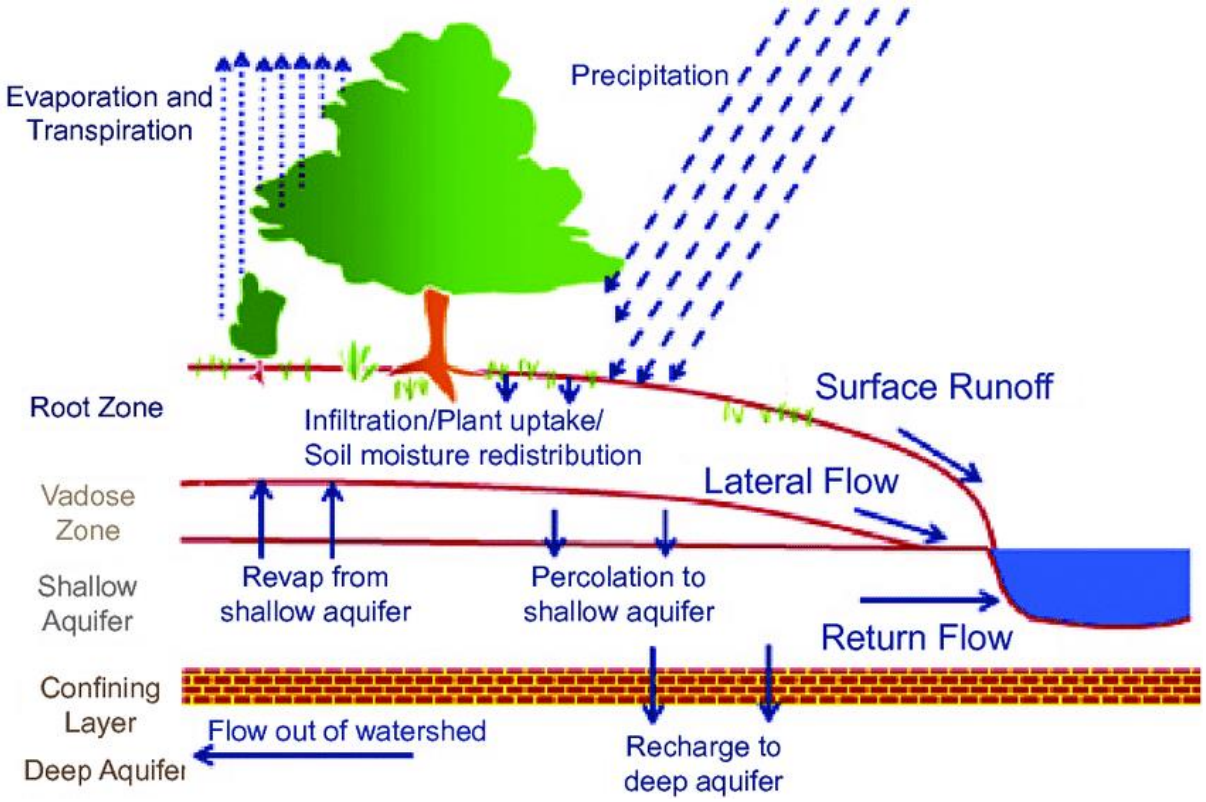

Figure 3.2: Hydrologic process in SWAT.

3.2.2 Snow

Swat classifies precipitation as rain or freezing rain/snow using the average daily temperature. The snowmelt is calculated in the SWAT model by considering the air and snowpack temperature, a melting factor, and the snow cover. In the SWAT model, the melted snow (snow water equivalent) is added to the precipitation input in the calculation of surface runoff and percolation. The snowpack increases with additional snowfall but decreases with snowmelt or sublimation. The mass balance for the snowpack is computed as:

$$SNO_i = SNO_{i-1} + R_{Sfi} - E_{subi} + SNO_{mlti} \quad \ldots\ldots\ldots\ldots\ldots\ldots\ldots\ldots \quad (3.2)$$

where SNO_i and SNO_{i-1} are the water equivalents of the snowpack on the current day (i) and previous day (i−1), respectively, R_{Sfi} is the water equivalent of the snow precipitation on day i, E_{subi} is the water equivalent of the snow sublimation on day i, and SNO_{mlti} is the water equivalent of the snowmelt on the day i.

3.2.3 Canopy Storage

Canopy storage is the water intercepted by vegetative surfaces (the canopy) where it is held and made available for evaporation. When using the curve number method to compute surface runoff, canopy storage is taken into account in the term initial abstractions. However, if methods such as Green & Ampt are used to model infiltration and runoff, canopy storage must be modeled separately. SWAT allows the user to input the maximum amount of water that can be stored in the canopy at the maximum leaf area index for the land cover. This value and the leaf area index are used by the model to compute the maximum storage at any time in the growth cycle of the land cover/crop. When evaporation is computed, water is first removed from canopy storage.

3.2.4 Infiltration

Infiltration refers to the entry of water into a soil profile from the soil surface. As infiltration continues, the soil becomes increasingly wet, causing the rate of infiltration to decrease with time until it reaches a steady value. In the SWAT model, the amount of water infiltrating into the soil profile is calculated indirectly because the surface runoff is computed directly using either of the previously mentioned methods (Neitsch et al., 2005). Hence, the infiltrated water is calculated as a difference between the amount of rainfall and the amount of surface runoff. The Green and Ampt infiltration equation (Green and Ampt, 1911) models infiltration directly, but it requires precipitation data in smaller time increments.

3.2.5 Evapotranspiration

Evapotranspiration is a collective term for all processes by which water in the liquid or solid phase at or near the earth's surface becomes atmospheric water vapor. Evapotranspiration includes evaporation from rivers and lakes, bare soil and vegetative surfaces, evaporation from within the leaves of plants (transpiration), and sublimation from ice and snow surfaces. The model computes evaporation from soils and plants separately, as described by Ritchie (1972). Potential soil water evaporation is estimated as a function of potential evapotranspiration and leaf area index (area of plant leaves relative to the area of the HRU). Actual soil water evaporation is estimated by using exponential functions of soil depth and water content. Plant transpiration is simulated as a linear function of potential evapotranspiration and leaf area index. Numerous methods have been developed to estimate ET. Three of these methods have been incorporated into SWAT2000: The Penman-Monteith method (Monteith, 1965; Allen, 1986;

Allen et al., 1989), the Priestley-Taylor method (Priestley and Taylor, 1972), and the Hargreaves method (Hargreaves et al., 1985).

3.2.6 Lateral Subsurface Flow

Lateral subsurface flow, or interflow, is a streamflow contribution that originates below the surface but above the zone where rocks are saturated with water. Lateral subsurface flow in the soil profile (0-2m) is calculated simultaneously with redistribution. Lateral subsurface flow or interflow in the soil profile is calculated using a kinematic storage model developed by Sloan and Moore (1984). The kinematic wave approximation of saturated subsurface or lateral flow assumes that the lines of flow in the saturated zone are parallel to the impermeable boundary, and the hydraulic gradient equals the slope of the bed.

3.2.7 Surface Runoff

Surface runoff, or overland flow, is a flow that occurs along a sloping surface. Using daily or sub-daily rainfall amounts, SWAT simulates surface runoff volumes and peak runoff rates for each HRU. The surface runoff component simulates the surface runoff volume, and the peak runoff rates provided daily rainfall data are fed. Surface runoff is computed using a modification of the SCS curve number (USDA Soil Conservation Service, 1972) or the Green & Ampt infiltration method (green and Ampt, 1911). In the curve number method, the curve number varies none linearly with the moisture content of the soil. The curve number drops as the soil approaches the wilting point and increases to near100 as the soil approaches saturation. The Green & Ampt method requires sub-daily precipitation data and calculates infiltration as a function of the wetting front matric potential and effective hydraulic conductivity.

3.2.8 Return Flow

Return flow, or base flow, is the volume of streamflow originating from groundwater. SWAT partitions groundwater into two aquifer systems: a shallow, unconfined aquifer that contributes return flow to streams within the watershed and a deep, confined aquifer that contributes return flow to streams outside the watershed (Arnold et al., 1993). Water percolating past the bottom of the root zone is partitioned into two fractions—each fraction becomes recharged for one of the aquifers. In addition to return flow, water stored in the shallow aquifer may replenish moisture in the soil profile in very dry conditions or be directly removed by the plant. Water in the shallow or deep aquifer may be removed by pumping.

3.3 Routing Phase of the Hydrologic Cycle

Once the SWAT determines the loading of water, sediment, nutrients, and pesticides to the main channel, the loading is routed through the stream network of the watershed. As water flows downstream, a portion may be lost due to evaporation and transmission through the bed of the channel. Another potential loss is the removal of water for agricultural or human use. Flow may be supplemented by the fall of rainfall or the addition of water from a point source. In SWAT, flow is routed using the variable storage coefficient method developed by Williams (1969) or the Muskingum routing method (Figure 3.3).

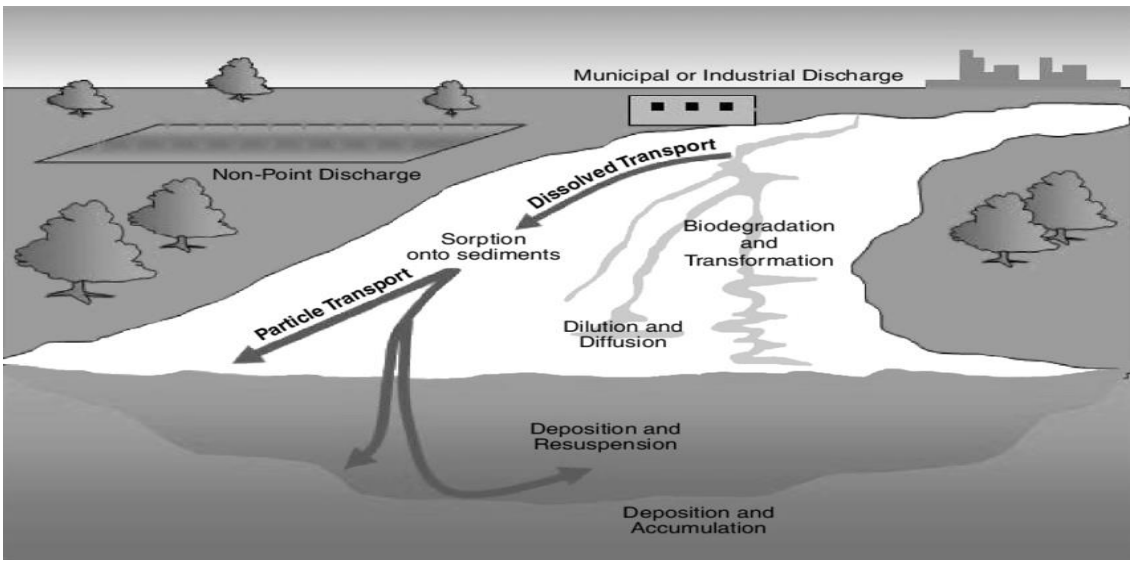

Figure 3.3: The routing phase of the hydrological cycle is used in the SWAT model.

3.4 Hydrology

3.4.1 Rainfall Intensity

The rainfall intensity is the average rainfall rate during the time of concentration. Based on this definition, it can be calculated with the equation (Eqn. 3.3)

$$I = R_{tc} / t_{con} \quad \text{.....(3.3)}$$

Where I is the rainfall intensity (mm/hr), R_{tc} is the amount of rain falling during the time of concentration (mm H2O), and t_{conc} is the time of concentration for the sub-basin (hr).

3.4.2 Percolation

Percolation is calculated for each soil layer in the profile. Water is allowed to percolate if the water content exceeds the field capacity water content for that layer and the layer below is not saturated. The volume of water available for percolation in the soil layer is calculated (Eqn. 3.4 and 3.5)

$$SW_{ly,\,access} = SW_{ly} - FC_{ly}\; if\; SW_{ly} > FC_{ly} \quad \text{(3.4)}$$

$$SW_{ly,\,access} = 0\; if\; SW_{ly} <= FC_{ly} \quad \text{(3.5)}$$

Where $SW_{ly,\,access}$ is the drainable volume of water on a given day (mm H2O), SW_{ly} is the water content of the soil layer on a given day (mm H2O). The amount of water that moves from one layer to the underlying layer is calculated using the storage routing methodology.

3.4.3 Lateral Flow

The lateral flow will be significant in areas with soils having high hydraulic conductivities in surface layers and an impermeable semi-permeable layer at a shallow depth. In such a system, rainfall will percolate vertically until it encounters the impermeable layer. The water then ponds above the impermeable layer forming a saturated zone of water, 39, i.e., a perched water table. This saturated zone is the source of water for lateral subsurface flow. SWAT incorporates a kinematic storage model for subsurface flow developed by Sloan et al. (1983) and summarized by Sloan and Moore (1984). This model simulates subsurface flow in a two-dimensional cross-section along a flow path down a steep hillslope.

3.4.4 Shallow Aquifer

The water balance for the shallow aquifer is (Eqn. 3.6)

$$aq_{sh,\,i} = aq_{sh,\,i-1} + w_{rchrg,\,sh} - Q_{gw} - w_{revap} - w_{pump,\,sh} \quad \text{(3.6)}$$

Where $aq_{sh,i}$ is the amount of water stored in the shallow aquifer on the day i (mm H2O), $aq_{sh,i-1}$ is the amount of water stored in the shallow aquifer on day i-1 (mm H2O), $w_{rchrg,\,sh}$ is the amount of recharge entering the shallow aquifer on the day I (mm H2O), Q_{gw} is the groundwater flow, or base flow, into the main channel on the day i (mm H2O), w_{revap} is the amount of water moving into the soil zone in response to water deficiencies on the day (mm H2O) and $w_{pump,\,sh}$ is the amount of water removed from the shallow aquifer by pumping on the day i (mm H2O).

3.4.5 Deep Aquifer

The water balance for the deep aquifer is (Eqn. 3.7)-

$$aq_{dp,\,i} = aq_{dp,\,i-1} + w_{deep} - w_{pump,\,dp} \quad \text{(3.7)}$$

Where $aq_{dp,i}$ is the amount of water stored in the deep aquifer on the day i (mm H2O), $aq_{dp,i-1}$ is the amount of water stored in the deep aquifer on day i-1(mm H2O), w_{deep} is the amount of water percolating from the shallow aquifer into the deep aquifer on the day i (mm H2O), and $w_{pump,dp}$ is the amount of water removed from the deep aquifer by pumping on the day i (mm H2O). If the deep aquifer is specified as the source of irrigation water or water removed for use outside the watershed, the model will allow an amount of water up to the total volume of the deep aquifer to be removed on any given day.

3.4.6 Transmission Loss

Transmission losses are estimated with the equation (Eqn. 3.8)-

$$T_{loss} = K_{ch} \times TT \times P_{ch} \times L_{ch} \quad \text{(3.8)}$$

Where T_{loss} is the channel transmission losses (m2 H2O), K_{ch} is the effective hydraulic conductivity of the channel alluvium (mm/hr), TT is the flow travel time (hr), P_{ch} is the wetted perimeter (m), and L_{ch} is the channel length (km). Transmission losses from the main channel are assumed to enter bank storage or the deep aquifer.

3.4.7 Evaporation Loss

Evaporation losses from the reach are calculated (Eqn. 3.9)-

$$E_{ch} = coef_{ev} \times E_o \times L_{ch} \times W \times fr_{\Delta t} \quad \text{(3.9)}$$

Where E_{ch} is the evaporation from the reach for the day (m3 H2O), $coef_{ev}$ is an evaporation coefficient, E_o is the potential evaporation (mm H2O), L_{ch} is the channel length (km), W is the channel width at water level (m), and $fr_{\Delta t}$ is the fraction of the time step in which water is flowing in the channel.

The evaporation coefficient is a calibration parameter for the user and is allowed to vary between 0 and 1. The fraction of the time step in which water is flowing in the channel is calculated by dividing the travel time by the length of the time step.

3.4.8 Bank Storage

The amount of water entering bank storage on a given day is calculated (Eqn. 3.10)-

$$bnk_{in} = T_{loss} \times (1 - fr_{trans}) \quad \text{..... (3.10)}$$

Where bnk_{in} is the amount of water entering bank storage (m3 H2O), T_{loss} is the channel transmission losses (m3 H2O), and fr_{trans} is the fraction of transmission losses portioned to the deep aquifer.

The volume entering the reach from bank storage is calculated (Eqn. 3.11)-

$$V_{bnk} = bnk \times (1 - exp[-\alpha_{bnk}]) \quad \text{..... (3.11)}$$

Where V_{bnk} is the volume of water added to the reach via return flow from bank storage (m3 H2O), bnk is the total amount of water in bank storage (m3 H2O), and α_{bnk} is the bank flow recession constant or constant of proportionality.

3.4.9 Channel Water Balance

Water storage in the reach at the end of the time step is calculated (Eqn. 3.12)-

$$V_{stored,2} = V_{stored,1} + V_{in} - V_{out} - T_{loss} - E_{ch} + div + V_{bnk} \quad \text{..... (3.12)}$$

Where $V_{stored,2}$ is the volume of water in the reach at the end of the time step (m3 H2O), $V_{stored,1}$ is the volume of water in the reach at the beginning of the time step (m3 H2O), V_{in} is the volume of water flowing into the reach during the time step (m3 H2O), V_{out} is the volume of water flowing out of reach during the time step (m3 H2O), T_{loss} is the volume of water lots from the reach via transmission through the bed(m3 H2O), E_{ch} is the evaporation from the reach for the day (m3 H2O), div is the volume of water added or removed from the reach for the day through diversions (m3 H2O), and V_{bnk} is the volume of water added to the reach via return low from bank storage (m3 H2O). As the transmission losses, evaporation, and other water losses for the reach segment are calculated, the amount of outflow to the next reach segment is reduced by the amount of the loss.

3.5 Steps of SWAT Modeling

The steps followed in the present research can be described as the following:

Step 1-Data Collection: This includes DEM, land use pattern, soil distribution, climate data, and flows time series.

Step 2- Bias Correction: Correcting bias in climate data (e.g., precipitation).

Step 3-Model Setup: Model setup, which includes watershed delineation, weather data setup, HRU definition, and selection of calculation methods.

Step 4-Sensitivity Analysis, Calibration, and Validation: Sensitivity analysis of the calibration parameters, calibration using the selected parameters, validation of the model, and evaluation of the performance.

Step 5-Scenario Selection: Selection of scenarios for climate change impact assessment.

Step 6-Pattern Scaling: Obtaining high-resolution projected climate data of selected scenarios.

Step 7-Climate Change Impact Assessment: Run the model with high-resolution projected data and analyze the impact of climate change on the flow of the Brahmaputra river basin.

3.5.1 Data Collection

Assessment of the impact of climate change on the flow of any river basin using a hydrological model involves several steps. Numerous amounts of preprocessing and post-processing are one of the major difficulties faced by the researchers. In the present study, several types of data, such as the Digital Elevation Model, land use pattern, soil distribution, climate data, and flow time series, were collected to set up a semi-distributed model using SWAT.

3.5.2 Digital Elevation Model, Land use, and Soil Data

Digital Elevation Model (DEM) of 3 arc second or 90 m grid resolution was downloaded from Shuttle Rudder Topography Mission (SRTM) website (http://srtm.csi.cgiar.org). Collected DEM was resampled to obtain relatively coarser resolution data in order to increase the computation efficiency (Figure 3.4 (a)). This was further used to delineate the watershed and the drainage pattern for the surface area analysis. A soil map of the selected area was collected from the Harmonized World Soil Database (HWSD). It has a 1km grid resolution and provides soil properties of two layers (0-30 cm) and (30-100 cm) depth. It includes soil properties like particle-size distribution, bulk density, organic carbon content, available water capacity, soil texture, available water content, saturated hydraulic conductivity, etc. There are 29 types of soil class data in the GBM basins (Figure 3.4 (c)).

Land use is one of the most important factors that affect surface erosion, runoff, and evapotranspiration in a watershed. Existing land use percentage collected was about: Agricultural land- 23%, Deciduous forest- 0%, Evergreen forest- 17%, Mixed forest- 6%, Herbaceous land- 36%, Shrub Land- 9%, Pasture- 0%, Water bodies- 0%, Snow and ice- 5%, Bare land- 2%, others- 2%. Parameters like infiltration and root depth have been collected from USGS (United States Geological Survey) - Global Land Cover 2000 database (Figure 3.4 (b)). The required area is available from the South-Central Asia dataset. The data is available in the geographic coordinate system - WGS84 datum. There are 11 types of land use data in the GBM basin. Land use classes have been parameterized based on existing SWAT land use classes.

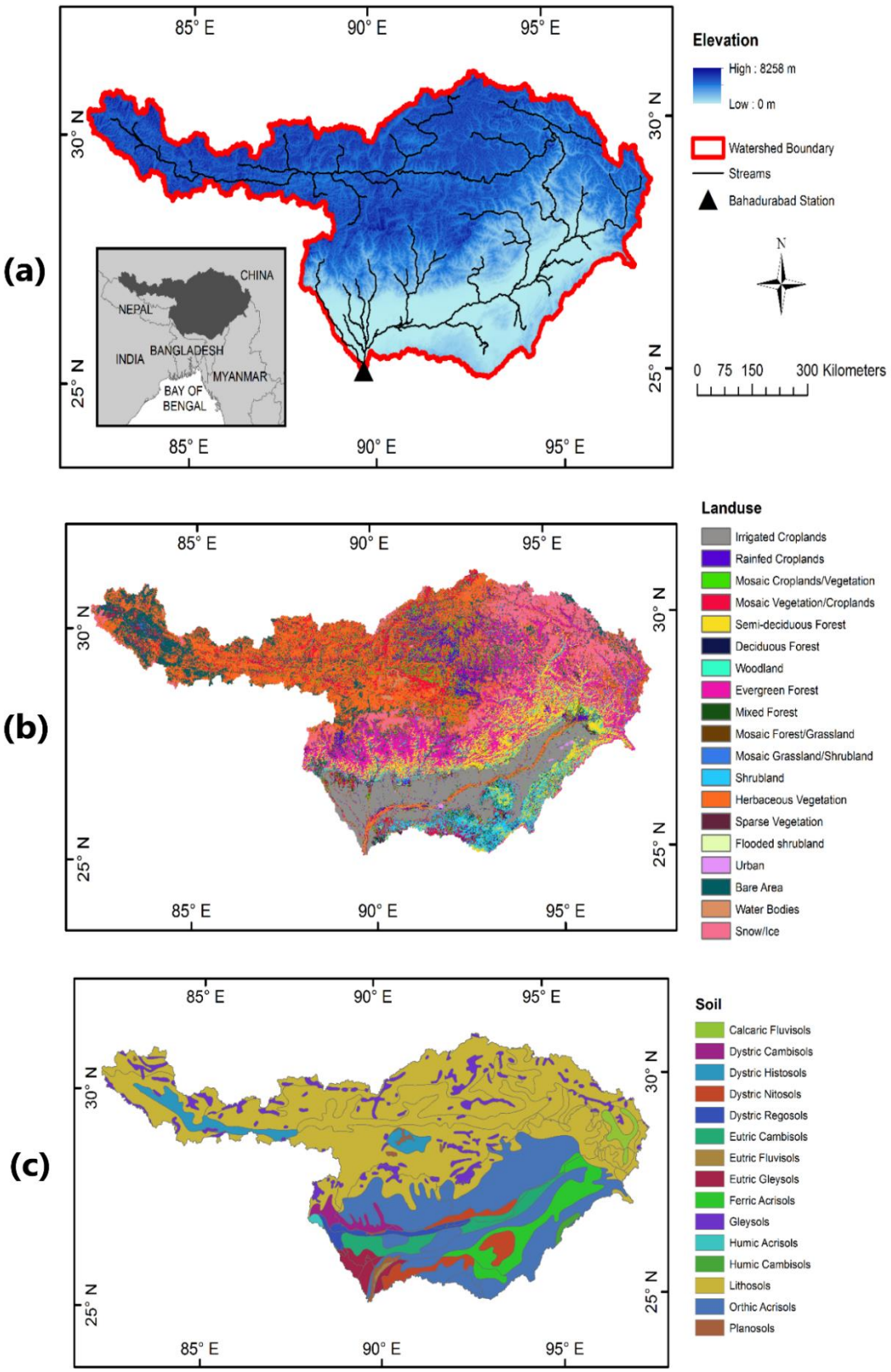

Figure 3.4: (a) DEM, (b) land use map, and (c) soil map of Brahmaputra River Basin.

SWAT model stores the information required to simulate plant growth in the plant growth database file for an individual plant. The plant growth database distributed with SWAT includes parameters for most of the common plant species.

3.5.3 Weather and Discharge data

The SWAT model requires different types of meteorological data to simulate the hydrological processes. These include daily values of precipitation, maximum and minimum temperature, solar radiation, relative humidity, and wind speed. For this study, meteorological data such as precipitation, maximum temperature, and minimum temperature for the Brahmaputra River Basin (BRB) have been collected and pre-processed from CMIP6 projections. After downloading the data for the GBM basin, the required data for the Brahmaputra basin has been pre-processed using Climate Data Operator (CDO) and MATLAB to prepare the SWAT inputs. The observed discharge data collected from Bangladesh Water Development Board (BWDB) has been compared to the discharge outputs from the model run using different climate projection data.

3.6 Climate Model Data

3.6.1 CMIP6 Global Climate Models

Climate models are one of the primary ways for scientists to understand how the climate has changed in the past and may change in the near and far future. These models simulate the physics, chemistry, and biology of the atmosphere, land, and oceans in great detail and need some of the largest and fastest supercomputers in the world to generate their projections. Climate models are constantly being updated as different modeling groups around the world incorporate higher spatial resolution, new physical processes, and biogeochemical cycles. These modeling groups coordinate their updates around the schedule of the Intergovernmental Panel on Climate Change (IPCC) assessment reports. All of these coordinated efforts are part of the Coupled Model Intercomparison Projects (CMIP). The 2013 IPCC fifth assessment report (AR5) featured climate models from CMIP5, while the upcoming 2021 IPCC sixth assessment report (AR6) will feature the brand new CMIP6 models. Global climate models (GCMs) have been used as a primary tool for examining the past and future changes in climate extremes, and the comprehensive evaluation of GCM performances is important for the proper interpretation of the simulated results. A new generation of GCMs has been developed for the CMIP6 experiments (Eyring et al., 2016). CMIP6 models have an increased range of complexity from GCMs to Earth System Models with improvements in physical processes and higher spatial

resolution. CMIP6 consists of the "runs" from around 100 distinct climate models being produced across 49 different modeling groups. In the lead-up to the IPCC AR6, the energy modeling community has developed a new set of emissions scenarios driven by different socioeconomic assumptions. These have been defined as "Shared Socioeconomic Pathways" (SSPs). A number of these SSP scenarios have been selected to drive climate models for CMIP6. Specifically, a set of scenarios were chosen to provide a range of distinct end-of-century climate change outcomes. The IPCC AR5 featured four Representative Concentration Pathways (RCPs) that examined different possible future greenhouse gas emissions.

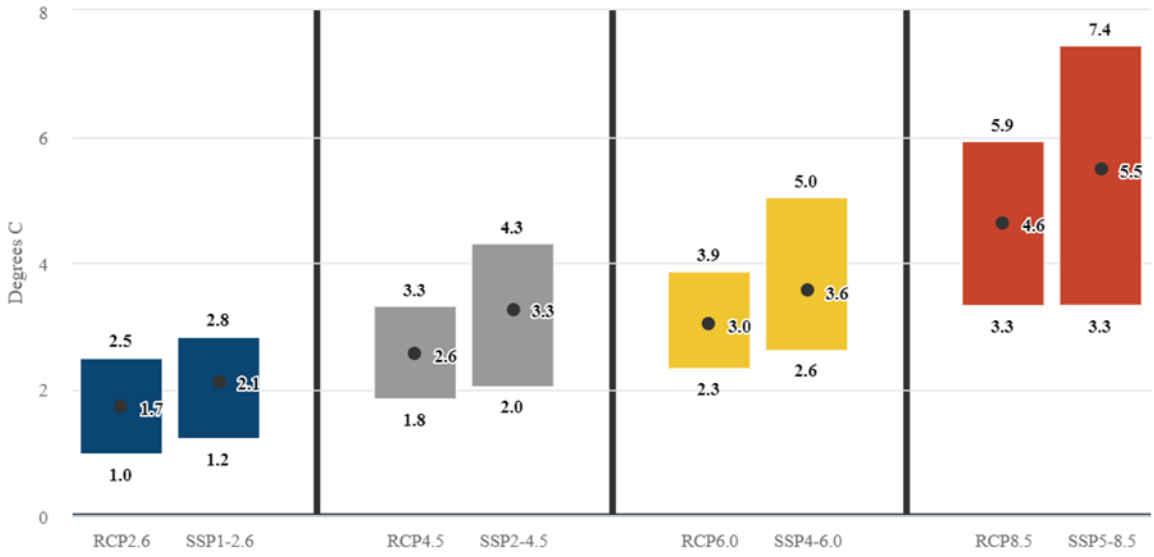

Figure 3.5: Comparing CMIP5 and CMIP6 scenarios from 1880-1900 and 2090-2100 for currently available runs. (Source: Carbon Brief).

These scenarios – RCP2.6, RCP4.5, RCP6.0, and RCP8.5 – have new versions in CMIP6. These updated scenarios are called SSP1-2.6, SSP2-4.5, SSP4-6.0, and SSP5-8.5, each of which result in similar 2100 radiative forcing levels as their predecessor in AR5. For the PROVATI3 project, 13 CMIP6 models from different modeling groups around the world have been used under ScenarioMIP for the baseline (1985-2014) and future period (2015-2100) based on (Mishra et al., 2020). Daily bias-corrected data of precipitation, maximum and minimum temperatures at 0.25° spatial resolution for South Asia (India, Pakistan, Bangladesh, Nepal, Bhutan, and Sri Lanka) and 18 river basins located in the Indian sub-continent have been downloaded from CMIP6 bias-corrected products developed by Mishra et al. (2020). The bias-corrected dataset is developed using Empirical Quantile Mapping (EQM) for the historical (1951–2014) and projected (2015–2100) climate for the four scenarios (SSP126, SSP2-45, SSP370, SSP5-85)

using output from 13 General Circulation Models (GCMs) of CMIP6. Daily datasets, including three variables, i.e., pr (total precipitation), tasmax (maximum temperature), and tasmin (minimum temperature), have been downloaded and processed to feed the SWAT model for the Brahmaputra basin developed by IWFM. The list of CMIP6 models that have been considered for this study is provided in Table 3.3.

Table 3.3: List of CMIP6 Climate Models used in the study.

Serial	Model Name	Country	Scenarios	Resolution (Degree)
1	ACCESS-CM2	Australia	SSP2-45, SSP5-85	0.25
2	ACCESS-ESM1-5	Australia	SSP2-45, SSP5-85	0.25
3	BCC-CSM2-MR	China	SSP2-45, SSP5-85	0.25
4	CanESM5	Canada	SSP2-45, SSP5-85	0.25
5	EC-Earth3	EU	SSP2-45, SSP5-85	0.25
6	EC-Earth3-Veg	EU	SSP2-45, SSP5-85	0.25
7	INM-CM4-8	Russia	SSP2-45, SSP5-85	0.25
8	INM-CM5-0	Russia	SSP2-45, SSP5-85	0.25
9	MPI-ESM1-2-HR	Germany	SSP2-45, SSP5-85	0.25
10	MPI-ESM1-2-LR	Germany	SSP2-45, SSP5-85	0.25
11	MRI-ESM2-0	Japan	SSP2-45, SSP5-85	0.25
12	NorESM2-LM	Norway	SSP2-45, SSP5-85	0.25
13	NorESM2-MM	Norway	SSP2-45, SSP5-85	0.25

Note: Frequency- Daily, Variables- pr, tasmax, tasmin

3.7 Bias Correction of climate data

The GCMs often show a considerable systematic error that limits their application in impact studies. In climate change impact studies, the most common way to deal with this error is to apply bias correction on GCM outputs. Both the parametric and nonparametric quantile mapping methods are widely used for bias correction of the climate model. Outputs of the various atmospheric (e.g., maximum and minimum temperatures and precipitation) variables obtained from GCMs are known to exhibit systematic biases. Hence, these outputs need to be bias-corrected to produce reliable estimates at regional and local scales for climate impact assessment.

Mishra et al. (2020) used Empirical Quantile Mapping (EQM) to statistically downscale the daily maximum and minimum temperatures and precipitation for South Asia and Indian sub-continental river basins. The outputs from 13 CMIP6-GCMs have been used, which are available at different resolutions (https://esgf-node.llnl.gov/search/cmip6/). Observations for the three variables at the resolution of 0.25-degree are obtained from the IMD (Pai et al., 2014) for Indian Region and (Sheffield et al., 2006) for grid points within and outside India, respectively. To maintain consistency with the observed data, all the variables from CMIP6 GCMs have been regridded to a 1-degree spatial resolution. (1951–2014) period has been used to obtain the transformation function to map the distribution of the outputs. For precipitation, the drizzle effect is corrected by using a wet day threshold of 1mm/day. If the values from model projections are larger (smaller) than the training values used to estimate the empirical CDF, the correction found for the highest (lowest) quantile of the training period is used. They have used mapped transformation to bias correct the outputs for the historical period and the SSP126, SSP2-45, SSP370, and SSP5-85 scenarios for the 2015–2100 period for all three variables. The bias-corrected model outputs have shown an excellent correlation with the observed data for the period of 1985-2014, shown in Figure 3.6.

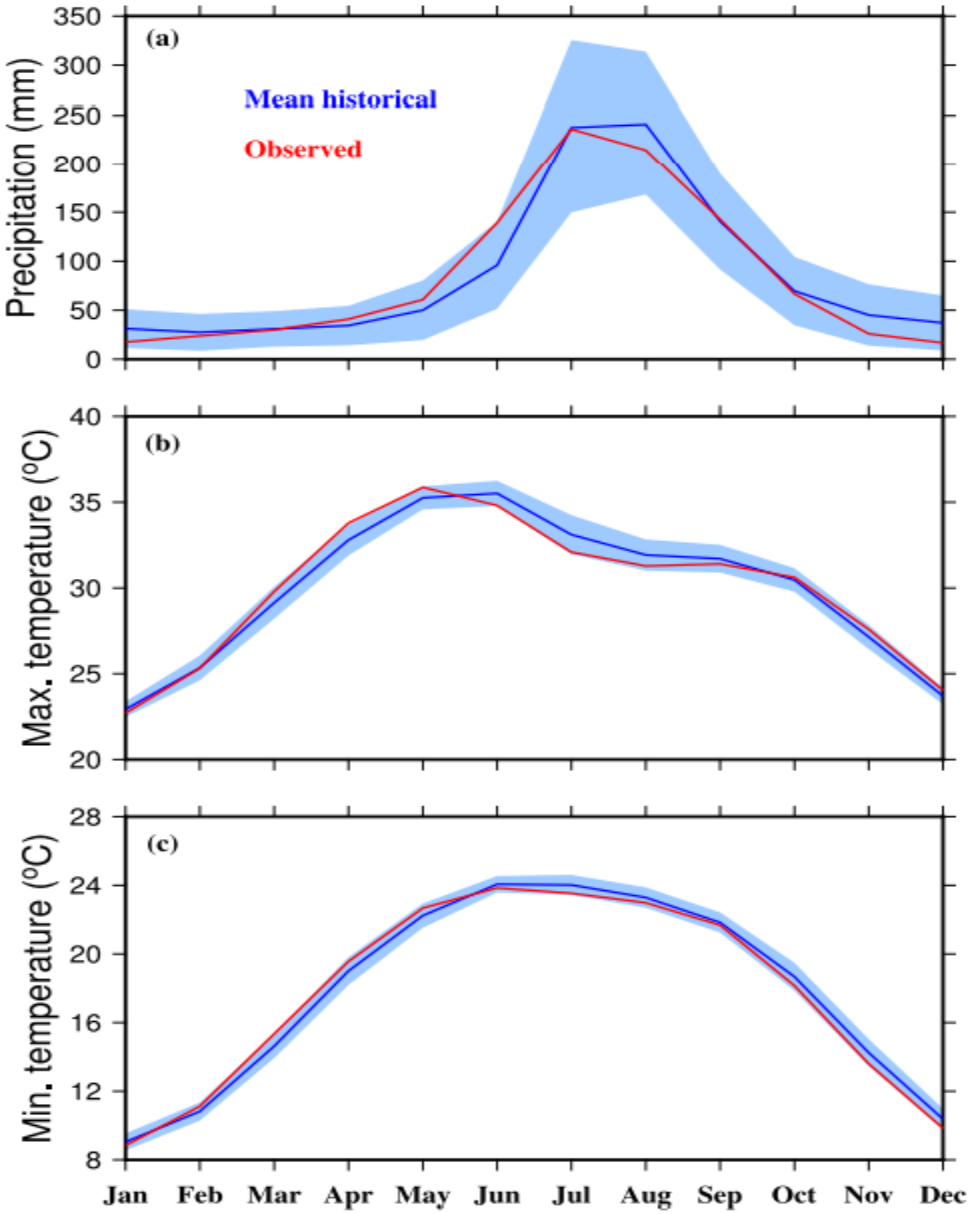

Figure 3.6: Comparison of the multi-model model ensemble (blue) mean seasonal cycle of bias-corrected (a) precipitation, (b) maximum temperature, and (c) minimum temperature against the observations for the 1985–2014 period. The shaded area represents the uncertainty of all the used CMIP6 Global Circulation Models (Mishra et al., 2020).

3.8 Steps of Model Setup

Five sequential steps have been followed to set up the SWAT model, which are (1) watershed delineation, (2) weather data definition, (3) editing of SWAT inputs and simulation, (4) model calibration and validation, and (5) Finally, streamflow simulation (both for present condition as well as in future) at different crucial points in some major rivers which are basically outflow of different sub-catchments.

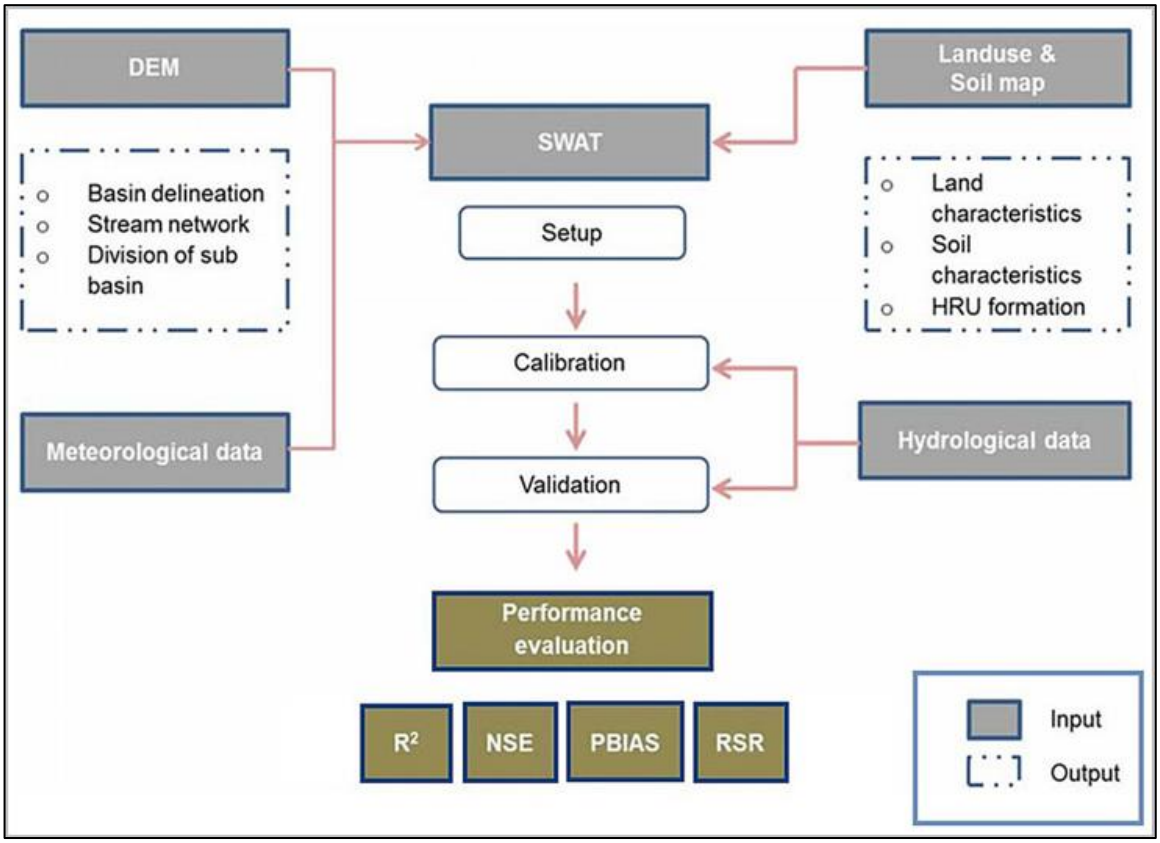

Figure 3.7: A brief framework of the SWAT model (Aqnouy, 2019).

3.8.1 Watershed Delineation

The first step in the model setup involves a delineation of the basin and sub-basin boundaries. This is accomplished using the automatic watershed delineation tool of ArcSWAT 2012.10.2.16 employing a 900 m DEM (resampled from 90 m DEM) for GBM basins and 200 m DEM (resampled from 300 m DEM) for Bangladesh. The Universal Transverse Mercator (UTM) projection has been used for the DEM and all other GIS layers. All the watershed delineation steps, such as filling the sink, defining flow direction, and accumulation, have been done automatically through the user interface. After watershed delineation, BRB basins have been divided into 149 watersheds based on the threshold area of 200,000 ha. After delineation, the basin was divided into 149 sub-basins, as shown in Figure 3.7. Soil and land use maps were loaded into SWAT to extract the land use and soil information of the BRB. The land use, soil layer, and slope class were overlaid to define the HRUs of the BRB. A total of 1020 HRUs (Average area of 687 km^2) were produced and included in the simulation. The discretization of the basin into HRUs allows a detailed simulation of the hydrological processes.

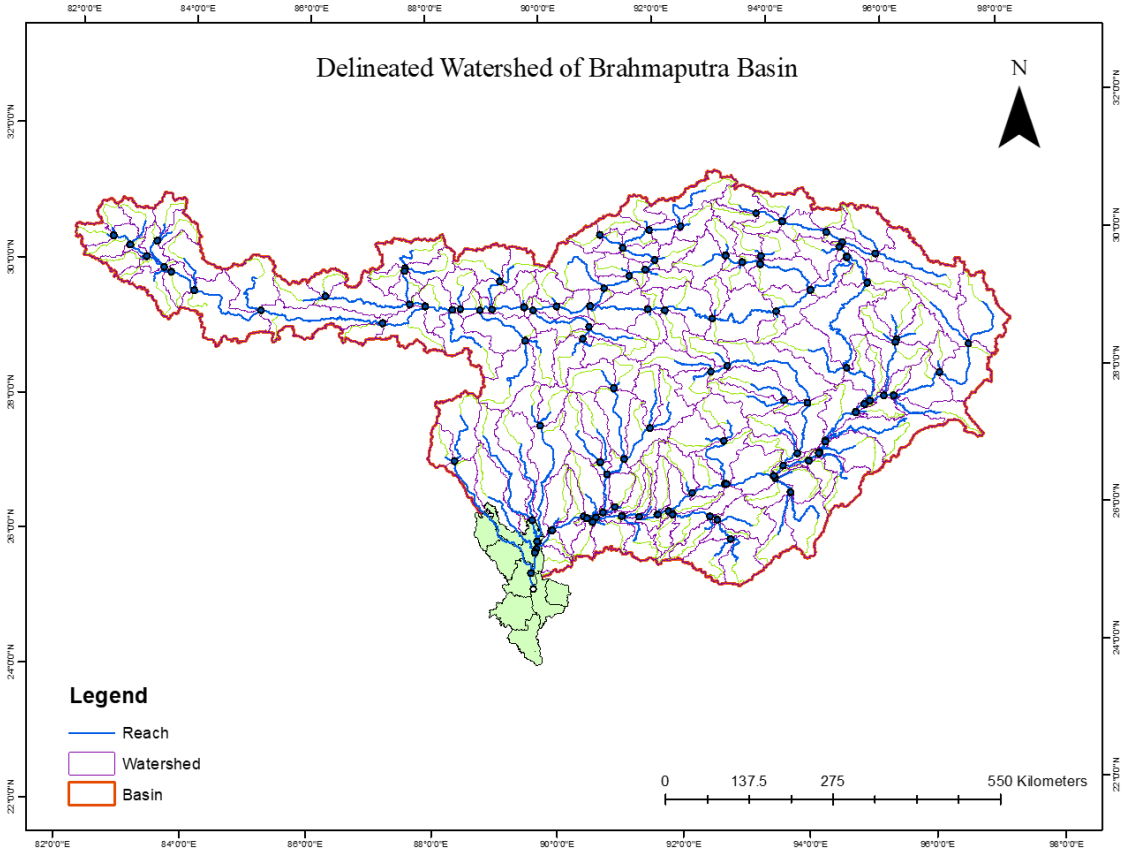

Figure 3.8: Sub-basins and delineated stream network of Brahmaputra River Basin.

3.8.2 Weather Data Definition

The climate of a watershed provides the moisture and energy inputs that control the water balance and determine the relative importance of the different components of the hydrologic cycle. The climatic variables required by SWAT consist of daily precipitation, maximum/minimum air temperature, solar radiation, wind speed, and relative humidity. The model allows values for daily precipitation, maximum/minimum air temperatures, solar radiation, wind speed, and relative humidity to be input from records of observed or generated data using weather generator tools (WXGEN) (Arnold et al., 2009b). WFDE5 over land merged with ERA5 over the ocean (W5E5) (Lange, 2019). The W5E5 dataset was compiled to support the bias adjustment of climate input data for the impact assessments carried out in phase 3b of the Inter-Sectoral Impact Model Intercomparison Project (ISIMIP3b). The data includes daily weather data (precipitation, minimum, and maximum temperature), which is used for SWAT modeling calibration and validation.

3.8.3 Simulation Method Selection

To describe the distribution of rainfall, SWAT provides two options: a skewed normal distribution and a mixed exponential distribution. Water is routed through the channel network using the variable storage routing method or the Muskingum River routing method. In the simulation for the present study, the skewed normal probability distribution function has been used. Again, the variable storage method has been used for channel routing. For estimating runoff, the SCS curve number method has been used. The Hargreaves method has been used to calculate potential evapotranspiration (PET) as it requires fewer weather parameters.

3.8.4 Model Calibration and Validation

The available weather and discharge data were divided equally into two segments, one for calibration (1985-1999) and the other for validation (2000-2014). Before starting the calibration of the model, a global sensitivity analysis was performed on selected hydrology-related parameters of SWAT to determine the sensitivity of simulated discharges to each of those parameters. A separate independent tool called SWAT-CUP (Calibration and Uncertainty Program) was used for this purpose (Abbaspour, 2015). From the results of the global sensitivity analysis, the 6 most sensitive parameters were chosen for performing calibration. The Sequential Uncertainty Fitting II (SUFI-2) algorithm of SWAT-CUP was used to calibrate the model. Upon completion of the calibration process, the SWAT model was run for the duration of the validation period, with the optimized parameters kept unchanged. To assess the performance of the models in calibration and validation, the Nash-Sutcliffe efficiency (NSE) and the coefficient of determination (R^2) were used. P-factor and R-factor values were used in this study to serve as an indicator of the uncertainties inherent in the calibration process.

3.8.4.1 SWAT-CUP

The SWAT-CUP package is developed for SWAT, which can be used for calibration, validation, sensitivity analysis, and uncertainty analysis. In short, uncertainty analysis is the process of estimating the error of the model input parameters, while calibration is the process of adjusting the model input parameters by minimizing error to achieve the best possible values compared to observation. Sensitivity analysis is the process of determining which processes or parameters govern the river basin. Finally, validation is the process of testing the calibrated parameters with a different dataset.

The SWAT-CUP model follows the stochastic approach for calibration rather than the deterministic approach, as in this process, the errors & uncertainties are recognized, and the degree of their uncertainty is captured (Abbaspour, 2015). As the model output, an envelope of good solutions, named 95% Prediction Uncertainty (95PPU), is provided rather than a single value, and this is performed using the SUFI-2 algorithm.

In Sequential Uncertainties Fitting (SUFI-2) algorithm, the uncertainty in parameters, which accounts for all the sources of error, are mapped into parameter ranges (Abbaspour et al., 2004). The aim is to capture most of the data within the 95PPU calculated at 2.5% and 97.5% levels of the cumulative distribution of an output variable. This process follows the Latin Hypercube method, which is a method that combines global and local sensitivity analysis methods (Abbaspour, 2013). The uncertainties are quantified by two statistics; P-factor, which is the percentage of the observed data bracketed by the 95PPU envelope, and R-Factor, which is the thickness of the 95PPU envelope. The P factor has a theoretical range of 0 to 100%, while the R factor has a theoretical range of 0 to infinity. A simulation with a P-factor of one and an R-factor of zero is one that exactly corresponds to the measured data (Khoi et al., 2015). The larger the P-factor, the higher the model prediction accuracy, while the larger the R-factor, the higher the model prediction uncertainty (Figure 3.9). The recommended value of the P-factor is to be larger than 0.7, and R-factor is to be less than 1.2 for the flow variable, whereas for the sediment, nitrate, and phosphor variables, a smaller P-factor and larger R-factor could be acceptable.

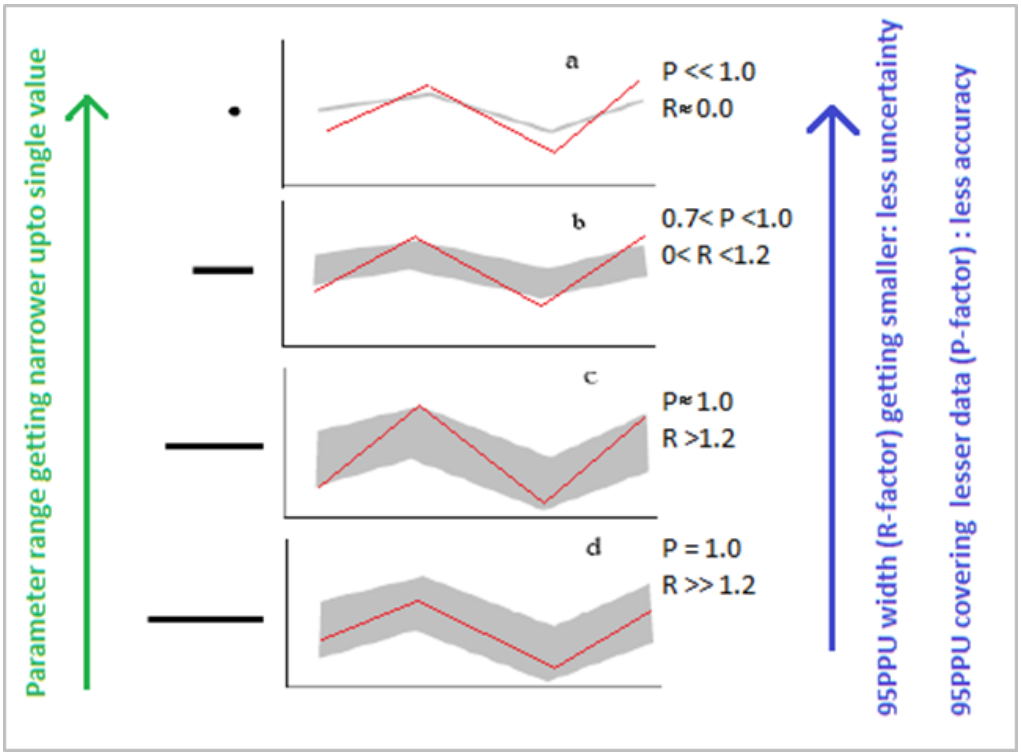

Figure 3.9: A conceptual illustration of the relationship between parameter uncertainty and prediction uncertainty (Abbaspour, 2007).

3.8.4.2 Performance Evaluation of the Model using Statistical Indicators

Statistically, the performance of the model is evaluated using the Nash-Sutcliffe Efficiency value (NSE), the coefficient of determination (proportion of the variance in the observations explained by the model, R^2), percent bias (PBIAS), and the ratio of the root mean square error between the simulated and the observed values to the standard deviation of the observations (RSR) (Moriasi et al., 2007 and Krauseet et al., 2005).

Coefficient of determination (R^2)

R^2 estimates the combined dispersion against the single dispersion of the observed and predicted series and provides the relationship strength between observed and simulated values. Its value ranges from 0 to 1; a value close to 0 means a very low correlation, whereas a value close to 1 represents a high correlation between observed and simulated discharge.

Nash–Sutcliffe efficiency (NSE)

NSE determines the relative magnitude of the residual variance compared to that of the measured data (Moriasi et al., 2007) and is one of the most widely used statistical indicators for hydrological model performance (Shrestha et al., 2013). Its value ranges from ∞ 1, where 1

indicates a perfect model, and a value of less than 0 indicates that the mean value of the observed time series would have been a better predictor than the model.

Percentage bias (PBIAS)

PBIAS indicates the average tendency of the simulated results to be greater or larger than their observed data. It measures the difference between the simulated and observed quantity, and its optimum value is 0. The positive value of the model represents underestimation, whereas the negative value represents overestimation.

RMSE-observation standard deviation ratio (RSR)

The lower value of RMSE (root mean square error) is commonly accepted and one of the widely used error parameters. However, the satisfactory threshold of RMSE as 46 is case-specific. Therefore, RSR is chosen as a complementary indicator to RMSE. The optimum value of RSR is 0, and a higher value indicates lower model performance.

The threshold value of goodness-of-fit for all models was based on Moriasi et al. (2007), as shown in Table 3.4.

Table 3.4: Model performance rating.

Performance	**NSE**	**PBIAS**	**RSR**
Very good	0.75	<±10	0 to 0.5
Good	0.65-0.75	± 10 to ± 15	0.5 to 0.6
Acceptable	0.5 to 0.65	15 to ±25	0.6 to 0.7
Unsatisfactory	<0.5	>±25	> 0.7

3.8.4.3 Sensitive Parameter Selection for Calibration

Model users are often faced with the different tasks of determining which parameters to calibrate so that the model response mimics the actual field, subsurface, and channel conditions as closely as possible. When the number of parameters in a model is substantial as a result of either a large number of sub-processes being considered or because of the model structure itself, the calibration process becomes complex and computationally extensive (Rosso, 1994; Sorooshian and Gupta, 1995). In such cases, sensitivity analysis is helpful for identifying and ranking parameters that have a significant impact on specific model outputs of interests (Saltelli

et al., 2000). Sensitivity analysis can be performed for many inputs, such as flow, sediment discharge, Organic Nitrogen, Phosphorus, etc.

For the present study, a sensitivity analysis was performed using the Latin hypercube one-factor-at-a- time (LH-OAT) (Van Griensven et al., 2002, 2005) method to rank the simulation parameters of the model for each sub-basin. In this study, sensitivity analysis is performed only for streamflow, as the study objective is to assess the availability of water. This analysis was done by using the SWAT-Cup tool. In this process, a multiple regression system regresses Latin hypercube-generated parameters against objective function to determine the sensitivity of the parameters. As statistical measurements, t-stat and p-value were used. A total of 14 parameters have been selected to find out their sensitivity to flow conditions given in Table 3.5. Parameters represented by the bold text have been found as the "most sensitive" to the basin flow determined by means of an LH-OAT analysis. It has been observed that the parameters representing the soil properties, surface runoff, groundwater, and evaporation are more sensitive than others and accurate estimation of these parameters is important for streamflow simulation with the SWAT model in the watershed. The parameters having P-value < .05 have been considered sensitive to the basin flow.

Table 3.5: Parameters used for calibration of the SWAT model.

Sl No.	**Parameter Name**	**Parameter Range**		**Fitted Value**
		Minimum	**Maximum**	
1	R_ESCO.hru (Soil evaporation compensation factor)	-0.238980	1.318980	0.306306
2	R_SOL_AWC(..).sol (Available water capacity of the soil layer)	-3.594597	0.154597	-3.032218
3	R_CN2.mgt (SCS runoff curve number)	-0.091305	0.131305	0.115722
4	V_GW_DELAY.gw (Groundwater delay)	148.312057	390.487915	242.760651
5	V_CH_K2.rte (Channel hydraulic conductivity)	48.950741	138.549255	105.397804
6	V_GW_REVAP.gw (Groundwater "revap" coefficient)	-0.019714	0.127714	0.096754
7	R_EPCO.hru (Plant uptake compensation factor)	-1.000000	1.000000	-0.42
8	R_SOL_BD(..).sol (Moist bulk density)	-2.000000	2.000000	0.04
9	R_SLSUBBSN.hru (Average slope length)	0.000000	1.000000	0.25
10	V_GWQMN.gw (Threshold depth of water in the shallow aquifer required for return flow to occur)	0.000000	2.000000	0.94

Sl No.	Parameter Name	Parameter Range		Fitted Value
		Minimum	Maximum	
11	R_HRU_SLP.hru (Average slope steepness)	0.000000	1.000000	0.47
12	V_REVAPMN.gw (Threshold depth for “revap”)	0.000000	10.000000	6.3
13	R_CH_N2.rte (Manning's ‘n’ value for the main channel)	0.000000	1.000000	0.47
14	R_OV_N.hru (Manning's ‘n’ value for overland flow)	0.000000	1.000000	0.57
15	R_ALPHA_BNK.rte (Base flow alpha factor for bank storage)	0.000000	1.000000	0.59
16	R_SOL_K(..).sol (Saturated hydraulic conductivity)	-2.000000	2.000000	-0.52
17	V_ALPHA_BF.gw (Base flow alpha factor)	0.000000	1.000000	0.17

3.8.4.4 Calibration and Validation Using SWAT-cup

The simulated streamflow needs to be calibrated to match the observed flow. That can be possible by getting fitted catchment parameters. Two approaches are available for calibration and validation. One is to use the whole observed data as calibration, and the second is to split data for validation. Both use almost the same methodology. The objective is to obtain fitted parameters. Automated model calibration requires that the uncertain model parameters are systematically changed, the model is run, and the required outputs (corresponding to measured data) are extracted from the model output files. The main function of a calibration interface is to provide a link between the input /output of a calibration program and the model. The simplest way of handling the file exchange is through text file formats. For this study, SWAT-CUP does the calibration and validation. Using the SWAT-CUP interface, any calibration or sensitivity program can easily be linked to SWAT. The program links various algorithms to SWAT. Among those algorithms, SUFI-2 has been used to perform the calibration and validation for this study. There was only one variable of our concern which was discharge. A total of 180 data points from the year 1985 to 1999 (15 years and monthly data) are used for model calibration. The NSE (Nash-Sutcliffe efficiency) was used as the objective function with a minimum threshold value of 0.5. Table 3.6 shows the 5 sensitive parameters with their respective P-values and t-stats.

Table 3.6: List of most sensitive parameters according to their P-values and t-stats.

Sl No.	Parameter Name	t-Stat	P-Value	Minimum Value	Maximum Value	Fitted Value
1	**R__ESCO.hru** (Soil evaporation compensation factor)	5.443671	0.000005	-0.238980	1.318980	0.306306
2	**R__SOL_AWC(..).sol** (Available water capacity of the soil layer)	-3.092078	0.004100	-3.594597	0.154597	-3.032218
3	**R__CN2.mgt** (SCS runoff curve number)	3.082941	0.004198	-0.091305	0.131305	0.115722
4	**V__GW_DELAY.gw** **(**Groundwater delay)	-2.716145	0.010562	148.312057	390.487915	242.760651
5	**V__CH_K2.rte** (Channel hydraulic conductivity)	2.453488	0.019777	48.950741	138.549255	105.397804
6	**V__GW_REVAP.gw** (Groundwater “revap” coefficient)	2.035426	0.050160	-0.019714	0.127714	0.096754
7	R__EPCO.hru (Plant uptake compensation factor)	1.673414	0.103995	-1.000000	1.000000	-0.42
8	R__SOL_BD(..).sol (Moist bulk density)	1.626659	0.113618	-2.000000	2.000000	0.04
9	R__SLSUBBSN.hru (Average slope length)	-1.100179	0.279462	0.000000	1.000000	0.25
10	V__GWQMN.gw (Threshold depth of water in the shallow aquifer required for return flow to occur)	0.972897	0.337902	0.000000	2.000000	0.94
11	R__HRU_SLP.hru (Average slope steepness)	0.949488	0.349489	0.000000	1.000000	0.47
12	V__REVAPMN.gw (Threshold depth for “revap”)	-0.912950	0.368096	0.000000	10.000000	6.3
13	R__CH_N2.rte (Manning's ‘n’ value for the main channel)	-0.875105	0.388038	0.000000	1.000000	0.47
14	R__OV_N.hru (Manning's ‘n’ value for overland flow)	-0.367328	0.715792	0.000000	1.000000	0.57
15	R__ALPHA_BNK.rte (Base flow alpha factor for bank storage)	0.361641	0.719997	0.000000	1.000000	0.59
16	R__SOL_K(..).sol (Saturated hydraulic conductivity)	-0.260563	0.796099	-2.000000	2.000000	-0.52
17	V__ALPHA_BF.gw (Base flow alpha factor)	0.1944591	0.847045	0.000000	1.000000	0.17

Just before the next iteration, the default values of those sensitive parameters are replaced with the fitted values obtained from the first iteration. The first iteration conducted 100 simulations after changing the values of sensitive parameters, and a second iteration where 200 simulations were conducted. After the second iteration, an excellent performance for calibration was

observed both statistically and graphically. The outflow comparison with the observed BWDB data at Bahadurabad station (SW 46.9 L) has been shown in Figure 3.10.

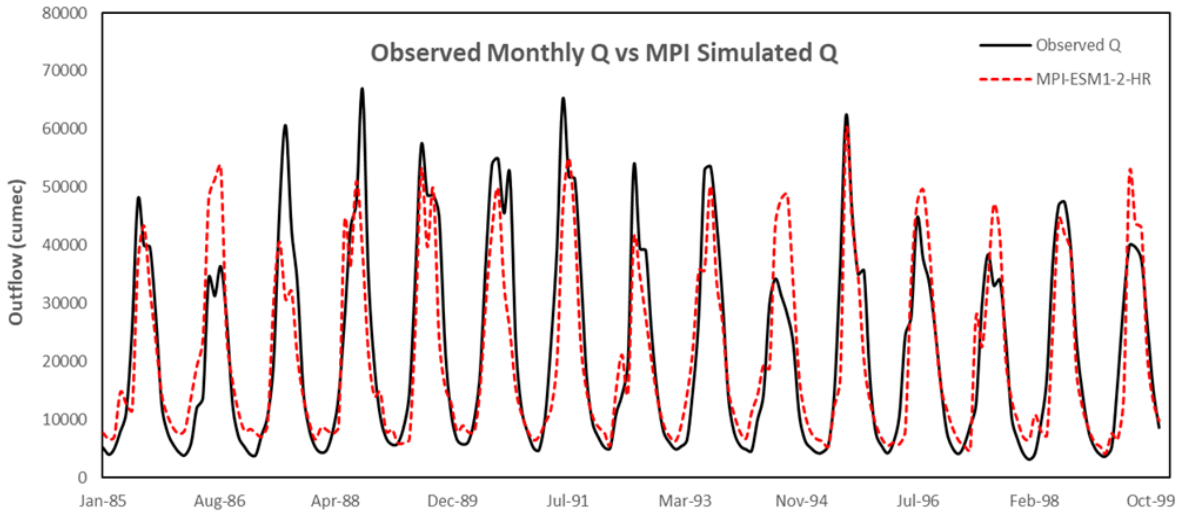

Figure 3.10: Comparison of the simulated flow with the observed for calibration (1985-1999).

During model validation, monthly averaged data of that time period were imported from the given database (data obtained from BWDB stations) into an observation file in text format. Then using the swat-cup interface, the model was validated for another 15 years (2000-2014). The outflow comparison with the observed BWDB data at Bahadurabad station (SW 46.9 L) for the validation period has been shown in Figure 3.11.

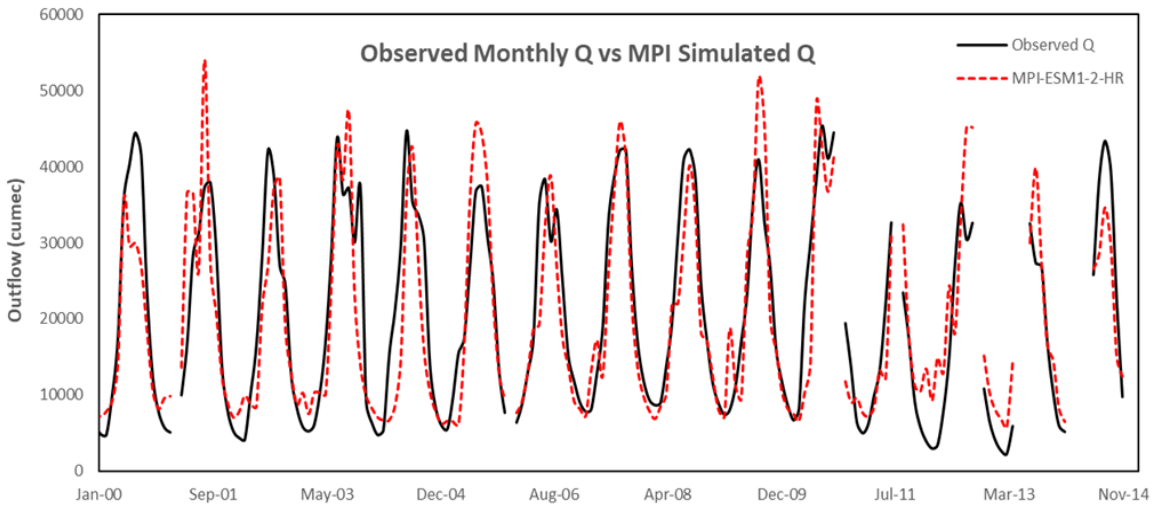

Figure 3.11: Comparison of the simulated flow with the observed for validation (2000-2014).

3.8.4.5 Performance of the Model

A comparison of observed and simulated hydrographs for calibration and validation periods has been shown in Figures 3.10 and Figure 3.11. The NSE values of 0.90 and 0.86 during calibration and validation periods, respectively, indicate a very good agreement between the observed and simulated discharges. The coefficient of determination values (R^2) values is 0.91 for calibration and 0.90 for validation which is also very good. The PBIAS values are found to be 3.5 and 3.1 for the calibration and validation stages, respectively. These statistics demonstrate that the SWAT model generally performed very well in both calibration and validation stages based on historical measured data for Brahmaputra River Basin.

Table 3.7: Model performance analysis.

Parameters	**Calibration**	**Validation**	**Performance**
R^2	0.91	0.90	Very good
NSE	0.90	0.86	Very good
PBIAS	3.50	3.10	Very Good

3.9 SWAT Model Simulation and Outputs

After adjusting the values of the sensitive parameters to the basin flow, the calibrated SWAT model has been simulated using 13 CMIP6 models for five scenarios: baseline (1985-2014), SSP2-45 near (2025-2054), SSP2-45 far (2071-2100), SSP5-85 near (2025-2054) and SSP5-85 far (2071-2100). Then the percent change in the flow for the future periods compared to the baseline (1985-2014) has been evaluated. Figure 3.12 shows the multi-model maximum simulated annual discharge starting from baseline to the future periods under the SSP245 scenario. Figure 3.13 exhibits the multi-model maximum simulated annual discharge starting from baseline to the future periods under the SSP585 scenario.

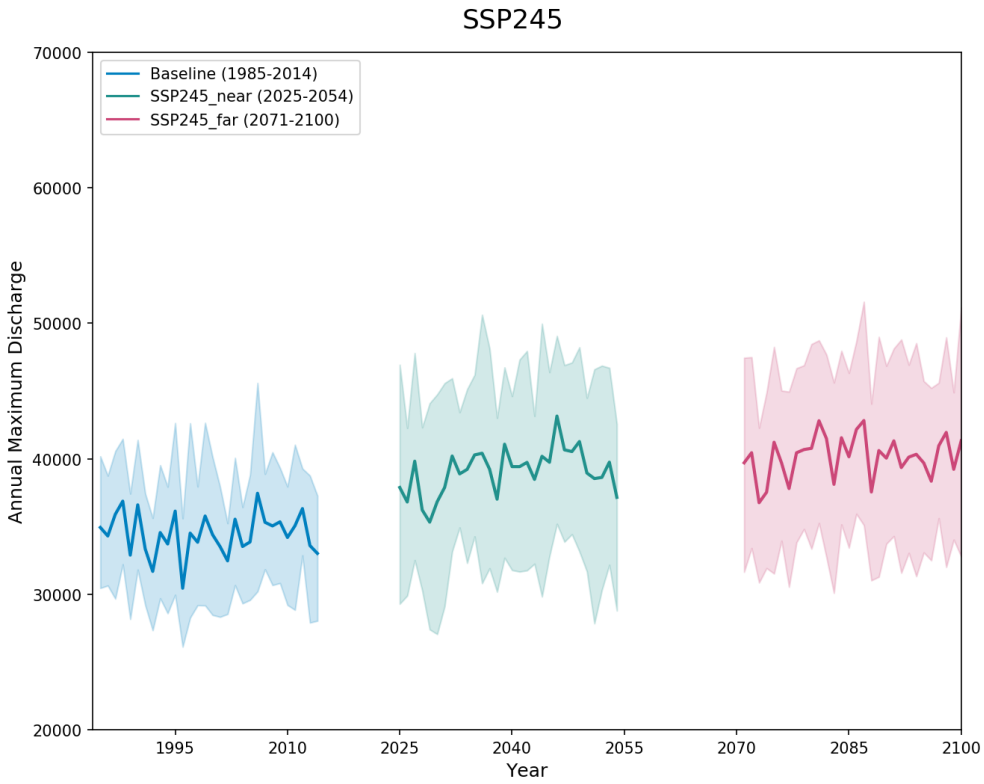

Figure 3.12: Simulated maximum annual discharge (cumec) for the baseline (1985-2014), near-future period (2025-2054), and far-future period (1971-2014) under SSP245.

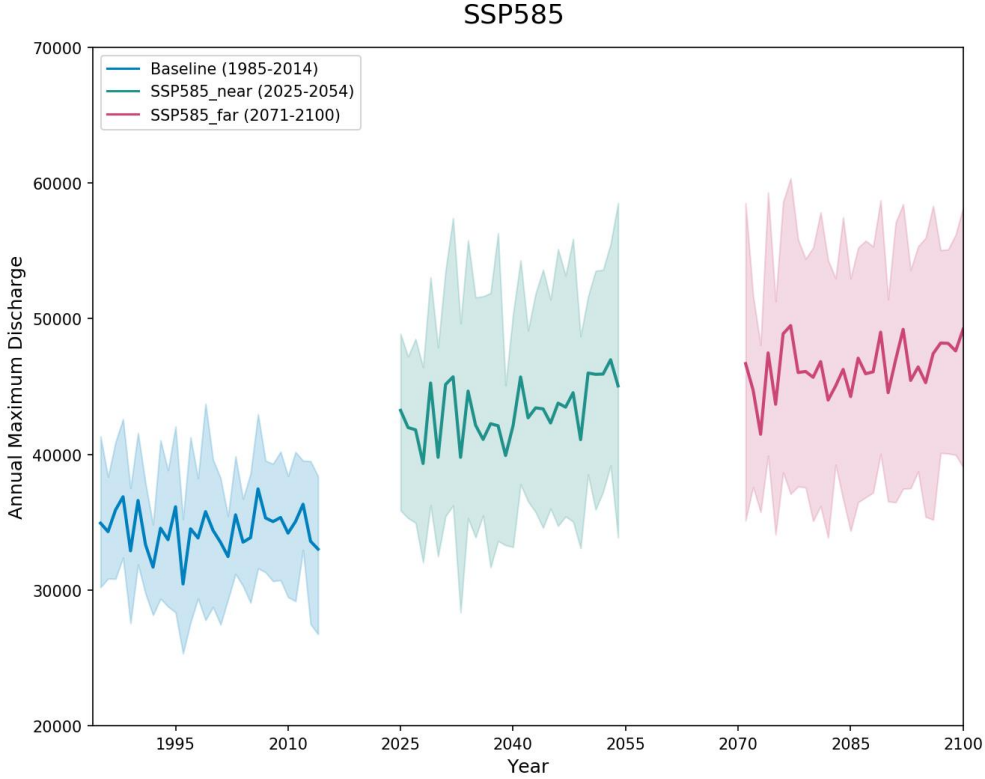

Figure 3.13: Simulated maximum annual discharge (cumec) for the baseline (1985-2014), near-future period (2025-2054), and far-future period (1971-2014) under SSP245.

Figure 3.14 illustrates the multi-model mean monthly percentage increase in flow for different simulation scenarios at Bahadurabaad station (SW 46.9L) compared to the baseline period. Under moderate scenario SSP2-45, the flow has been observed to increase from 10%-45% in the future. Considering the extreme climate change scenario SSP5-85, the mean monthly percentage increase ranges from 15%-75% at the end of the century. The maximum increase has been observed for the monsoon month of March and April under the SSP5-85 far (2071-2100) scenario.

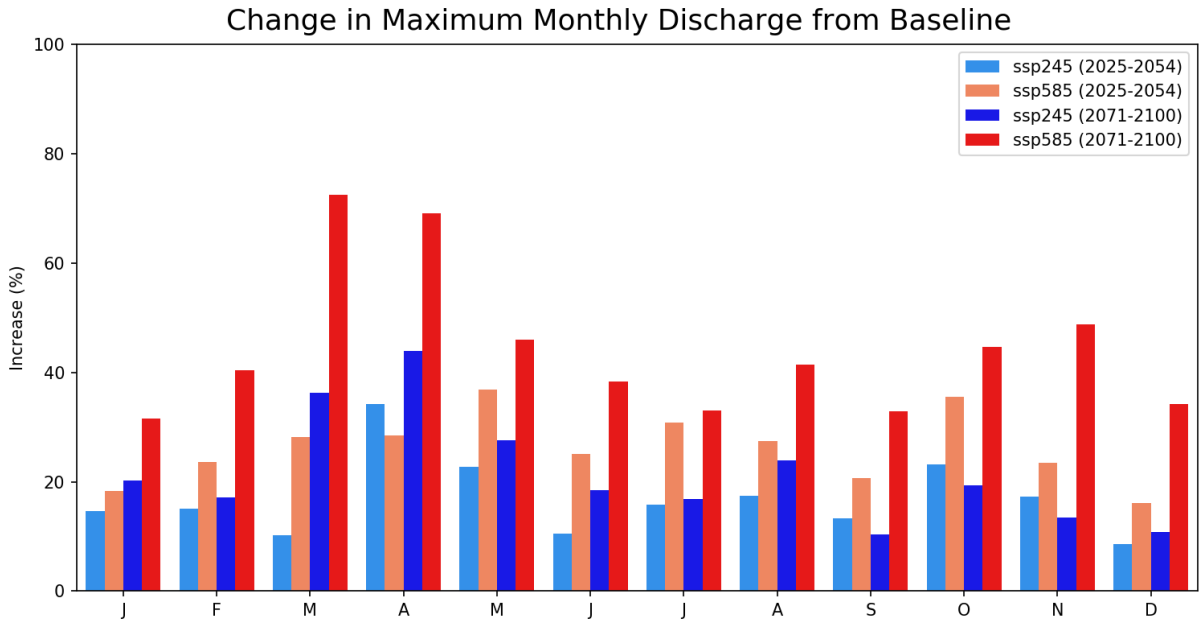

Figure 3.14: Multi-model ensemble mean monthly percentage increase of flow at Bahadurabad (SW 46.9L) in the Brahmaputra-Jamuna river in the near (2025-2054) and far future (2071-2100) with respect to the baseline period (1985-2014) under SSP2-45 and SSP5-85 scenarios.

CMIP6 models have an increased range of complexity from GCMs to Earth System Models, with improvements in physical processes and higher spatial resolution compared to the previous CMIP5 models. Different models have different climate sensitivity based on their forcing and corresponding shared socio-economic pathways (SSP). Figure 3.15 illustrates the change in the maximum monthly discharge of the climate models for the near future period (2025-2054) under SSP2-45 and SSP5-85 scenarios compared to the baseline (1985-2014). The change in maximum monthly flow has been observed to vary significantly for the months of May, June, and July for most of the models for both scenarios. In the dry season, climate models have shown less variability.

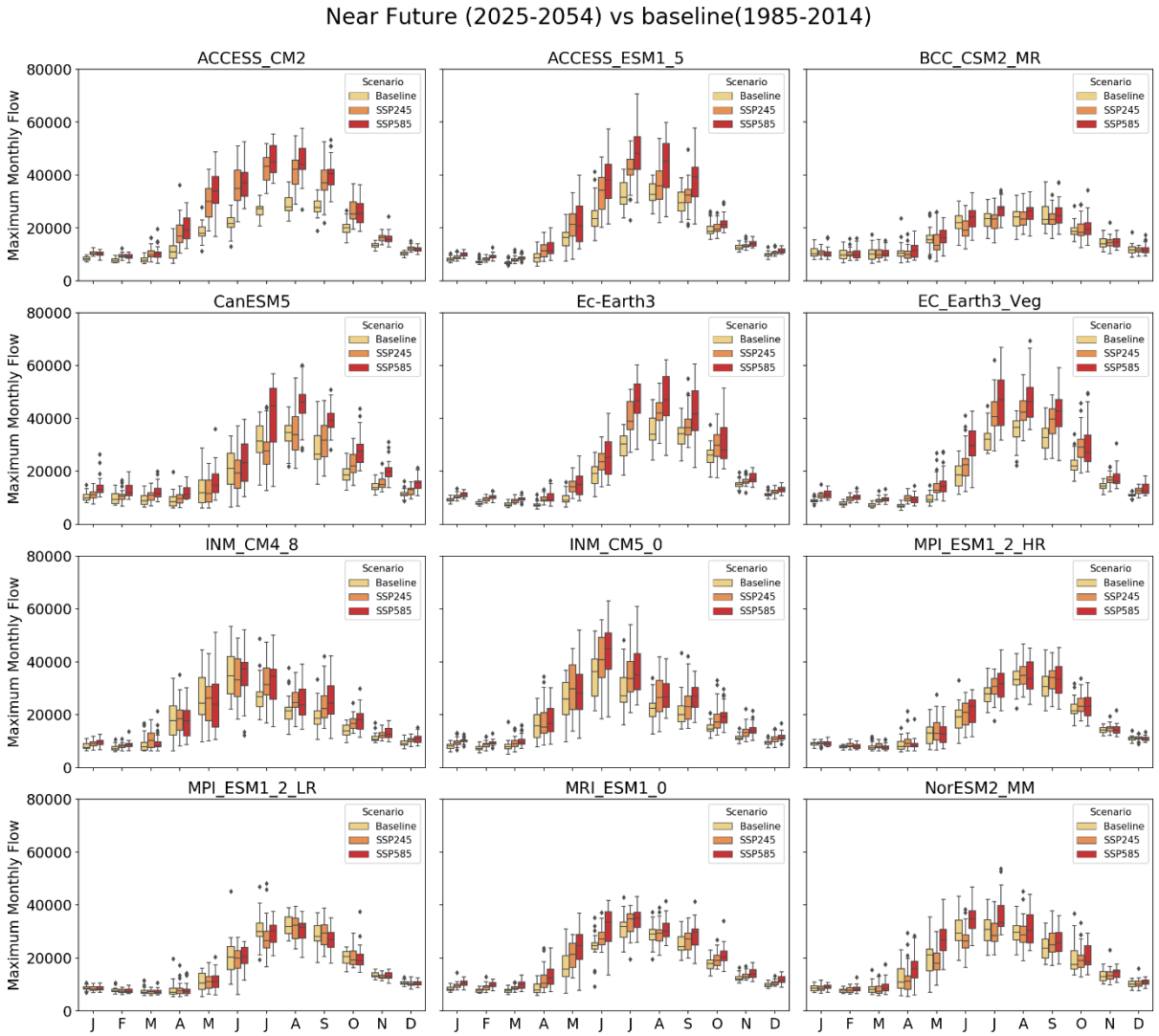

Figure 3.15: Simulated maximum monthly discharge (cumec) for the near future period (2025-2054) compared to baseline (1985-2014).

Figure 3.16 illustrates the change of the maximum monthly discharge of the climate models for the far future period (2071-2100) under SSP2-45 and SSP5-85 scenarios. Compared to the baseline period (1985-2014), the change has been observed to vary ominously for the pre-monsoon and early monsoon months of April, May, and June for maximum models, especially ACCESS-ESM1-5, Ec-Earth3, and MRI-ESM-1-0. For the far future period, the variability extent in a change of maximum flow for the SSP5-85 scenario is more intense than the SSP2-45 for both wet and dry months.

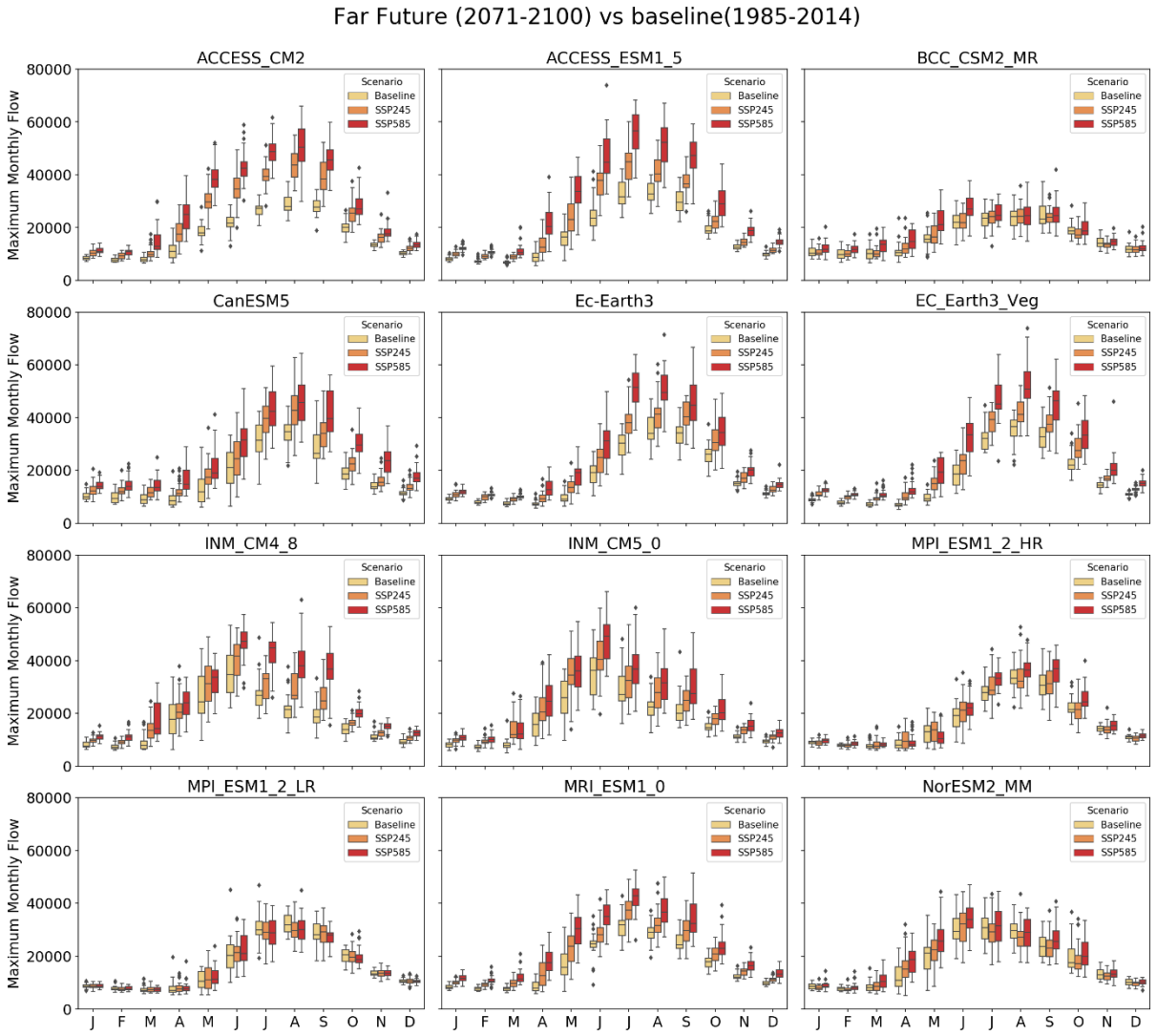

Figure 3.16: Percentage change in mean monthly discharge (cumec) for the far future period (2071-2100) compared to baseline (1985-2014).

Figure 3.17 illustrates the comparison of the simulated multi-model maximum monthly discharge of the climate models for the near future period (2025-2054) under SSP2-45 and SSP5-85 scenarios. Similarly, figure 3.18 shows the variability of the simulated multi-model maximum monthly discharge of the climate models for the far future period (2071-2100) under SSP2-45 and SSP5-85 scenarios.

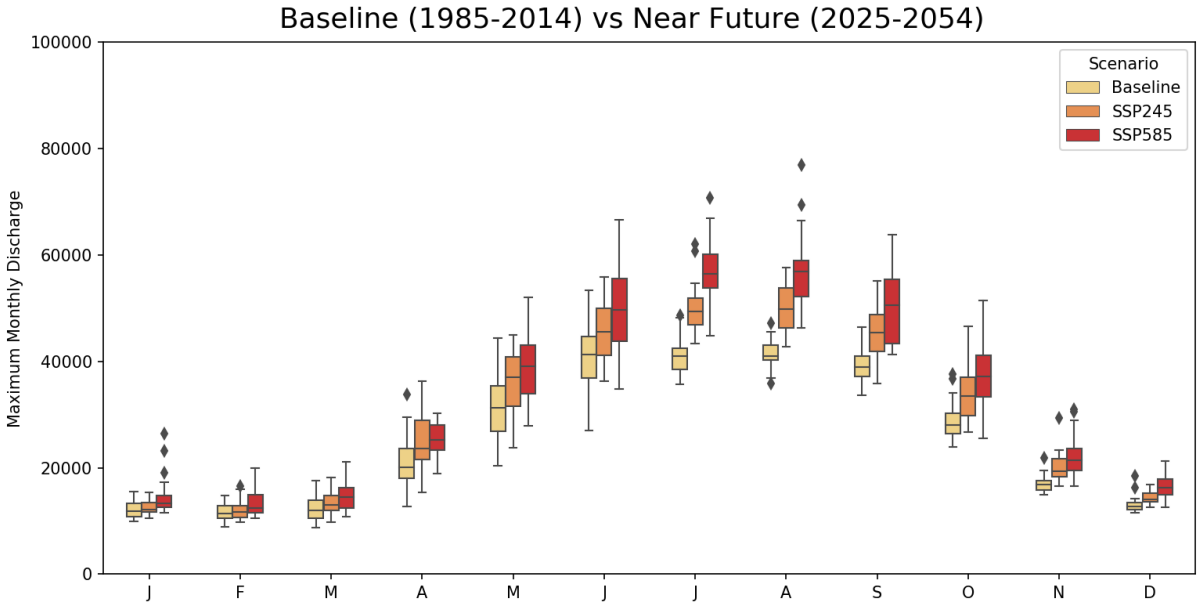

Figure 3.17: Variability in multi-model maximum monthly discharge (cumec) for the near future period (2025-2054) compared to baseline (1985-2014).

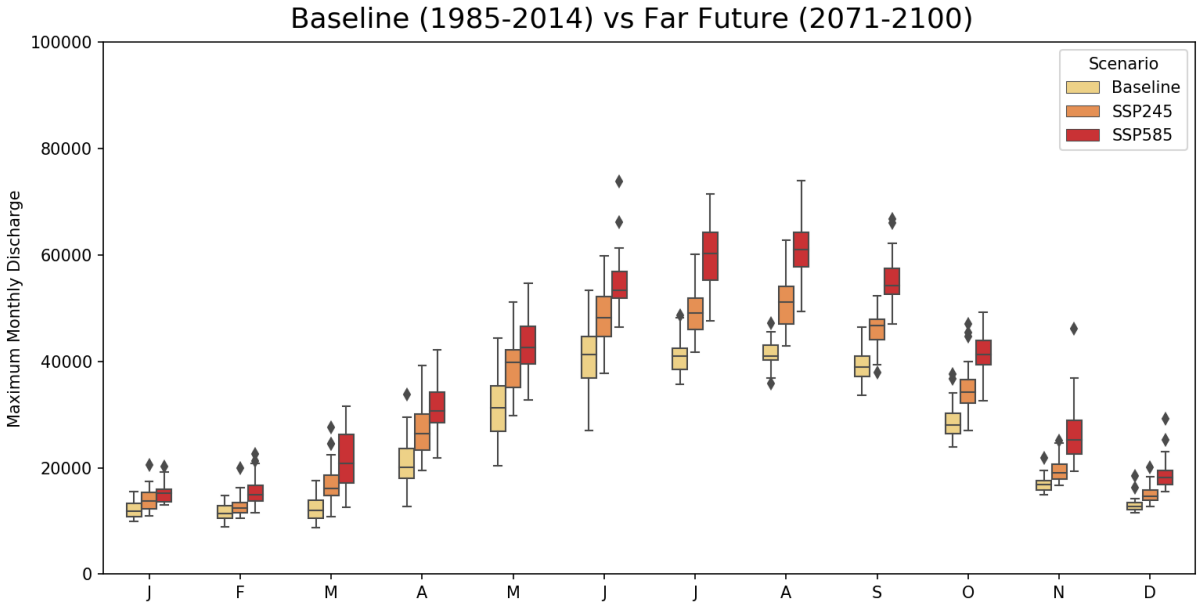

Figure 3.18: Variability in multi-model maximum monthly discharge (cumec) for the far future period (2071-2100) compared to baseline (1985-2014).

Probability density functions (PDF) of maximum, mean, and minimum monthly discharge for the near (2025-2054) and far future period (2071-2100) compared to baseline (1985-2014) are shown in Figures 3.19, 3.20, and 3.21, respectively. It was found that probabilities of the occurrences of peak flow in the future have been reduced for all scenarios under global warming compared to the baseline scenario.

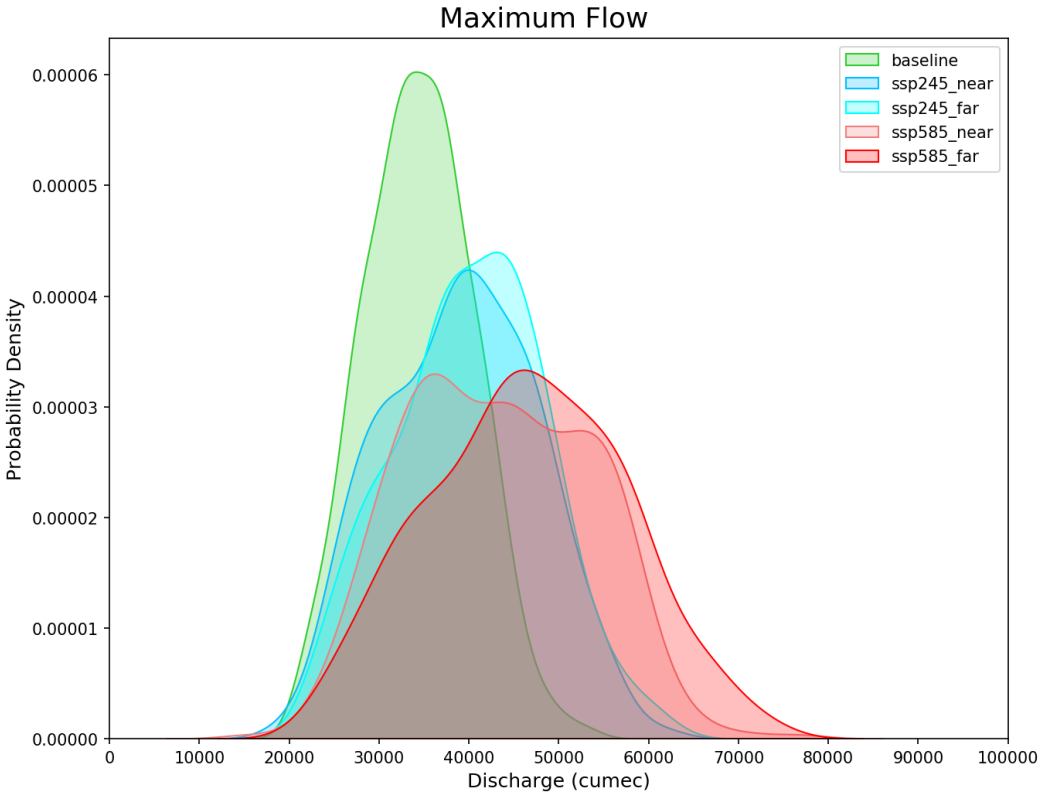

Figure 3.19: Probability density functions (PDF) of maximum monthly discharge (cumec) for the near (2025-2054) and far future period (2071-2100) compared to baseline (1985-2014).

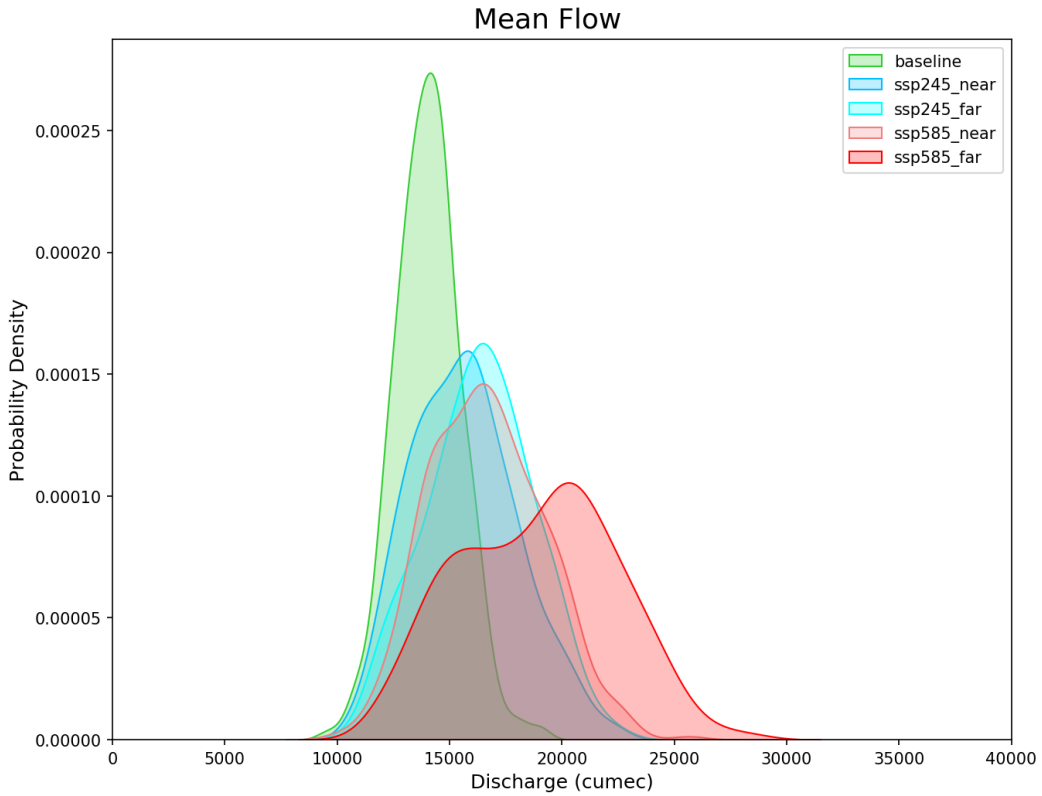

Figure 3.20: Probability density functions (PDF) of mean monthly discharge (cumec) for the near (2025-2054) and far future period (2071-2100) compared to baseline (1985-2014).

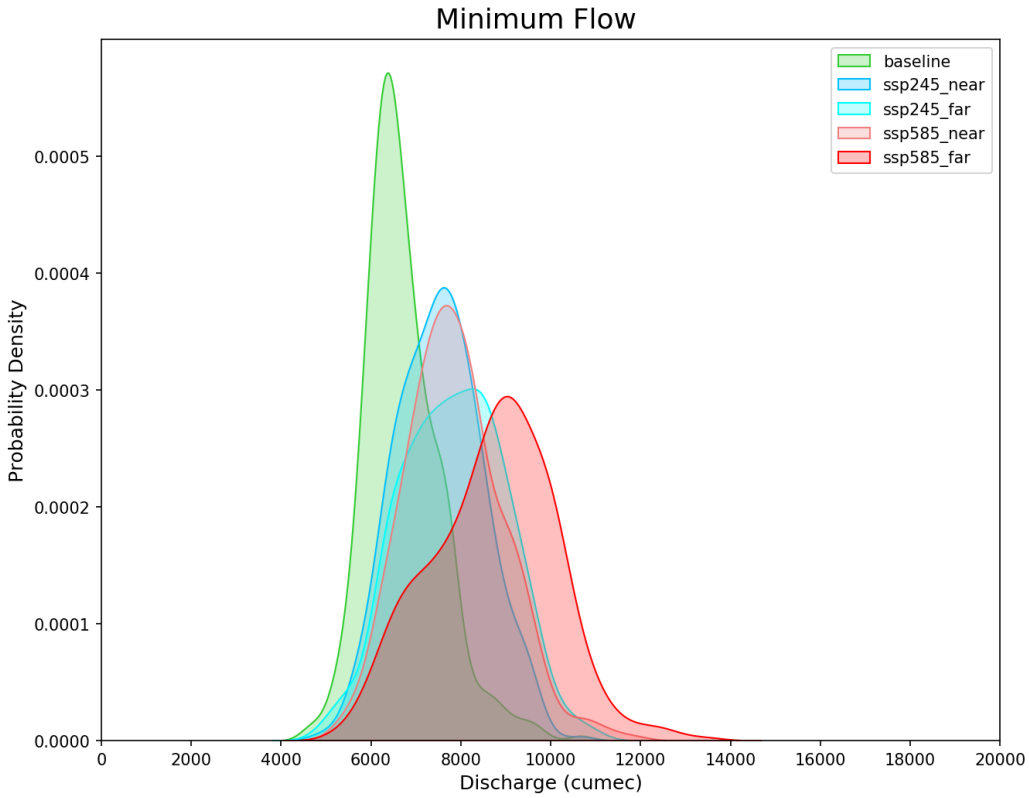

Figure 3.21: Probability density functions (PDF) of minimum monthly discharge (cumec) for the near (2025-2054) and far future period (2071-2100) compared to baseline (1985-2014).

CHAPTER FOUR
HYDRODYNAMIC MODELING FOR FLOODING

4.1 Introduction

Hydrodynamic modeling of the flooding in the study area will be conducted for the major rivers, namely, Teesta, Dharala, Dudhkumar, Brahmaputra-Jamuna, and Old Brahmaputra, Ghaghat, Bangali, and Jhenai rivers. Several numbers of commercial and non-commercial software tools are available for hydrodynamic modeling and analysis. However, open-source software HEC-RAS (Hydrologic Engineering Center River's Analysis System) has been chosen to carry out this study due to its accuracy in the analysis of river systems and special features of 1D-2D river-floodplain coupling simulation (HEC-RAS, 2016). The major tools used in this study are one and two-dimensional numerical models HEC-RAS 5.0.7 beta version and Arc GIS for spatial data processing and HEC-GeoRAS for interfacing between HEC-RAS and Arc GIS. HEC-RAS and HEC-GeoRAS, an open-source model which has excellent Graphical User Interfaces (GUI), were developed by the US Army Corps of Engineers. Arc GIS was developed Environmental Systems Research Institute (ESRI), which enables to view, editing, creation, and analyze geospatial data. Descriptions of these software tools are presented below.

CHAPTER FOUR
HYDRODYNAMIC MODELING FOR FLOODING

4.1 Introduction

Hydrodynamic modeling of the flooding in the study area will be conducted for the major rivers, namely, Teesta, Dharala, Dudhkumar, Brahmaputra-Jamuna, and Old Brahmaputra, Ghaghat, Bangali, and Jhenai rivers. Several numbers of commercial and non-commercial software tools are available for hydrodynamic modeling and analysis. However, open-source software HEC-RAS (Hydrologic Engineering Center River's Analysis System) has been chosen to carry out this study due to its accuracy in the analysis of river systems and special features of 1D-2D river-floodplain coupling simulation (HEC-RAS, 2016). The major tools used in this study are one and two-dimensional numerical models HEC-RAS 5.0.7 beta version and Arc GIS for spatial data processing and HEC-GeoRAS for interfacing between HEC-RAS and Arc GIS. HEC-RAS and HEC-GeoRAS, an open-source model which has excellent Graphical User Interfaces (GUI), were developed by the US Army Corps of Engineers. Arc GIS was developed Environmental Systems Research Institute (ESRI), which enables to view, editing, creation, and analyze geospatial data. Descriptions of these software tools are presented below.

4.2 HEC-RAS Model

HEC-RAS is a computer program that models the hydraulics of water flow through natural rivers and other channels. Prior to the recent update to Version 5.0, the program was one-dimensional, meaning that there is no direct modeling of the hydraulic effect of cross-section shape changes, bends, and other two- and three-dimensional aspects of flow. The release of version 5.0 introduced two-dimensional modeling of flow as well as sediment transfer modeling capabilities. The program was developed by the US Department of Defense, and the Army Corps of Engineers in order to manage the rivers, harbors, and other public works under their jurisdiction; it has found wide acceptance by many others since its public release in 1995. HEC-RAS is designed to perform one and two-dimensional hydraulic calculations for a full network of natural and constructed channels. The following is a description of the major capabilities of HEC-RAS.

The user interacts with HEC-RAS through a graphical user interface (GUI). The main focus in the design of the interface was to make it easy to use the software while still maintaining a high level of efficiency for the user. The interface provides the following functions:
i) File Management, ii) Data Entry and Editing, iii) Hydraulic Analyses iv) Tabulation and Graphical Displays of Input and Output Data, v) Inundation mapping and animations of water propagation, vi) Reporting Facilities, and vii) Context-Sensitive Help.

The HEC-RAS system contains several river analysis components for (i) steady flow water surface profile computations; (ii) one- and two-dimensional unsteady flow simulation; (iii) movable boundary sediment transport computations; and (iv) water quality analysis. A key element is that all four components use a common geometric data representation and common geometric and hydraulic computation routines. In addition to these river analysis components, the system contains several hydraulic design features that can be invoked once the basic water surface profiles are computed.

HEC-RAS has the capability to perform inundation mapping of water surface profile results directly from HEC-RAS (Appendix A-4). Using the HEC-RAS geometry and computed water surface profiles, inundation depth and floodplain boundary datasets are created through the RAS Mapper.

4.3 HEC-GeoRAS

GISs are defined as computer systems capable of assembling, storing, manipulating, and displaying geographically referenced information (USGS, 1998). Originally developed as a tool for cartographers, GIS has recently gained widespread use in engineering design and analysis, especially in the fields of water quality, hydrology, and hydraulics. GIS provides a setting in which to overlay data layers and perform spatial queries and thus create new spatial data. The results can be digitally mapped and tabulated, facilitating efficient analysis and decision-making. Structurally, GIS consists of a computer environment that joins graphical elements (points, lines, polygons) with associated tabular attribute descriptions. This characteristic sets GIS apart from both computer-aided design software (geographic representation) and databases (tabular descriptive data). For example, in a GIS view of a river network, the graphical elements represent the location and shape of the rivers, whereas the attributes might describe the stream name, length, and flow rate. This one-tone relationship between each feature and its associated

attributes makes the GIS environment unique. In order to provide a conceptual framework, it is necessary first to define some basic GIS constructs.

HEC-GeoRAS is an ArcGIS extension specifically designed to process geospatial data for use with the Hydrologic Engineering Center River's Analysis System (HEC-RAS). The extension allows users to create an HEC-RAS import sample containing geometric attribute data from an existing digital terrain model (DTM) and complementary data sets. Water surface profile results may also be processed to visualize inundation depths and boundaries. HEC-GeoRAS extension for ArcGIS used an interface method to provide a direct link to transfer information between the ArcGIS and the HEC-RAS.

HEC-GeoRAS requires a DTM in the form of a TIN or a GRID. The DTM must be a continuous surface that includes the bottom of the river channel and the floodplain to be modeled. Because all cross-sectional data will be extracted from the DTM, only high-resolution DTMs that accurately represent the ground surface should be considered for hydraulic modeling.

The HEC-GeoRAS menu options are RAS Geometry, RAS Mapping, ApUtilities, and Help. The RAS Geometry menu is for pre-processing geometric data for import into HEC-RAS. The RAS Mapping menu is for post-processing exported HEC-RAS results.

4.4 Methodology

4.4.1 Data collection

In order to develop the mathematical flood model, various kinds of data from recent and previous years have been collected and compiled. These data also form the basis for further analysis and interpretation of the model results leading to an accurate assessment of the hydrological condition of the river floodplain. According to the modeling requirements, a significant amount of data, including water level, discharge, and cross-section, have been collected and set up in a flood model using this Data. A summary of data sets that will be used for hydrodynamic modeling is presented in Table 4.1. Details of the hydrological and morphological data collected in this study have been presented in Appendix A.

Table 4.1: Summary of data sets that are available to be used for hydrodynamic modeling.

Data Type	**Data Source**	**Data Location**	**Periods (Year)**
Discharge Data	BWDB	1. Dalia 2. Bahadurabad 3. Pateswari 4. Taluk Simulbari	1996-2019
Water Level Data	BWDB	1. Noonkhawa 2. Chilmari 3. Bahadurabad 4. Sirajganj 5. Kaunia 6. Kaliganj 7. Haripur 8. Gaibandha 9. Offtake Jhenai 10. Jamalpur 11. Kurigram	1996-2019
Cross Section	BWDB	1. Jamuna 2. Teesta 3. Dudhkumar 4. Dharala 5. Ghaghat 6. Old Brahmaputra 7. Jhenai 8. Bangali	2014-2018
DEM	USGS	Bangladesh	
Satellite Image	Earth Explorer / Copernicus	North-Central (NC) of Bangladesh	

4.5 Setting up HEC-GeoRAS

4.5.1 Pre-processing the DEM

In this study, the Digital Elevation Model (DEM) of Bangladesh in raster format has been collected from the FTP server of the Shuttle Radar Topographic Mission (SRTM) of the National Aeronautics and Space Administration (NASA). DEMs are commonly built using data collected using remote sensing techniques, but they may also be built from land surveying. This data is required to formulate mathematical models for the study area. Each cell, and cell face, of the computational mesh of the 2D flow area is pre-processed in order to develop detailed hydraulic property tables based on the underlying terrain used in the modeling process. The raster file was projected into WGS 1984 UTM 45N coordinate system. The collected DEM was at MSL Datum. So, it was converted into PWD datum by adding 0.46m. The DEM of the Study Area to be used for HEC-RAS modeling is shown in Figure 4.4.

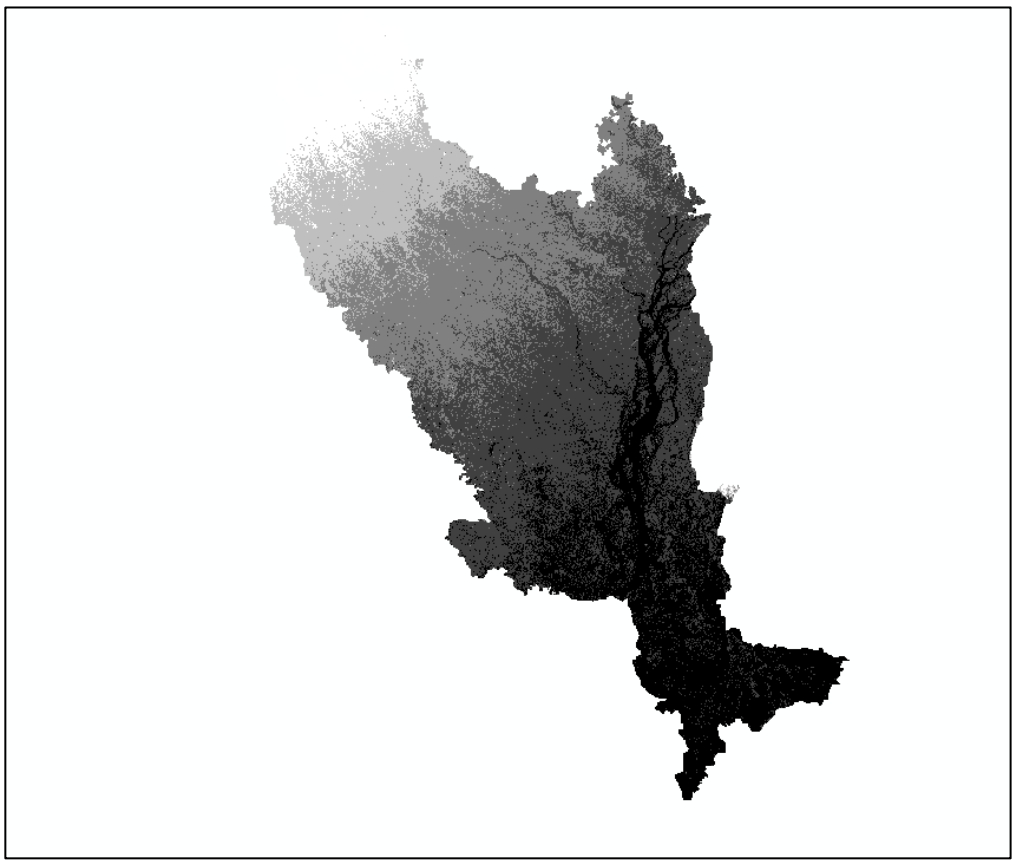

Figure 4.1: DEM of the Study Area is used for HEC-RAS modeling.

4.5.2 Creating RAS layers for geometric data using HEC-GeoRAS

In this study, only the preprocessing is done in HEC-GeoRAS. HEC-GeoRAS requires a DTM in the form of a TIN or a GRID. The DTM must be a continuous surface that includes the

bottom of the river channel and the floodplain to be modeled, as all cross-sectional data have been extracted from the DTM (Figure 4.5). A TIN is a triangulated mesh constructed on the (x, y) locations of a set of data points. By including the dimension of height (z) for each triangle vertex, the triangles can be raised and tilted to form a plane. The collection of all such triangular planes forms a representation of the land surface terrain in a considerable degree of detail. The TIN triangles are small where the land surface is complex and detailed, such as river channels, and larger in flat or gently sloping areas. Break lines represent significant terrain features like streams or roads.

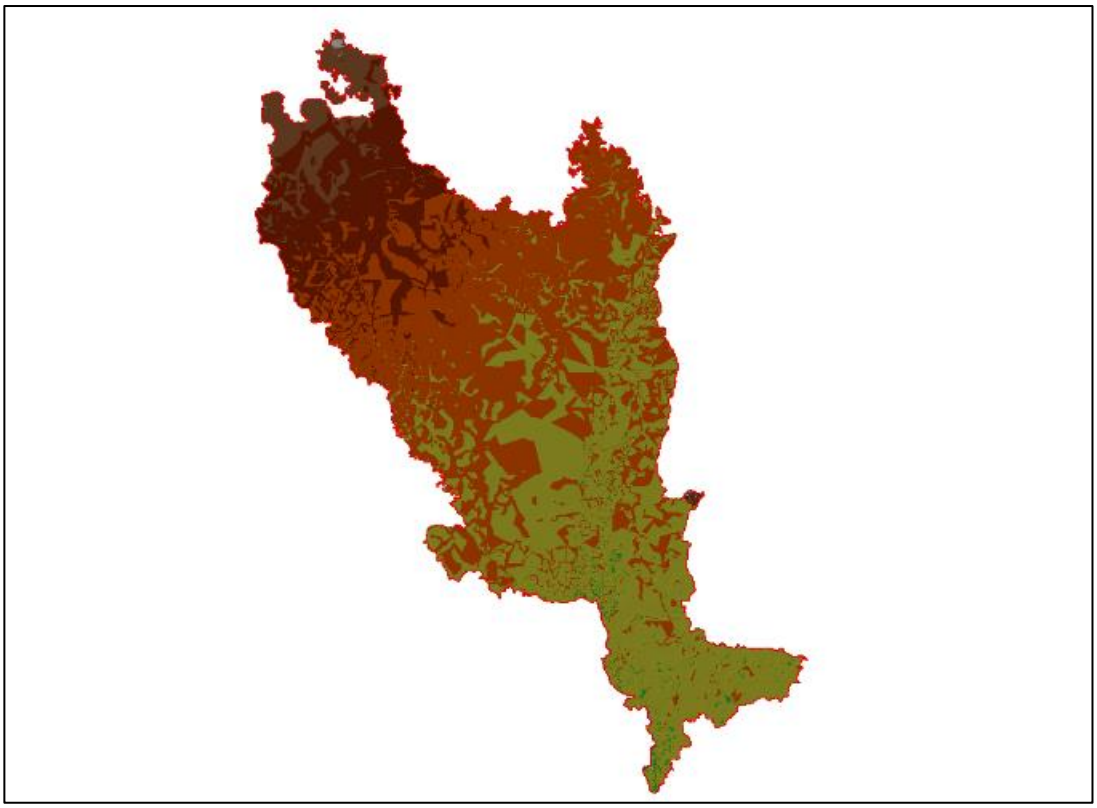

Figure 4.2: Pre-processing with HEC-GeoRAS.

Finally, river center lines, bank lines, flow paths, and cross-section cut lines were assigned in the HEC-GeoRAS window. And later, generated layers were exported to HEC-RAS. The developed RAS layers are shown in figure 4.3.

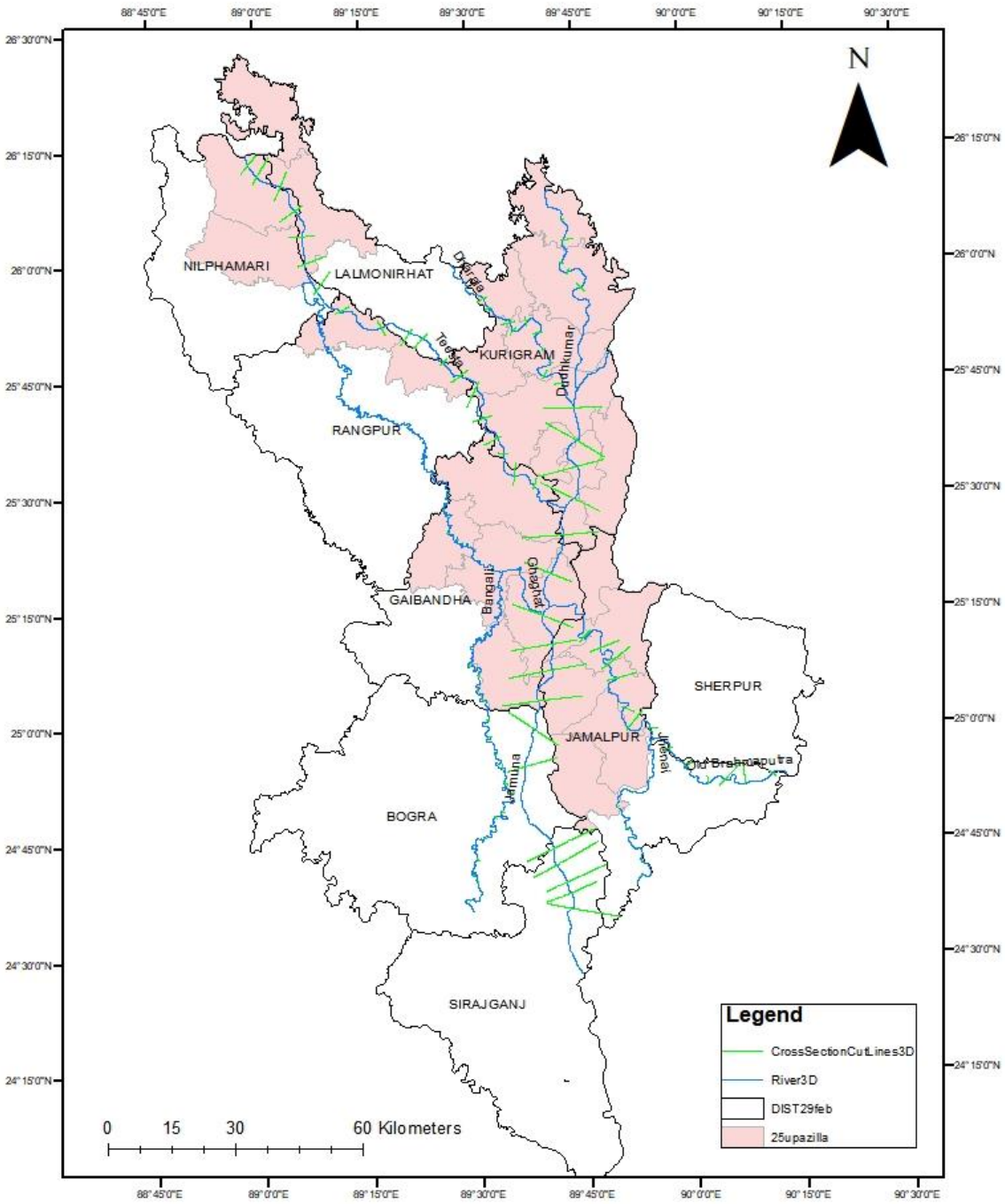

Figure 4.3: Generating RAS layers with HEC-GeoRAS.

4.6 HEC-RAS 1D Model Setup

4.6.1 Exporting and Modifying Geometry Data

Exported bathymetry data from HEC-GeoRAS were further modified in HEC-RAS using BWDB cross-section data. The latest available River cross-sections of Jamuna, Teesta, Dudhkumar, Dharala, Ghaghat, Old Brahmaputra, Bangali, and Jhenai Rivers were collected from Bangladesh Water Development Board (BWDB). BWDB collects cross-section data at 21 different stations in the Jamuna River, 20 different stations in the Teesta River, 5 different stations in Dudhkumar River, 10 different stations in the Dharala River, and 12 different stations in the Ghaghat River, and 13 different stations in Old Brahmaputra River. Details of the morphological data collected in this study have been presented in Appendix A3. The most recent x-section data has been used for model development, as this has been the baseline condition for future simulation.

4.6.2 Boundary Condition and Model Simulation

As boundary conditions, discharge data were provided at the upstream boundary conditions, while the water-level data were provided at the downstream boundary conditions. The flow data of the Teesta River at Dalia gauge station, the Dudhkumar River at Pateswari gauge station, and the Dharala River at Taluk Simulbari gauge station, as shown in Figure 4.4, have been used as the upstream boundary condition in the model. Details of the daily discharge data collected in this study have been presented in Appendix A2. On the other hand, the water level data of the Jamuna River at Sirajganj station, the Old Brahmaputra River at Jamalpur gauge station, the Jhenai river at Offtake Bangshi, and the Bangali river at Khanpur gauge station, as shown in Figure 4.4, have been used as the downstream boundary condition in the model. Details of the daily water level data collected in this study have been presented in Appendix A1.

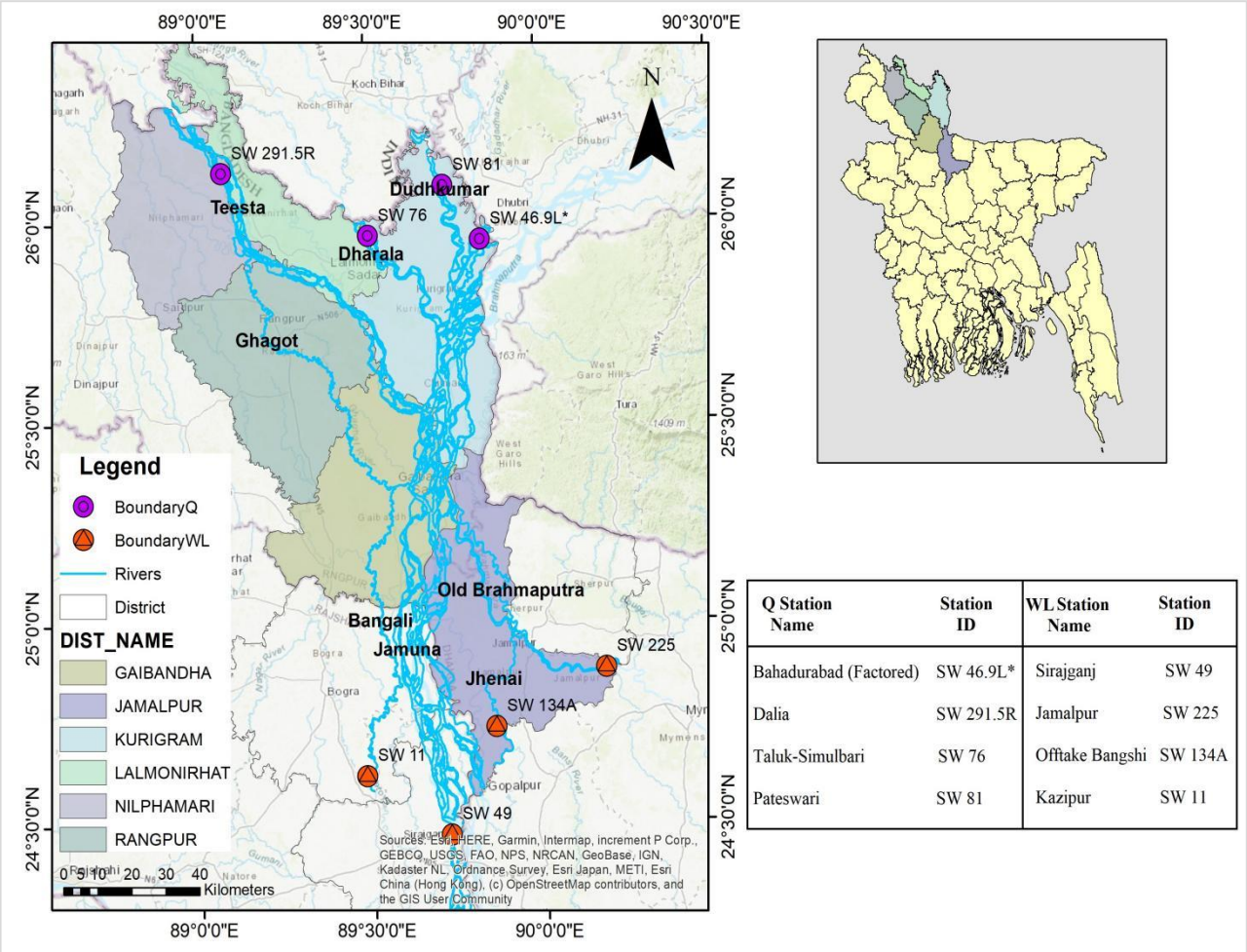

Q Station Name	Station ID	WL Station Name	Station ID
Bahadurabad (Factored)	SW 46.9L*	Sirajganj	SW 49
Dalia	SW 291.5R	Jamalpur	SW 225
Taluk-Simulbari	SW 76	Offtake Bangshi	SW 134A
Pateswari	SW 81	Kazipur	SW 11

Figure 4.4: Discharge and Water-level stations of the study area.

Finally, the model was simulated for the monsoon season (1st June - 15 October) for the period 2010 to 2019. After simulating the model primarily, further calibration-validation procedures of the 1D HEC-RAS model were followed, which will be discussed in the following section.

4.7 Calibration and Validation of HEC-RAS 1D Model

Model calibration is done where the model-generated water level at a specific location and a specific time range is compared with the measured water level at that location and at the same time range. Here, the model has been calibrated using the observed water level and flows of the river at various stations. The calibration of the hydrodynamic model includes the choice of an appropriate value of Manning's 'n' such that simulated results from the HEC RAS model should be close to the observed stages along the river. Channel roughness is a sensitive parameter in the development of the hydraulic model for flood forecasting and flood inundation mapping. The requirement of multiple channel roughness coefficient Manning's 'n' values along the river have been adjusted depending on the observed water level. It must be confirmed that the

parameters assigned during the calibration period could also replicate the real physical scenario at the same location but at a different time range. Thus, validation is done, which, again, compares the model-generated water level with the measured water level. In this study, the Calibration period is considered from 2010 to 2014. The performance of the calibrated model has been verified for the flood of the year 2015 to 2019. In this study, flood frequency analysis was conducted in 12 stations of 7 rivers, which are shown in Table 4.2.

Table 4.2: Summary of Model calibration and validation.

River Name	**Station Name**	**Station ID**	**R^2 for Model Calibration (2010 – 2014)**	**R^2 for Model Validation (2010 – 2014)**
Jamuna	Noonkhawa	SW45	0.9350	0.9062
Jamuna	Chilmari	SW45.5	0.9465	0.9405
Jamuna	Bahadurabad	SW46.9L	0.9385	0.9448
Jamuna	Kazipur	SW49A	0.9276	0.9765
Dudhkumar	Pateswari	SW81	0.7191	0.8804
Dharala	Kurigram	SW77	0.8503	0.8161
Teesta	Kaliganj	SW 293	0.9317	-
Teesta	Kaunia	SW294	0.8911	0.8295
Teesta	Haripur	SW294.5	0.8014	0.8278
Ghaghat	Gaibandha	SW97	0.7828	0.4920
Bangali	Simulbari	SW10	0.5549	0.7137
Old Brahmaputra	Jamalpur	SW225	0.9447	0.8970

Simulated results have been obtained close to the observed stages. The performance is reasonably good for many stations. Most of the stations provided very good results in terms of R^2 (>0.8) except Simulbari (SW 10) station in the Bangali river and Gaibandha (SW 97) station in the Ghaghat river. Although Jamalpur (SW 225) station in the Old Brahmaputra river provided a good R^2 value, in reality, the simulated stage hydrograph doesn't match accurately with the observed water-level data-set pattern. This is mainly due to the unavailability of cross-section data of the upper portion of the Ghaghat river and the Bangali river's unavailability of daily discharge data at the upstream locations of the study area, which has been solved by generating yearly rating curves for the upstream boundary stations. There still remain some uncertainties as the study area consists of a really complex river system in this study. A comparison of R^2 during the calibration and validation period in the Jamuna, Ghaghat, and Bangali rivers is shown in Figure 4.5 and Teesta, Dharala, and Dudhkumar rivers in Figure 4.6.

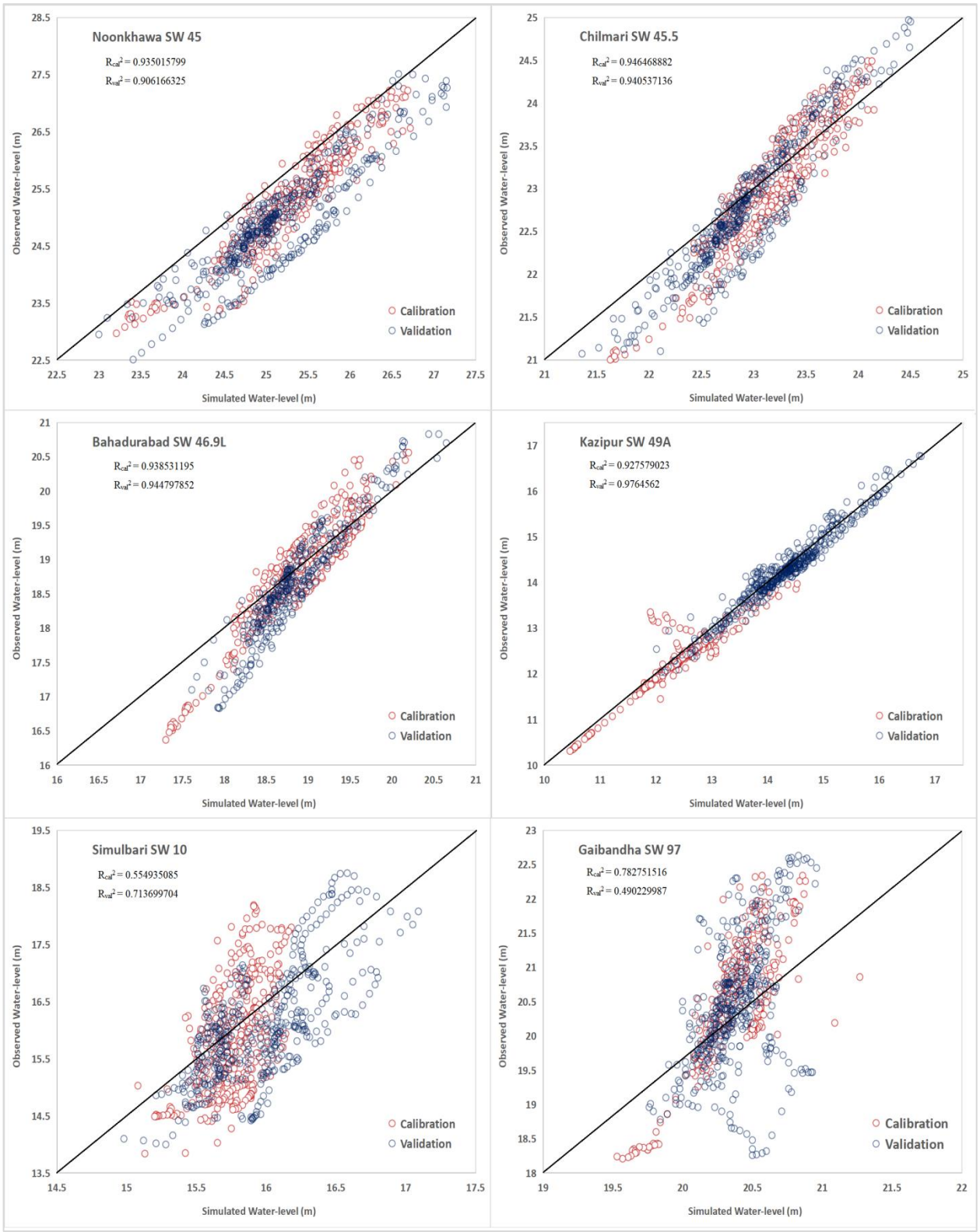

Figure 4.5: Comparison of R^2 during calibration and validation period in the Jamuna, Ghaghat, and Bangali rivers.

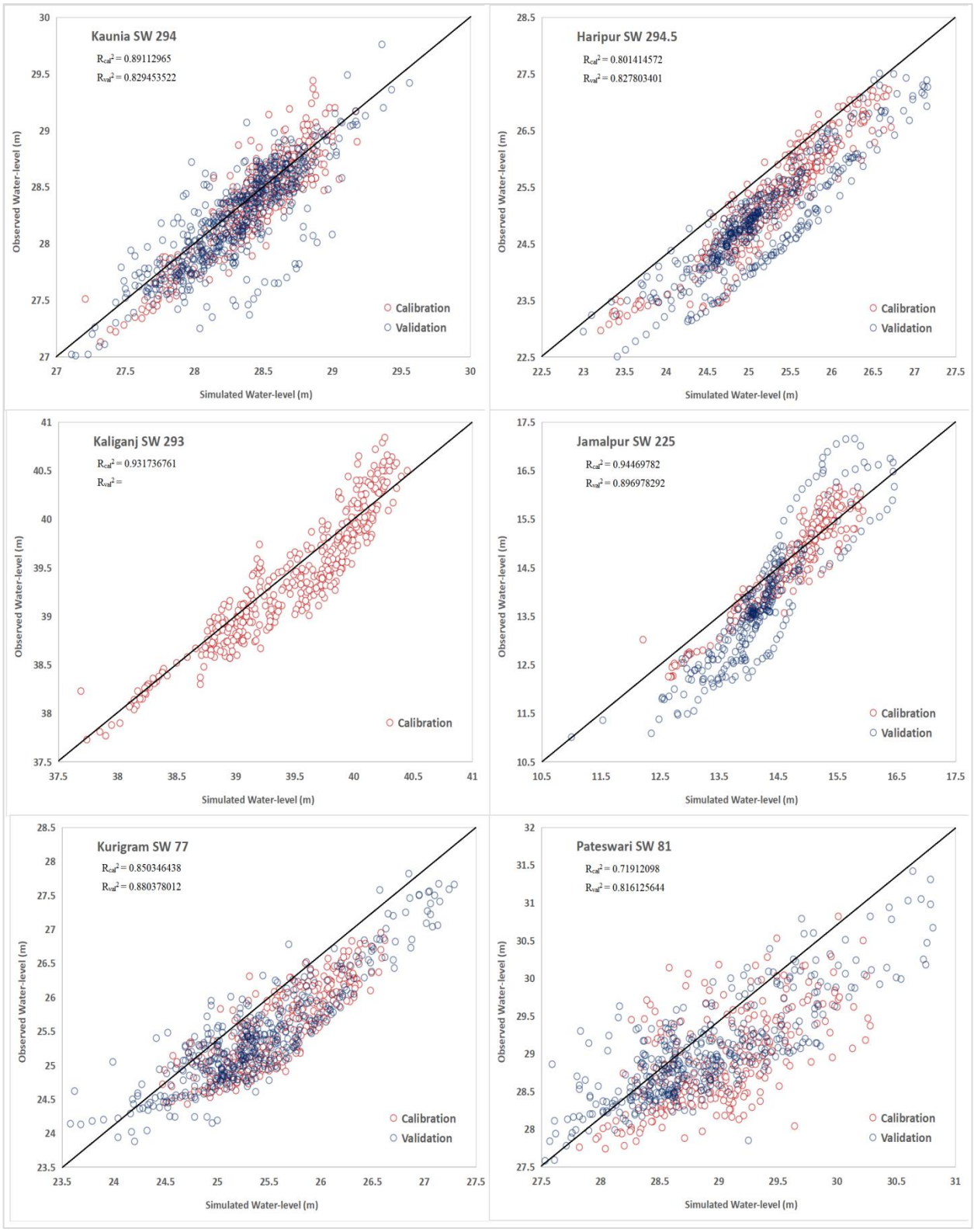

Figure 4.6: Comparison of R^2 during calibration and validation period in the Teesta, Dharala, and Dudhkumar rivers.

4.8 Performance Evaluation of HEC-RAS 1D Model during Major Flood Years

After the calibration and validation, the model was simulated for two recent major flood years, 2017 and 2019, to evaluate the 1D HEC-RAS model performance using four statistical parameters, which are the following:

1. Percent Bias (PBIAS)
2. Coefficient of Determination (R^2)
3. RMSE-observations Standard Deviation Ratio (RMSE)
4. Nash-Sutcliff Efficiency (NSE)

PBIAS or Percent Bias is done to check the average tendency of the simulated data to be higher or lower than the observed data, that is, the bias of the model against the observed discharge data. R^2 or the Coefficient of Determination, the value was checked to determine how well the observed versus simulated data fits the 1:1 line and R^2 ranges from 0 to 1, with higher values indicating less error variance, and typically values greater than 0.5 are considered acceptable.

NSE or Nash-Sutcliff Efficiency was calculated to check the efficiency of the model at projecting the observed discharge. NSE ranges between $-\infty$ and 1.0 (1 inclusive), with NSE as 1 being the optimal value. Values between 0.0 and 1.0 are generally viewed as acceptable levels of performance, whereas values less than 0.0 indicate that the mean observed value is a better predictor than the simulated value, which indicates unacceptable performance.

RSR or RMSE-observations Standard Deviation Ratio is calculated as the ratio of the RMSE and standard deviation of measured data. RSR was used as it standardizes RMSE using the standard deviation of the observed term so that the resulting statistic and reported values could apply to various constituents. The ideal ranges of each of the parameters are shown in Table 4.3, adopted by Moriasi et al. (2007).

Table 4.3: Performance rating of different evaluation parameters.

Performance Rating	R^2	**RSR**	**NSE**	**PBIAS (%)**
Very Good	$0.80 \leq R^2 \leq 1.00$	0.00 < RSR < 0.50	0.75 < NSE < 1.00	PBIAS < ±10
Good	$0.70 \leq R^2 \leq 0.80$	0.50 < RSR < 0.60	0.65 < NSE < 0.75	±10 < PBIAS < ±15
Satisfactory	$0.50 \leq R^2 \leq 0.70$	0.60 < RSR < 0.70	0.50 < NSE < 0.65	±15 < PBIAS < ±25
Unsatisfactory	$R^2 \leq 0.50$	RSR > 0.70	NSE < 0.50	PBIAS > ±25

In this study, model performance was evaluated in the previously mentioned 12 observed stations, which were used for model calibration validation. The summary of the result is presented in Table 4.4. A comparison between simulated and observed water levels has been provided in Figures 4.7 and 4.8.

Table 4.4: A summary of the Performance Evaluation of the model.

River Name	**Station Name (Station ID)**	**Evaluation parameters for a flood event in 2017**				**Evaluation parameters for a flood event in 2019**			
		R^2	**NSE**	**PBIAS (%)**	**RSR**	R^2	**NSE**	**PBIAS (%)**	**RSR**
Jamuna	Noonkhawa (SW45)	0.9134	0.9995	-0.0018	0.0228	0.9760	0.9998	0.0039	0.0124
Jamuna	Chilmari (SW45)	0.9572	0.9996	-0.0047	0.0210	0.9770	0.9998	0.0002	0.0128
Jamuna	Bahadurabad (SW46.9)	0.9518	0.9994	-0.0051	0.0251	0.9850	0.9994	-0.0116	0.0255
Jamuna	Kazipur (SW49A)	0.9578	0.9994	-0.0063	0.0250	0.9808	0.9998	0.0015	0.0123
Dudhkumar	Pateswari (SW81)	0.7056	0.9640	-0.0045	0.1898	0.8748	0.9999	0.0051	0.0093
Dharala	Kurigram (SW77)	0.8113	0.9996	-0.0018	0.0194	0.9145	0.9999	-0.0033	0.0101
Teesta	Kaunia (SW294)	0.8080	0.9651	-0.0235	0.1867	0.7957	1.0000	0.0012	0.0062
Teesta	Haripur (SW294.5)	0.7152	0.9978	-0.0047	0.0469	0.6464	0.9995	-0.0040	0.0216
Ghagat	Gaibandha (SW97)	0.8391	0.9968	0.0118	0.0564	0.7493	0.9981	0.0148	0.0434
Bangali	Simulbari (SW10)	0.5211	0.9912	0.0083	0.0938	0.7953	0.9946	0.0132	0.0736
Old Brahmaputra	Jamalpur (SW225)	0.5466	0.9721	0.0138	0.1672	0.8792	0.9950	-0.0226	0.0707

According to Table 4.3, it can be stated that the model provided "**very good**" values of the statistical parameters at most of the stations except R^2 were found to be somehow "**satisfactory**" at Simulbari and Jamalpur, **PBIAS** in the range of **"good"** at Jamalpur, Gaibandha and Simulbari. Hence, it's quite evident that the model performed quite well according to these statistical indices.

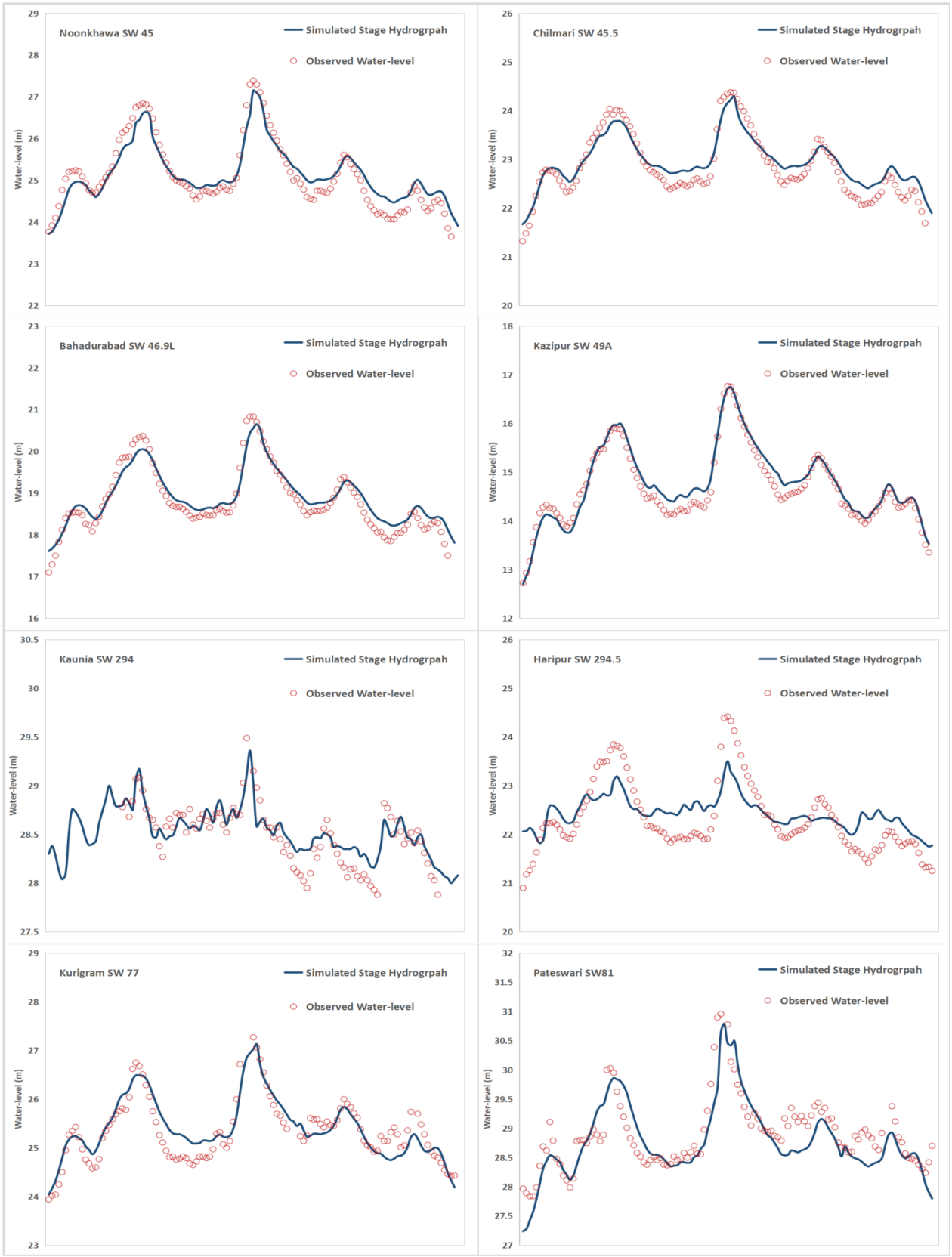

Figure 4.7. Comparison of Simulated Hydrograph and Observed Water-level on 2017 Flood event.

Figure 4.8. Comparison of Simulated Hydrograph and Observed Water-level on 2019 Flood event.

4.9 Summary and Discussions

The Hydrodynamic model using the HEC-RAS 1-D module to simulate water level has been discussed in this chapter. The aim is to predict water levels based on input flow data and analyze flood levels using measured cross-section and stream-flow data of the river network. The performance of the model has been determined through statistical indicators. Values of statistical indicators obtained for most of the stations during the calibration and validation period showed good agreement between observations and model results. There's still room for improvement in this study as the calibration result wasn't satisfactory in the Ghaghat river, the Jhenai river, and the Bangali river. This is mainly due to the unavailability of cross-section data of the upper portion of the Ghaghat river and the Bangali river and the unavailability of daily discharge data at the upstream locations of the study area, which has been solved by generating yearly rating curves for the upstream boundary stations. Further efforts will be made to resolve the remaining uncertainties of modeling this complex river system.

CHAPTER FIVE
RAPID FLOOD MAPPING USING SENTINEL-1 SAR IMAGES

5.1 Introduction

Flooding is one of the most important types of disasters that have provoked extended damage over the last centuries. Floods are the most visible and destructive hydrologic phenomenon in terms of human and economic loss. Over 75% of natural disasters that occur worldwide involve flooding. Bangladesh is part of the world's most dynamic hydrological and the biggest active delta system. The topography, location, and outfall of the three great rivers shape the annual hydrological cycle of the land. Too much and too little water in a hydrological cycle is an annual phenomenon. A regular monsoon event is a flood; the depth and duration of inundation are the deciding factors on whether it is affecting beneficially or adversely. Monsoon inflow, along with rainfall, historically shapes the civilization, development, environment, ecology, and economy of the country. Extreme events of floods adversely affect the development, economy, food security, poverty, and almost every sector. In flood management, Bangladesh has taken structural and non-structural measures. The country is mostly flat, with few hills in the southeast and the northeast part. Generally, the ground slopes of the country extend from the north to the south, and the elevation ranges from 60 meters to one meter above Mean Sea Level (MSL) at the Northwest boundary of the country and the coastal areas in the south. The land in the west of the Brahmaputra is higher than in the eastern part.

Within Bangladesh, the Brahmaputra receives four major Right Bank tributaries - the Dudkumar, the Dharla, the Teesta, and the Hurasagar. The first is flashy rivers, rising in steep catchments on the southern side of the Himalayans between Darjeeling and Bhutan. The Hurasagar River is the outlet to the Karatoya-Atrai river system, which comprises much of the internal drainage of northwest Bangladesh.

There are four distinct climatic seasons in Bangladesh (i) Winter, November to February, (ii) Pre-monsoon, March to May, (iii) Monsoon, June to September (iv) Post monsoon. Over 80% of the rainfall occurs during the monsoon or rainy season, also known as the flood season. The normal annual rainfall of the country varies approximately from 1,200 mm in the west to over 5,000 mm in the east. Long periods of steady rainfall persisting over several days are common

during the monsoon, but sometimes local high-intensity rainfall of short duration also occurs. Floods in Bangladesh occur for several reasons. The main causes are excessive precipitation, low topography, and the flat slope of the country. Excessive rainfall for upstream reasons is another cause.

Remote Sensing techniques provide safe and cost-effective tools for monitoring, mapping, and assessing the evolution and damages caused by flood events (Casagli, Nicola et al., 2017). The Earth Observation (EO) data required for such purposes include both optical and radar data, but preference is given to all-weather radar data due to the high probability of cloud cover. SAR is an active microwave remote sensing instrument that can provide high-resolution images of the Earth's surface during both day and night and virtually under all-weather day-night conditions (Psomiadis, Emmanouil, 2016). The sensor's ability to penetrate cloud cover and detect water makes an airborne or satellite SAR system a powerful tool for flood monitoring, as floods are often associated with heavy rain, where it is almost impossible for optical remote sensing instruments to image the water (Townsend, P. A., 2002). Although flood mapping with optical remote sensing has also been very common, SAR systems are more advanced than optical systems with all-weather monitoring capability. The first methods and algorithms for flood detection with SAR were introduced in the early 1980s and have been developed further ever since (Tavus, B. et al.,2018). Nowadays, SAR systems are widely used for flood mapping (Nasirzadehdizaji, R., Akyuz, D. E., & Cakir, Z., 2019) and are proven especially useful in small- to medium-sized drainage basins where inundation often recedes before meteorological conditions improve (Martinis, S., 2010). The European Space Agency (ESA), through the Copernicus program, provides accurate, timely, and easily accessible information to improve the management of the environment, understand and mitigate the effects of climate change and ensure civil security. Each mission of Sentinels (till now, Sentinel 1, 2, and 3 exist) focuses on a different aspect of Earth observation; Atmospheric, Oceanic, and Land monitoring, and the data will be of use in many applications. The contribution of Sentinel-1 SAR data products to this application arises from the sensitivity of the backscatter signal to open water. Through radar intensity imagery, in the absence of wind, the specular reflection of C-band signals over open water means that the signal is significantly lower than average. In the present study, the Sentinel-1 Level-1 Ground Range Detected (GRD) products have been utilized. They consist of focused SAR data, multi-looked, and projected to ground range using an Earth ellipsoid model such as WGS84. The images have been acquired through the Sentinels Scientific Data Hub. The data were processed to reveal and delineate the flooded areas. The Sentinel's

Application Platform (SNAP), which is an open-source-based common architecture for ESA Toolboxes, was used for the exploitation of EO data. This work is focused on flood extension mapping, using two different methods implemented on Sentinel-1 radar data. The first one deals with the determination of a threshold on the image acquired during the flood, while the second one has to do with the image difference between the image before and the image during the flood. Figure 5.1 shows a map of the study area that will be used for satellite image analysis.

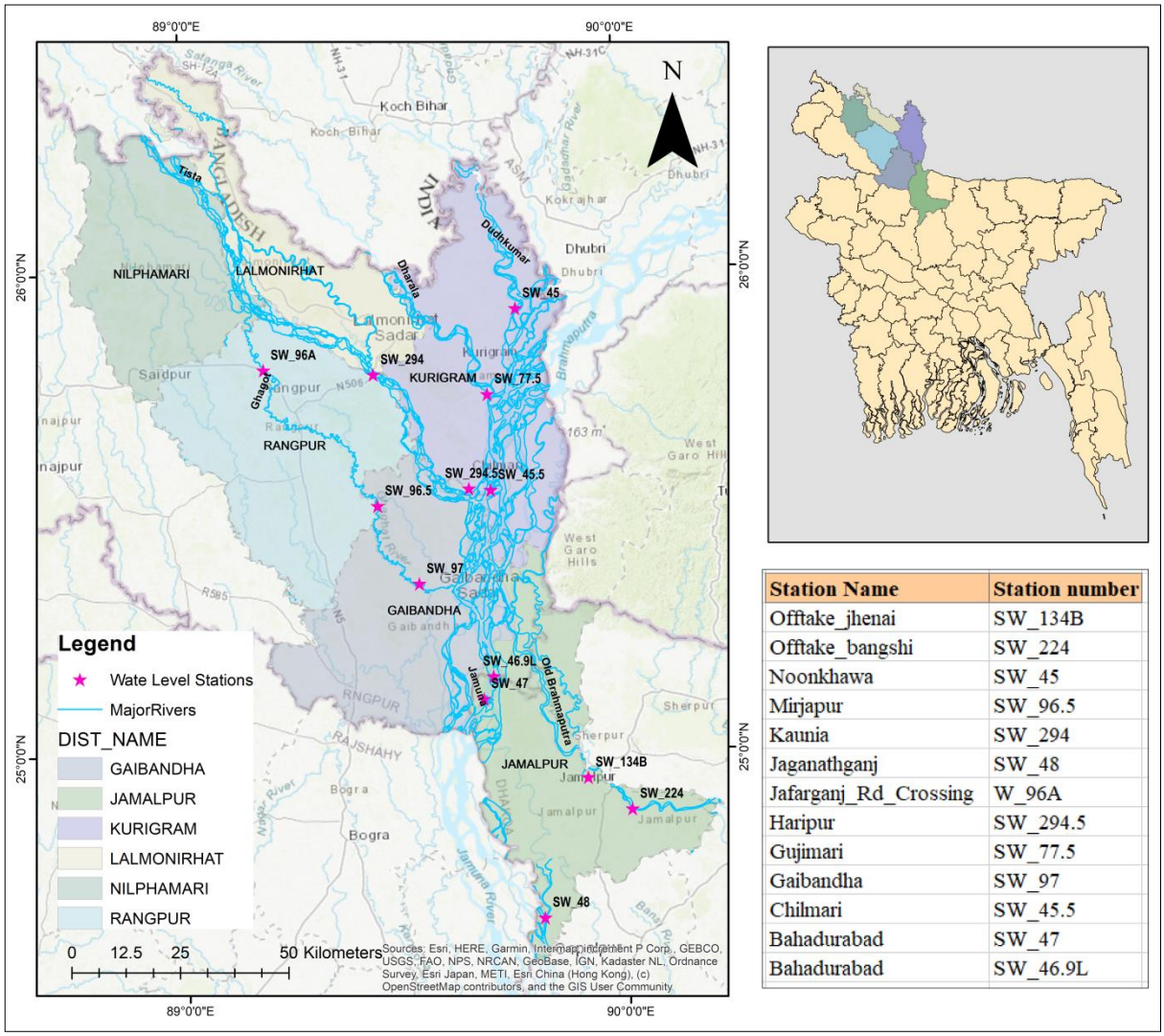

Station Name	Station number
Offtake_jhenai	SW_134B
Offtake_bangshi	SW_224
Noonkhawa	SW_45
Mirjapur	SW_96.5
Kaunia	SW_294
Jaganathganj	SW_48
Jafarganj_Rd_Crossing	W_96A
Haripur	SW_294.5
Gujimari	SW_77.5
Gaibandha	SW_97
Chilmari	SW_45.5
Bahadurabad	SW_47
Bahadurabad	SW_46.9L

Figure 5.1: Study area map used for satellite image analysis.

5.2 Methodology for flood inundation mapping

One of the major advantages of using SAR images, apart from its all-weather capability, lies in its ability to sharply distinguish water from other classes, given the high contrast that exists. Water bodies act as mirror-reflecting surfaces; their response is low (low backscatter coefficient in SAR images) and thus looks like a dark area. The earth, for its part, gives a much greater

amount of radar energy due to the surface roughness, and this generates a high contrast between surfaces: soil and water (Vilches, J. P., 2013, March).

The pair of SAR images obtained from the Sentinel-1C-band comprises an image during the flood, which is called a "crisis image," and another one before the flood event, which is called "achieve an image." To distinguish the flooded area, two different methods were followed. The first method uses only the "flood image" and sets the threshold value (that was established manually) of radar backscatter, which is followed by a binary algorithm (band math equation) to determine whether a given raster pixel is flooded or not. The second method deals with the separation of water from non-water areas by comparing the "reference image" with the "flood image," making use of a change detection technique.

SAR polarization is a key factor in flood detection. In this study, the available image during the flood had an Intensity of VV and VH polarization. The VV polarization was preferred because the medium incident angle of the data makes this image suitable for flood monitoring. Moreover, the same polarization (VV) was chosen for both dates to achieve the same co-polarization (VV-VV) comparison that gives better results than the cross-polarization (VH-VV).

The European Space Agency (ESA), through the Copernicus program, provides accurate, timely, and easily accessible information to improve the management of the environment, understand and mitigate the effects of climate change and ensure civil security. Each mission of Sentinels (till now, Sentinel 1, 2, and 3 exist) focuses on a different aspect of Earth observation; Atmospheric, Oceanic, and Land monitoring, and the data will be of use in many applications. The contribution of Sentinel-1 SAR data products to this application arises from the sensitivity of the backscatter signal to open water. Through radar intensity imagery, in the absence of wind, the specula reflection of C-band signals over open water means that the signal is significantly lowered than average. In the present study, the Sentinel-1 Level-1 Ground Range Detected (GRD) products have been utilized. They consist of focused SAR data, multi-looked, and projected to ground range using an Earth ellipsoid model such as WGS84. The images have been acquired through the Sentinels Scientific Data Hub. The data were processed to reveal and delineate the flooded areas. The Sentinel's Application Platform (SNAP), which is an open-source-based common architecture for ESA Toolboxes, was used for the exploitation

of EO data. A flow diagram of the methodology for flood inundation mapping is presented in Figure 5.2

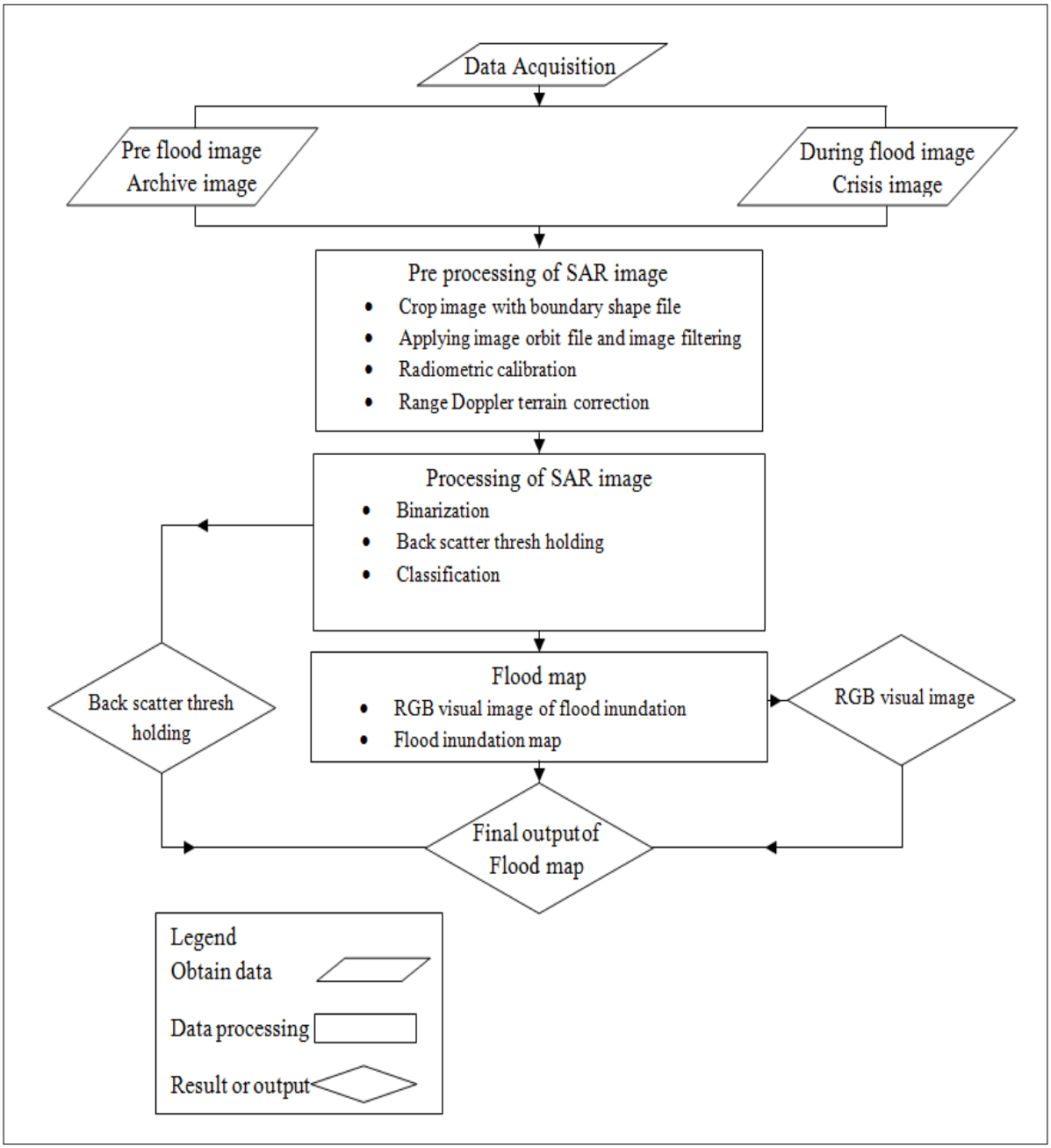

Figure 5.2: Methodology for flood inundation mapping

5.2.1 Data acquisition

Two types of Sentinel-1 images have been acquired to assess the final flood inventory map. One type is just before the flood image, named pre-flood or archive image, and another is during a flood situation, named crisis image. In this study, the date of acquiring an image through

secondary information is chosen considering major flood events. Detailed data information on acquired data is presented in Table 5.1.

Table 5.1: Detailed data information on acquired data.

Date of Acquisition	Acquisition Mode	Product Type	Polarization used	Relative orbit	Slice number	Pass direction	Note
31 March 2017	IW	GRD	VV	114	4	Ascending	Archive image
31 March 2017	IW	GRD	VV	114	5	Ascending	Archive image
22 August 2017	IW	GRD	VV	114	4	Ascending	Crisis image
22 August 2017	IW	GRD	VV	114	5	Ascending	Crisis image
28 June 2019	IW	GRD	VV	114	4	Ascending	Archive image
28 June 2019	IW	GRD	VV	114	5	Ascending	Archive image
19 July 2019	IW	GRD	VV	114	4	Ascending	Crisis image
19 July 2019	IW	GRD	VV	114	5	Ascending	Crisis image

5.2.3 Pre-processing of SAR image

After gaining the image, different types of correction methods have been used for Sentinel-1 data. Thermal noise removal, TOPSAR deburst, geometric correction, radiometric correction, and spectral correction are the main part of this process. SNAP S1TBX is used for this pre-process (Figure 5.3).

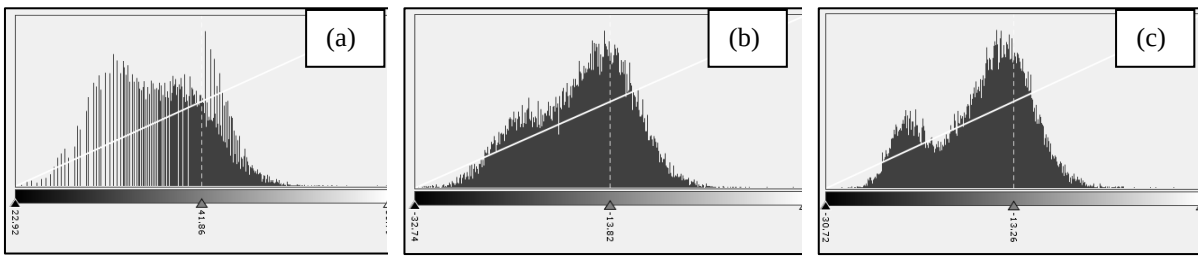

Figure 5.3: Pre-processing of the image, orbit files, image filtering (a), radiometric calibration (b), and terrain correction (c).

5.2.4 Processing of SAR image

In our processing part of the SAR image, three major parts are considered, which are described as follows.

a) Binarization of image

The backscatter value has been converted from a linear scale to a nonlinear logarithm scale. Before conversion and after the conversion of the images are shown in Figure 5.4.

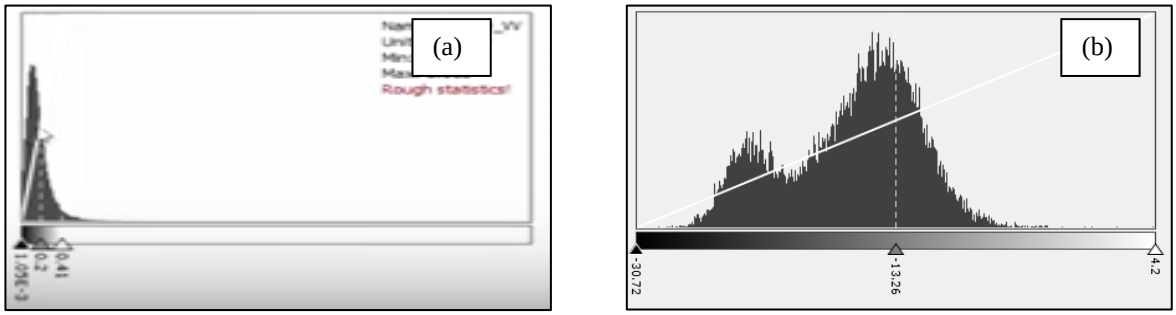

Figure5.4: Backscatter value has been converted from a linear scale to a nonlinear logarithm scale, before conversion (a) and after the conversion (b).

b) Backscatter thresh holding

A histogram of pixel values in a non-linear logarithm scale has been generated to detect the backscatter thresh hold as it gives two high peak values, one for the water body and another for the land surface. For low scattering from the water surface, the lowest peak always represents the thresh hold for the water body (Figure 5.5).

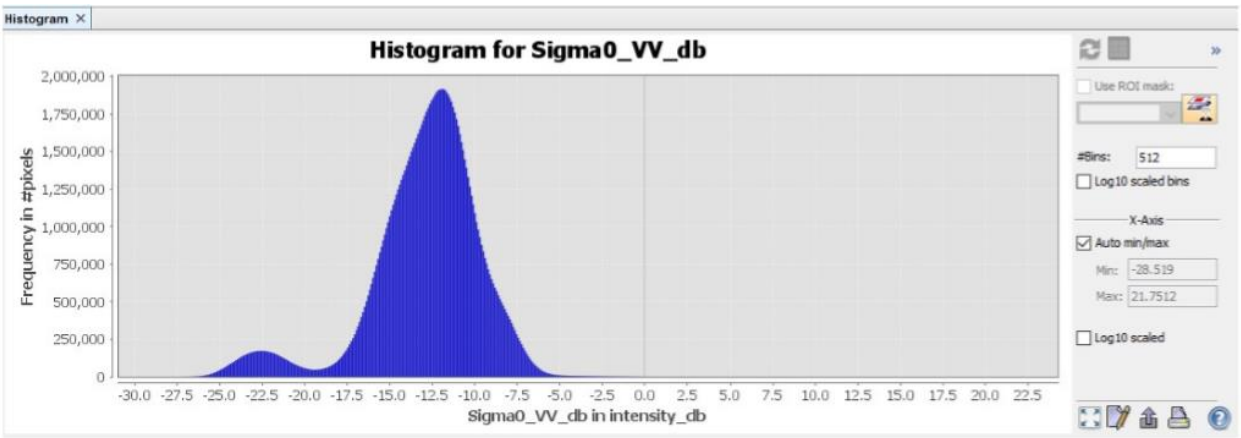

Figure 5.5: Histogram of pixel values in a nonlinear logarithm scale.

c) Classification method

Image classification is the process of assigning land cover classes to pixels. For example, classes include water, urban, forest, agriculture, and grassland. Unsupervised and supervised image classifications are the two most common approaches. In unsupervised classification, it first groups pixels into “clusters” based on their properties. Then, each cluster is classified into

a land cover class. In supervised classification, we select representative samples for each land cover class. The software then uses these “training sites” and applies them to the entire image. Overall, unsupervised classification is the most basic technique. Because you don’t need samples for unsupervised classification, it’s an easy way to segment and understand an image. Using remote sensing software, we first create “clusters.” After picking a clustering algorithm, we identify the number of groups we want to generate. For example, we create 32 clusters. The next step is to assign land cover classes to each cluster manually.

d) Final flood inventory map

In this part, first, the RGB visualization image of a flood is created. For this process, we use the non-linear logarithm values of VV polarization from the archive image in the red band and non-linear logarithm values of VV polarization from the crisis image in the green and blue bands. Through this process, we have an image of the flooded area represented in red color as there is a difference between backscattering in the red band due to the difference between the archive and crisis image. The flooded areas represent the water body in the crisis image, but the same place in the archive image represents a land part. This difference can be visualized in RGB to visualize the image. The map is finalized by cross-checking the unsupervised classification with a visual RGB image and backscatter threshold by a value that has been assessed previously (Figure 5.6).

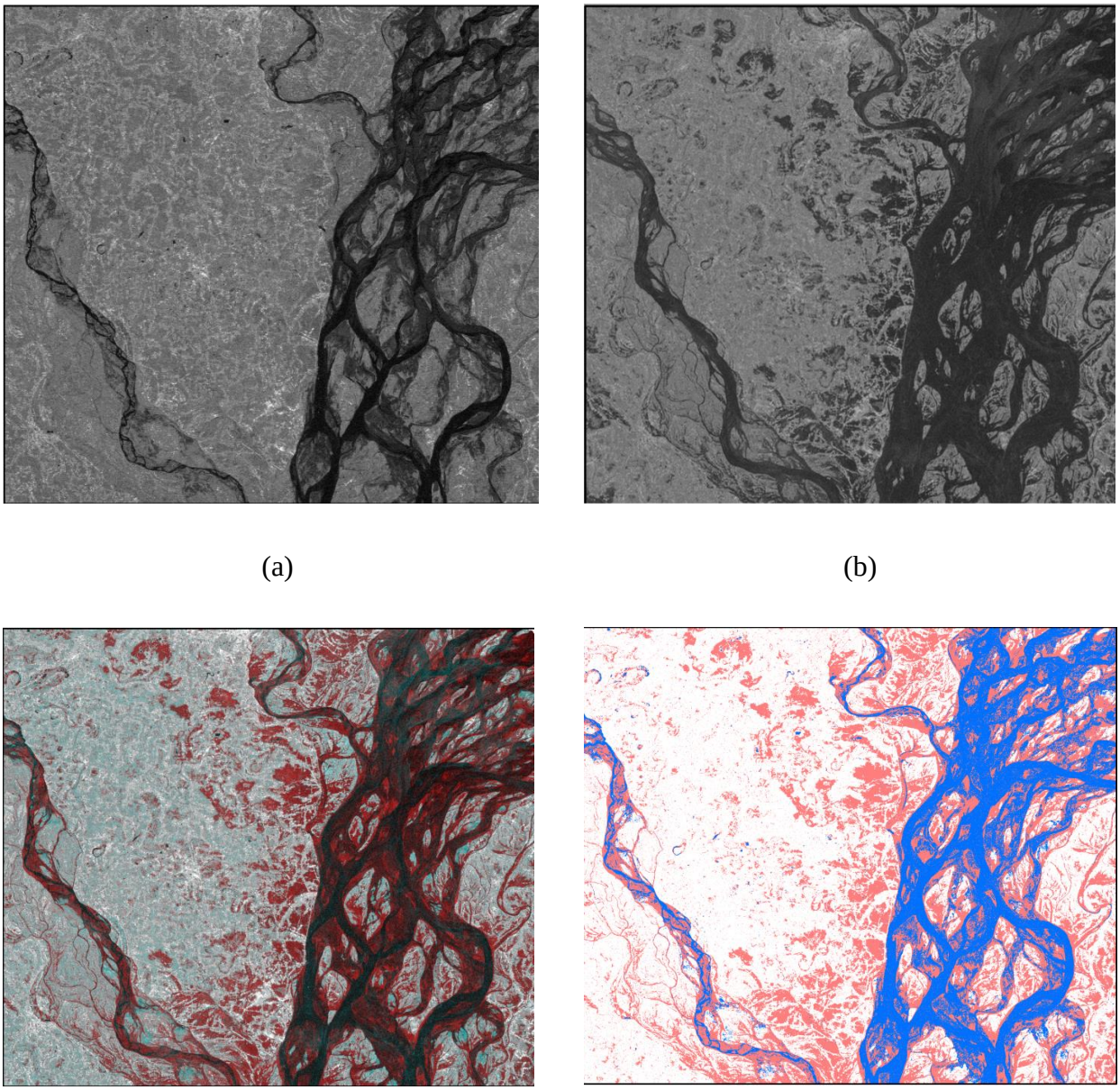

(a) (b)

(c) (d)

Figure 5.6: Preprocessed archive or pre-flood image (a), preprocessed crisis or during flood image (b), RGB visual flood map (c), final flood map (d).

Map the flood inundation over the study area for 2004, 2007, 2017, 2019, and 2020 floods are prepared using Google Earth Engine (GEE) using python environment due to its easy interface and linkage with wider applications. Details of this process have been described in the next section.

5.2.5. Cloud-based platform for flood mapping

In recent times using, Google Earth Engine (GEE), a cloud-based platform, has been widely used due to its accessibility, performance, and quick response. As a program-based platform, it is very easy to modify and conduct analysis in your way of understanding. Google Earth Engine is an online platform that helps researchers with geographical research by providing easy access to a server with a huge geographical dataset with their catalog for big data analysis.

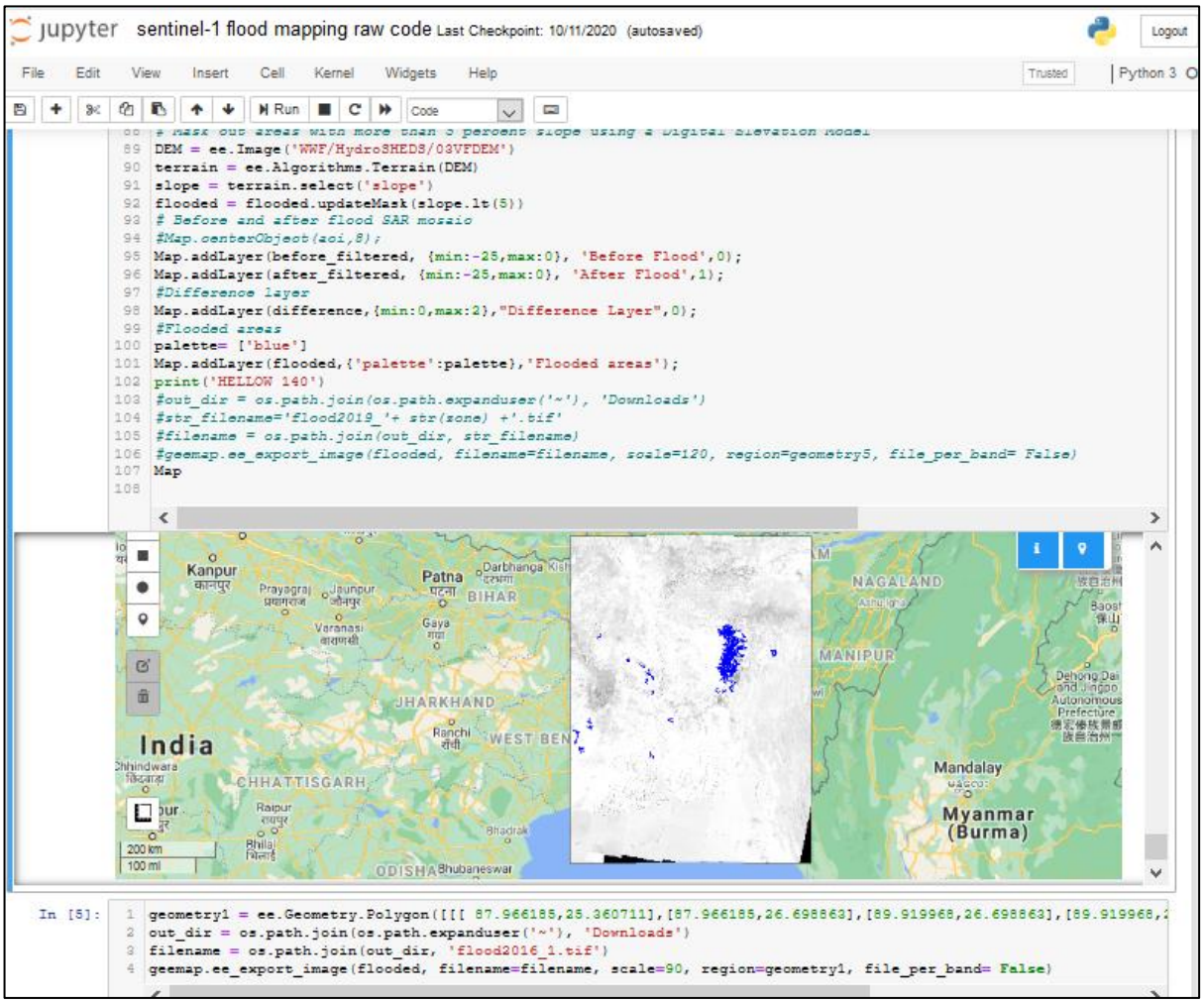

Figure 5.7: A working window of Google Earth Engine (GEE) using python API using Jupiter notebook.

Google Earth Engine is also a cloud-based geospatial analysis platform that enables users to visualize and analyze satellite images of our planet. Scientists and non-profits use Earth Engine for remote sensing research, predicting disease outbreaks, natural resource management, and more. There are several examples in recent days that the GEE platform has been used in various research, especially in disaster management, especially floods, drought, river erosion, and many more. It also opens a new window for resource management as well. Some examples have been described as well.

Studies that directly address disaster extent and response were done across the globe and reported in this issue. A snow cloud hydro model, applicable to different environments in Chile, Spain, and the USA, was developed using MOD10A1 (Sproles et al., 2018). The cloud-based model forecasts monthly stream flows in snow areas and mapped snow cover areas and is generally applicable. Concerning disasters, (Liu et al., 2018) developed a good prevention and response system using the cloud-based GEE platform. The system integrates a whole range of datasets from remote sensing and ancillary sources at each stage of flood events (before, during, and after), including Formosat-2, Synthetic aperture radar, and GIS topographic data, and was successfully tested to manage the Typhoon Souder in August 2015. The GEE platform was also used to assess drought occurrence using soil moisture as an indicator on a global scale (Sazib et al., 2018). The cloud-based engine facilitated the integration of soil moisture global data sets and web-based processing tools to forecast drought duration, as well as the intensity and the model, which was successfully tested in Ethiopia and South Africa (Sazib et al., 2018). Other applications in this issue include cloud masking using multi-temporal approaches (Mateo-García et al., 2018), surface sediment monitoring (Markert et al., 2018), and mining area mapping using Sentinel data (Lobo et al., 2017).

The GEE platform is capable of handling huge data sets at various scales and building automated programs that can be used at an operational level. This is a great step in solving environmental problems affecting the earth and is critical in achieving the UN millennium development goals. The applications demonstrated are wide-ranging, from mining, agriculture, ecosystem services, and drought monitoring, among others. Day-to-day, monthly, seasonal, and long-term monitoring of phenomena at high spatial resolution and covering large extents is now possible with the availability of such platforms that can handle big data.

5.3 Flood inundation mapping for 2004, 2007, 2016, 2017 and 2019 and 2020

5.3.1 Floods in 2004

The 2004 monsoon floods commenced around 8 July. This followed early flooding in the northwest districts of Bangladesh in April that had destroyed much of the main annual rice crop in that region just before it was harvested. They rose more swiftly than usual in the same area and in the northern districts on either side of the Brahmaputra/Jamuna River. Water persisted in these regions for some 3 to 4 weeks whilst gradually draining southwards, severely flooding most of Central Bangladesh and the Greater Dhaka area, especially districts adjacent to the two confluence points of the three great rivers. The high-water level and widest extent of the flood - about 35,000 km^2 - was reached on 24 July. The water had receded in most places by mid-August, although it persisted and stagnated in areas behind protective embankments without adequate drainage. In total, 39 out of 64 districts and 36 million people (25% of the total population) were affected. In mid-September, a localized depression caused continuous torrential rain and high winds over a six-day period, bringing renewed flooding to many parts of Central Bangladesh, but also flooding areas never normally flooded by the rivers, including Dhaka and other urban areas and some of the most productive agricultural land.

The worst impact of this rain-fed flooding was in Comilla and Feni to the east, where the Meghna River breached embankments already weakened by the earlier floods, and in the southwest border districts of Jessore, Satkhira, and Magura and parts of three others. Here the impact was a combination of the rainfall, water released from West Bengal, and poor drainage because of the region's low elevation and inappropriate coastal protection. Although the monsoon normally ends by mid-October, there is still the risk of heavy rainfall upstream in the catchment areas of the major rivers and the attendant risk of water being released without warning, as occurred in 2000. The cyclone season then prevails until the end of the year, posing a significant threat to coastal communities.

5.3.2 Floods in 2007

The 2007 floods came in two waves. The first wave commenced around the 24th of July 2007 and initially affected Nilphamari, Lalmonirhat, and Kurigram, Sherpur, Jamalpur, Sylhet, Sunamgonj districts. In the following days, Rangpur Gaibandha, Bogra, and Sirajgonj were flooded, and subsequently, the other districts were inundated up until about the 6th of August. This represented about 39 districts. The second wave commenced on the 5th of September and

continued up until the 15th of September 2007, when some new districts apart from the previous 39 were flooded. A total of 46 districts were affected to varying degrees during both flood waves.

By the report of the ministry of food and disaster management published in November 2007, The flood inundated about 32000 Sq. Km, including the char areas of 6000 sq. km affecting almost 16 million people in around 3 million households. Thousands of people also suffered from flood-related health hazards. Eighty-five thousand (85,000) houses were completely damaged, while almost one million suffered partial damage. Six hundred forty-nine persons were reported to have perished either as a direct impact of the flood or through flood-related causes, including bridge collapse or boat capsizing. Several children drowned as a result of swimming in flood areas. A number, in addition to this, perished as a result of diseases caused by contaminated water and poor sanitation.

To the situation report published on 31 august 2007 by all Indian disaster mitigation institutes in Bangladesh, floods affected tens of millions of people, displacing eight million people and over 340 reported deaths. About half of the country is inundated. In Bangladesh, floods affected tens of millions of people, displacing eight million people and over 340 reported deaths. About half of the country is inundated. The floods are caused by the heavy rains at the beginning of August and water coming from rivers. Additionally, many people suffered from snakebites in the floodwaters. Myanmar has also been hit by floods, especially in areas around the City of Mandalay. Outbreaks of diseases in the 2nd week of July have been reported. Further data on affected and/or people killed by floods or other natural disasters are unfortunately unavailable. In Nepal, flash floods and landslides affected over 330,000 and killed over 90 people. Floods mainly affect the southern part of the country; landslides mainly affect the north.

5.3.3 Floods in 2016

In July 2016, Bangladesh was hit by one of the worst floods in recent history. At least 820,000 people have been affected by the floods in Bangladesh, and the situation is deteriorating daily. Dangerously high river levels have forced thousands of people from their homes. River levels are forecast to continue rising over the next few days. Many families are living under the open sky, and there are shortages of clean water, food, medicine, and fuel. The Bangladesh Red Crescent is distributing food in seven affected districts: Kurigram, Bogra, Sirajganj, Jamalpur,

Nilphamari, Lalmonirhat, and Sunamganj, according to a Reifelweb report on 29th July 2016 (https://reliefweb.int/report/nepal/millions-south-asia-hit-floods-and-landslides-after-severe-monsoon-rains).

As of 3 August, some 3.2 million people across 16 districts of Bangladesh were affected by monsoon-induced floods that began around 22 July. Forty-two deaths were recorded, and 38 officially confirmed, including mostly drowned minors, as nearly 7,400 people sought refuge in 69 flood shelters. Some 250,000 houses were destroyed or damaged. The affected populations are mainly in need of food, water, and emergency shelter. More than 300,000 people are stranded in Shariatpur and Faridpur districts, according to a Reliefweb report on 3rd August 2016 (https://reliefweb.int/report/bangladesh/acaps-briefing-note-bangladesh-floods-3-august-2016)

On 11 August, HCTT Humanitarian Response Plan, requiring US$ 13,620,052, was presented to the HCTT. 3.7 million people across 19 districts of Bangladesh are affected by monsoon-induced floods. One hundred six people died to date as a consequence of the floods. As of 7 August, 16,770 houses/homesteads were reported completely lost, with a further 65,156 partially damaged by erosion. The districts which have experienced the greatest impact of the floods are Jamalpur, Kurigram, Sirajgonj, Tangail, and Gaibanda. Together, these five districts account for more than 70% of the affected people, according to the Reliefweb report on 15th August 2016 (https://reliefweb.int/report/bangladesh/2016-humanitarian-response-plan-bangladesh-monsoon-floods-15th-august-2016).

As of September, roughly 4.2 million people have been affected by flooding in at least 19 districts since July, according to the government and aid agencies. The flooding has wiped out entire villages and crops, sending farmers deeper into debt, according to the Reliefweb report on 8th September 2016 (https://reliefweb.int/report/bangladesh/bangladeshi-farmers-drown-debt-floods-destroy-crops).

WFP, together with UNICEF, is responding to significant monsoon flooding in northwest Bangladesh. Food Security, Nutrition, and WASH assistance will be provided to 150,000 people following confirmation of funding from the United Kingdom. The joint response has been informed by a Multi-sector Rapid Needs Analysis undertaken in August. WFP will provide food assistance to 42,500 people in the four most affected districts with unconditional cash

transfers for three months beginning in November, according to the Reliefweb report on 30th September 2016 (https://reliefweb.int/report/bangladesh/wfp-bangladesh-country-brief-september-2016)

On 16 August, an Emergency Appeal was launched for CHF 1,637,374 to support the Bangladesh Red Crescent Society (BDRCS) in scaling up the delivery of humanitarian assistance to 105,000 people. By the end of October, BDRCS-led assistance had reached 62,000 people, according to the Reliefweb report on 18th November 2016 (https://reliefweb.int/report/bangladesh/bangladesh-floods-emergency-appeal-operations-update-n-2-mdrbd017)

5.3.4 Floods in 2017

Bangladesh experienced a severe flood in 2017, which made the country adrift. As monsoon rain kept on pouring and overflowing the rivers in the country as well as the upstream hilly regions of neighboring countries, Bangladesh faced a flood affecting the Brahmaputra-Jamuna river basin. The northern, northeastern, and central parts of the country had experienced that flood. Approximately 3.9 million people were affected, and 531,517 houses were damaged in 24 districts. The most affected districts are Dinajpur, Kurigram, Lalmonirhat, Rangpur, Naogaon, Sirajganj, Jamalpur, Bogra, Tangail, Netrokona, Sylhet and Sunamganj, Gaibandha and Thakurgaon, Panchagarh. A total of 56 people were reported killed in this current flooding. Table 5.2 presents damage information at a glance for flood 2017.

Table 5.2: Damage information at a glance for flood 2017.

District	No. of affected Upazila	No. of affected families		No. of affected people		No. of the affected house		No. of death
		Total	Partial	Total	Partial	Total	Partial	
Nilphamari	6	301	41234	1204	164936	301	38050	5
Lalmonirhat	5	-	102750	-	411000	-	-	5
Kurigram	9	-	102743	-	421584	22075	80668	8

District	No. of affected Upazila	No. of affected families		No. of affected people		No. of the affected house		No. of death
		Total	Partial	Total	Partial	Total	Partial	
Gaibandha	6	-	60417	-	252103	-	314809	2
Jamalpur	7	-	105441	-	565502	210	9505	1
Rangpur	-	-	-	-	-	-	-	-

Source: Reliefweb (2021)

In our study area, 2017 was an early flood that damaged the main crop of this region (Figure 5.7). Literally, in monsoon, our study area has to face regular flooding, but the 2017 flood was different for its early arrival. About 20% of the total area was inundated in this flood (Figure 5.8).

5.3.5. Floods in 2019

As compared to the 2017 monsoon floods, the 2019 floods were not that widespread. However, they could have a greater intensity for fewer but highly impacted districts, and the distress to the people and disruption created could be severe and last for a longer period. This is notable since large sections of embankments were rapidly washed away upstream. That situation might lead to prolonged flooding and waterlogging issues in these districts, with all the consequences it could have. Continuous monitoring of the situation was therefore required.

Latest estimates from the National Disaster Response Coordination Centre (NDRCC) of the Ministry of Disaster Management and Relief (MoDMR) inform that 21 districts across the country were affected by the monsoon floods and that the death toll of 71 people (56 from drowning, eight from snake-bite and seven from Lightning). It is estimated that 5.3 million (5,302,698) people were directly affected, that 419,336 houses were damaged, and that an estimated 287,513 people were displaced (UNRCO, 2020).

Floods and landslides damaged roads and vital infrastructure, leaving hundreds of thousands stranded and without power and electricity (Gaibandha and Bandarban). According to NDRCC, 6,655 km of road were damaged and destroyed, and 1,463 km of the embankment was either fully or partially destroyed. Besides, 308 bridges and culverts were damaged. Moreover, 203 education institutions are either damaged or are serving as emergency shelters, and 44,106 tube wells were damaged. From the image processing result, we can find that the level of inundation and the 2019 flood was much more devastating than the flood in 2017. But the difference was while 2017, it was a pre-monsoon flood, and in 2019 it was a regular monsoon flood (Figure 5.9). In 2019 it inundated about 29% of the total area in the major six districts, which was 9% more than we experienced in 2017 (Figure 5.10). A summary of the area affected during the 2017 and 2019 floods in 6 districts of our study area is presented in Table 5.3.

Table 5.3. Area affected during the 2017 and 2019 floods in 6 districts of our study area.

Class name	**Area in hectare**		**Area (%)**	
	2017	2019	2017	2019
Flood	234211	336684	20%	29%
Water	66764	107272	5.7%	6%

5.3.6. Floods in 2020

Monsoon rainfall and an onrush of water from hilly areas upstream have inundated districts in the northern and eastern areas of Bangladesh, causing extensive damage. Thousands of people in 7 districts of the country are marooned or displaced, and their homes are flooded. Over 164,000 people are marooned across Jamalpur District and Rangpur Division. On 30 June, the river water levels were above danger in 14 locations across the country. International humanitarian organizations are assisting the national government with preparedness measures while relief items have been distributed to the affected communities. On 1-2 July, rainfalls and thunderstorms are forecast over north and east Bangladesh. Water levels are expected to rise further over the coming days, according to the Reliefweb report on 1st July 2020 (https://reliefweb.int/report/bangladesh/bangladesh-floods-dg-echo-bmd-ifrc-floodlist-media-echo-daily-flash-1-july-2020)

According to the Bangladesh Meteorological Department (BMD), due to the strong monsoon, a steep pressure gradient lies over the North Bay of Bengal. Maritime ports have been advised to hoist local cautionary signal No 3. Due to its influence, moderately heavy to very heavy falls are likely to occur in many places all over the country. The National Disaster Response Coordination Centre (NDRCC) of Bangladesh reports that on 5 July, more than 15 districts were affected, with a caseload of 356,451 households representing more than 1.5 million people in these districts, according to the Reliefweb report on 6th July 2020 (https://reliefweb.int/report/bangladesh/bangladesh-flood-dg-echo-modmr-bmd-ffwc-media-echo-daily-flash-06-july-2020).

Earlier, during the last week of June 2020, BDRCS, based on the forecast, activated its Early Action Protocol (EAP) to support 3,800 households in three districts that have more than 25 percent of household assets damaged. After showing a slight improvement last week, the flood situation has deteriorated again as major rivers in the country are flowing above the danger level. According to the current forecast, this flood has a 50 percent chance of crossing 1 in 10 years on 21 July. Thousands of people in low-lying areas are witnessing the second phase of floods this season due to the rise of water levels of major rivers in the country, according to the Reliefweb report on 20th July 2020 (https://reliefweb.int/report/bangladesh/bangladesh-monsoon-floods-information-bulletin-0)

Over a million people were marooned in dozens of villages from 10 to 11 July 2020 as roaring rivers swept away embankments in the districts where some of the embankments were already underwater since 26 June. Thousands of people are expected to leave their homes throughout the beginning of this week to seek shelter on higher grounds as the Water Development Board warned that the onrush of water from upstream would further intensify.

Monsoon rainfall and an onrush of water from hilly areas upstream have inundated districts in the northern and eastern areas of Bangladesh, causing extensive damage. The situation is still evolving and is yet to reach its peak. The National Disaster Response Coordination Centre (NDRCC) of Bangladesh reported that as of 13 July, more than 15 districts with some 1.3 million people are affected. NDRCC also informed that more than 280,000 people are marooned in floodwater. On 11 July, the final activation trigger for the Anticipatory Action Pilot 2020 was reached, initiating cash assistance, interventions to support food security and agriculture, and ensuring continued access to lifesaving SRHR, GBV, and PSS services,

according to the Reliefweb report on 14th July 2020 (https://reliefweb.int/report/bangladesh/asia-and-pacific-weekly-regional-humanitarian-snapshot-7-13-july-2020).

As of 16 July, a total of 2,246,472 people in 18 districts have been affected by fresh floods, and six people have died. A total of 1,086 flood shelters are opened in 18 districts, and 55,930 people have taken refuge there. New flooding areas in Nilphamari, Jamalpur, Kurigram, Lalmonirhat, Sylhet, Sunamganj, Natore, Gaibandha, Bogra, Netrokona, Feni, Habiganj, and Sirajganj were inundated further due to overflow of major rivers on 13 July. As the flood inundated many low-lying areas in northern and northeastern regions over the past few days, marooned people have set up basic shelter on embankments, roads, highlands, and flood centers with their domestic animals and valuables, according to the Reliefweb report on 18th July 2020 (https://reliefweb.int/report/bangladesh/bangladesh-monsoon-floods-emergency-plan-action-epoa-dref-operation-n-mdrbd025).

According to National Disaster Response Coordination Center (NDRCC) report issued on July 17, 18 districts (Lalmonirhat, Kurigram, Gaibandha, Nilphamari, Naogaon, Rangpur, Sirajganj, Bogra, Jamalpur, Tangail, Netrokona, Rajbari, Faridpur, Madaripur, Manikganj, Feni, Sunamganj, Sylhet) of Northern, NorthEastern and South-Eastern Bangladesh are most affected due to continuation of weeklong monsoon rains in the upstream regions and throughout the country. The flood situation is currently worsening in those districts where roads are cut off, and hundreds of thousands of people are stranded. NDRCC preliminary report informs that 2.4 million people are affected in the 18 districts, and 548,816 families lost their houses, according to the Reliefweb report on 18th July 2020 (https://reliefweb.int/report/bangladesh/office-un-resident-coordinator-flash-update-no-1-bangladesh-2020-severe-monsoon).

Flooding in Bangladesh continues to grow more severe, with about 1.4 million people currently affected. Current estimates indicate that nearly half of all districts in the country have been affected in the coming weeks, according to the Reliefweb report on 17th July 2020 (https://reliefweb.int/report/bangladesh/daily-noon-briefing-highlights-bangladesh-nepal-syria-17-july-2020).

Monsoon rain continues to hit Bangladesh. According to the media, the number of fatalities has reached 67. Thousands of people in low-lying areas are affected by flood or landslide events.

Approximately 56,000 people were displaced to 1,086 flood shelters across 18 Districts. Road communication in some areas was damaged by floods, isolating several sub-districts. According to Flood Forecasting and Warning Centre (FFWC), the water level of major river basins is at severe flood risk in at least three localities and flood risk in 17 points across the country. The flood situation is likely to worsen over the north-west and central Bangladesh in the coming days, until the end of July, according to the Reliefweb report on 20th July 2020 (https://reliefweb.int/report/bangladesh/bangladesh-floods-update-ifrc-ffwc-media-echo-daily-flash-20-july-2020).

According to the National Disaster Response Coordination Center (NDRCC), 2.4 million people are reportedly affected, and over 548,000 families had their homes flooded or water-logged. Flood protection infrastructures such as embankments and dykes are already damaged. The COVID-19 pandemic context creates further challenges to disaster response and recovery efforts as measures such as physical distancing need to be observed to minimize the risk of infections among the affected people, especially those in emergency shelters, according to the Reliefweb report on 21st July 2020 (https://reliefweb.int/report/bangladesh/asia-and-pacific-weekly-regional-humanitarian-snapshot-14-20-july-2020).

Official Authorities reports, as of 25 July, 93 fatalities, around 3.3 million affected people, and around 732,000 waterlogged people across 21 districts of the country. The worst affected Districts by the flood are the Jamalpur (Mymensingh Division) and the Sunamganj Districts (Sylhet Division), according to the Reliefweb report on 27th July 2020 (https://reliefweb.int/report/bangladesh/bangladesh-monsoon-rain-update-un-ocha-humanitarian-response-hctt-nawg-bmd).

As of 28 July, 4.7 million people were affected, and 984,819 houses were inundated. More than 150,000 ha of paddy fields were damaged, along with thousands of latrines and tube wells. As per the Needs Assessment Working Group report, 24% of the country is inundated, and approximately 56,000 people have been displaced in 1,086 flood shelters. Several districts are isolated due to road communication damage. Over 1,900 schools are damaged, leaving 807,467 children without access to education, according to the Reliefweb report on 28th July 2020 (https://reliefweb.int/report/bangladesh/bangladesh-floods-update-dg-echo-modmr-bmd-ffwc-media-echo-daily-flash-28-july).

Heavy monsoon rains in upstream regions continue to cause flooding in 30 districts in the north, northeast, and southeast of the country, affecting some 5.4 million people. As of 2 August, 135 deaths, mostly as a result of drowning, have been reported. Flooding has damaged houses, dykes and embankments, water sources, and hygiene facilities and has severely impacted livelihoods, especially in the agricultural sector. Access to basic services such as health care and education has been disrupted. Humanitarian partners continue to respond to the needs of affected people in coordination with the Government of Bangladesh, according to the Reliefweb report on 4th August 2020 (https://reliefweb.int/report/bangladesh/asia-and-pacific-weekly-regional-humanitarian-snapshot-28-july-3-august-2020).

According to the Ministry of Health and Family Welfare (MoHFW), the ongoing floods resulted in over 220 deaths so far. More than 1.27 million houses have been partially or fully damaged by the floods, and over 167,000 families remain displaced. Besides, over 170,000 hectares of agricultural land have been affected. While floodwaters are receding in some areas, riverbanks continue to erode and pose risks to surrounding communities, according to the Reliefweb report on 19th August 2020 (https://reliefweb.int/report/bangladesh/asia-and-pacific-weekly-regional-humanitarian-snapshot-11-18-august-2020).

Heavy rain and gusty winds over the Rohingya refugee camps in Cox's Bazar this week have affected 10,117 people (1,208 households), including 775 displaced people across 34 Rohingya refugee camps in Ukhia and Teknaf. One thousand nine hundred shelters were damaged as well as other infrastructure. Flooding has also been reported at the Bangladesh-Myanmar border in Naikhongchhari Upazila of Cox's Bazar, where thousands of Rohingya refugees remain stranded. The ongoing monsoon and COVID-19 pandemic are exacerbating the suffering of affected refugees, according to the Reliefweb report on 19th August 2020 (https://reliefweb.int/report/bangladesh/asia-and-pacific-weekly-regional-humanitarian-snapshot-11-18-august-2020).

About 101,400 people have been affected in the Rohingya camps in Cox's Bazar, including 8,736 who have been displaced, 41 injured, and 14 deaths, according to the Reliefweb report on 20th August 2020 (https://reliefweb.int/report/bangladesh/bangladesh-monsoon-rains-update-un-ocha-bmd-floodlist-echo-daily-flash-20-august).

Flooding due to heavy rains and high tides in low-lying areas of Satkhira districts in Southwest Bangladesh has marooned about 100,000 people. Many houses, fish farms, betel vines, and vast tracts of croplands have been damaged. Intermittent heavy rains and gusty winds continue to affect the Rohingya camps in Cox's Bazar. With 3,490 newly affected in the last 48 hours, the total number of people affected by the 2020 monsoon in the refugee camps has risen to 109,312, while 8,911 are displaced, 41 injured, and 14 have died, according to the Reliefweb report on 24th August 2020 (https://reliefweb.int/report/bangladesh/bangladesh-severe-weather-dg-echo-iscg-bmd-echo-daily-flash-24-august-2020).

As of 1 October, media reports around 125,000 people affected, of which 100,000 in Rangpur District (particularly in Rangpur City) and 25,000 more across Nilphamari, Lalmonirhat, and Thakurgaon Districts. Also, hundreds of damaged buildings and several flooded roads were reported across all of the aforementioned District and in the Kurigram District, according to the Reliefweb report on 1st October 2020 (https://reliefweb.int/report/bangladesh/bangladesh-floods-bmd-floodlist-media-echo-daily-flash-1-october-2020).

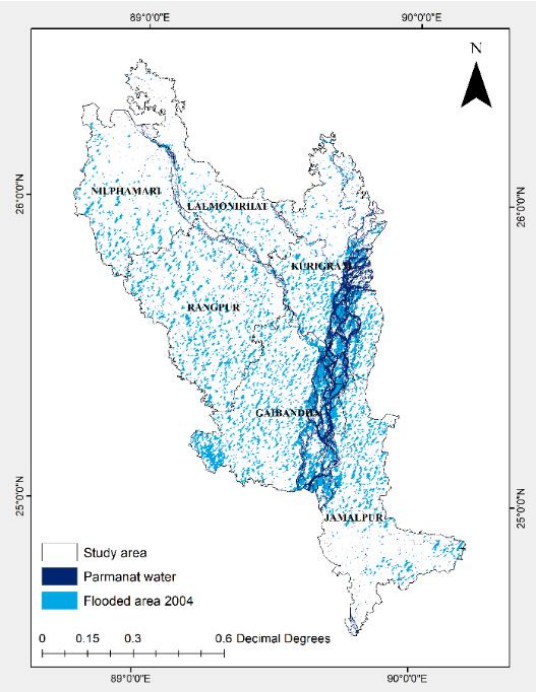

(a)

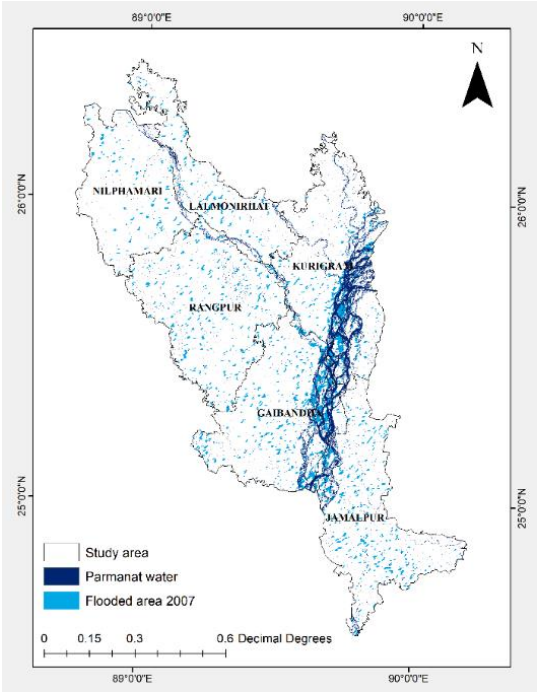

(b)

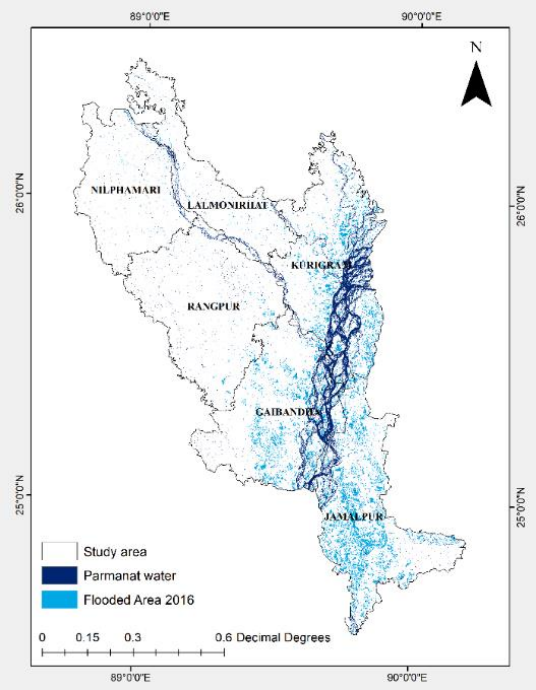

(c)

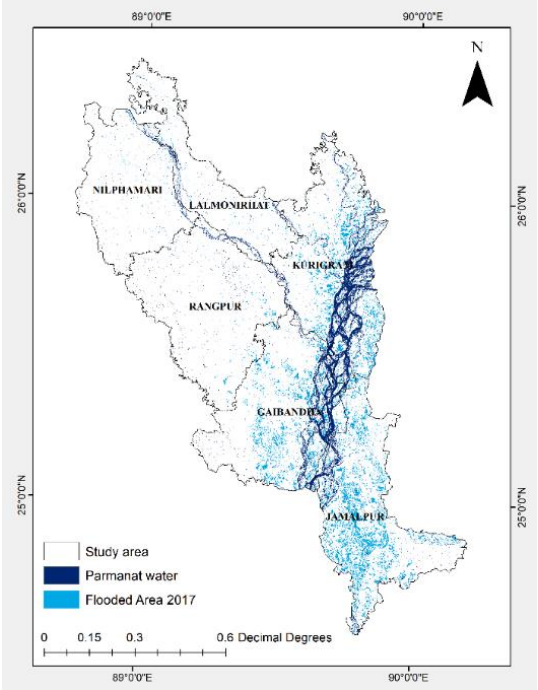

(d)

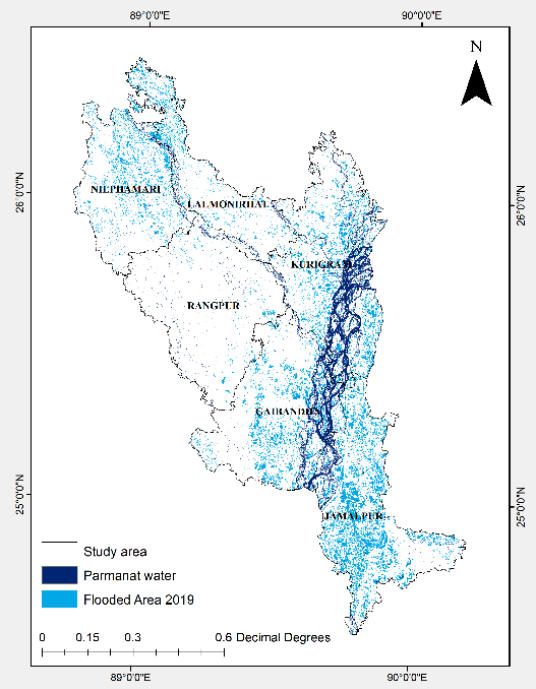

(e)

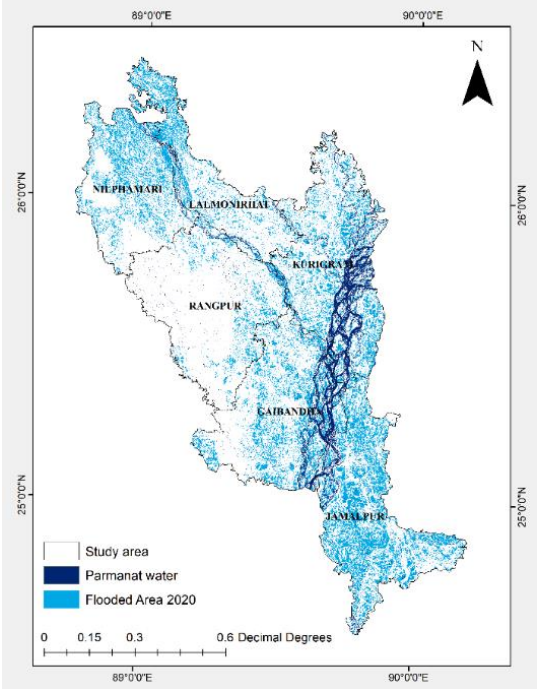

(f)

Figure 5.8: The flood map of (a) 2004, (b) 2007 developed using the MODIS images and (c) 2016, (d) 2017, (e) 2019, (f) 2020 developed using Sentinel-1 image

5.4 Accuracy assessment of Flood Maps using ground truthing

After the generation of the flood map for the study area from SAR satellite images (i.e., Sentinel-1), we also performed the accuracy assessment of the flood map to validate the level of accuracy of this task. For this analysis, the confusion matrix technique is applied through the use of both map and observed data. A confusion matrix is a specified table (i.e., Table 5.4) that is used to define the performance of a classification algorithm by comparing the observed and predicted data providing categories like a true positive, true negative, false positive, and false negative.

Table-5.4: Framework of the confusion matrix

Predicted / **Actual**	**Positive**	**Negative**
Positive	True Positive	False Positive
Negative	False Negative	True Negative

Note:

- True Positive = the number of predicted values correctly predicted as actual positive values;
- False Positive = the number of Predicted values incorrectly predicted Negative values as positive;
- False Negative= the number of predicted values incorrectly predicted negative values as positive; and
- True Negative= the number of predicted values correctly predicted as actual negative values

Finally, Parameters like precision, recall, F-1 score and overall accuracy are calculated to validate the flood map of 2021. Here, Precision parameters in the confusion matrix are defined as the accuracy of the positive class. It measures how likely the prediction of the positive class is correct. A recall is used to calculate the model's ability to predict positive values. This parameter presents how good the model is at recognizing a positive class. The F-1 score is a weighted average score of recall and precision. It is useful when need to take both Precision and Recall into account. The accuracy is used to find the portion of correctly classified values. It tells us how often our classifier is right. The statistical analysis of these above parameters can be calculated by using the following equations below-

$$\text{Precision} = \frac{\text{True positive}}{\text{True positive + False positive}} = \frac{\text{True positive}}{\text{Total predicted positive}} \quad (5.1)$$

$$\text{Recall} = \frac{\text{True positive}}{\text{True positive + False negative}} = \frac{\text{True positive}}{\text{Total actual positive}} \quad (5.2)$$

$$\text{F1} = 2 * \frac{\text{Precision} * \text{Recall}}{\text{Precision + Recall}} \quad (5.3)$$

$$\text{Overall accuracy} = \frac{\text{True positive+False positive}}{\text{Total observed}} \quad (5.4)$$

There are a total of 159 observed points data were used in this analysis, as presented in Table 5.5. Results of the accuracy assessment of 2019 and 2020 flood maps are given summarized in Table 5.6 and 5.7, respectively. Updated maps with the least errors for floods in 2016, 2017, 2019 and 2020 are presented in Figures 5.9, 5.10, 5.11 and 5.12, respectively.

Table 5.5: Location of ground truthing of flood inundation.

No	**Latitude**	**Longitude**	**Flood 2019**	**Flood 2020**
1	25°35'4.174"N	89°39'41.6"E	Yes	Yes
2	25°36'21.44"N	89°39'55.32"E	Yes	Yes
3	25°37'51"N	89°40'28.1"E	Yes	Yes
4	25°37'32.66"N	89°40'31.71"E	Yes	Yes
5	25°33'28.4"N	89°40'1.383"E	Yes	Yes
6	25°33'11.29"N	89°39'37.42"E	Yes	Yes
7	26°13'57.19"N	88°56'37.58"E	Yes	Yes
8	26°13'57.19"N	88°56'37.58"E	Yes	Yes
9	26°13'57.19"N	88°56'37.58"E	Yes	Yes
10	26°11'5.521"N	88°59'4.635"E	Yes	Yes
11	26°11'5.521"N	88°59'4.635"E	Yes	Yes
12	26°10'31.12"N	88°58'20.46"E	Yes	Yes
13	26°10'39.36"N	88°55'53.96"E	Yes	Yes
14	26°9'5.6"N	89°2'2.5738"E	Yes	Yes
15	26°10'43.26"N	88°59'35.21"E	Yes	Yes
16	26°5'1.631"N	89°2'1.7786"E	Yes	No
17	26°11'5.521"N	88°59'4.635"E	Yes	Yes
18	25°9'5.148"N	89°52'17.96"E	Yes	Yes
19	25°7'1.581"N	89°52'13.45"E	Yes	Yes
20	25°10'33.99"N	89°49'20.03"E	Yes	Yes
21	25°10'27.38"N	89°49'40.81"E	Yes	Yes
22	25°8'3.816"N	89°52'27.66"E	Yes	Yes
23	25°10'31.25"N	89°51'7.246"E	Yes	Yes
24	25°12'19.47"N	89°50'56.32"E	Yes	Yes
25	25°13'55.97"N	89°51'7.362"E	Yes	Yes

26	25°13'55.97"N	89°51'7.362"E	Yes	Yes
27	25°12'50.25"N	89°52'10.38"E	Yes	No
28	25°13'30.81"N	89°59'5.848"E	Yes	Yes
29	25°34'2.837"N	89°49'47.53"E	Yes	Yes
30	25°34'28.77"N	89°49'51.68"E	Yes	Yes
31	25°34'33.47"N	89°49'42.26"E	Yes	Yes
32	25°36'46.39"N	89°50'56.44"E	Yes	Yes
33	25°36'33.84"N	89°50'57.39"E	Yes	Yes
34	25°35'25.18"N	89°49'1.869"E	Yes	Yes
35	25°34'46.01"N	89°49'24.52"E	Yes	Yes
36	25°35'23.41"N	89°49'1.243"E	Yes	Yes
37	25°29'25.24"N	89°48'44.87"E	Yes	Yes
38	25°29'47.34"N	89°48'45.33"E	Yes	Yes
39	26°7'5.217"N	89°37'20.61"E	Yes	Yes
40	26°5'5.024"N	89°43'9.112"E	Yes	Yes
41	26°3'5.275"N	89°45'1.054"E	Yes	Yes
42	26°6'1.685"N	89°45'23.14"E	Yes	Yes
43	26°5'5.692"N	89°45'16.68"E	Yes	Yes
44	26°3'5.295"N	89°45'2.131"E	Yes	No
45	26°4'4.459"N	89°52'13.34"E	Yes	No
46	26°7'3.789"N	89°38'33.6"E	Yes	No
47	26°4'1.906"N	89°40'4.18"E	Yes	Yes
48	26°3'4.841"N	89°39'59.89"E	Yes	Yes
49	25°57'34.45"N	89°35'9.603"E	Yes	No
50	26°0'4.822"N	89°35'52.2"E	NO	No
51	25°55'30.13"N	89°34'13.51"E	Yes	No
52	25°55'57.18"N	89°36'22.97"E	Yes	No
53	25°56'13.76"N	89°31'51.34"E	Yes	Yes
54	25°56'2.353"N	89°30'53.13"E	Yes	Yes
55	25°58'47.84"N	89°30'54.54"E	Yes	No
56	25°59'23.94"N	89°31'10.48"E	Yes	No
57	25°59'1.744"N	89°31'21.22"E	Yes	Yes
58	25°57'50.29"N	89°31'27.71"E	Yes	Yes
59	25°14'9.996"N	89°34'57.86"E	Yes	No
60	25°14'2.716"N	89°34'57.62"E	Yes	No
61	25°15'31.53"N	89°36'14.2"E	Yes	No
62	25°16'27.67"N	89°36'14.56"E	Yes	No
63	25°15'55.56"N	89°36'4.348"E	Yes	No
64	25°16'26.37"N	89°36'15.13"E	Yes	No
65	25°16'4.778"N	89°35'19.83"E	Yes	No
66	25°16'55.45"N	89°34'26.22"E	Yes	No
67	25°19'5.372"N	89°43'57"E	Yes	Yes
68	25°19'0.238"N	89°44'14.88"E	Yes	Yes

69	25°18'45.77"N	89°42'52.19"E	Yes	Yes
70	25°11'11.34"N	89°38'1.017"E	Yes	Yes
71	25°11'8.206"N	89°38'6.295"E	Yes	Yes
72	25°11'11.13"N	89°37'56.78"E	Yes	Yes
73	25°11'14.61"N	89°37'58.92"E	Yes	Yes
74	25°11'20.46"N	89°37'49.35"E	Yes	Yes
75	26°4'4.86"N	89°8'3.785"E	Yes	No
76	26°7'2.637"N	89°8'3.224"E	Yes	No
77	26°10'11.73"N	89°6'5.036"E	Yes	No
78	26°10'11.73"N	89°5'5.812"E	Yes	No
79	26°4'4.86"N	89°8'3.785"E	Yes	No
80	24°58'47.69"N	89°49'42.13"E	Yes	Yes
81	24°58'20.12"N	89°45'46.09"E	Yes	Yes
82	24°58'47.69"N	89°49'42.13"E	Yes	Yes
83	24°58'20.12"N	89°45'46.09"E	Yes	Yes
84	24°59'32.52"N	89°49'43.77"E	Yes	Yes
85	25°54'56.82"N	89°39'35.96"E	No	No
86	26°0'1.182"N	89°37'3.705"E	No	No
87	26°0'2.998"N	89°39'18.53"E	Yes	No
88	25°59'36.34"N	89°40'12.61"E	No	No
89	26°0'1.380"N	89°37'1.556"E	No	No
90	25°57'30.78"N	89°42'13.13"E	Yes	Yes
91	25°55'41.42"N	89°44'41.04"E	Yes	Yes
92	25°56'35.16"N	89°43'32.23"E	Yes	Yes
93	25°56'47.01"N	89°44'45.6"E	Yes	Yes
94	25°57'18.59"N	89°44'2.468"E	Yes	Yes
95	25°57'18.77"N	89°43'59.03"E	Yes	Yes
96	25°57'47.93"N	89°43'0.501"E	Yes	Yes
97	25°21'24.28"N	89°33'23.94"E	Yes	Yes
98	25°21'46.13"N	89°35'11.51"E	Yes	Yes
99	25°21'46.14"N	89°35'11.51"E	Yes	Yes
100	25°21'30.82"N	89°36'12.36"E	Yes	Yes
101	25°21'50.09"N	89°35'42.15"E	Yes	Yes
102	25°24'35.52"N	89°34'33.98"E	No	No
103	25°25'48"N	89°34'23.38"E	Yes	No
104	25°17'43.54"N	89°31'57.16"E	No	No
105	25°15'31.69"N	89°32'50.12"E	No	No
106	25°15'59.33"N	89°32'3.3"E	No	No
107	25°35'2.021"N	89°36'2.901"E	Yes	Yes
108	25°35'7.339"N	89°36'18.84"E	Yes	Yes
109	25°35'7.126"N	89°36'19.26"E	Yes	Yes
110	25°35'10.4"N	89°36'42.57"E	Yes	Yes
111	25°35'25.07"N	89°36'44.29"E	Yes	Yes

112	25°41'46.03"N	89°39'41.88"E	Yes	Yes
113	25°41'51.47"N	89°39'57.82"E	Yes	Yes
114	25°41'49.65"N	89°40'15.79"E	Yes	Yes
115	25°41'48.62"N	89°40'26"E	Yes	Yes
116	25°41'49.47"N	89°40'36.23"E	Yes	Yes
117	25°38'17.75"N	89°34'47.23"E	No	No
118	25°33'49.08"N	89°34'44.49"E	No	No
119	25°38'2.979"N	89°34'40.9"E	No	No
120	25°40'19.12"N	89°41'11.18"E	Yes	Yes
121	25°40'19.4"N	89°41'11.04"E	Yes	Yes
122	25°40'20.17"N	89°41'13.81"E	Yes	Yes
123	25°43'21.95"N	89°32'58.41"E	Yes	Yes
124	25°43'23.76"N	89°32'47.98"E	Yes	Yes
125	25°43'22.14"N	89°32'28.93"E	Yes	Yes
126	25°43'21.15"N	89°32'20.77"E	Yes	No
127	25°44'5.672"N	89°32'8.869"E	Yes	Yes
128	25°40'41.62"N	89°40'34"E	Yes	Yes
129	25°40'31.43"N	89°40'34.25"E	Yes	Yes
130	25°40'50.31"N	89°40'35.34"E	Yes	Yes
131	25°40'24.12"N	89°40'53.46"E	Yes	Yes
132	25°40'21.39"N	89°41'4.7"E	Yes	Yes
133	25°40'8.158"N	89°34'8.428"E	No	No
134	25°40'8.425"N	89°34'8.464"E	No	No
135	25°39'44.56"N	89°34'7.118"E	No	No
136	25°39'37.1"N	89°34'4.868"E	No	No
137	25°39'27.24"N	89°34'2.431"E	No	No
138	25°26'36.36"N	89°47'37.28"E	Yes	Yes
139	25°26'34.01"N	89°47'26.49"E	Yes	Yes
140	25°26'33.75"N	89°47'24.29"E	Yes	No
141	25°26'35.99"N	89°48'1.533"E	Yes	Yes
142	25°26'24.1"N	89°48'10.42"E	Yes	Yes
143	25°26'45.87"N	89°48'6.674"E	Yes	Yes
144	25°29'11" N	89°26'11" E	Yes	Yes
145	25°29'12" N	89°26'8" E	Yes	Yes
146	25°29'7" N	89°26'40" E	Yes	Yes
147	25°28'23" N	89°28'10" E	Yes	No
148	25°28'15" N	89°28'11" E	Yes	No
149	25°28'15" N	89°28'11" E	Yes	No
150	25°24'27" N	89°27'29" E	Yes	No
151	25°23'6" N	89°28'11" E	Yes	Yes
152	25°23'6" N	89°28'8" E	No	No
153	25°23'10" N	89°28'10" E	No	No
154	24°53'01 5" N	89°42'71.1"E	Yes	Yes

155	24°53'17.0"N	89°42'22.4"E	Yes	Yes
156	24°54'40.1"N	89°43'19.7"E	Yes	Yes
157	24°56'58 0"N	89°41'19.3"E	Yes	Yes
158	24°56'24 9" N	89°40'52 5'E	Yes	Yes
159	24°55'59.6"N	89°42'44.5"E	Yes	Yes

Table 5.6: Accuracy assessment of Flood map of 2019.

Parameters	Flood	Non-flood
Precision	0.98	0.33
Recall	0.75	0.89
F-1 score	0.85	0.49
Overall accuracy	0.76	

Table 5.7: Accuracy assessment of Flood map of 2020

Parameters	Flood	Non-flood
Precision	0.92	0.63
Recall	0.76	0.86
F-1 score	0.83	0.73
Overall accuracy	0.79	

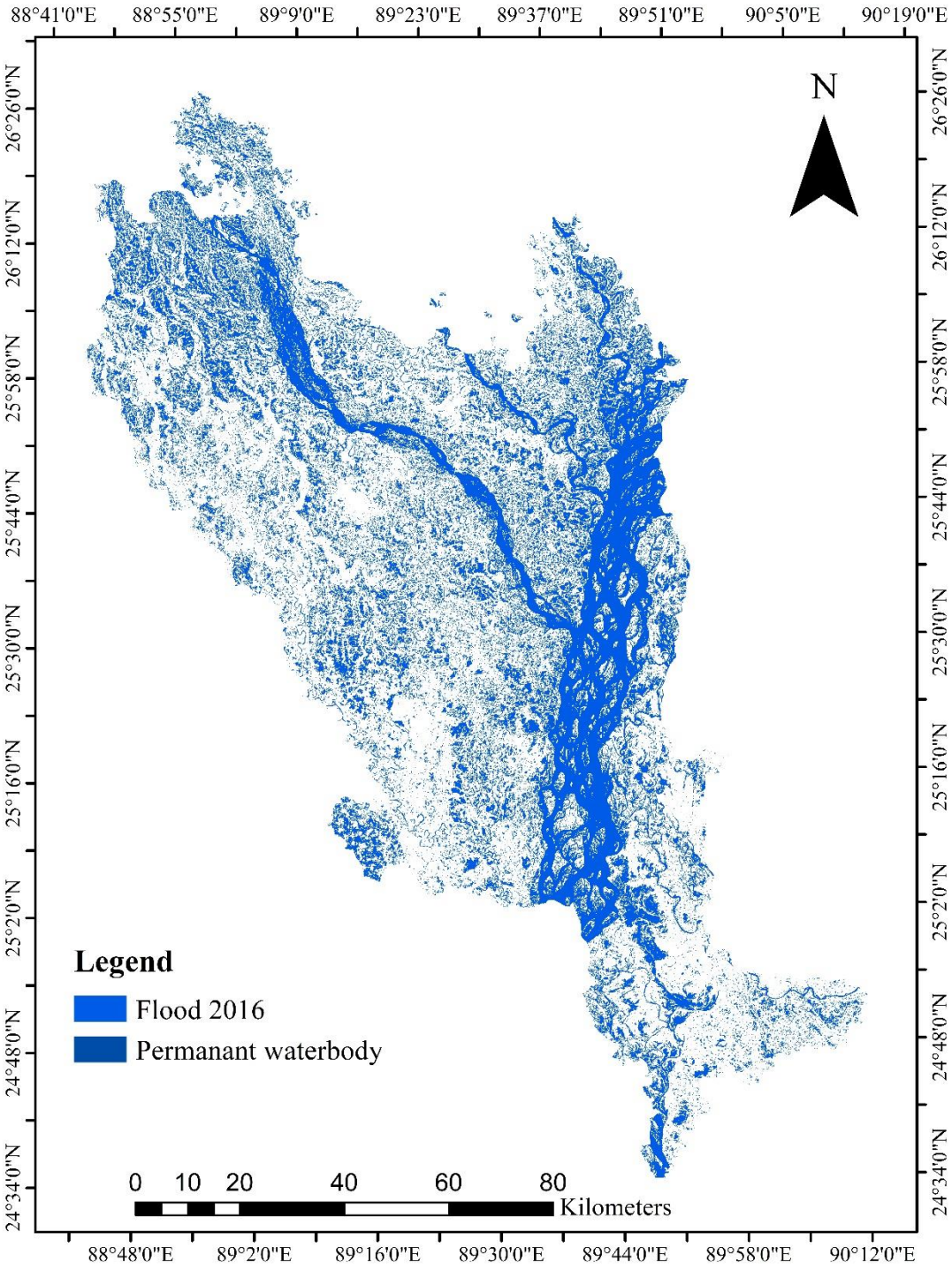

Figure 5.9: Update flood map of 2016 developed using Sentinel-1 image.

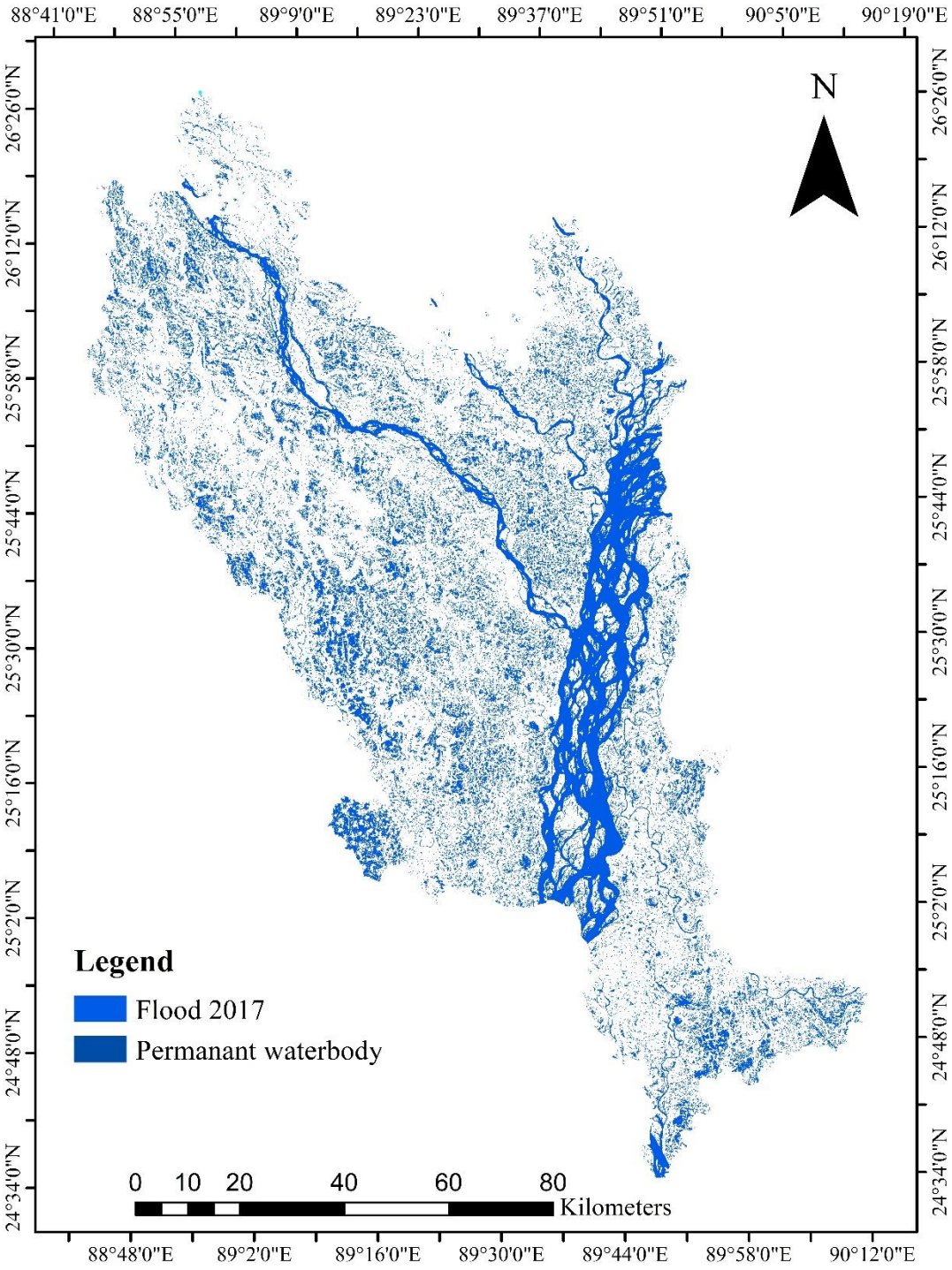

Figure 5.10: Update flood map of 2017 developed using Sentinel-1 image.

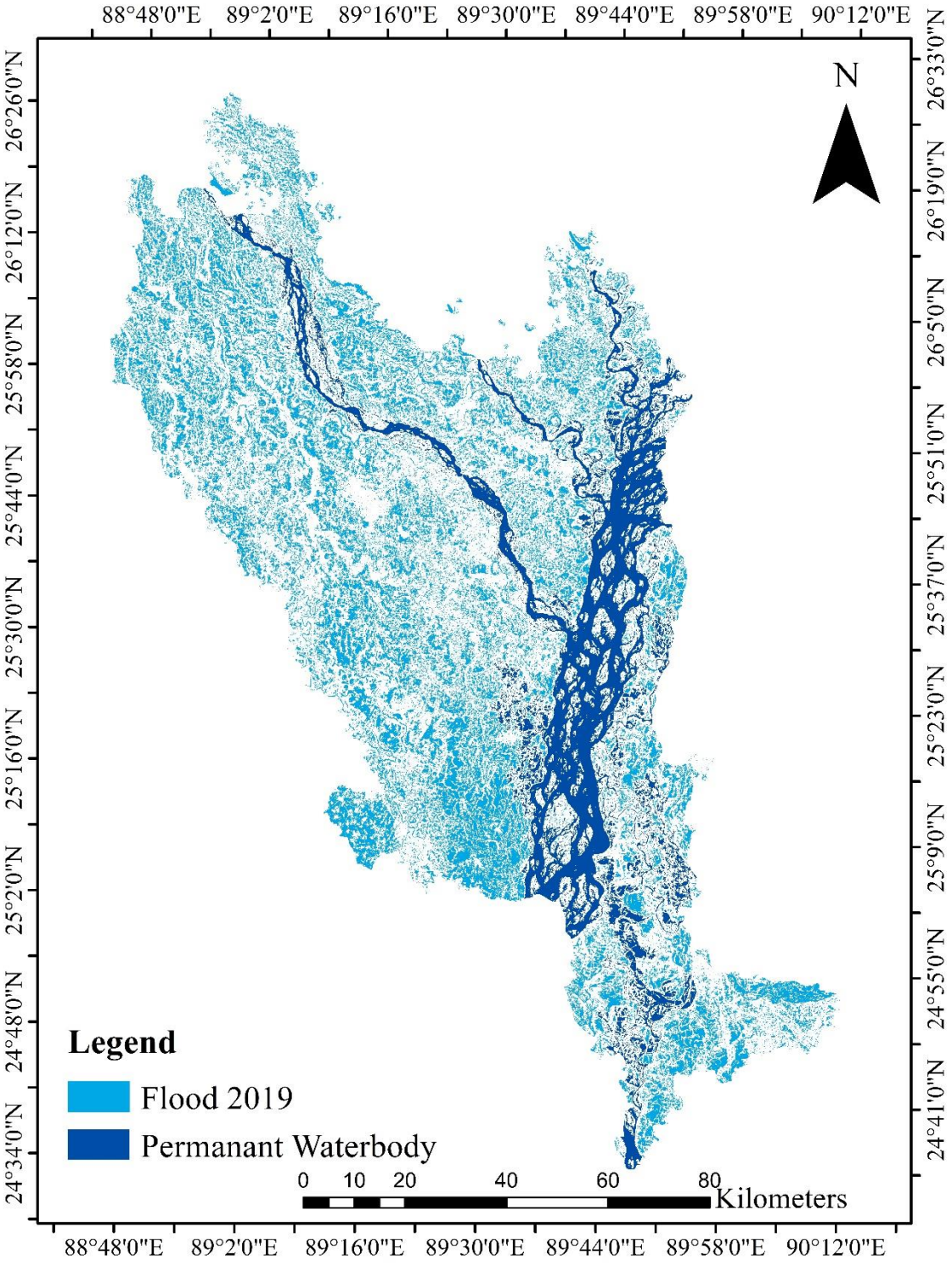

Figure 5.11: Update flood map of 2019 developed using Sentinel-1 image.

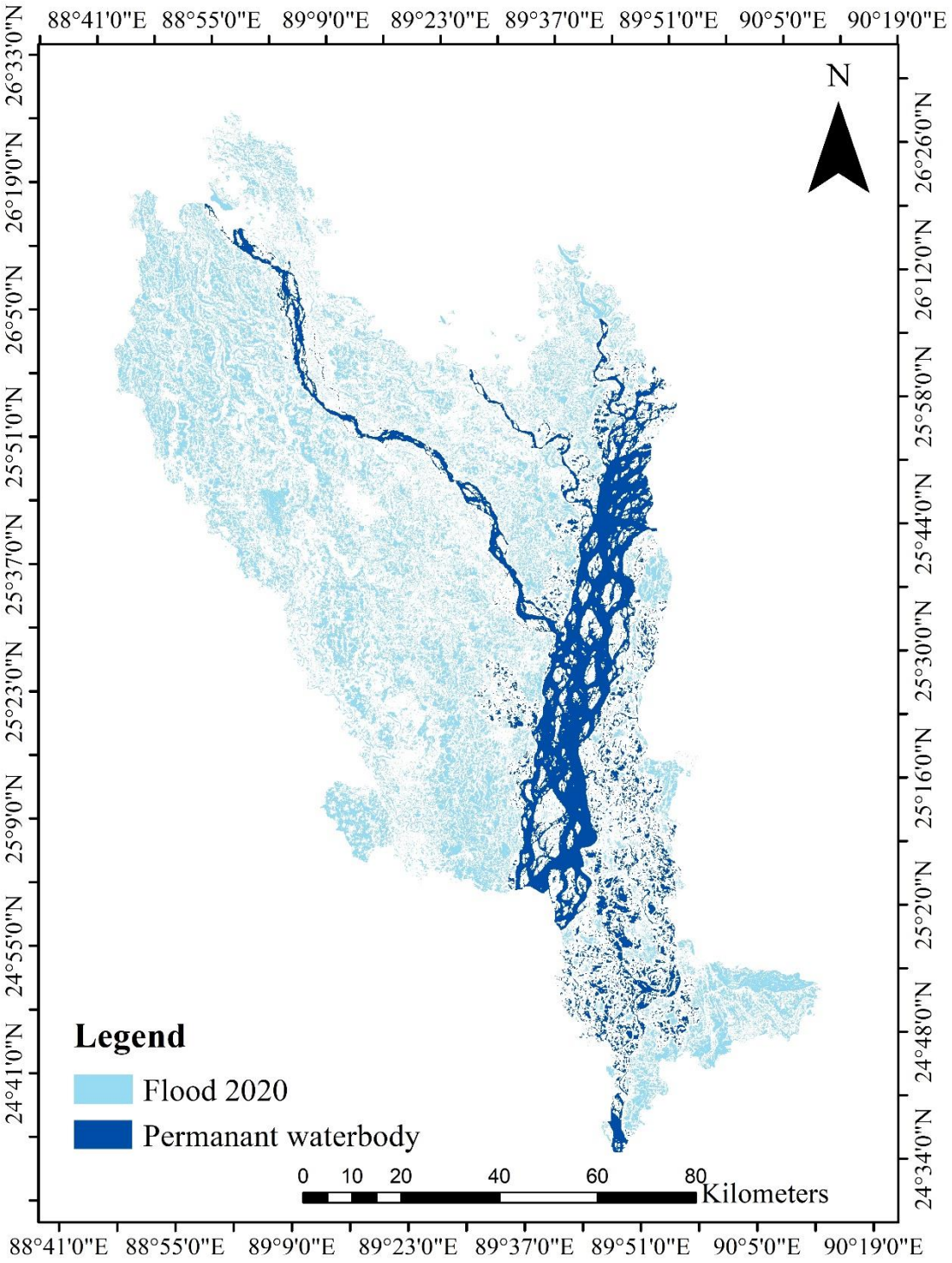

Figure 5.12: Update flood map of 2020 developed using Sentinel-1 image.

5.4 Flood Vulnerability Mapping

A flood vulnerability map has been developed for the project area based on the frequency of flooding during the last six major floods in the recent past. The area which is severely flooded in every major flood is considered a more risk zone, and the area which is flooded by a single flood during this time has been considered a low-risk zone (Figure 5.13).

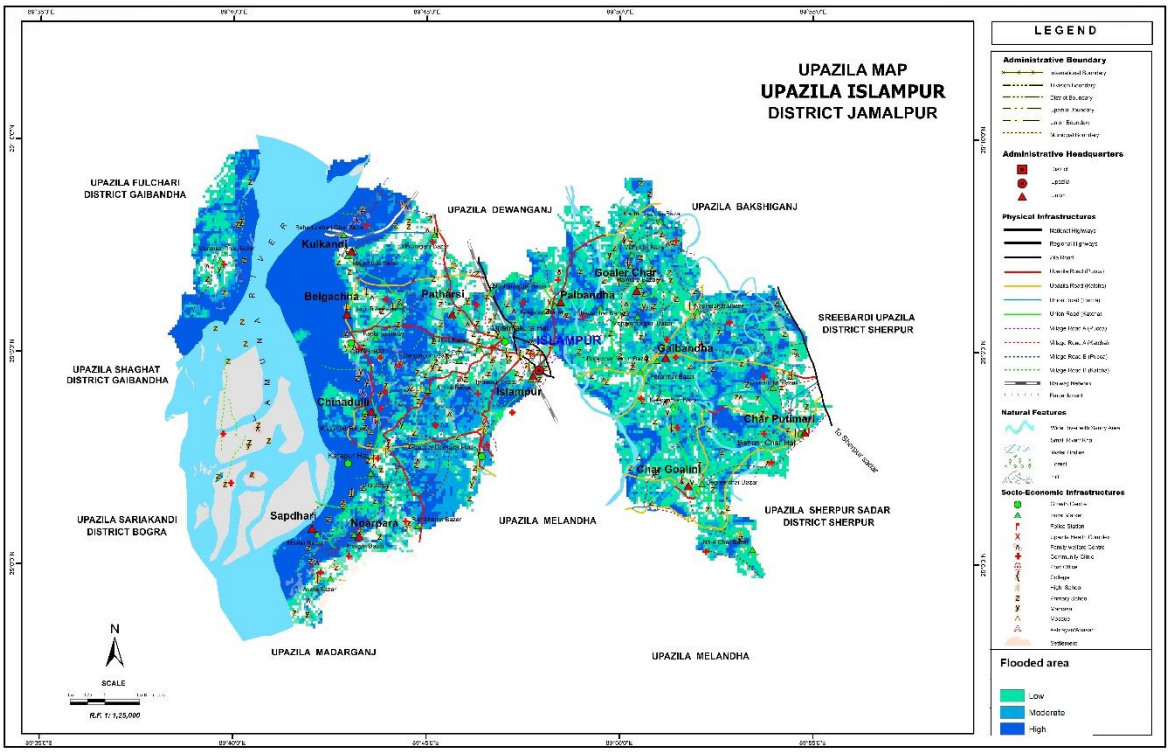

Figure 5.13: Flood vulnerability mapping based on inundation frequency.

A flood vulnerability map of individual Upazila has also been conducted for detailed information. Figures 5.14 and 5.38 show the detailed flood information with other detailed information about critical infrastructure and growing centers which help to understand the overall situation within a single look. The inundation vulnerability map has also been converted to KML format so that it can be observed in detail with fine resolution visual satellite data set provided by Google Earth which will help the decision-maker to have a quick understanding of that area. **All of these composite flood vulnerability maps are prepared in an open source-based Google KML format which can be easily visualized and shared across many applications.**

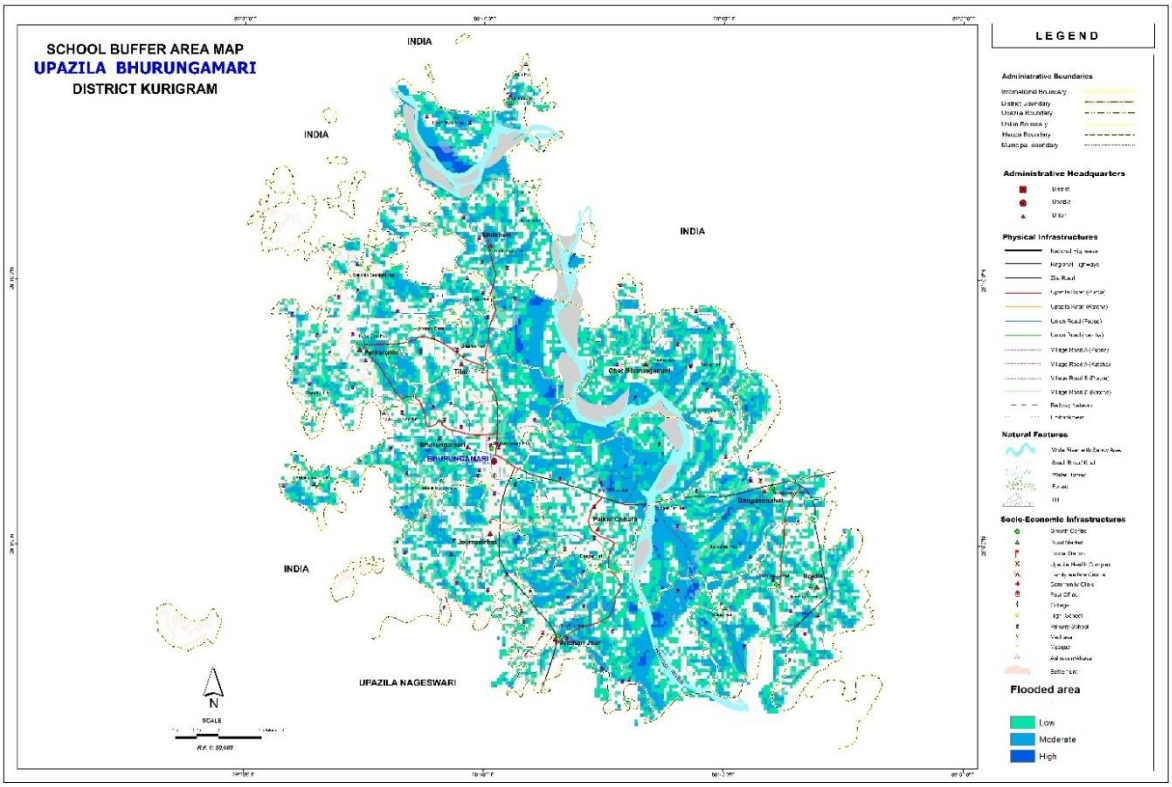

Figure 5.14: Flood vulnerability mapping for Bhurungamari Upazila of Kurigram district.

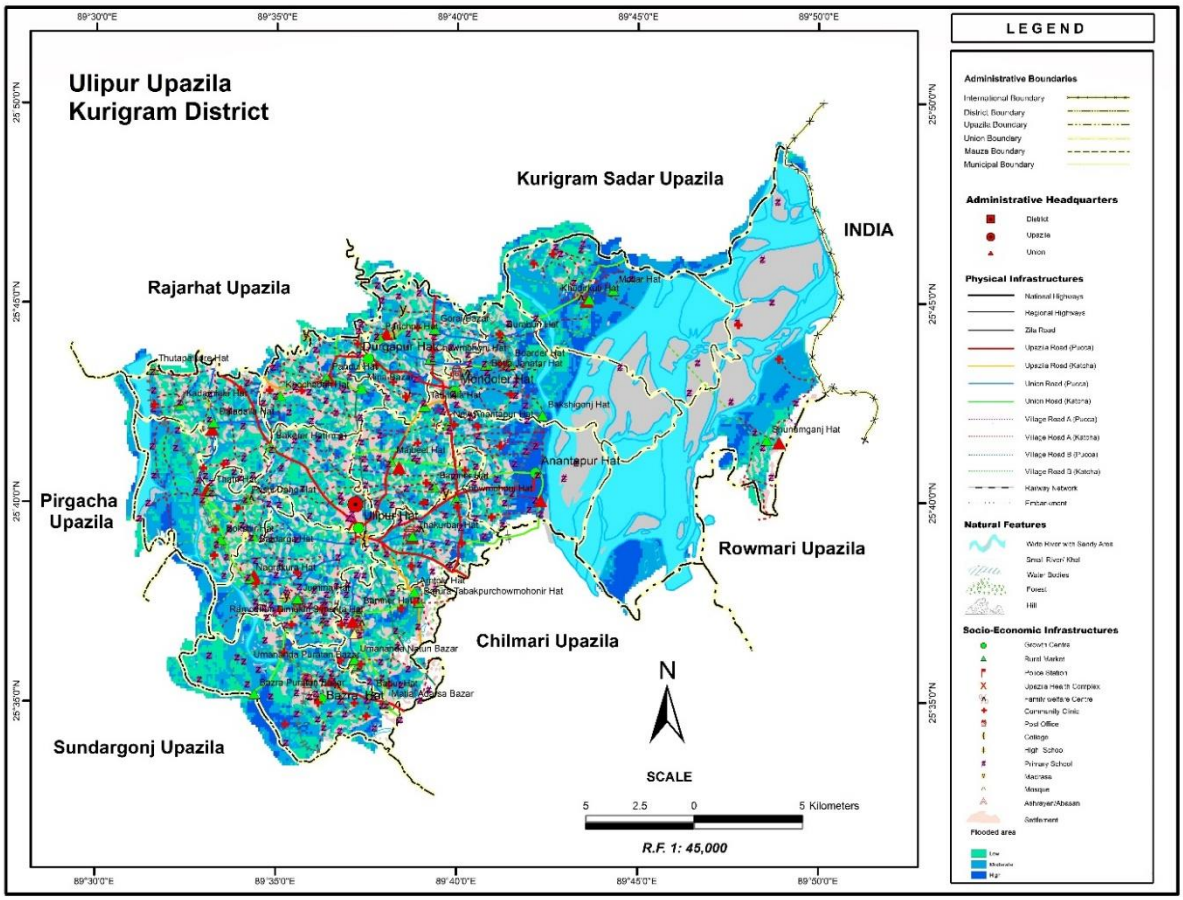

Figure 5.15: Flood vulnerability mapping for Sadar Upazila of Kurigram district.

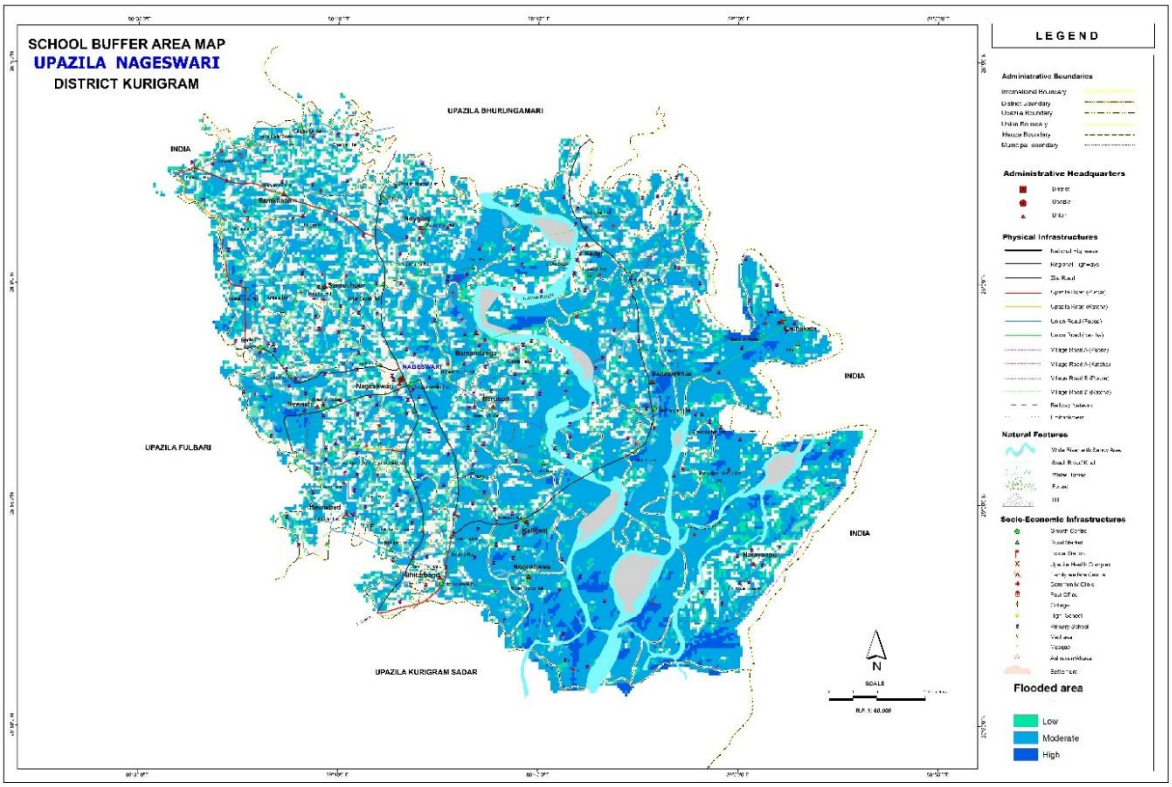

Figure 5.16: Flood vulnerability mapping for Nageswari Upazila of Kurigram district.

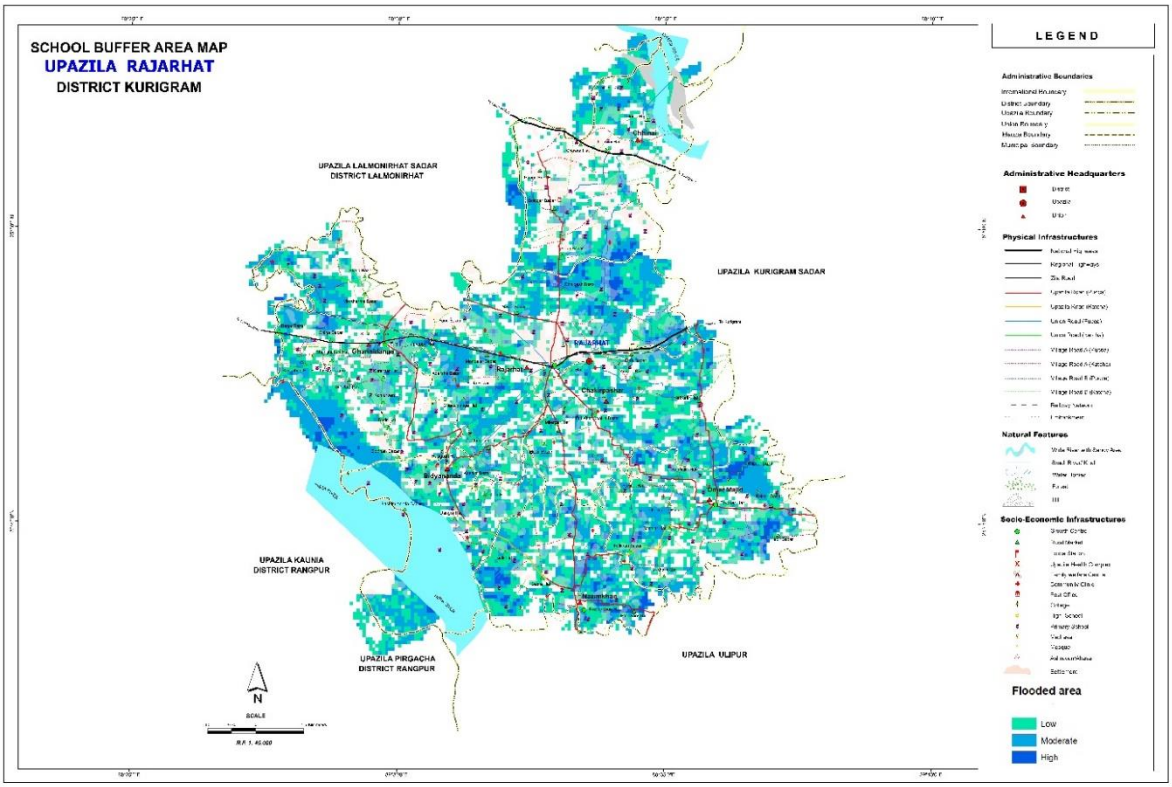

Figure 5.17: Flood vulnerability mapping for Rajarhat Upazila of Kurigram district.

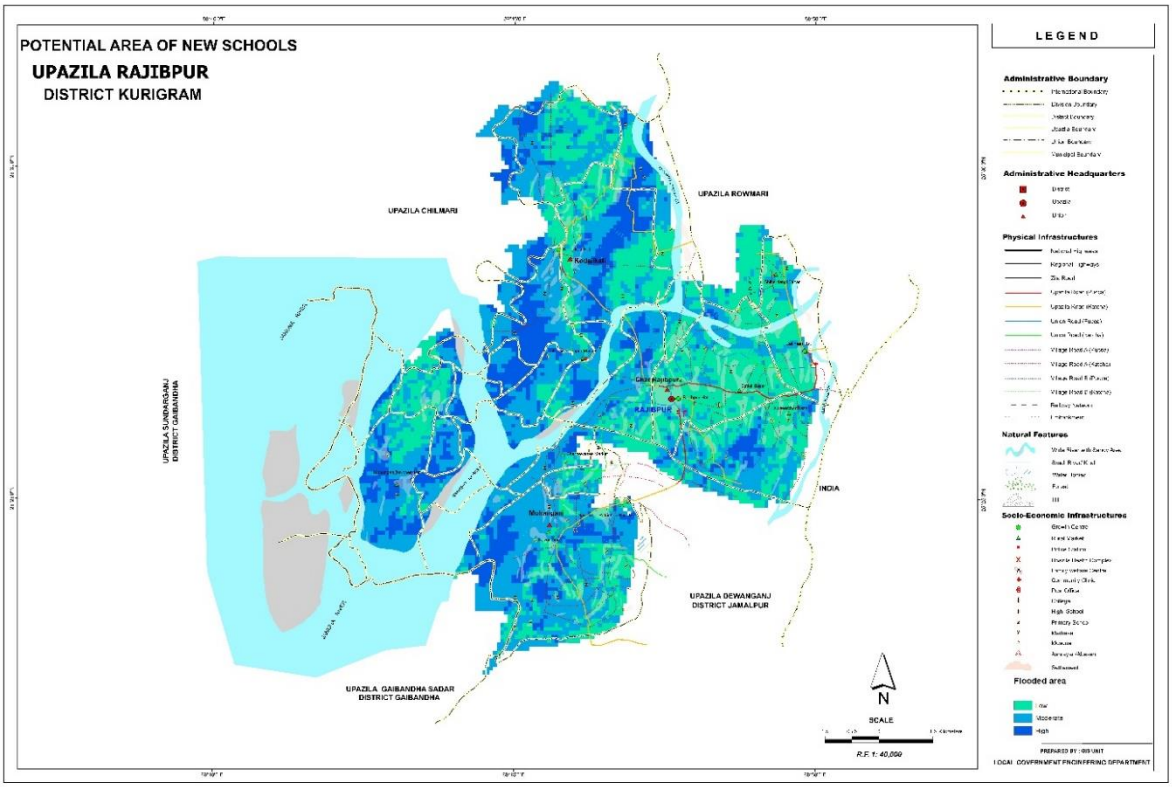

Figure 5.18: Flood vulnerability mapping for Rajibpur Upazila of Kurgram district.

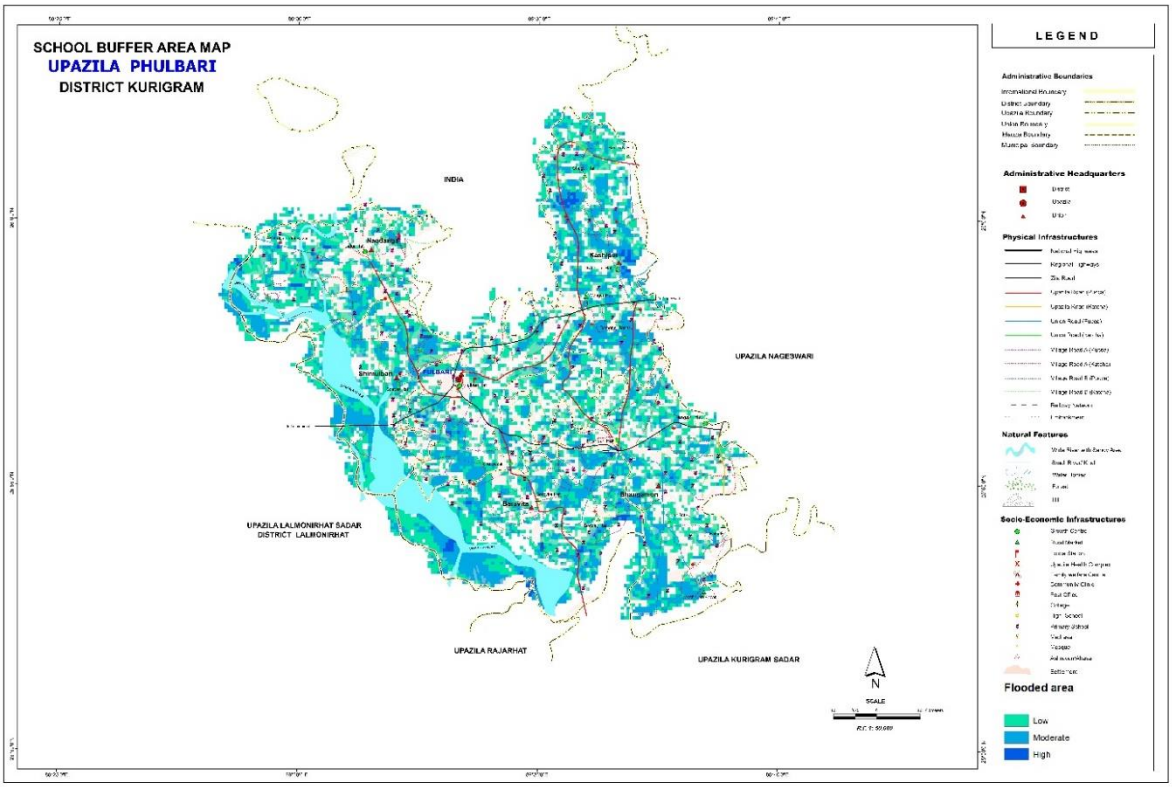

Figure 5.19: Flood vulnerability mapping for Phulbari Upazila of Kurigram district.

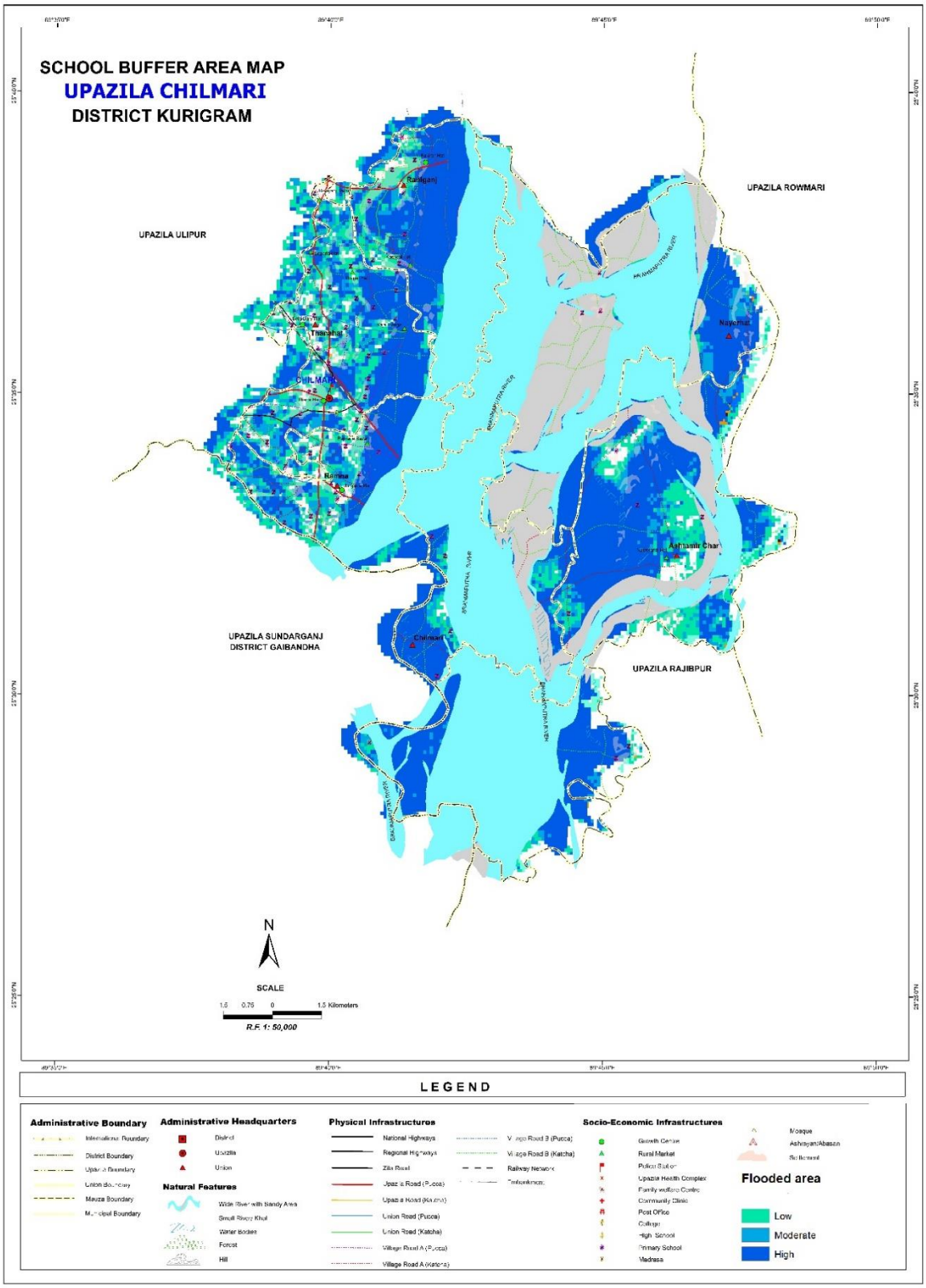

Figure 5.20: Flood vulnerability mapping for Chilmari Upazila of Kurigram district.

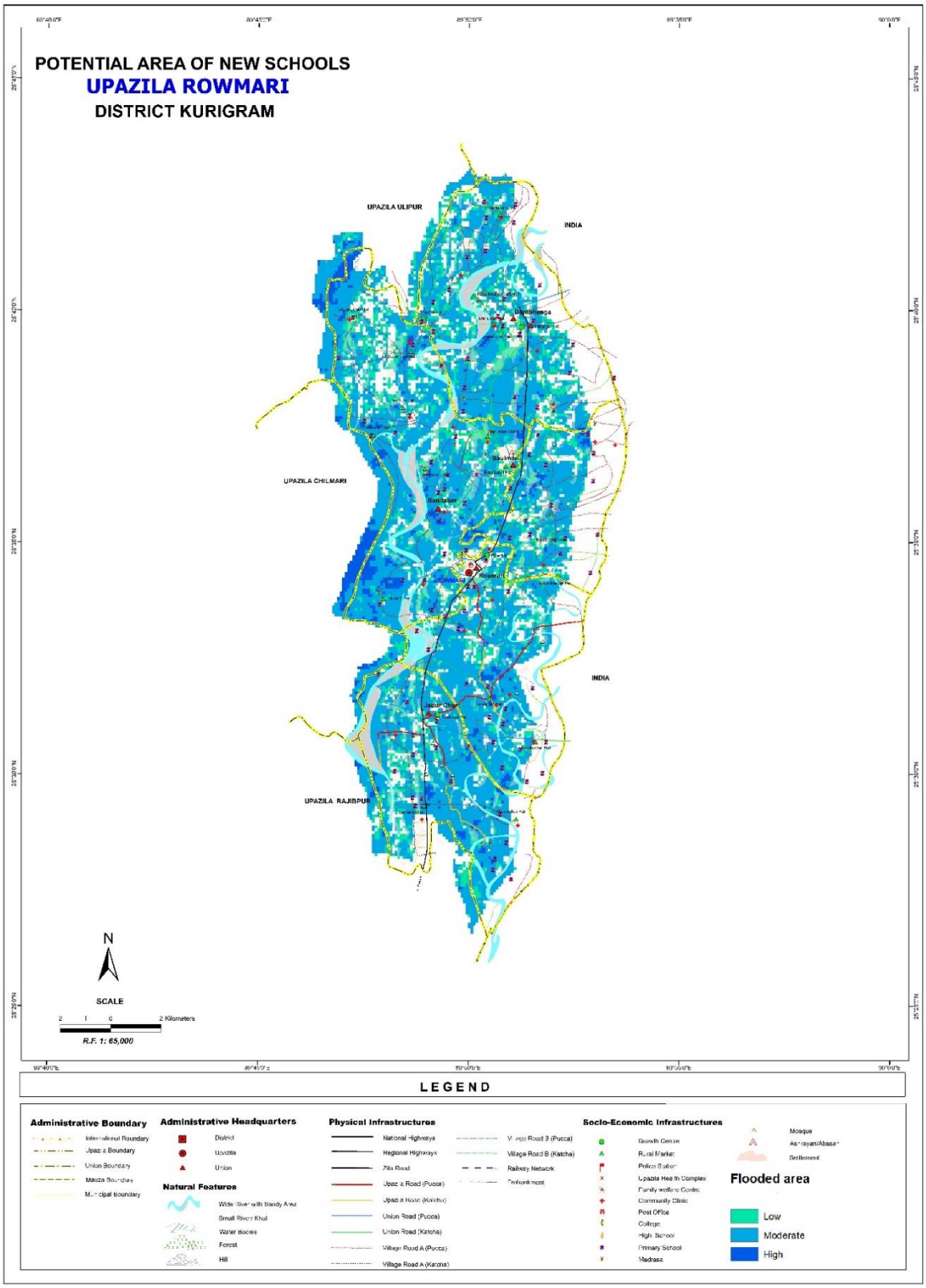

Figure 5.21: Flood vulnerability mapping for Rowmari Upazila of Kurigram district.

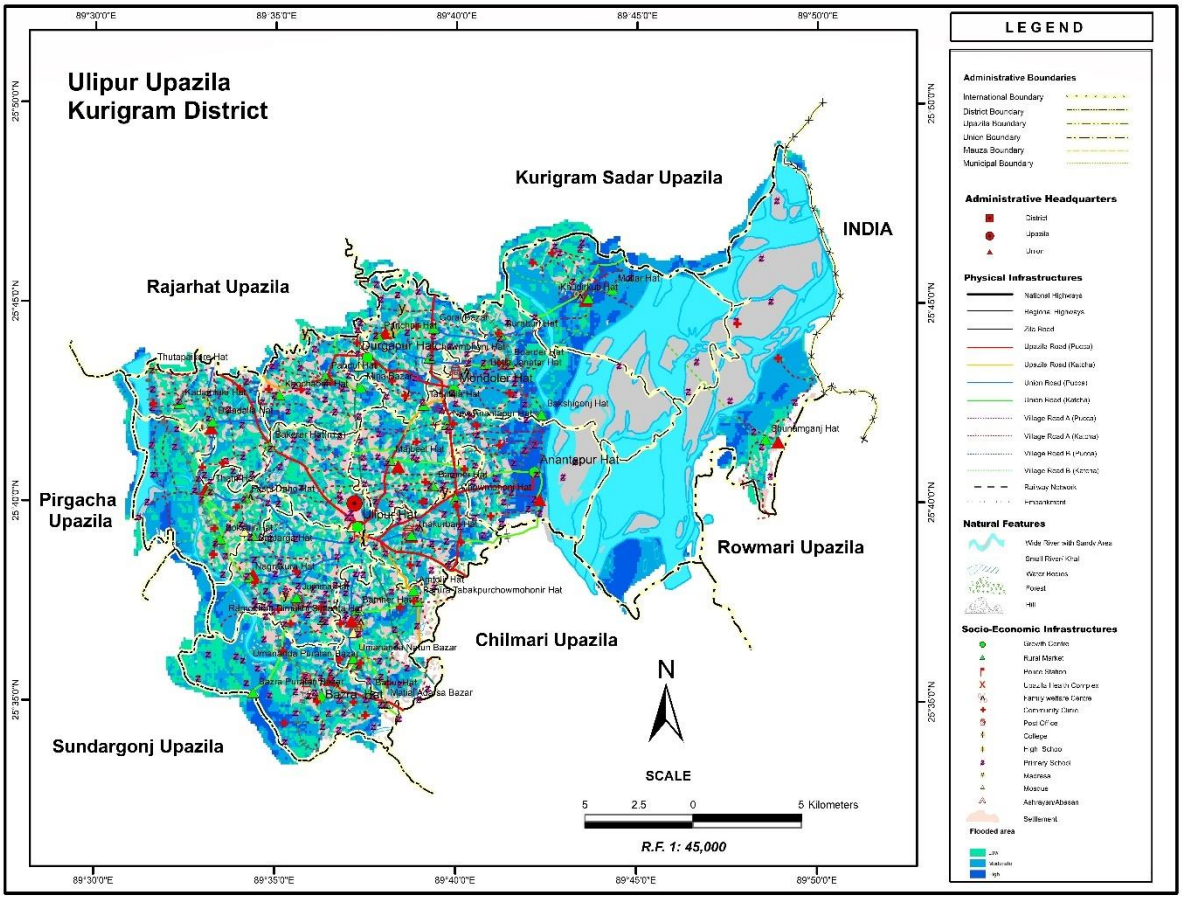

Figure 5.22: Flood vulnerability mapping for Ulipur Upazila of Kurigram district.

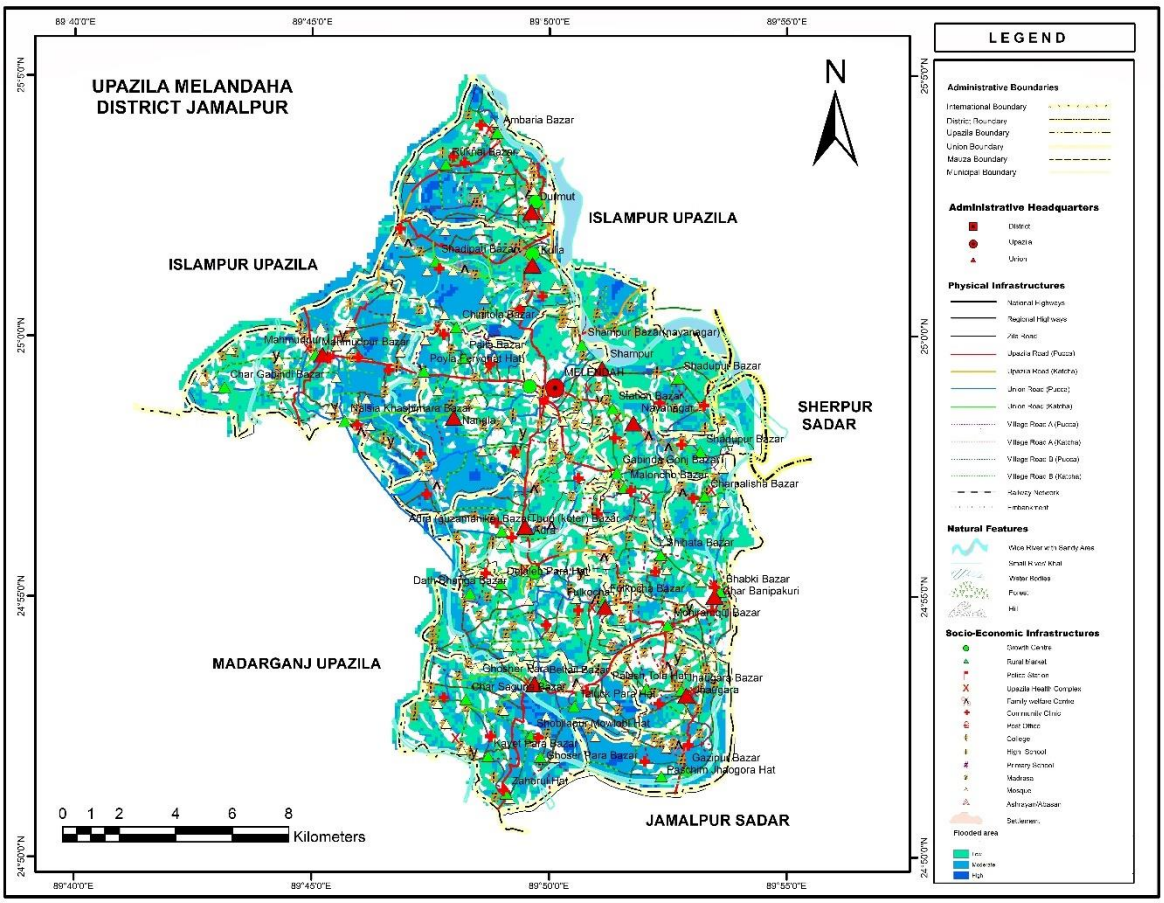

Figure 5.23: Flood vulnerability mapping for Melandah Upazila of Jamalpur district.

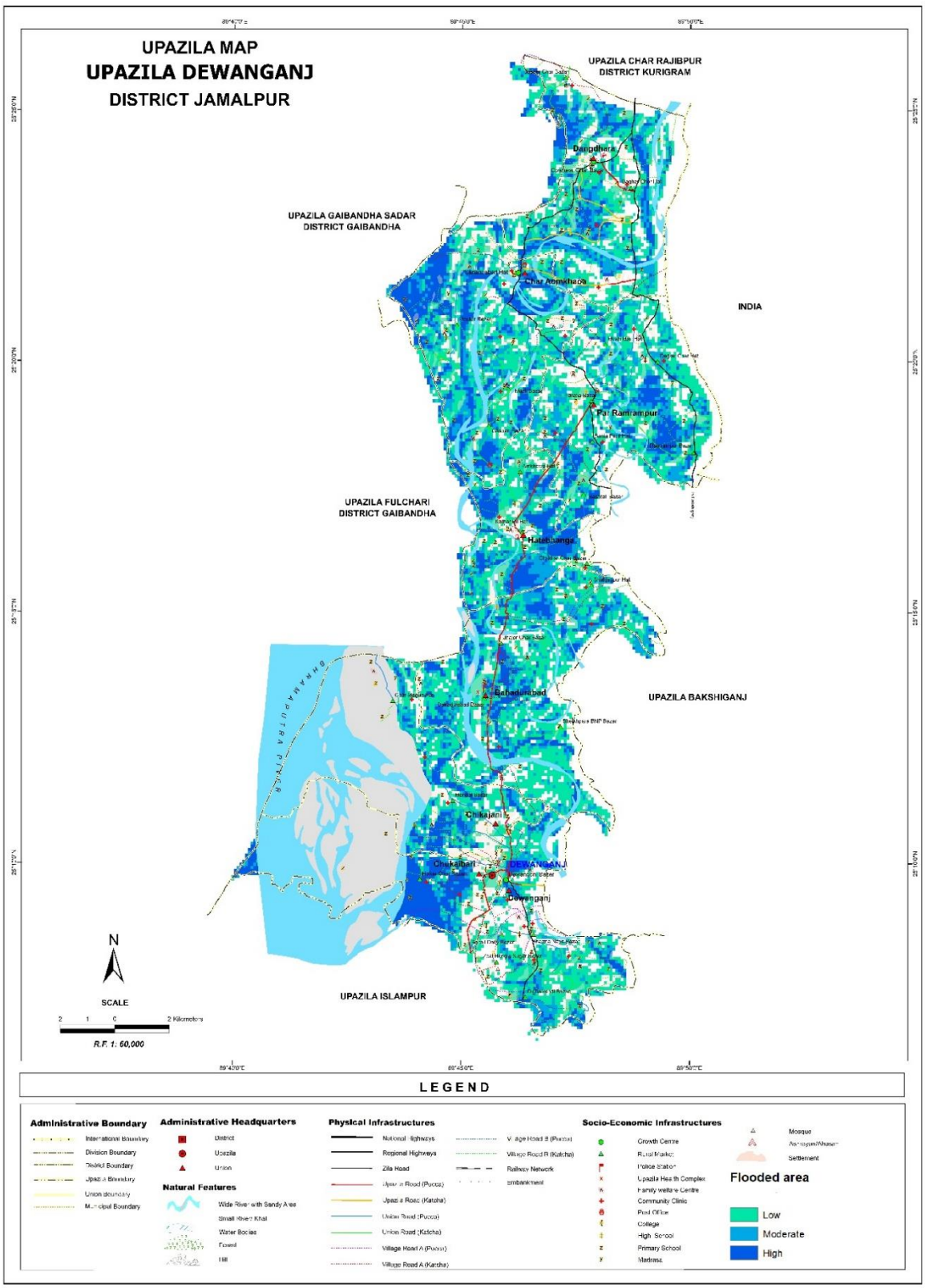

Figure 5.24: Flood vulnerability mapping for Dewanganj Upazila of Jamalpur district.

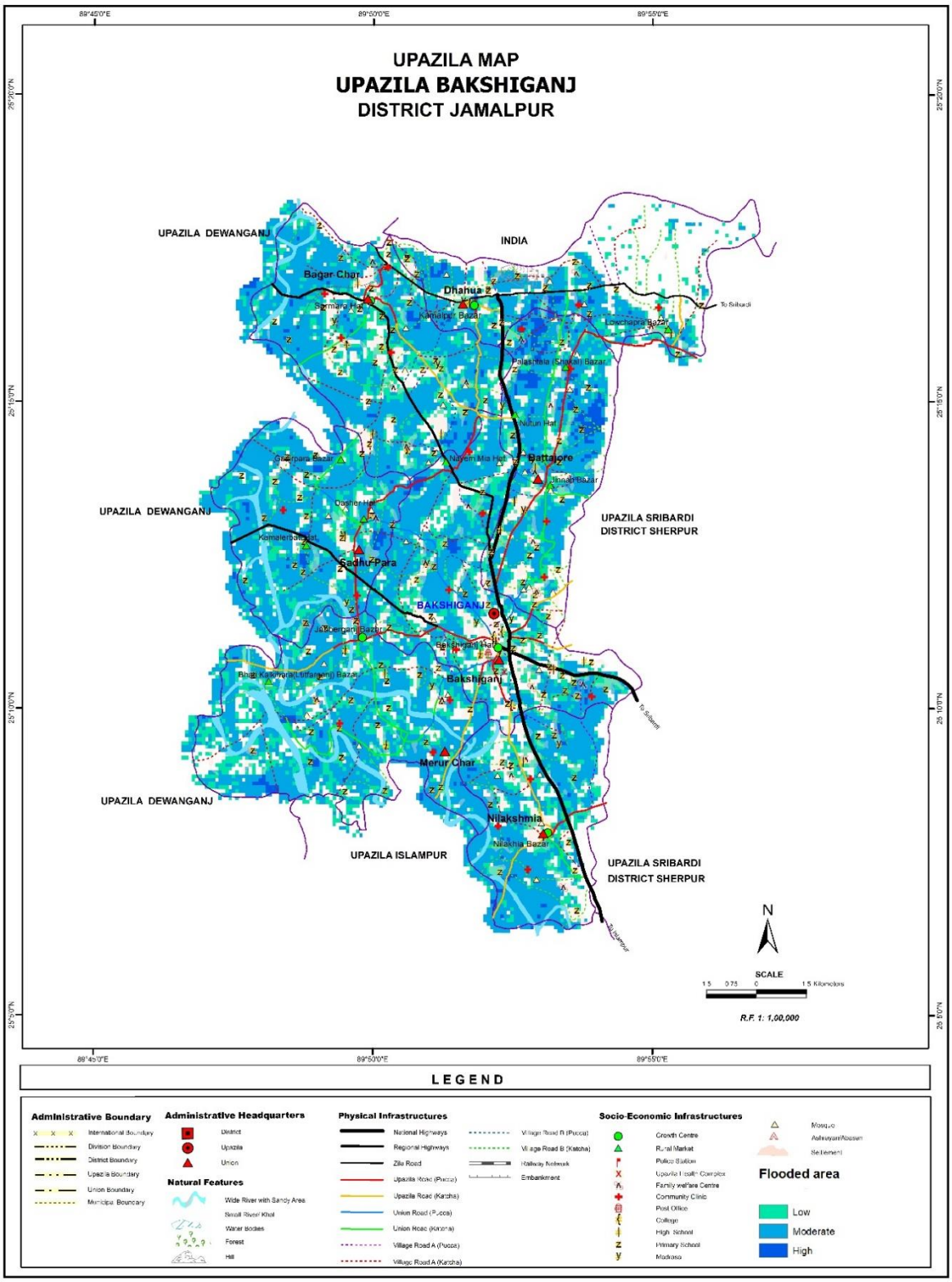

Figure 5.25: Flood vulnerability mapping for Bakshiganj Upazila of Jamalpur district.

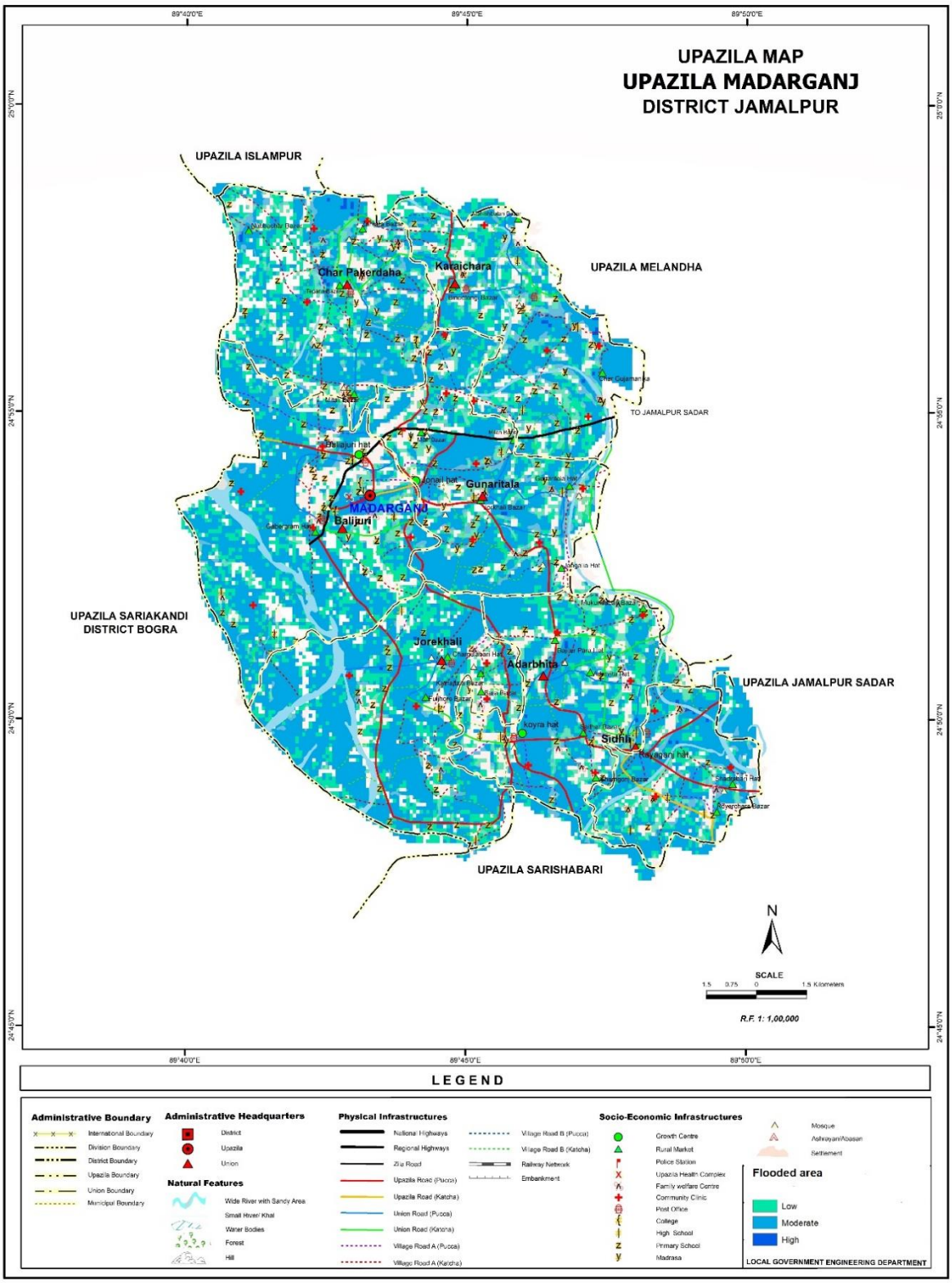

Figure 5.26: Flood vulnerability mapping for Madarganj Upazila of Jamalpur district.

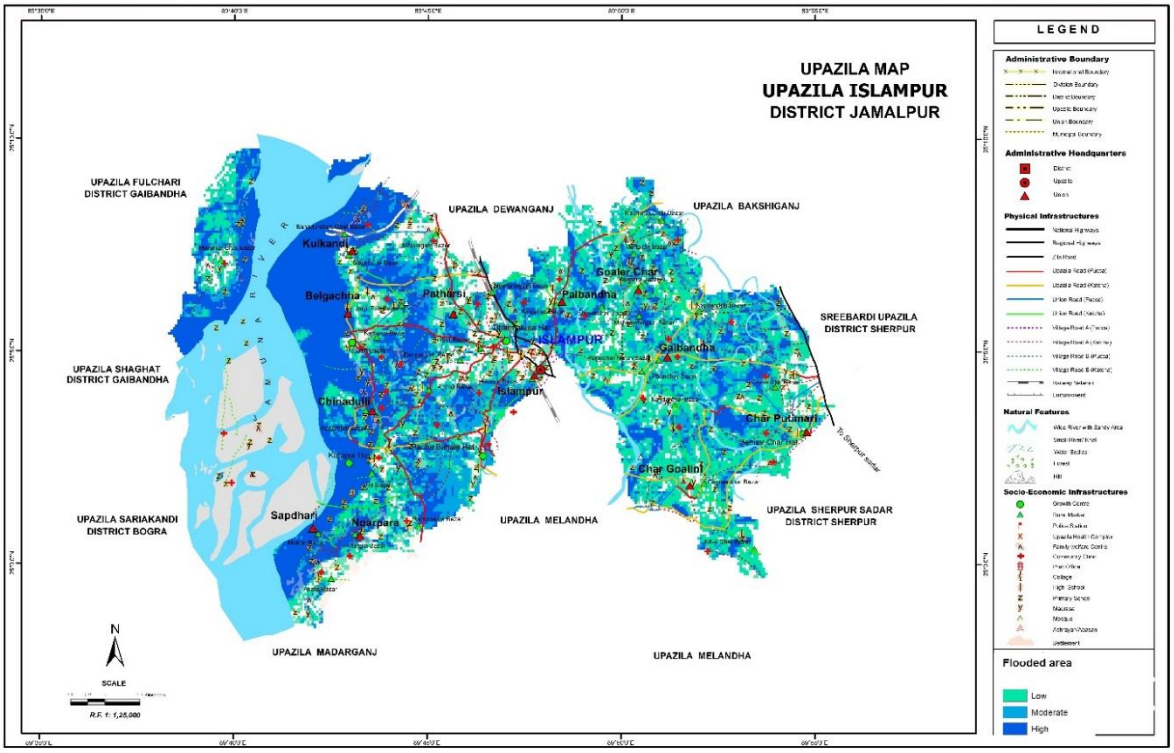

Figure 5.27: Flood vulnerability mapping for Islampur Upazila of Jamalpur district.

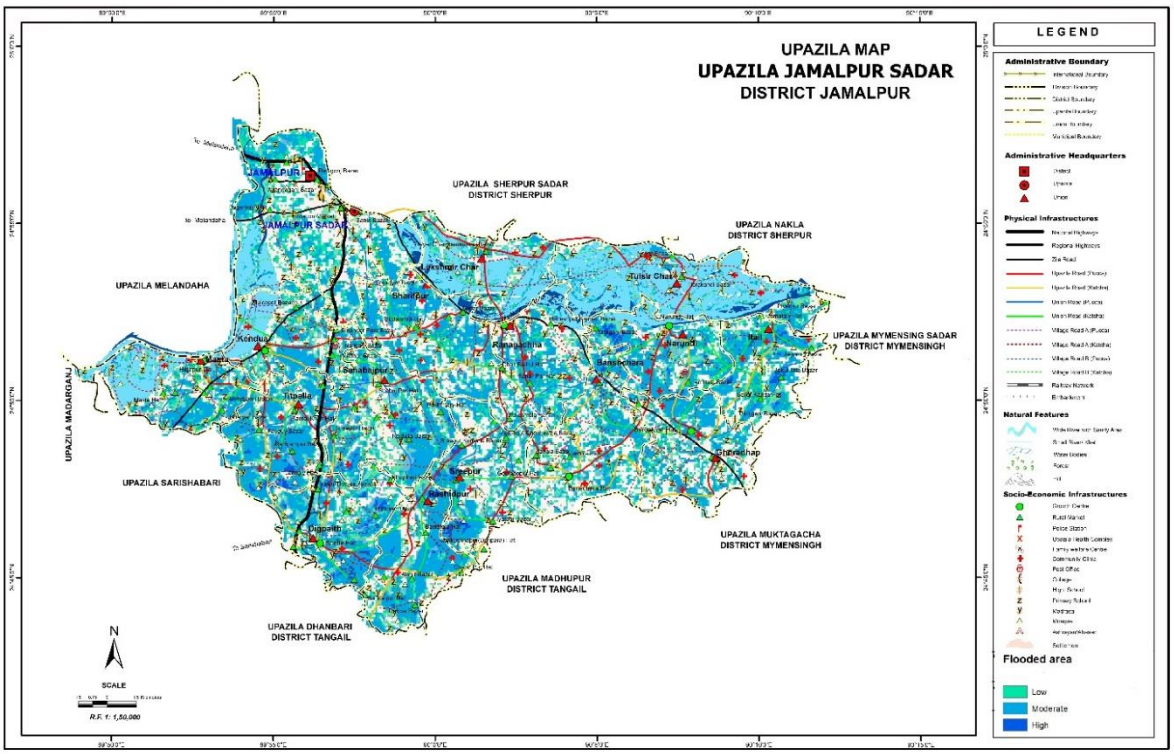

Figure 5.28: Flood vulnerability mapping for Sadar Upazila of Jamalpur district.

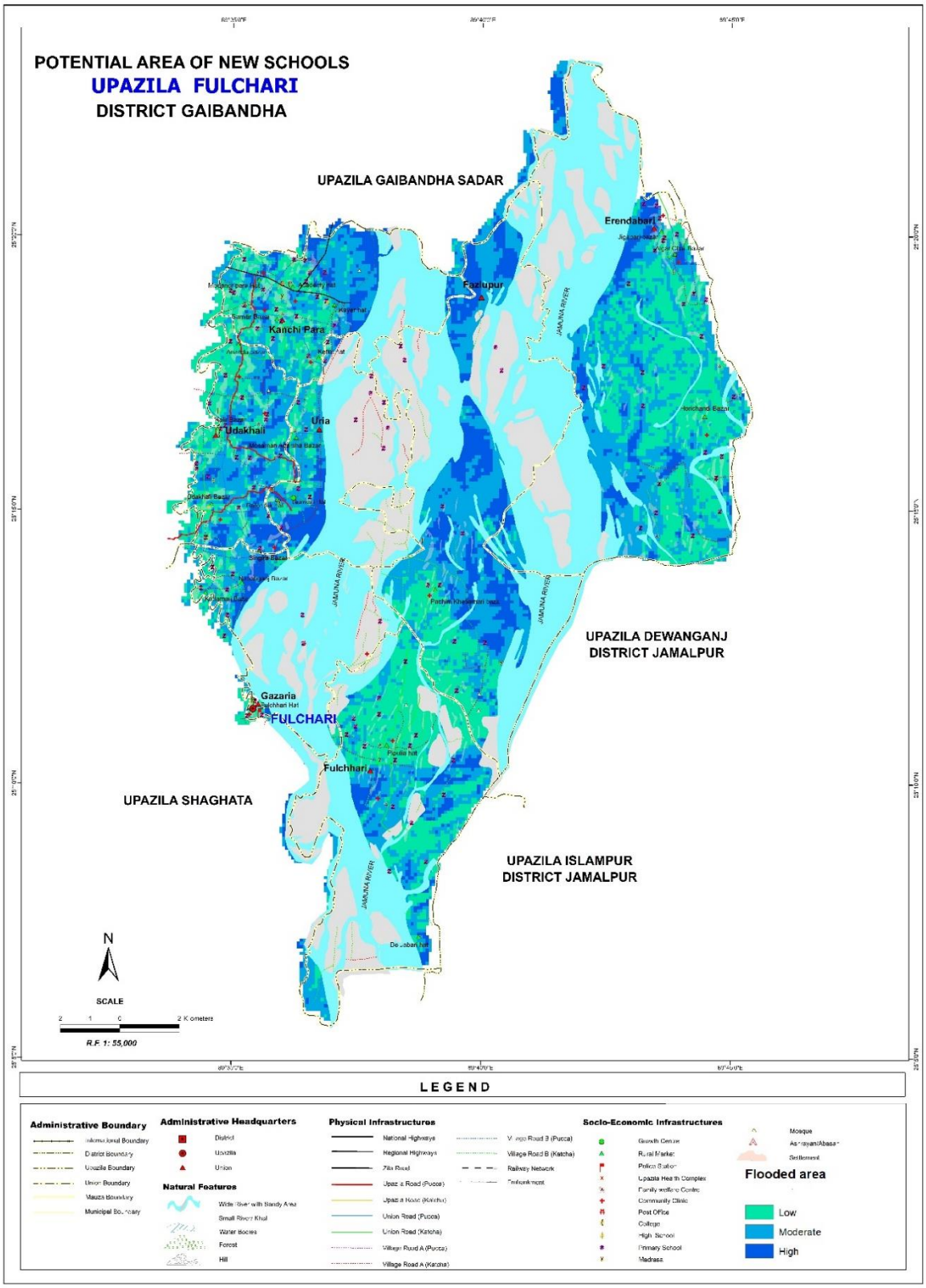

Figure 5.29: Flood vulnerability mapping for Fulchari Upazila of Gaibandha district.

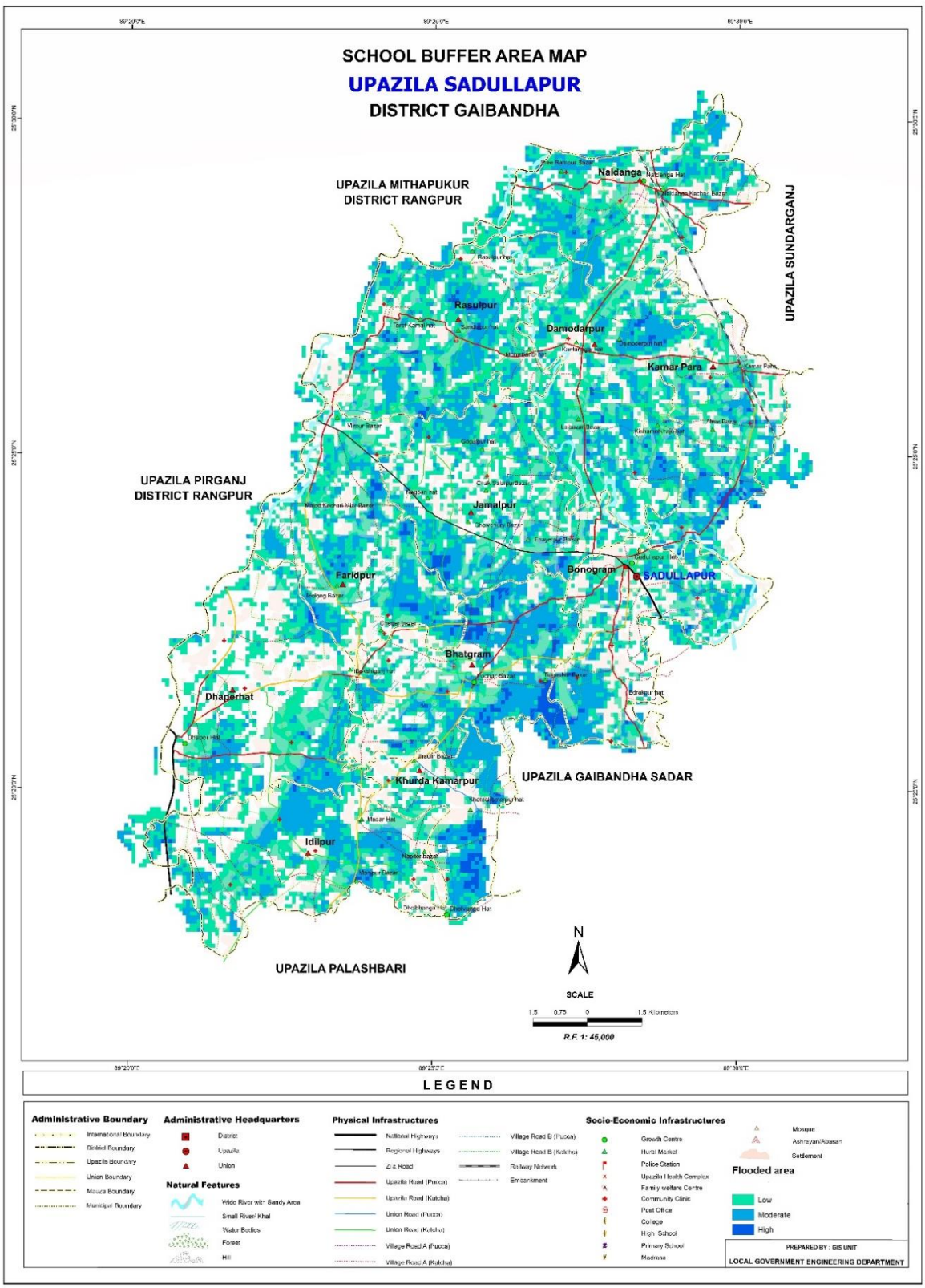

Figure 5.30: Flood vulnerability mapping for Sadullahpur Upazila of Gaibandha district.

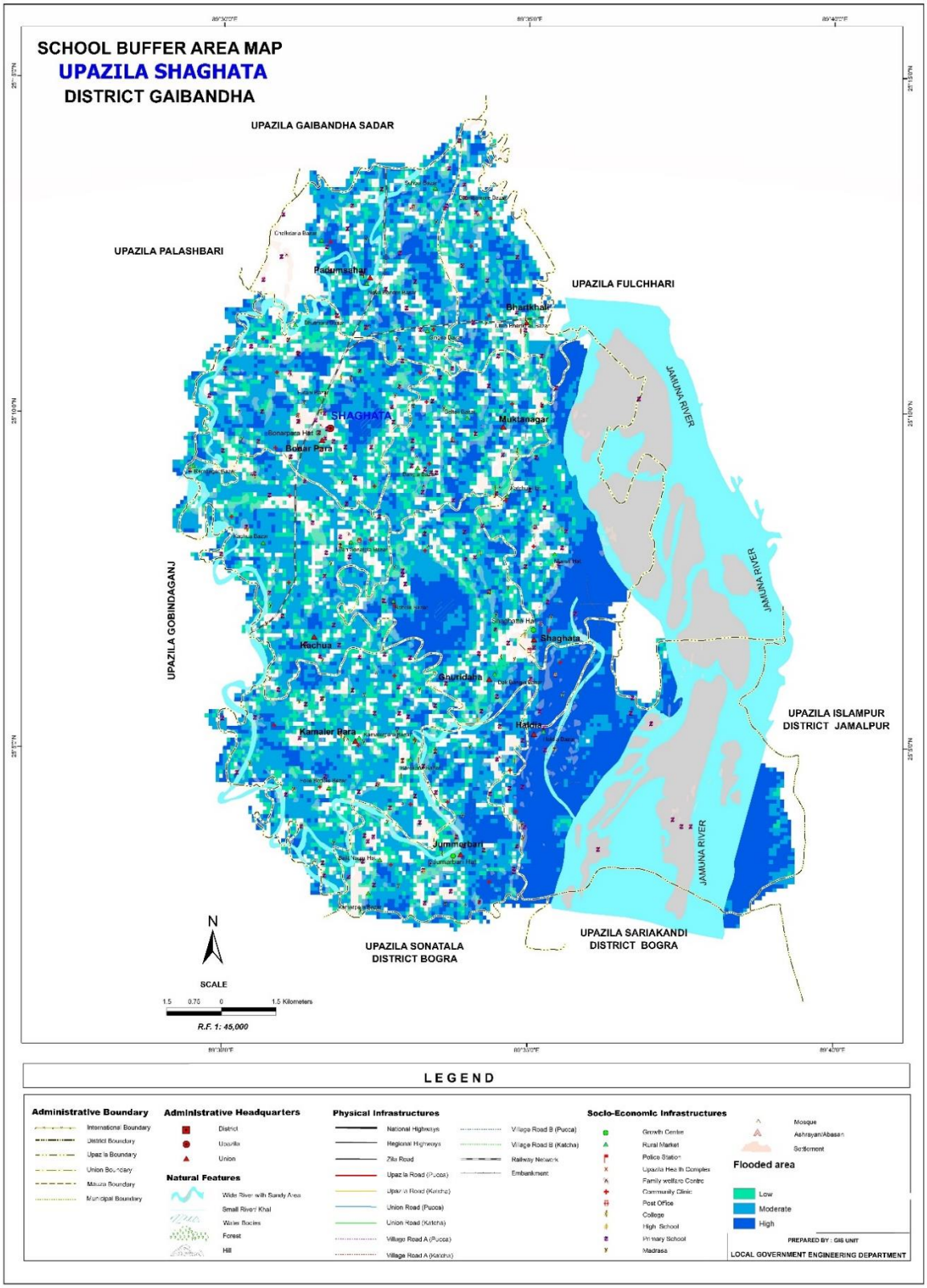

Figure 5.31: Flood vulnerability mapping for Shaghata Upazila of Gaibandha district.

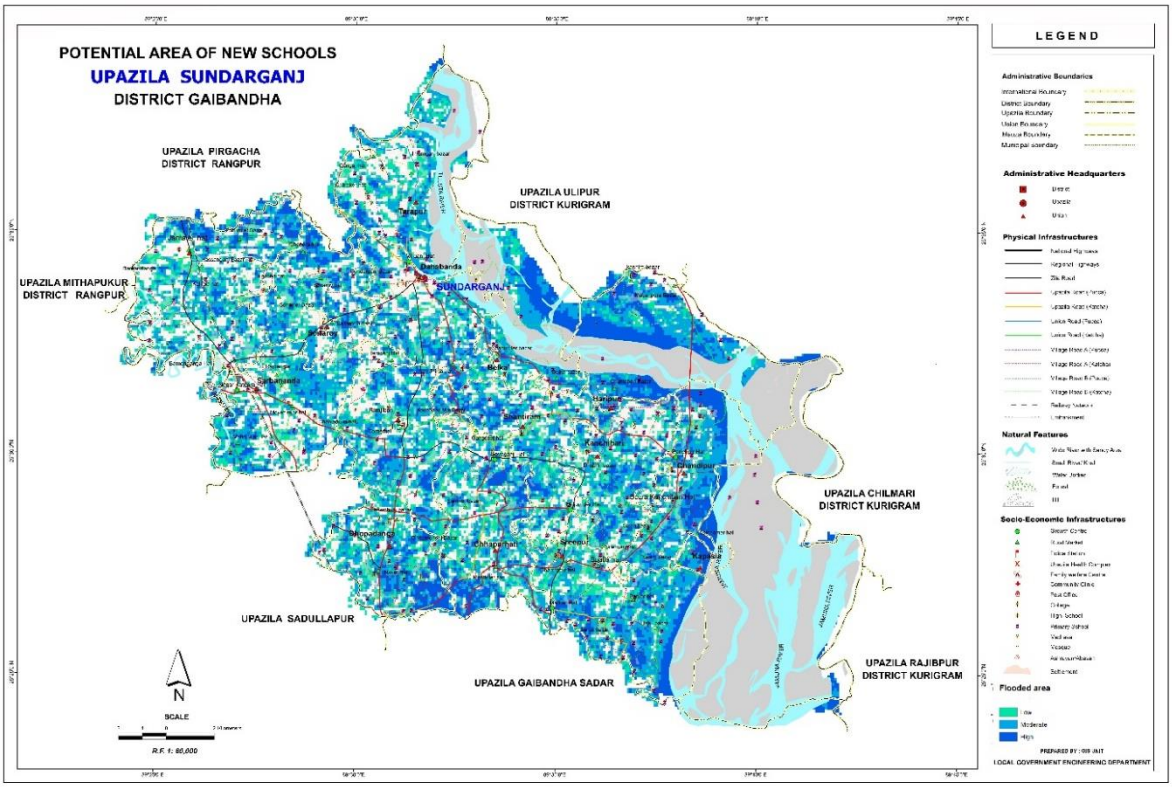

Figure 5.32: Flood vulnerability mapping for Sundarganj Upazila of Gaibandha district.

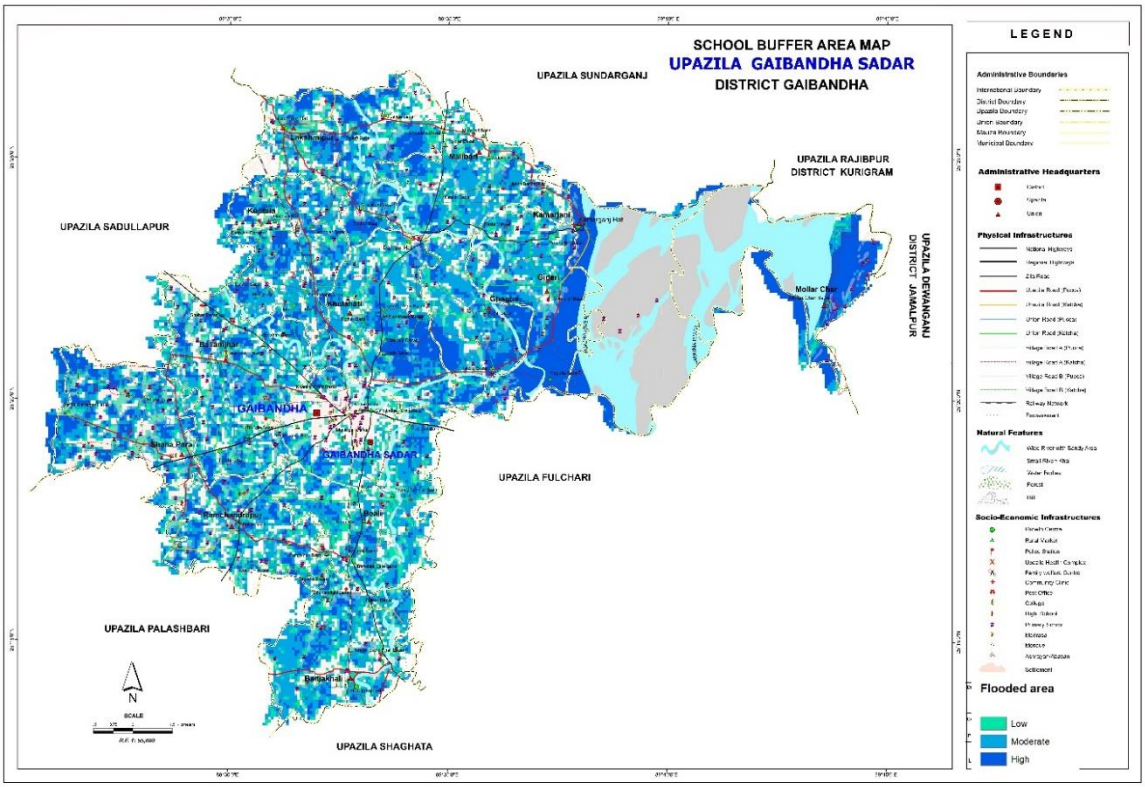

Figure 5.33: Flood vulnerability mapping for Sadar Upazila of Gaibandha district.

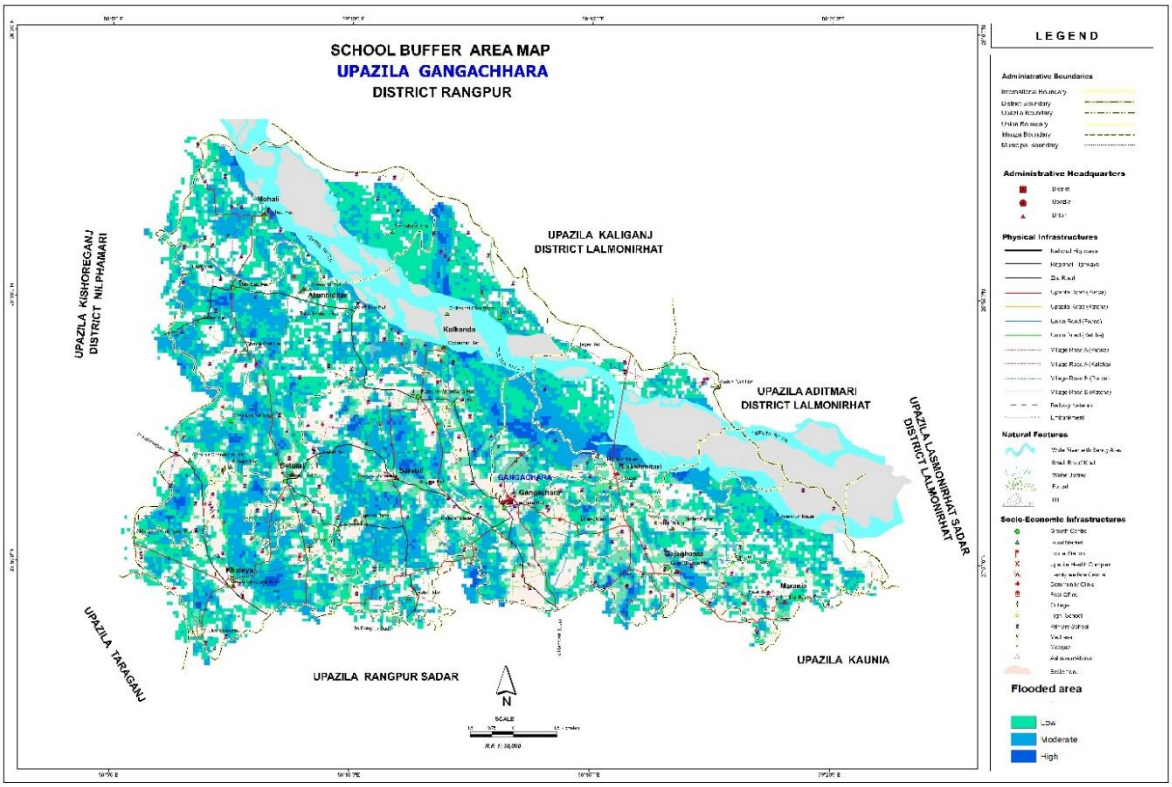

Figure 5.34: Flood vulnerability mapping for Gangachra Upazila of Rangpur district.

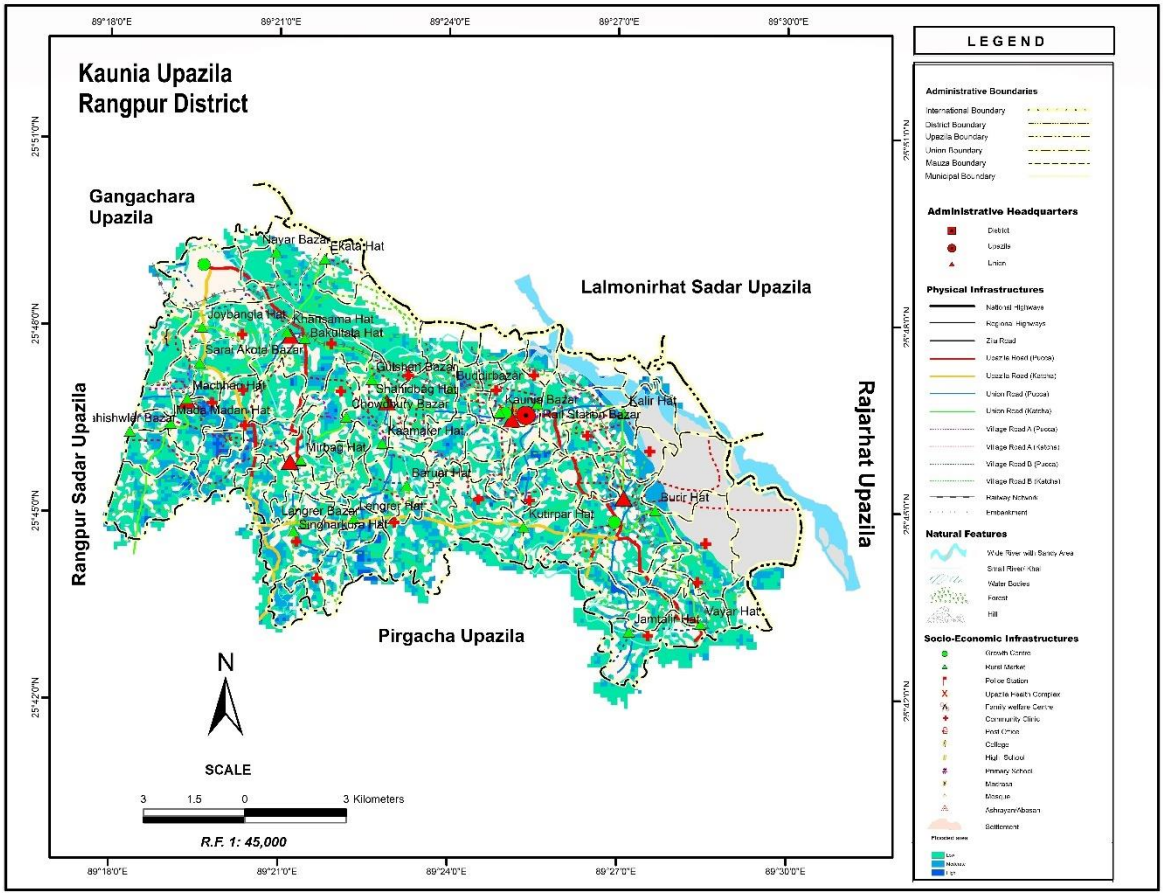

Figure 5.35: Flood vulnerability mapping for Kaunia Upazila of Rangpur district.

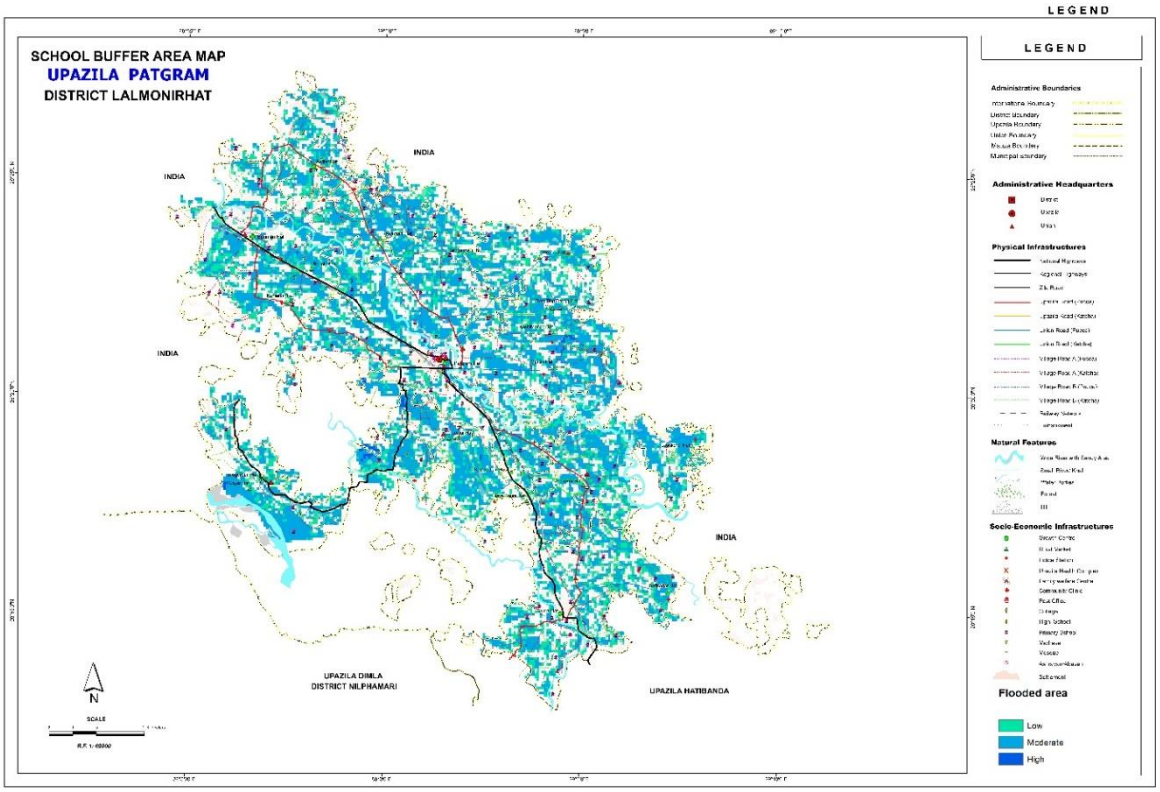

Figure 5.36: Flood vulnerability mapping for Patgram Upazila of Lalmonirhat district.

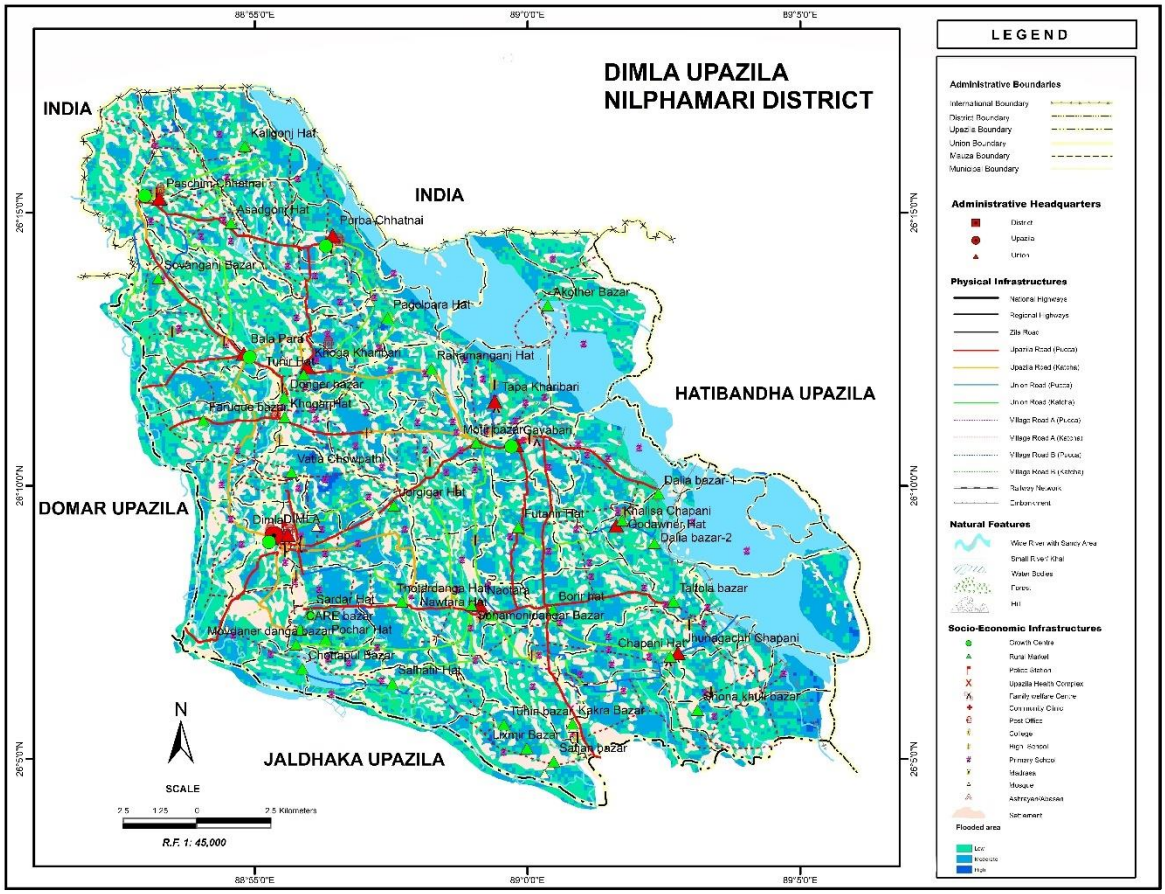

Figure 5.37: Flood vulnerability mapping for Dimla Upazila of Nilphamari district.

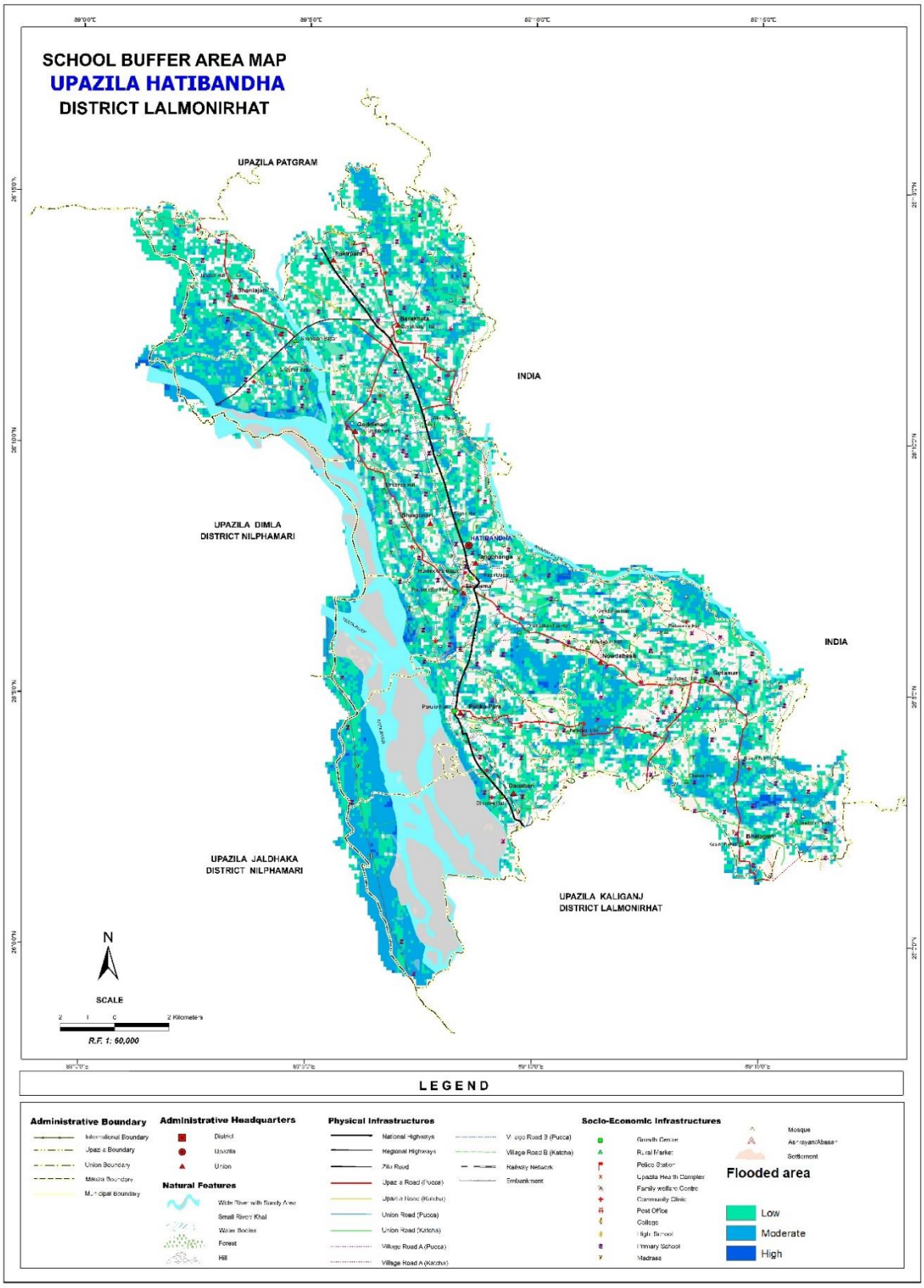

Figure 5.38: Flood vulnerability mapping for Hatibandha Upazila of Lalmonirhat district.

5.5 Planform Analysis for estimation of erosion and accretion of river

Channel dynamics and its evolution are perhaps the most investigated planform morphology in geomorphological research for decades (Xu et al., 2011). In order to understand the river morphology, a holistic but multidisciplinary approach is necessary that helps to understand the channel planform dynamics (Sinha et al., 2010). For the past few decades, remote sensing and GIS technology are playing a very important role in the study of river morphology (Sinha and Ghosh, 2012; Thakur et al., 2012; Gupta et al., 2013; Hossain et al., 2013). Remote sensing techniques provide a great possibility to analyze environmental processes on a local or global scale. Landsat images with their 30 m resolution are suitable, among others, for land cover mapping and change monitoring.

Identification of the channel migration pattern of rivers from satellite images of different years using GIS and Remote Sensing technology is found very much useful for studying the fluvial geomorphology of a river. For this study, the dry season satellite images from 1988 to 2018 have been collected. Bank lines of these years were digitized from the geo-referenced satellite imageries using the ARC GIS, and the erosion-accretion pattern due to the lateral movement of the active river channel has been estimated using the GIS software.

5.5.1 Modified Normalized Difference Water Index (MNDWI)

In this study, Modified Normalized Difference Water Index (MNDWI) was investigated from the aspect of the water body. To assess the situation, initially, two bands, band 3 and band 6 from LANDSAT 8 and LANDSAT 7 Images and band 2 and band 5 from LANDSAT, have been used, which is available on the USGS earth explorer website (http://earthexplorer.usgs.gov) then a field observation will be conducted later. For detecting the erosion, two images have been cast off. Modified normalized difference water index (MNDWI) has been carried out to detect the bank shifting during this time (Pal, R. and Pani, P., 2016; Pal, R. and Pani, P., 2018; Islam, M.K., Dustegir, M.M., Rahman, M.M. and Rahman, M., 2018). Two different bands, band 3 (green) with the wavelength of 0.53-0.59 µm and band 6 (short wave infrared 1) as MIR with the wavelength of 1.57-1.65 µm, have been used in this study (Eqn. 5.1)-

$$\mathrm{MNDWI} = \mathrm{Green} - \mathrm{MIR}/\mathrm{Green} + \mathrm{MIR} \quad (5.1)$$

All available satellite images will be georeferenced. For error measurement, a second-order polynomial equation will be used in Arc map software with the nearest neighbor resampling method considering less than one-pixel average root mean square error (RMSE). As different period of data has different resolution, ground resolution standardization will be done, and all images will be transferred into the same ground resolution for channel migration visualization.

a) Geomorphologic analysis

For the analysis of the channel geometry tree, geomorphological properties will be examined and taken into account, and they are presented below.

b) *Sinuosity index (p) for single-channel river*

It is the measurement of the bending of a channel. It can be defined as

$P = L_{cmax}/L_R$

Where P is the sinuosity index, L_{cmax} is the mid-channel length in a reach, and L_R is the straight-line length of the channel belt for the same reach. For sinuosity, high values indicate the high meandering geometry, and low values go toward straightness.

c) *Braid-channel index (Bfd) for multi-channel river*

Channel braiding is the multiplicity of a channel. On the basis of this method, the braid-channel index (Bfd) can be derived as (Eqn. 5.2)-

$$Bfd = L_{ctot}/ L_{cmax} \quad (5.2)$$

Where Bfd is the braid-channel index, L_{ctot} is the mid-channel length of all the segments of main channels in a reach, and L_{cmax} is the mid-channel length of the primary channel in that reach. A higher value indicates the high multiplicity and braidness of a channel where the lowest value of this ratio is 1, which means the channel is single-threaded and has no channel bars.

d) *B-W ratio*

In order to historical dynamics of a channel, in-land channel island area and channel area analysis are vital. B-W ratio is the ratio of the bar-covered area and the water-covered area in a significant segment of a river (Eqn. 5.3).

B-W radio = B/W (5.3)

Where B is the bar-covered area, and W is the water-covered area.

5.5.2 Satellite Image Processing for Planform Analysis

The sentinel image of 2020 has been processed for planform analysis. Results for the Dudhkumar, Dharala, Teesta, Jamuna, and Old Brahmaputra rivers have been presented in Figures 5.39(a)-(d), respectively. It was not possible to process the satellite image for the Ghaghot river as the river width is very narrow compared to the satellite resolution.

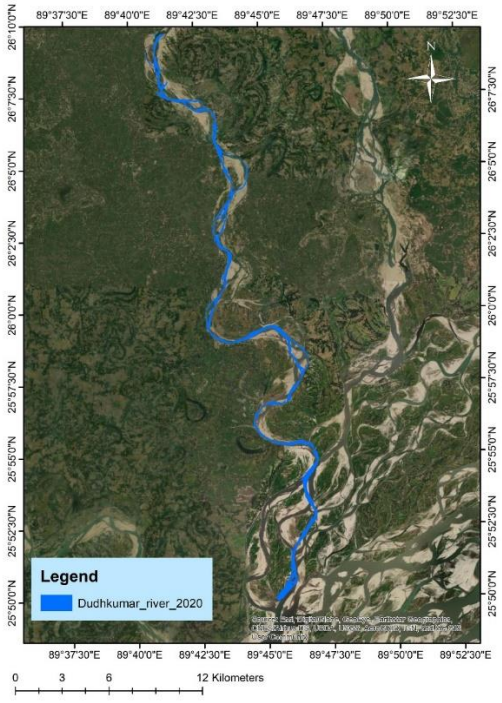

(a)

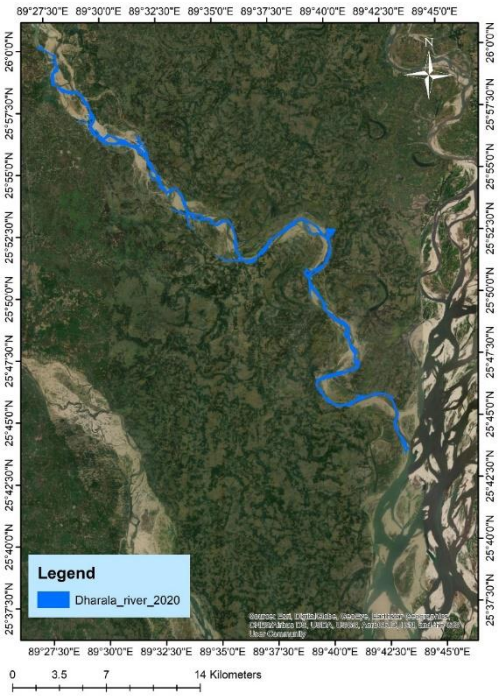

(b)

(c)

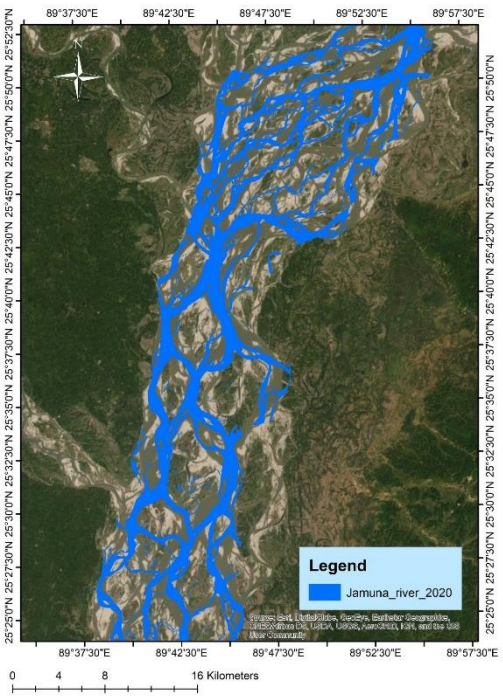

(d)

(e)

Figure 5.39: Satellite image processing for planform analysis of different rivers for the year 2020, (a) Dudhkumar, (b) Dharala, (c) Teesta, (c) Jamuna, (d) Old Brahmaputra.

5.5.3 Planform Analysis of different Flood Shelters and Markets

Channel dynamics and its evolution are perhaps the most investigated planform morphology in geomorphological research for decades (Xu et al., 2011). In order to understand the river morphology, a holistic but multidisciplinary approach is necessary that helps to understand the channel planform dynamics (Sinha et al., 2010). For the past few decades, remote sensing and GIS technology are playing a very important role in the study of river morphology (Sinha and Ghosh, 2012; Thakur et al., 2012; Gupta et al., 2013; Hossain et al., 2013). Remote sensing techniques provide a great possibility to analyze environmental processes on a local or global scale. Landsat images with their 30 m resolution are suitable, among others, for land cover mapping and change monitoring.

Identification of the channel migration pattern of rivers from satellite images of different years using GIS and Remote Sensing technology is found very much useful for studying the fluvial geomorphology of a river. For this study, the dry season satellite images from 1989 to 2020 have been collected. Bank lines of these years were digitized from the geo-referenced satellite imageries using the ARC GIS. Shifting of the bank lines due to the lateral movement of the active river channel has been estimated using GIS software.

Using satellite and remote sensing technology has a great advantage in studying river bank lines shifting as it has access to the historical data in a cost and time-effective manner. In the following figures (Figure 5.40-5.57), we have analyzed the changes in river banks near different markets and flood shelters located in Jamalpur, Kurigram and Gaibandha districts. Satellite images have been analyzed from 1989 to 2020 to determine the shift of the bank lines. We also included the flood vulnerability based on flood inundation maps of 6 major floods in recent times, which occurred in 2004, 2007, 2016, 2017, 2019 and 2020 in the Brahmaputra-Teesta river basin.

5.5.4 Combined flood and erosion risk of the infrastructure

Based on flood inundation vulnerability maps, we have calculated flood risks for the rural infrastructures using the following criteria as presented in Table 5.8. High, moderate and low risks on the infrastructure are based on the location of the infrastructure within different flood-vulnerable areas. River bank erosion risks of the infrastructure have been calculated using the criteria presented in Table 5.9. Depending on the locations of the infrastructure and type of rivers, bank erosion patterns are considered to estimate bank erosion risks.

Table 5.8: Criteria for assessing flood risks based on flood inundation mapping.

Flood Risk Criteria
High Risk: • If a major flood occurs at least five times out of 6 major floods in the last two decades within 100m peripheries. Moderate Risk: • If a major flood occurred at least three times out of 6 major floods in the last two decades within 100m peripheries. Low Risk: • If a major flood occurs at most two times out of 6 major floods in the last two decades within 100m peripheries. It is noteworthy to mention that major floods in the last two decades (2000-2020) occurred in 2004, 2007, 2016, 2017, 2019 and 2020.

Table 5.9: Criteria for assessing river bank erosion risk based on planform analysis.

River Bank Erosion Risk Criteria
High Risk: • Major Rivers: Historically, bank lines were within 1000m of the market or shelter. • Moderate Rivers: Historically, bank lines were within 300m of the market or shelter. • Minor Rivers: Historically, bank lines were within 50m of the market or shelter. Moderate Risk: • Major Rivers: Historically, bank lines were within 2000m of the market or shelter. • Moderate Rivers: Historically, bank lines were within 1000m of the market or shelter. • Minor Rivers: Historically, bank lines were within 100m of the market or shelter. Low Risk: • Major Rivers: Historically, bank lines were more than 3000m from the market or shelter. • Moderate Rivers: Historically, bank lines were within 1500m of the market or shelter. • Minor Rivers: Historically, bank lines were more than 200m from the market or shelter.

However, if any interventions in the river, such as the construction of a dam, barrage, bridge, bank protection, or unplanned sand mining or dredging in the river, the risk may be changed, any record-breaking extreme events occur, and the morphology of the river may abruptly change, which would change the degree of vulnerability criteria. Here, the major rivers in the study area as Brahmaputra, Jamuna, and Teesta. Moderate rivers are Dharla, Dudhkumar, Old Brahmaputra, Ghagat, and Bangali, while minor rivers are their distributaries and tributaries.

5.5.5 Combined Flood and Bank Erosion Risks for School cum Flood Shelters

Based on planform analysis using historical satellite images, bank erosion risks are identified for the proposed school cum flood shelters in the above-selected locations on a scale of low, moderate and high. Finally, combined flood and bank erosion risks on the school cum flood shelters are presented in Table 5.28.

The details of the analysis of the following locations are given in the next sections-

- Location 1: Abdul Gani Govt. Primary school, Jamalpur District
- Location 2: Chinarchar Uttarpara Govt. Primary school, Jamalpur District
- Location 3: Shapdhori Govt. Primary school, Jamalpur District
- Location 4: Shuknagori Govt. Primary school, Jamalpur District
- Location 5: All Haz Gohor Uddin Junior School, Lalmonirhat District
- Location 6: Ajam Kha Government Primary School, Rangpur District
- Location 7: Dalia Baish Pukure Tistarchar Government Primary School, Nilphamari District
- Location 8: Char Holdibari Government Primary School, Nilphamari District
- Location 9: Jongra 3 No Battala Government Primary School, Lalmonirhat District
- Location 10: Pollimari Government Primary School, Rangpur District
- Location 11: Shoulmari Charvorot Government Primary School, Nilphamari District
- Location 12: Tapakharibari 1 No Government Primary School, Nilphamari District
- Location 13: Jotindra Naraya Government Primary School, Kurigram District
- Location 14: Kochabari Bhurongamari Government Primary School, Kurigram District
- Location 15: Sayadpur Government Primary School cum Flood Shelter
- Location 16: Bashir Nagar Government Primary School cum Flood Shelter
- Location 17: Bekrir Char Government Primary School cum Flood Shelter
- Location 18: Chinirpatol Government Primary School cum Flood Shelter

Location 1: Abdul Gani Govt. Primary school, Jamalpur District

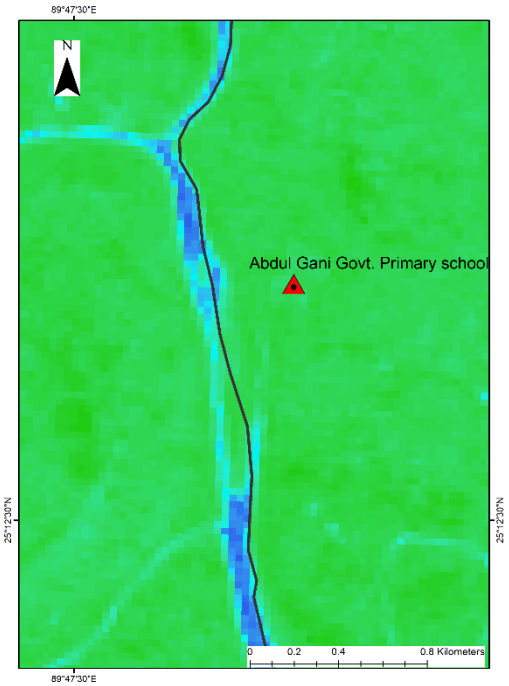

(a)

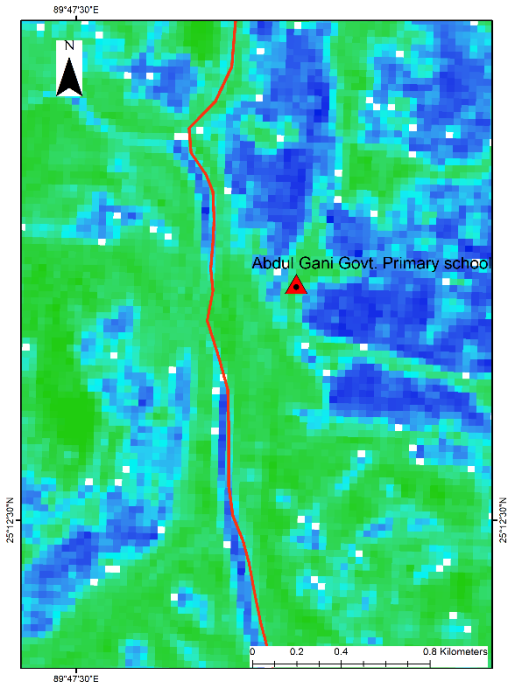

(b)

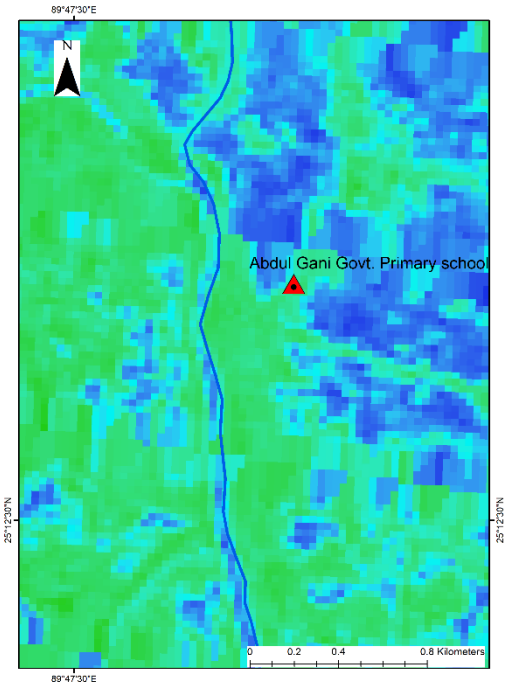

(c)

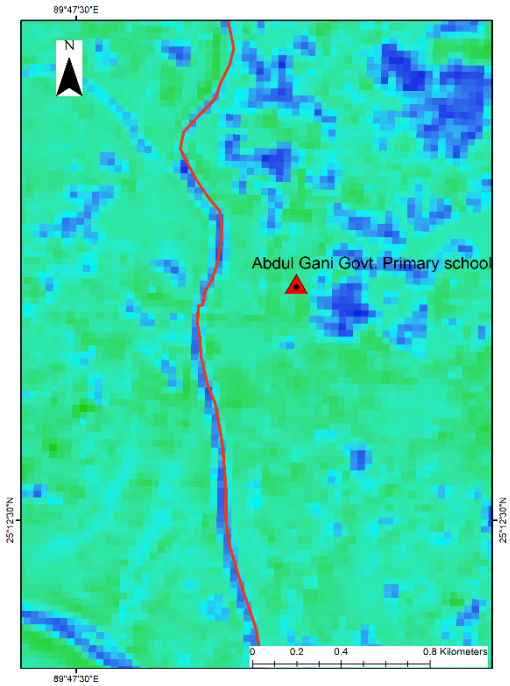

(d)

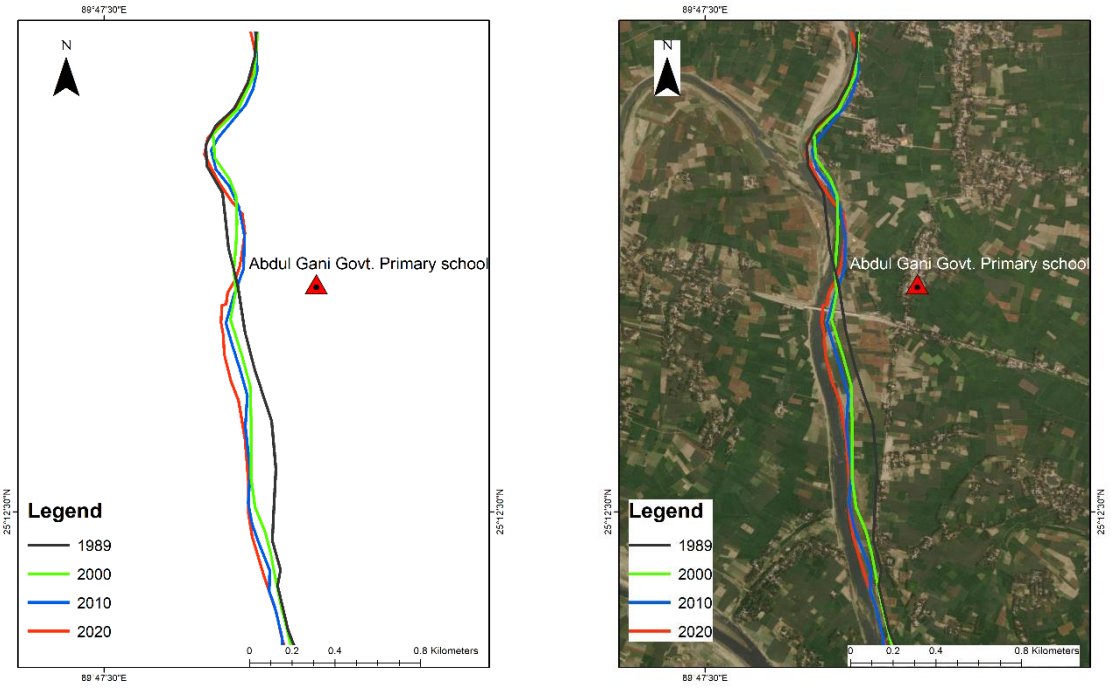

(e) (f)

Figure 5.40: River planform analysis near Abdul Gani Govt. Primary school from the year 1989 to 2020 using satellite data. Here river bank line for years (a)1989, (b) 2000, (c) 2010 and (d) 2020, (e) bank line shifting from the year 1989 to 2020 and (f) on google earth image.

Table 5.10: Shifting of the river banks and flood vulnerability of the Abdul Gani Govt. Primary school (North direction).

Abdul Gani Govt. Primary school (North direction)			
Year	Distance of riverbank from Bazar (km)	Riverbank shifting (m)	Flood risk zone
1989	0.33	-	Moderate risk (2/6)
2000	0.34	10 (away from school)	
2010	0.34	0	
2020	0.36	20 (away from school)	

Based on the above analysis, the flood and erosion risks of the school are as follows-

- Flood Risk: The school is located in a **low** flood-risk area, considering the inundation patterns of all major floods in recent times. However, the surrounding area is at high flood risk.
- Bank Erosion Risk: Based on planform analysis using historical satellite images, the school is located in the **low** bank erosion risk area.

Location 2: Chinarchar Uttarpara Govt. Primary school, Jamalpur District

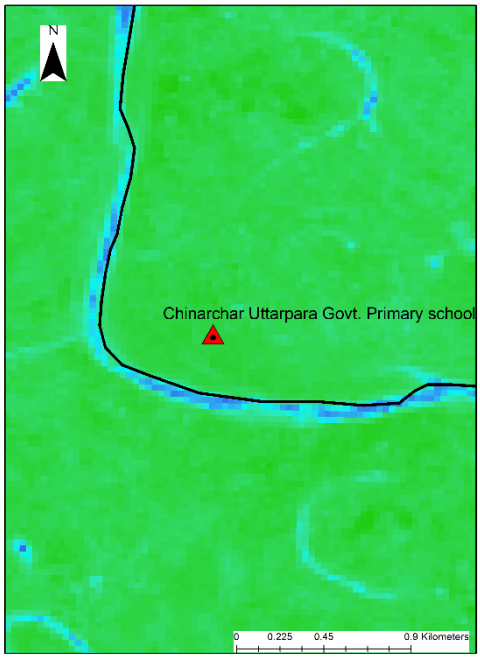

(a)

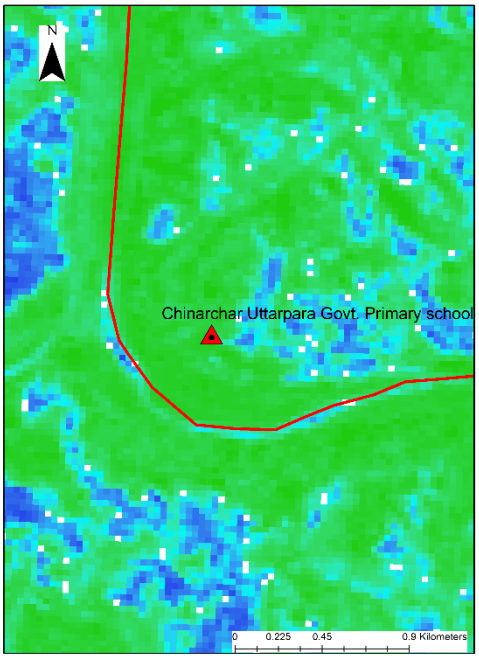

(b)

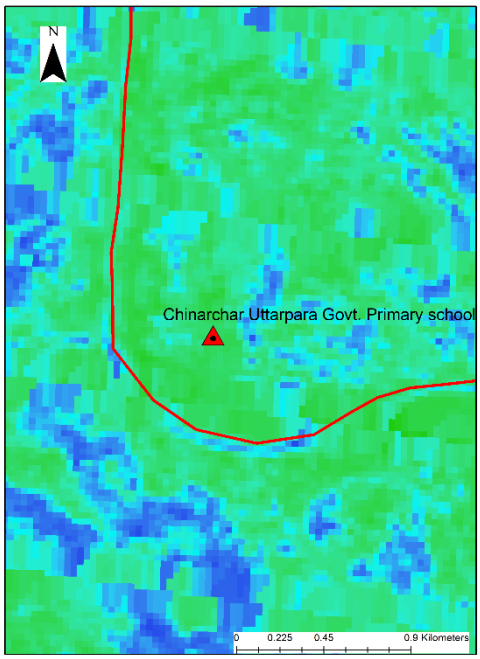

(c)

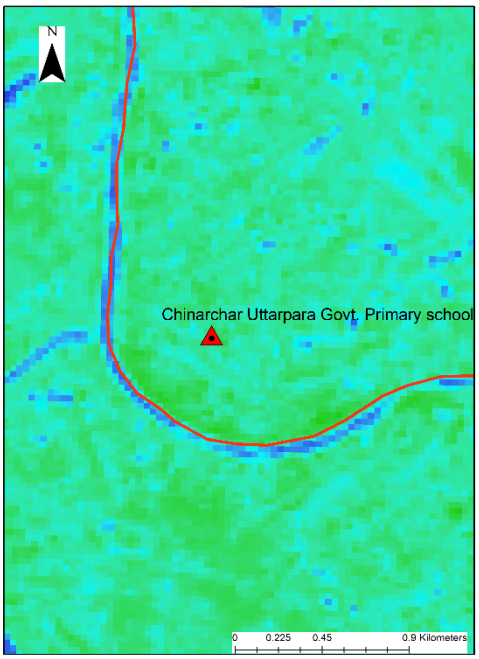

(d)

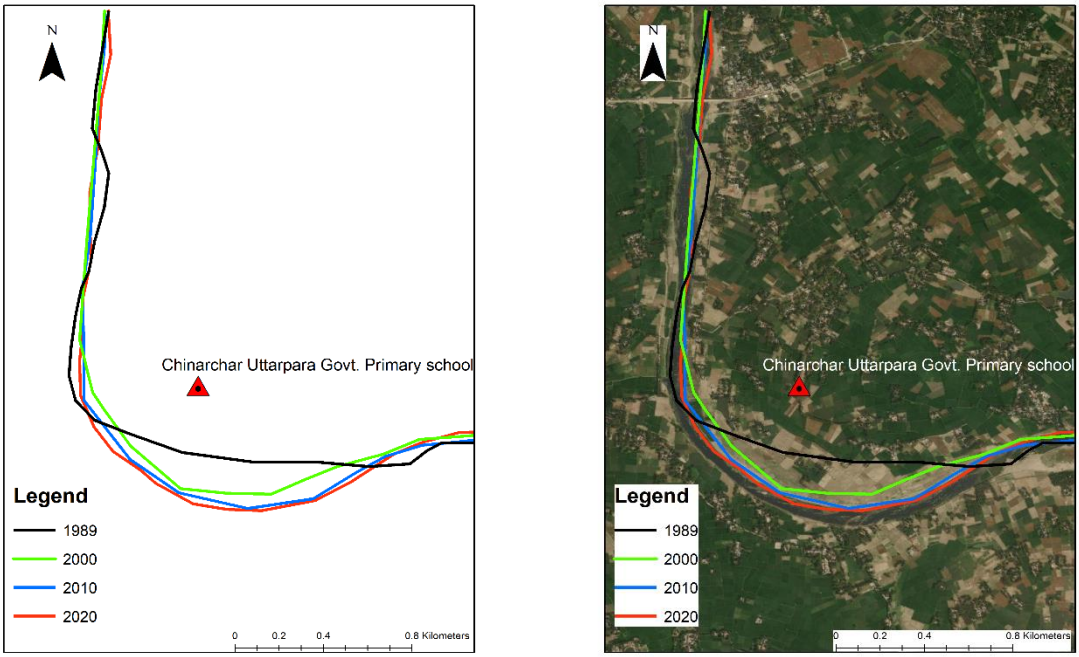

(e) (f)

Figure 5.41: River planform analysis near Chinarchar Uttarpara Govt. Primary school from the year 1989 to 2020 using satellite data. Here is the river bank line of years (a)1989, (b) 2000, (c) 2010 and (d) 2020, and (e) bank line shifting from the year 1989 to 2020 and (f) on google earth image.

Table 5.11: Shifting of the river banks and flood vulnerability of the Chinarchar Uttarpara Govt. Primary school (Southeast direction).

Chinarchar Uttarpara Govt. Primary school (Southeast direction)			
year	Distance of riverbank from Bazar (km)	Riverbank shifting (m)	Flood risk zone
1989	0.3	-	Low risk (1/6)
2000	0.37	70 (away from school)	
2010	0.41	40 (away from school)	
2020	0.42	10 (away from school)	

Based on the above analysis, the flood and erosion risks of the school are as follows-

- Flood Risk: The school is located in a **low** flood-risk area, considering the inundation patterns of all major floods in recent times. However, the surrounding area is at high flood risk.
- Bank Erosion Risk: Based on planform analysis using historical satellite images, the school is located in the **low** bank erosion risk area.

Location 3: Shapdhori Govt. Primary school, Jamalpur District

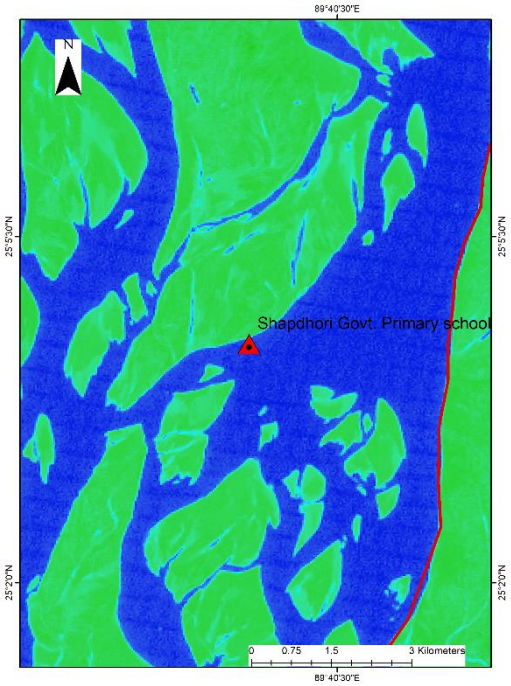

(a)

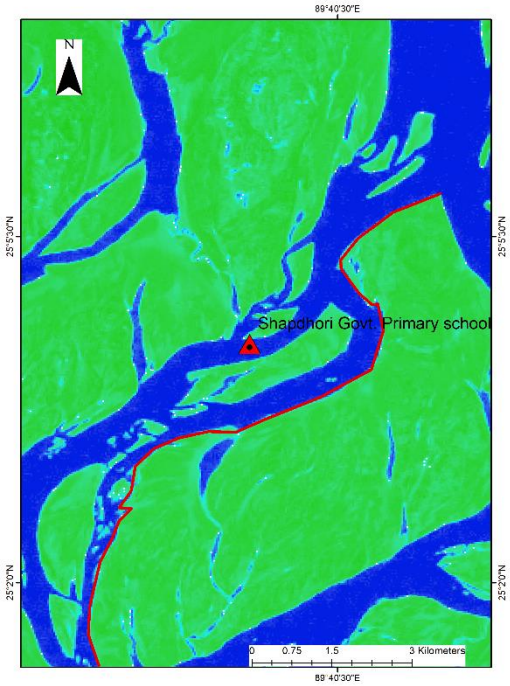

(b)

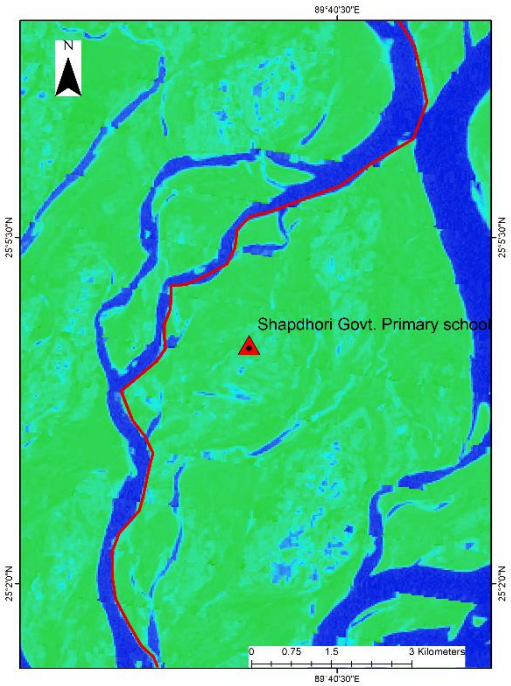

(c)

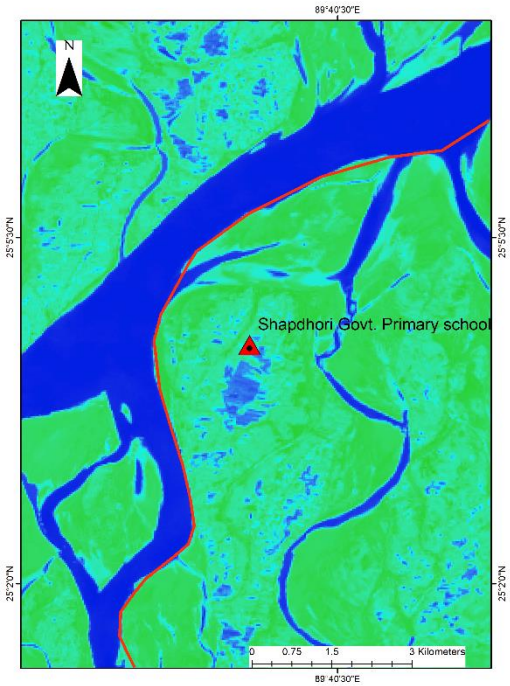

(d)

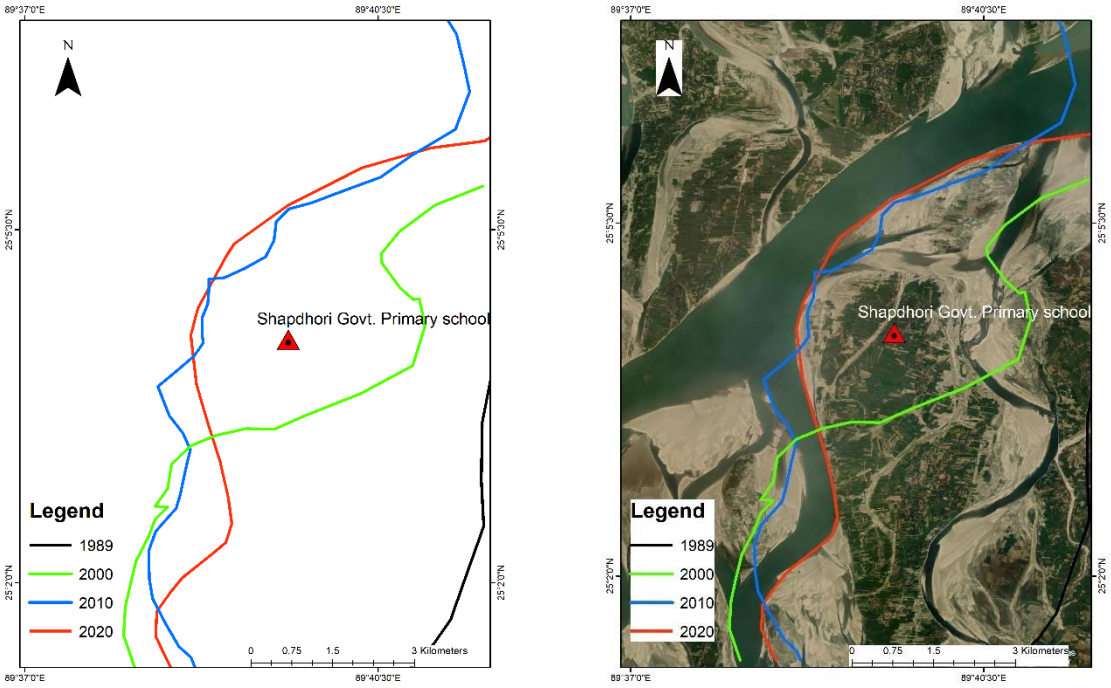

(e) (f)

Figure 5.42: River planform analysis near Shapdhori Govt. Primary school from the year 1989 to 2020 using satellite data. Here is the river bank line of years (a)1989, (b) 2000, (c) 2010 and (d) 2020, and (e) bank line shifting from 1989 to 2020 and (f) on google earth image.

Table 5.12: Shifting of the river banks and flood vulnerability of the Shapdhori Govt. Primary school (East direction)

Shapdhori Govt. Primary school (East direction)			
year	Distance of riverbank from Bazar (km)	Riverbank shifting (m)	Flood risk zone
1989	0	Inside the main river	High risk (3/6)
2000	0	Inside the main river	
2010	1.41	1411.3 (away from school)	
2020	1.59	191.3 (away from school)	

Based on the above analysis, the flood and erosion risks of the school are as follows-

- Flood Risk: The school is located in a **high** flood-risk area, considering the inundation patterns of all major floods in recent times. However, the surrounding area is at high flood risk.
- Bank Erosion Risk: Based on planform analysis using historical satellite images, the school is located in the **high** bank erosion risk area.

Location 4: Shuknagori Govt. Primary school, Jamalpur District

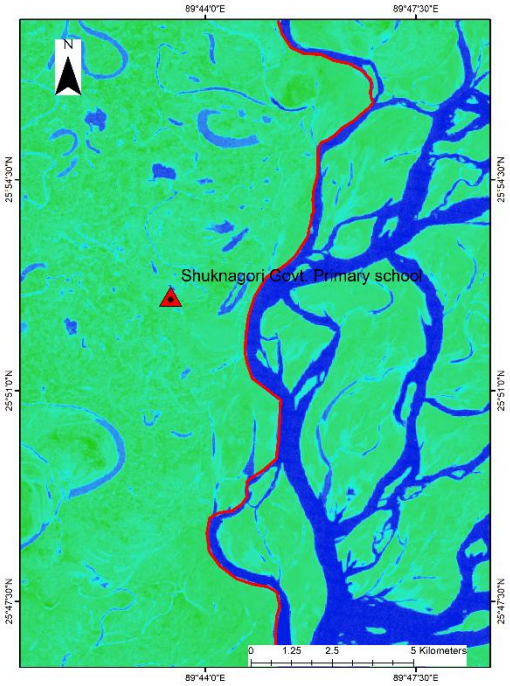

(a)

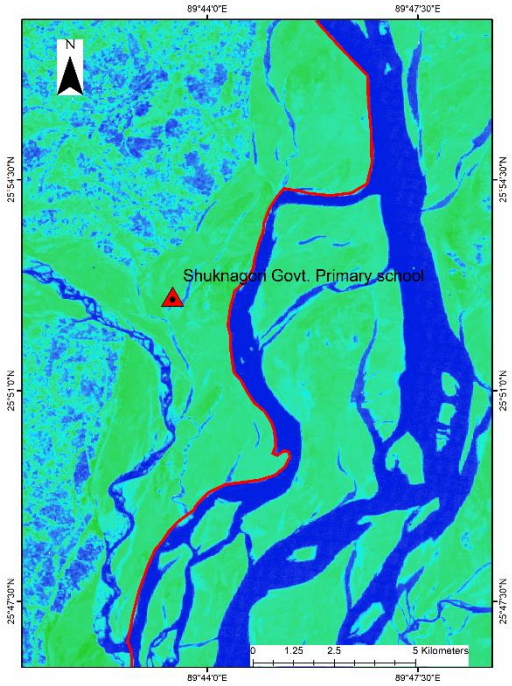

(b)

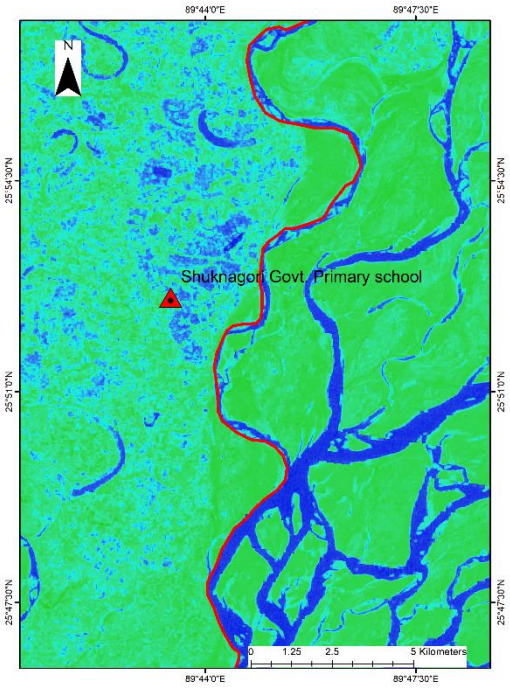

(c)

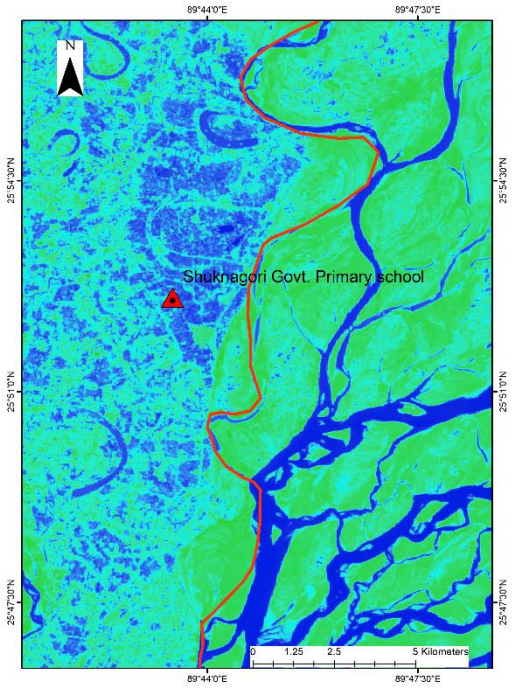

(d)

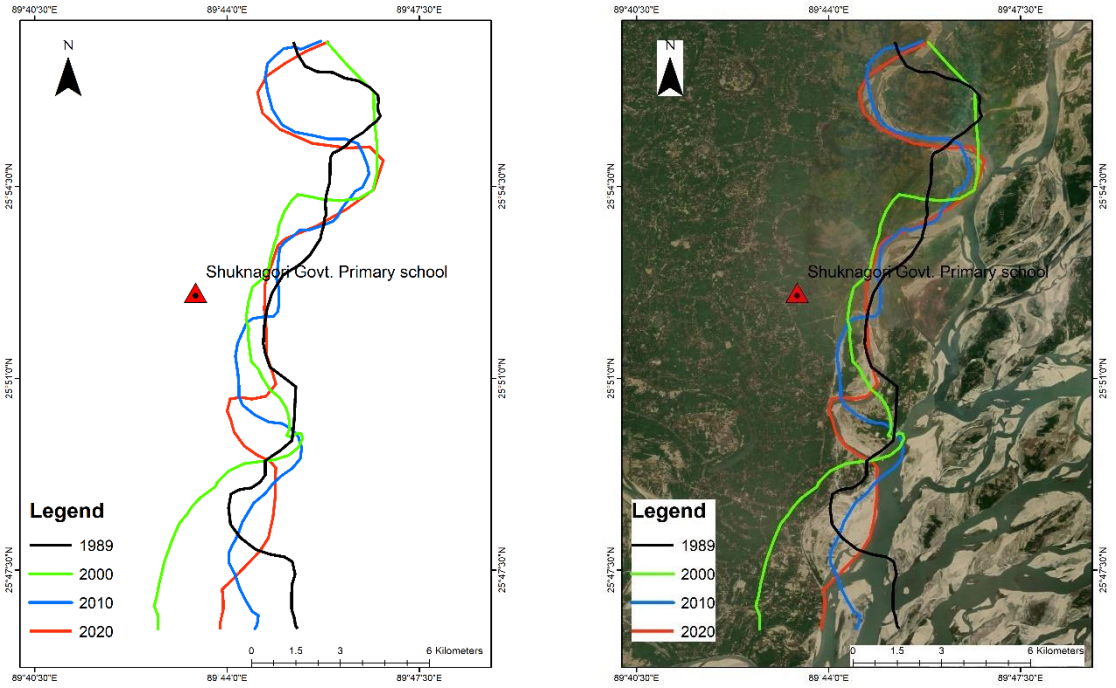

(e) (f)

Figure 5.43: River planform analysis near Shuknagori Govt. Primary school from the year 1989 to 2020 using satellite data. Here is the river bank line of years (a)1989, (b) 2000, (c) 2010 and (d) 2020, and (e) bank line shifting from the year 1989 to 2020 and (f) on google earth image.

Table 5.13: Shifting of the river banks and flood vulnerability of the Shuknagori Govt. Primary school (West direction).

Shuknagori Govt. Primary school (West direction)			
year	Distance of riverbank from Bazar (km)	Riverbank shifting (m)	Flood risk zone
1989	2.24	-	High risk (3/6)
2000	1.65	590	
2010	2.51	860 (away from school)	
2020	2.07	440	

Based on the above analysis, the flood and erosion risks of the school are as follows-

- Flood Risk: The school is located in a **moderate** flood risk area, considering the inundation patterns of all major floods in recent times. However, the surrounding area is at high flood risk.
- Bank Erosion Risk: Based on planform analysis using historical satellite images, the school is located in the **low** bank erosion risk area.

Location 5: All Haz Gohor Uddin Junior School, Lalmonirhat District

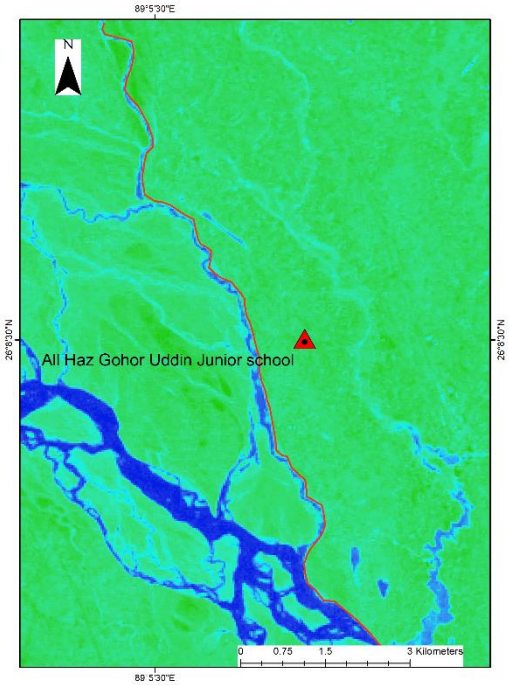

(a)

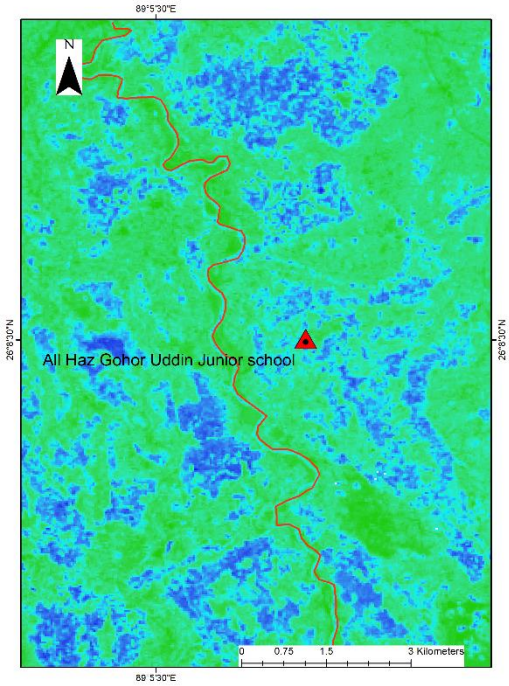

(b)

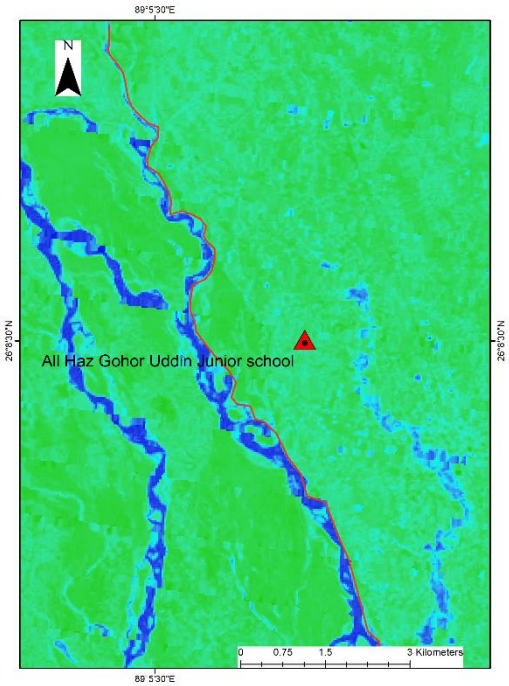

(c)

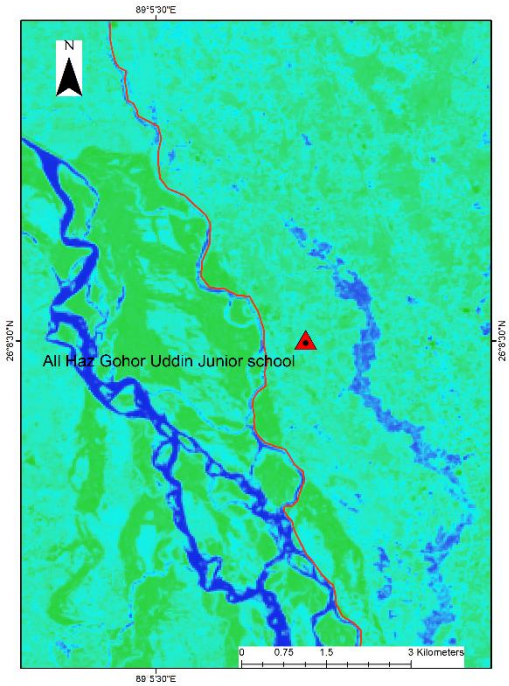

(d)

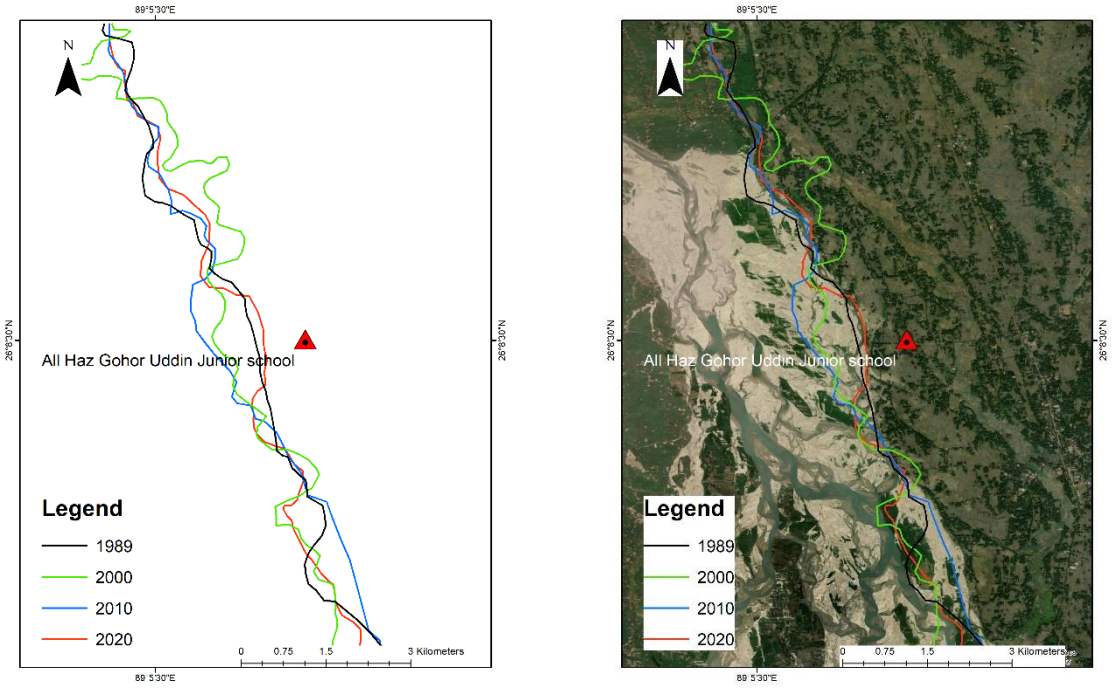

(e) (f)

Figure 5.44: River planform analysis near All Haz Gohor Uddin Junior school from the year 1989 to 2020 using satellite data. Here is the river bank line of years (a)1989, (b) 2000, (c) 2010 and (d) 2020, and (e) bank line shifting from the year 1989 to 2020 and (f) on google earth image.

Table 5.14: Shifting of the river banks and flood vulnerability of the All Haz Gohor Uddin Junior school (West direction).

All Haz Gohor Uddin Junior School (west direction)			
year	Distance of riverbank from Bazar (km)	Riverbank shifting (m)	Flood risk zone
1989	0.8	-	Moderate risk (2/6)
2000	1.47	670 (away from school)	
2010	1.63	160 (away from school)	
2020	0.67	960	

Based on the above analysis, the flood and erosion risks of the school are as follows-

- Flood Risk: The school is located in a **low** flood-risk area, considering the inundation patterns of all major floods in recent times. However, the surrounding area is at high flood risk.
- Bank Erosion Risk: Based on planform analysis using historical satellite images, the school is located in the **moderate** bank erosion risk area.

Location 6: Ajam Kha Government Primary School, Rangpur District

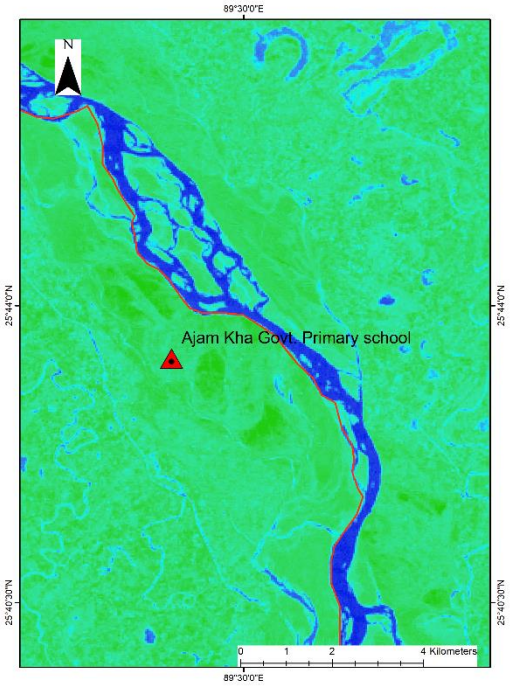

(a)

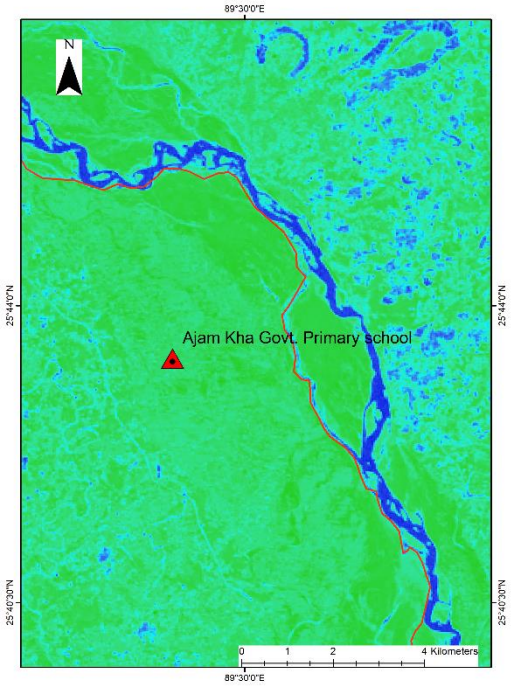

(b)

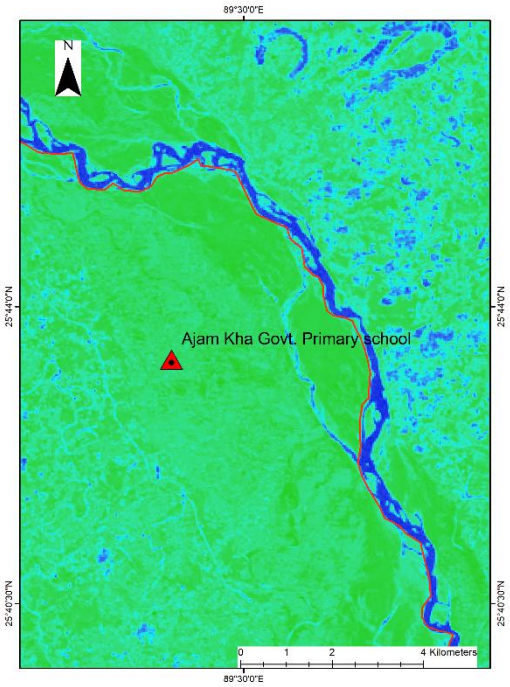

(c)

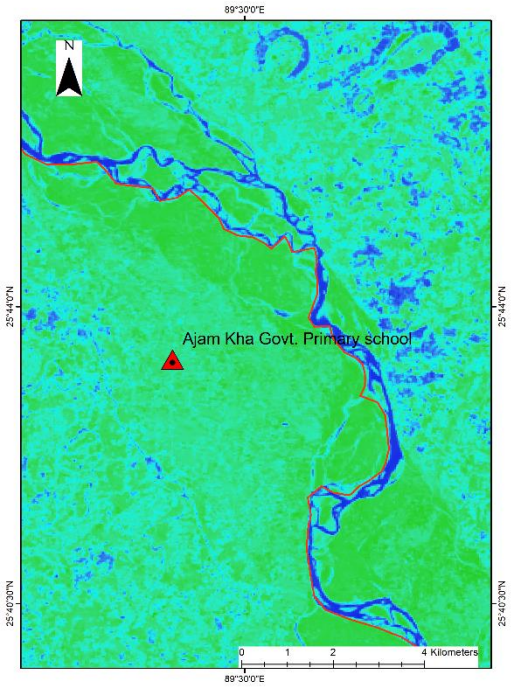

(d)

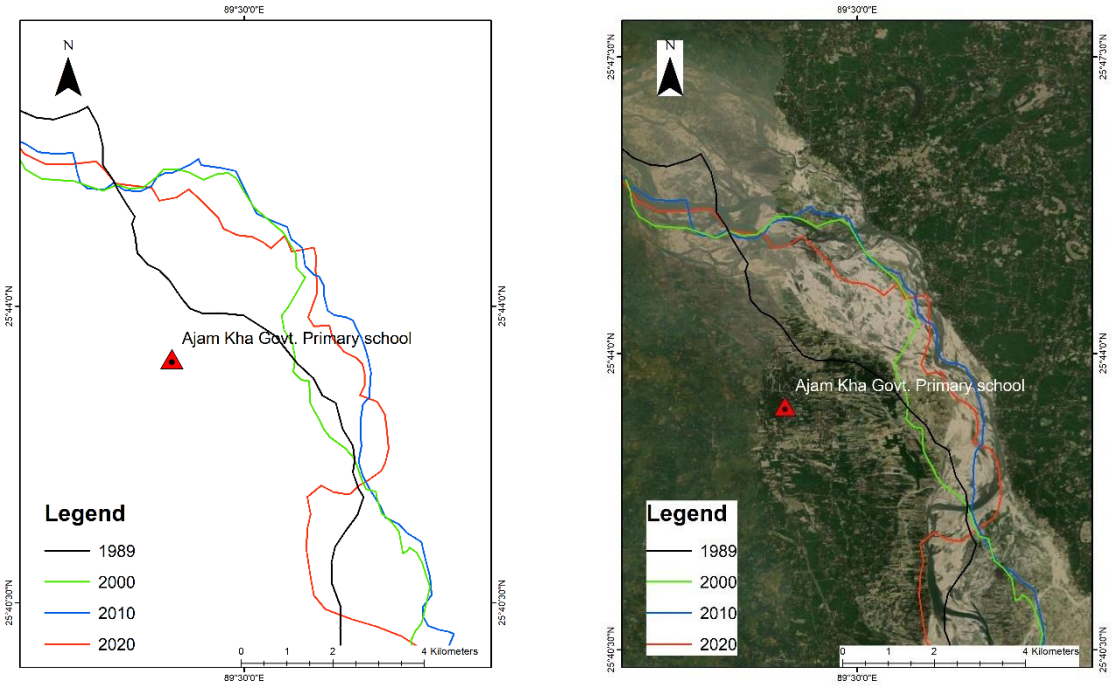

(e) (f)

Figure 5.45: River planform analysis near Ajam Kha Government Primary school from the year 1989 to 2020 using satellite data. Here is the river bank line of years (a)1989, (b) 2000, (c) 2010 and (d) 2020, and (e) bank line shifting from the year 1989 to 2020 and (f) on google earth image.

Table 5.15: Shifting of the river banks and flood vulnerability of the Ajam Kha Government Primary school (West direction).

Ajam Kha Government Primary School (west direction)			
year	Distance of riverbank from Bazar (km)	Riverbank shifting (m)	Flood risk zone
1989	2.15	-	Low risk (1/6)
2000	2.34	190 (away from school)	
2010	3.34	1000 (away from school)	
2020	2.88	460	

Based on the above analysis, the flood and erosion risks of the school are as follows-

- Flood Risk: The school is located in a **low** flood-risk area, considering the inundation patterns of all major floods in recent times. However, the surrounding area is at high flood risk.
- Bank Erosion Risk: Based on planform analysis using historical satellite images, the school is located in the **moderate** bank erosion risk area.

Location 7: Dalia Baish Pukure Tistarchar Government Primary School, Nilphamari District

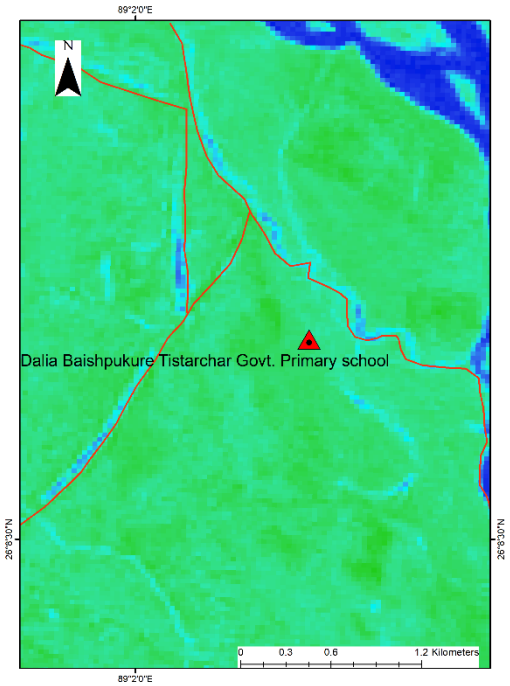

(a)

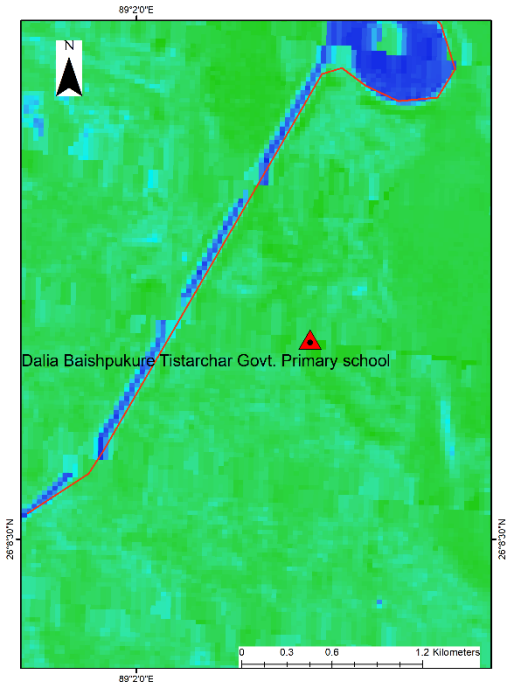

(b)

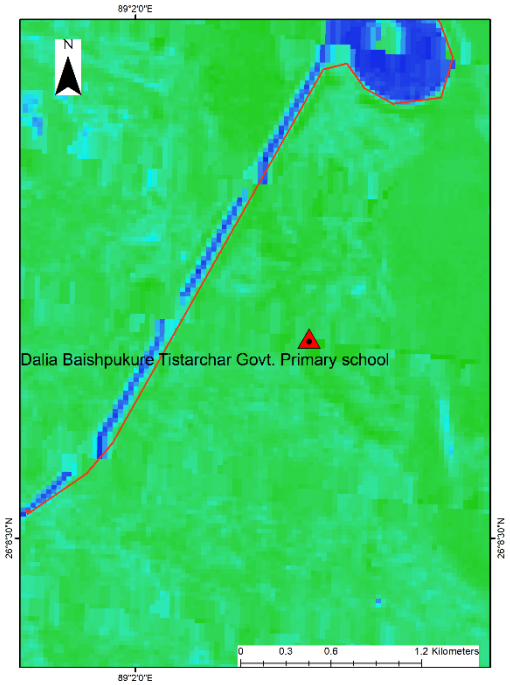

(c)

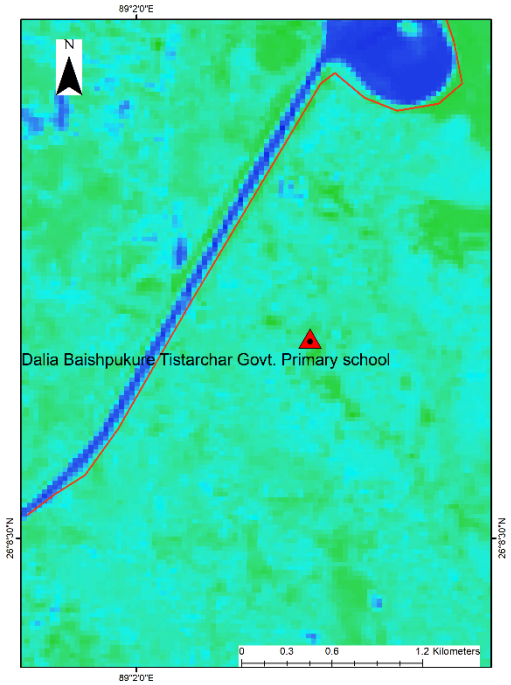

(d)

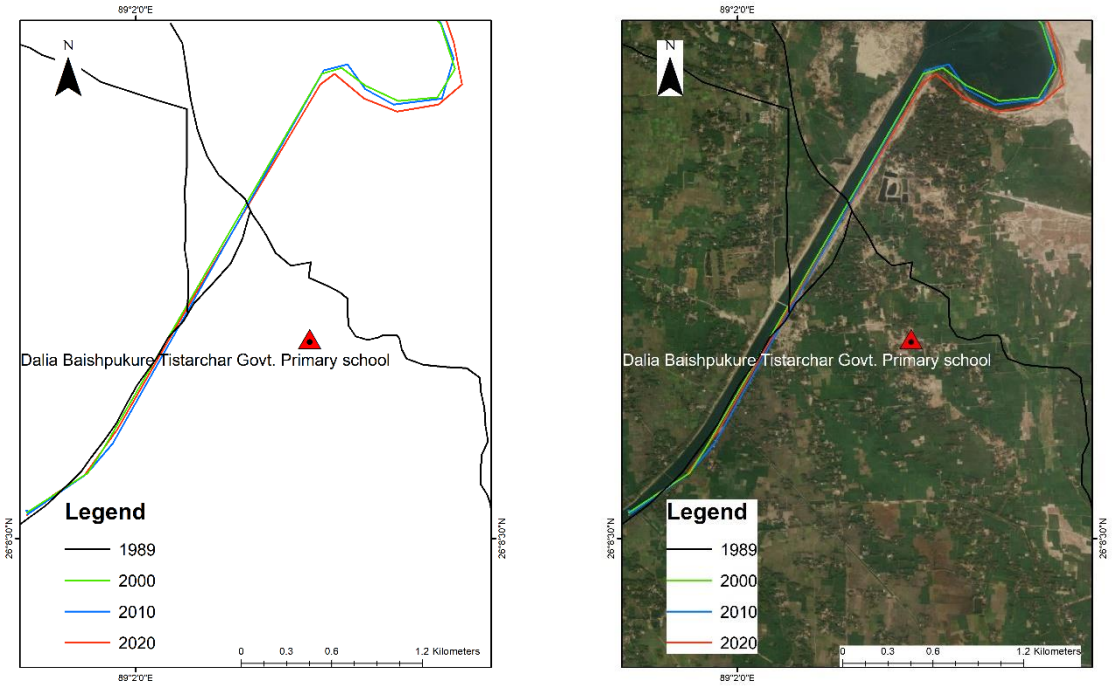

(e) (f)

Figure 5.46: River planform analysis near Dalia Baishpukure Tistarchar Government Primary school from the year 1989 to 2020 using satellite data. Here is the river bank line of years (a)1989, (b) 2000, (c) 2010 and (d) 2020, and (e) bank line shifting from the year 1989 to 2020 and (f) on google earth image.

Table 5.16: Shifting of the river banks and flood vulnerability of the Dalia Baishpukure Tistarchar Government Primary school (West direction).

Dalia Baishpukur Tistarchar Government Primary School (west direction)			
year	Distance of riverbank from Bazar (km)	Riverbank shifting (m)	Flood risk zone
1989	0.843	-	Low risk (1/6)
2000	0.84	3	
2010	0.81	30	
2020	0.83	20 (away from school)	

Based on the above analysis, the flood and erosion risks of the school are as follows-

- Flood Risk: The school is located in a **low** flood-risk area, considering the inundation patterns of all major floods in recent times. However, the surrounding area is at high flood risk.
- Bank Erosion Risk: Based on planform analysis using historical satellite images, the school is located in the **low** bank erosion risk area.

Location 8: Char Holdibari Government Primary School, Nilphamari District

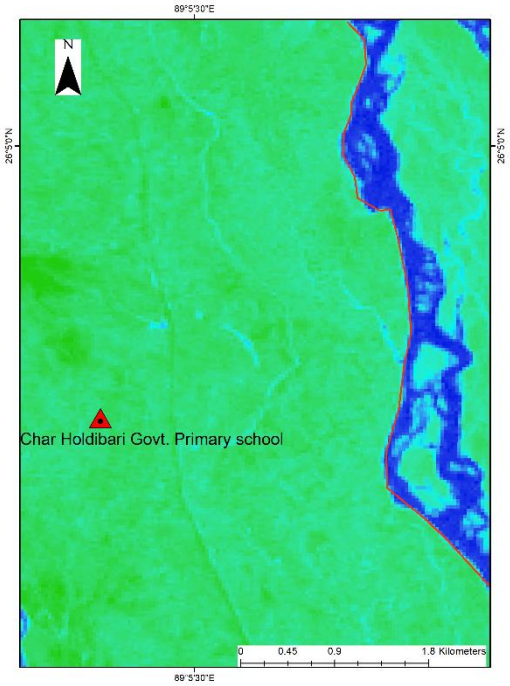

(a)

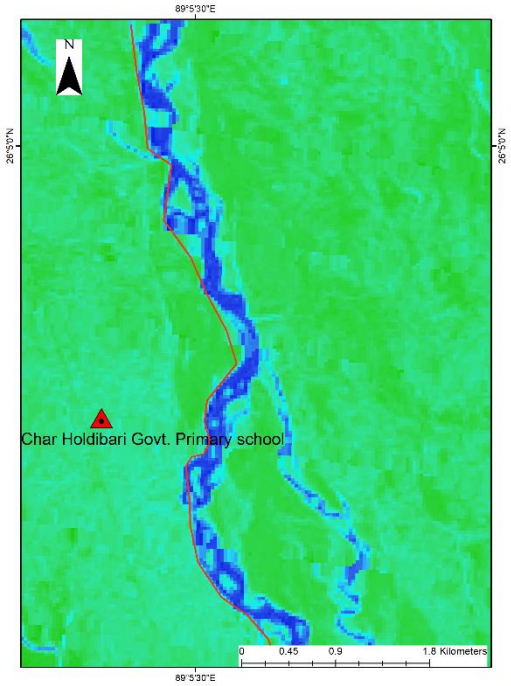

(b)

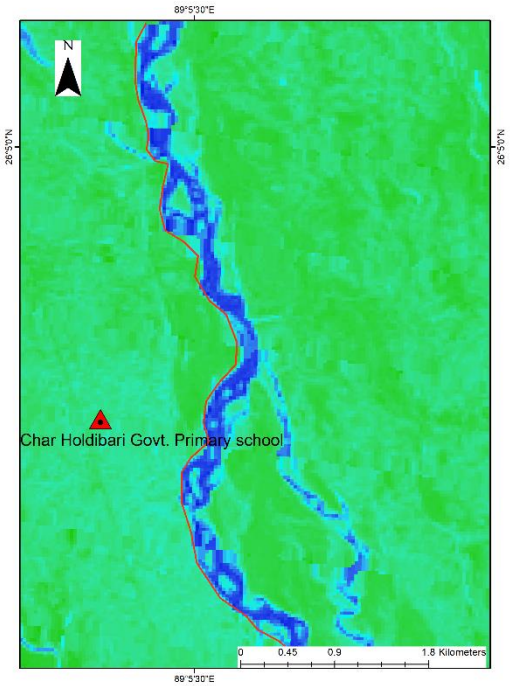

(c)

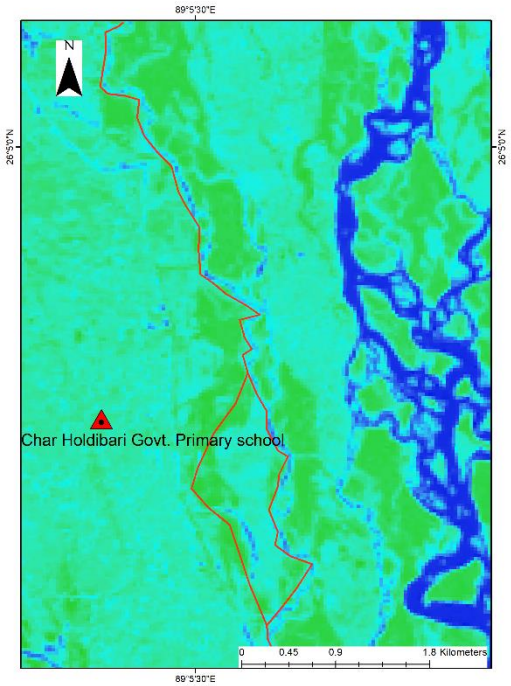

(d)

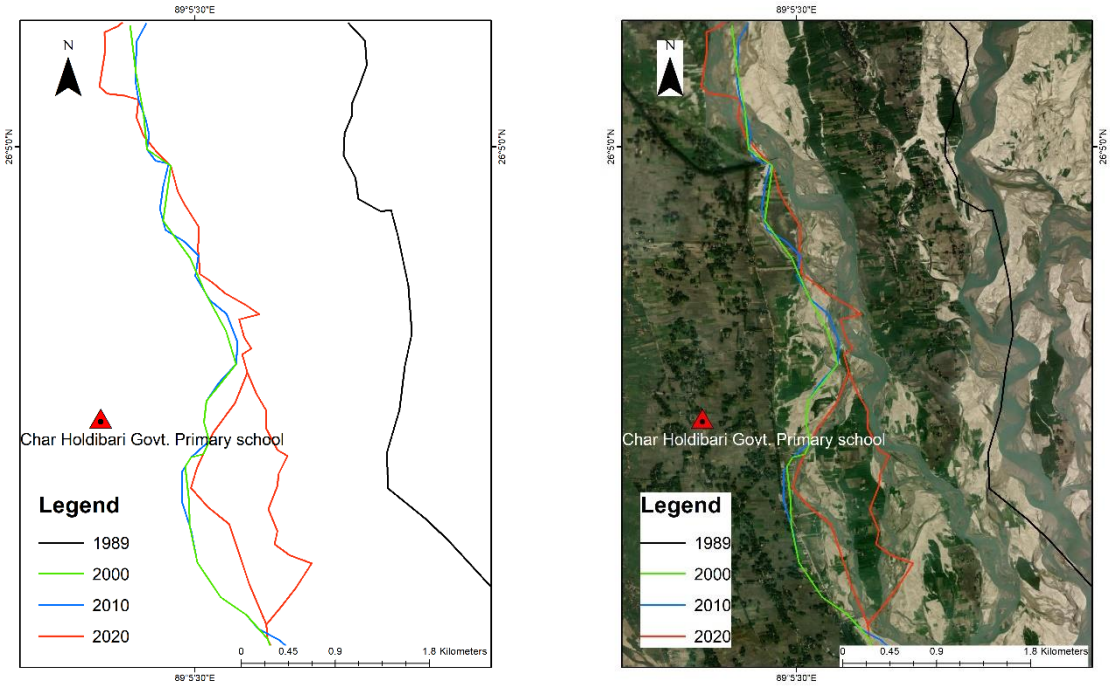

(e) (f)

Figure 5.47: River planform analysis near Dalia Baishpukure Tistar char Government Primary school from the year 1989 to 2020 using satellite data. Here is the river bank line of years (a)1989, (b) 2000, (c) 2010 and (d) 2020, and (e) bank line shifting from the year 1989 to 2020 and (f) on google earth image.

Table 5.17: Shifting of the river banks and flood vulnerability of the Dalia Baishpukure Tistar char Government Primary school (West direction).

Char Holdibari Government Primary School (west direction)			
year	Distance of riverbank from Bazar (km)	Riverbank shifting (m)	Flood risk zone
1989	2.54	-	High risk (3/6)
2000	0.89	1650	
2010	0.89	0	
2020	1.04	150 (away from school)	

Based on the above analysis, the flood and erosion risks of the school are as follows-

- Flood Risk: The school is located in a **moderate** flood risk area, considering the inundation patterns of all major floods in recent times. However, the surrounding area is at high flood risk.
- Bank Erosion Risk: Based on planform analysis using historical satellite images, the school is located in the **moderate** bank erosion risk area.

Location 9: Jongra 3 No Battala Government Primary School, Lalmonirhat District

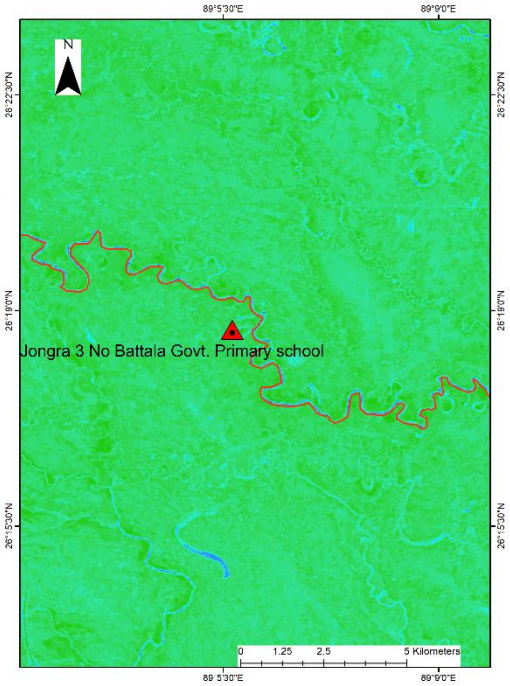

(a)

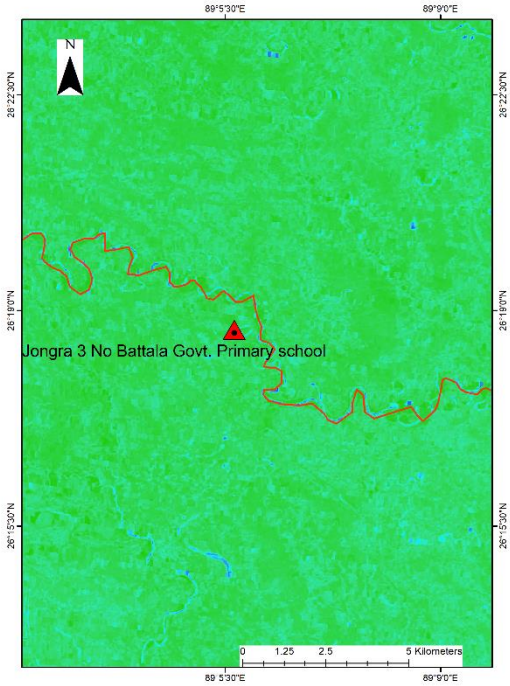

(b)

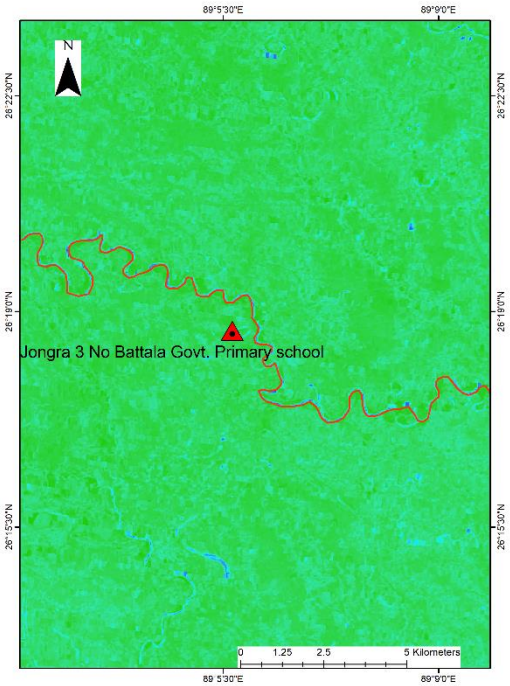

(c)

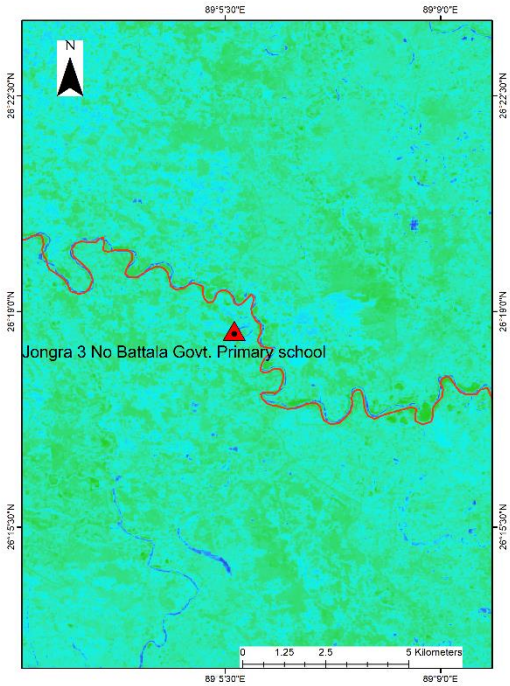

(d)

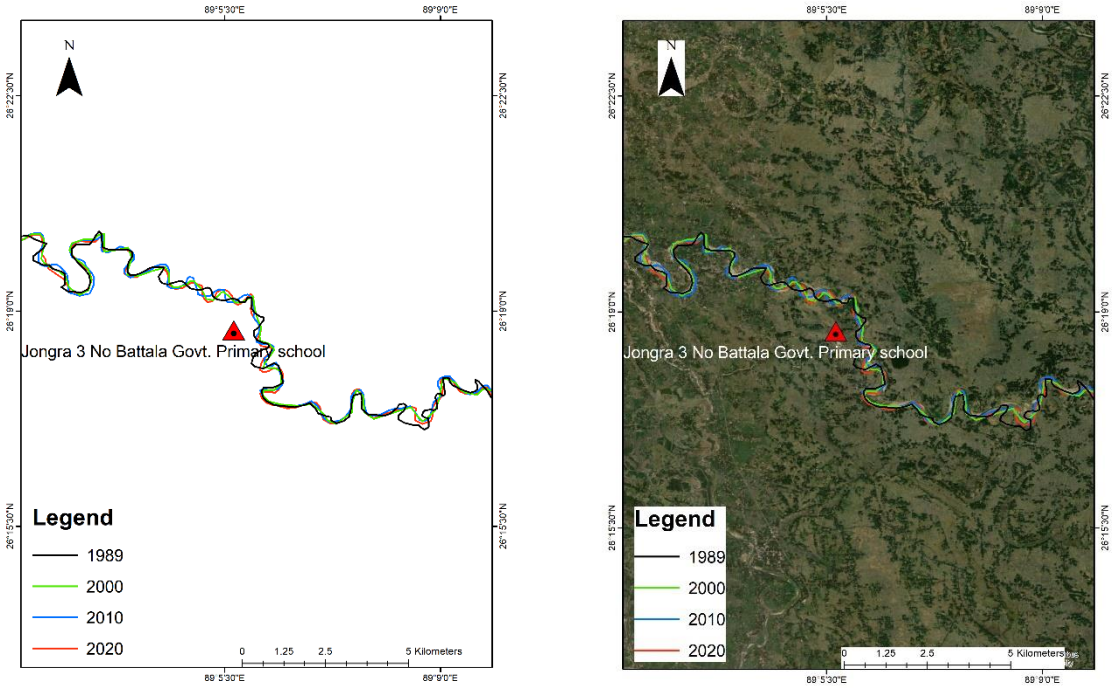

(e) (f)

Figure 5.48: River planform analysis near Jongra 3 No Battala Government Primary school from the year 1989 to 2020 using satellite data. Here is the river bank line of years (a)1989, (b) 2000, (c) 2010 and (d) 2020, and (e) bank line shifting from the year 1989 to 2020 and (f) on google earth image.

Table 5.18: Shifting of the river banks and flood vulnerability of Jongra 3 No Battala Government Primary school (West direction).

Jongra 3 No Battala Government Primary School (west direction)			
year	Distance of riverbank from Bazar (km)	Riverbank shifting (m)	Flood risk zone
1989	0.55	-	Low risk (1/6)
2000	0.73	180 (away from school)	
2010	0.69	40	
2020	0.72	30 (away from school)	

Based on the above analysis, the flood and erosion risks of the school are as follows-

- Flood Risk: The school is located in a **low** flood-risk area, considering the inundation patterns of all major floods in recent times. However, the surrounding area is at high flood risk.
- Bank Erosion Risk: Based on planform analysis using historical satellite images, the school is located in the **moderate** bank erosion risk area.

Location 10: Pollimari Government Primary School, Rangpur District

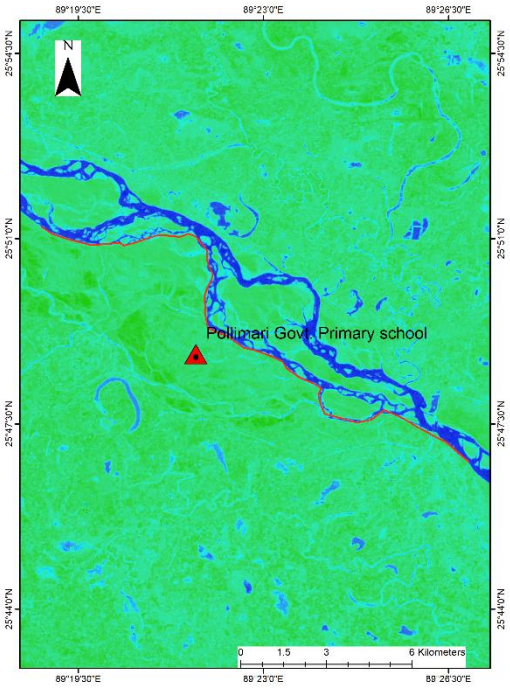

(a)

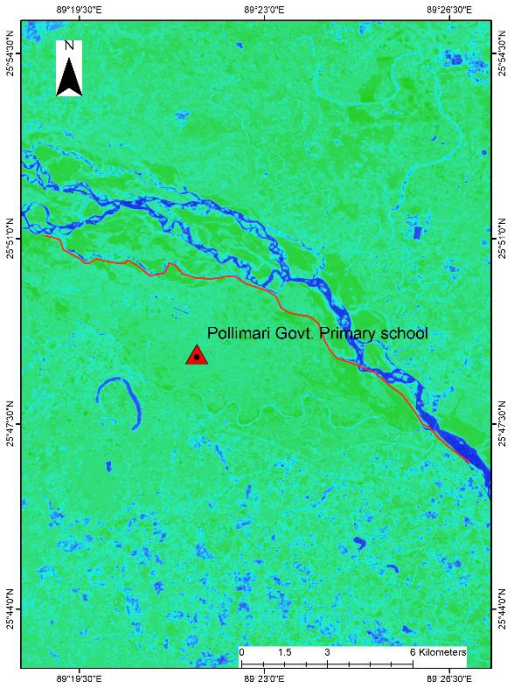

(b)

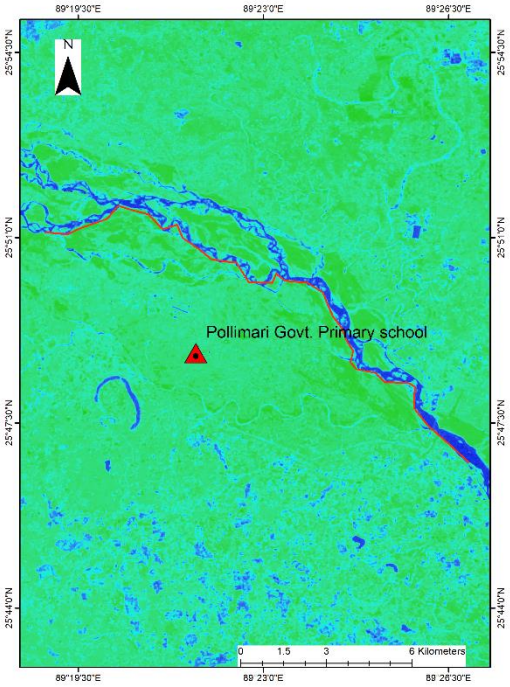

(c)

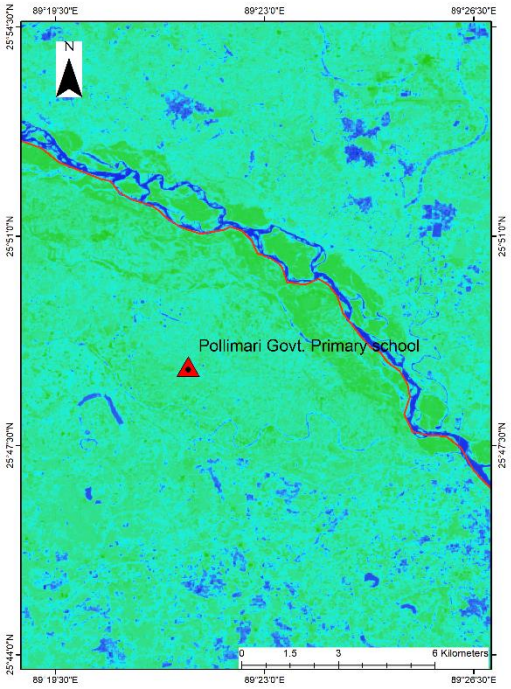

(d)

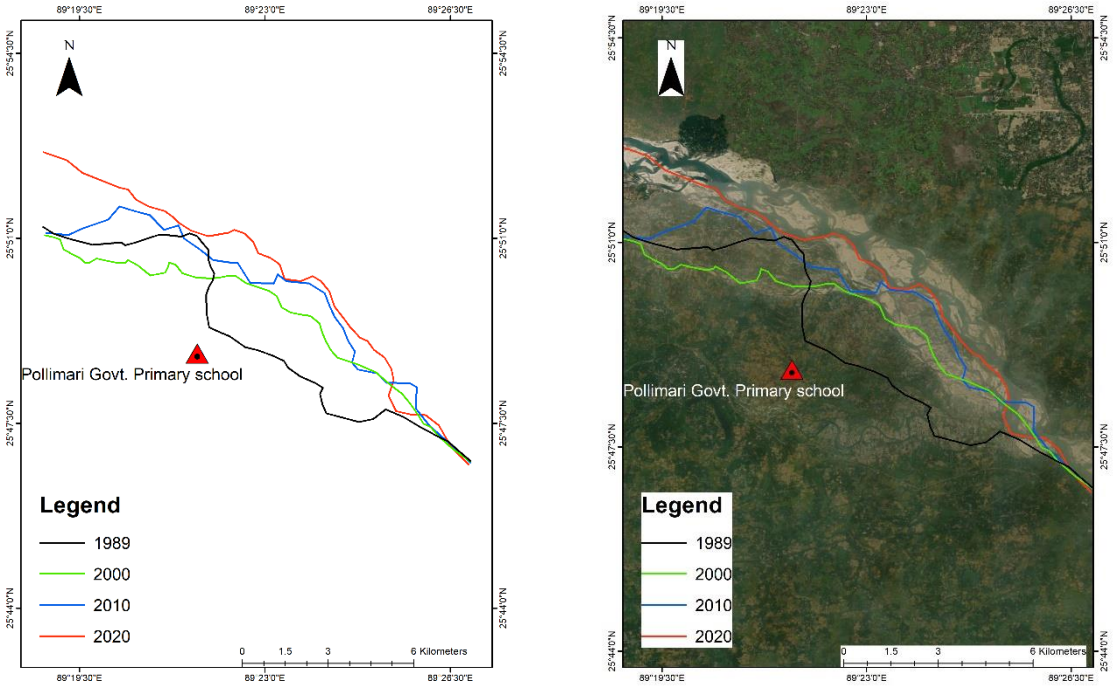

(e) (f)

Figure 5.49: River planform analysis near Pollimari Government Primary school from the year 1989 to 2020 using satellite data. Here is the river bank line of years (a)1989, (b) 2000, (c) 2010 and (d) 2020, and (e) bank line shifting from the year 1989 to 2020 and (f) on google earth image.

Table 5.19: Shifting of the river banks and flood vulnerability of Pollimari Government Primary school (West direction).

Pollimari Government Primary School (west direction)			
year	Distance of riverbank from Bazar (km)	Riverbank shifting (m)	Flood risk zone
1989	1.52	-	Low risk (1/6)
2000	4.04	2520(away from school)	
2010	4.64	600 (away from school)	
2020	4.86	220 (away from school)	

Based on the above analysis, the flood and erosion risks of the school are as follows-

- Flood Risk: The school is located in a **low** flood-risk area, considering the inundation patterns of all major floods in recent times. However, the surrounding area is at high flood risk.
- Bank Erosion Risk: Based on planform analysis using historical satellite images, the school is located in the **moderate** bank erosion risk area.

Location 11: Shoulmari Charvorot Government Primary School, Nilphamari District

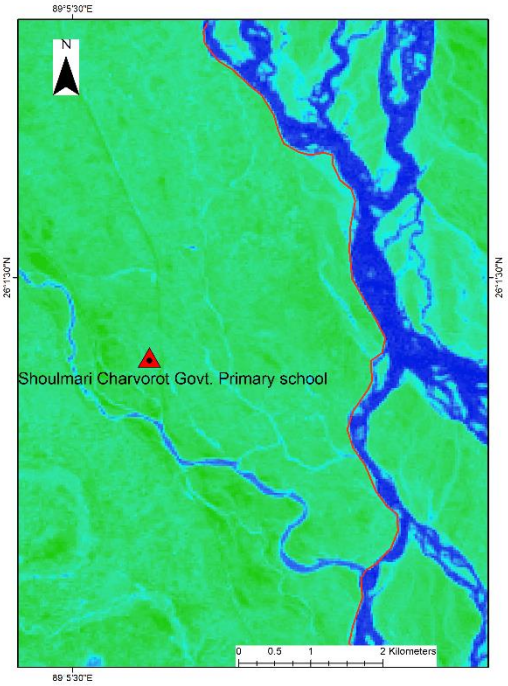

(a)

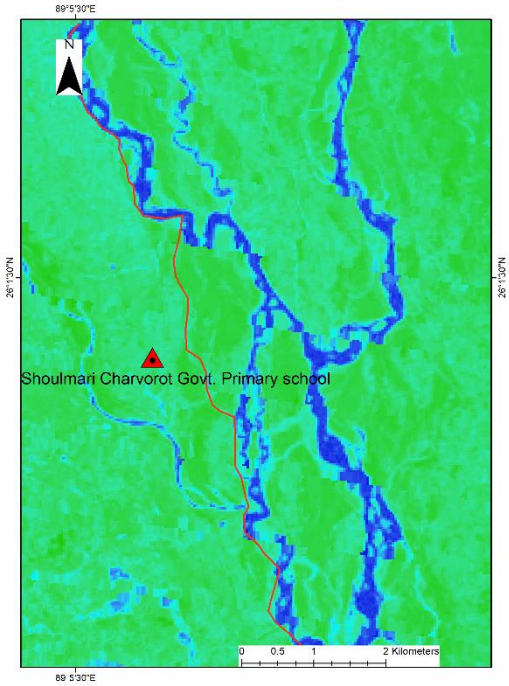

(b)

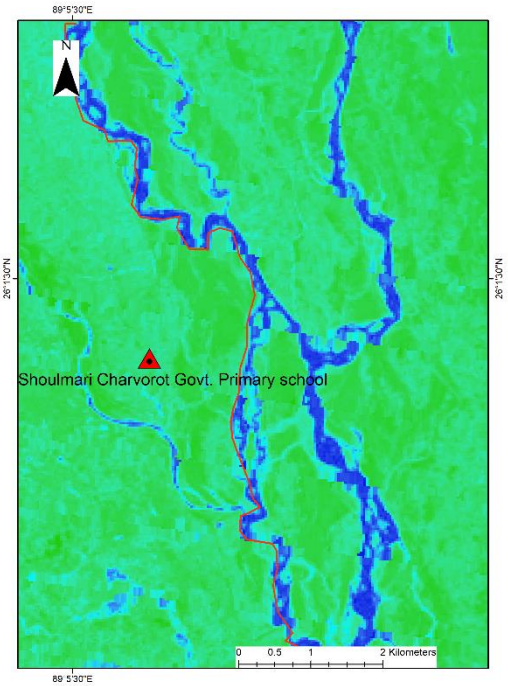

(c)

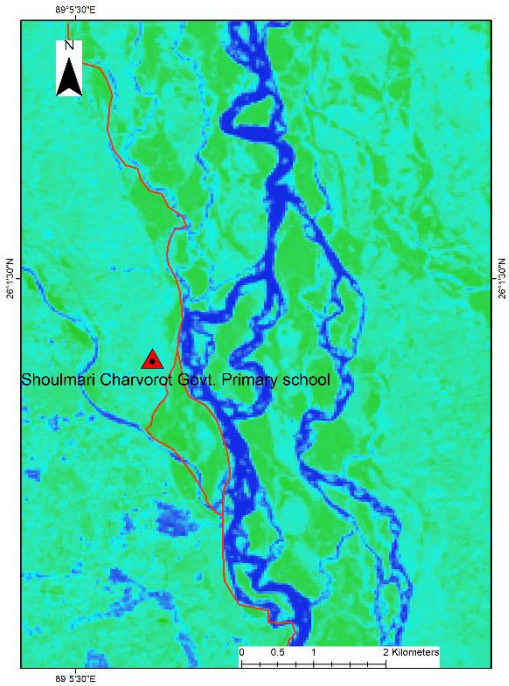

(d)

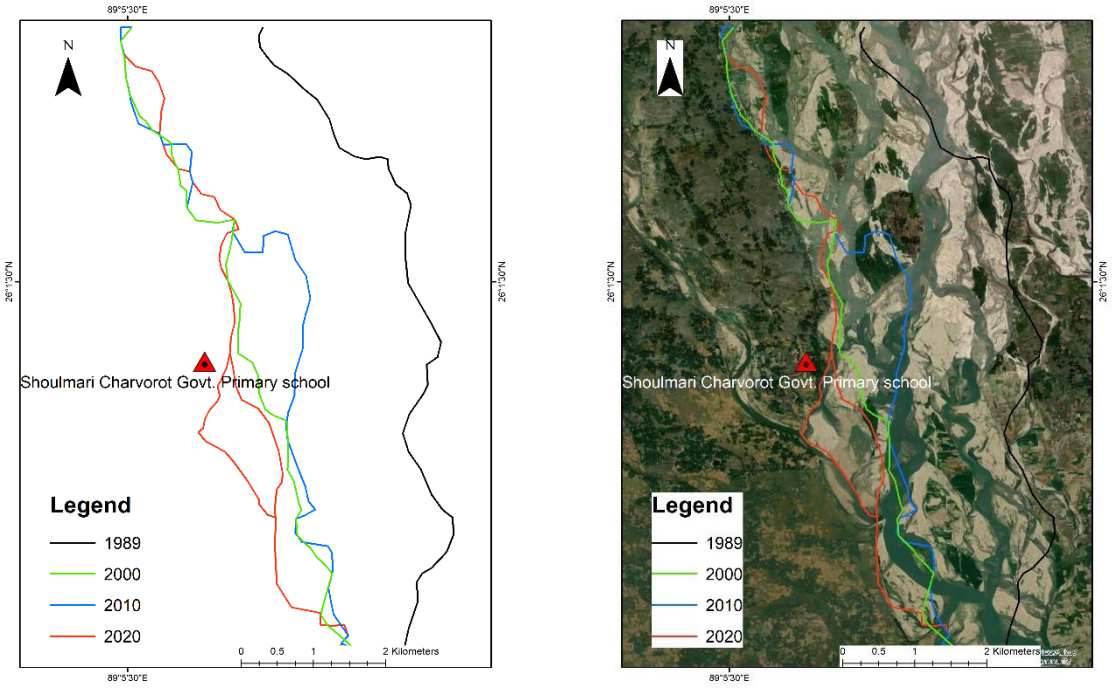

(e) (f)

Figure 5.50: River planform analysis near Shoulmari Charvorot Government Primary school from the year 1989 to 2020 using satellite data. Here is the river bank line of years (a)1989, (b) 2000, (c) 2010 and (d) 2020, and (e) bank line shifting from the year 1989 to 2020 and (f) on google earth image.

Table 5.20: Shifting of the river banks and flood vulnerability of Shoulmari Charvorot Government Primary school (West direction).

Shoulmari Charvorot Government Primary School (west direction)			
year	Distance of riverbank from Bazar (km)	Riverbank shifting (m)	Flood risk zone
1989	2.76	-	Moderate risk (2/6)
2000	0.56	2200	
2010	1.16	600 (away from school)	
2020	0.29	870	

Based on the above analysis, the flood and erosion risks of the school are as follows-

- Flood Risk: The school is located in a **low** flood-risk area, considering the inundation patterns of all major floods in recent times. However, the surrounding area is at high flood risk.
- Bank Erosion Risk: Based on planform analysis using historical satellite images, the school is located in the **high** bank erosion risk area.

Location 12: Tapakharibari 1 No Government Primary School, Nilphamari District

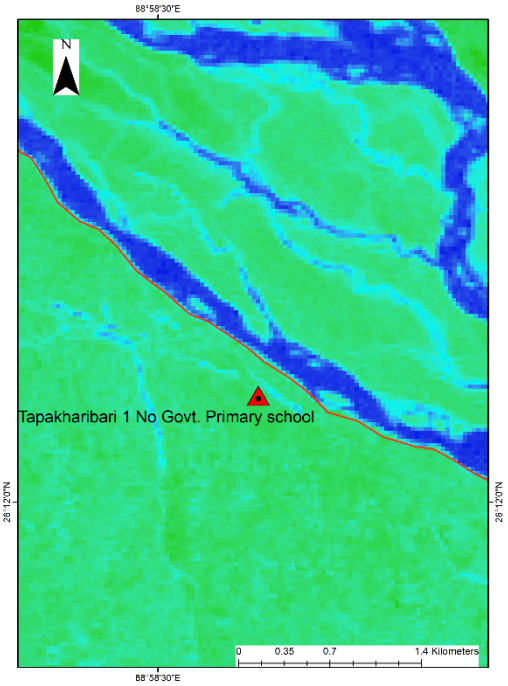

(a)

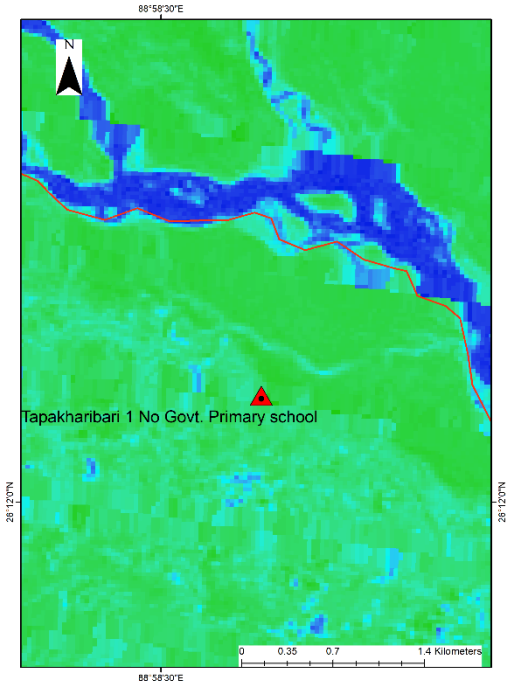

(b)

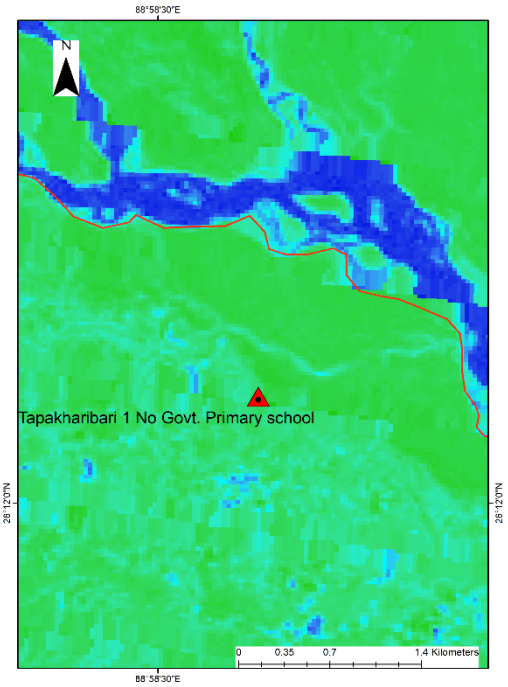

(c)

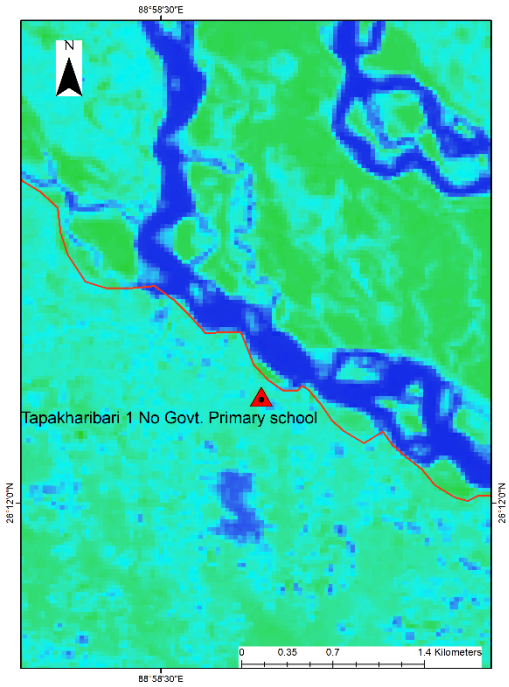

(d)

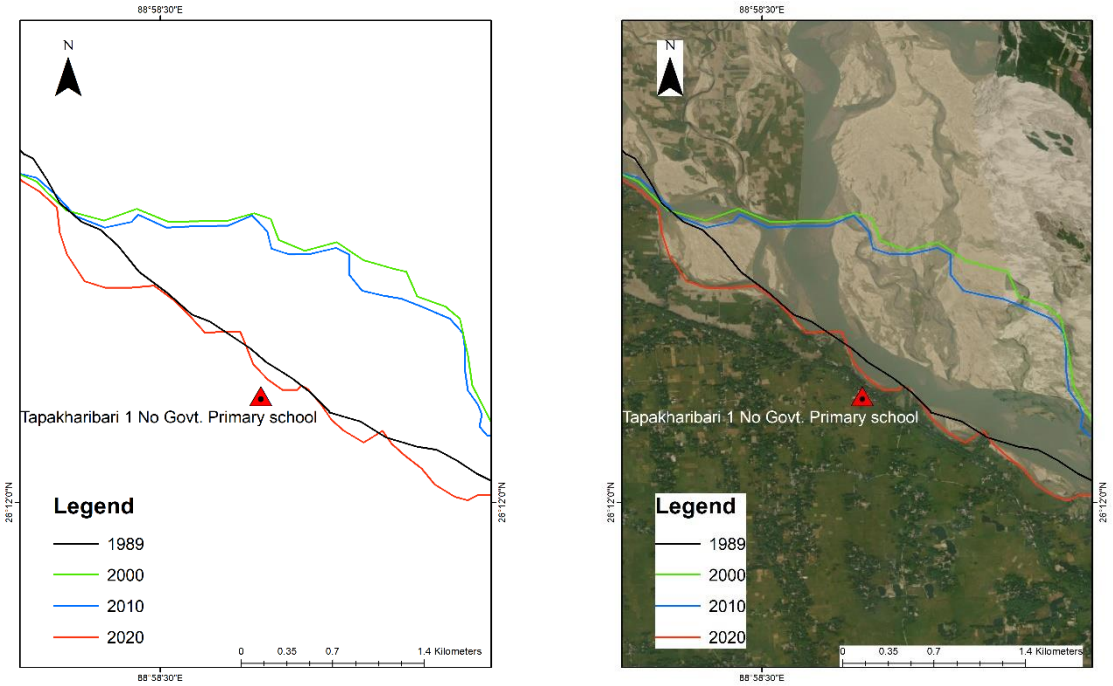

(e) (f)

Figure 5.51: River planform analysis near Tapakharibari 1 No Government Primary school from the year 1989 to 2020 using satellite data. Here is the river bank line of years (a)1989, (b) 2000, (c) 2010 and (d) 2020, and (e) bank line shifting from the year 1989 to 2020 and (f) on google earth image.

Table 5.21: Shifting of the river banks and flood vulnerability of Tapakharibari 1 No Government Primary school (North East direction).

Tapakharibari 1 No Government Primary School (North East direction)			
year	Distance of riverbank from Bazar (km)	Riverbank shifting (m)	Flood risk zone
1989	0.24	-	Moderate risk (2/6)
2000	1.33	1090 (away from school)	
2010	1.22	110	
2020	0.13	1090	

Based on the above analysis, the flood and erosion risks of the school are as follows-

- Flood Risk: The school is located in a **low** flood-risk area, considering the inundation patterns of all major floods in recent times. However, the surrounding area is at high flood risk.
- Bank Erosion Risk: Based on planform analysis using historical satellite images, the school is located in the **high** bank erosion risk area.

Location 13: Jotindra Naraya Government Primary School, Kurigram District

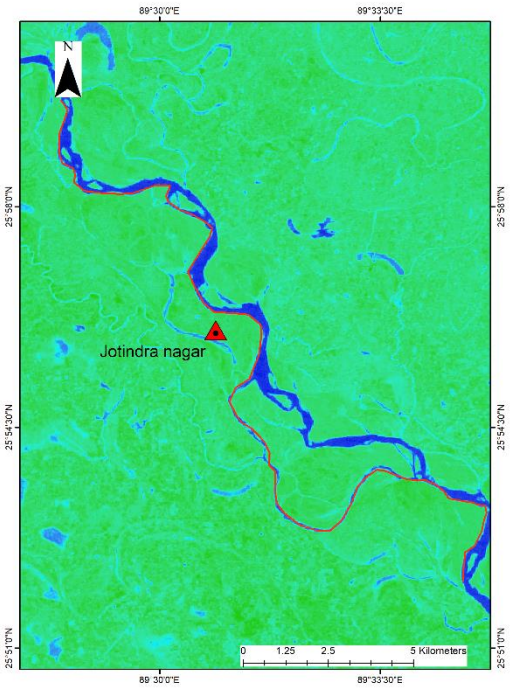

(a)

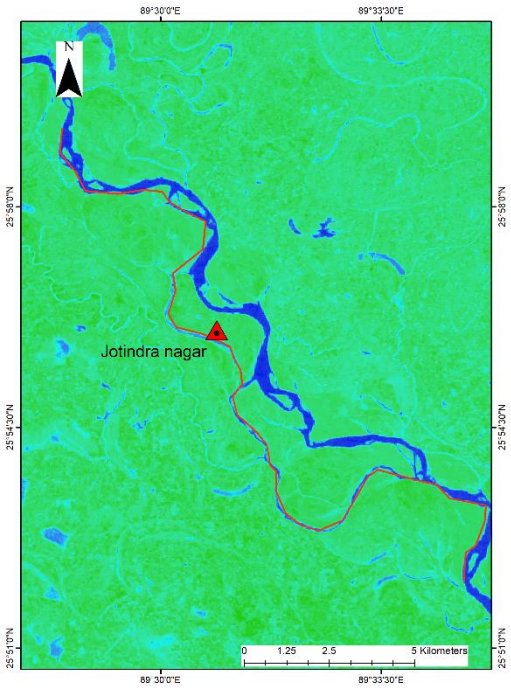

(b)

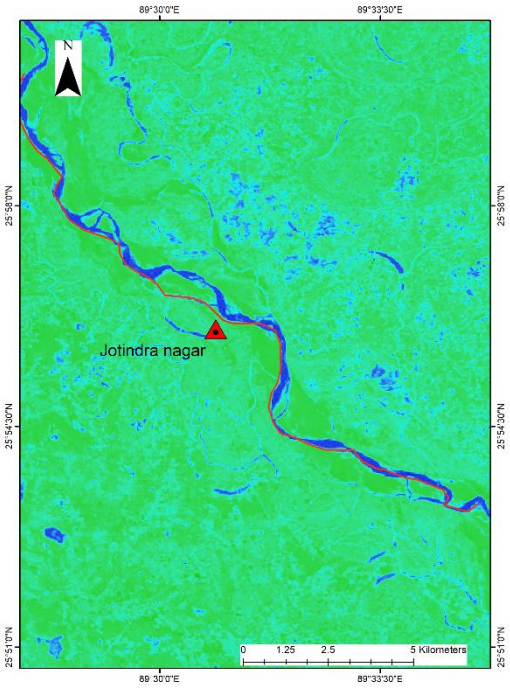

(c)

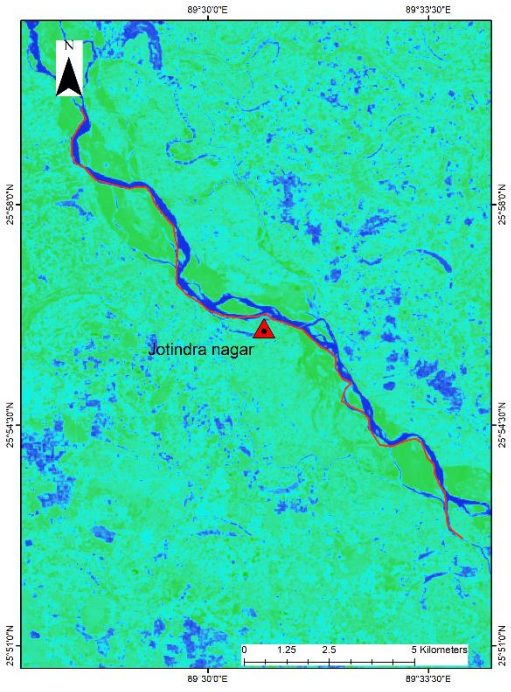

(d)

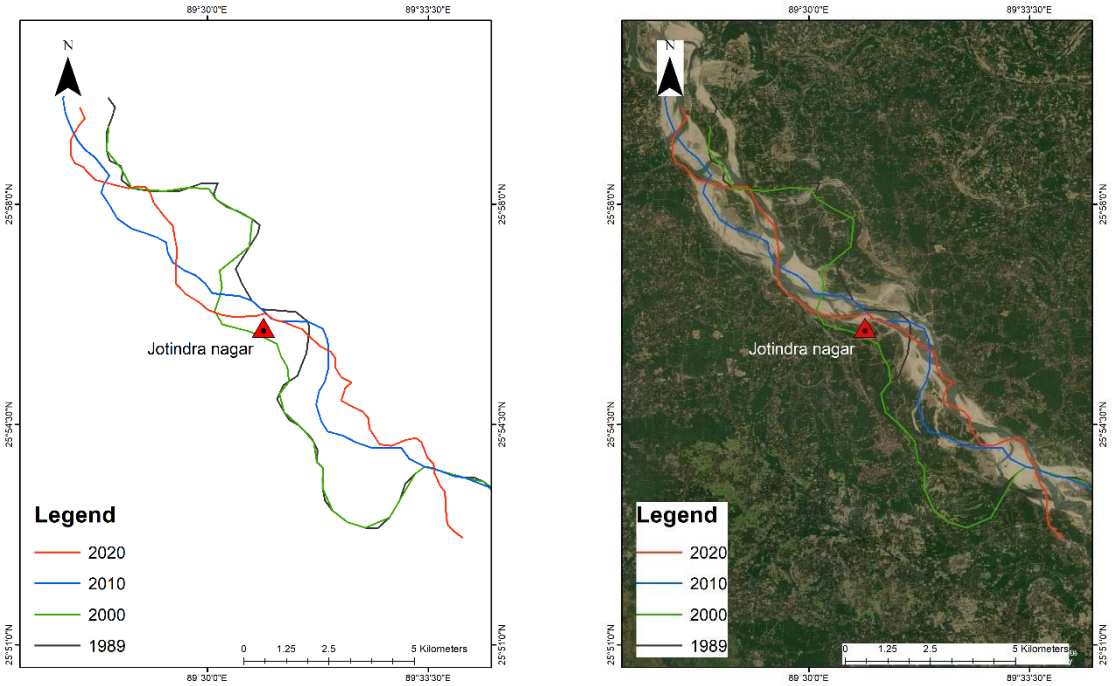

(e) (f)

Figure 5.52: River planform analysis near Jotindra Naraya Government Primary School, Kurigram District, from the year 1989 to 2020 using satellite data. Here river bank line of years (a)1989, (b) 2000, (c) 2010 and (d) 2020, and (e) bank line shifting from the year 1989 to 2020 and (f) on Google Earth image.

Table 5.22: Shifting of the river banks and flood vulnerability of Jotindra Naraya Government Primary School, Kurigram District (East direction)

Jotindra Naraya Government Primary School, Kurigram District (East direction)			
year	Distance of river bank from bazar (km)	River bank shifting (m)	Flood risk zone
1989	0.66		Low risk (1/6)
2000	0	660 (away from the location)	
2010	0.33	330 (away from the location)	
2020	0.35	20 (away from the location)	

Based on the above analysis, flood and erosion risks of the market are as follows-

- Flood Risk: The school is located in a **low** flood-risk area, considering the inundation patterns of all major floods in recent times. However, the surrounding area is at high flood risk.
- Bank Erosion Risk: Based on planform analysis using historical satellite images, the school is located in the **high** bank erosion risk area.

Location 14: Kochabari Bhurongamari Government Primary School, Kurigram District

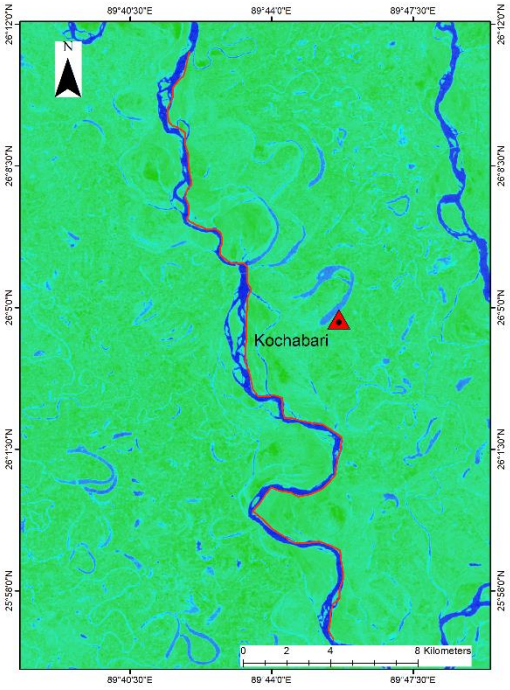

(a)

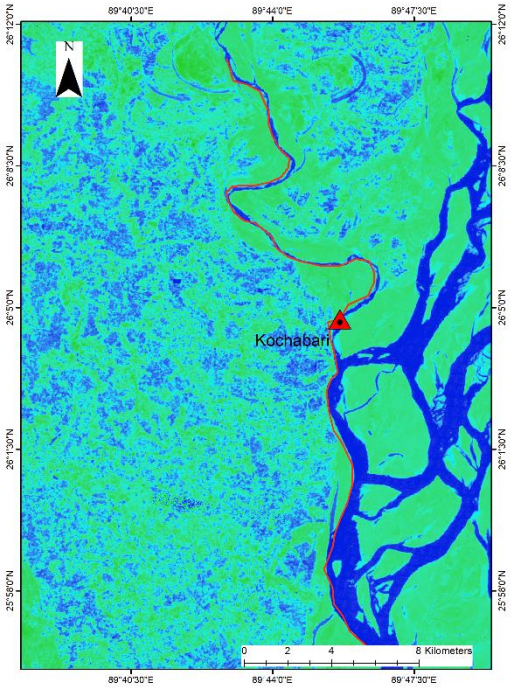

(b)

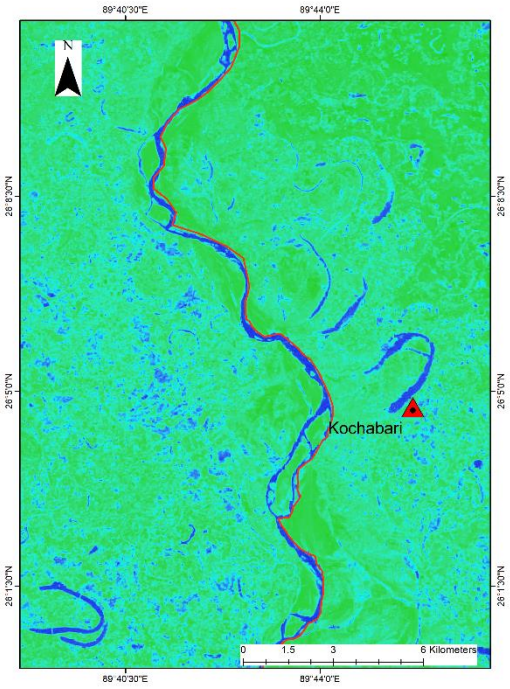

(c)

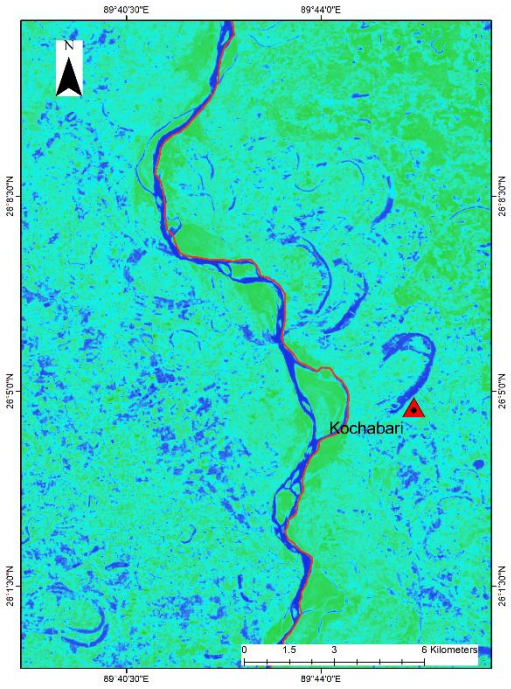

(d)

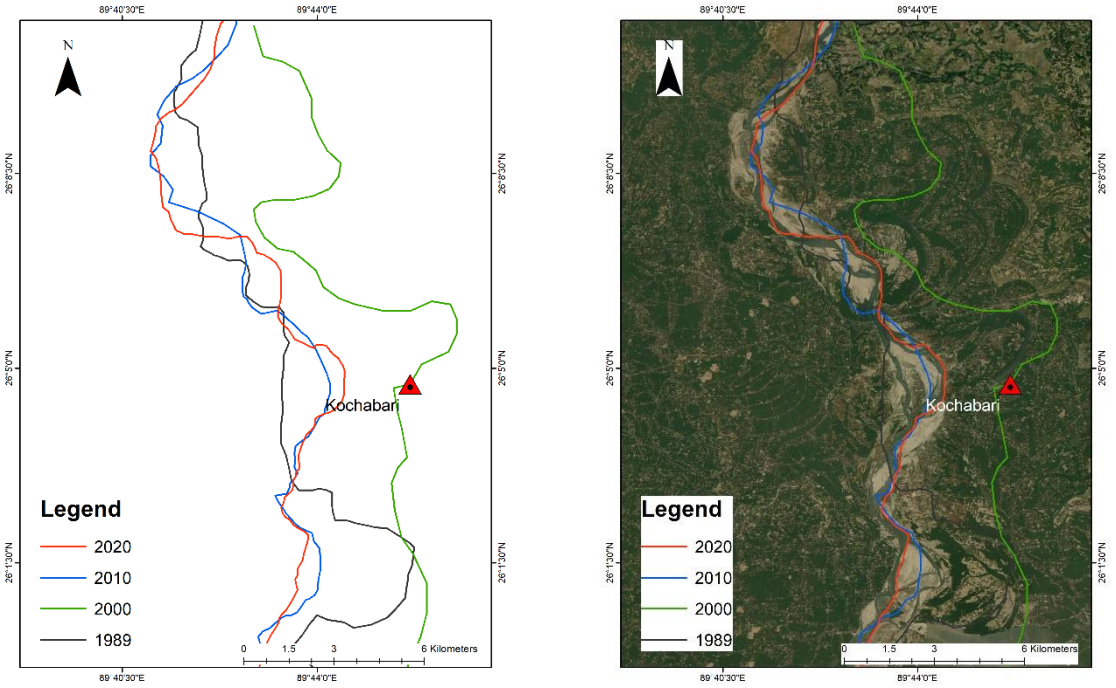

(e) (f)

Figure 5.53: River planform analysis near Kochabari Bhurongamari Government Primary School, Kurigram District, from the year 1989 to 2020 using satellite data. Here river bank line of years (a)1989, (b) 2000, (c) 2010 and (d) 2020, and (e) bank line shifting from the year 1989 to 2020 and (f) on Google Earth image.

Table 5.23: Shifting of the river banks and flood vulnerability of Kochabari Bhurongamari Government Primary School (East direction).

Kochabari Bhurongamari Government Primary School (East direction)			
year	Distance of river bank from bazar (km)	River bank shifting (m)	Flood risk zone
1989	3.82		Low risk (1/6)
2000	0	3820	
2010	2.39	2390 (away from the location)	
2020	1.96	0430	

Based on the above analysis, the flood and erosion risks of the school are as follows-

- Flood Risk: The school is located in a **low** flood-risk area, considering the inundation patterns of all major floods in recent times. However, the surrounding area is at high flood risk.
- Bank Erosion Risk: Based on planform analysis using historical satellite images, the school is located in the **low** bank erosion risk area.

Location 15: Sayadpur Government Primary School cum Flood Shelter

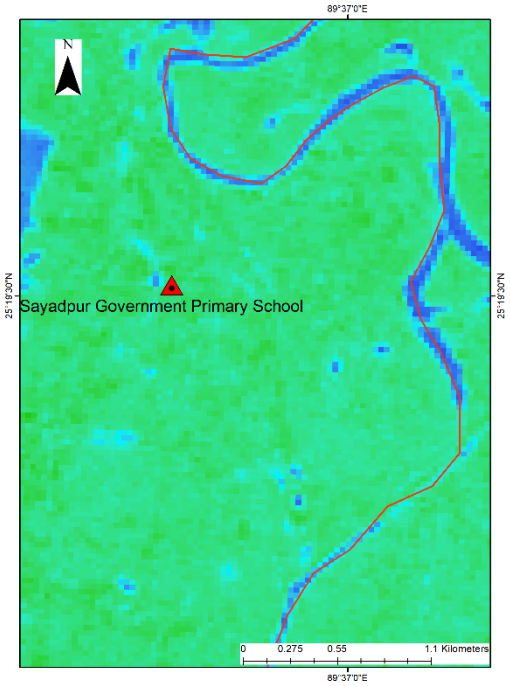

(a)

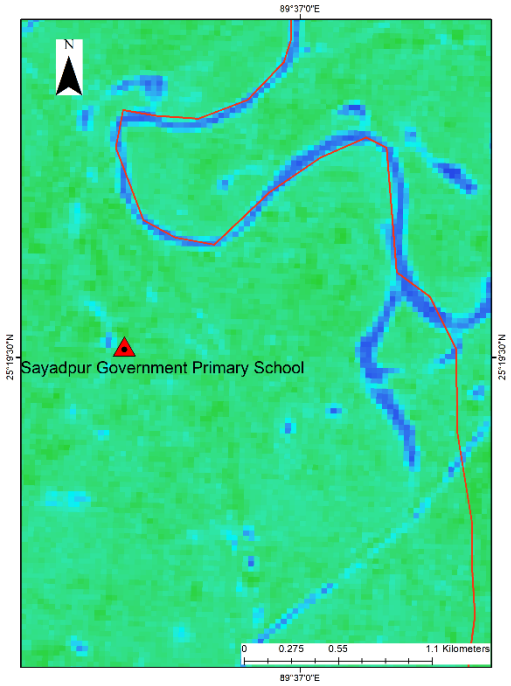

(b)

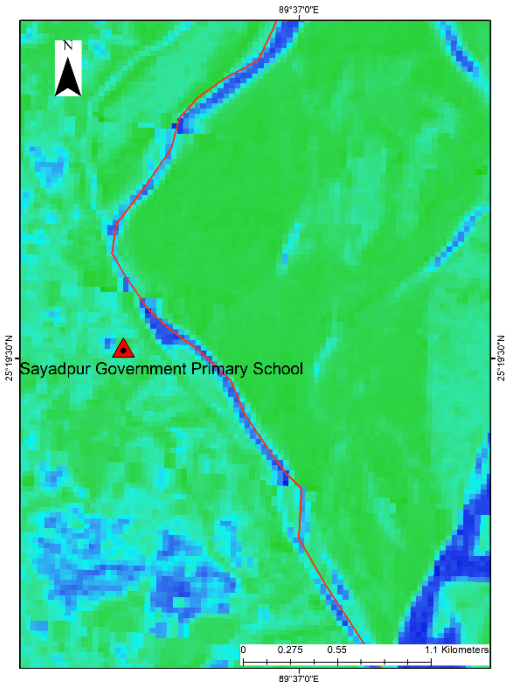

(c)

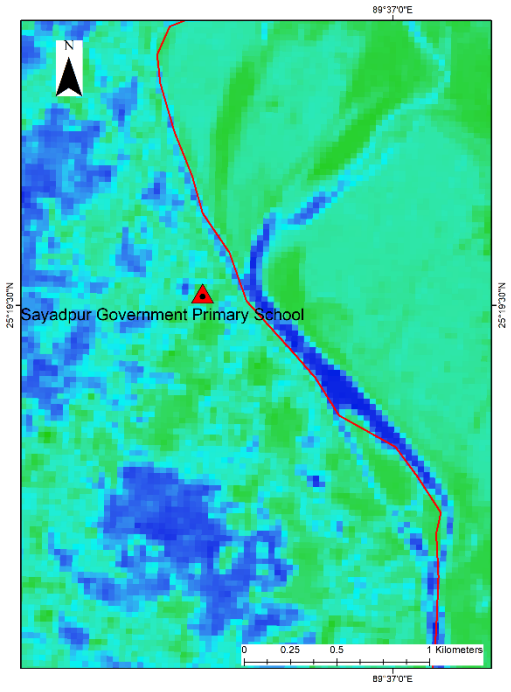

(d)

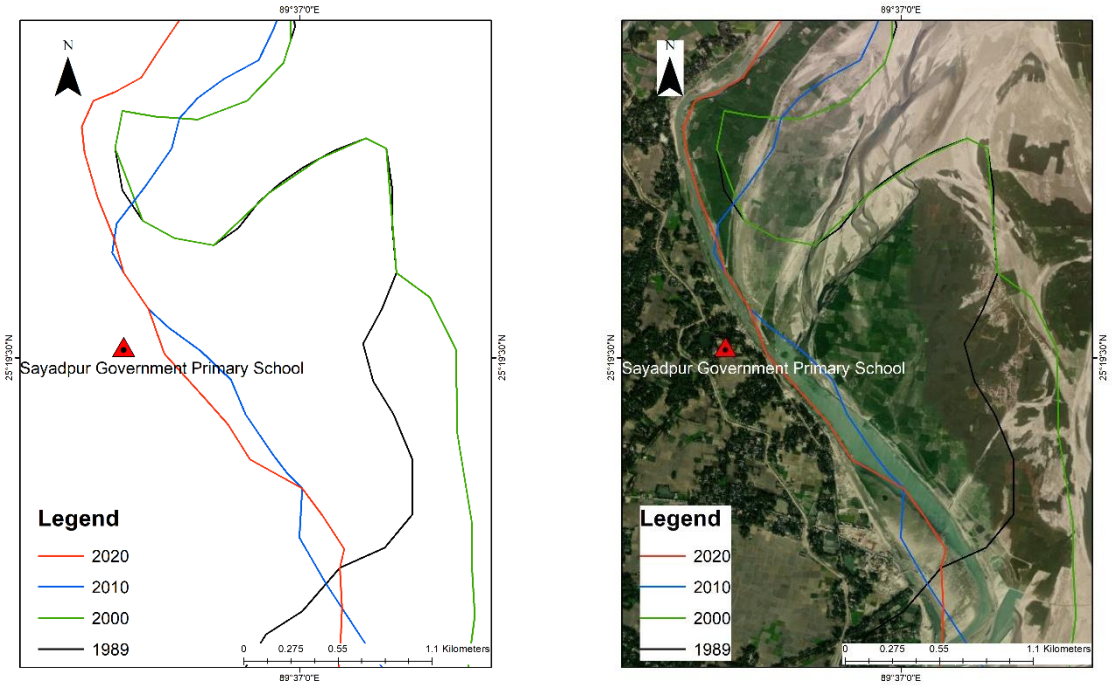

(e) (f)

Figure 5.54: River planform analysis near Sayadpur Government Primary School from the year 1989 to 2020 using satellite data. Here river bank line of years (a)1989, (b) 2000, (c) 2010 and (d) 2020, and (e) bank line shifting from the year 1989 to 2020 and (f) on Google Earth image.

Table 5.24: Shifting of the river banks and flood vulnerability of Sayadpur Government Primary School (East direction).

Sayadpur Government Primary School (East direction)			
year	Distance of river bank from bazar (km)	River bank shifting (m)	Flood risk zone
1989	1.26		Low risk (1/6)
2000	1.72	460 (away from the location)	
2010	0.32	1400	
2020	0.19	130	

Based on the above analysis, the flood and erosion risks of the school are as follows-

- Flood Risk: The school is located in a **low** flood-risk area, considering the inundation patterns of all major floods in recent times. However, the surrounding area is at high flood risk.
- Bank Erosion Risk: Based on planform analysis using historical satellite images, the school is located in the **high** bank erosion risk area.

Location 16: Bashir Nagar Government Primary School cum Flood Shelter

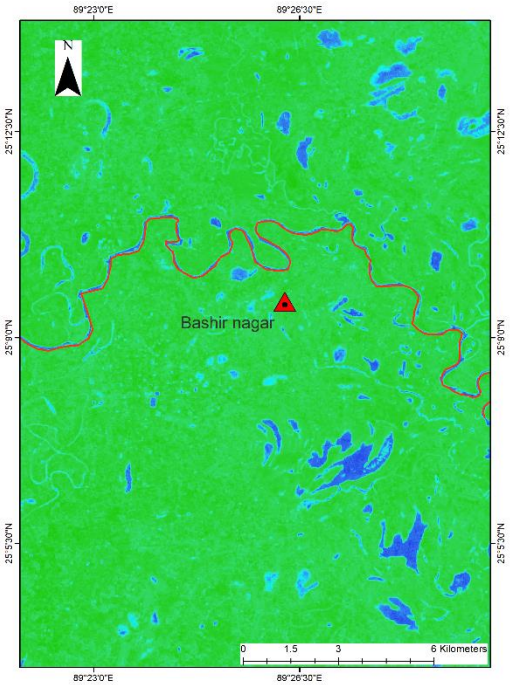

(a)

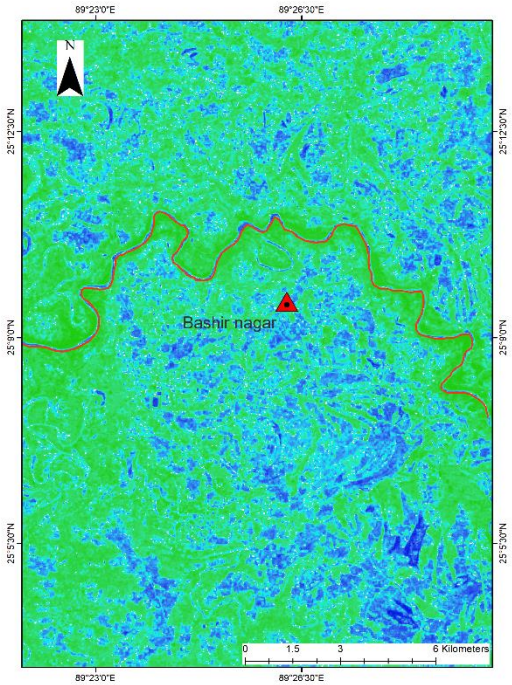

(b)

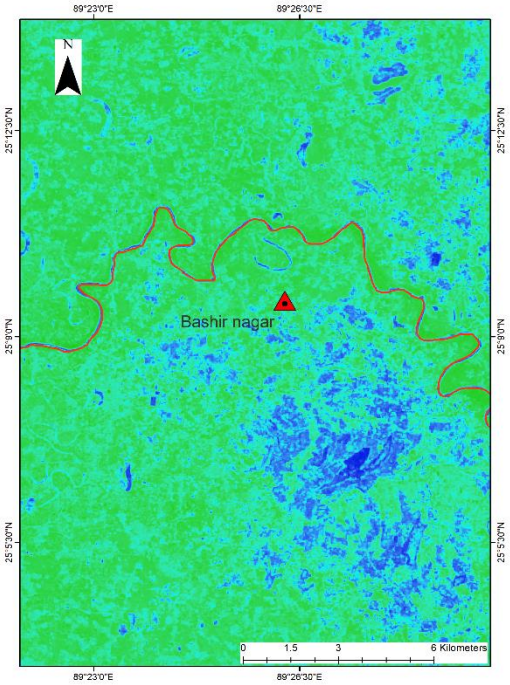

(c)

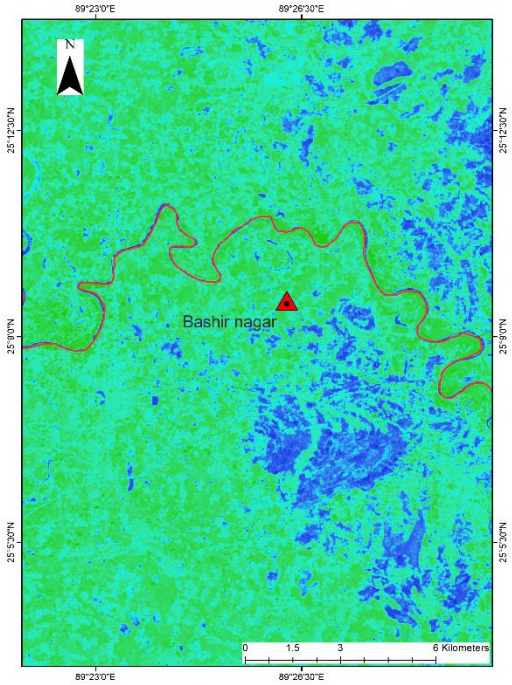

(d)

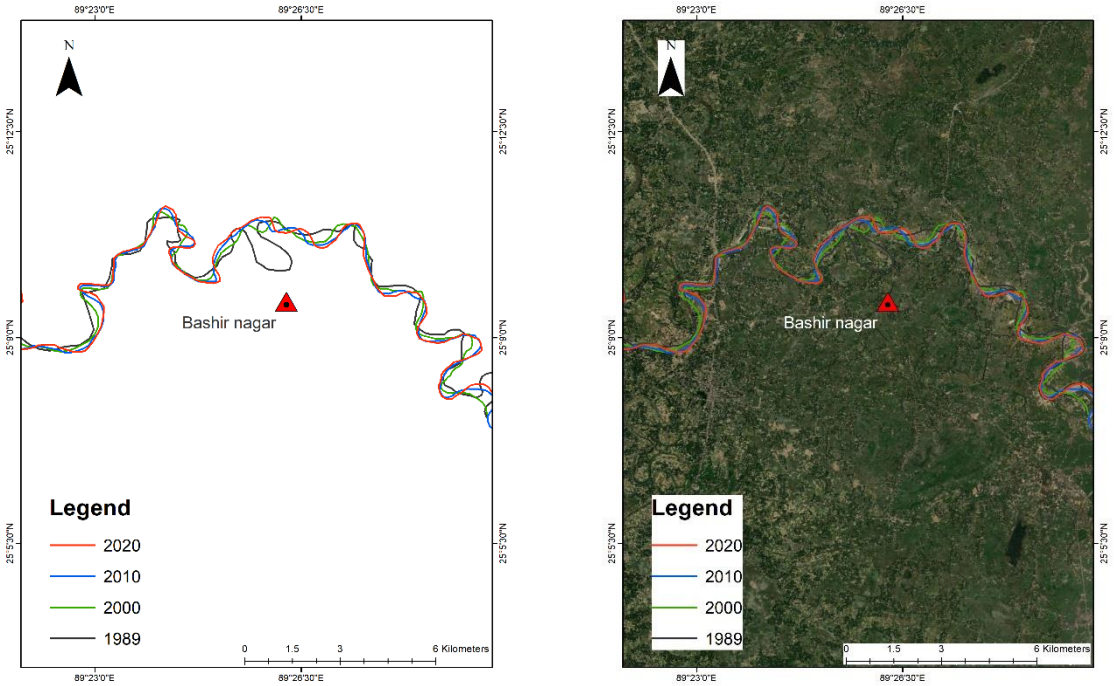

(e) (f)

Figure 5.55: River planform analysis near Bashir Nagar Government Primary School from the year 1989 to 2020 using satellite data. Here river bank line of years (a)1989, (b) 2000, (c) 2010 and (d) 2020, and (e) bank line shifting from the year 1989 to 2020 and (f) on Google Earth image.

Table 5.25: Shifting of the river banks and flood vulnerability of Bashir Nagar Government Primary School (East direction).

Bashir Nagar Government Primary School (North West direction)			
year	Distance of river bank from bazar (km)	River bank shifting (m)	Flood risk zone
1989	0.99		Moderate risk (2/6)
2000	2.27	1280 (away from the location)	
2010	2.15	120	
2020	2.02	130	

Based on the above analysis, the flood and erosion risks of the school are as follows-

- Flood Risk: The school is located in a **low** flood-risk area, considering the inundation patterns of all major floods in recent times. However, the surrounding area is at high flood risk.
- Bank Erosion Risk: Based on planform analysis using historical satellite images, the school is located in the **low** bank erosion risk area.

Location 17: Bekrir Char Government Primary School cum Flood Shelter

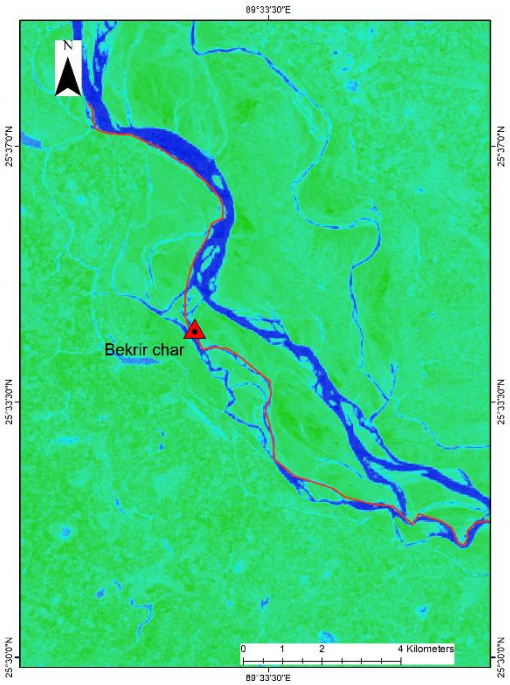

(a)

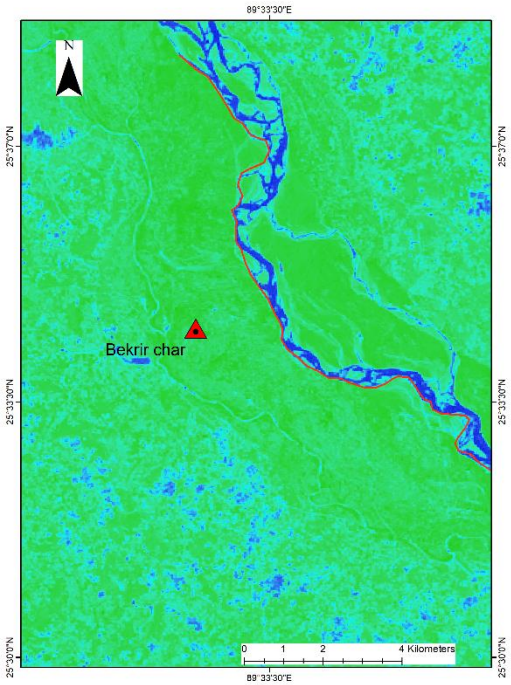

(b)

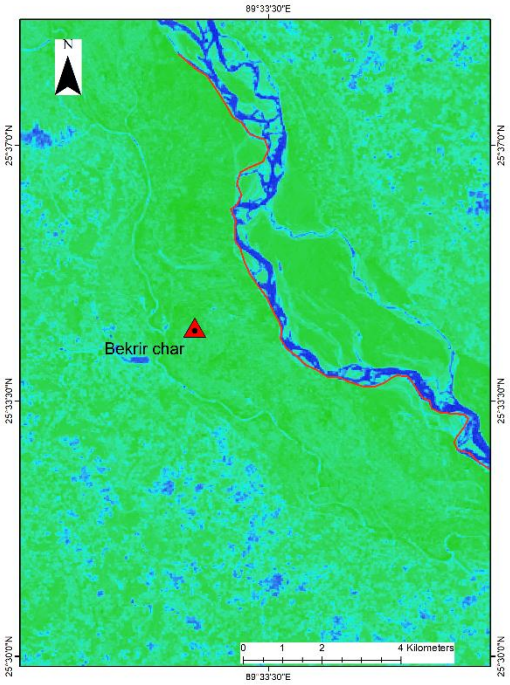

(c)

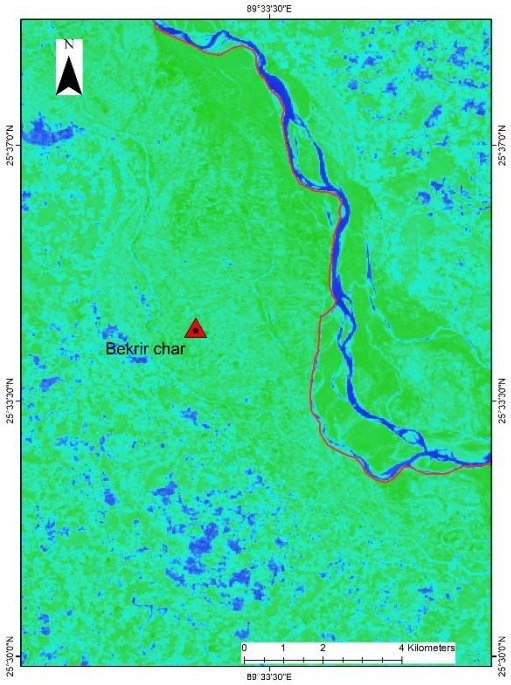

(d)

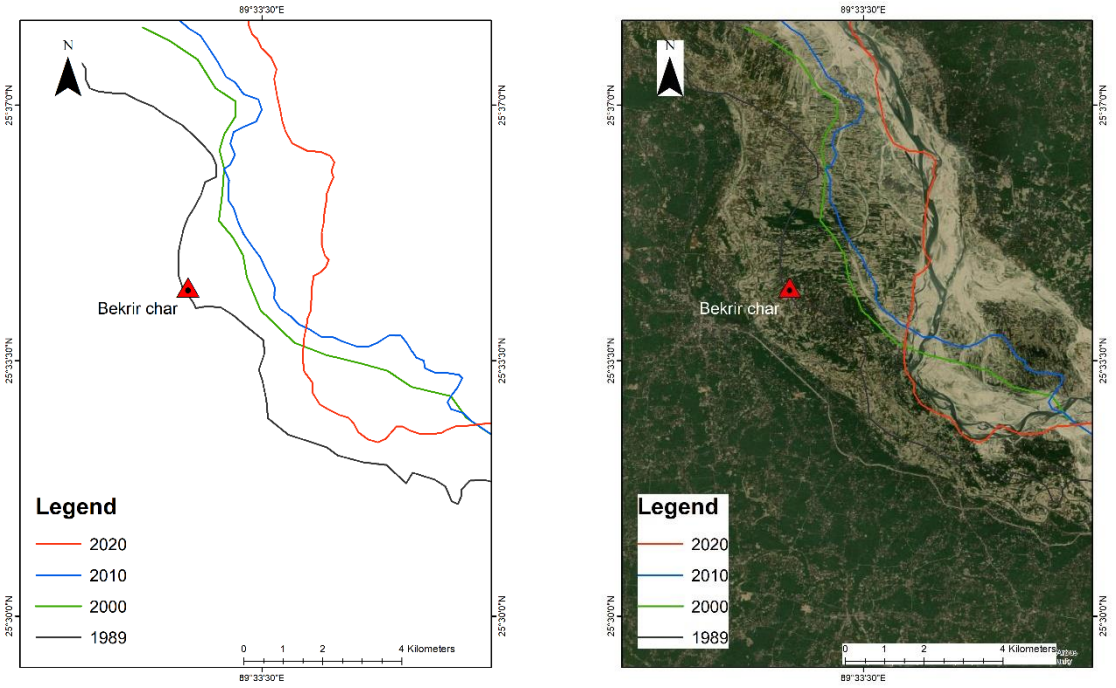

(e) (f)

Figure 5.56: River planform analysis near Bekrir Char Government Primary School from the year 1989 to 2020 using satellite data. Here river bank line of years (a)1989, (b) 2000, (c) 2010 and (d) 2020, and (e) bank line shifting from the year 1989 to 2020 and (f) on Google Earth image.

Table 5.26: Shifting of the river banks and flood vulnerability of Bekrir Char Government Primary School (East direction).

Bekrir Char Government Primary School (East direction)			
year	Distance of river bank from bazar (km)	River bank shifting (m)	Flood risk zone
1989	0		Low risk (1/6)
2000	1.41	1410 (away from the location)	
2010	1.94	530 (away from the location)	
2020	2.81	870 (away from the location)	

Based on the above analysis, the flood and erosion risks of the school are as follows-

- Flood Risk: The school is located in a **low** flood-risk area, considering the inundation patterns of all major floods in recent times. However, the surrounding area is at high flood risk.
- Bank Erosion Risk: Based on planform analysis using historical satellite images, the school is located in the **high** bank erosion risk area.

Location 18: Chinirpatol Government Primary School cum Flood Shelter

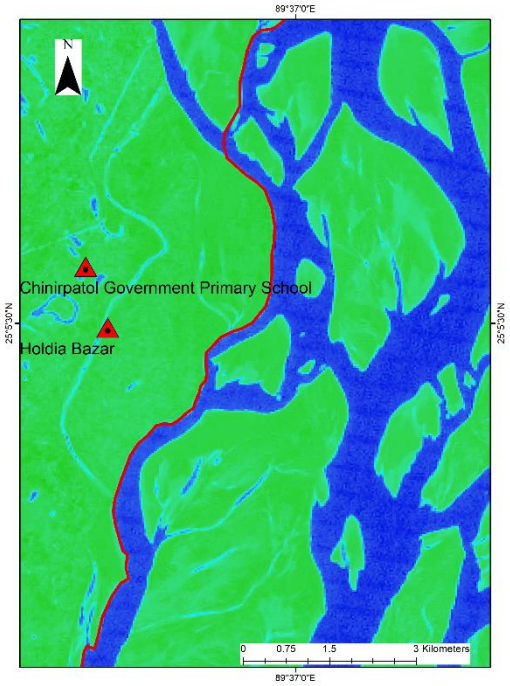

(a)

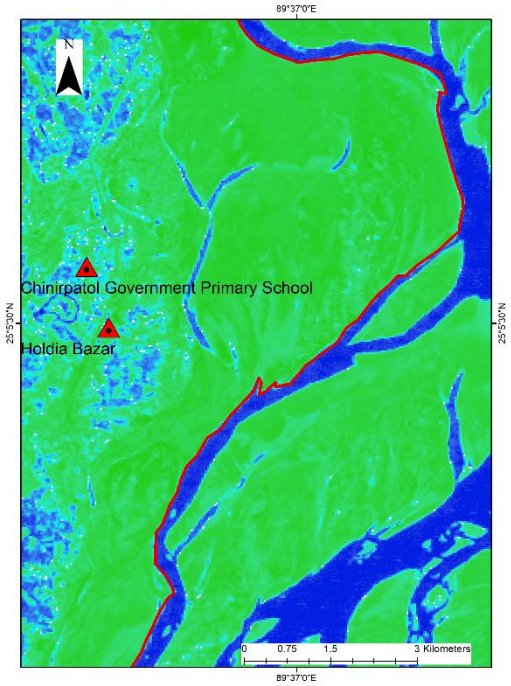

(b)

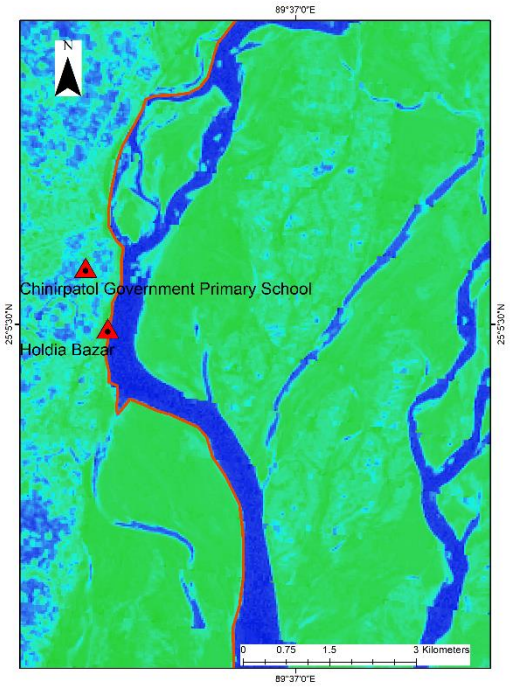

(c)

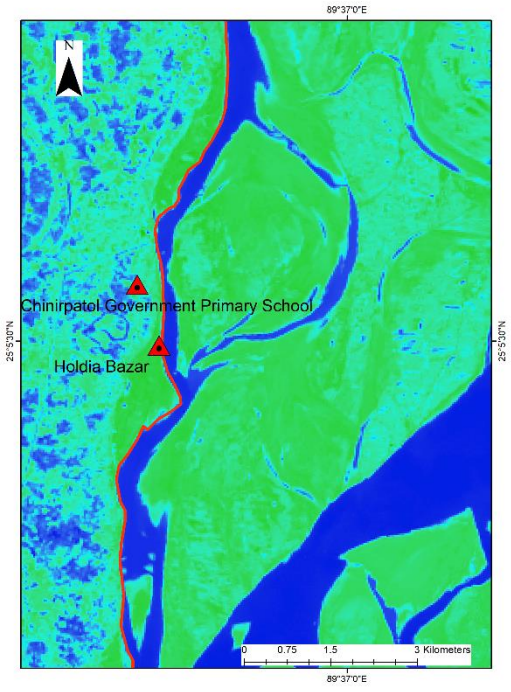

(d)

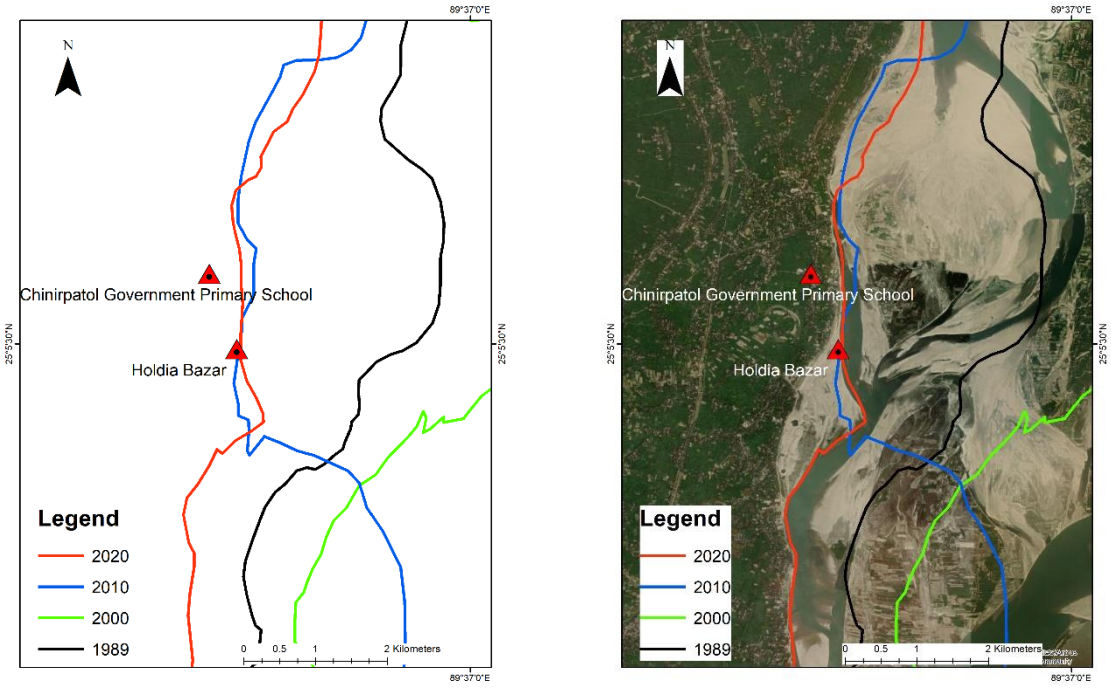

Figure 5.57: River planform analysis near Chinirpatol Government Primary School from the year 1989 to 2020 using satellite data. Here river bank line of years (a)1989, (b) 2000, (c) 2010 and (d) 2020, and (e) bank line shifting from the year 1989 to 2020 and (f) on Google Earth image.

Table 5.27: Shifting of the river banks and flood vulnerability of Chinirpatol Government Primary School (East direction).

Chinirpatol Government Primary School (East direction)			
year	Distance of river bank from bazar (km)	River bank shifting (m)	Flood risk zone
1989	2.92		Low risk (1/6)
2000	4.89	1970 (away from the location)	
2010	0.56	4330	
2020	0.41	150	

Based on the above analysis, the flood and erosion risks of the school are as follows-

- Flood Risk: The school is located in a **low** flood-risk area, considering the inundation patterns of all major floods in recent times. However, the surrounding area is at high flood risk.
- Bank Erosion Risk: Based on planform analysis using historical satellite images, the school is located in the **high** bank erosion risk area.

Table 5.28: Combined flood and bank erosion risks of the proposed school cum flood shelters in the selected locations.

No	Shelter name	Upazila	District	Distance from River (m)	River name	Flood Risk	Bank Erosion Risk
1	Abdul Gani GPS	Bakshigonj	Jamalpur	360	Dasani	Low	Low
2	Chinarchar Uttar para GPS	Bakshigonj	Jamalpur	420	Dasani	Low	Low
3	Shapdhori Govt. Primary school	Jamalpur	High	159	Brahmaputra	High	High
4	Shukhnogory GPS	Madargonj	Jamalpur	2007	Jamuna	Moderate	Low
5	All Haz Gohor Junior School	Hatibandha	Nilphamari	670	Teesta	Low	Moderate
6	Ajam Kha GPS	Kaunia	Rangpur	2880	Teesta	Low	Low
7	Dalia Baishpukure Tistarchar GPS	Dimla	Nilphamari	830	Minor River	Moderate	Low
8	Char Holdibari GPS	Jaldhaka	Nilphamari	1040	Teesta	Moderate	Moderate
9	Jongra 3 No Battala GPS	Patgram	Lalmonirhat	720	Dharala	Moderate	Moderate
10	Pollimari GPS	Kaunia	Rangpur	4860	Teesta	Low	moderate
11	Shoulmari Charvorot GPS	Jaldhaka	Nilphamari	290	Teesta	Low	High
12	Tapakharibari 1 No GPS	Dimla	Nilphamari	130	Teesta	Low	High
13	Jotindra Naraya Government Primary School	Kurigram	Phulbari	350	Teesta	Low	High
14	Kochabari GPS	Bhurongamari	Kurigram	1960	DudKumur	Low	Low
15	Saiyadpur GPS cum Shelter	Gaibandha Sadar	Gaibandha	190	Teesta	Low	High
16	Bashir Nagor GPS	Shadullahpur	Gaibandha	2020	Karotoya	Low	Low
17	Bekrir Chaer GPS	Sundorgonj	Gaibandha	2810	Teesta	Low	High
18	Chinirpatol Government Primary School	Shaghata	Gaibandha	410	Brahmaputra	Low	High

5.5.6 Combined Flood and Bank Erosion Risks for Markets

Based on planform analysis using historical satellite images, bank erosion risks are identified for the proposed markets in the selected locations on a scale of low, moderate and high. Finally, combined flood and bank erosion risks on the markets are presented in Table 5.29. The details of the analysis of the above-mentioned markets are given in the next sections.

Table 5.29: Combined flood and bank erosion risks of the proposed markets in the selected locations.

Sl.	District	Upazila	Market Name	Rivers	Distance from River (m)	Flood Risk	Bank Erosion Risk
1	Gaibandha	Sadullapur	Boxigonj Bazar	Minor river	105	Low	Low
2	Gaibandha	Sundarganj	Charokerhat Bazar	Minor river	2250	Low	Low
3	Gaibandha	Sundarganj	Jamaler Hat	Minor river	2350	Low	Low
4	Gaibandha	Saghatta	Dakhin Dighalkandi	Brahmaputra	10	Moderate	High
5	Gaibandha	Saghatta	Falia Bottala	Minor river	380	Low	Low
6	Gaibandha	Saghatta	Futani Bazar			Low	N/A***
7	Gaibandha	Saghatta	Ullah Bazar	Brahmaputra	400	Low	High*
8	Gaibandha	Saghatta	Nayabondar Bazar	Minor river	290	Low	Low
9	Gaibandha	Saghatta	Ullah Sonatala	Minor river	10	Low	High*
10	Gaibandha	Sadullapur	Kantanagar Bazar	Minor river	420	Low	Low
11	Gaibandha	Gaibandha Sadar	Lenga Bazar	Minor river	730	Low	Low
12	Gaibandha	Gaibandha Sadar	Puratan Badiakhali Hat	Minor river	30	Low	High
13	Gaibandha	Gaibandha Sadar	Balua Hat	Minor river	5800	Moderate	Low
14	Gaibandha	Fulchhari	Purbo Fulchori Bazar	Brahmaputra	1545	Low	Moderate
15	Rangpur	Gangachara	Bagerhat	Teesta	760	Low	High
16	Rangpur	Gangachara	Abuliarhat	Teesta	1170	Moderate	Moderate
17	Rangpur	Gangachara	Ichli Bazar (SKS Bazar)	Teesta	430	Low	High
18	Rangpur	Kaunia	Ekotarhat	Minor rivers	810	Low	Low
19	Rangpur	Kaunia	Haqueer Hat	Teesta	1100	Low	Moderate
20	Rangpur	Kaunia	Bhaier Hat	Minor river	65	Low	Moderate
21	Rangpur	Kaunia	Bhutsora (Mirbag) Hat	Minor river	200	Moderate	Moderate
22	Jamalpur	Islampur	Bulakip (ara Bazar)	Minor river	10	Low	High
23	Jamalpur	Islampur	Mondalpara Bazar	Brahmaputra	185	Low	High**
24	Jamalpur	Islampur	Napiterchar Bazar	Minor river	600	Low	Low
25	Jamalpur	Islampur	Shirajabad Bazar	Old Brahmaputra	760	Low	Moderate
26	Jamalpur	Islampur	Akota Bazar	Jamuna	835	Low	High
27	Jamalpur	Dewanganj	Amkhowa Bazar	Jinjiram	2100	Low	Low

Sl.	District	Upazila	Market Name	Rivers	Distance from River (m)	Flood Risk	Bank Erosion Risk
28	Jamalpur	Dewanganj	Molla Para Bazar(Tilokpur)	Old Brahmaputra	500	Low	High
29	Jamalpur	Dewanganj	Sanandabari	Minor river	240	Low	Low
30	Jamalpur	Dewanganj	Khorma bazar	Minor river	420	Low	Low
31	Jamalpur	Melandaha	Bhabki Bazar	Minor river	1375	Low	Low
32	Jamalpur	Melandaha	Bhaluka(Tarankandi Bazar)	Old Brahmaputra	1450	Low	Low
33	Jamalpur	Melandaha	Char Gobindi Bazar	Jamuna	1200	Low	Moderate
34	Jamalpur	Melandaha	Gazipur Bazar	Minor river	75	Low	Moderate
35	Jamalpur	Melandaha	Gobindoganj Bazar	Minor river	20	Low	High*
36	Jamalpur	Melandaha	Mahmudpur	Minor river	1850	Low	Low
37	Jamalpur	Melandaha	Jhawgora Bazar	Minor river	2430	Low	Low
38	Jamalpur	Melandaha	Kahetpara bazar	Minor river	35	Low	High
39	Jamalpur	Madarganj	Koali Kandi Bazar	Minor river	60	Low	Moderate
40	Jamalpur	Madarganj	Millon Bazar	Minor river	1550	Low	Low
41	Jamalpur	Madarganj	Nabbo Char Bazar	Minor river	500	Low	Low
42	Jamalpur	Madarganj	Rayerchara Bazar	Minor river	1250	Low	Low
43	Jamalpur	Madarganj	Tegharaia Bazar	Minor river		Low	N/A***
44	Jamalpur	Madarganj	Nalsia bazar	Minor river	550	Moderate	Low
45	Jamalpur	Melandaha	Talukpara Bazar	Minor river	70	Moderate	Moderate
46	Jamalpur	Melandaha	Tegharia Bazar	Minor river	775	Low	Low
47	Jamalpur	Bakshiganj	Duttapara Ananda Bazar	Minor river	205	Low	Low
48	Jamalpur	Bakshiganj	Parchim kamalerbatti Bazar	Jinjiram	1070	Low	Low
49	Jamalpur	Melandaha	Saguna Bazar	Minor river	1280	Low	Low
50	Lalmonirhat	Hatibandha	Dighir Hat	Teesta	2581	Low	Low
51	Lalmonirhat	Hatibandha	Chander Hat	Minor rivers	780	Low	Low
52	Lalmonirhat	Hatibandha	Muktijoddha Hat	Teesta	2400	Low	Low
53	Lalmonirhat	Hatibandha	Nowdabash Hat			Low	N/A***
54	Lalmonirhat	Patgram	Burimari Hat	Dharala	300	Low	Moderate
55	Lalmonirhat	Patgram	Kamarar Hat	Dharala	3000	No	Low
56	Lalmonirhat	Patgram	Kashirdangga Hat	Dharala	2650	Low	Low
57	Lalmonirhat	Patgram	Nayer Hat	Teesta	463	Moderate	High*
58	Lalmonirhat	Patgram	Shofinagar Hat	Minor river	1420	Low	Low
59	Lalmonirhat	Patgram	Sharkaar Hat	Dharala	1610	Low	Low
60	Lalmonirhat	Patgram	Loliter Hat	Dharala	2287	Low	Low
61	Kurigram	Bhurungamari	Baldia Bazar	Dudkumur	1350	Low	Low
62	Kurigram	Bhurungamari	Muktijodha Hat Bhurungamari	Minor river		Low	N/A***
63	Kurigram	Bhurungamari	Chowdhurir hat	Dudkumur	400	Low	Moderate
64	Kurigram	Nageshwari	Schooler Hat	Minor river		Moderate	N/A***
65	Kurigram	Nageshwari	Chilakhana Hat	Minor river	800	Moderate	Low
66	Kurigram	Nageshwari	Maniganj Bazar	Minor river	450	Low	Low
67	Kurigram	Nageshwari	Berubari Hat	Minor river	190	Low	Low
68	Kurigram	Phulbari	Bokultala Bazar	Dharala	770	Low	Moderate

Sl.	District	Upazila	Market Name	Rivers	Distance from River (m)	Flood Risk	Bank Erosion Risk
69	Kurigram	Phulbari	Ghogurhat Bazar	Minor river		Low	N/A***
70	Kurigram	Phulbari	Shiber Bazar	Minor river	410	Low	Low
71	Kurigram	Phulbari	Boroloi Bazar	Dharala	1770	Low	Low
72	Kurigram	Rajarhat	Chandamari Hat	Teesta	2750	Low	Low
73	Kurigram	Rajarhat	Panga	Minor river		Low	N/A***
74	Kurigram	Rajarhat	Sharishabari Hat	Teesta	1000	Low	High
75	Kurigram	Rajarhat	Chowrahat	Dharala	2470	Low	Low
76	Kurigram	Chilmari	Jorgach Hat	Brahmaputra	740	Low	High*
77	Kurigram	Chilmari	Karai Barisal	Brahmaputra	700	Low	High**
78	Kurigram	Chilmari	Thana Hat	Brahmaputra	2050	Low	Low
79	Kurigram	Chilmari	Fakirar Hat	Brahmaputra	350	Low	High*
80	Kurigram	Ulipur	Hatia Vobesh	Brahmaputra	590	Moderate	High*
81	Kurigram	Ulipur	Mollar Hat	Brahmaputra	330	Low	High
82	Kurigram	Ulipur	Jatiner Hat	Minor river	580	Low	Low
83	Kurigram	Kurigram Sadar	Panchgachi Bazar	Brahmaputra Dharala	2770	Low	Low
84	Kurigram	Kurigram Sadar	Rajmallir Hat	Dharala	50	Moderate	High
85	Kurigram	Kurigram Sadar	Rajarhat Bazar	Brahmaputra	2750	Moderate	Low
86	Kurigram	Kurigram Sadar	Masterer Hat	Dharala	1030	Low	Low
87	Kurigram	Raumari	Baraikandhi Hat	Jinjiram	1700	Low	Low
88	Kurigram	Raumari	Saydabad Bazar	Jinjiram	900	Moderate	Moderate
89	Kurigram	Char Rajibpur	Rajibpur GC	Brahmaputra	790	Low	High
90	Nilphamari	Jaldhaka	Balagram Bazar	Minor river	2000	Low	Low
91	Nilphamari	Jaldhaka	Bhabonchur Bazar	Minor river	68	Low	Moderate
92	Nilphamari	Jaldhaka	Dakligonj Hat	Teesta	830	Low	High
93	Nilphamari	Jaldhaka	Golmunda Bazar	Teesta	170	Low	High
94	Nilphamari	Jaldhaka	Kaligonj Bangha Bandhu Bazar	Minor rivers	2058	Low	Low
95	Nilphamari	Jaldhaka	Kathali Nayer Hat	Minor river	830	Low	Low
96	Nilphamari	Jaldhaka	Pathanpara Hat	Minor river	1930	Low	Low
97	Nilphamari	Jaldhaka	Shibur Hat	Minor river	2750	Low	Low
98	Nilphamari	Dimla	Tunirhat	Minor river	840	Low	Low

Notes:

** Protected by Embankment, which can be considered under "Low" risk*

*** Located on the island (char)*

****N/A (Not Applicable): Image resolution is not adequate to identify bank lines*

Market-1: Boxigonj Bazar in Sadullapur Upazila of Gaibandha District

- Flood Risk: The market is located in a **Low** flood-risk area, considering the inundation patterns of all major floods in recent times.
- Bank Erosion Risk: Based on planform analysis using historical satellite images, the market is located in the **Low** bank erosion risk area

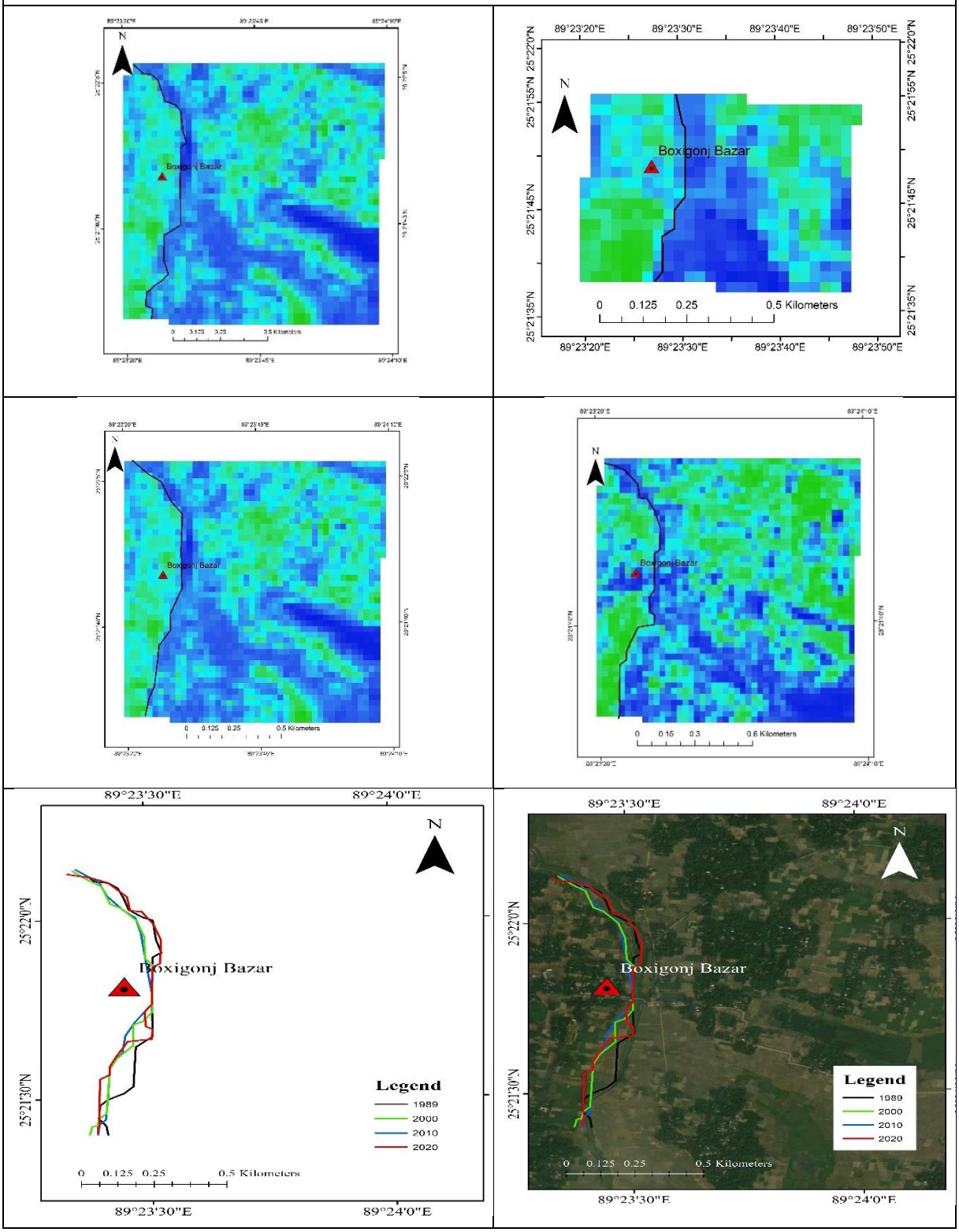

Market-2: Charokerhat Bazar in Sundarganj Upzila of Gaibandha District

- Flood Risk: The market is located in a **Low** flood-risk area, considering the inundation patterns of all major floods in recent times.
- Bank Erosion Risk: Based on planform analysis using historical satellite images, the market is located in the **Low** bank erosion risk area.

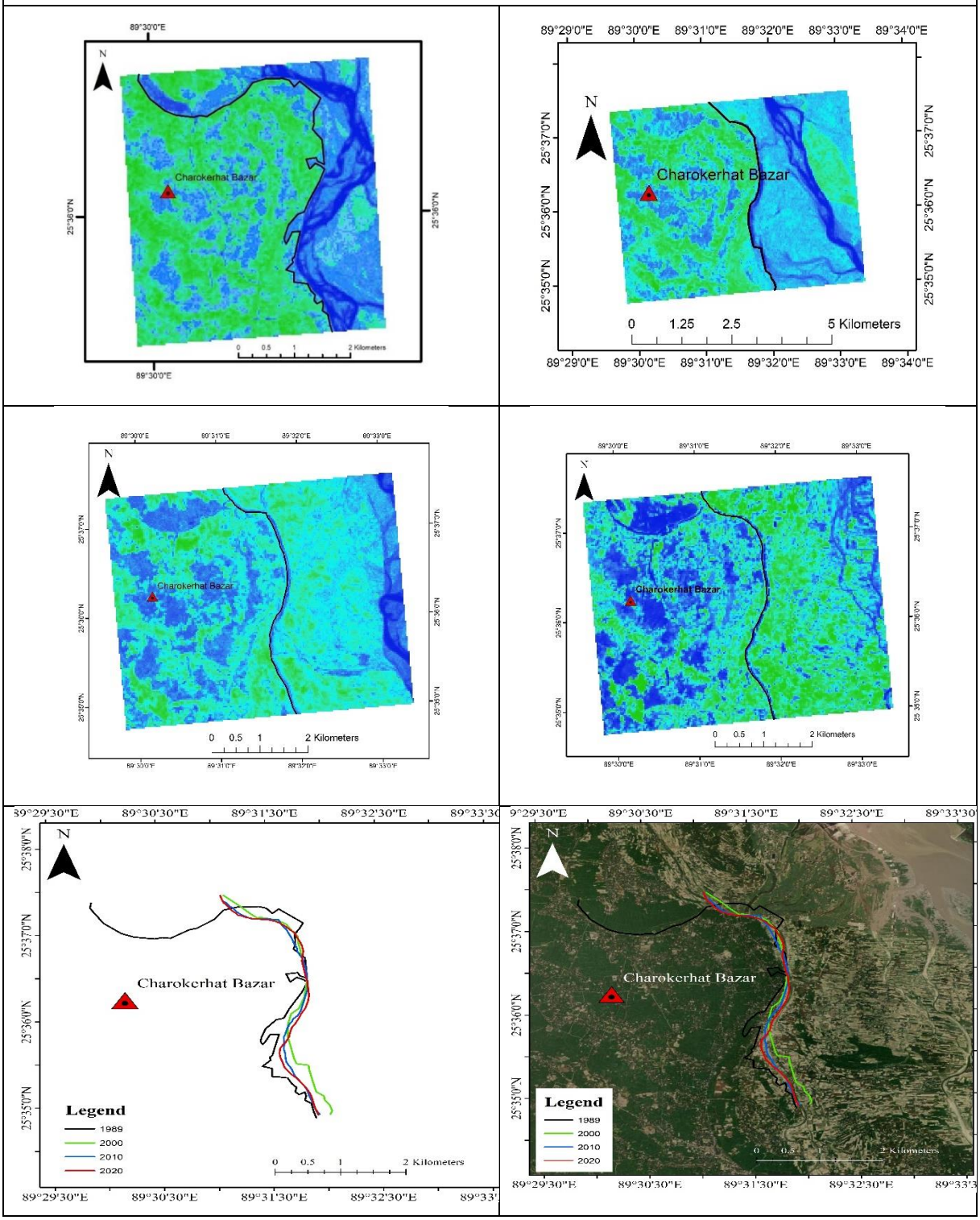

Market-3: Jamaler Hat in Sundarganj Upzila of Gaibandha District

- Flood Risk: The market is located in a **Low** flood-risk area, considering the inundation patterns of all major floods in recent times. However, the surrounding area is at low flood risk.
- Bank Erosion Risk: Based on planform analysis using historical satellite images, the market is located in the **Low** bank erosion risk area.

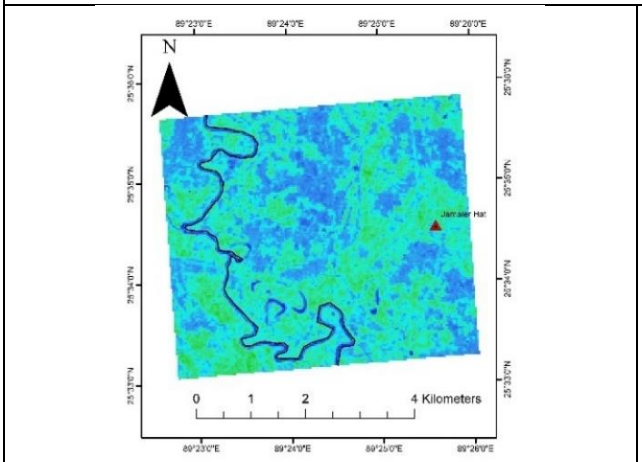

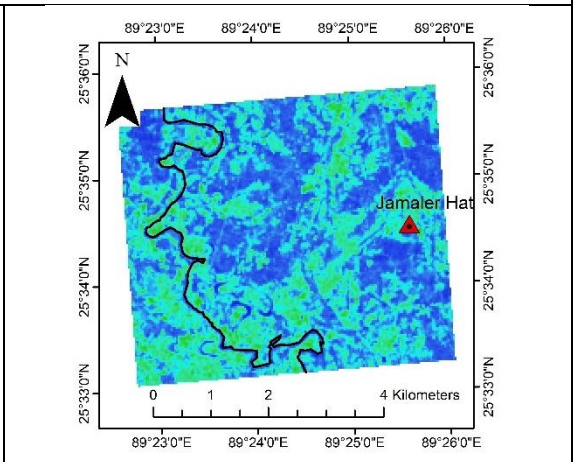

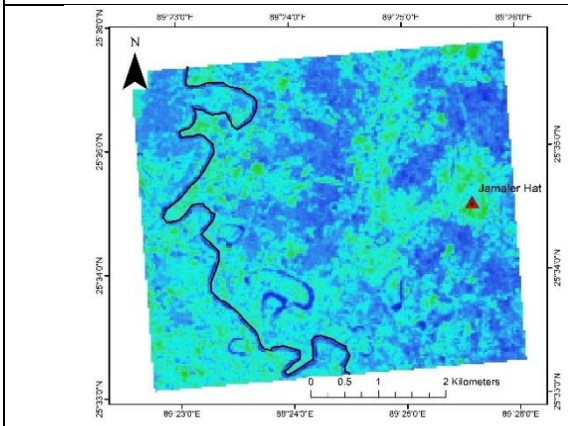

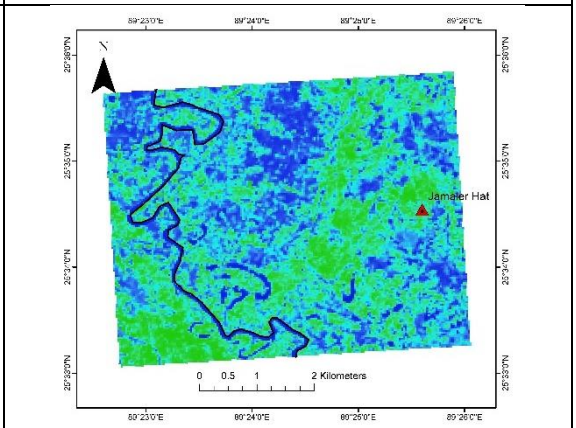

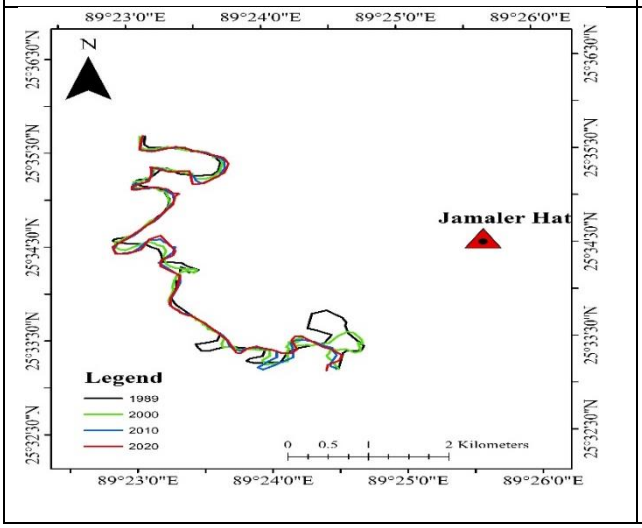

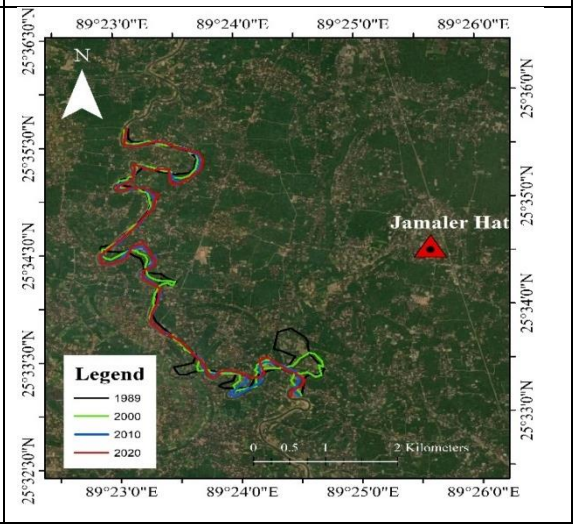

Market-4: Dakhin Dighalkandi Bazar in Saghatta Upzila of Gaibandha District

- Flood Risk: The market is located in a **Moderate** flood risk area, considering the inundation patterns of all major floods in recent times. However, the surrounding area is at low flood risk.
- Bank Erosion Risk: Based on planform analysis using historical satellite images, the market is located in the **High** bank erosion risk area

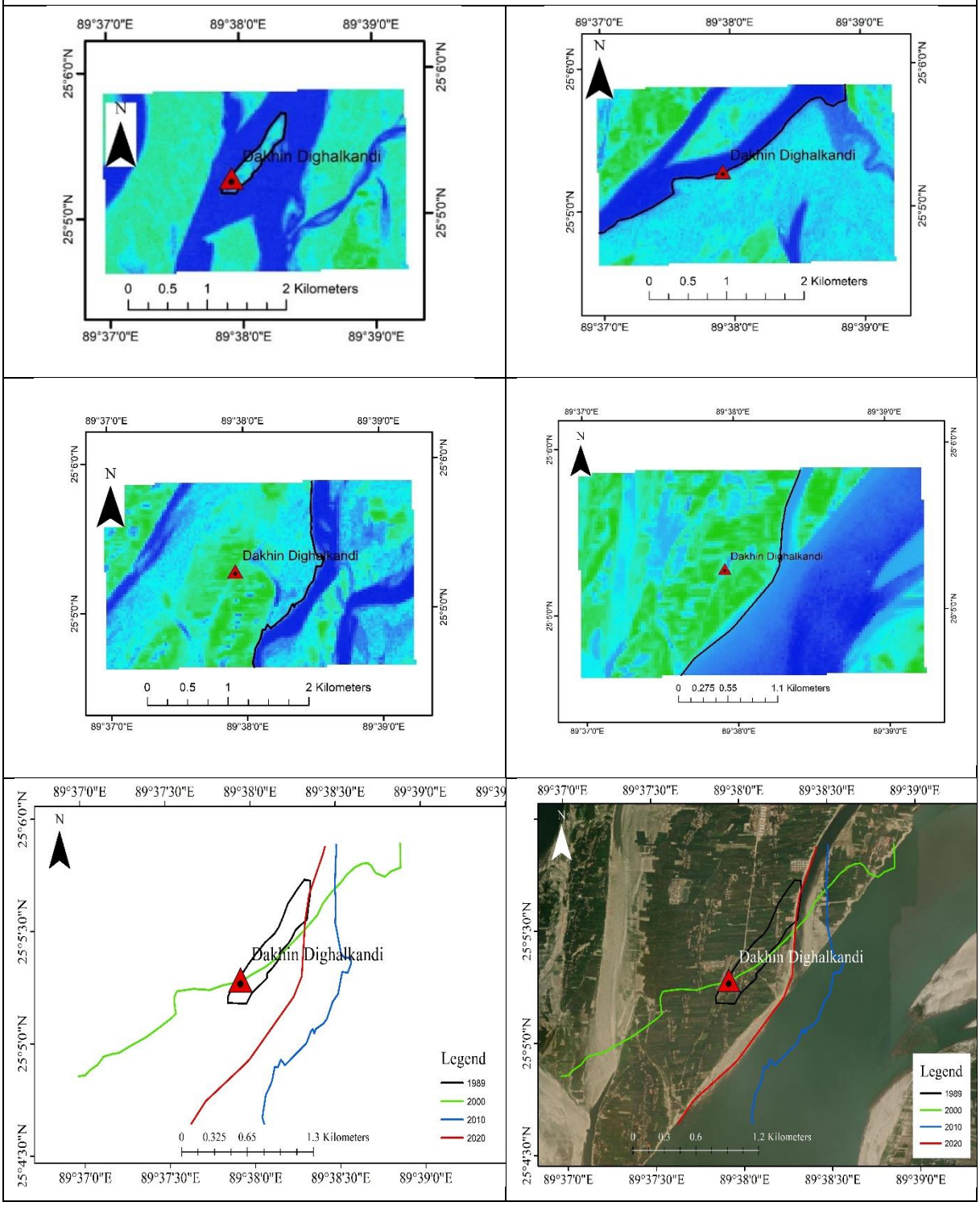

Market-5: Falia Bottala Bazar in Saghatta Upazila of Gaibandha District

- Flood Risk: The market is located in a **Low** flood-risk area, considering the inundation patterns of all major floods in recent times. However, the surrounding area is at low flood risk.
- Bank Erosion Risk: Based on planform analysis using historical satellite images, the market is located in the **Low** bank erosion risk area.

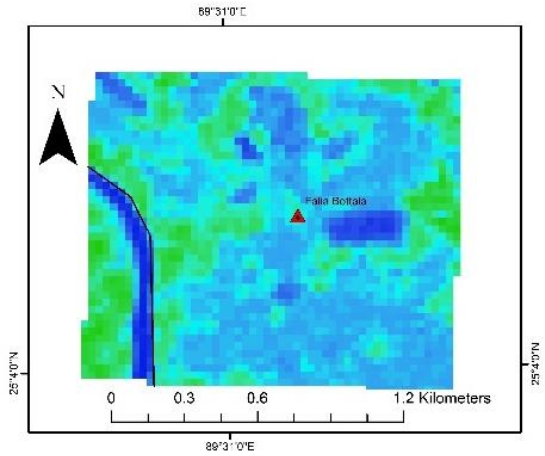

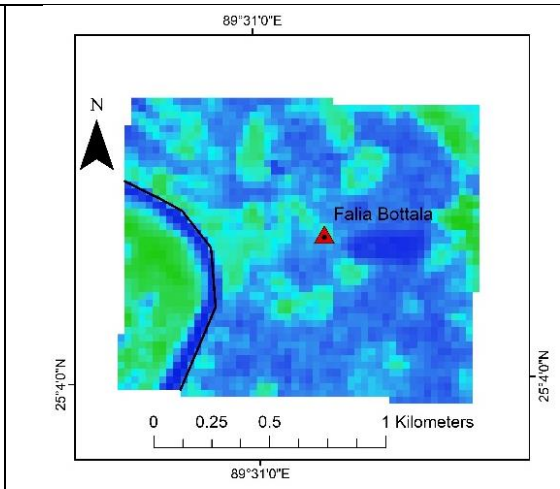

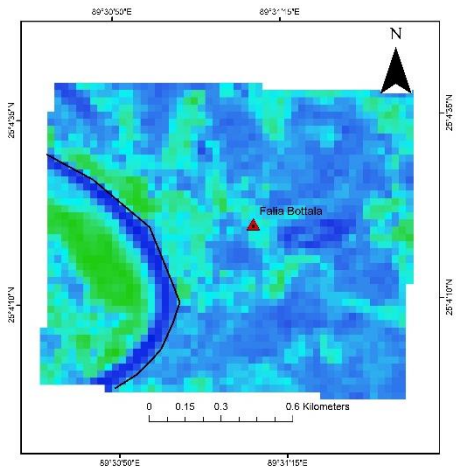

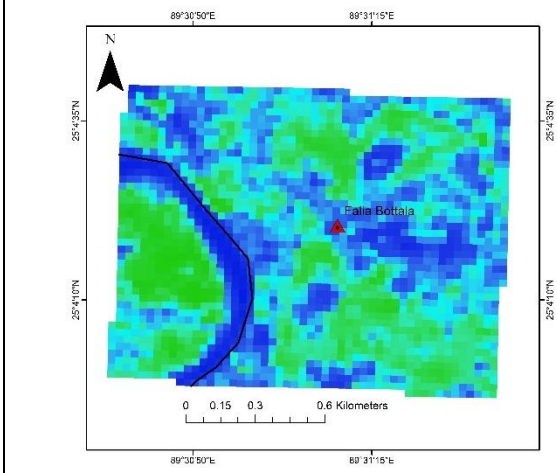

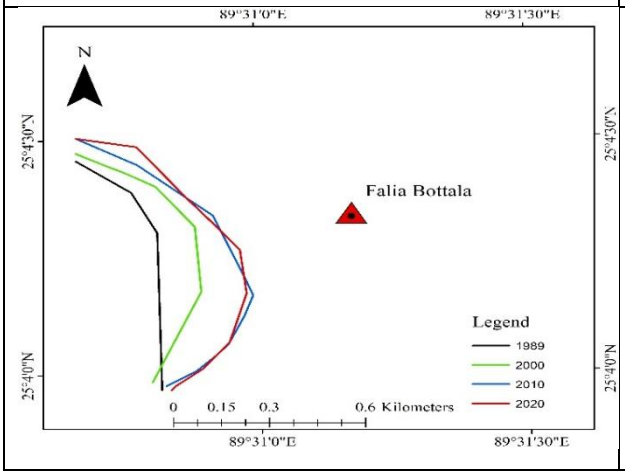

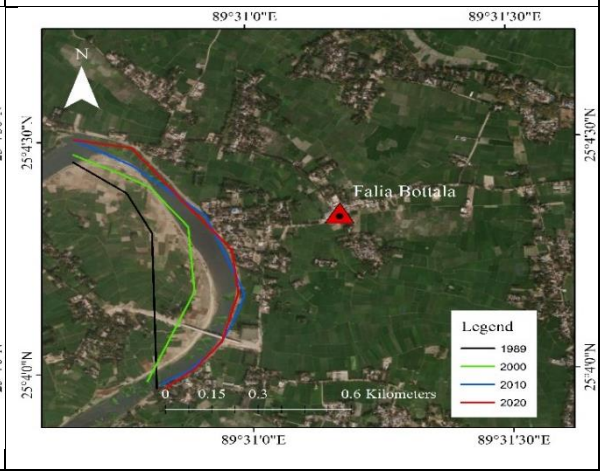

Market-6: Futani Bazar in Saghatta Upzila of Gaibandha District

- Flood Risk: The market is located in a **Low** flood-risk area, considering the inundation patterns of all major floods in recent times.
- Bank Erosion Risk: Due to satellite image limitation, the river bank erosion risk cannot be assessed **(N/A).**

<table>
<tr>
<td> 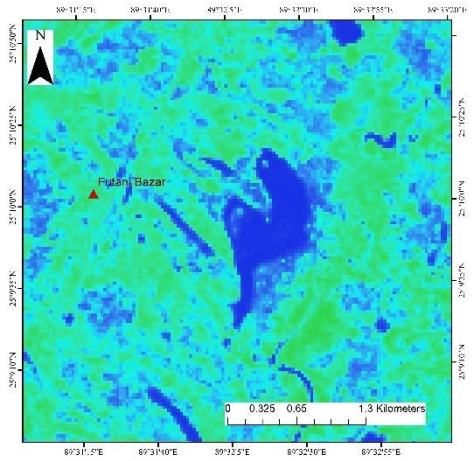
</td>
<td> 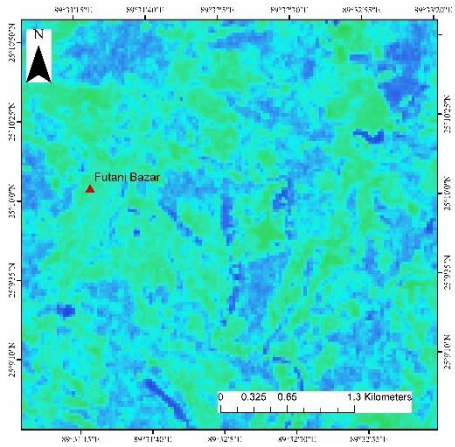
</td>
</tr>
<tr>
<td> 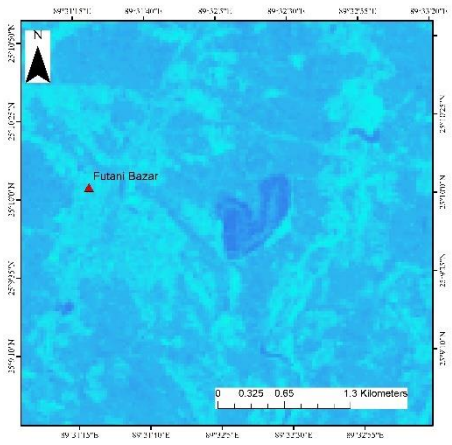
</td>
<td> 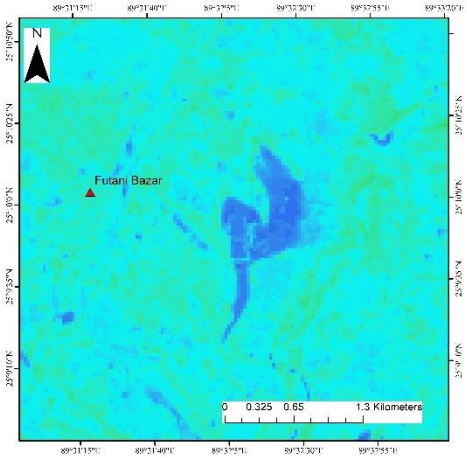
</td>
</tr>
<tr>
<td>It is not possible to detect changes in bank lines due to inadequate resolution of satellite image</td>
<td>It is not possible to detect changes in bank lines due to inadequate resolution of satellite image</td>
</tr>
</table>

Market-7: Ullah Bazar in Saghatta Upazila of Gaibandha District

- Flood Risk: The market is located in a **Low** flood-risk area, considering the inundation patterns of all major floods in recent times.
- Bank Erosion Risk: Based on planform analysis using historical satellite images, the Market is located in the **High** bank erosion risk area.

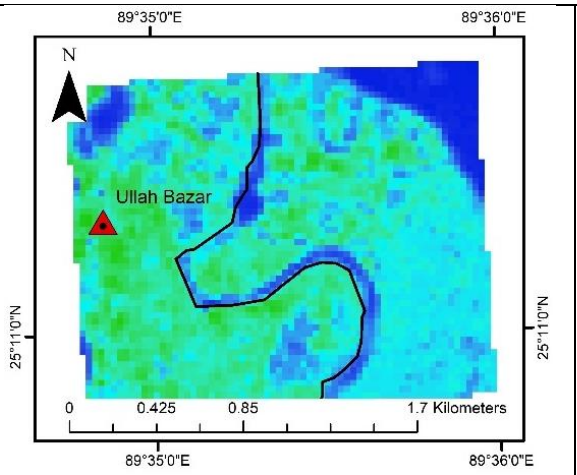

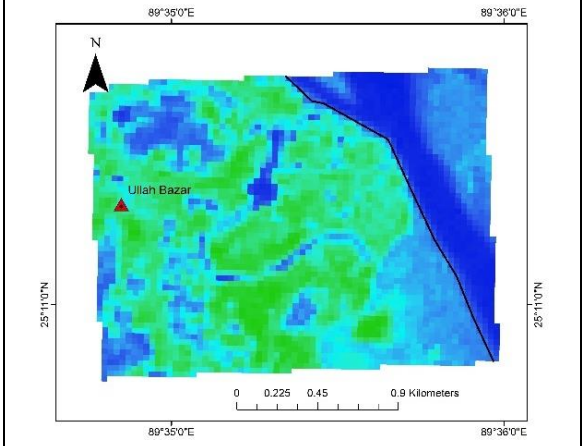

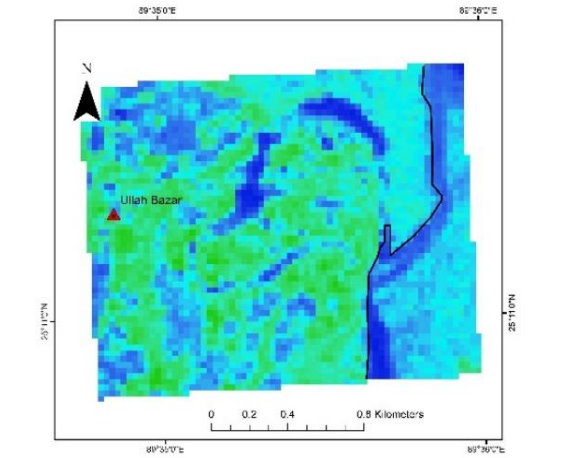

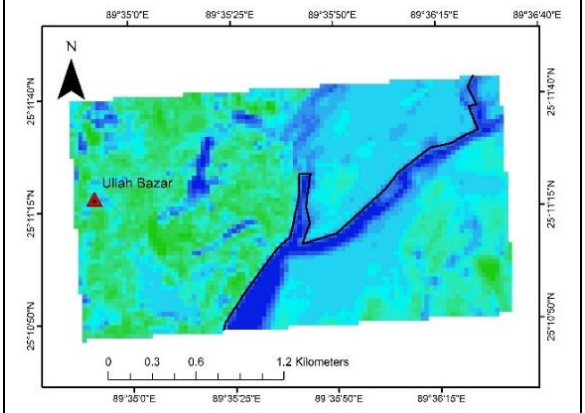

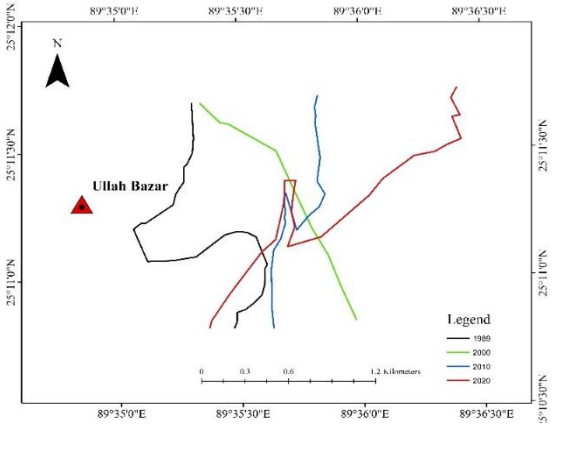

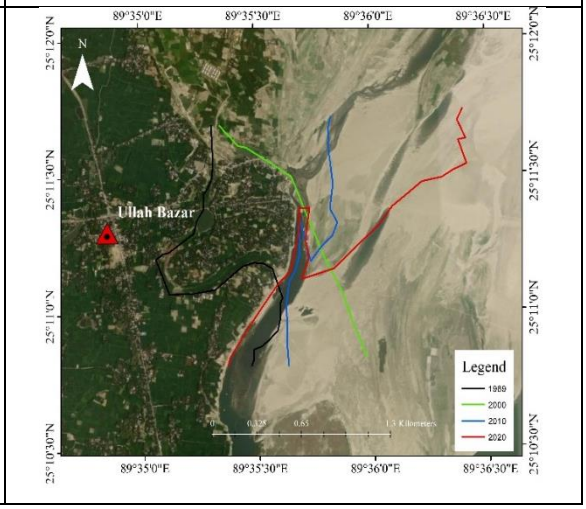

Market-8: Nayabondar Bazar in Palashbari Upazila of Gaibandha District

- Flood Risk: The market is located in a **Low** flood-risk area, considering the inundation patterns of all major floods in recent times.

  Bank Erosion Risk: Based on planform analysis using historical satellite images, the Market is located in the **Low** bank erosion risk area.

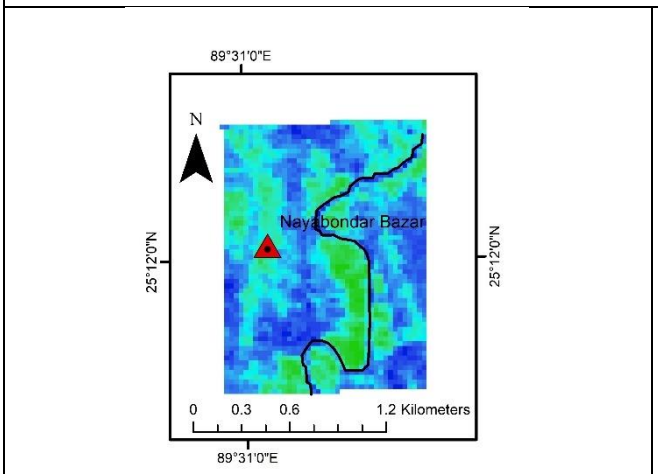

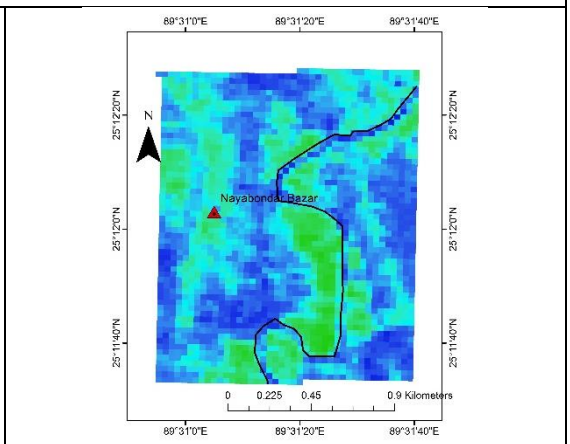

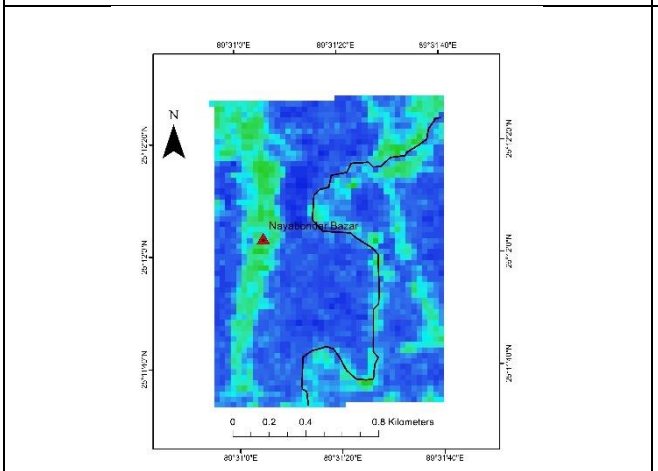

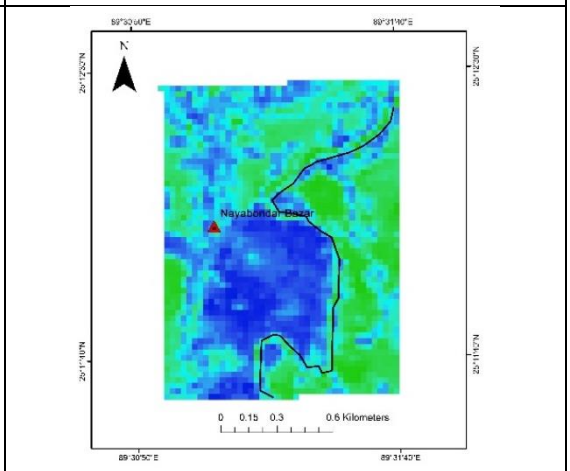

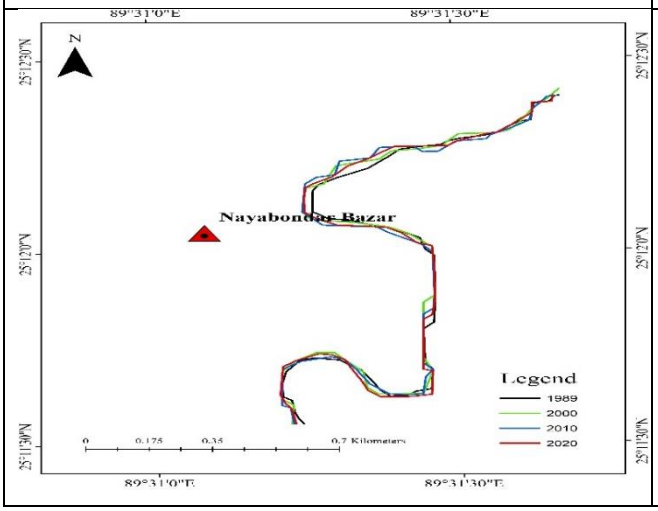

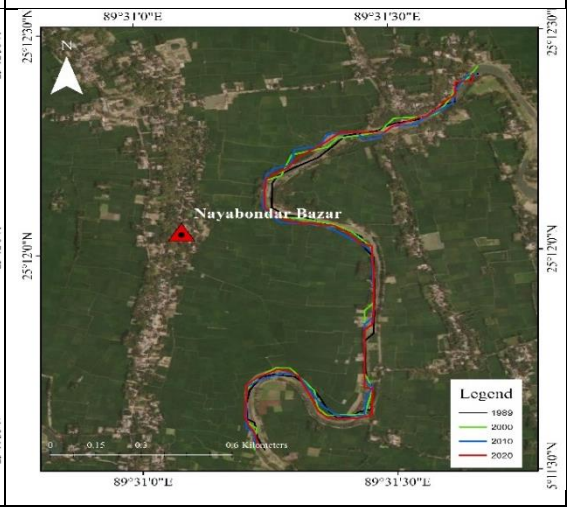

Market-9: Ullah Sonatala Bazar in Saghatta Upazila of Gaibandha District

- Flood Risk: The market is located in a **Low** flood-risk area, considering the inundation patterns of all major floods in recent times. However, the surrounding area is at low flood risk.
- Bank Erosion Risk: Based on planform analysis using historical satellite images, the Market is located in the **High** bank erosion risk area.

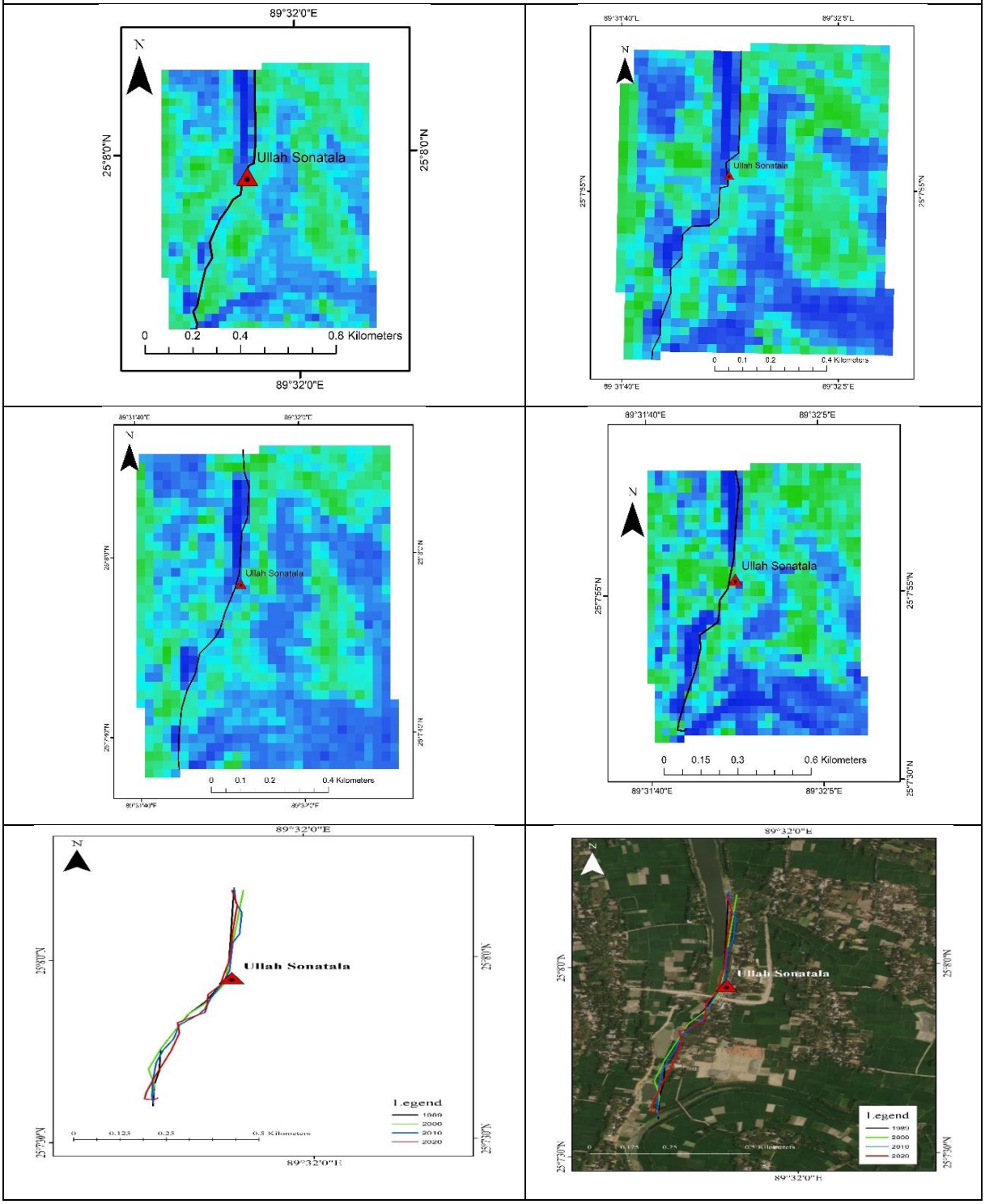

Market-10: Kantanagor Bazar in Sadullapur Upzila of Gaibandha District

- Flood Risk: The market is located in a **Low** flood-risk area, considering the inundation patterns of all major floods in recent times.
- Bank Erosion Risk: Based on planform analysis using historical satellite images, the market is located in the **Low** bank erosion risk area.

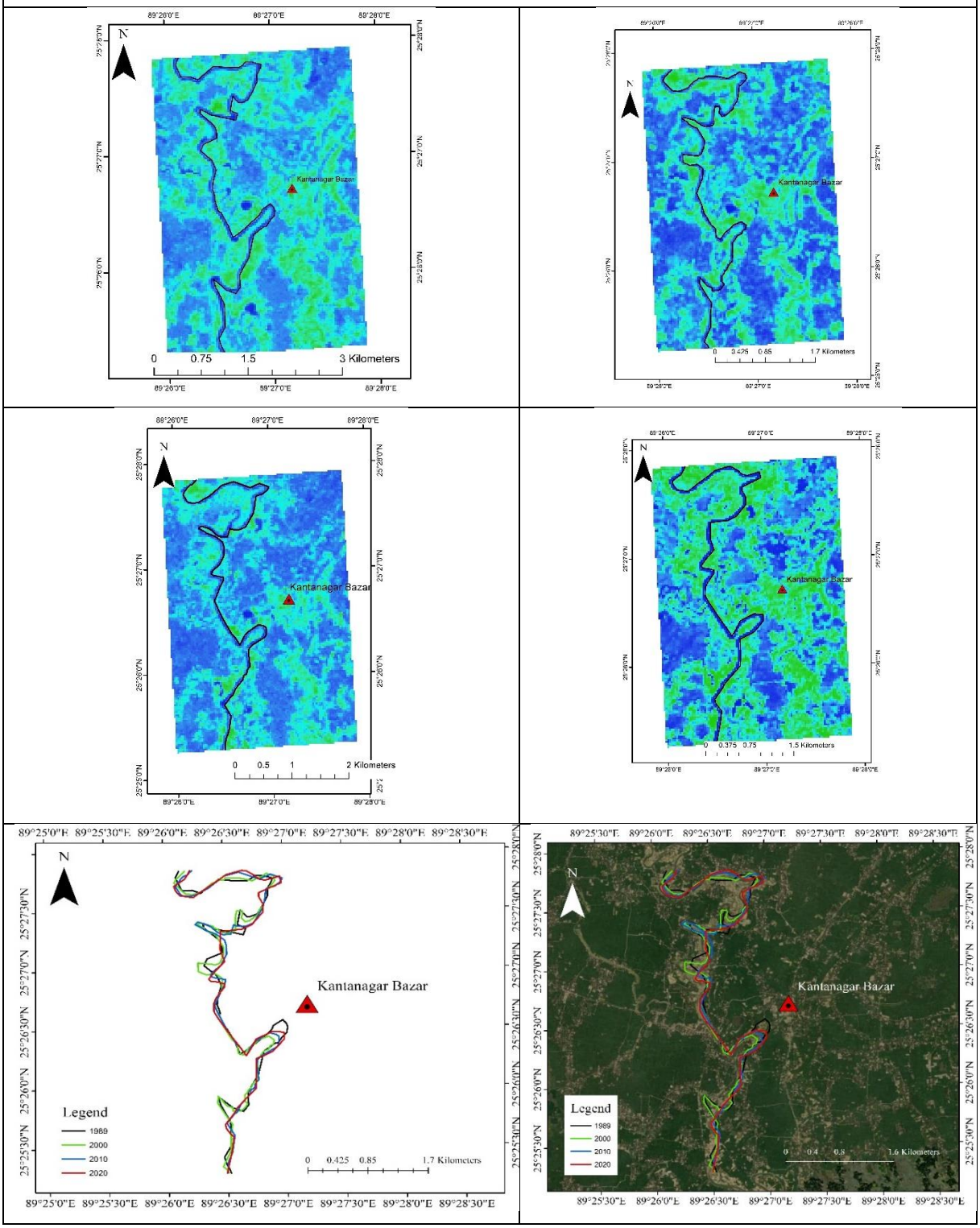

Market-11: Lenga Bazar in Gaibandha Sadar Upzila of Gaibandha District

- Flood Risk: The market is located in a **Low** flood-risk area, considering the inundation patterns of all major floods in recent times.
- Bank Erosion Risk: Based on planform analysis using historical satellite images, the market is located in the **Low** bank erosion risk area.

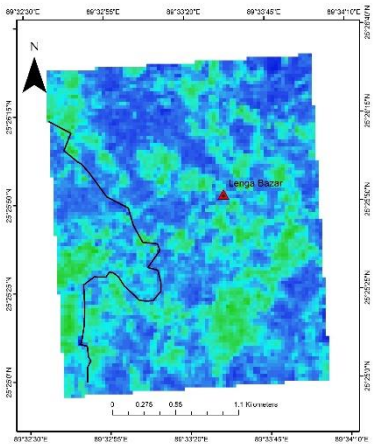

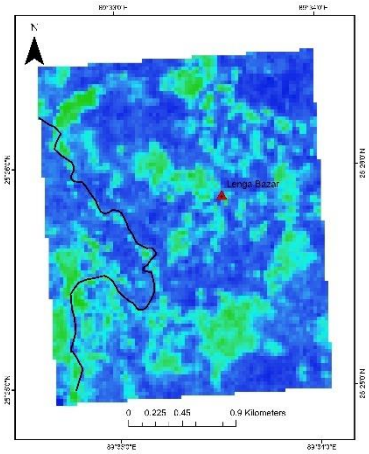

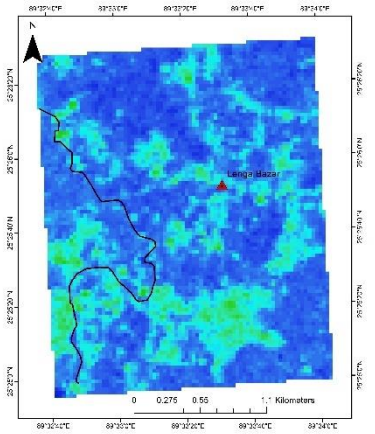

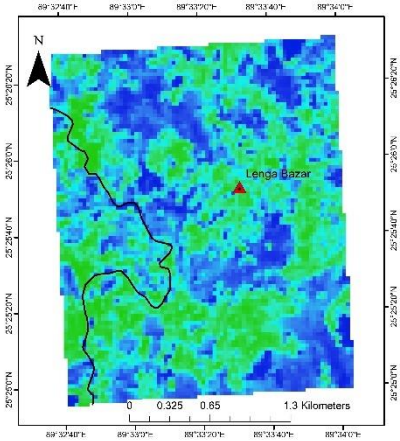

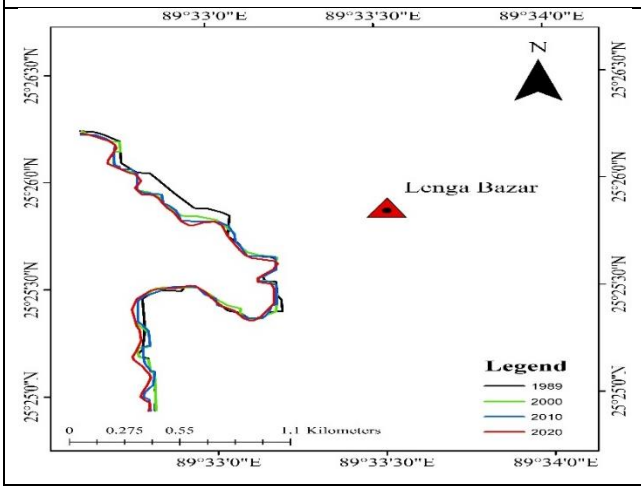

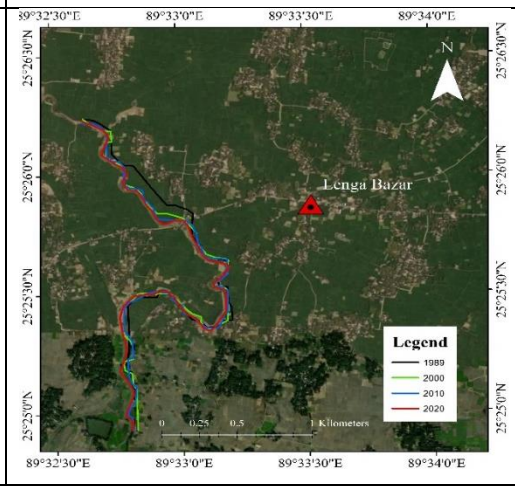

Market-12: Puratan Badiakhali Hat in Nilphamari Sadar Upzila of Nilphamari District

- Flood Risk: The market is located in a **Low** flood-risk area, considering the inundation patterns of all major floods in recent times.
- Bank Erosion Risk: Based on planform analysis using historical satellite images, the Market is located in the **High** bank erosion risk area.

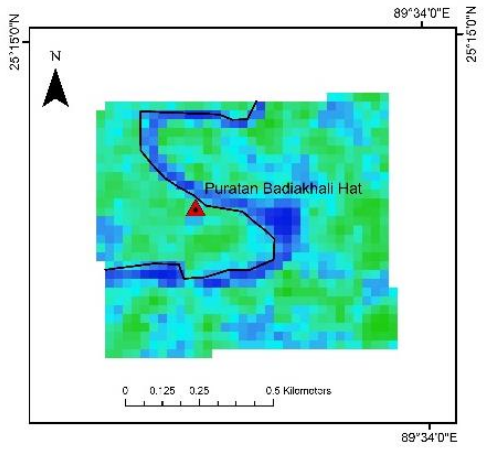

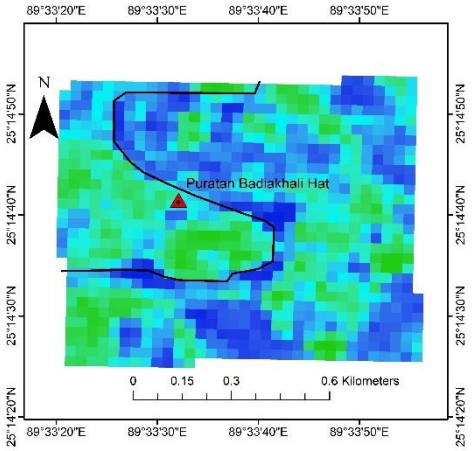

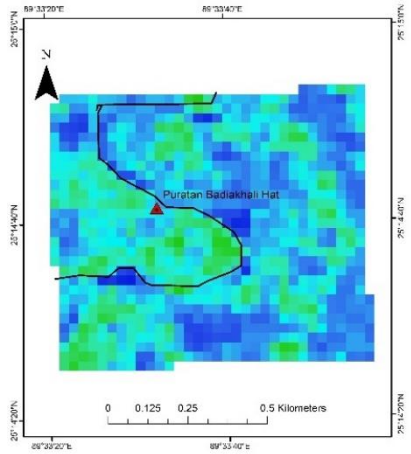

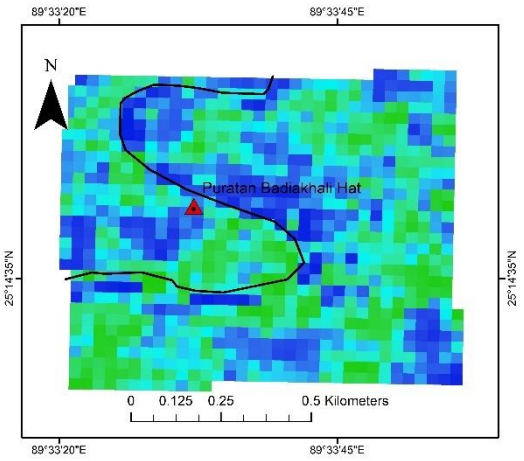

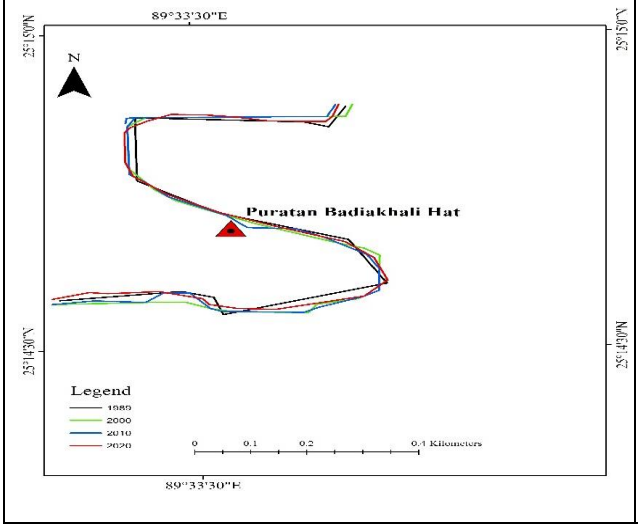

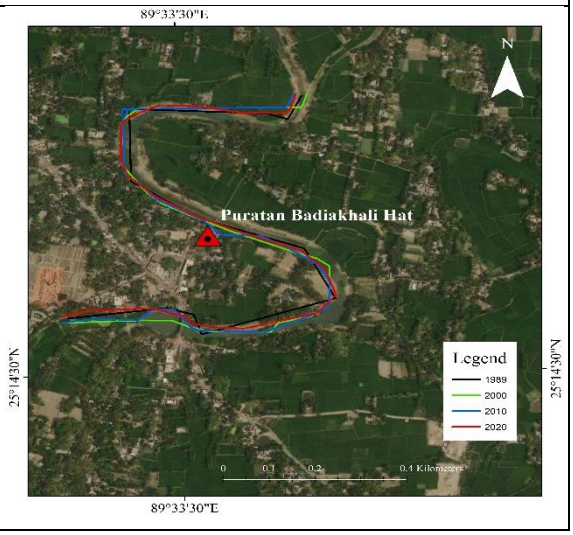

Market-13: Balua Hat in Gaibandha sadar Upzila of Gaibandha District

- Flood Risk: The market is located in a **Moderate** flood risk area, considering the inundation patterns of all major floods in recent times.
- Bank Erosion Risk: Based on planform analysis using historical satellite images, the market is located in the **Low** bank erosion risk area.

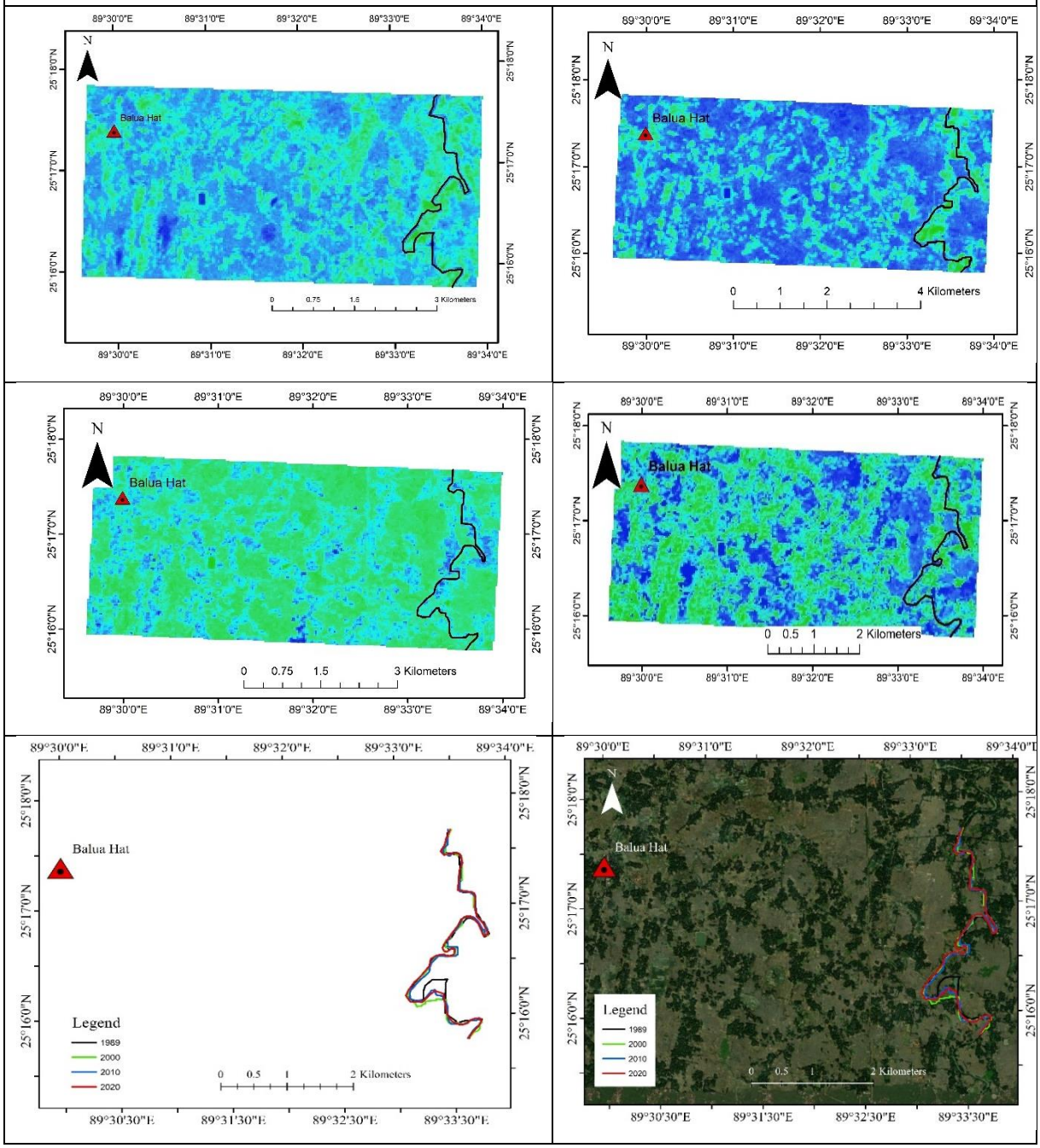

Market-14: Purbo Fulchori Bazar in Fulchori Upazila of Gaibandha District

- Flood Risk: The market is located in a **Low** flood-risk area, considering the inundation patterns of all major floods in recent times.
- Bank Erosion Risk: Based on planform analysis using historical satellite images, the Market is located in the **Moderate** bank erosion risk area.

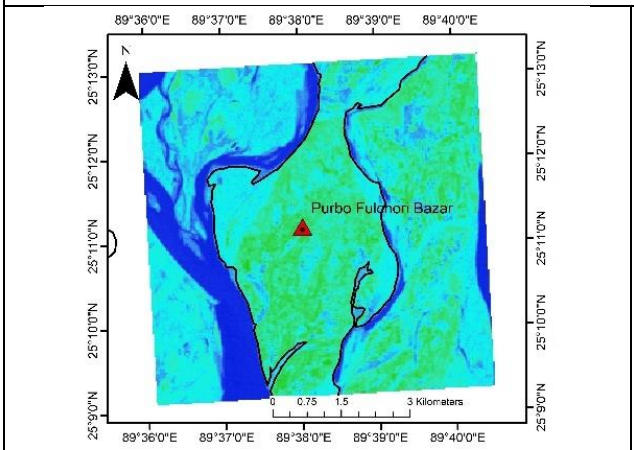

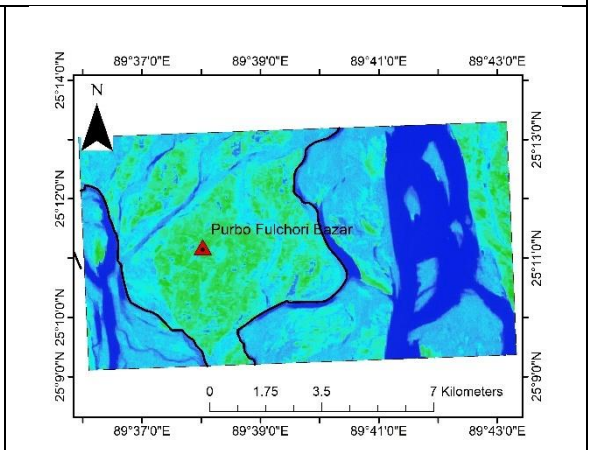

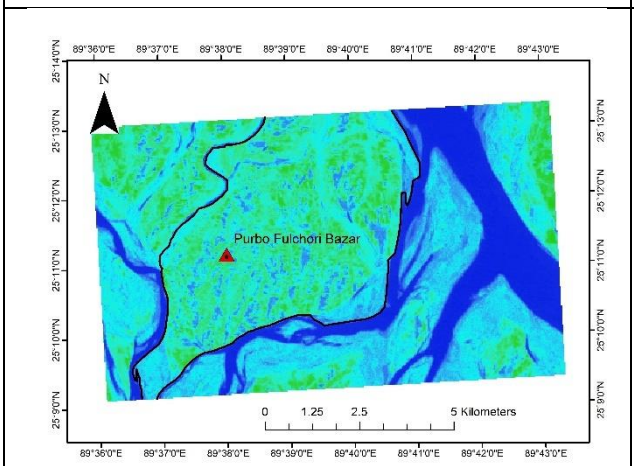

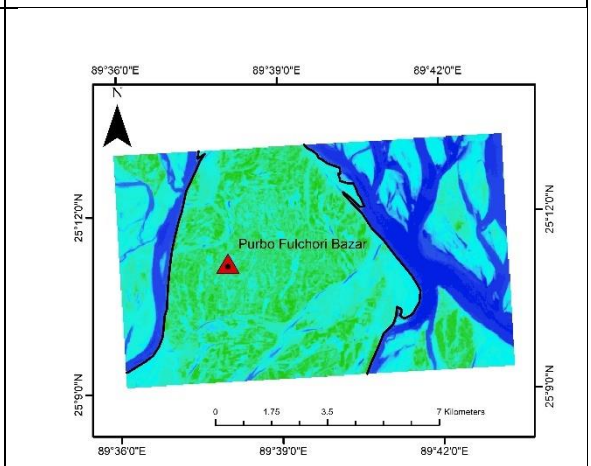

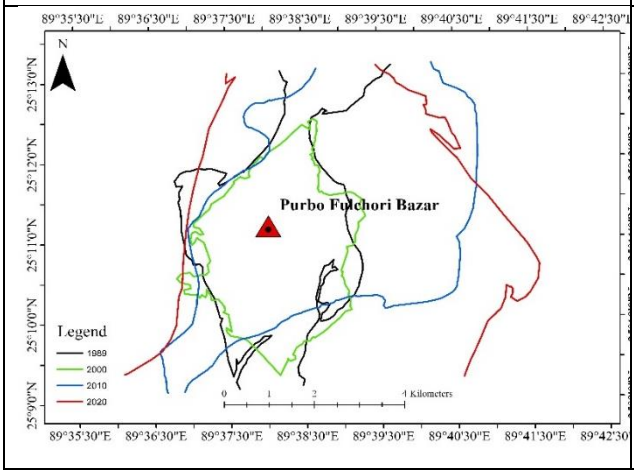

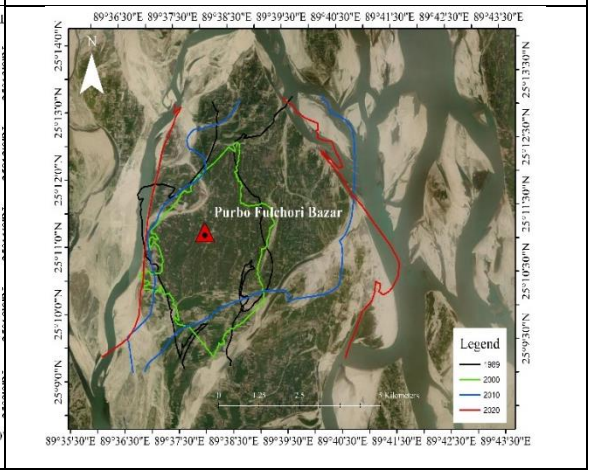

Market-15: Bagerhat in Gangachara Upzila of Rangpur District

- Flood Risk: The market is located in a **Low** flood-risk area, considering the inundation patterns of all major floods in recent times. However, the surrounding area is at low flood risk.
- Bank Erosion Risk: Based on planform analysis using historical satellite images, the market is located in the **High** bank erosion risk area.

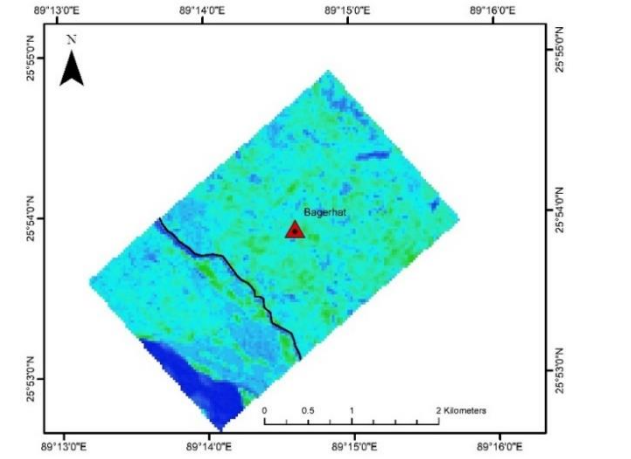

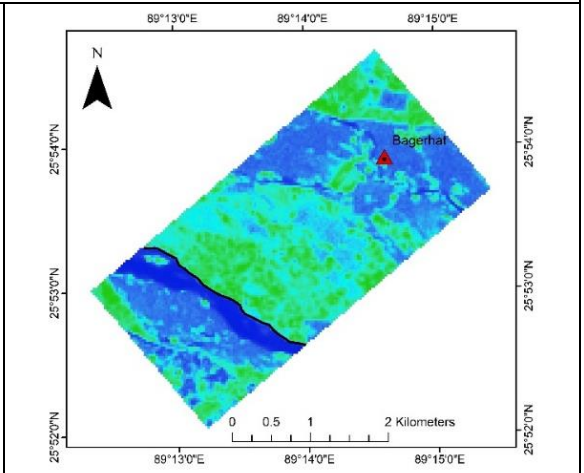

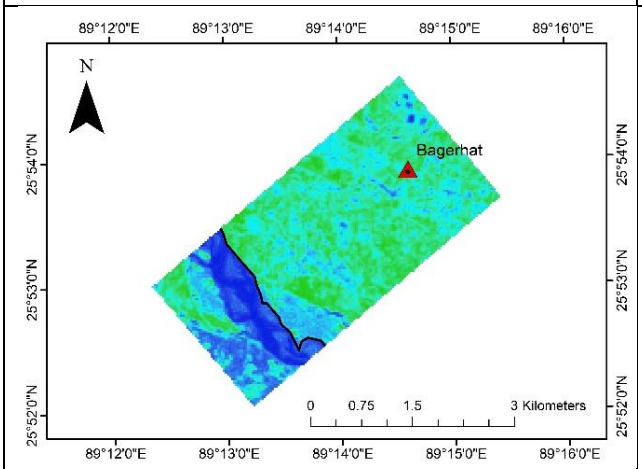

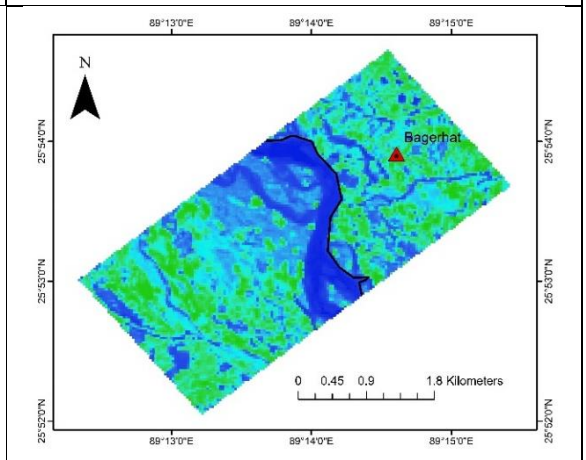

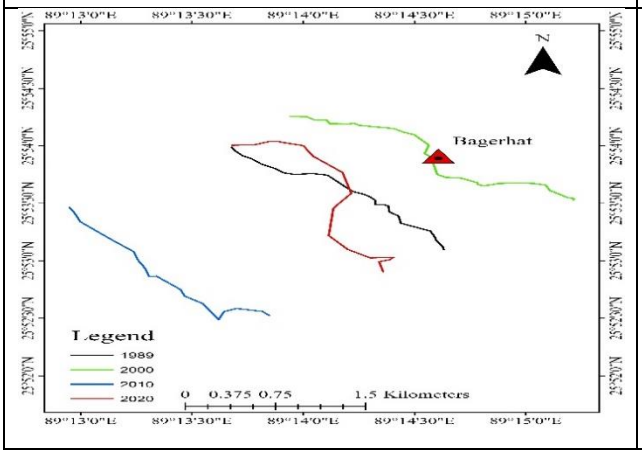

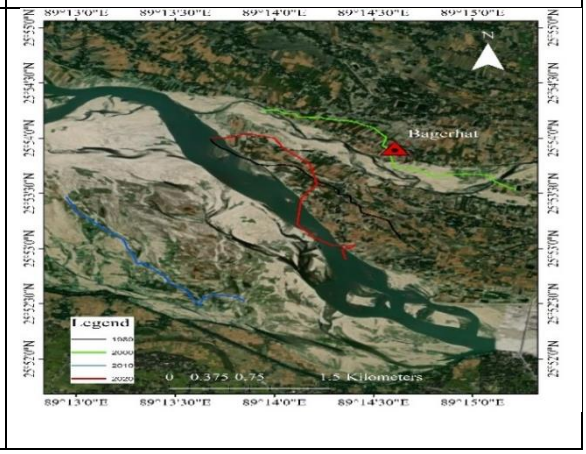

Market-16: Abuliarhat Hat in Kaliganj Upzila of Lalmonirhat District

- Flood Risk: The market is located in a **Moderate** flood risk area, considering the inundation patterns of all major floods in recent times.
- Bank Erosion Risk: Based on planform analysis using historical satellite images, the Market is located in the **Moderate** bank erosion risk area.

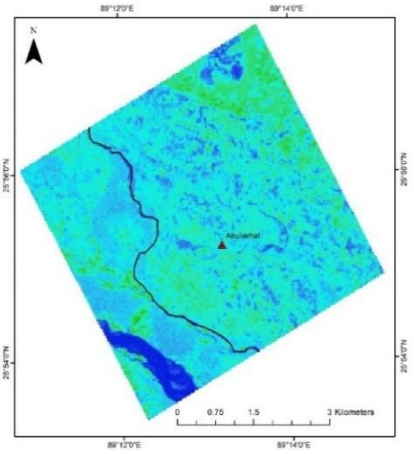

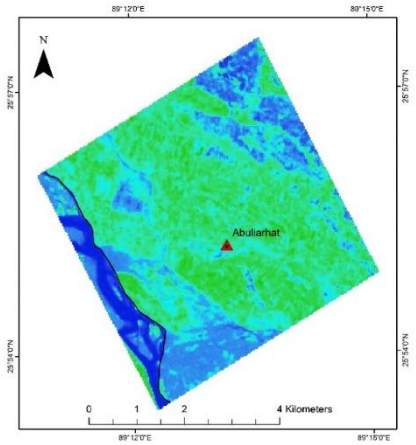

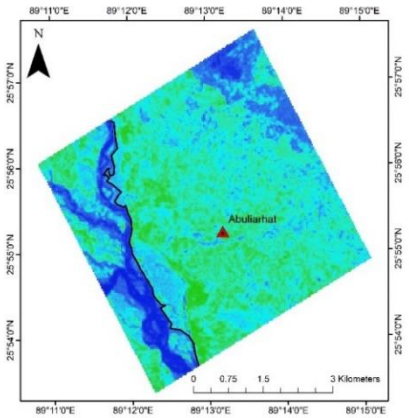

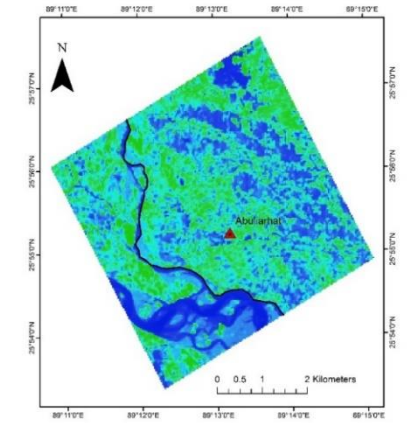

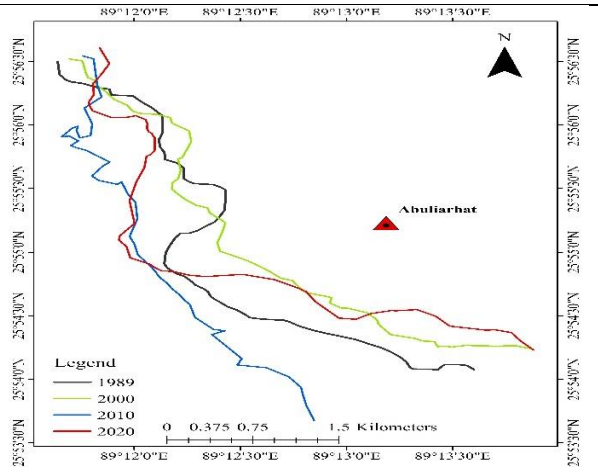

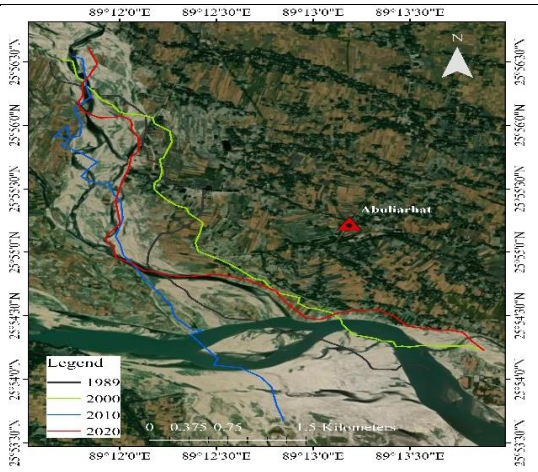

Market-17: Ichli Bazar (SKS Bazar) in Gangachara Upzila of Rangpur District

- Flood Risk: The market is located in a **Low** flood-risk area, considering the inundation patterns of all major floods in recent times.
- Bank Erosion Risk: Based on planform analysis using historical satellite images, the market is located in the **High** bank erosion risk area.

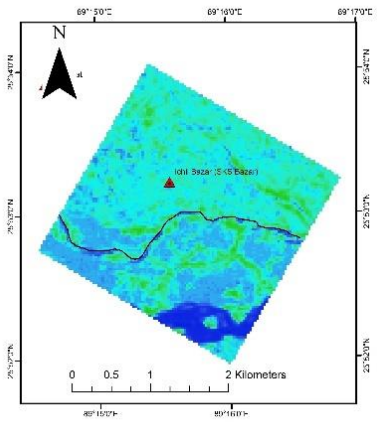

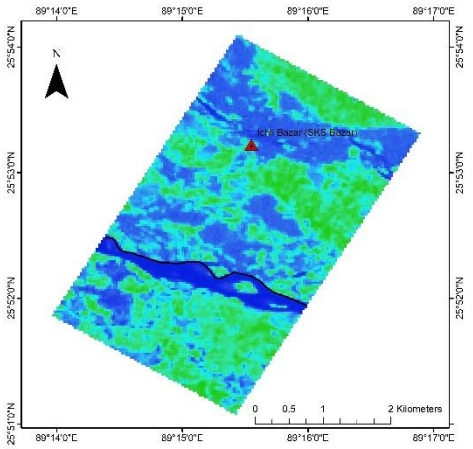

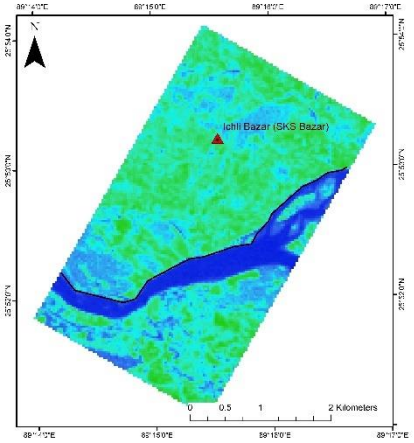

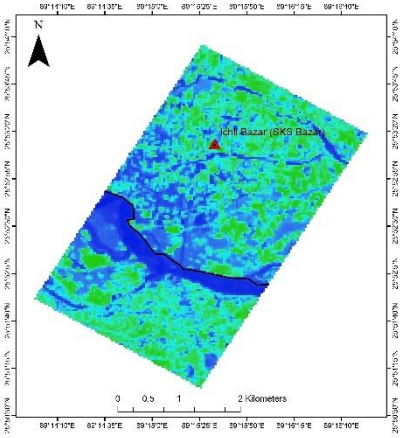

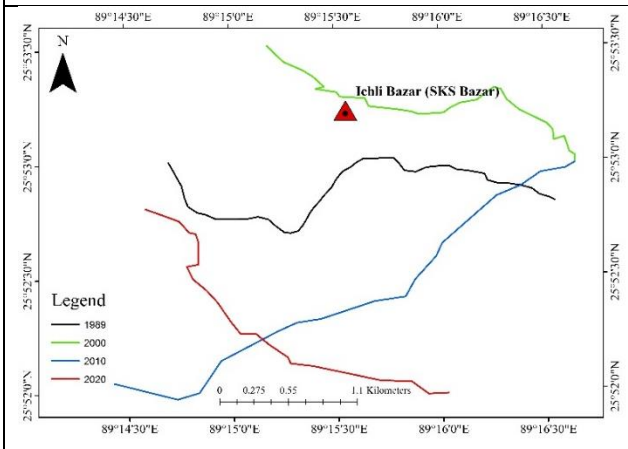

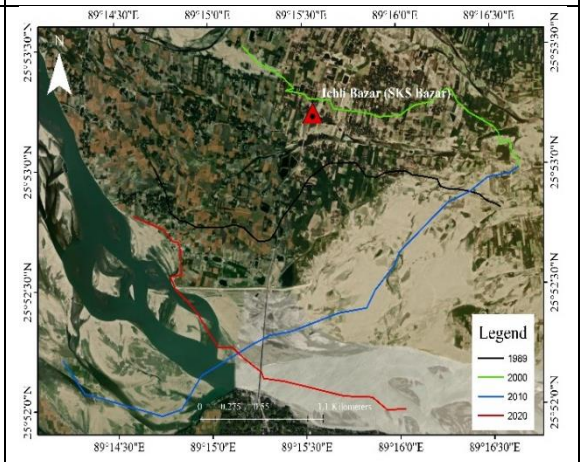

Market-18: Ekotarhat in Kaunia Upzila of Rangpur District

- Flood Risk: The market is located in a **Low** flood-risk area, considering the inundation patterns of all major floods in recent times.
- Bank Erosion Risk: Based on planform analysis using historical satellite images, the market is located in the **Low** bank erosion risk area.

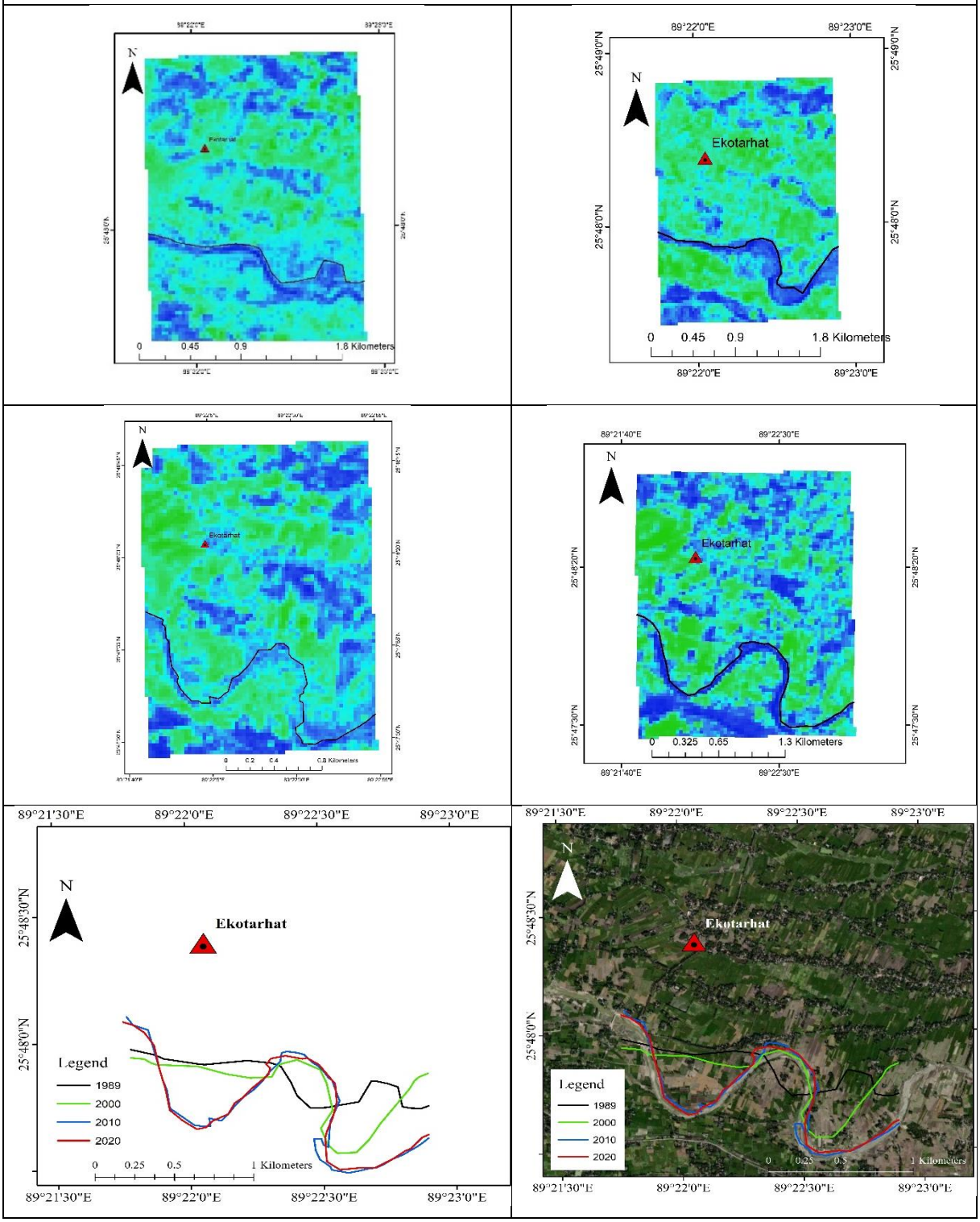

Market-19: Haqueer Hat in Lalmonirhat sadar Upzila of Lalmonirhat District

- Flood Risk: The market is located in a **Low** flood-risk area, considering the inundation patterns of all major floods in recent times.
- Bank Erosion Risk: Based on planform analysis using historical satellite images, the market is located in the **Moderate** bank erosion risk area.

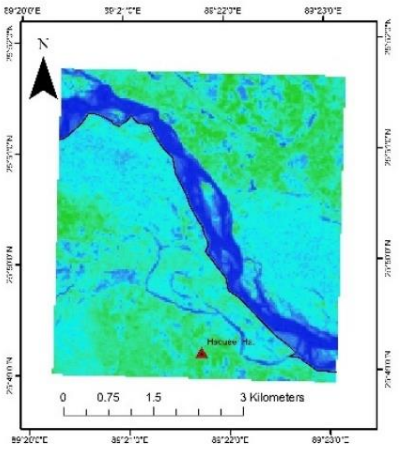

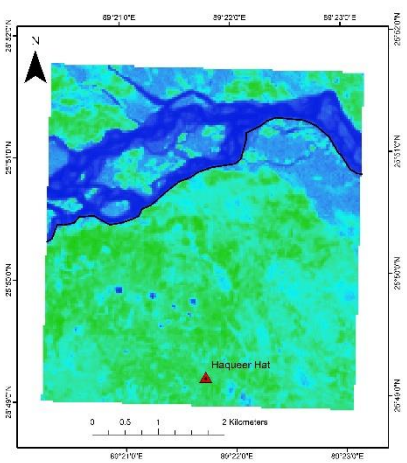

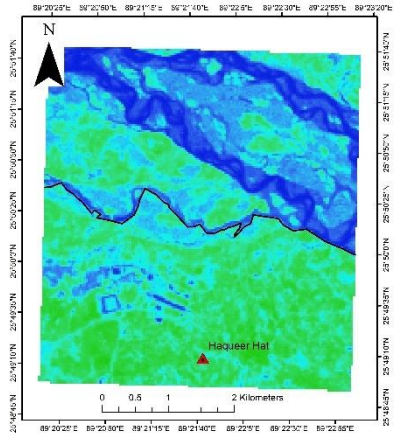

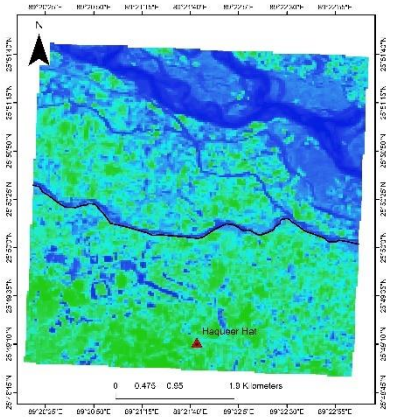

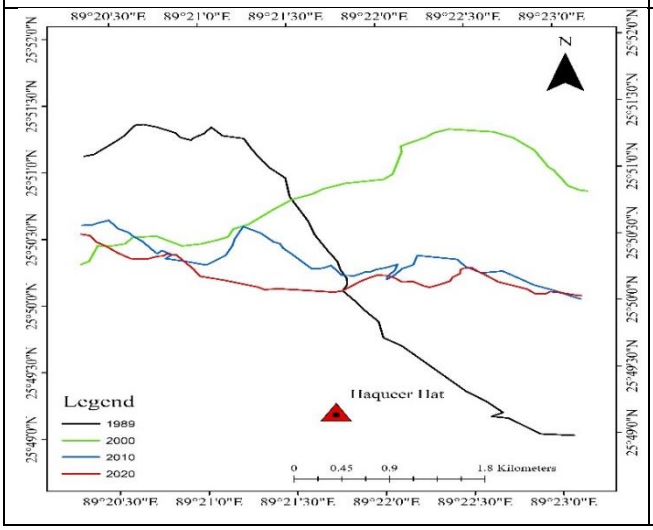

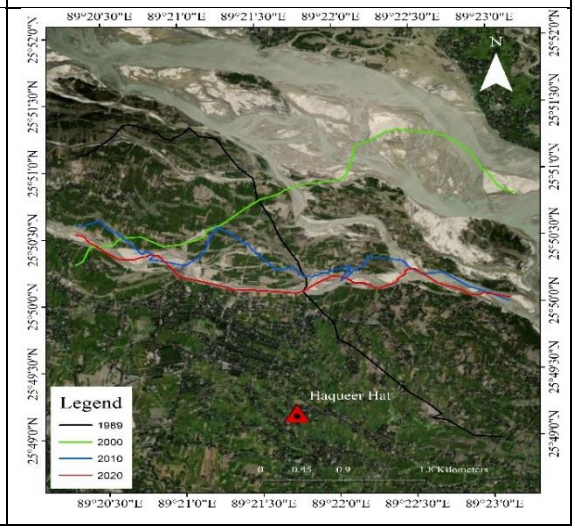

Market-20: Bhaier Hat in Kaunia Upzila of Rangpur District

- Flood Risk: The market is located in a **Low** flood-risk area, considering the inundation patterns of all major floods in recent times.
- Bank Erosion Risk: Based on planform analysis using historical satellite images, the market is located in the **Moderate** bank erosion risk area.

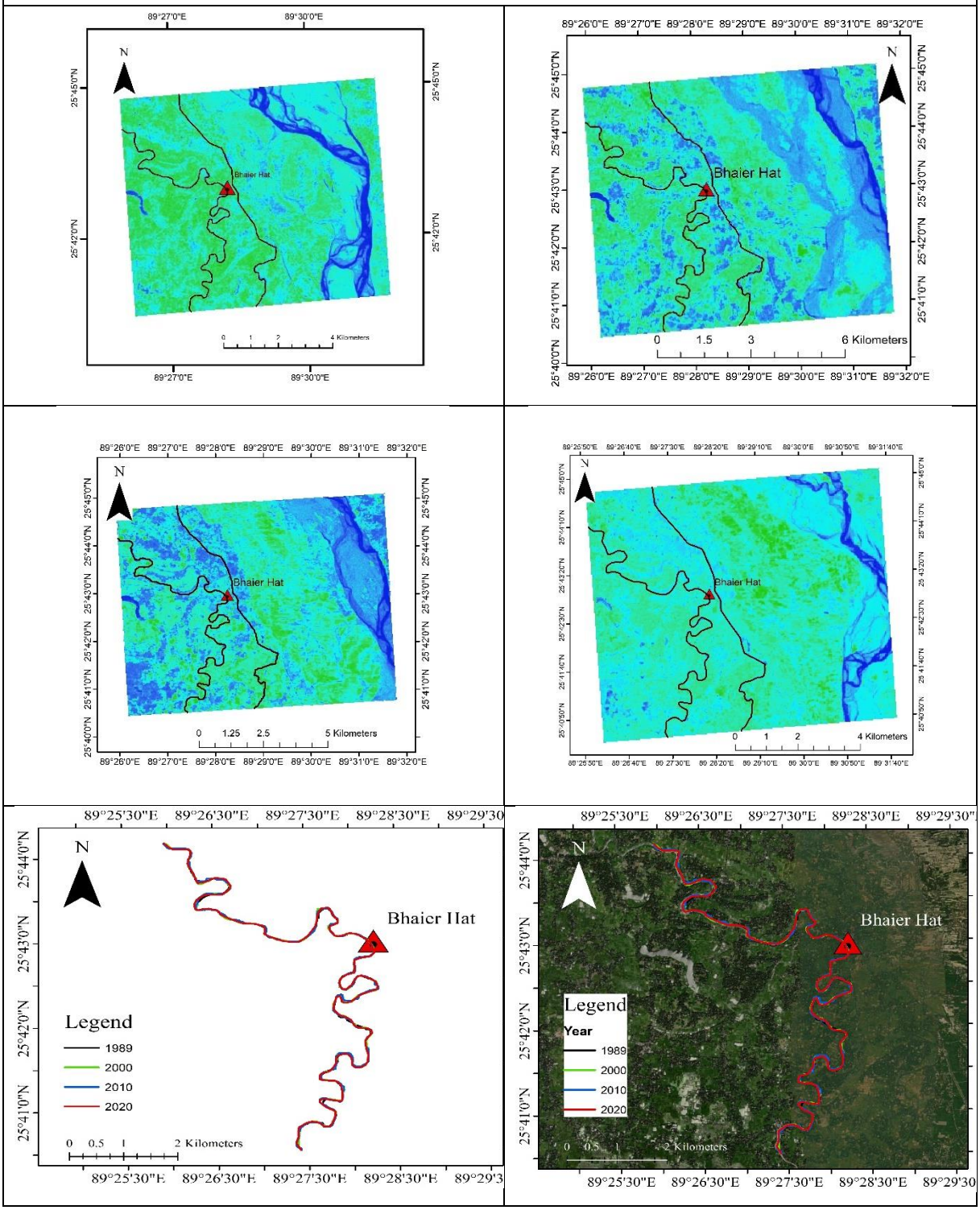

Market-21: Bhutsora (Mirbag hat) in Kaunia Upzila of Rangpur District

- Flood Risk: The market is located in a **Moderate** flood risk area, considering the inundation patterns of all major floods in recent times.
- Bank Erosion Risk: Based on planform analysis using historical satellite images, the market is located in the **Moderate** bank erosion risk area

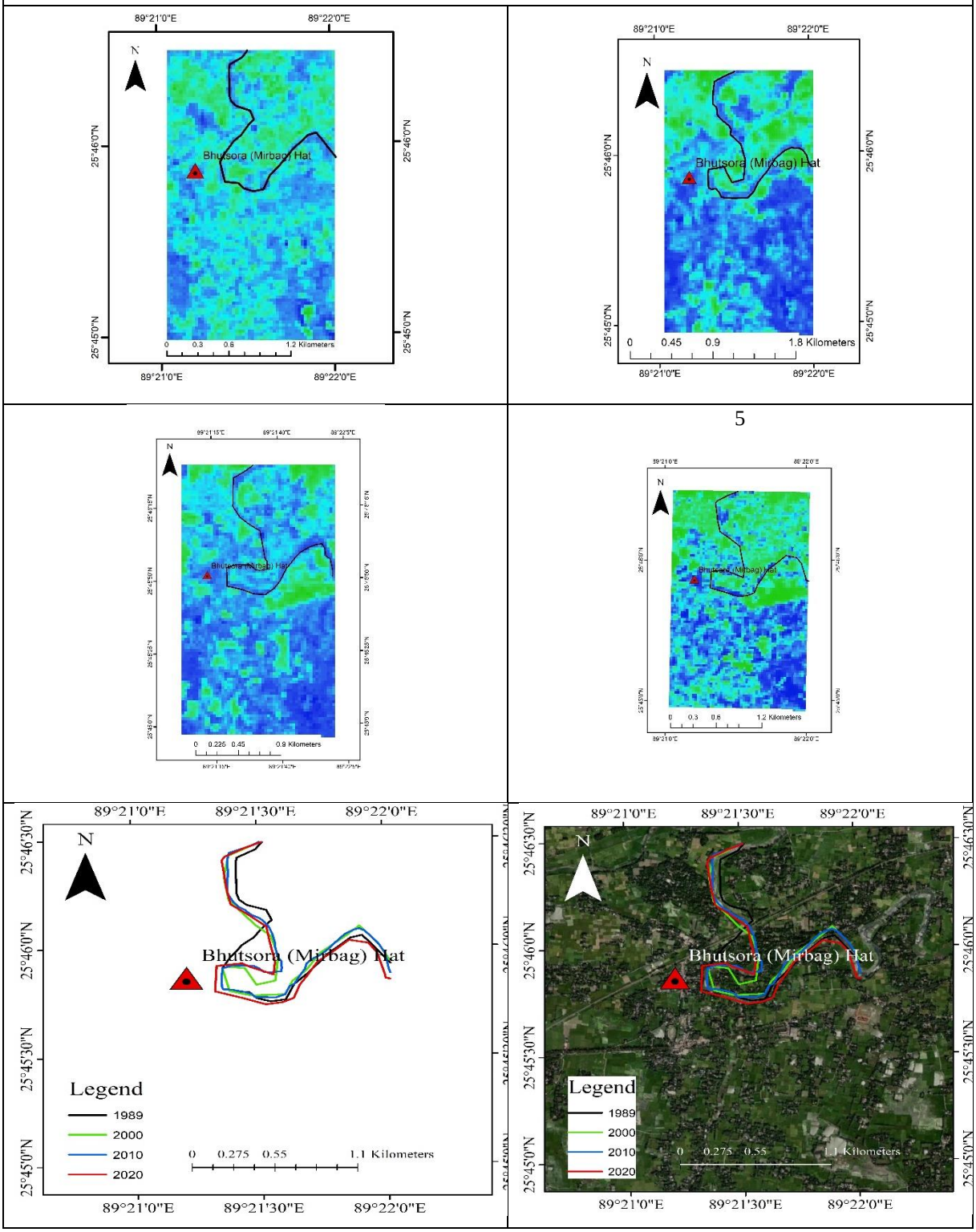

Market-22: Bulakip (ara Bazar) in Islampur Upzila of Jamalpur District

- Flood Risk: The market is located in a **Low** flood-risk area, considering the inundation patterns of all major floods in recent times.
- Bank Erosion Risk: Based on planform analysis using historical satellite images, the market is located in the **High** bank erosion risk area

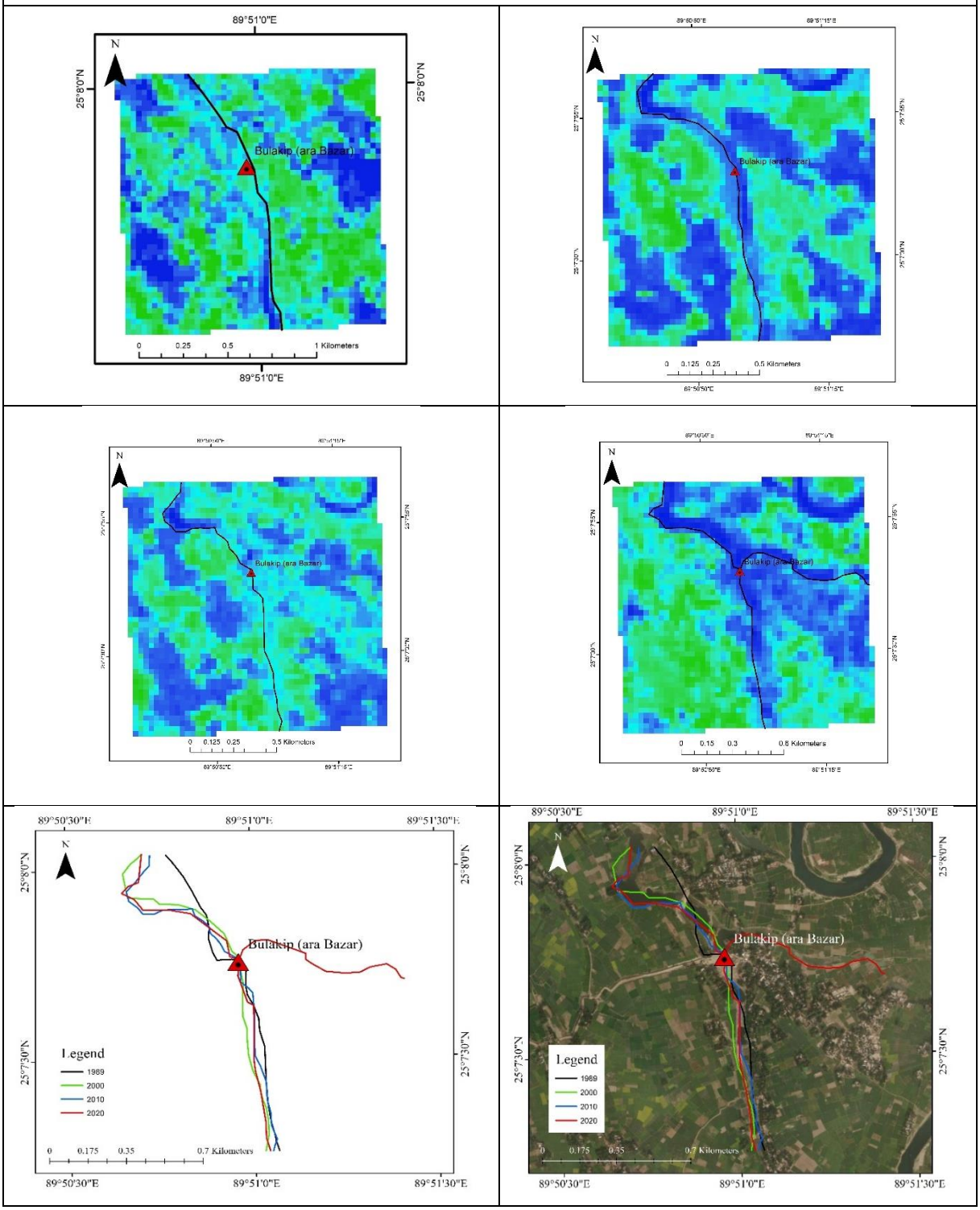

Market-23: Mondalpara Bazar in Islampur Upzila of Jamalpur District

- Flood Risk: The market is located in a **Low** flood-risk area, considering the inundation patterns of all major floods in recent times.
- Bank Erosion Risk: Based on planform analysis using historical satellite images, the Market is located in the **High** bank erosion risk area.

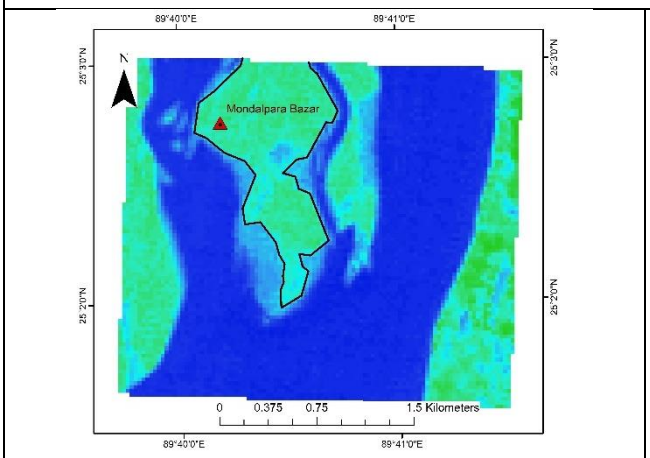

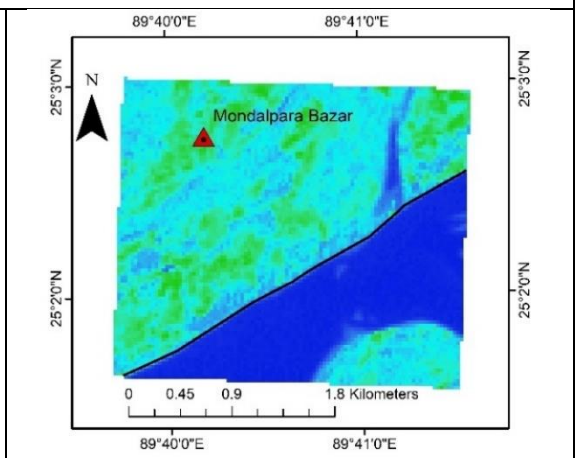

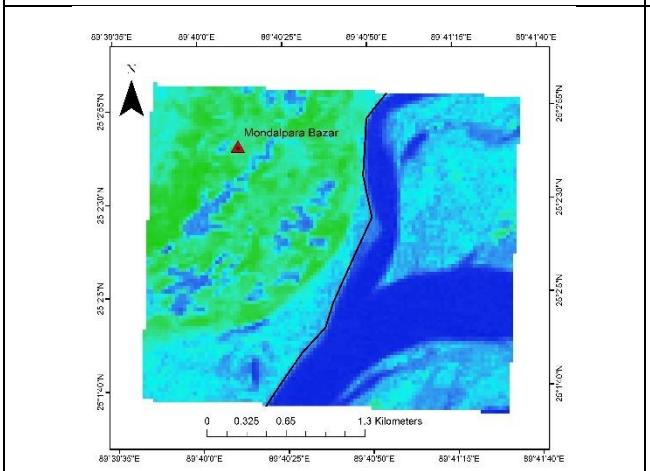

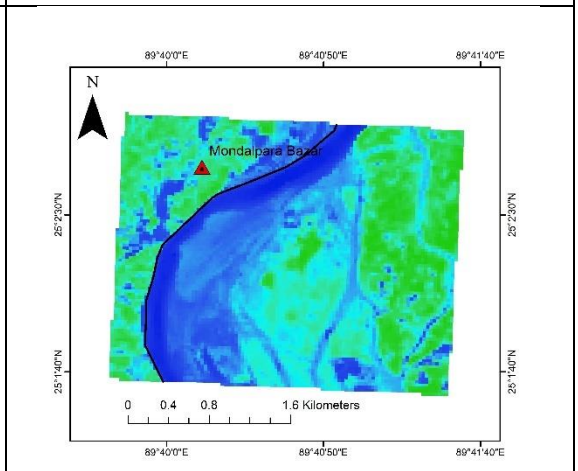

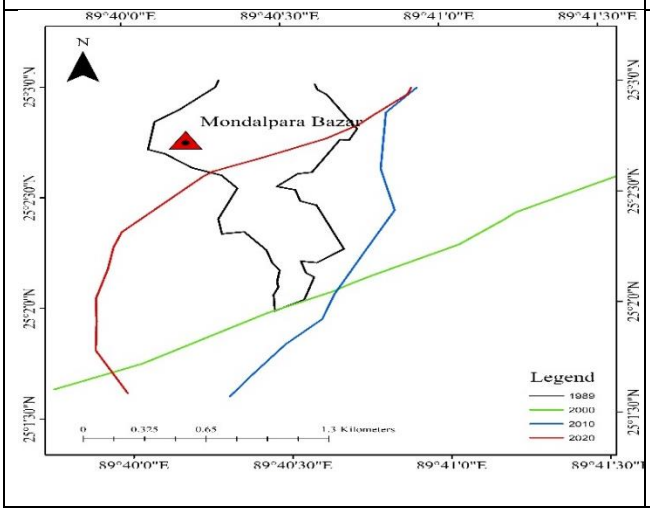

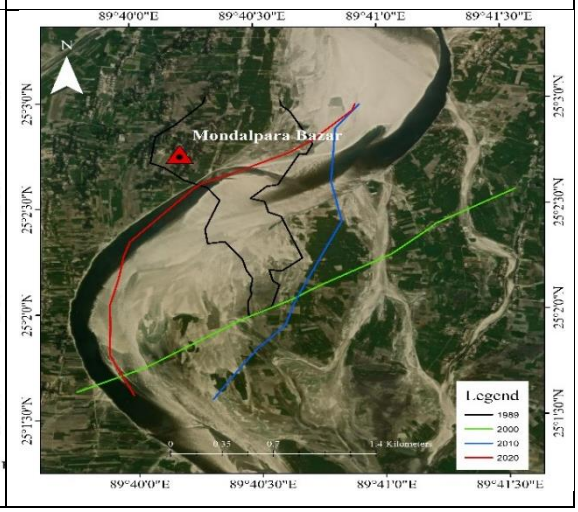

Market-24: Napiterchar Bazar in Islampur Upzila of Jamalpur District

- Flood Risk: The market is located in a **Low** flood-risk area, considering the inundation patterns of all major floods in recent times.
- Bank Erosion Risk: Based on planform analysis using historical satellite images, the Market is located in the **Low** bank erosion risk area.

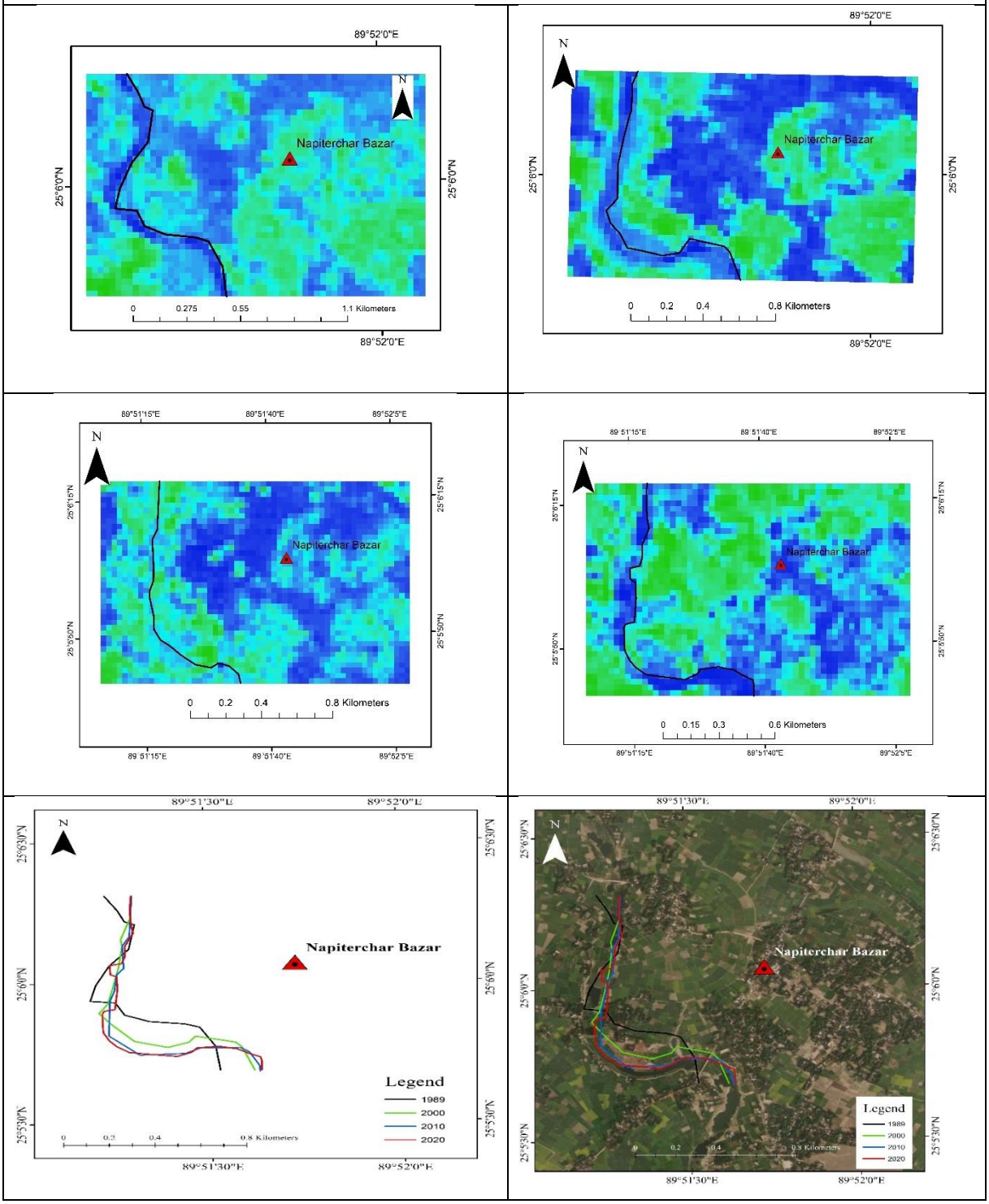

Market-25: Shirajabad Bazar in Islampur Upzila of Jamalpur District

- Flood Risk: The market is located in a **Low** flood-risk area, considering the inundation patterns of all major floods in recent times.
- Bank Erosion Risk: Based on planform analysis using historical satellite images, the Market is located in the **Moderate** bank erosion risk area.

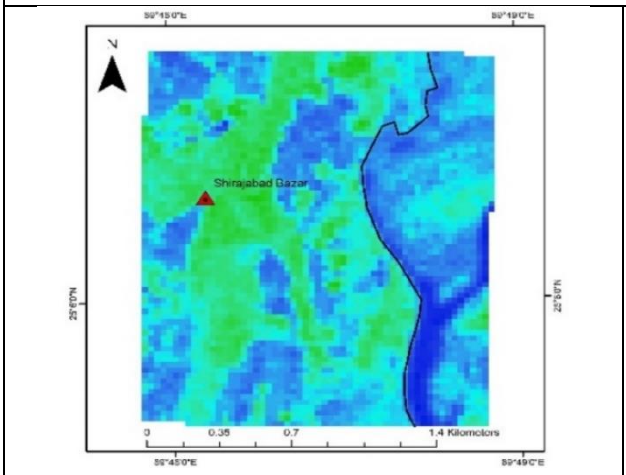

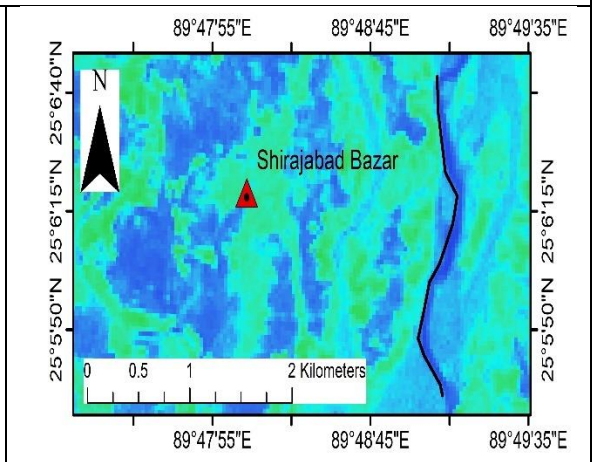

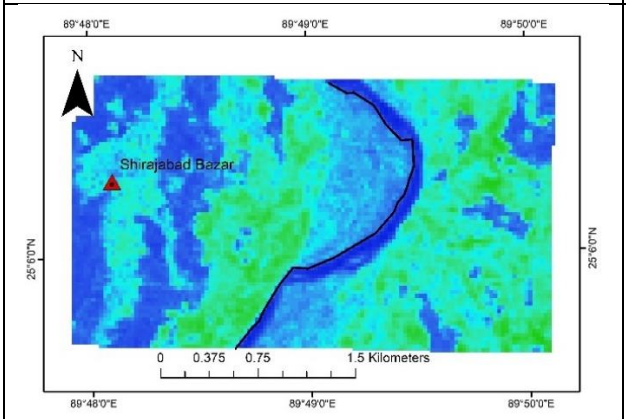

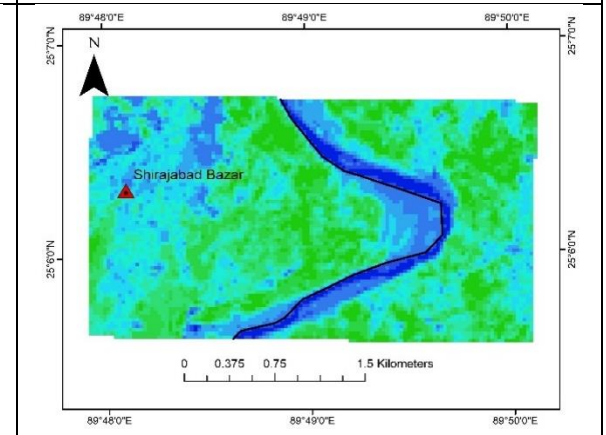

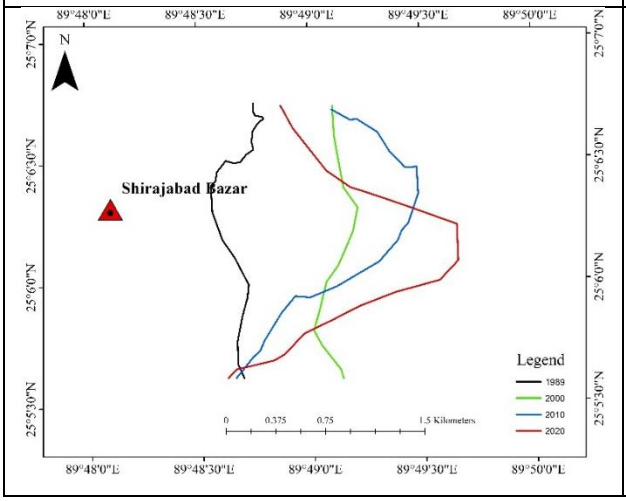

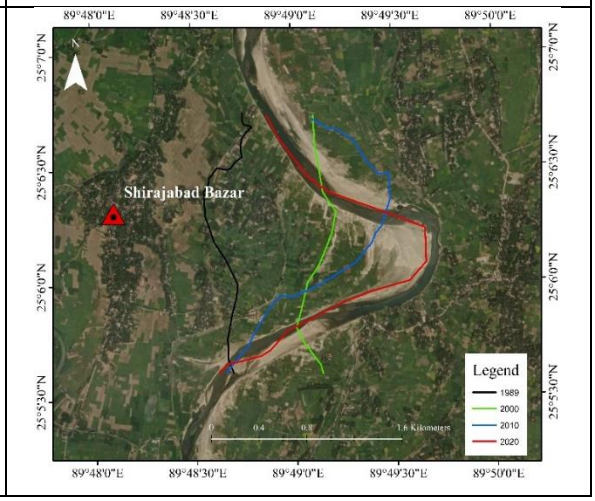

Market-26: Akota Bazar in Islampur Upzila of Jamalpur District

- Flood Risk: The market is located in a **Low** flood-risk area, considering the inundation patterns of all major floods in recent times.
- Bank Erosion Risk: Based on planform analysis using historical satellite images, the Market is located in the **High** bank erosion risk area.

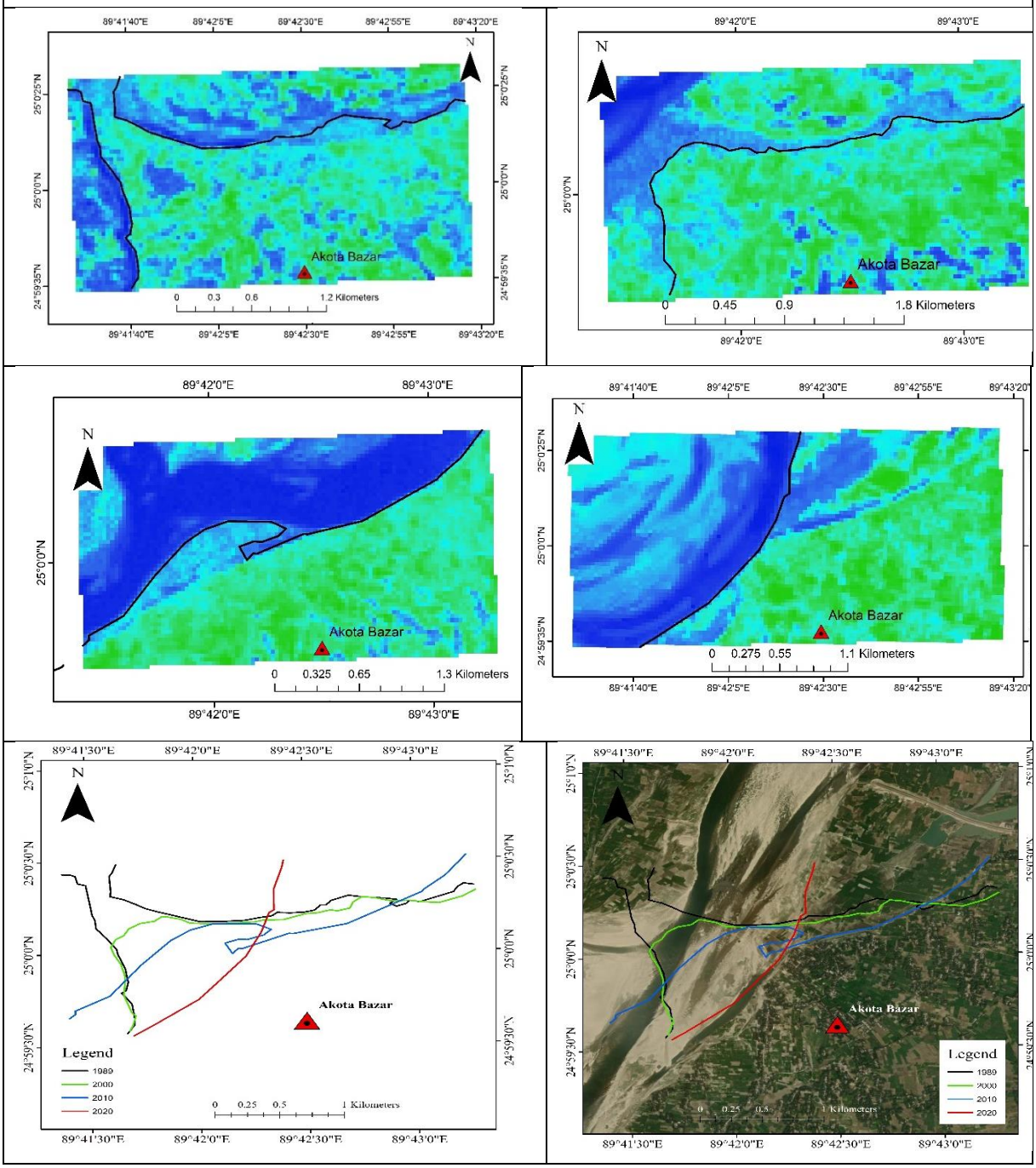

Market-27: Amkhowa Bazar in Dewanganj Upzila of Jamalpur District

- Flood Risk: The market is located in a **Low** flood-risk area, considering the inundation patterns of all major floods in recent times.
- Bank Erosion Risk: Based on planform analysis using historical satellite images, the market is located in the **Low** bank erosion risk area.

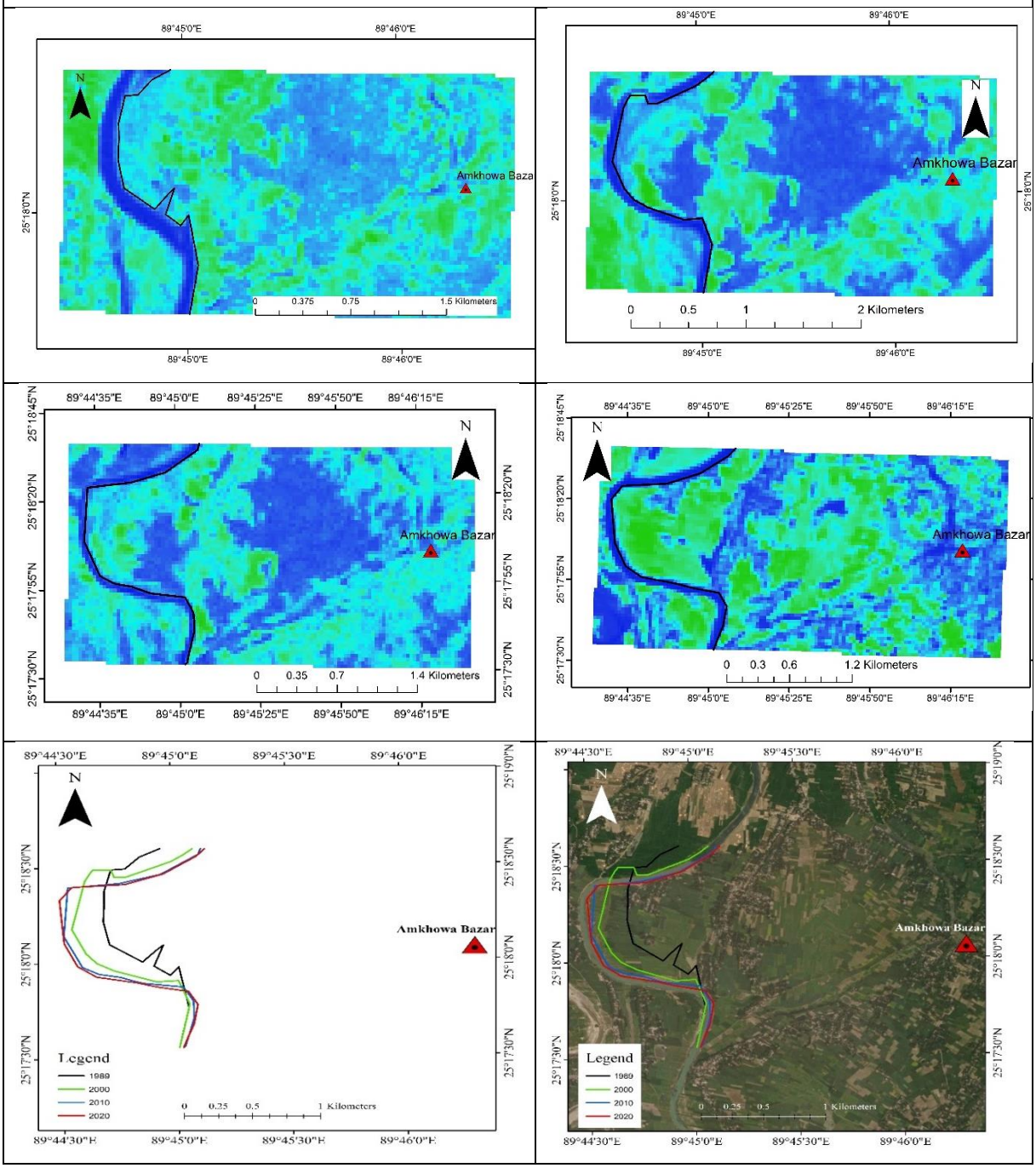

Market-28: Molla Para Bazar(Tilokpur) in Dewanganj Upzila of Jamalpur District

- Flood Risk: The market is located in a **Low** flood-risk area, considering the inundation patterns of all major floods in recent times.
- Bank Erosion Risk: Based on planform analysis using historical satellite images, the Market is located in the **High** bank erosion risk area.

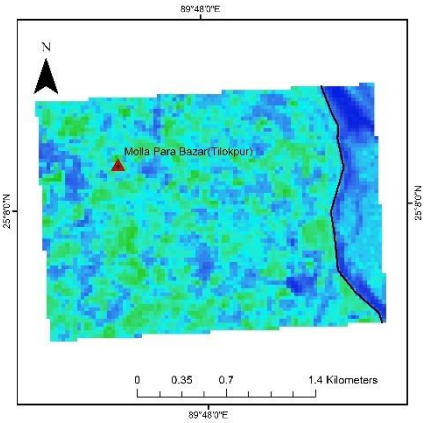

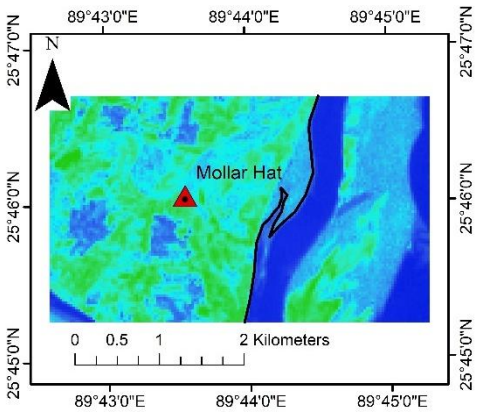

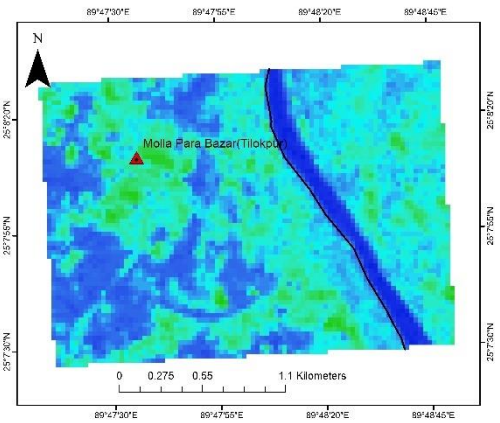

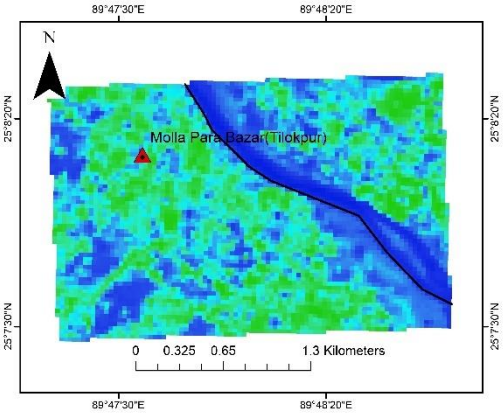

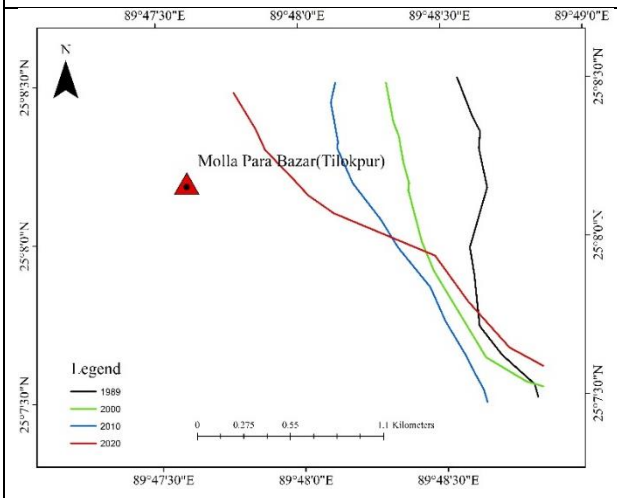

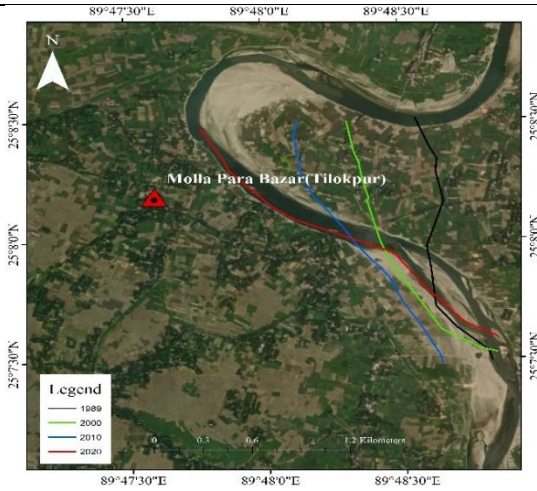

Market-29: Sunandabari Bazar in Dewanganj Upzila of Jamalpur District

- Flood Risk: The market is located in a **Low** flood-risk area, considering the inundation patterns of all major floods in recent times.
- Bank Erosion Risk: Based on planform analysis using historical satellite images, the Market is located in the **Low** bank erosion risk area.

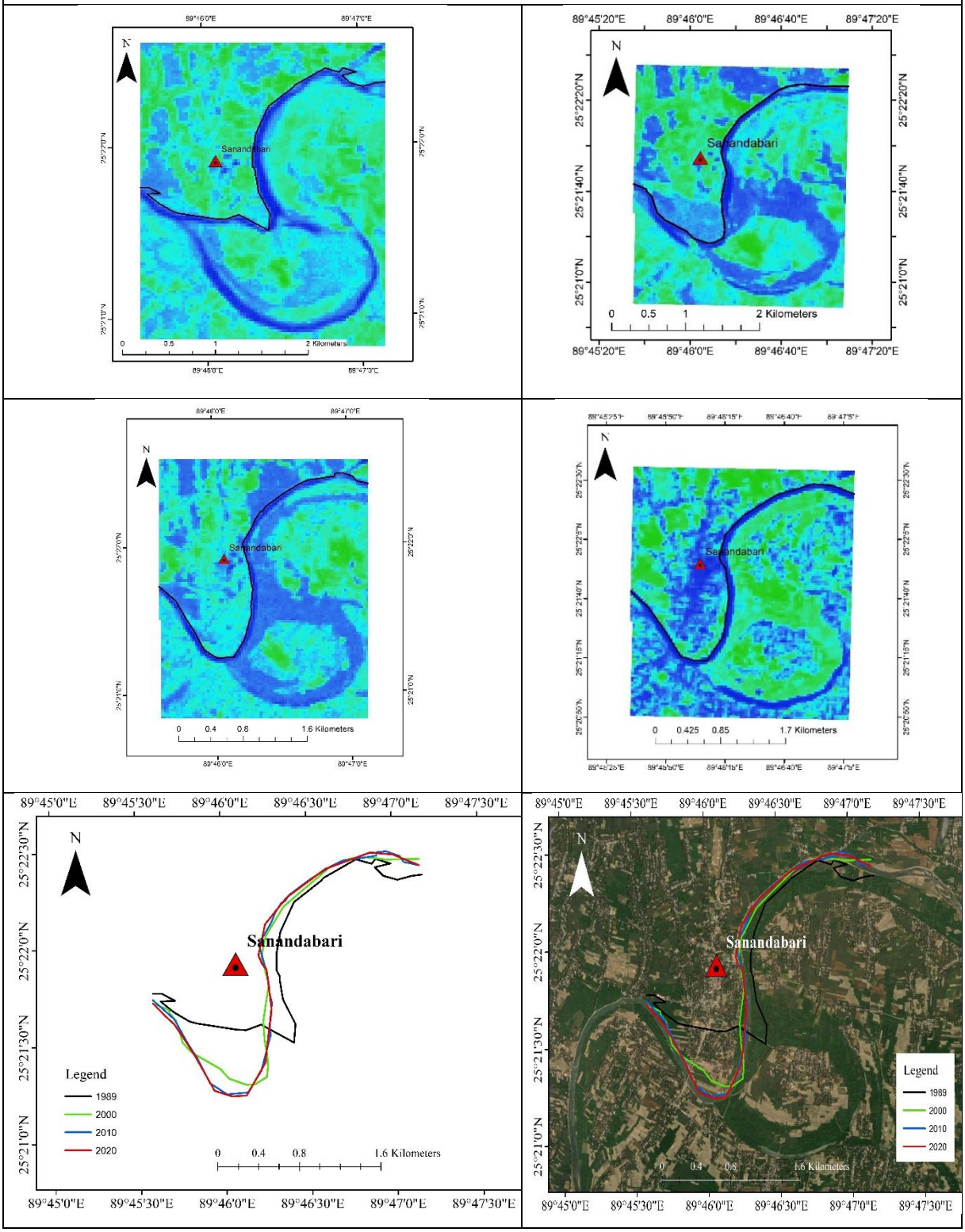

Market-30: Khorma Bazar in Dewanganj Upzila of Jamalpur District

- Flood Risk: The market is located in a **Low** flood-risk area, considering the inundation patterns of all major floods in recent times.
- Bank Erosion Risk: Based on planform analysis using historical satellite images, the market is located in the **Low** bank erosion risk area.

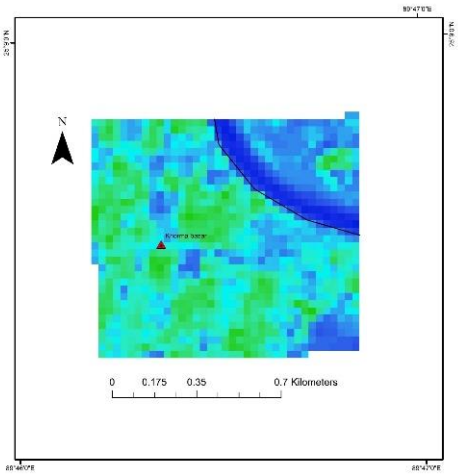

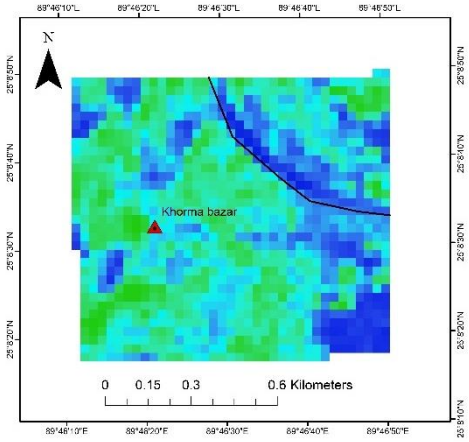

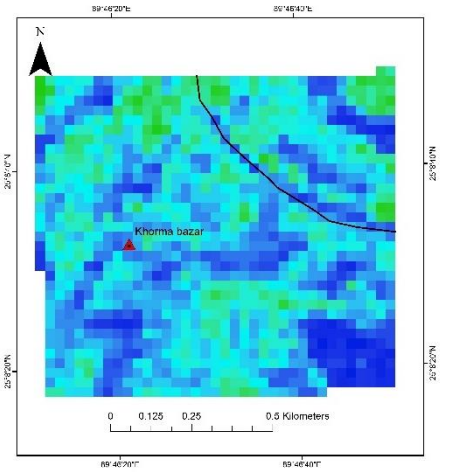

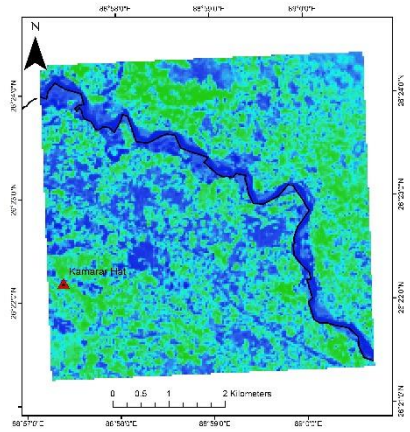

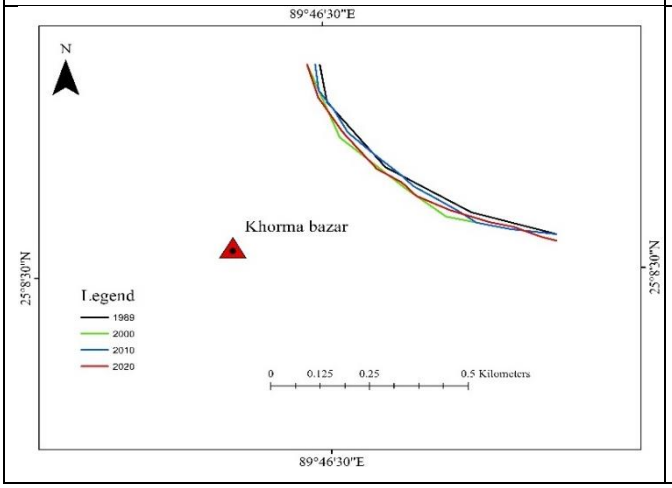

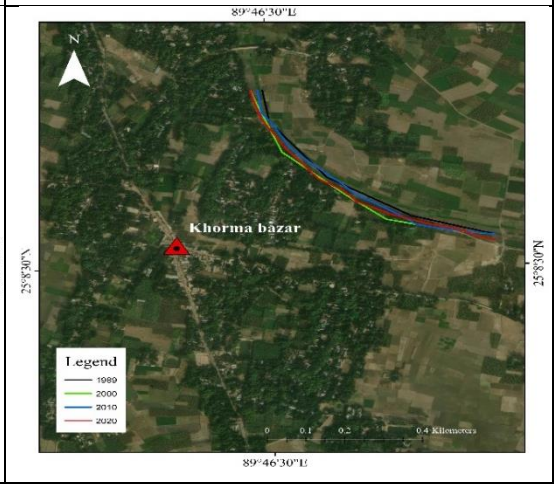

Market-31: Bhabki Bazar in Melandaha Upzila of Jamalpur District

- Flood Risk: The market is located in a **Low** flood-risk area, considering the inundation patterns of all major floods in recent times.
- Bank Erosion Risk: Based on planform analysis using historical satellite images, the market is located in the **Low** bank erosion risk area.

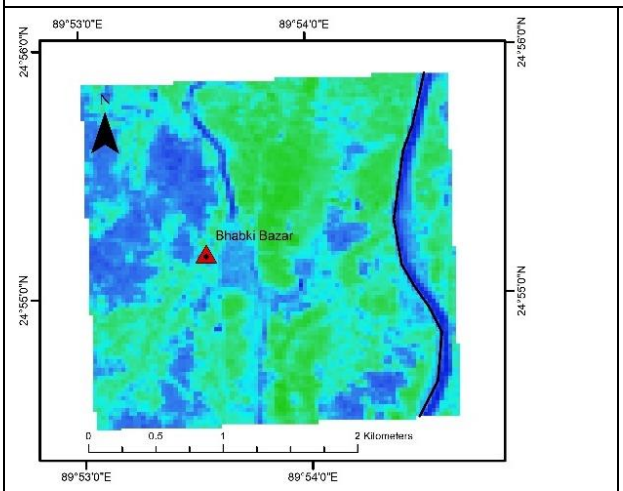

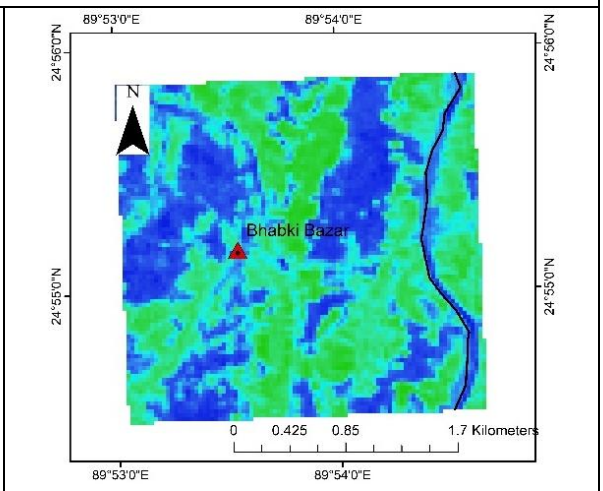

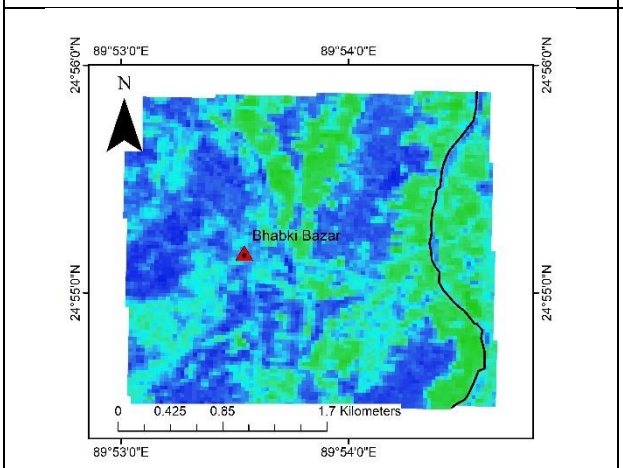

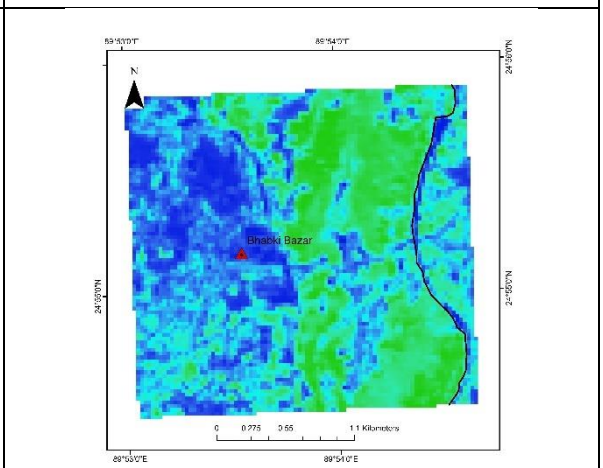

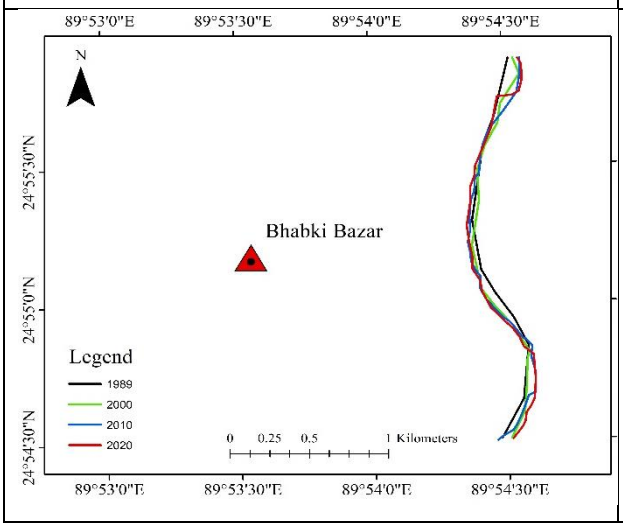

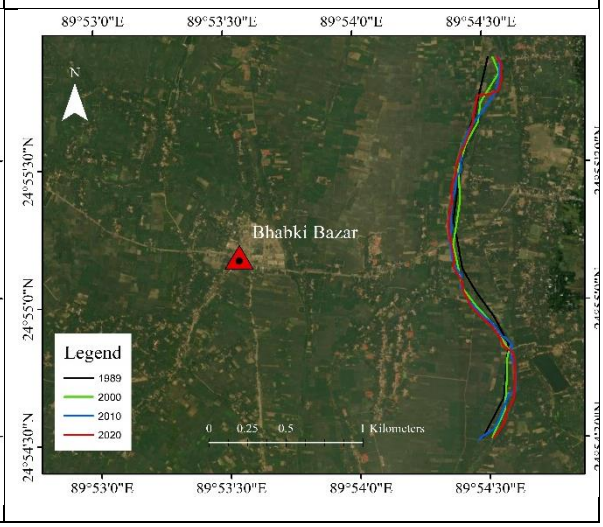

Market-32: Bhaluka (Tarankandi Bazar) in Melandaha Upzila of Jamalpur District

- Flood Risk: The market is located in a **Low** flood-risk area, considering the inundation patterns of all major floods in recent times.
- Bank Erosion Risk: Based on planform analysis using historical satellite images, the market is located in the **Low** bank erosion risk area

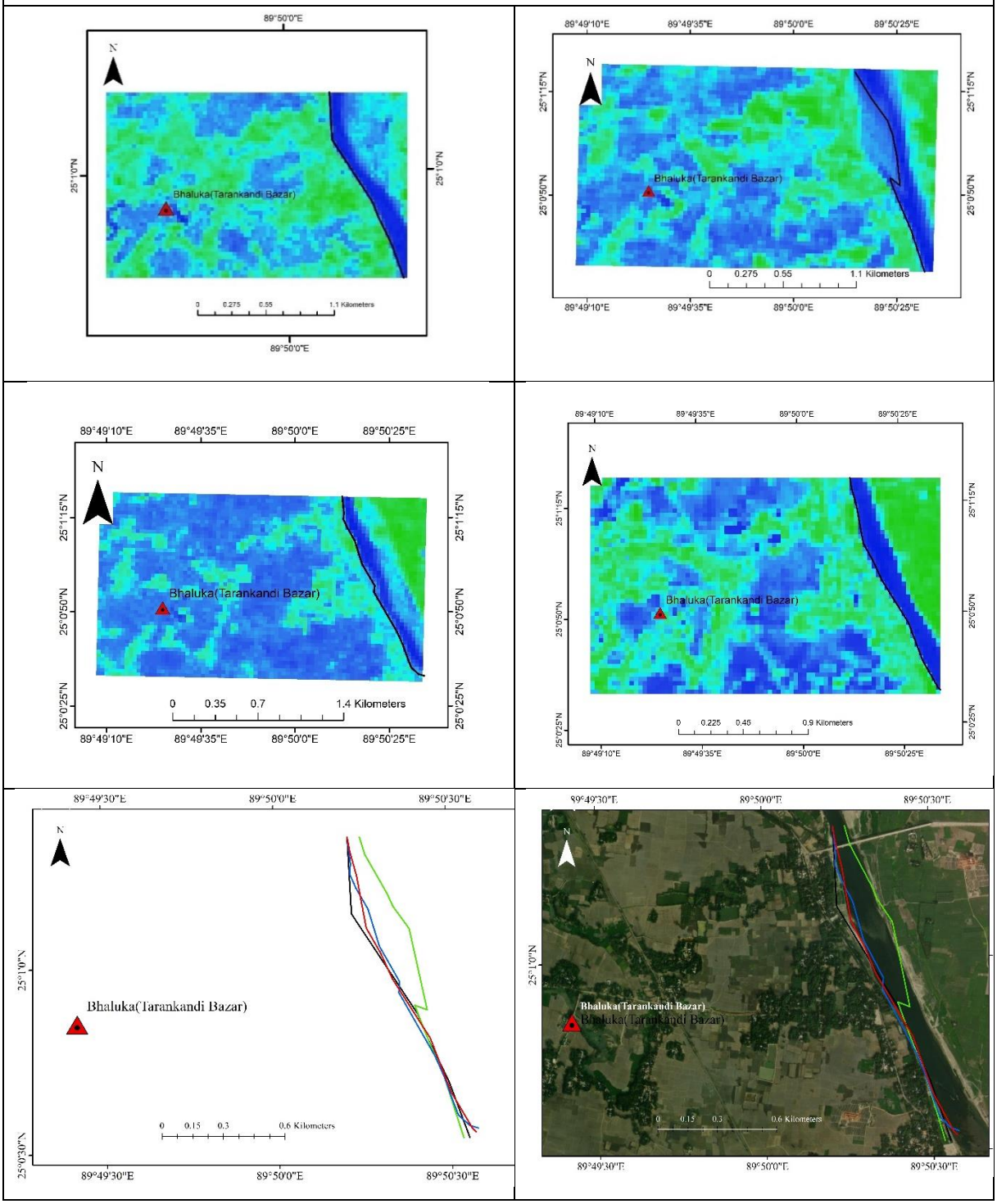

Market-33: Char Gobindi Bazar in Melandaha Upazila of Jamalpur District

- Flood Risk: The market is located in a **Low** flood-risk area, considering the inundation patterns of all major floods in recent times.
- Bank Erosion Risk: Based on planform analysis using historical satellite images, the market is located in the **Moderate** bank erosion risk area.

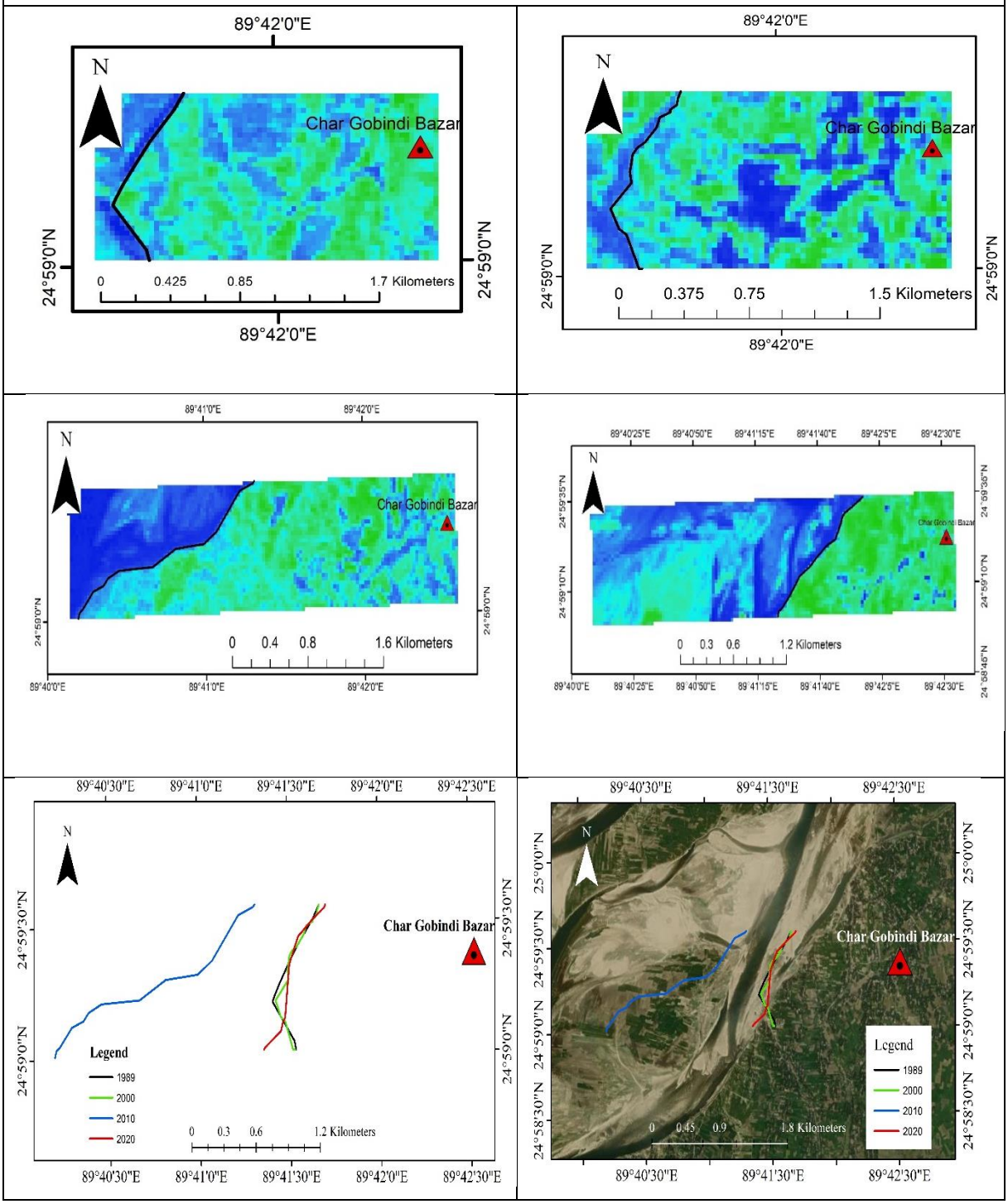

Market-34: Gazipur Bazar in Melandaha Upazila of Jamalpur District

- Flood Risk: The market is located in a **Low** flood-risk area, considering the inundation patterns of all major floods in recent times.
- Bank Erosion Risk: Based on planform analysis using historical satellite images, the market is located in the **Moderate** bank erosion risk area.

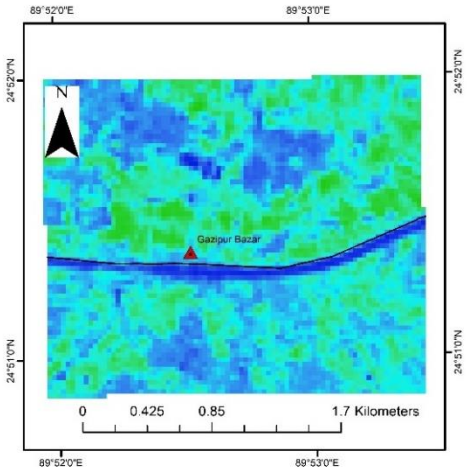

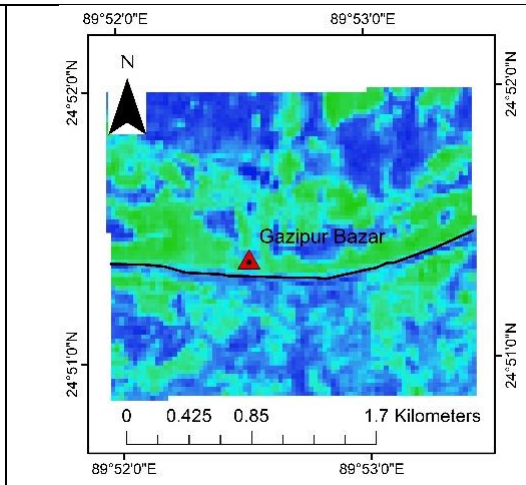

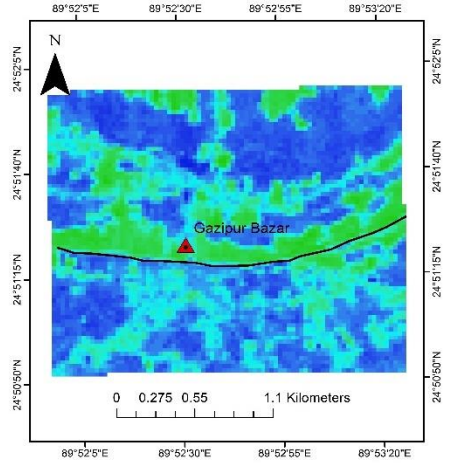

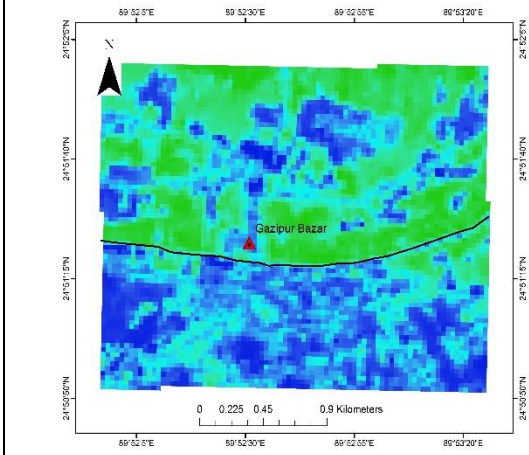

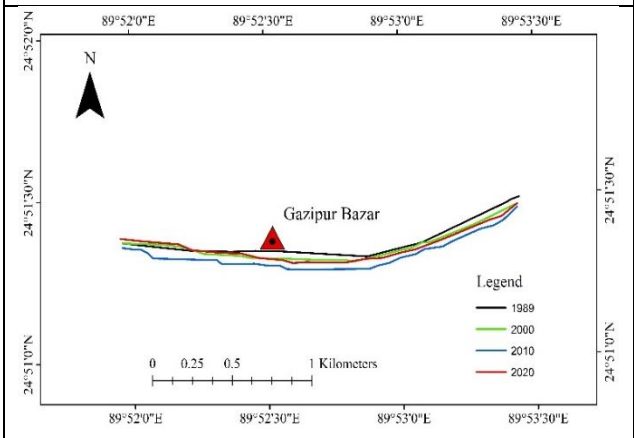

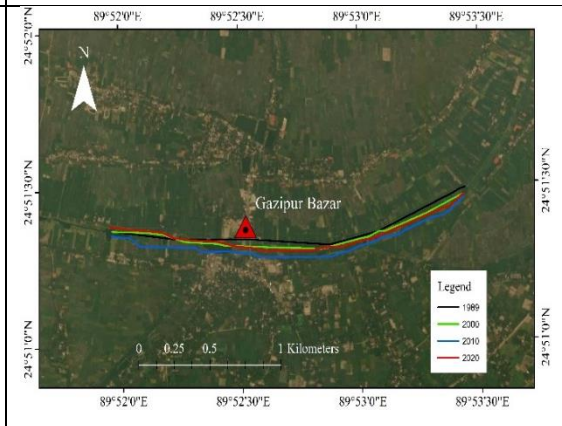

Market-35: Gobindoganj Bazar in Melandaha Upzila of Jamalpur District

- Flood Risk: The market is located in a **Low** flood-risk area, considering the inundation patterns of all major floods in recent times.
- Bank Erosion Risk: Based on planform analysis using historical satellite images, the market is located in the **High** bank erosion risk area

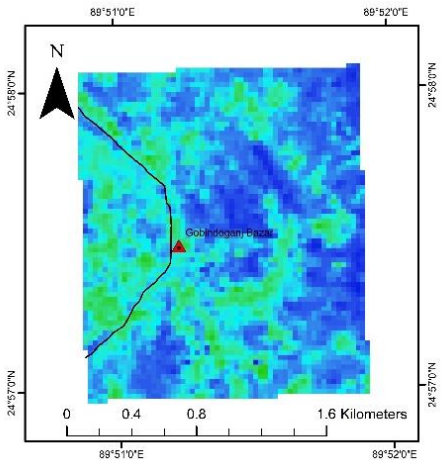

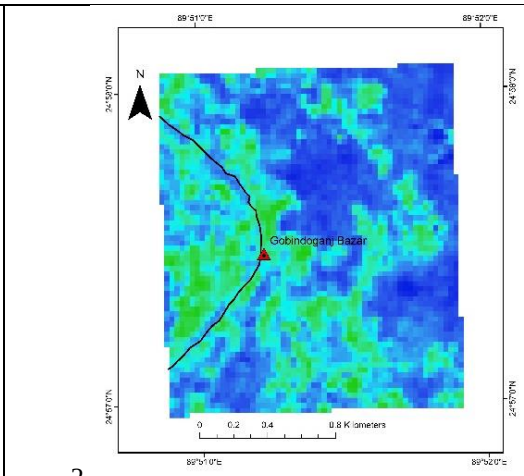

2.

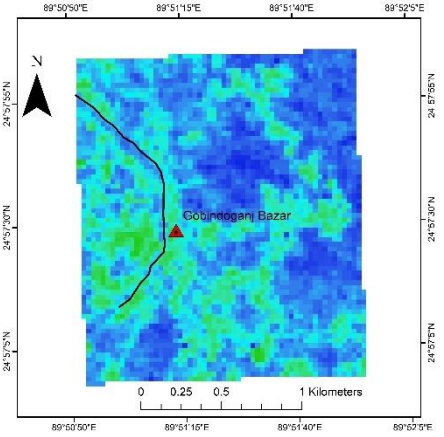

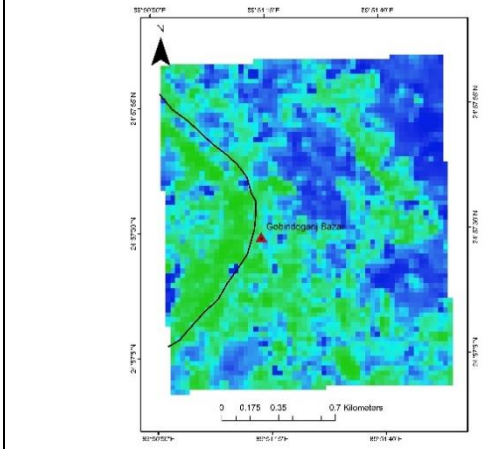

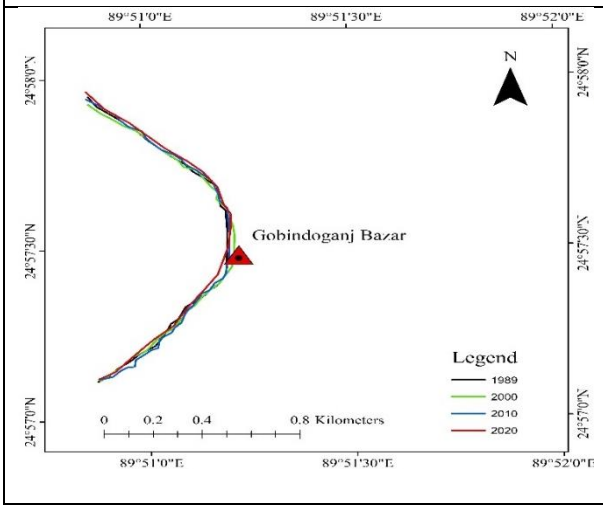

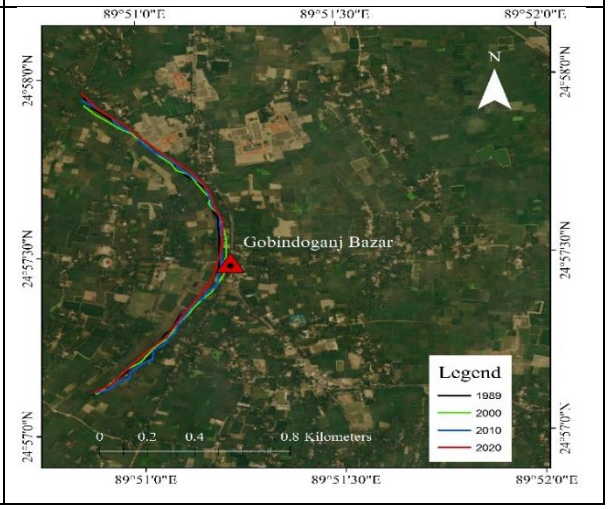

Market-36: Mahmudpur in Melandaha Upzila of Jamalpur District

- Flood Risk: The market is located in a **Low** flood-risk area, considering the inundation patterns of all major floods in recent times.
- Bank Erosion Risk: Based on planform analysis using historical satellite images, the market is located in the **Low** bank erosion risk area.

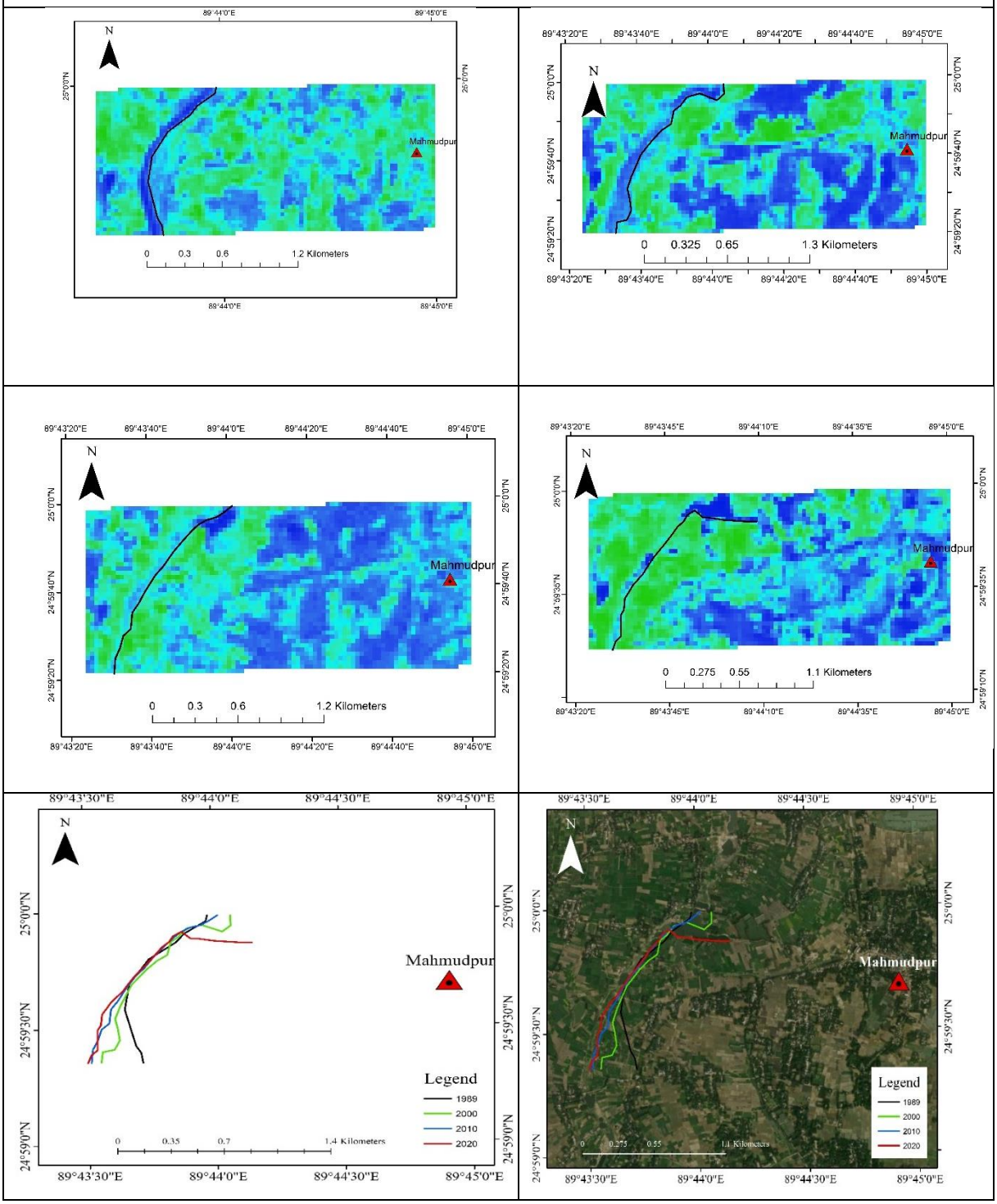

Market-37: Jhawgora Bazar in Melandaha Upzila of Jamalpur District

- Flood Risk: The market is located in a **Low** flood-risk area, considering the inundation patterns of all major floods in recent times.
- Bank Erosion Risk: Based on planform analysis using historical satellite images, the market is located in the **Low** bank erosion risk area.

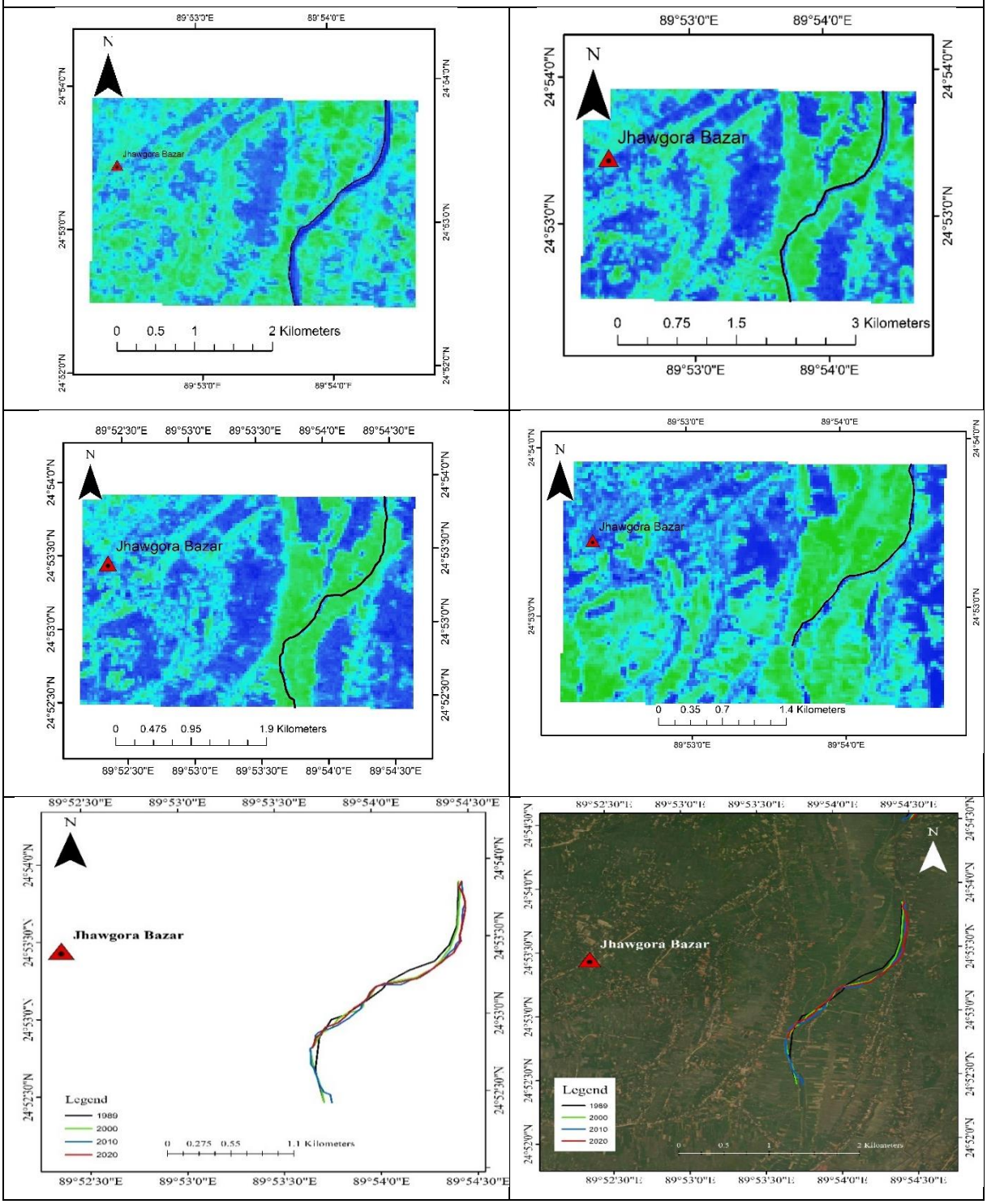

Market-38: Kahetpara Bazar in Melandaha Upzila of Jamalpur District

- Flood Risk: The market is located in a **Low** flood-risk area, considering the inundation patterns of all major floods in recent times.
- Bank Erosion Risk: Based on planform analysis using historical satellite images, the market is located in the **High** bank erosion risk area.

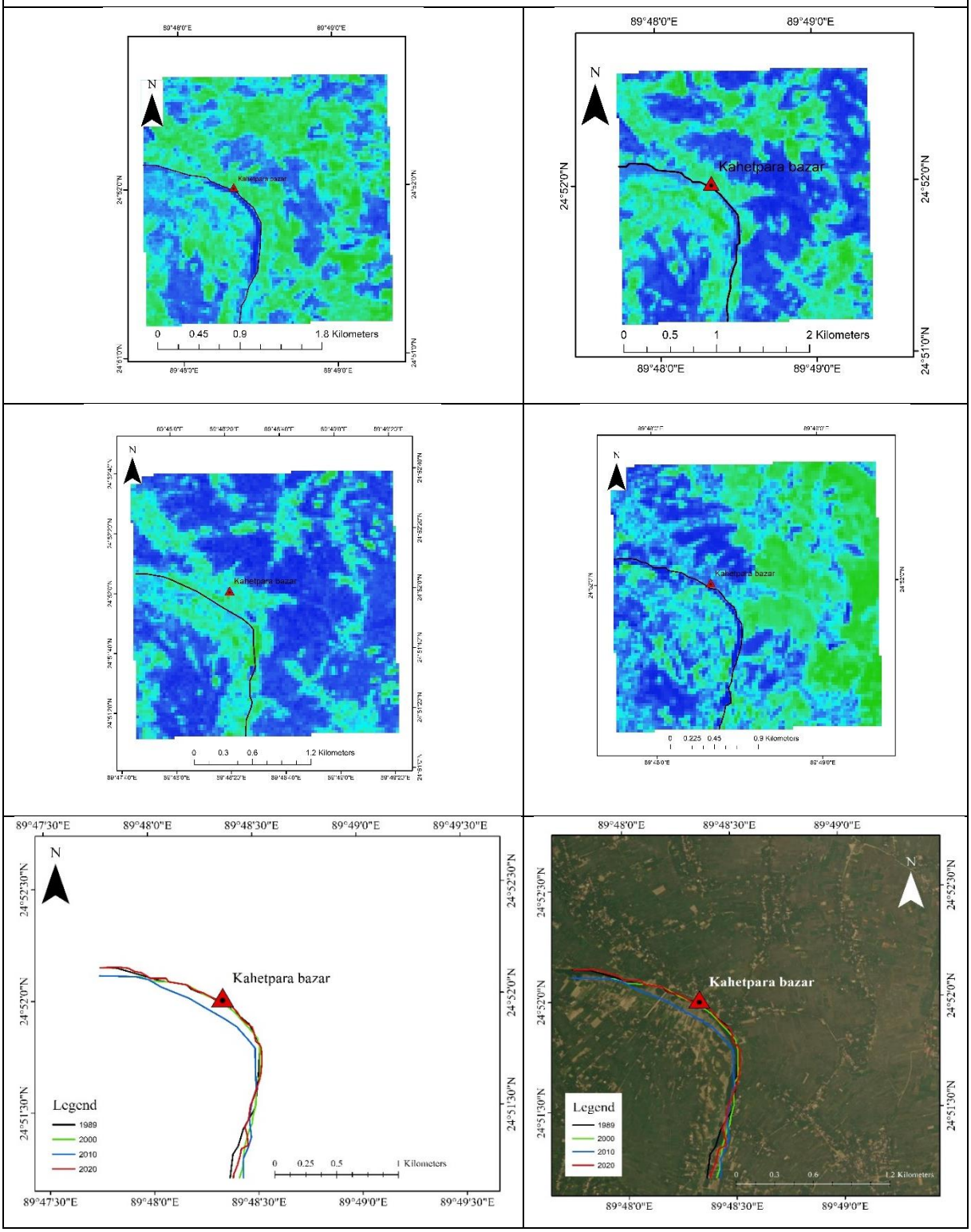

Market-39: Koali Kandi Bazar in Madarganj Upzila of Jamalpur District

- Flood Risk: The market is located in a **Low** flood-risk area, considering the inundation patterns of all major floods in recent times.
- Bank Erosion Risk: Based on planform analysis using historical satellite images, the market is located in the **Moderate** bank erosion risk area.

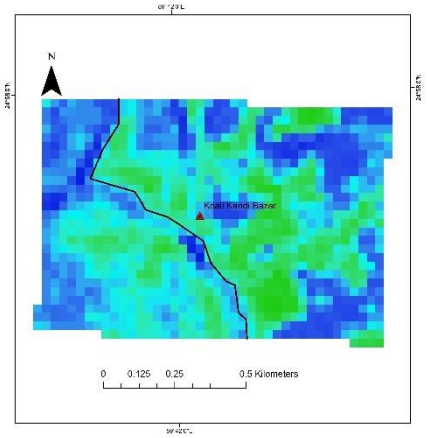

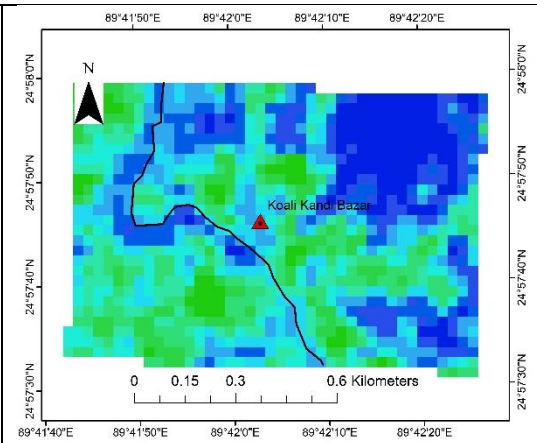

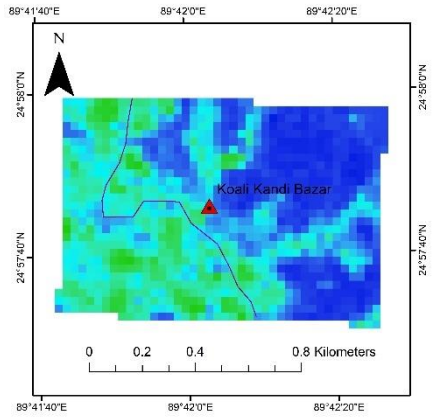

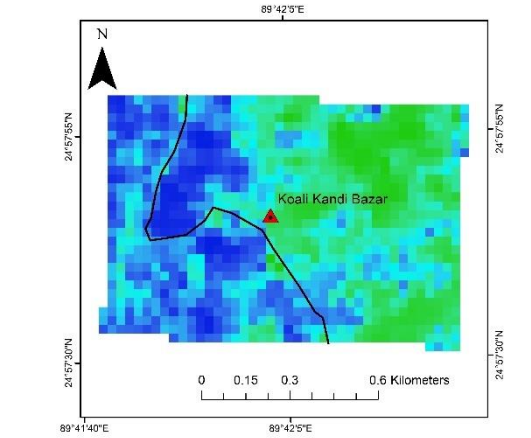

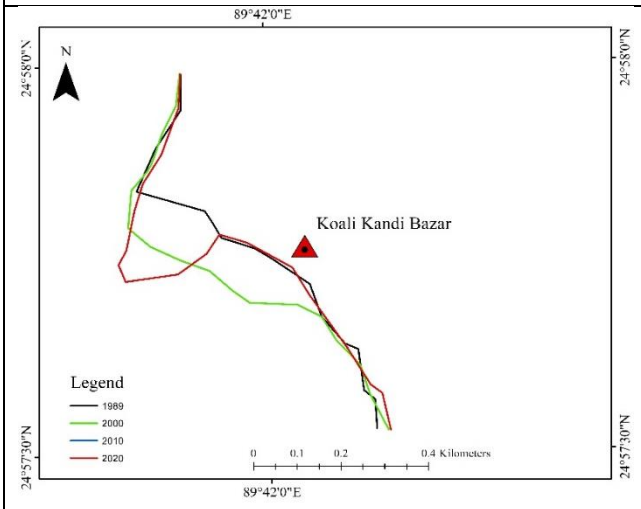

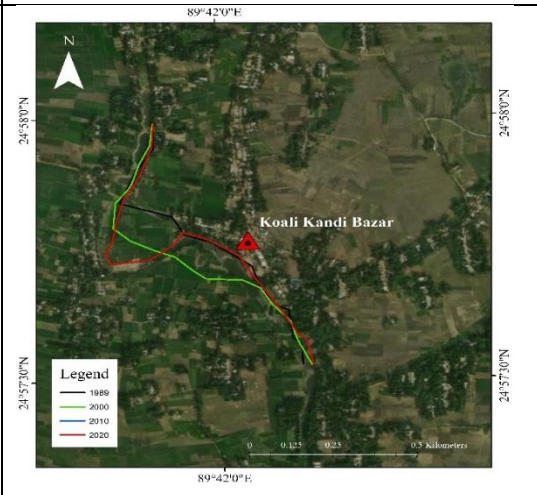

Market-40: Millon Bazar in Madarganj Upzila of Jamalpur District

- Flood Risk: The market is located in a **Low** flood-risk area, considering the inundation patterns of all major floods in recent times.
- Bank Erosion Risk: Based on planform analysis using historical satellite images, the Market is located in the **Low** bank erosion risk area.

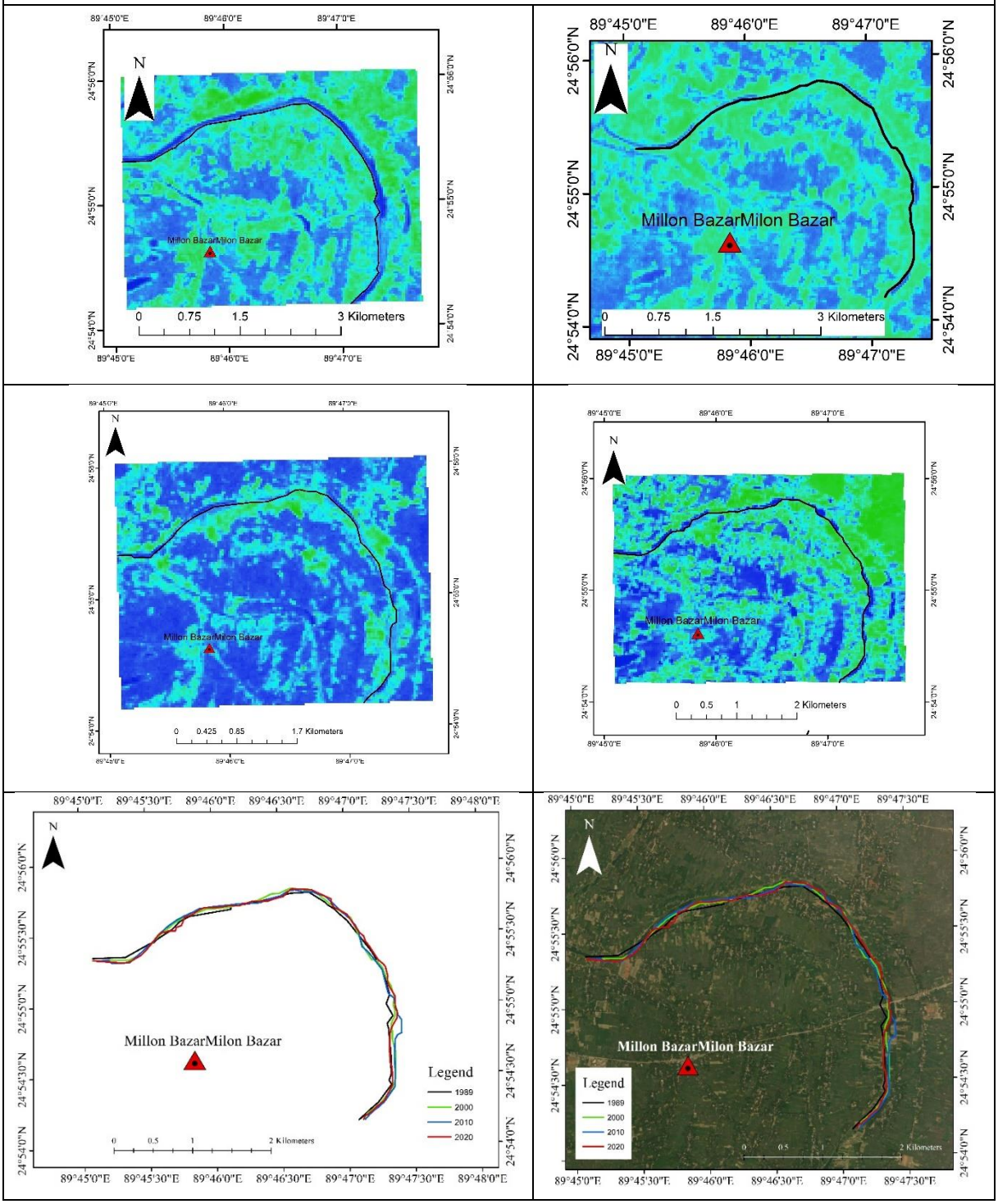

Market-41: Nabbo Char Bazar in Madarganj Upazila of Jamalpur District

- Flood Risk: The market is located in a **Low** flood-risk area, considering the inundation patterns of all major floods in recent times.
- Bank Erosion Risk: Based on planform analysis using historical satellite images, the Market is located in the **Low** bank erosion risk area.

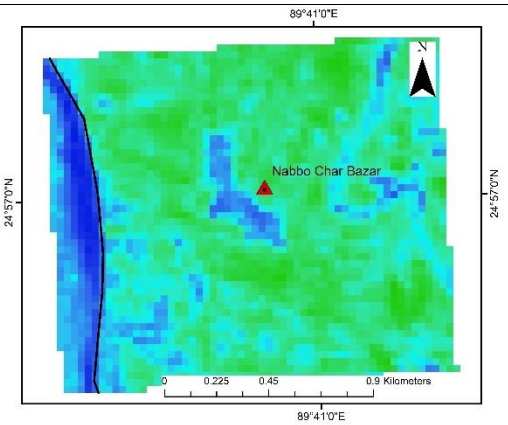

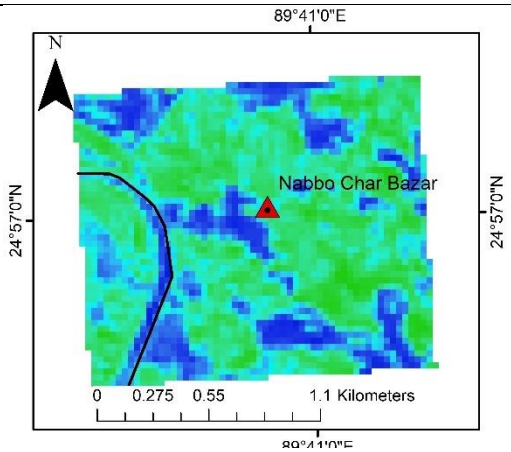

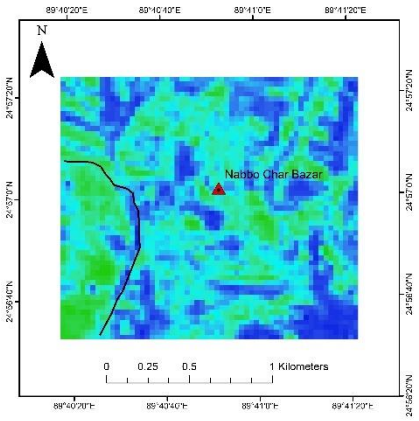

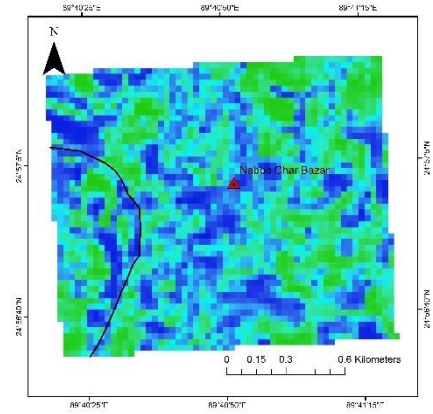

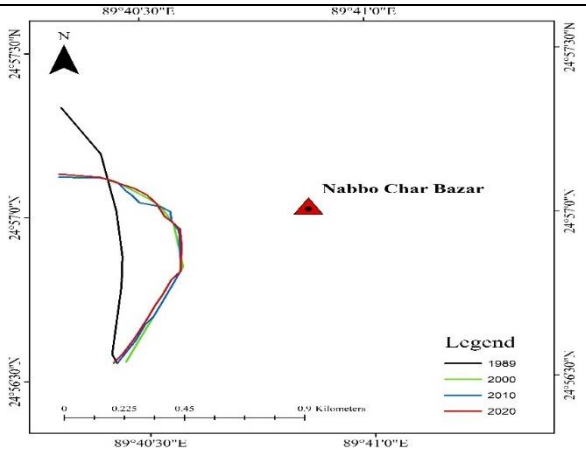

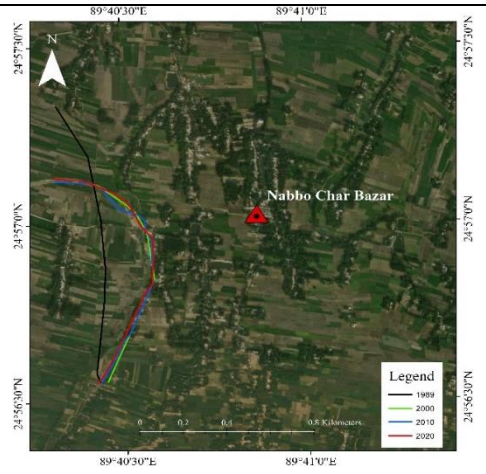

Market-42: Rayerchara Bazar in Madarganj Upzila of Jamalpur District

- Flood Risk: The market is located in a **Low** flood-risk area, considering the inundation patterns of all major floods in recent times.
- Bank Erosion Risk: Based on planform analysis using historical satellite images, the Market is located in the **Low** bank erosion risk area.

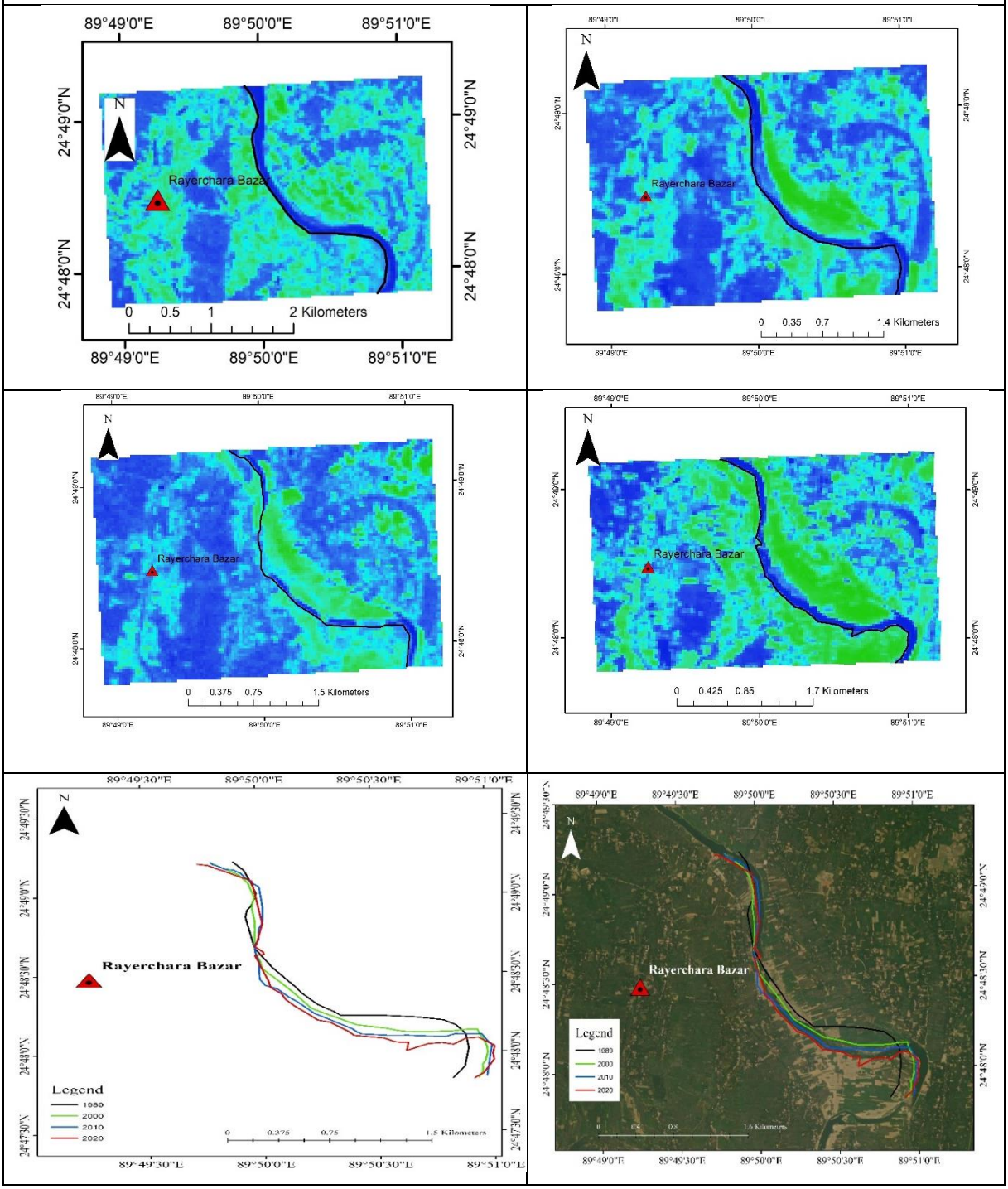

Market-43: Tegharaia Bazar in Madarganj Upzila of Jamalpur District

- Flood Risk: The market is located in a **Low** flood-risk area, considering the inundation patterns of all major floods in recent times.
- Bank Erosion Risk: Due to satellite image limitation, the river bank erosion risk cannot be assessed **(N/A)**.

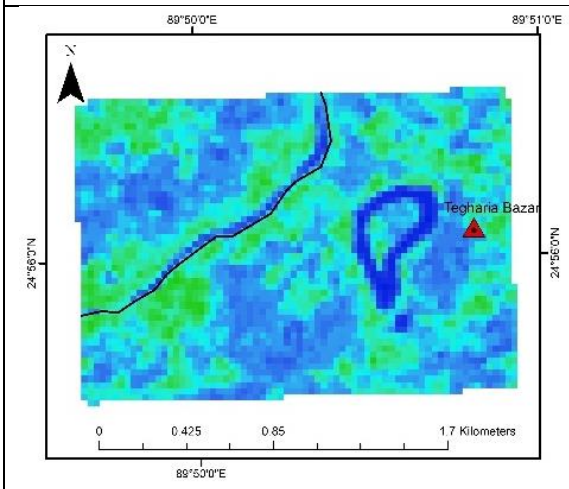

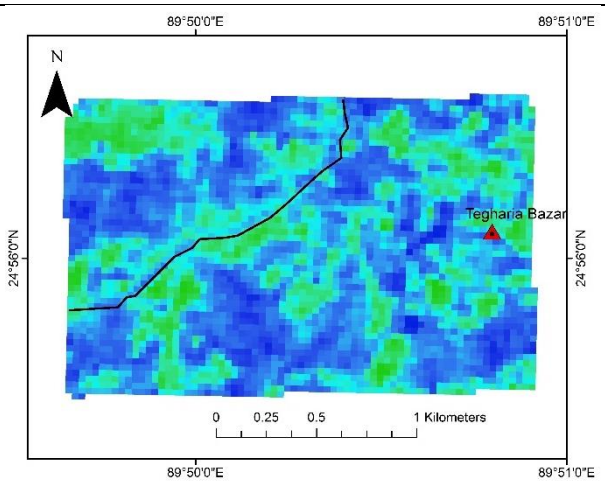

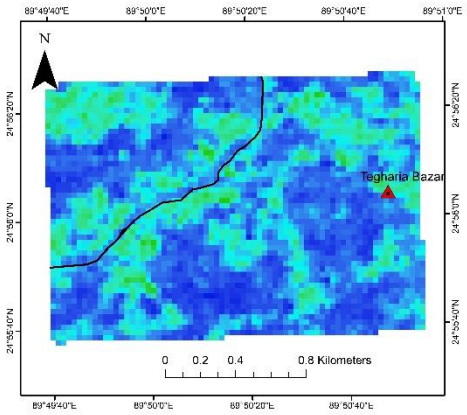

It is not possible to detect changes in bank lines due to inadequate resolution of satellite image

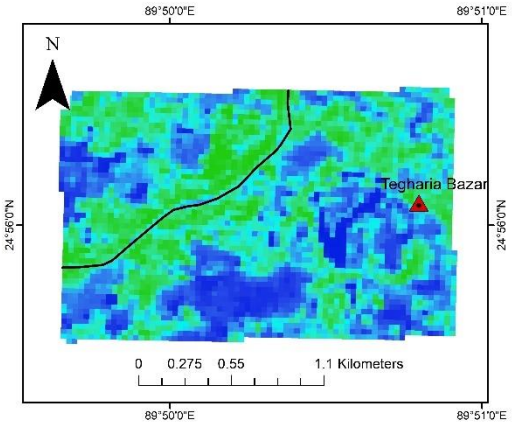

It is not possible to detect changes in bank lines due to inadequate resolution of satellite image

Market-44: Nalsia Bazar in Madarganj Upzila of Jamalpur District

- Flood Risk: The market is located in a **Moderate** flood risk area, considering the inundation patterns of all major floods in recent times.
- Bank Erosion Risk: Based on planform analysis using historical satellite images, the Market is located in the **Low** bank erosion risk area.

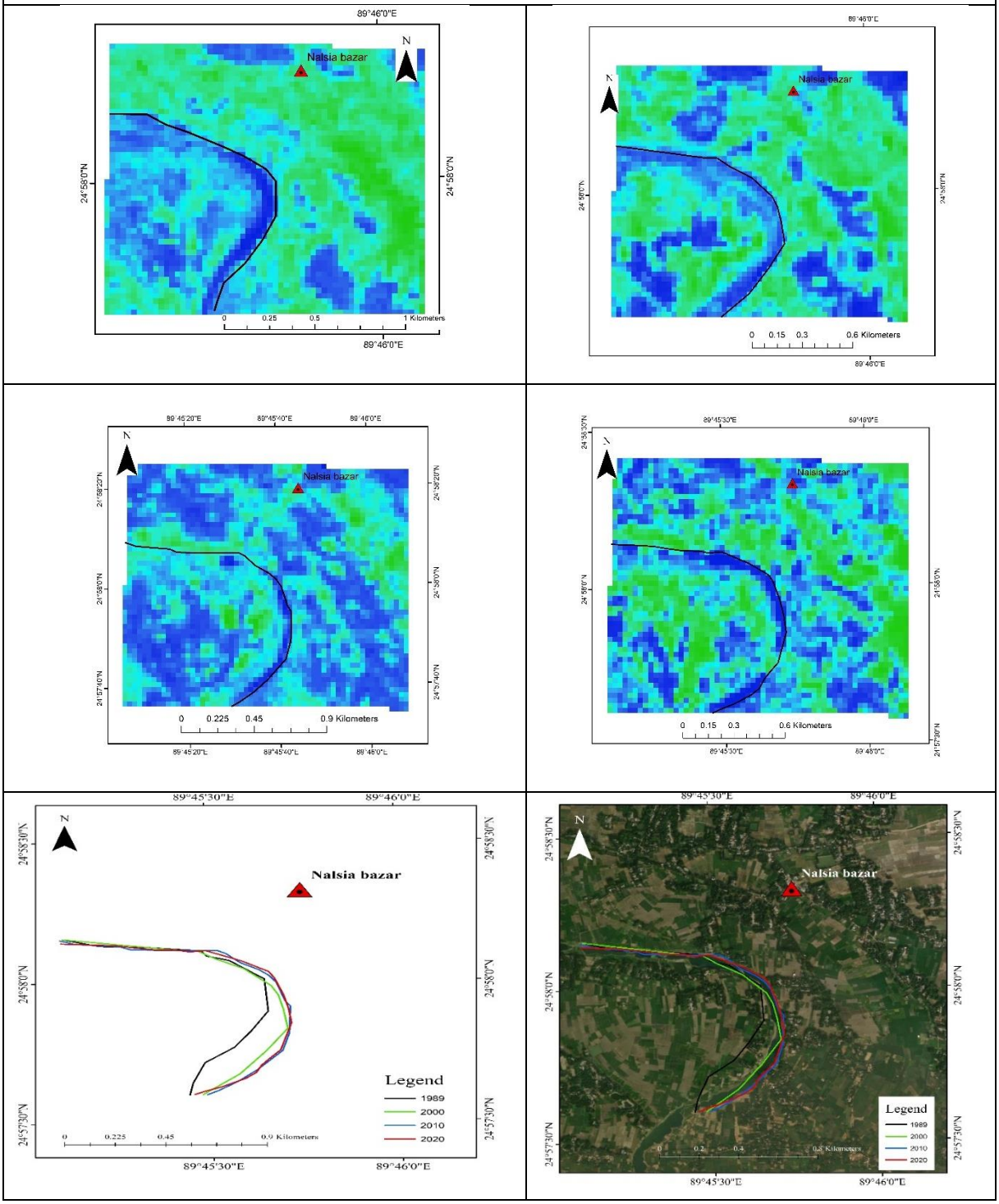

Market-45: Tulukpara Bazar in Melandaha Upzila of Jamalpur District

- Flood Risk: The market is located in a **Moderate** flood risk area, considering the inundation patterns of all major floods in recent times.
- Bank Erosion Risk: Based on planform analysis using historical satellite images, the Market is located in the **Moderate** bank erosion risk area.

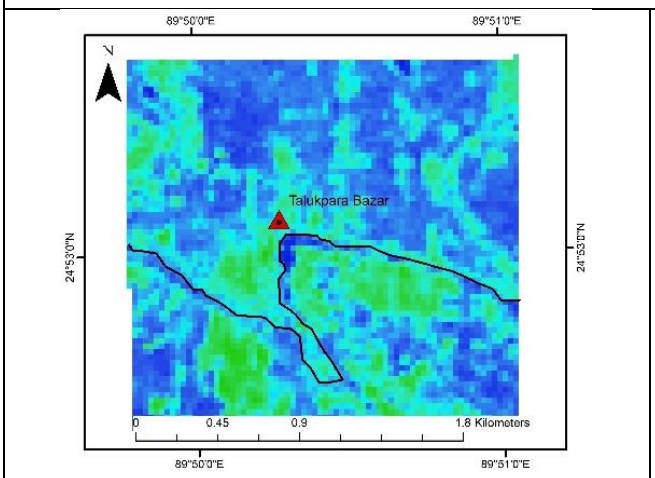

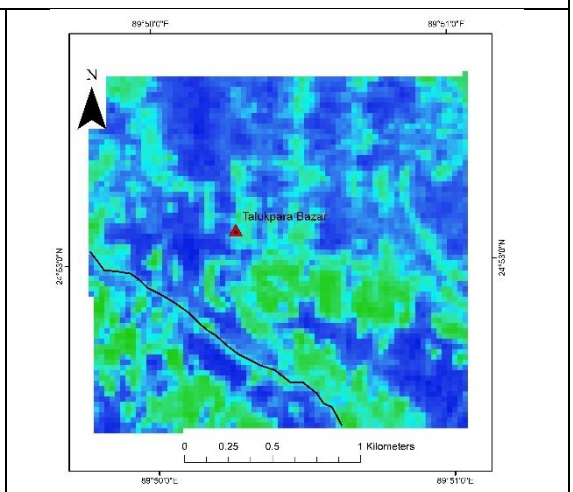

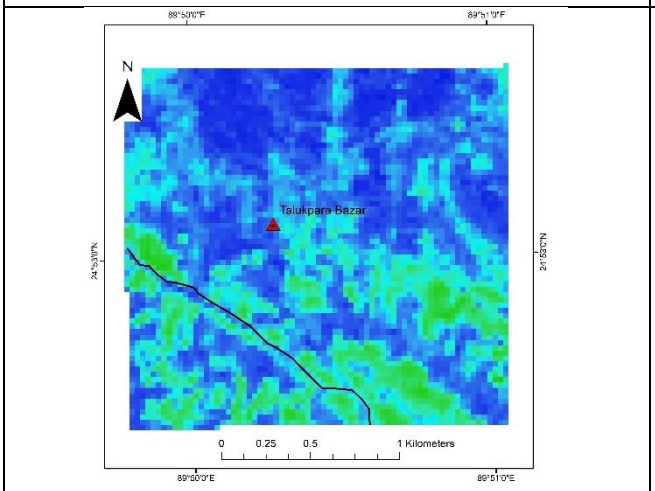

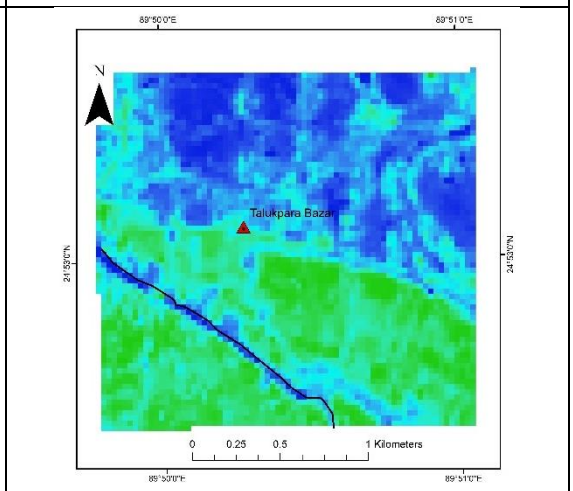

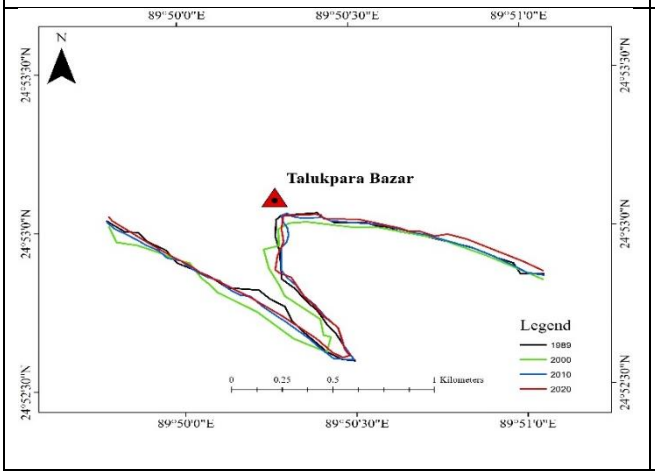

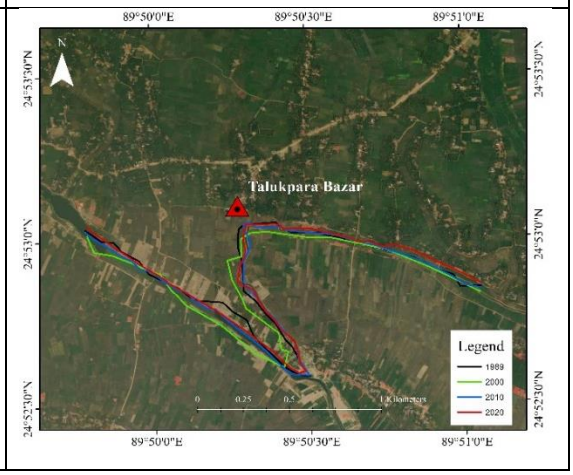

Market-46: Tegharia Bazar in Melandaha Upzila of Jamalpur District

- Flood Risk: The market is located in a **Low** flood-risk area, considering the inundation patterns of all major floods in recent times.
- Bank Erosion Risk: Based on planform analysis using historical satellite images, the Market is located in the **Low** bank erosion risk area.

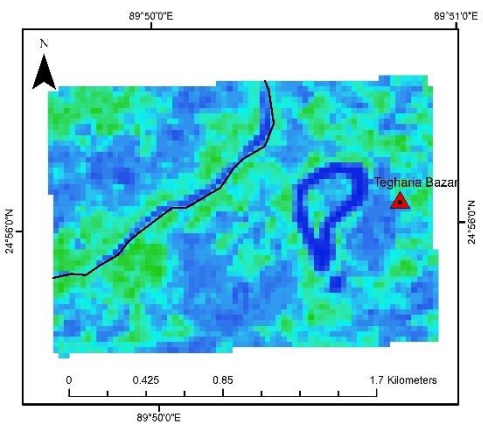

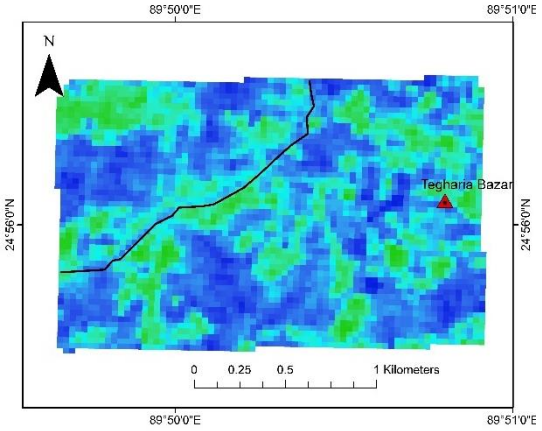

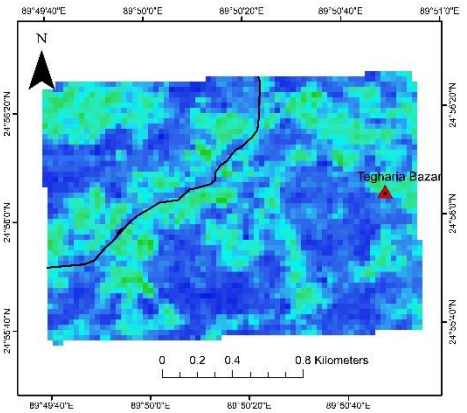

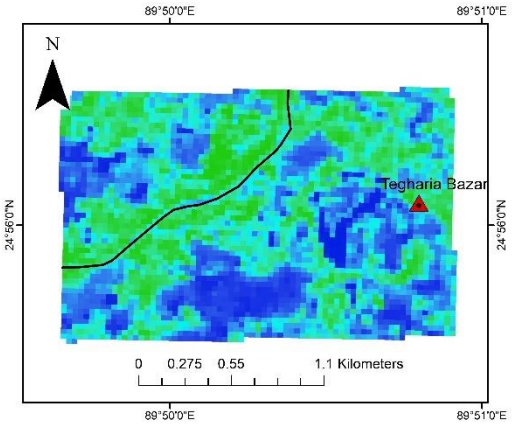

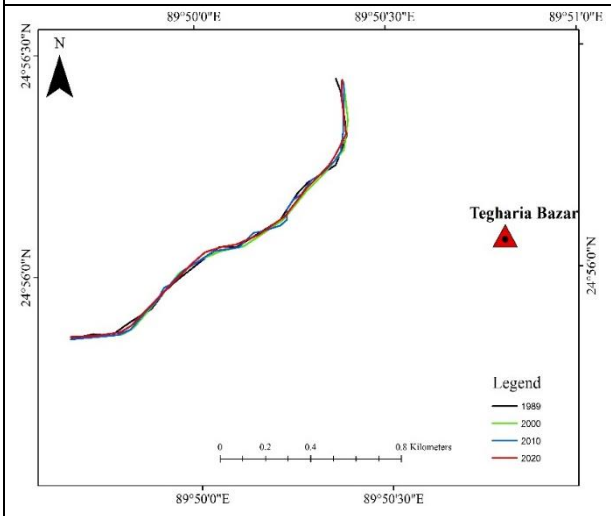

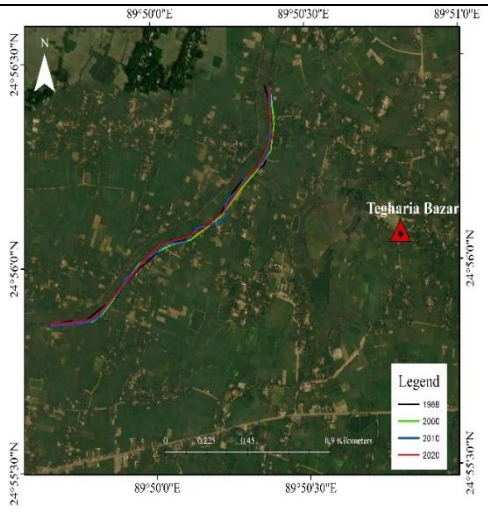

Market-47: Duttapara Ananda Bazar in Bakshiganj Upazila of Jamalpur District

- Flood Risk: The market is located in a **Low** flood-risk area, considering the inundation patterns of all major floods in recent times.
- Bank Erosion Risk: Based on planform analysis using historical satellite images, the market is located in the **Low** bank erosion risk area

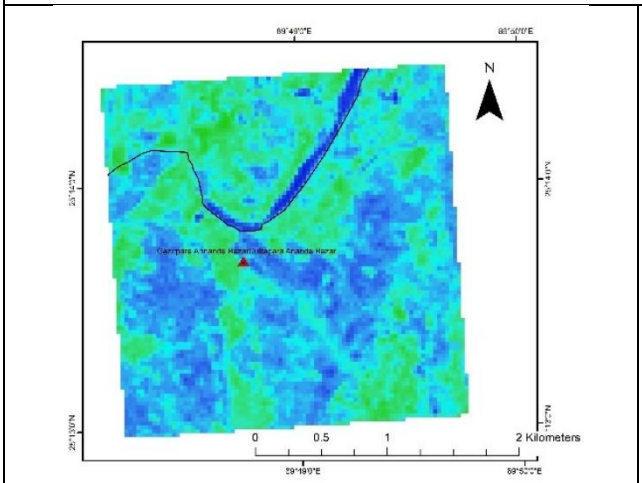

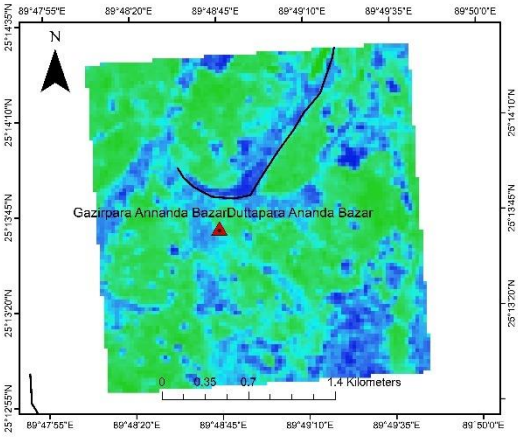

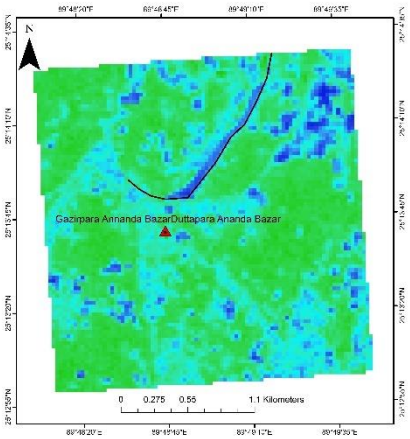

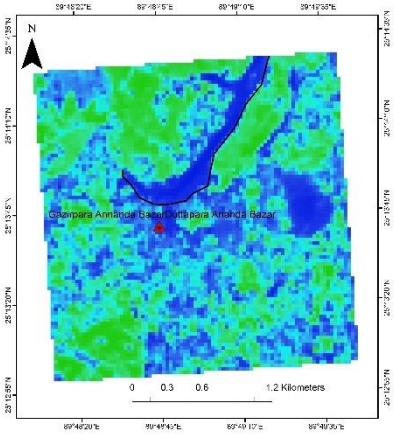

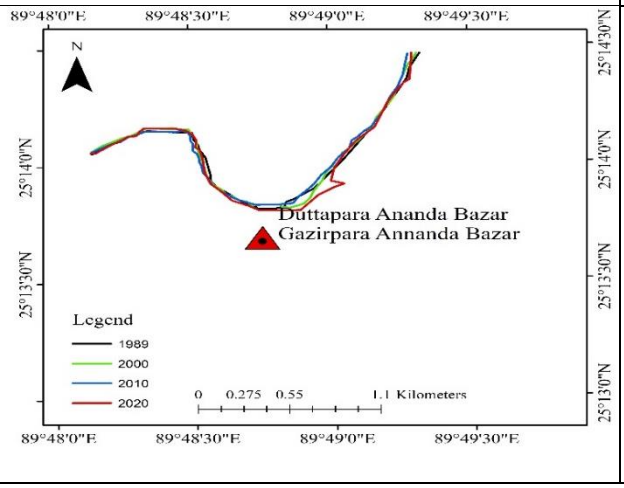

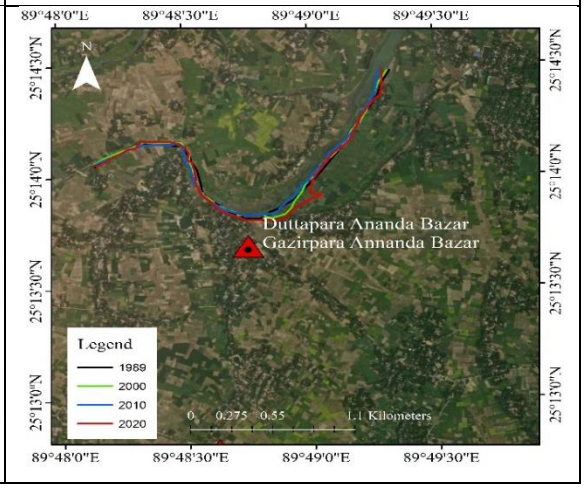

Market-48: Parchim Kamalerbatti Bazar in Bakshiganj Upzila of Jamalpur District

- Flood Risk: The market is located in a **Low** flood-risk area, considering the inundation patterns of all major floods in recent times. However, the surrounding area is at low flood risk.
- Bank Erosion Risk: Based on planform analysis using historical satellite images, the Market is located in the **Low** bank erosion risk area.

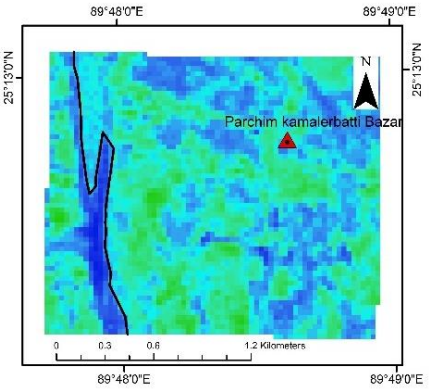

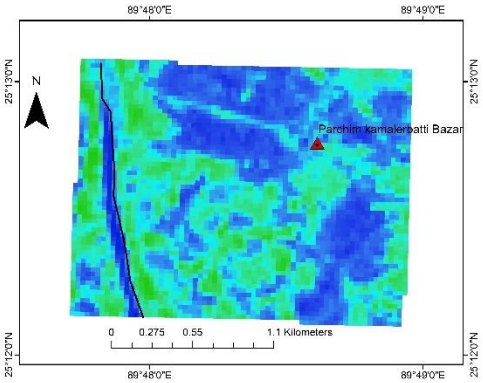

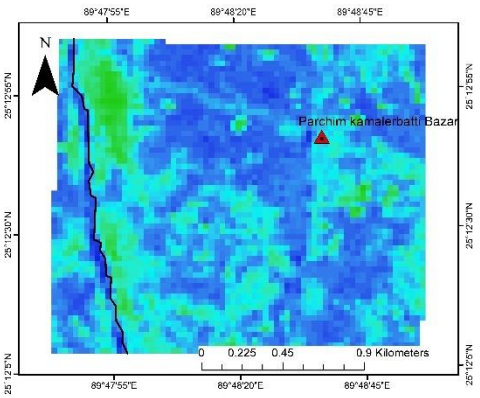

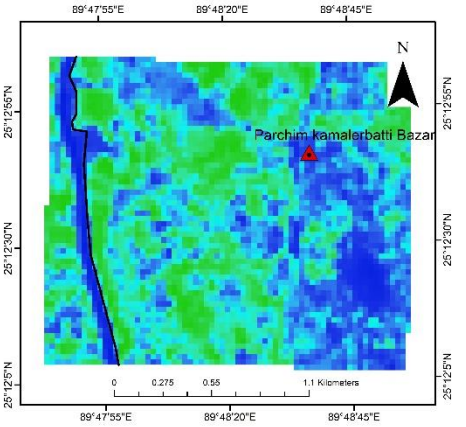

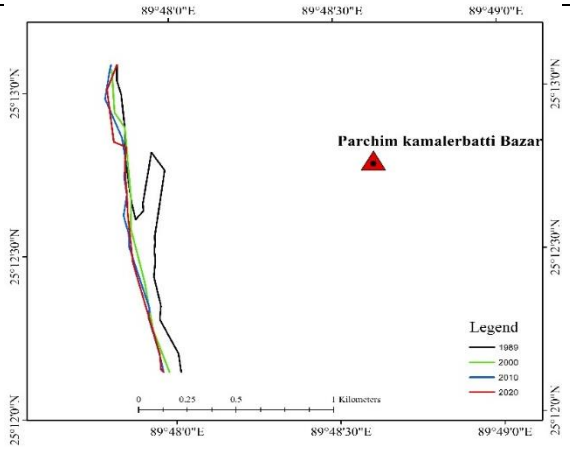

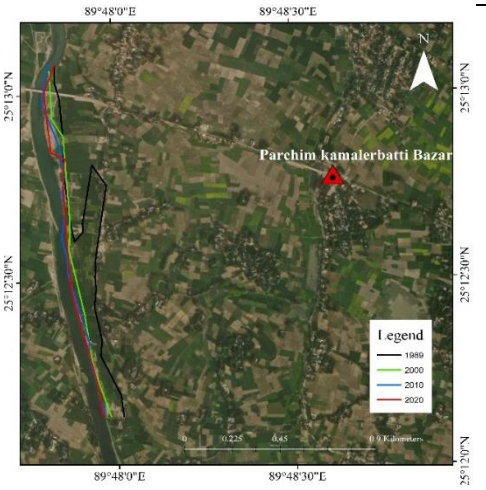

Market-49: Saguna Bazar in Melandaha Upzila of Jamalpur District

- Flood Risk: The market is located in a **Low** flood-risk area, considering the inundation patterns of all major floods in recent times.
- Bank Erosion Risk: Based on planform analysis using historical satellite images, the Market is located in the **Low** bank erosion risk area.

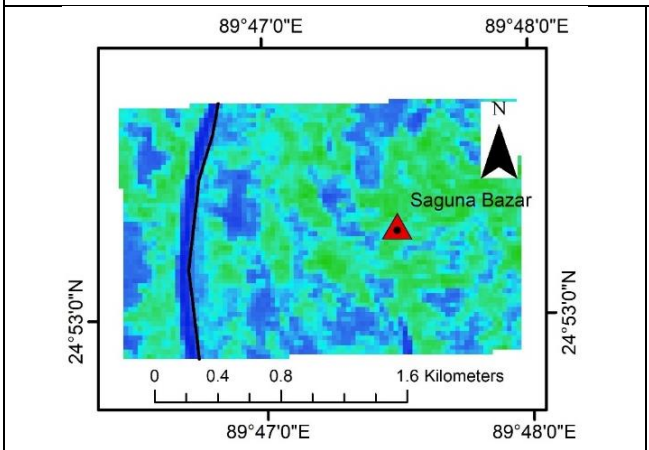

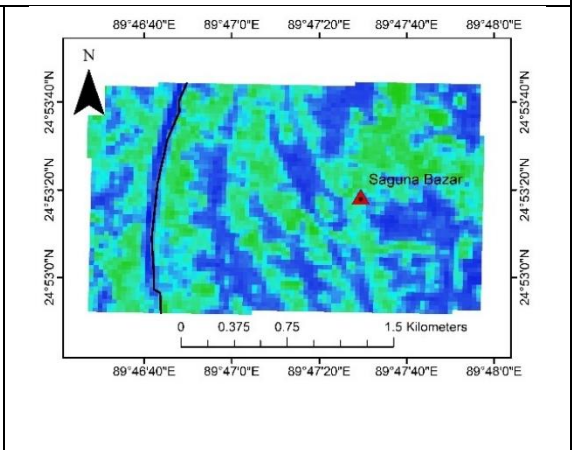

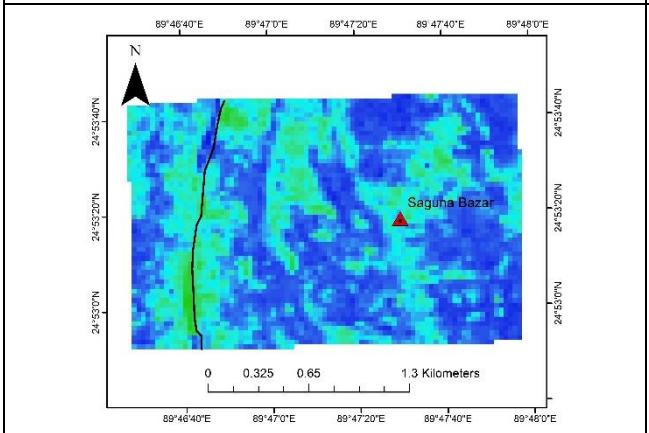

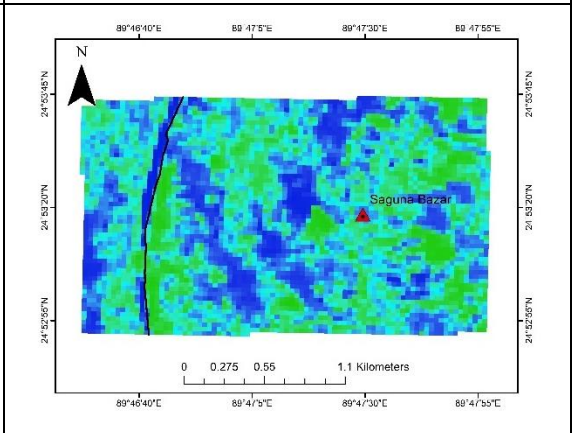

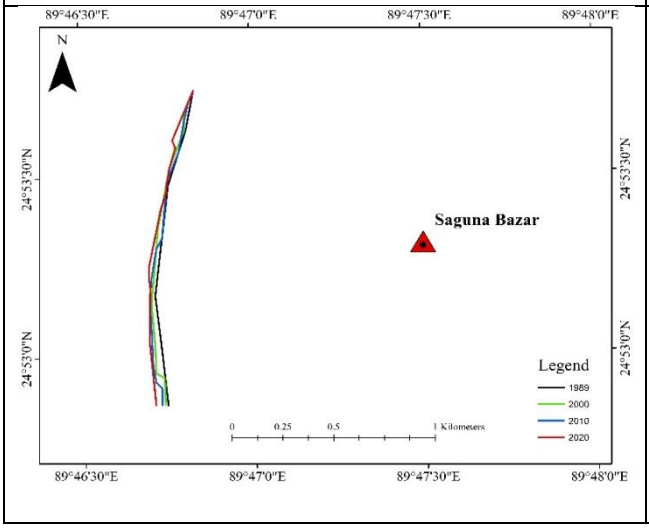

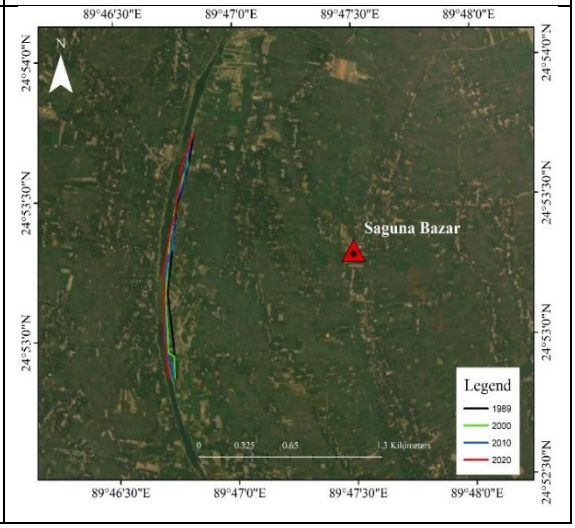

Market-50: Dighir Hat in Hatibandha Upazila of Lalmonirhat District

- Flood Risk: The market is located in a **Low** flood-risk area, considering the inundation patterns of all major floods in recent times.
- Bank Erosion Risk: Based on planform analysis using historical satellite images, the market is located in the **Low** bank erosion risk area.

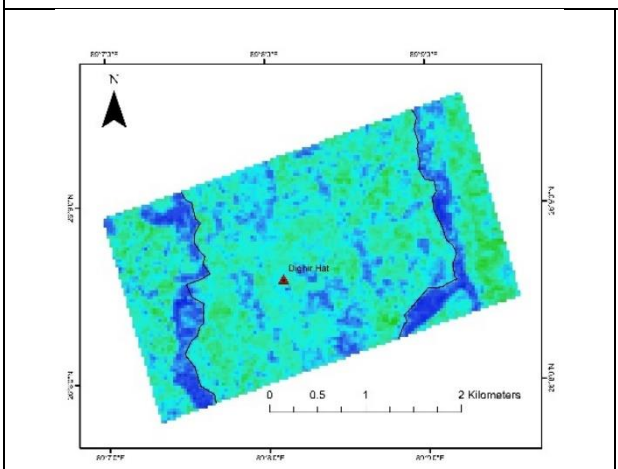

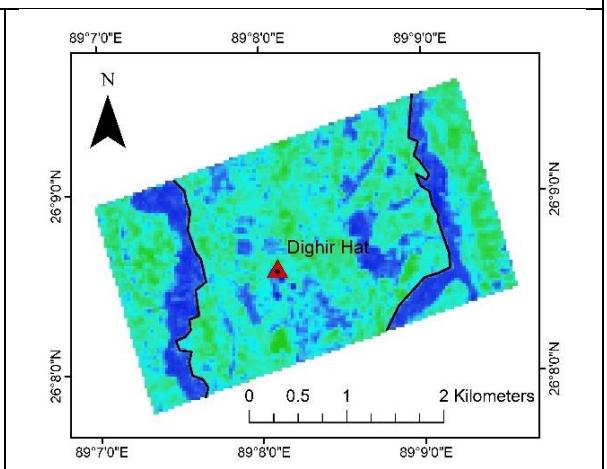

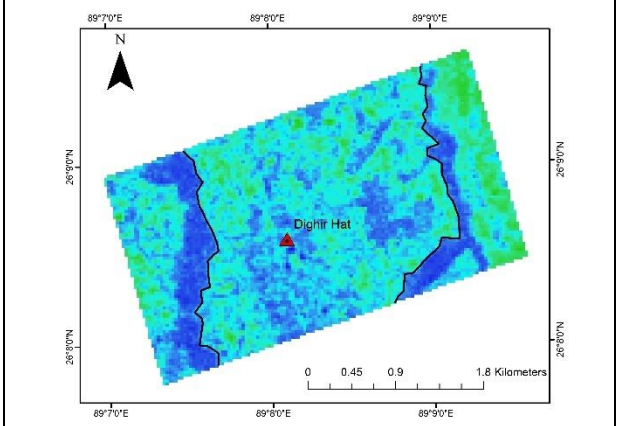

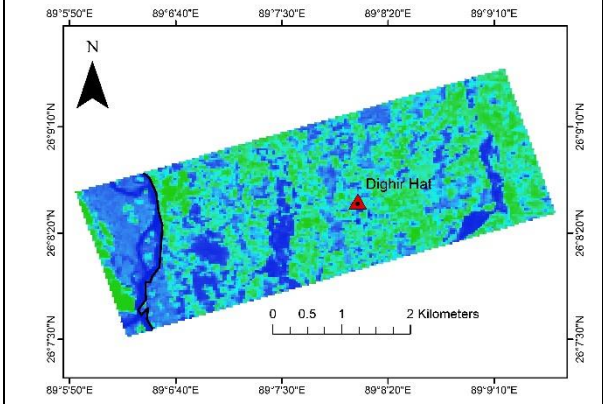

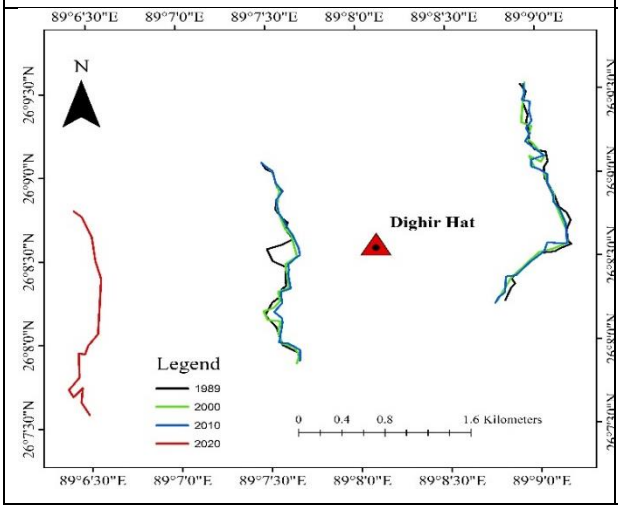

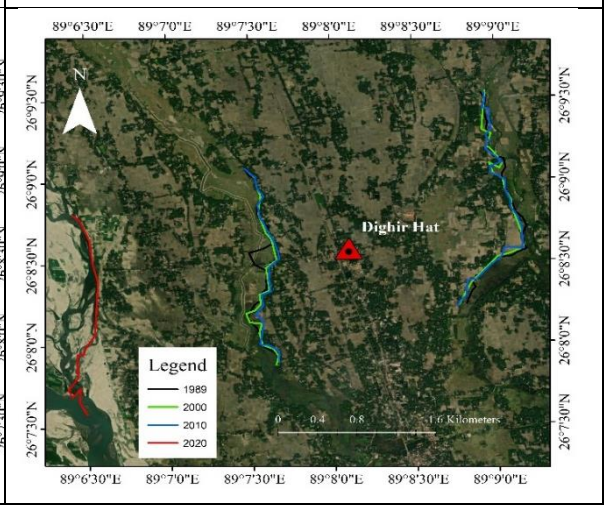

Market-51: Chander Hat in Hatibandha Upzila of Lalmonirhat District

- Flood Risk: The market is located in a **Low** flood-risk area, considering the inundation patterns of all major floods in recent times.
- Bank Erosion Risk: Based on planform analysis using historical satellite images, the market is located in the **Low** bank erosion risk area.

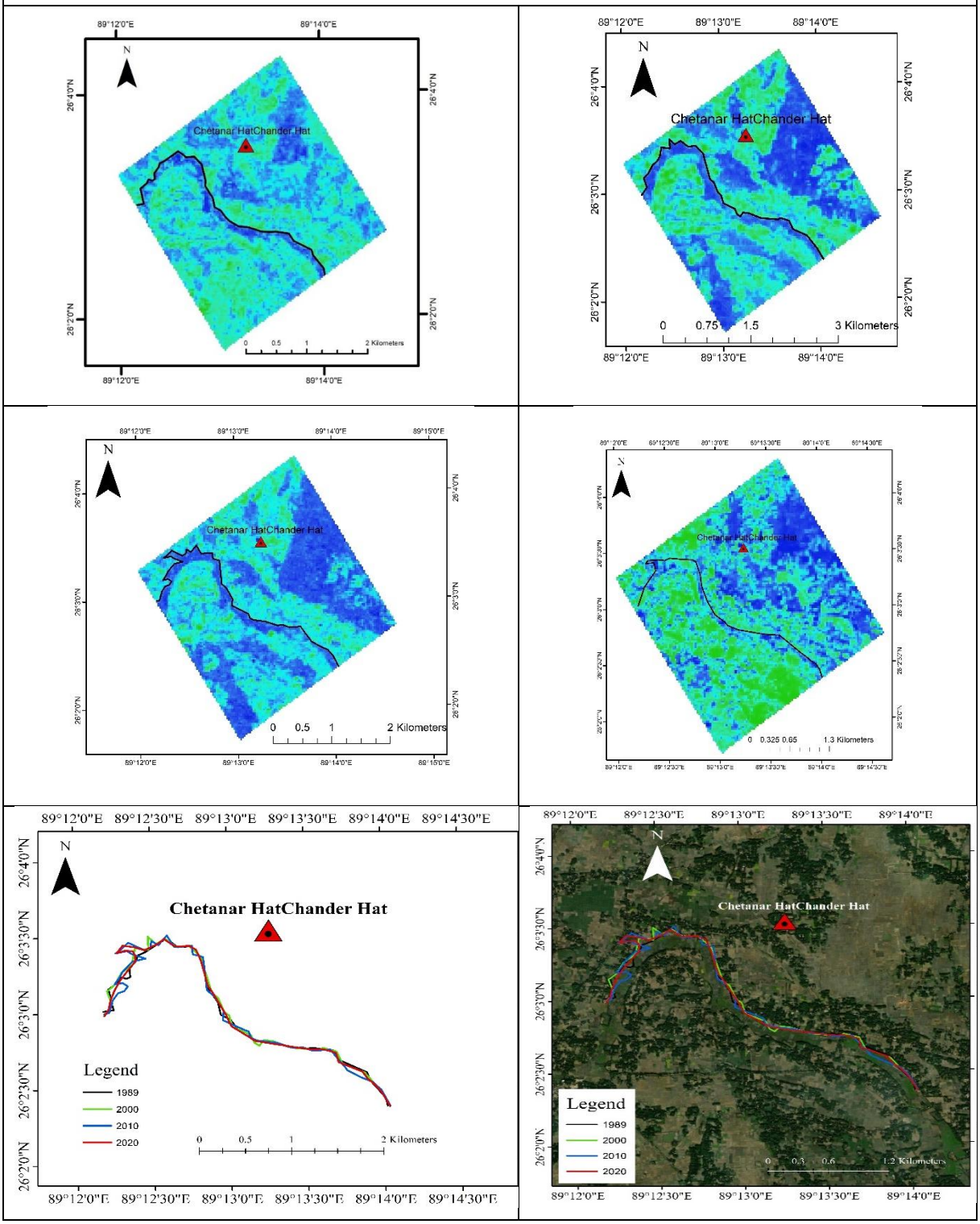

Market-52: Muktijoddha Hat in Hatibandha Upzila of Lalmonirhat District

- Flood Risk: The market is located in a **Low** flood-risk area, considering the inundation patterns of all major floods in recent times. However, the surrounding area is at low flood risk.
- Bank Erosion Risk: Based on planform analysis using historical satellite images, the Market is located in the **Low** bank erosion risk area.

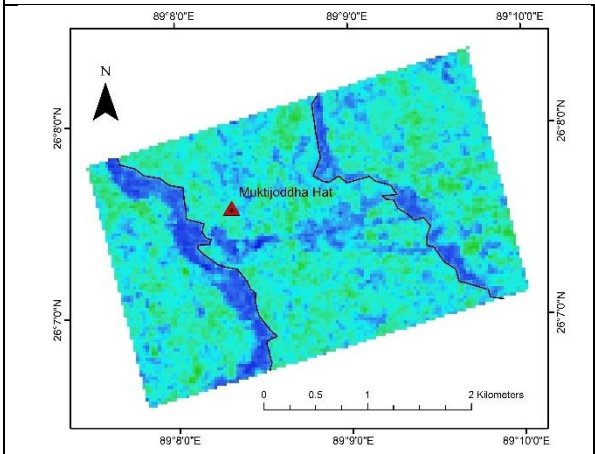

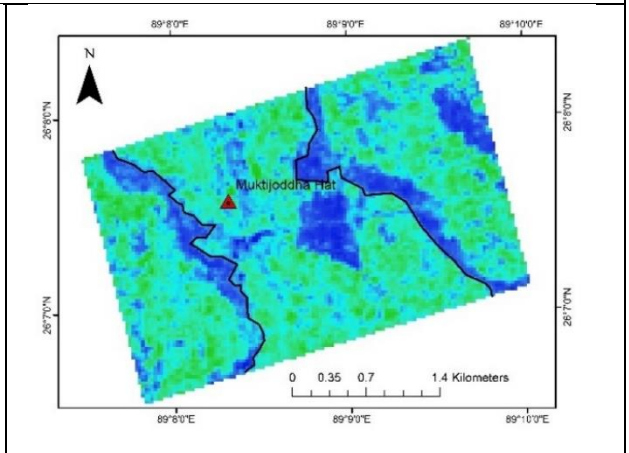

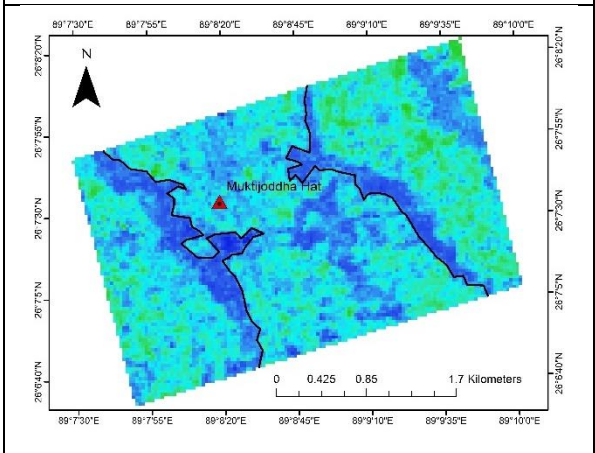

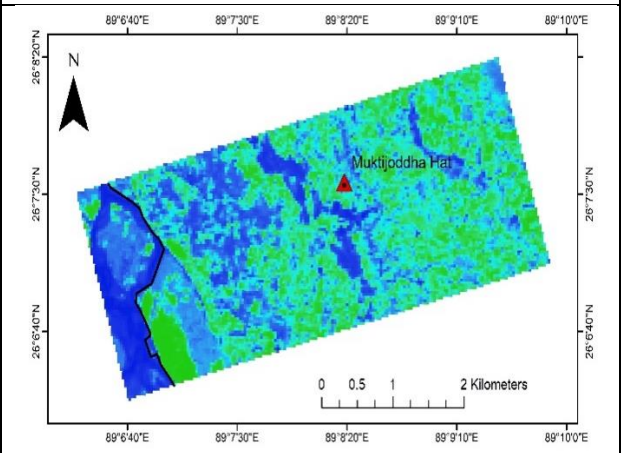

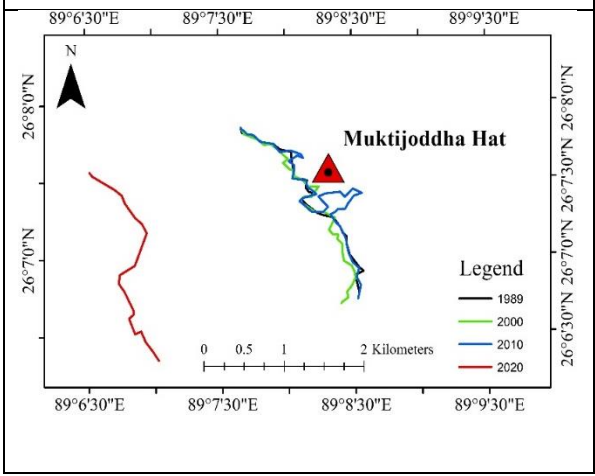

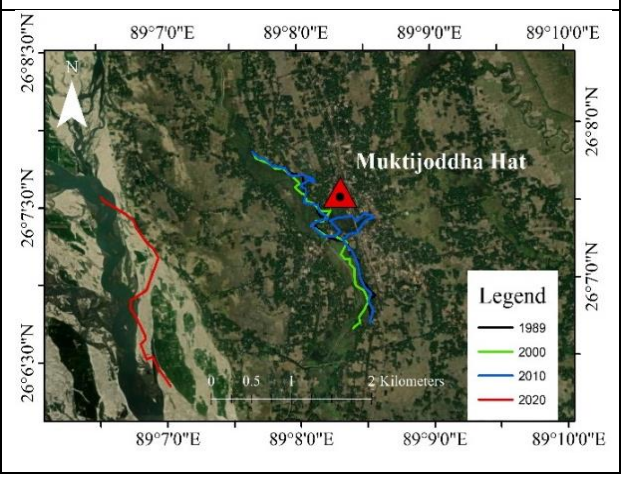

Market-53: Nowdabash Hat in Hatibandha Upazila of Lalmonirhat District

- Flood Risk: The market is located in a **Low** flood-risk area, considering the inundation patterns of all major floods in recent times.
- Bank Erosion Risk: Due to satellite image limitation, the river bank erosion risk cannot be assessed **(N/A)**.

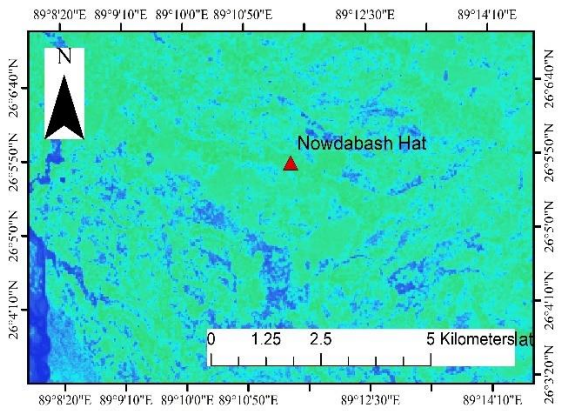

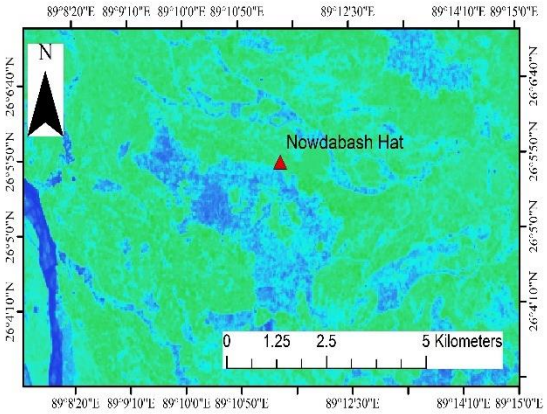

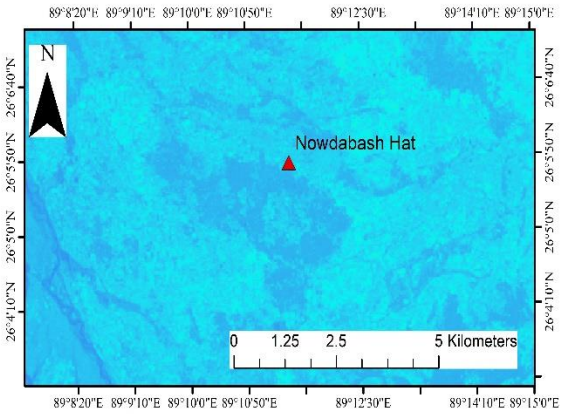

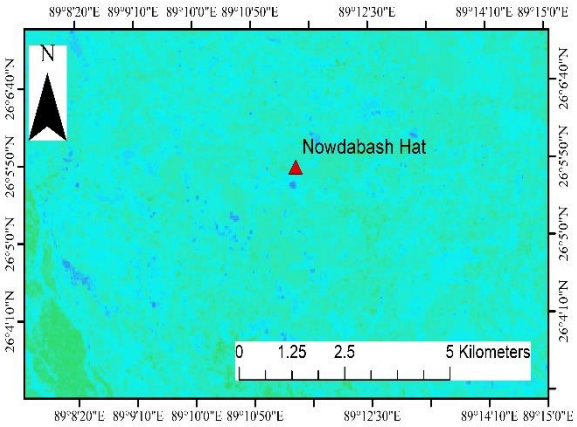

It is not possible to detect changes in bank lines due to inadequate resolution of satellite image

It is not possible to detect changes in bank lines due to inadequate resolution of satellite image

Market-54: Burimari Hat in Patgram Upazila of Lalmonirhat District

- Flood Risk: The market is located in a **Low** flood-risk area, considering the inundation patterns of all major floods in recent times.
- Bank Erosion Risk: Based on planform analysis using historical satellite images, the market is located in the **Moderate** bank erosion risk area

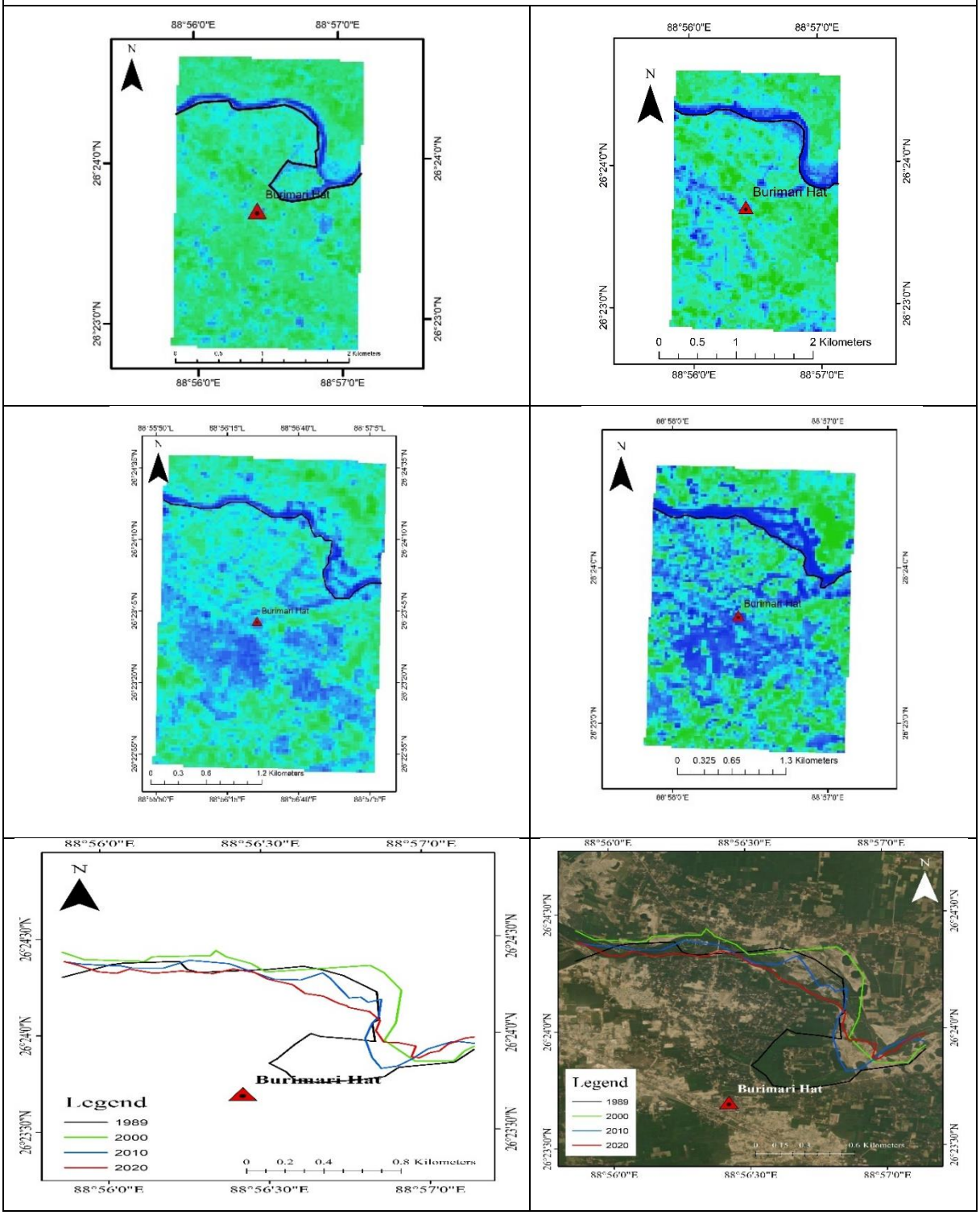

Market-55: Kamara Hat in Patgram Upzila of Lalmonirhat District

- Flood Risk: The market is located in a **Low** flood-risk area, considering the inundation patterns of all major floods in recent times.
- Bank Erosion Risk: Based on planform analysis using historical satellite images, the market is located in the **Low** bank erosion risk area

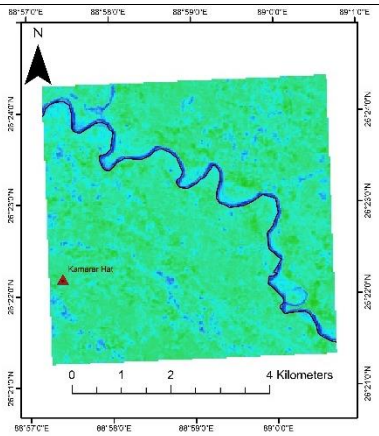

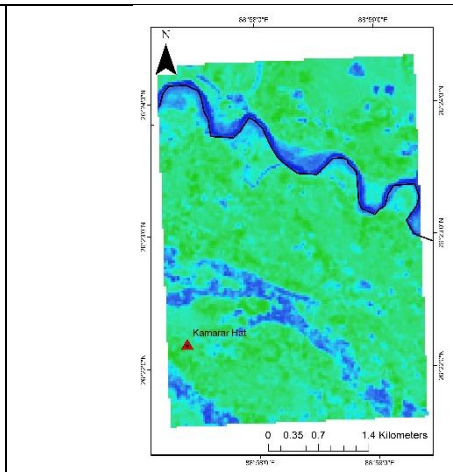

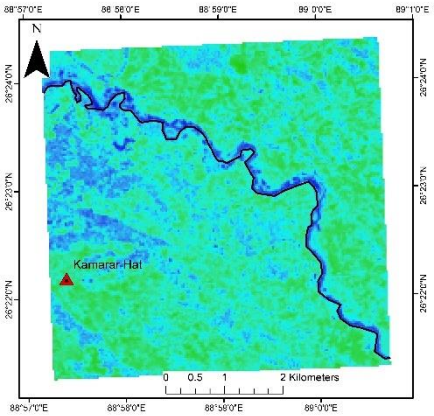

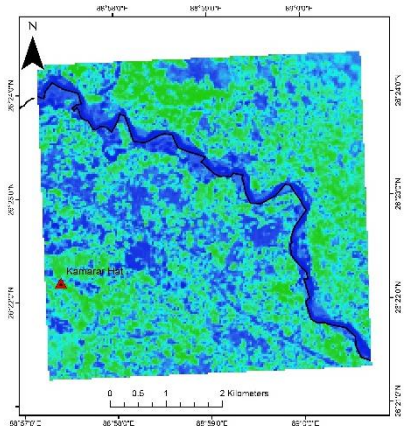

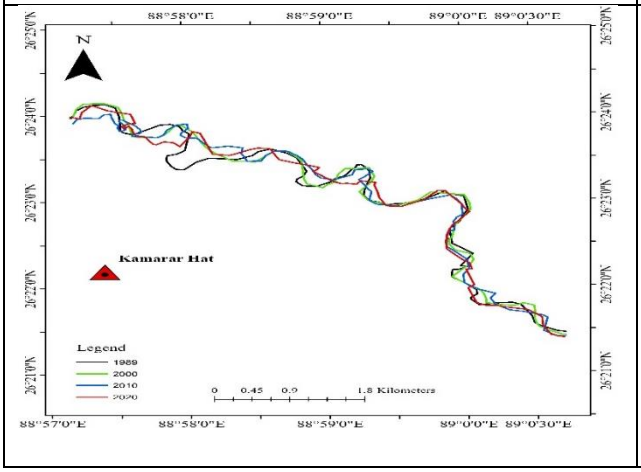

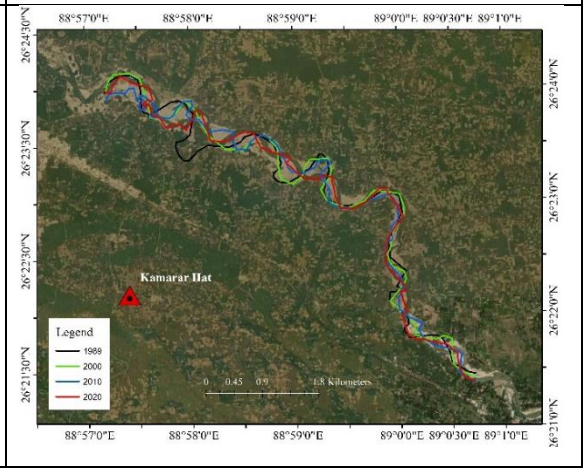

Market-56: Kashirdangga Hat in Patgram Upazila of Lalmonirhat District

- Flood Risk: The market is located in a **Low** flood-risk area, considering the inundation patterns of all major floods in recent times.
- Bank Erosion Risk: Based on planform analysis using historical satellite images, the market is located in the **Low** bank erosion risk area.

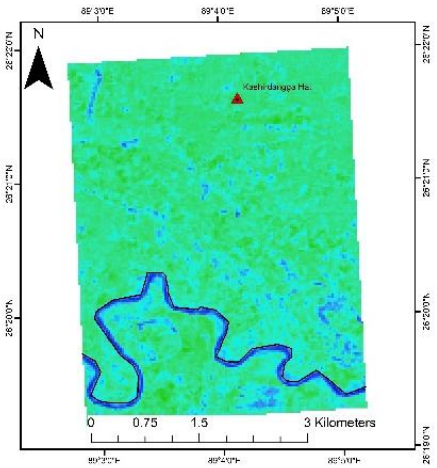

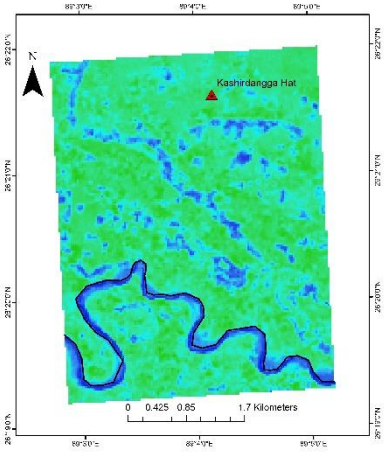

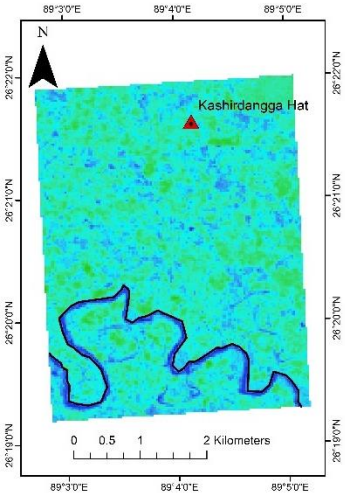

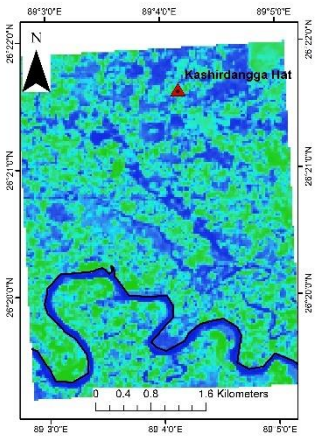

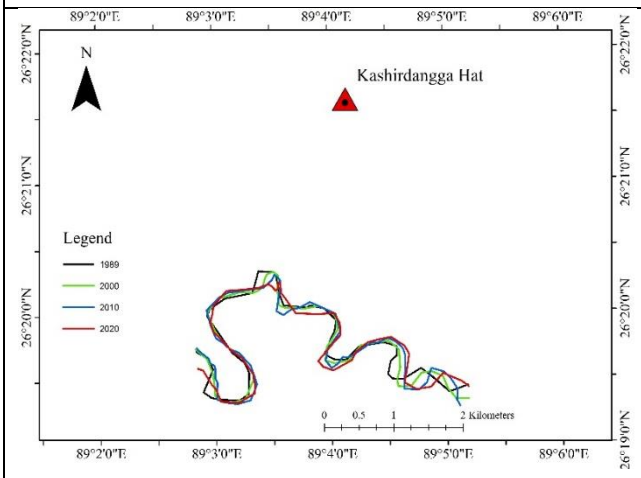

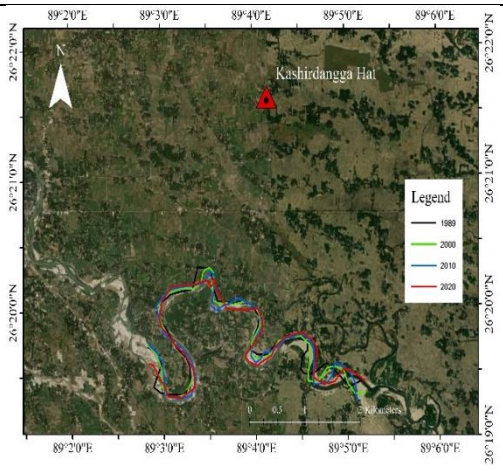

Market-57: Nayer Hat in Patgram Upzila of Lalmonirhat District

- Flood Risk: The market is located in a **Moderate** flood risk area, considering the inundation patterns of all major floods in recent times.
- Bank Erosion Risk: Based on planform analysis using historical satellite images, the Market is located in the **High** bank erosion risk area.

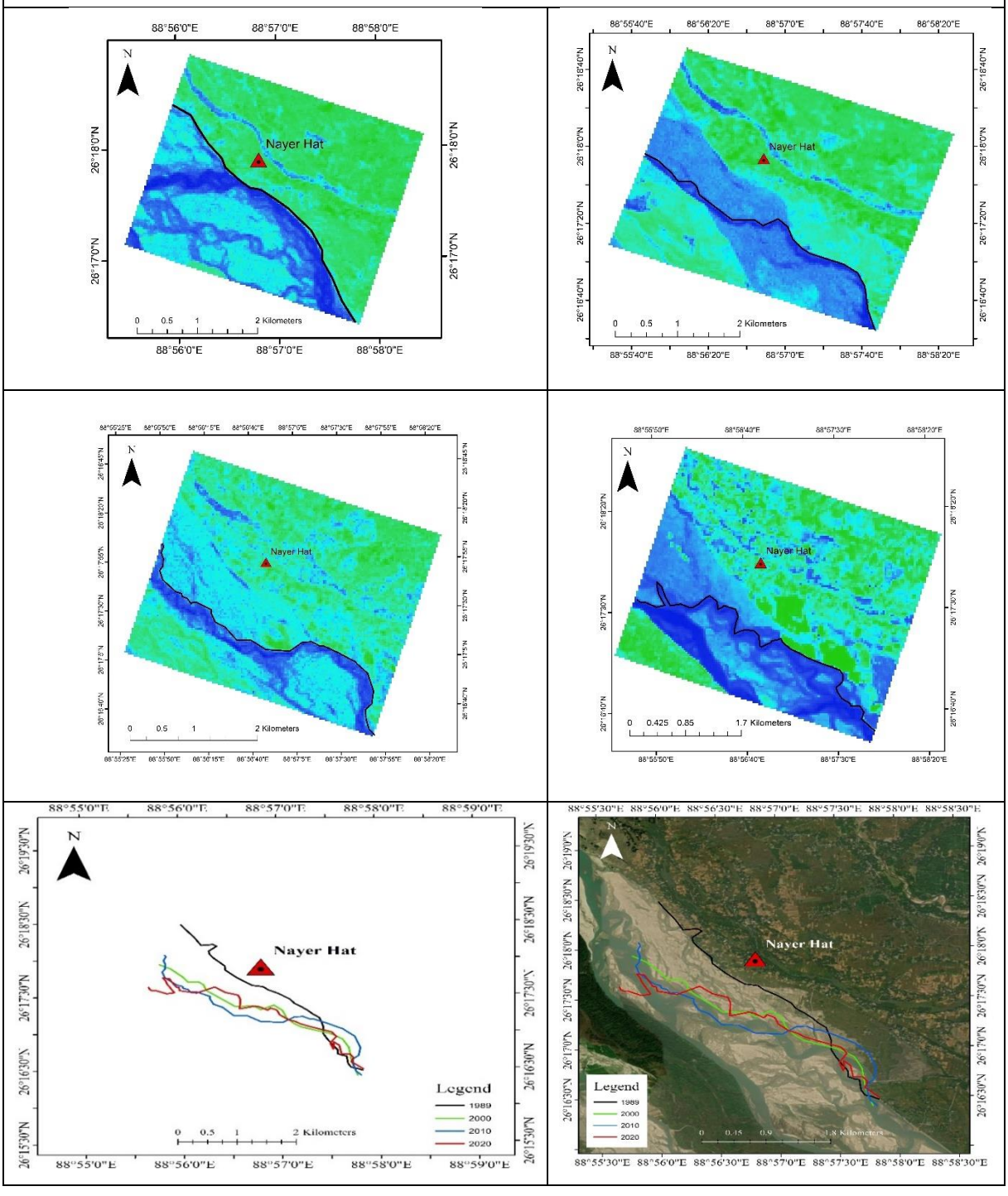

Market-58: Shofinagar Hat in Patgram Upazila of Lalmonirhat District

- Flood Risk: The market is located in a **Low** flood-risk area, considering the inundation patterns of all major floods in recent times.
- Bank Erosion Risk: Based on planform analysis using historical satellite images, the Market is located in the **Low** bank erosion risk area.

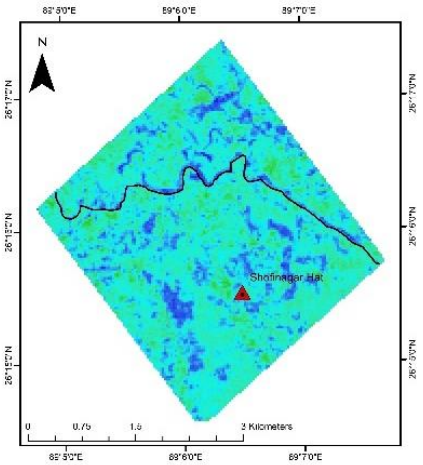

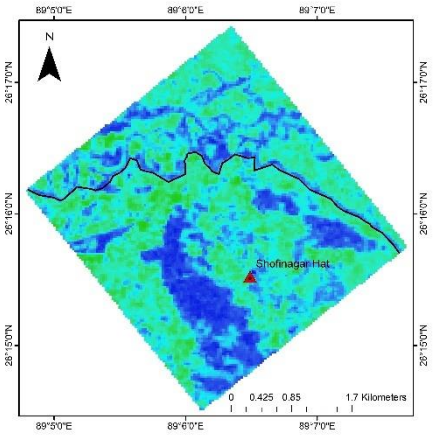

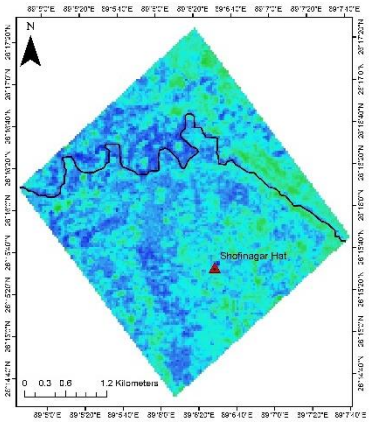

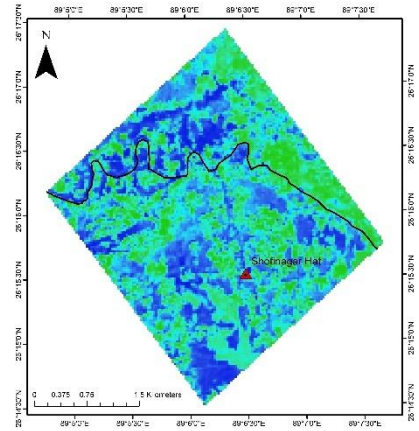

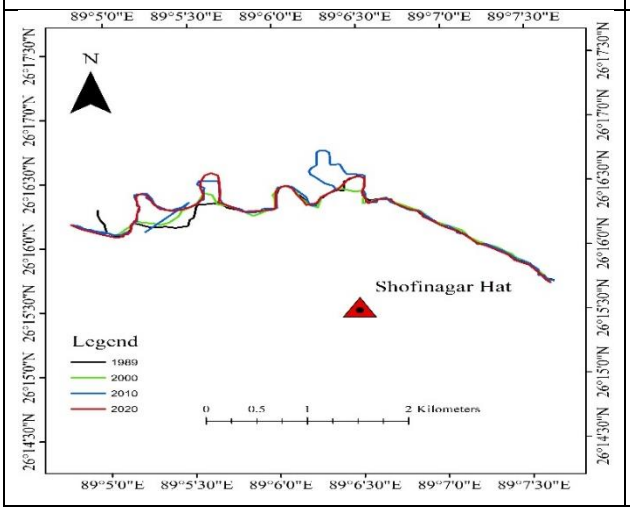

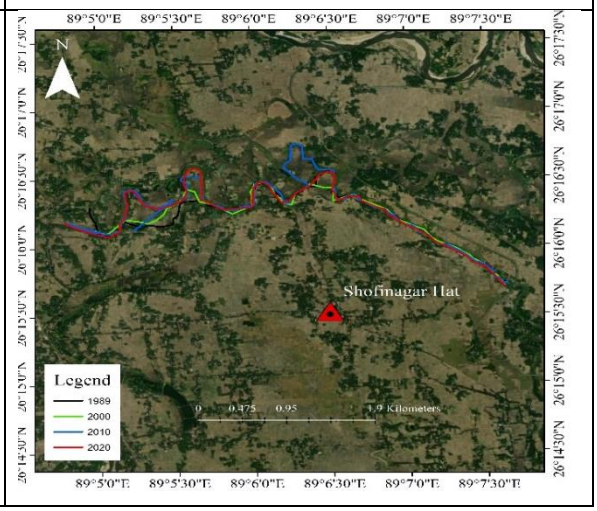

Market-59: Sharkaar Hat in Patgram Upzila of Lalmonirhat District

- Flood Risk: The market is located in a **Low** flood-risk area, considering the inundation patterns of all major floods in recent times.
- Bank Erosion Risk: Based on planform analysis using historical satellite images, the Market is located in the **Low** bank erosion risk area.

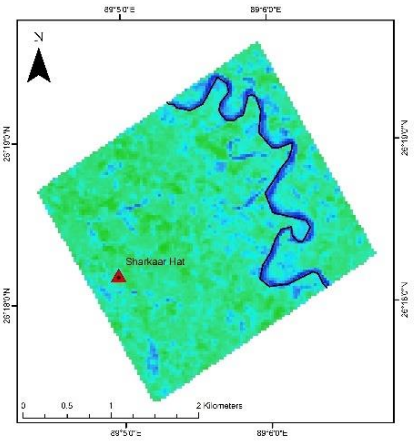

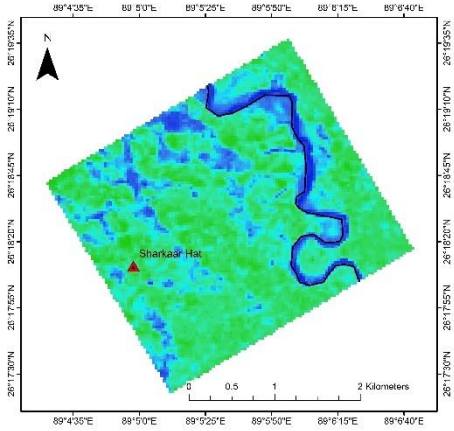

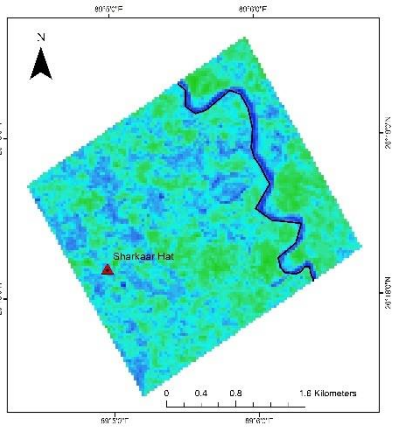

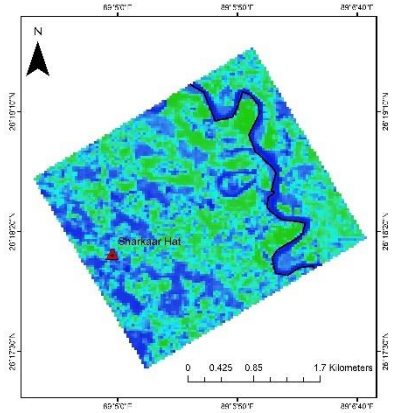

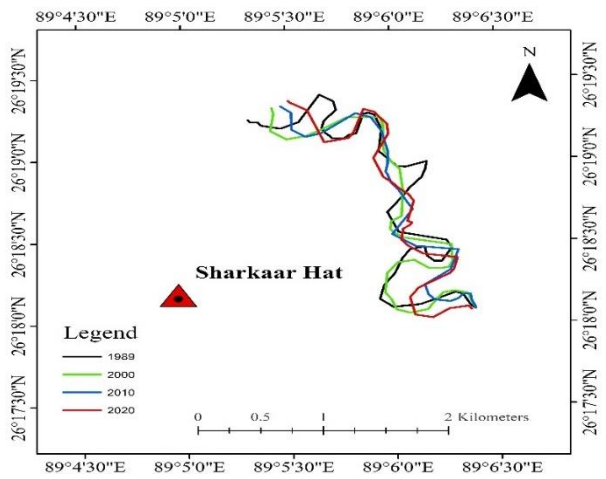

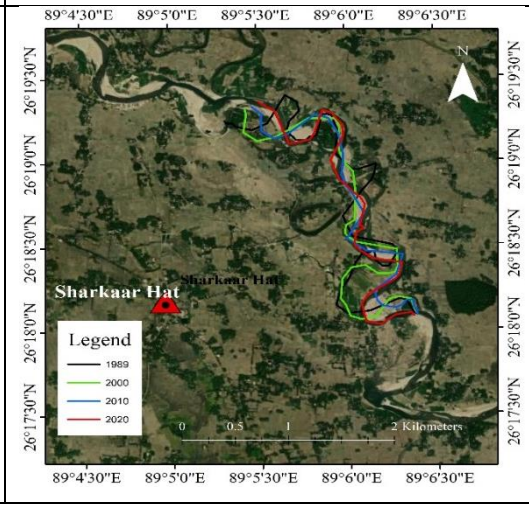

Market-60: Loliter Hat in Patgram Upzila of Lalmonirhat District

- Flood Risk: The market is located in a **Low** flood-risk area, considering the inundation patterns of all major floods in recent times.
- Bank Erosion Risk: Based on planform analysis using historical satellite images, the market is located in the **Low** bank erosion risk area.

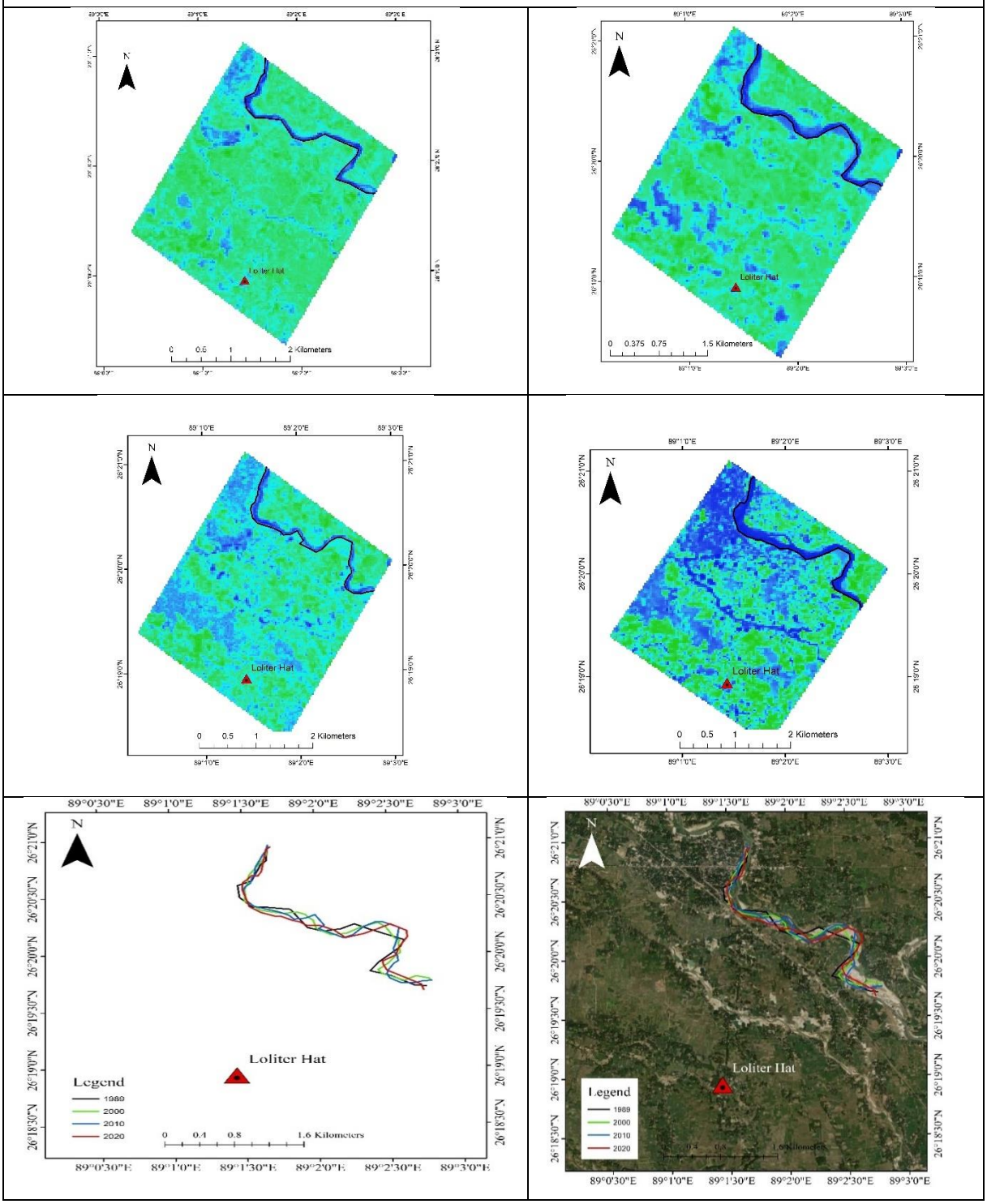

Market-61: Baldia Bazar in Bhurungamari Upzila of Kurigram District

- Flood Risk: The market is located in a **Low** flood-risk area, considering the inundation patterns of all major floods in recent times.
- Bank Erosion Risk: Based on planform analysis using historical satellite images, the market is located in the **Low** bank erosion risk area.

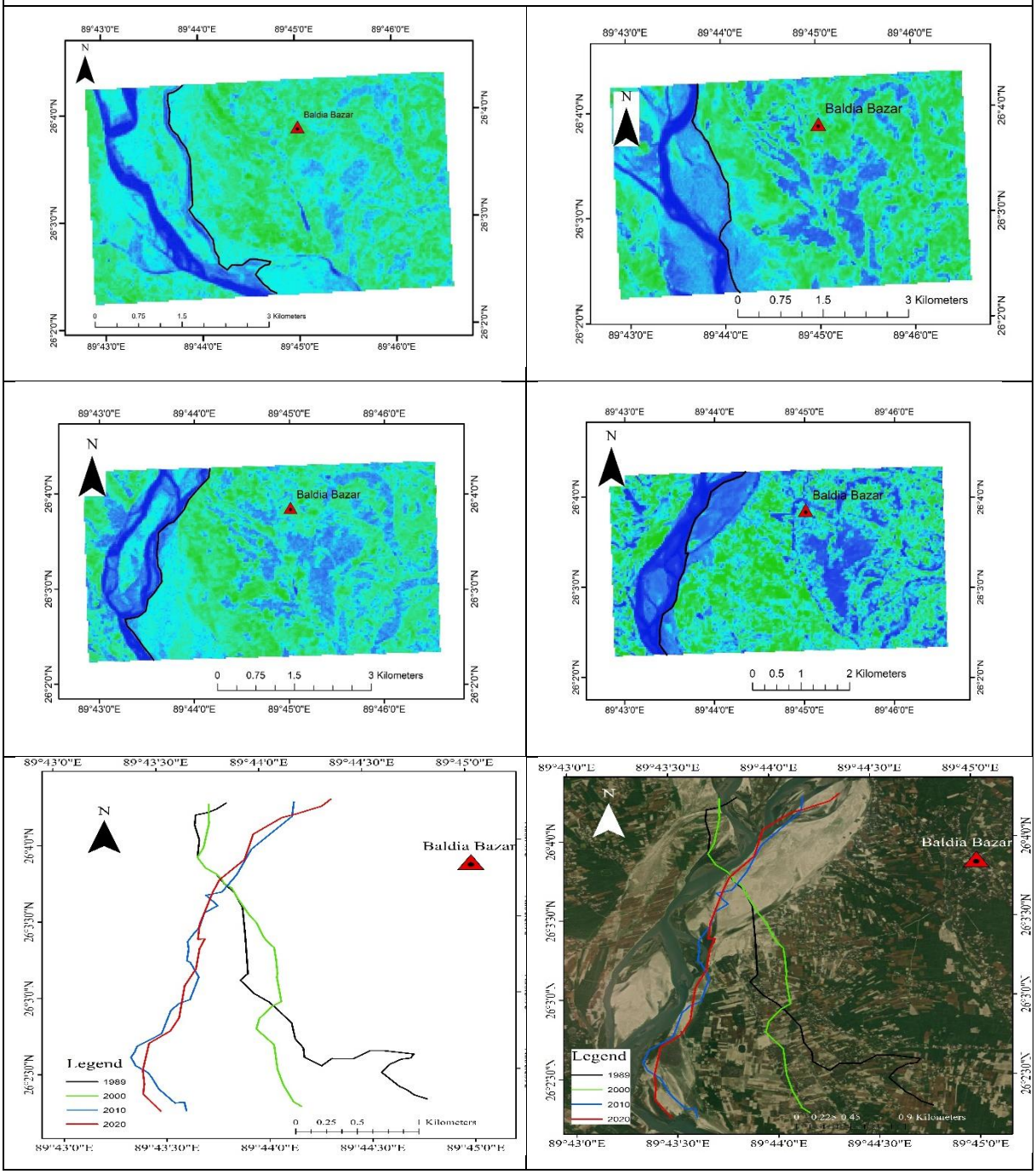

Market-62: Muktijoddha Hat in Bhurungamari Upzila of Kurigram District

- Flood Risk: The market is located in a **Low** flood-risk area, considering the inundation patterns of all major floods in recent times.
- Bank Erosion Risk: Due to satellite image limitation, the river bank erosion risk cannot be assessed **(N/A).**

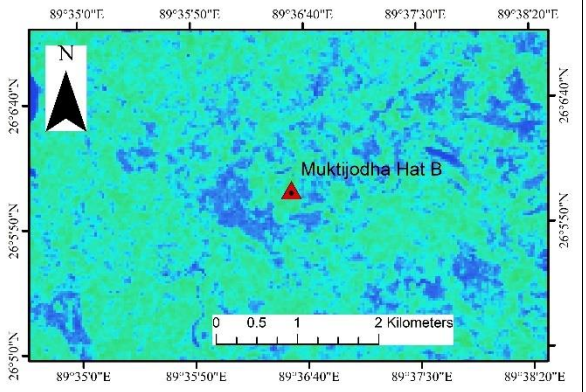

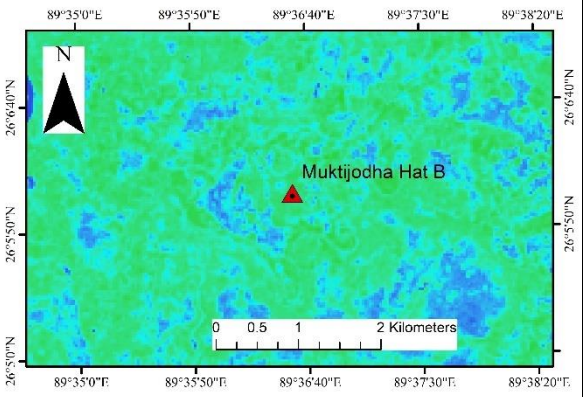

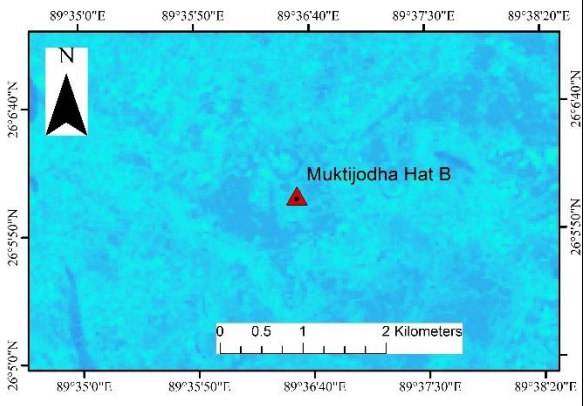

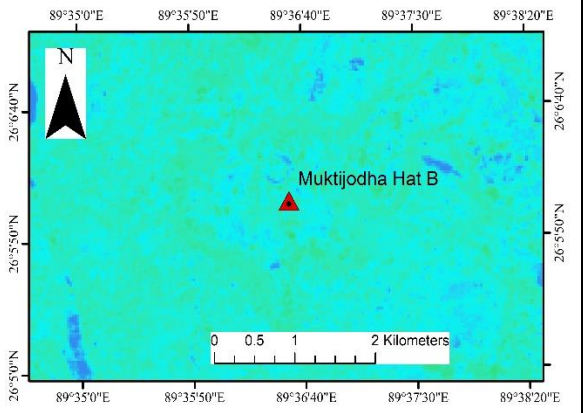

It is not possible to detect changes in bank lines due to inadequate resolution of satellite image

It is not possible to detect changes in bank lines due to inadequate resolution of satellite image

Market-63: Chowdhurir Hat in Bhurungamari Upazila of Kurigram District

- Flood Risk: The market is located in a **Low** flood-risk area, considering the inundation patterns of all major floods in recent times.
- Bank Erosion Risk: Based on planform analysis using historical satellite images, the market is located in the **Moderate** bank erosion risk area.

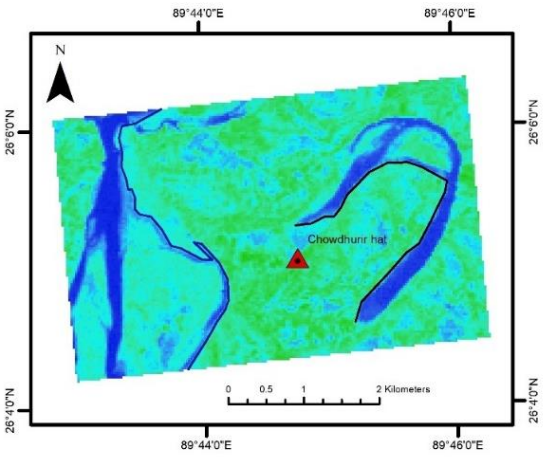

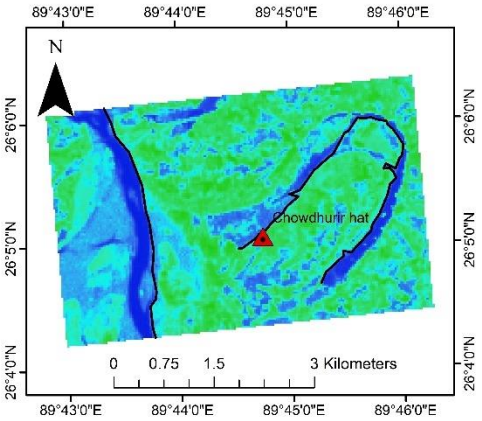

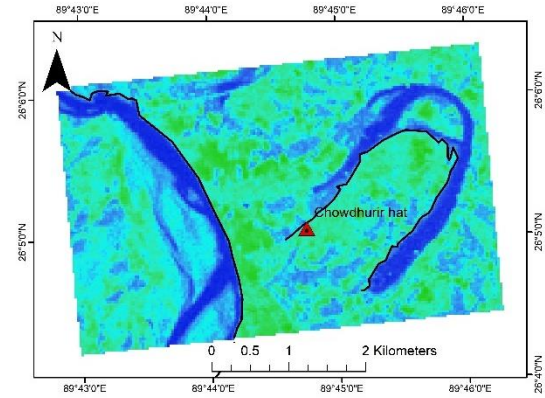

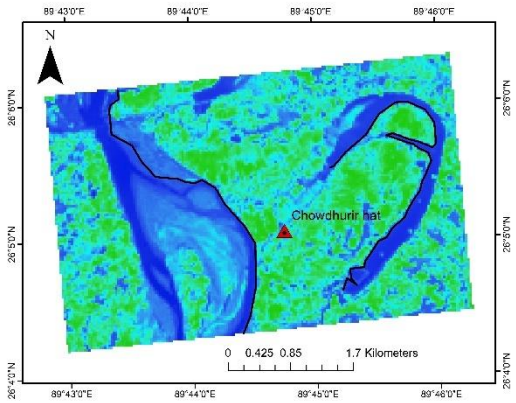

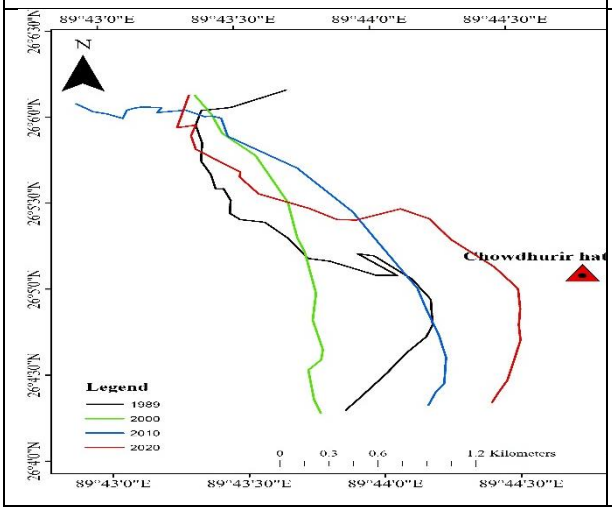

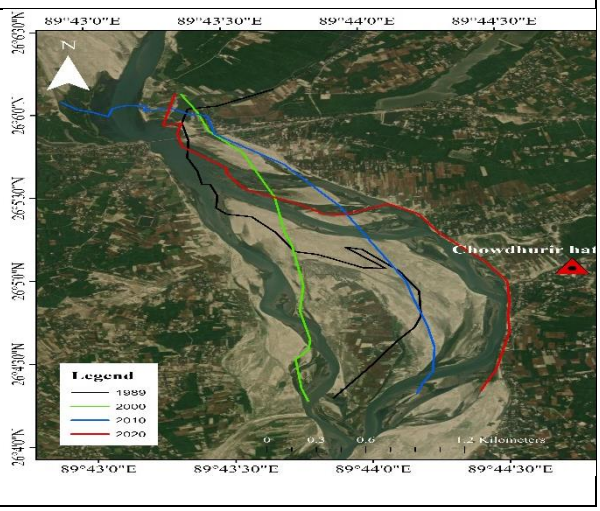

Market-64: Schooler hat in Nageshwari Upazila of Kurigram District

- Flood Risk: The market is located in a **Moderate** flood risk area, considering the inundation patterns of all major floods in recent times.
- Bank Erosion Risk: Due to satellite image limitation, the river bank erosion risk cannot be assessed **(N/A)**.

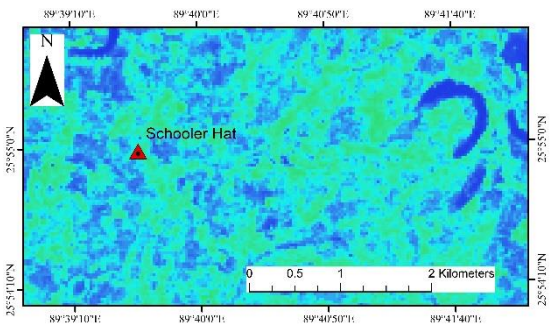

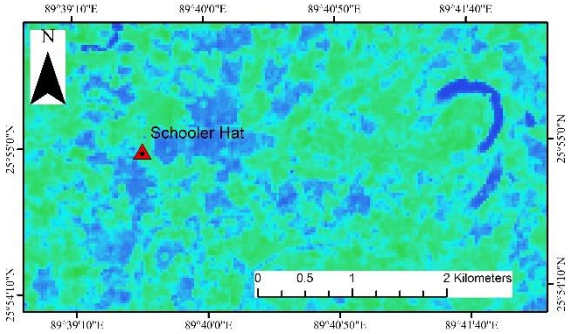

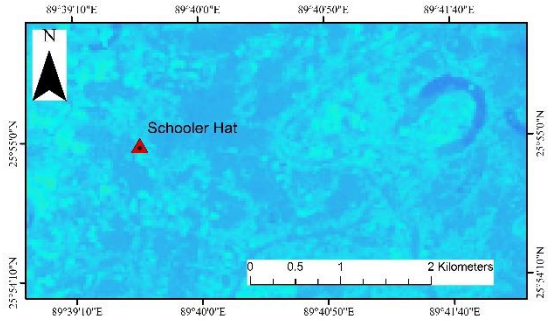

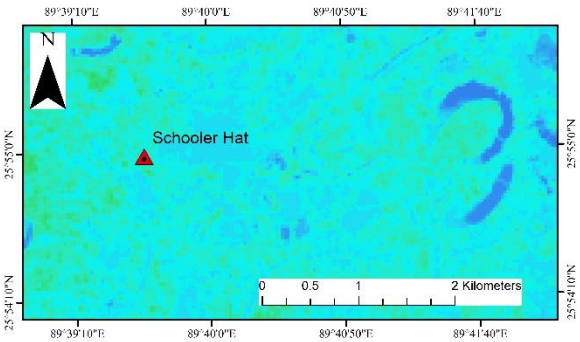

It is not possible to detect changes in bank lines due to inadequate resolution of satellite image

It is not possible to detect changes in bank lines due to inadequate resolution of satellite image

Market-65: Chilakhana Hat in Nageshwari Upazila of Kurigram District

- Flood Risk: The market is located in a **Moderate** flood risk area, considering the inundation patterns of all major floods in recent times.
- Bank Erosion Risk: Based on planform analysis using historical satellite images, the market is located in the **Low** bank erosion risk area.

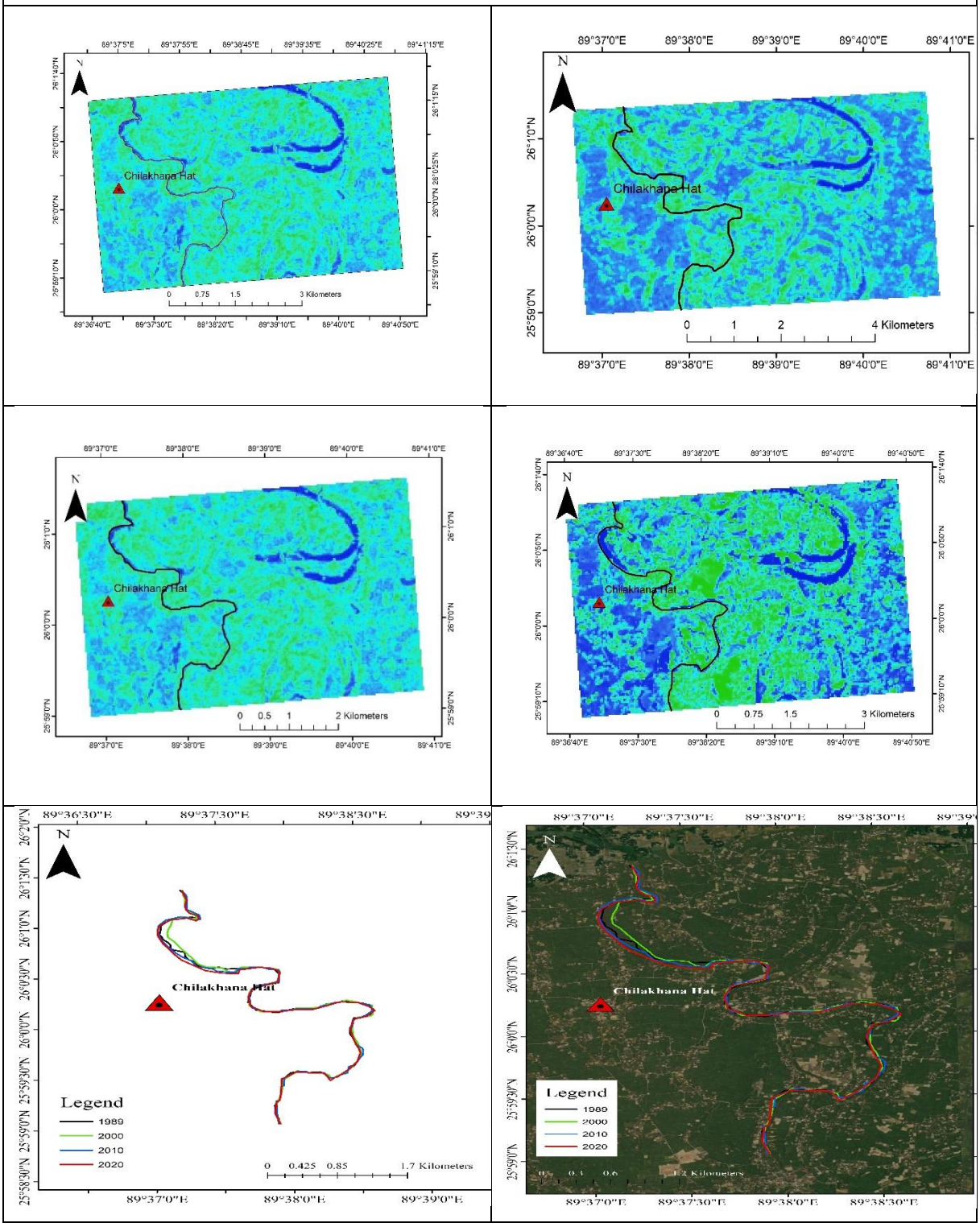

Market-66: Manigonj Bazar in Nageshwari Upazila of Kurigram District

- Flood Risk: The market is located in a **Low** flood-risk area, considering the inundation patterns of all major floods in recent times.
- Bank Erosion Risk: Based on planform analysis using historical satellite images, the market is located in the **Low** bank erosion risk area.

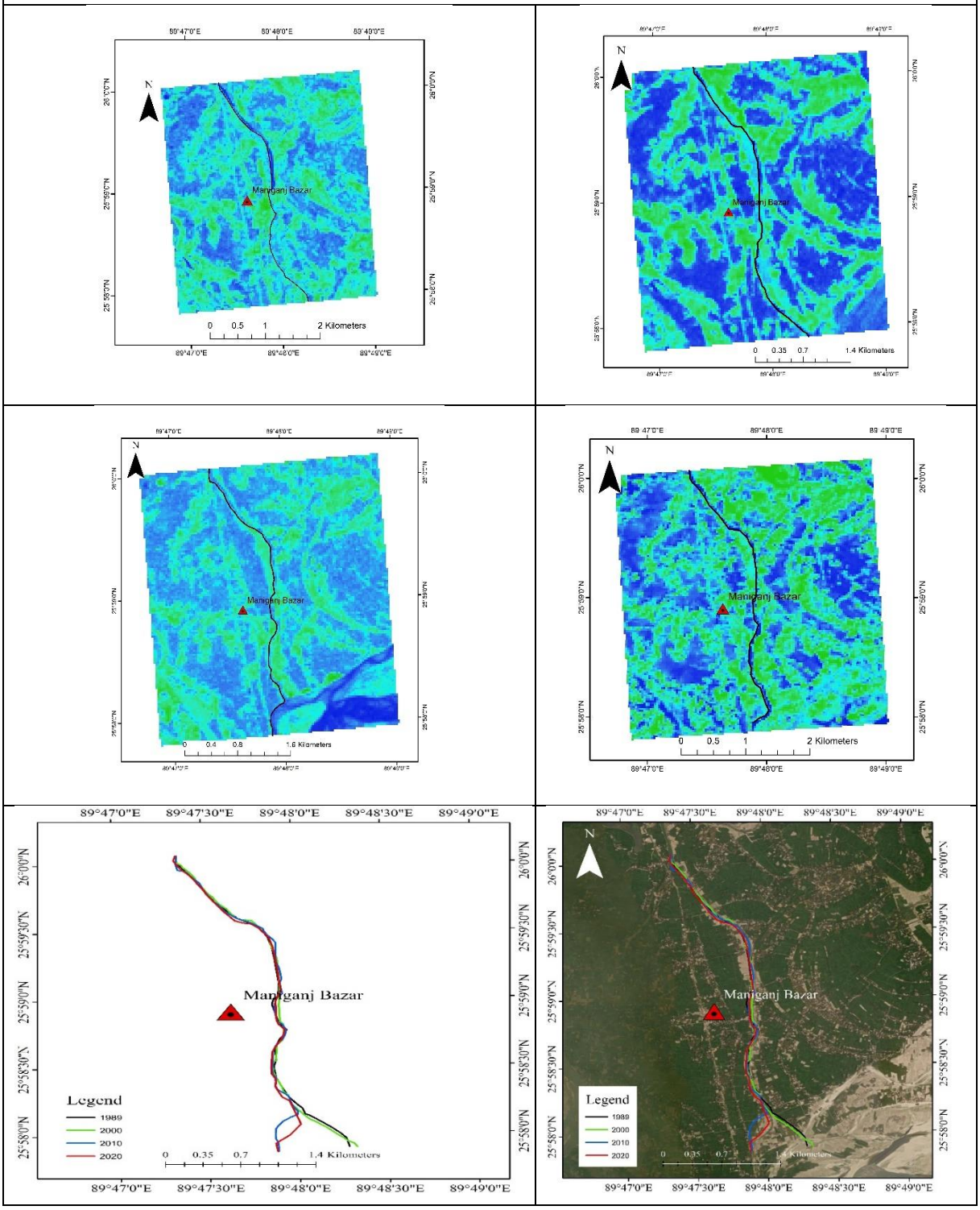

Market-67: Berubari Hat in Nageshwari Upazila of Kurigram District

- Flood Risk: The market is located in a **Low** flood-risk area, considering the inundation patterns of all major floods in recent times.
- Bank Erosion Risk: Based on planform analysis using historical satellite images, the market is located in the **Low** bank erosion risk area.

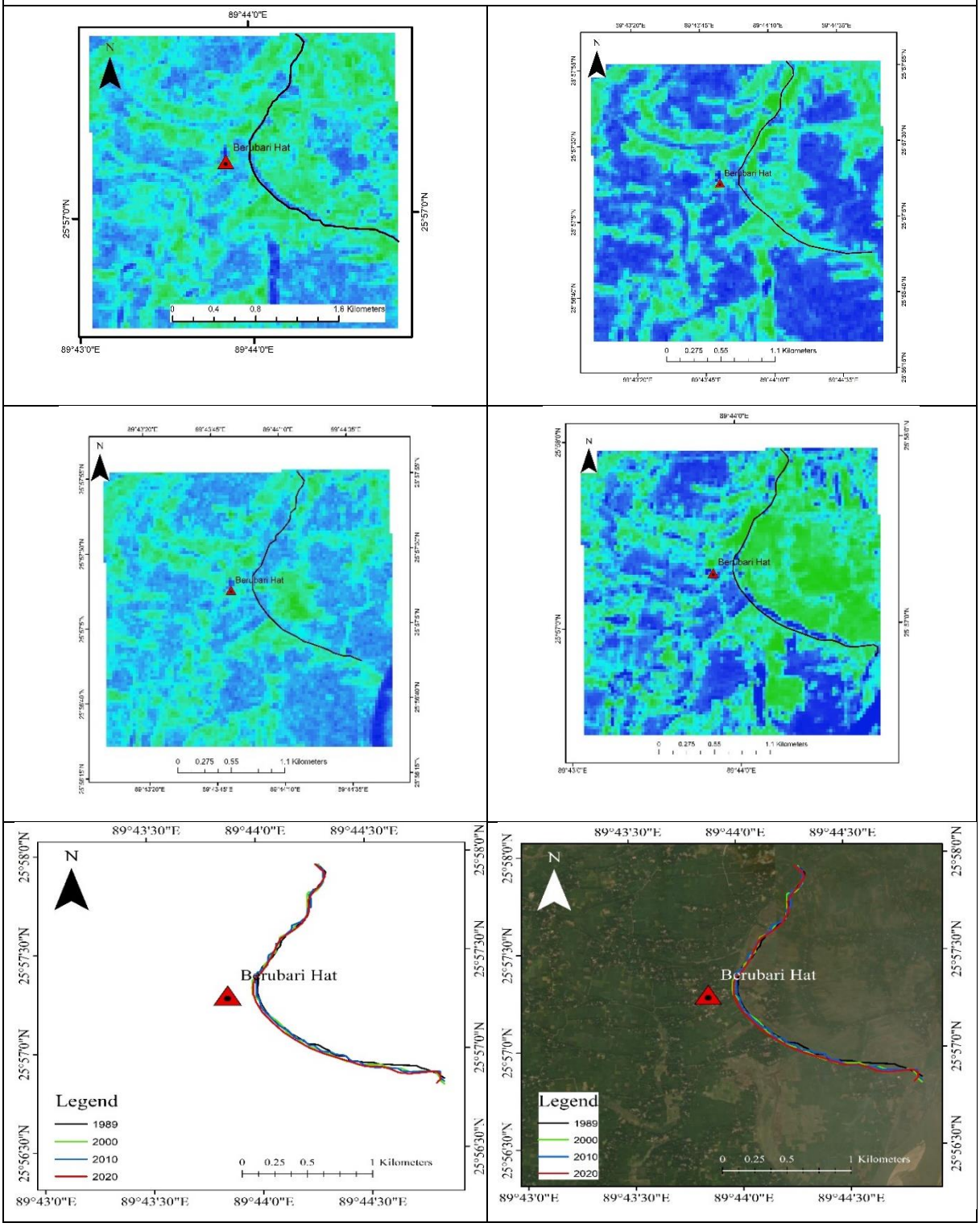

Market-68: Bakultala Bazar in Phulbari Upzila of Kurigram District

- Flood Risk: The market is located in a **Low** flood-risk area, considering the inundation patterns of all major floods in recent times.
- Bank Erosion Risk: Based on planform analysis using historical satellite images, the market is located in the **Moderate** bank erosion risk area

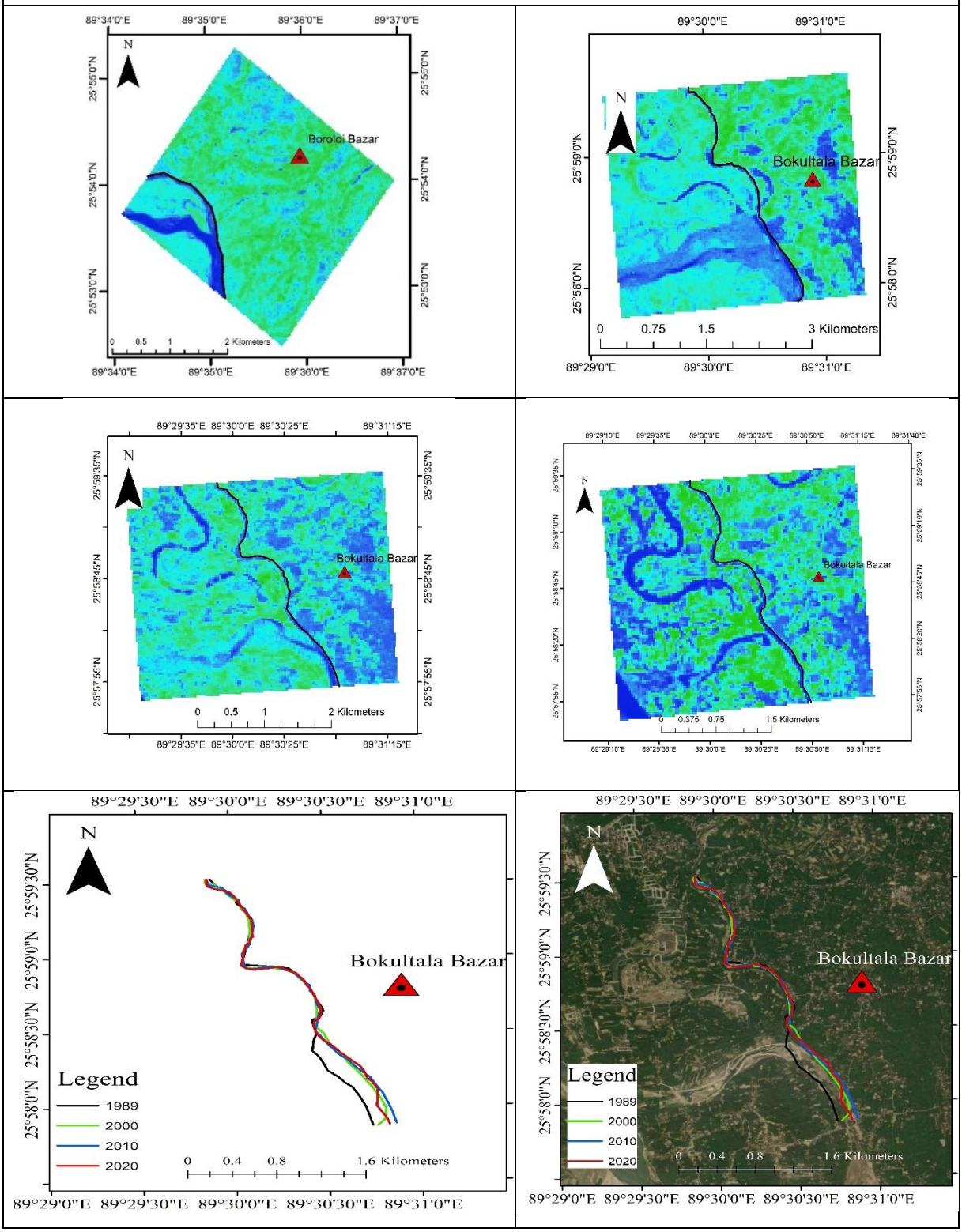

Market-69: Ghogurhat Bazar in Phulbari Upzila of Kurigram District

- Flood Risk: The market is located in a **Low** flood-risk area, considering the inundation patterns of all major floods in recent times.
- Bank Erosion Risk: Due to limitations of satellite image resolution, the river bank erosion risk cannot be assessed **(N/A).**

<table>
<tr>
<td> 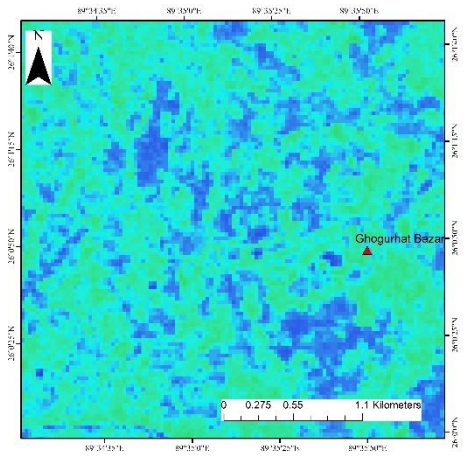
</td>
<td> 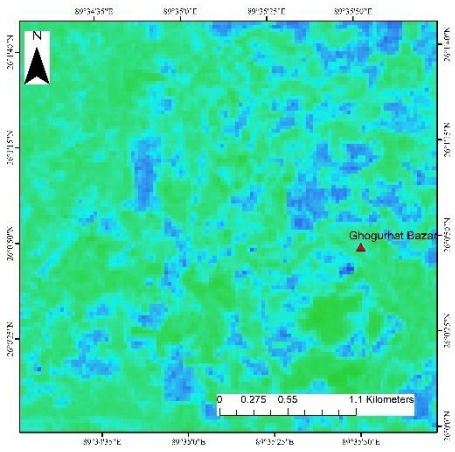
</td>
</tr>
<tr>
<td> 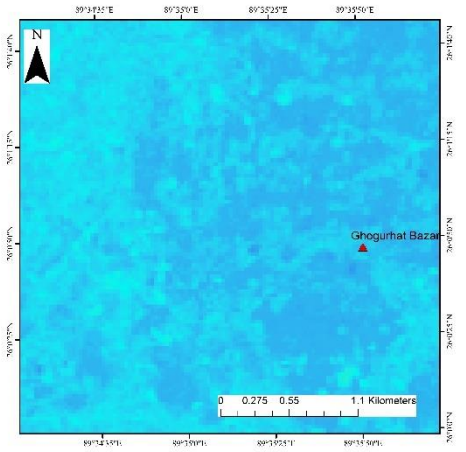
</td>
<td> 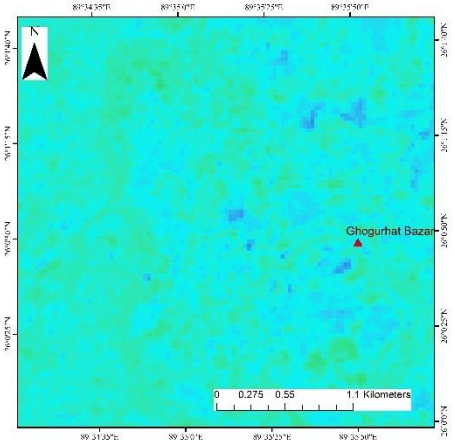
</td>
</tr>
<tr>
<td>It is not possible to detect changes in bank lines due to inadequate resolution of satellite image</td>
<td>It is not possible to detect changes in bank lines due to inadequate resolution of satellite image</td>
</tr>
</table>

Market-70: Shiber Bazar in Phulbari Upzila of Kurigram District

- Flood Risk: The market is located in a **Low** flood-risk area, considering the inundation patterns of all major floods in recent times.
- Bank Erosion Risk: Based on planform analysis using historical satellite images, the Market is located in the **Low** bank erosion risk area.

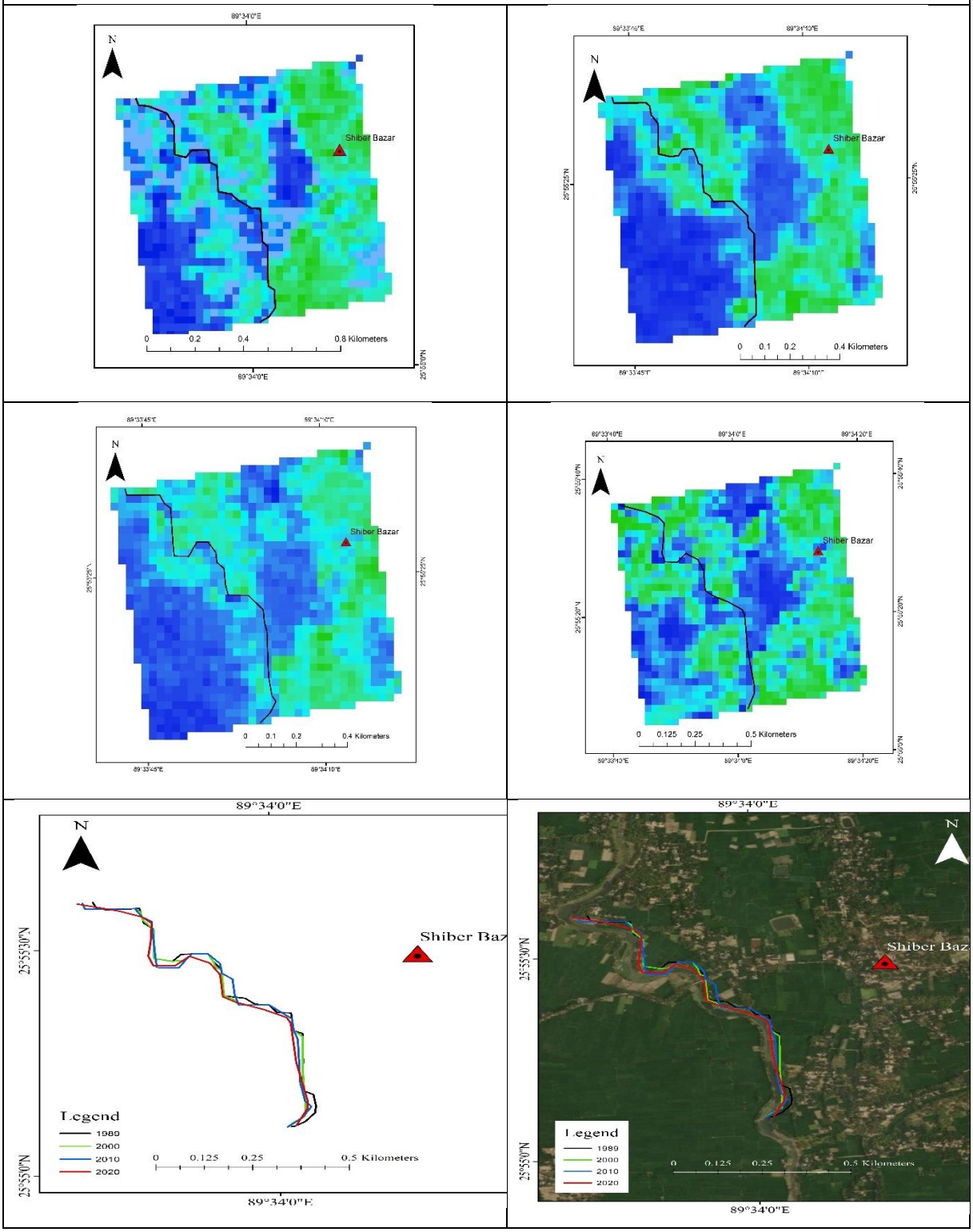

Market-71: Boroloi Bazar in Phulbari Upzila of Kurigram District

- Flood Risk: The market is located in a **Low** flood-risk area, considering the inundation patterns of all major floods in recent times.
- Bank Erosion Risk: Based on planform analysis using historical satellite images, the market is located in the **Low** bank erosion risk area

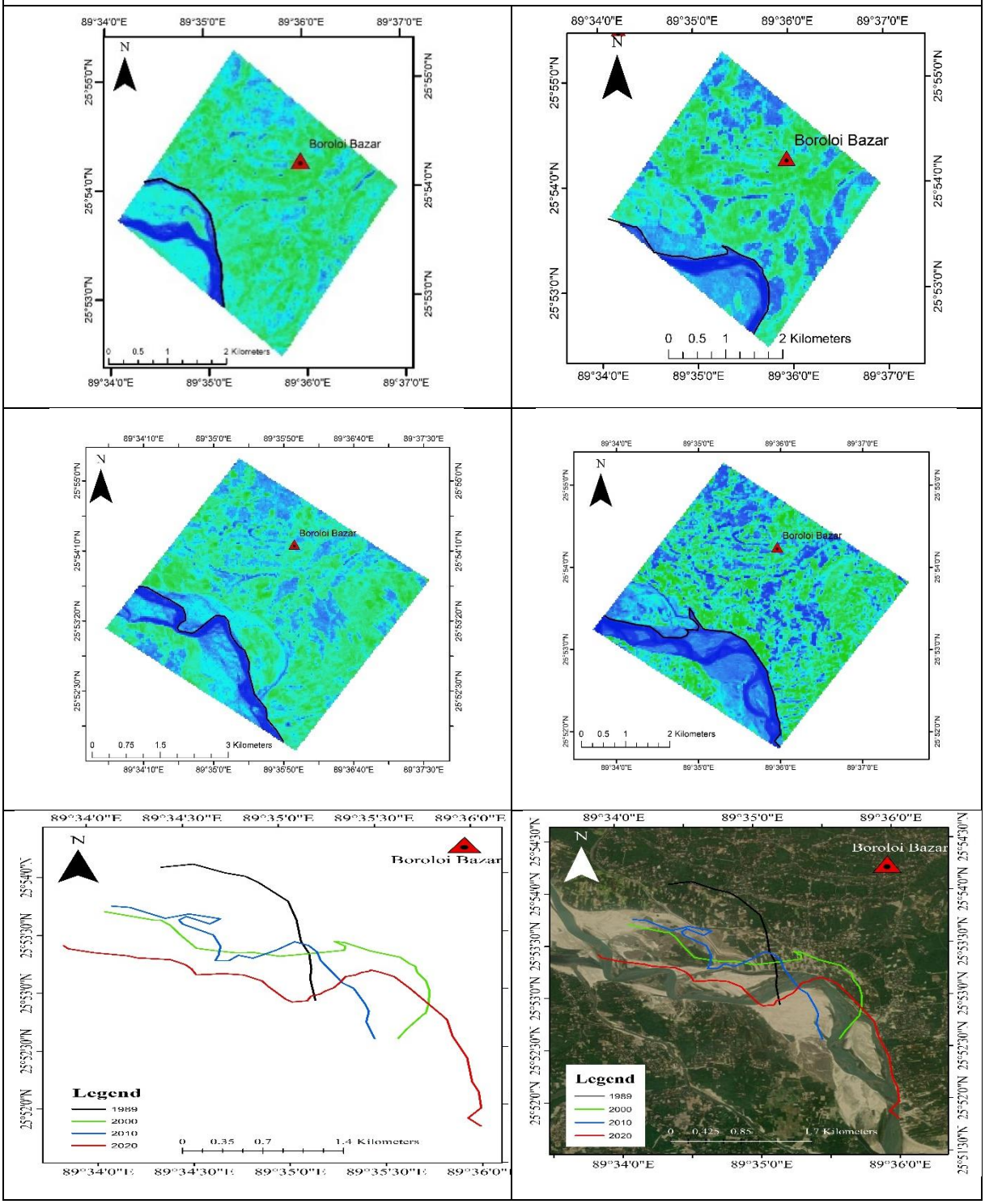

Market-72: Chandamari Hat in Rajarhat Upzila of Kurigram District

- Flood Risk: The market is located in a **Low** flood-risk area, considering the inundation patterns of all major floods in recent times.
- Bank Erosion Risk: Based on planform analysis using historical satellite images, the market is located in the **Low** bank erosion risk area

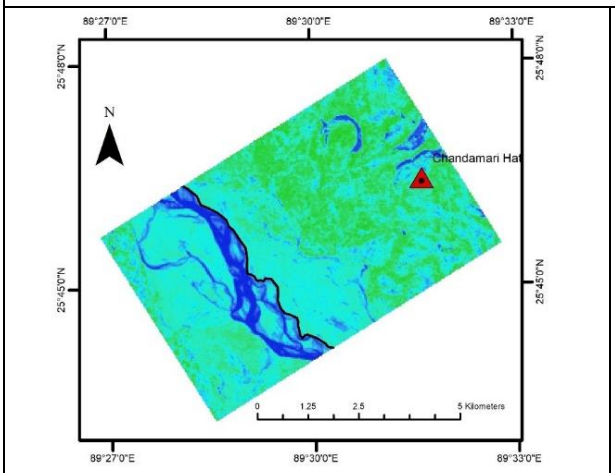

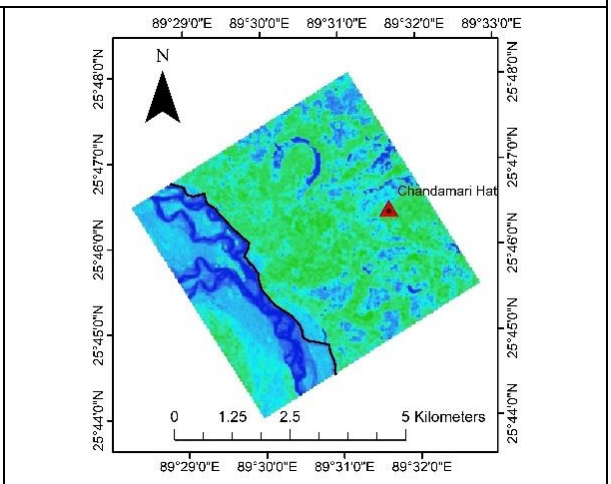

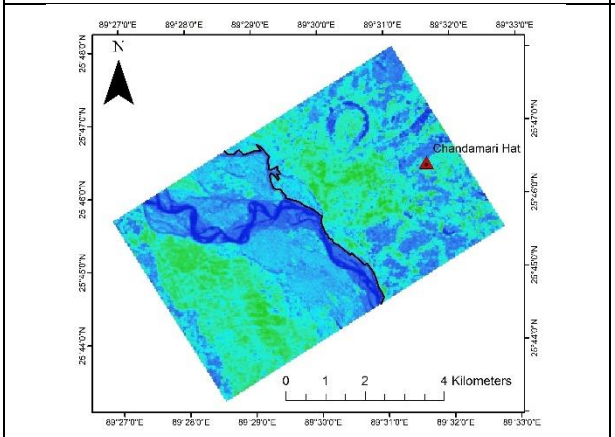

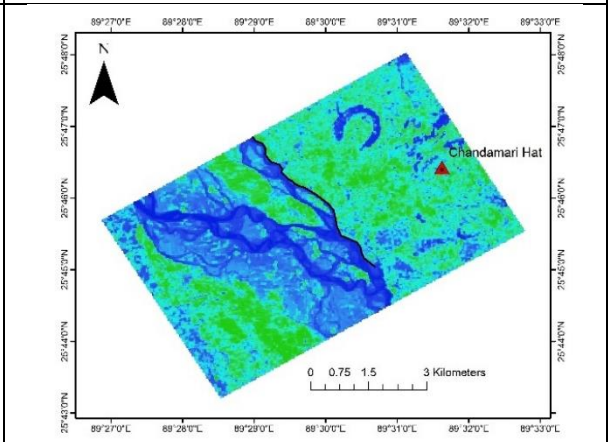

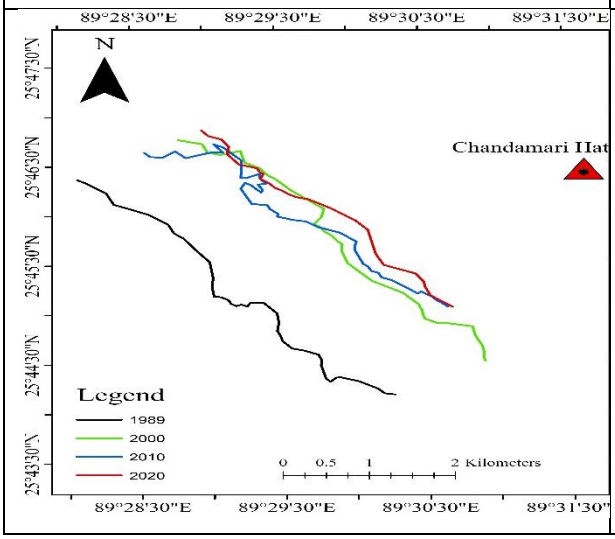

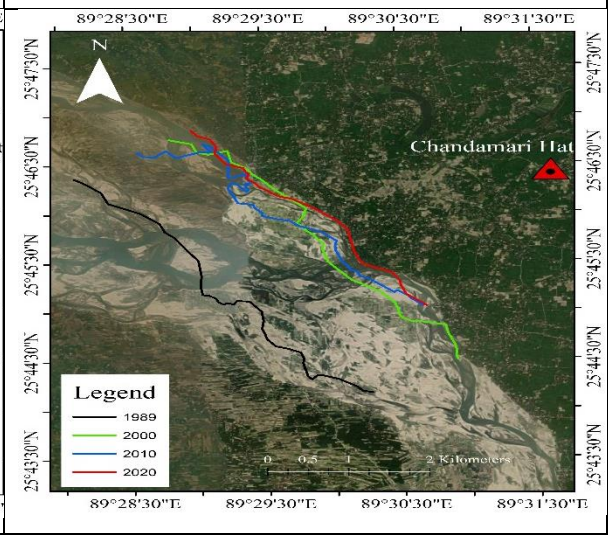

Market-73: Panga Bazar in Rajarhat Upzila of Kurigram District

- Flood Risk: The market is located in a **Low** flood-risk area, considering the inundation patterns of all major floods in recent times.
- Bank Erosion Risk: Due to satellite image limitation, the river bank erosion risk cannot be assessed **(N/A)**.

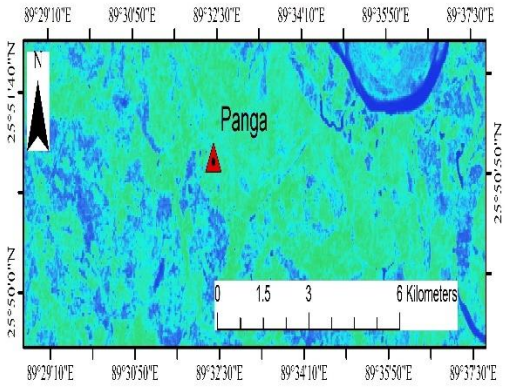

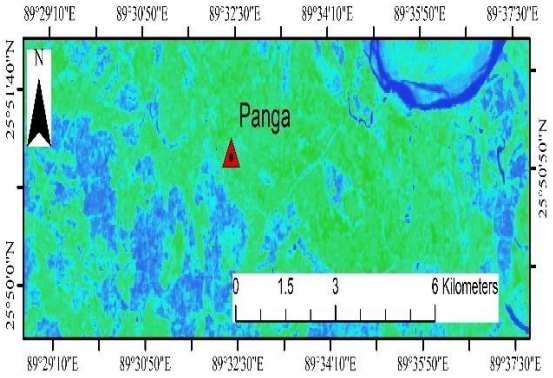

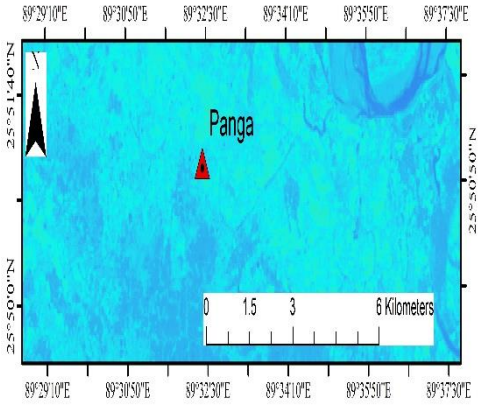

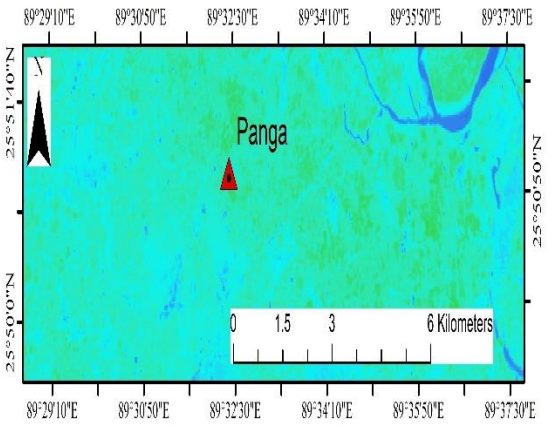

It is not possible to detect changes in bank lines due to inadequate resolution of satellite image

It is not possible to detect changes in bank lines due to inadequate resolution of satellite image

Market-74: Sharishabari Hat in Rajarhat Upazila of Kurigram District

- Flood Risk: The market is located in a **Low** flood-risk area, considering the inundation patterns of all major floods in recent times.
- Bank Erosion Risk: Based on planform analysis using historical satellite images, the Market is located in the **High** bank erosion risk area.

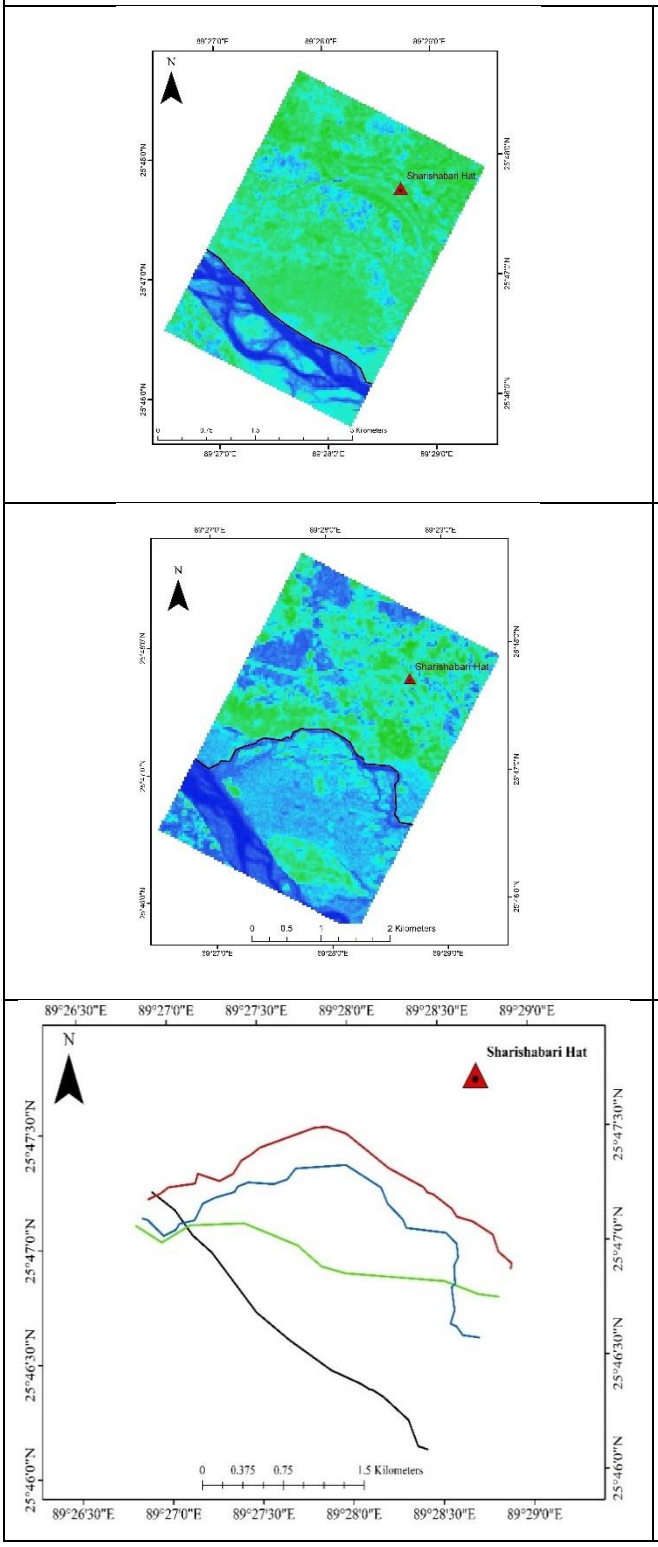

Market-75: Chowrahat in Rajarhat Upazila of Kurigram District

- Flood Risk: The market is located in a **Low** flood-risk area, considering the inundation patterns of all major floods in recent times.
- Bank Erosion Risk: Based on planform analysis using historical satellite images, the market is located in the **Low** bank erosion risk area

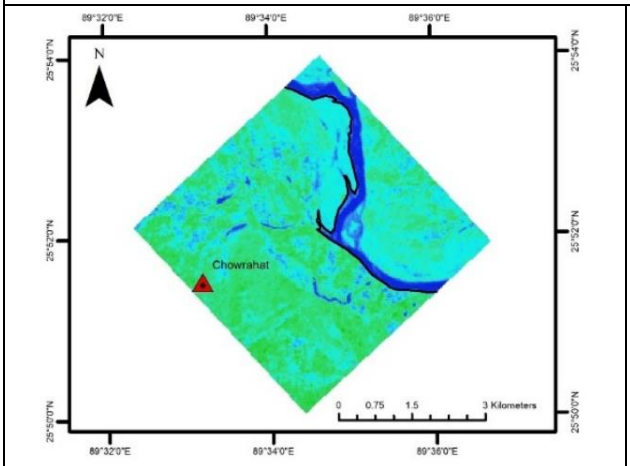

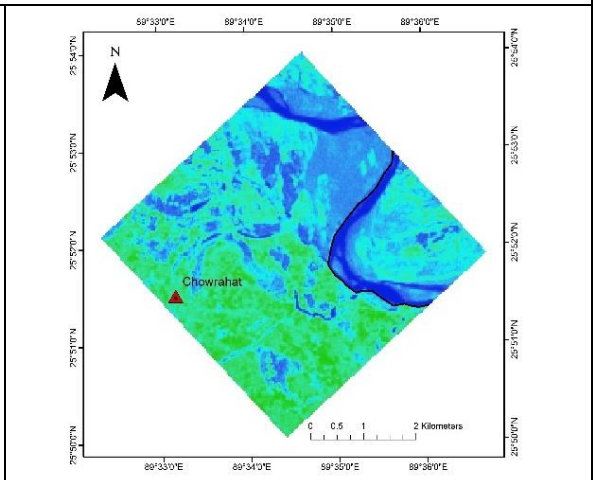

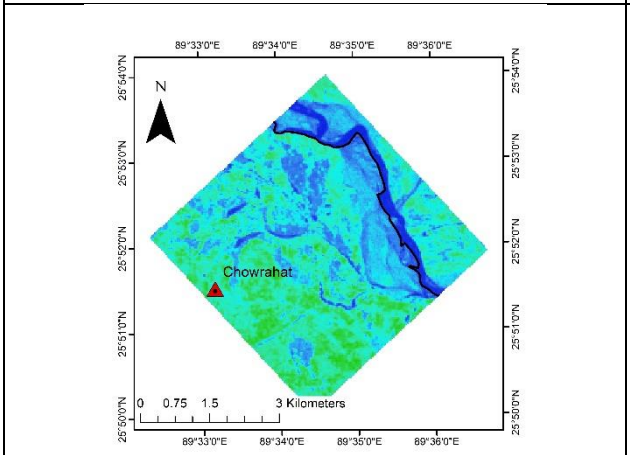

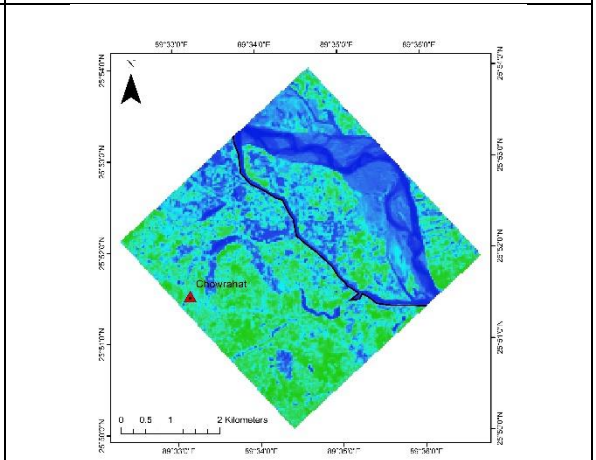

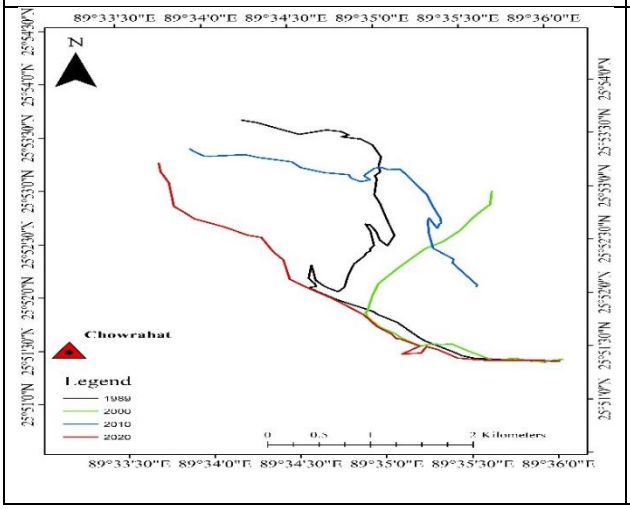

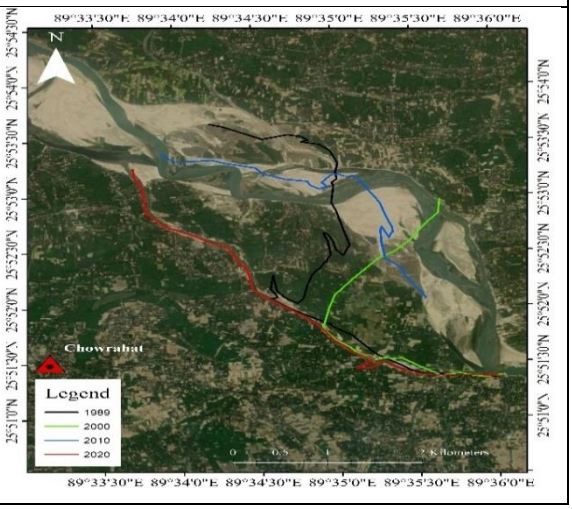

Market-76: Jorgach Hat in Chilmari Upzila of Kurigram District

- Flood Risk: The market is located in a **Low** flood-risk area, considering the inundation patterns of all major floods in recent times.
- Bank Erosion Risk: Based on planform analysis using historical satellite images, the market is located in the **High** bank erosion risk area.

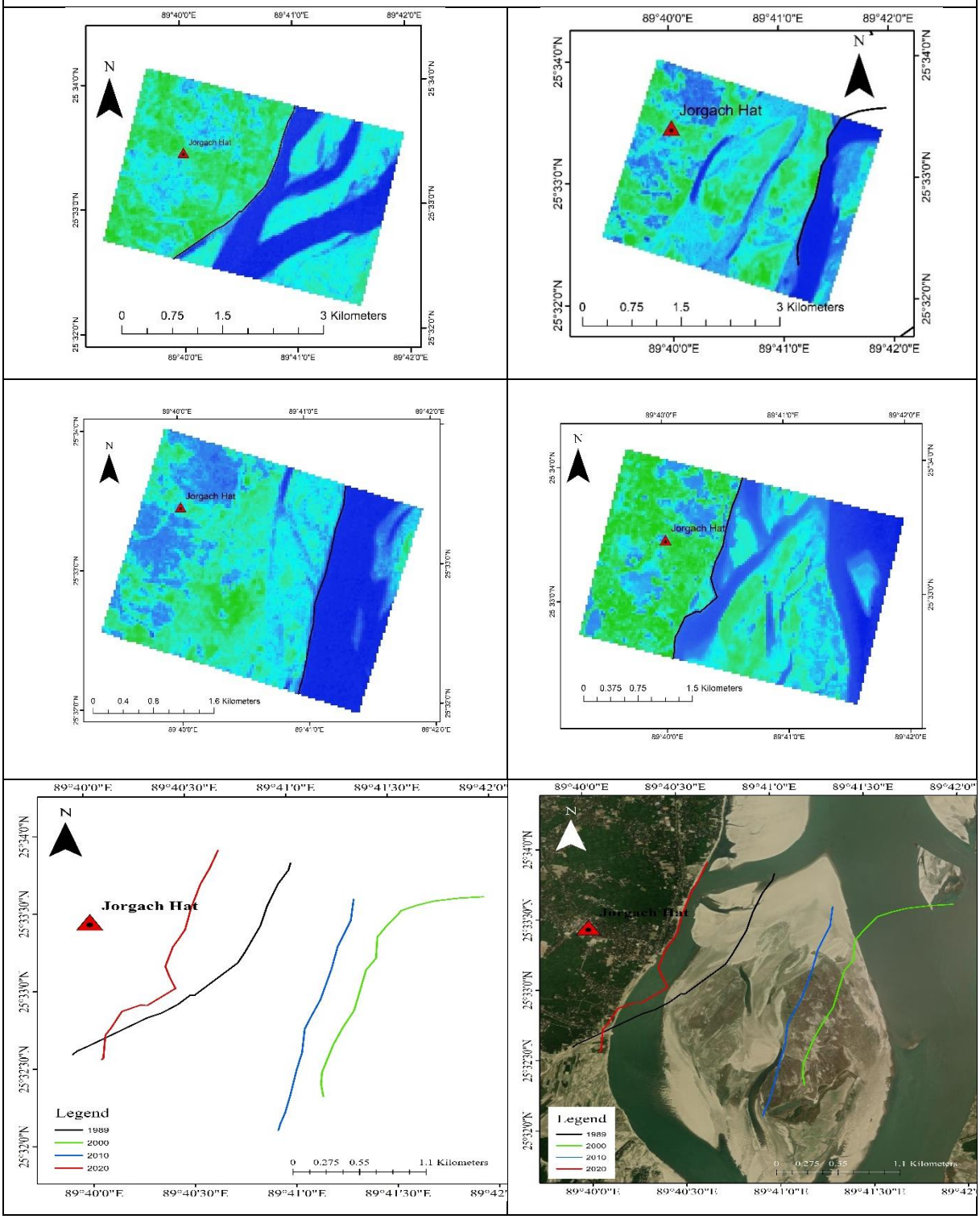

Market-77: Karai Barisal Bazar in Chilmari Upzila of Kurigram District

- Flood Risk: The market is located in a **Low** flood-risk area, considering the inundation patterns of all major floods in recent times.
- Bank Erosion Risk: Based on planform analysis using historical satellite images, the market is located in the **High** bank erosion risk area.

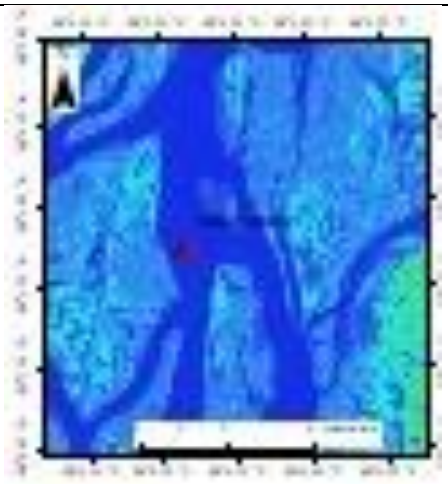

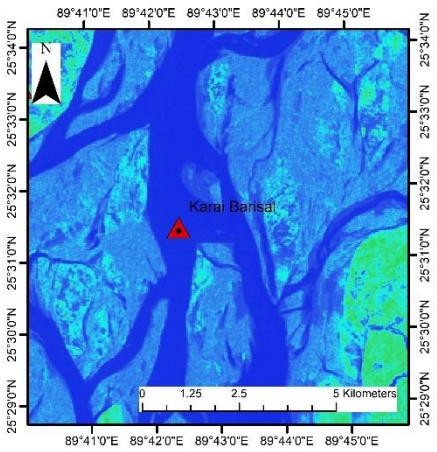

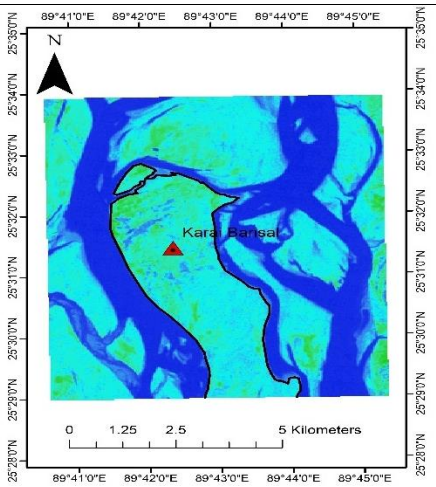

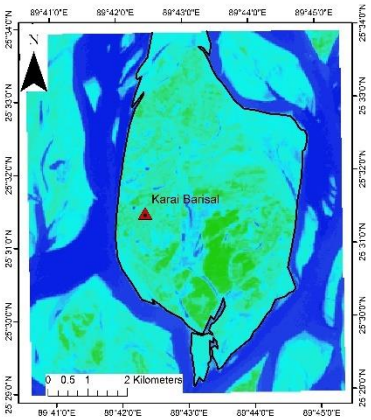

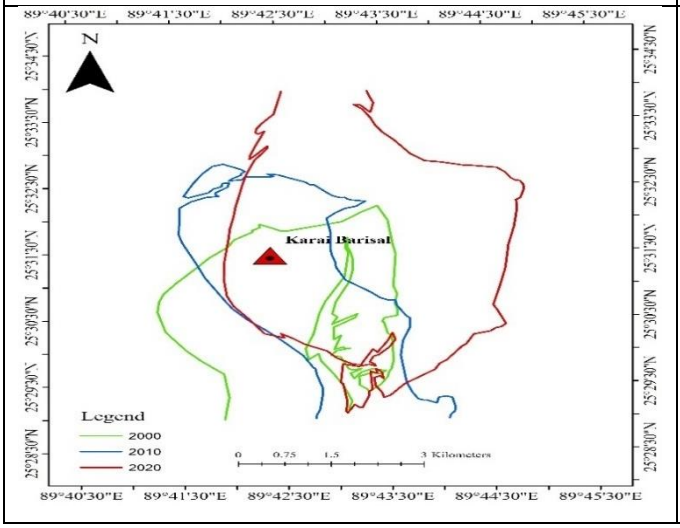

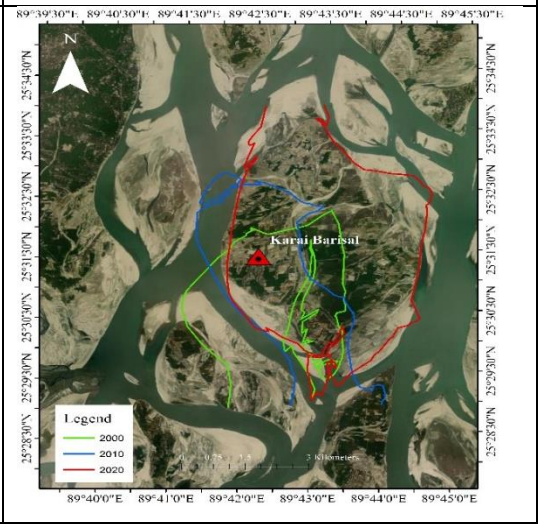

Market-78: Thana Hat in Chilmari Upzila of Kurigram District

- Flood Risk: The market is located in a **Low** flood-risk area, considering the inundation patterns of all major floods in recent times.
- Bank Erosion Risk: Based on planform analysis using historical satellite images, the Market is located in the **Low** bank erosion risk area.

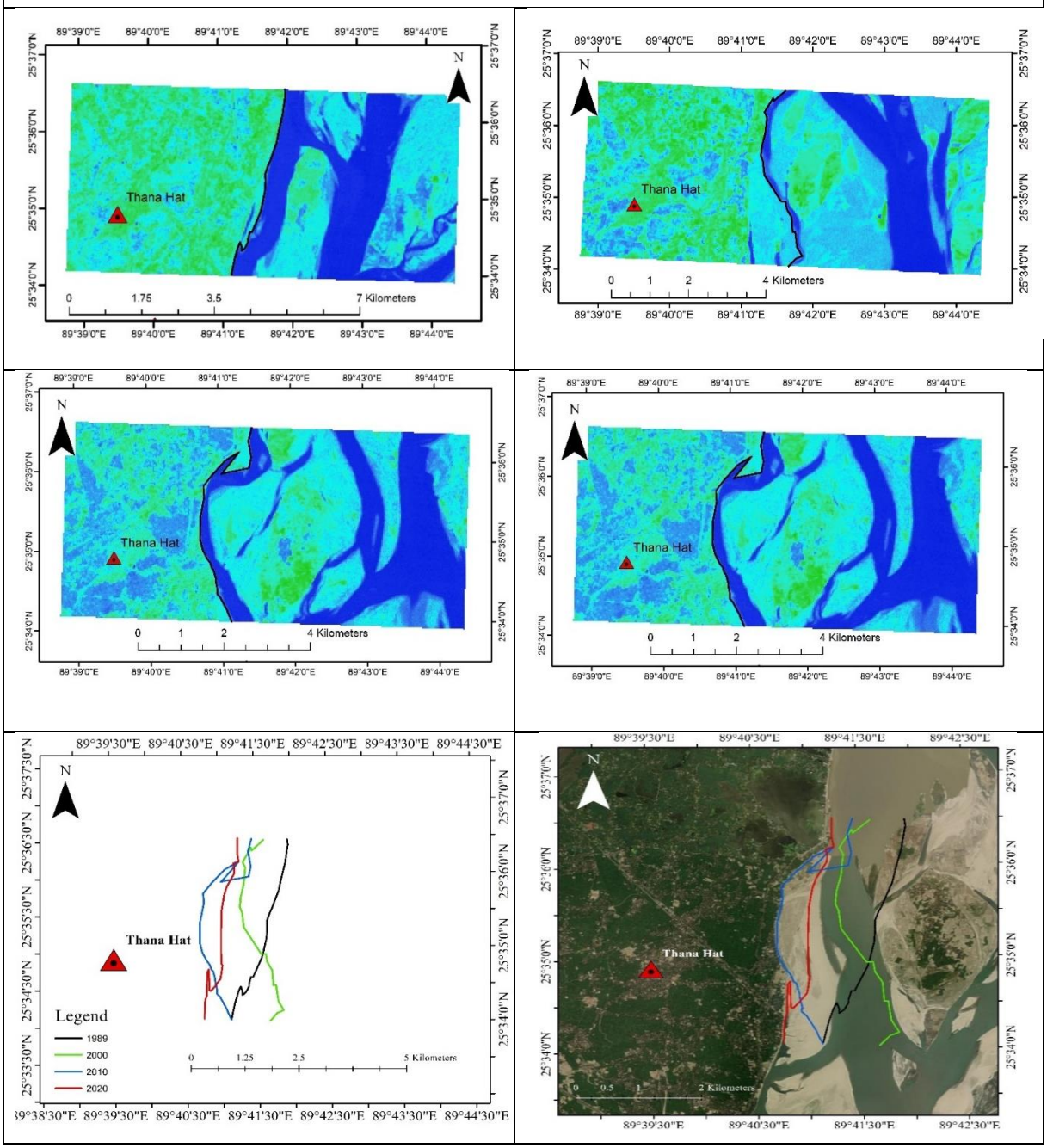

Market-79: Fakirarhat in Chilmari Upzila of Kurigram District

- Flood Risk: The market is located in a **Low** flood-risk area, considering the inundation patterns of all major floods in recent times.
- Bank Erosion Risk: Based on planform analysis using historical satellite images, the market is located in the **High** bank erosion risk area.

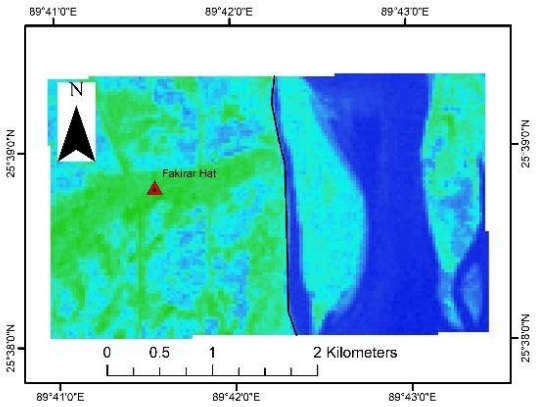

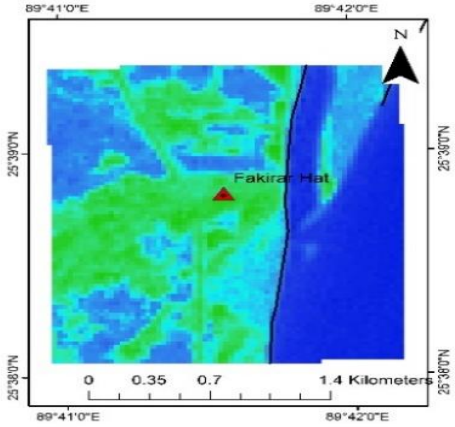

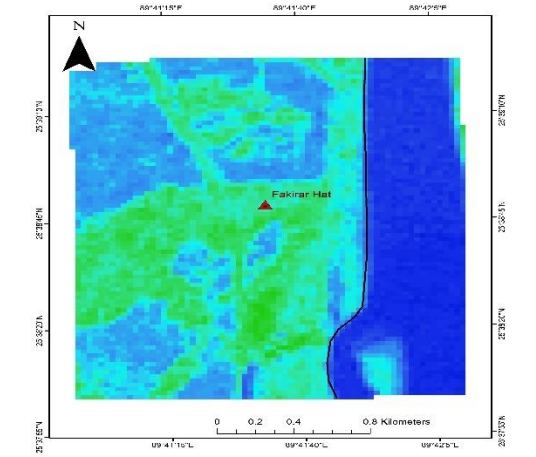

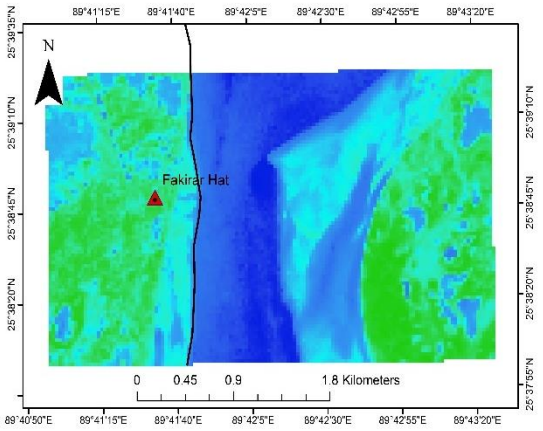

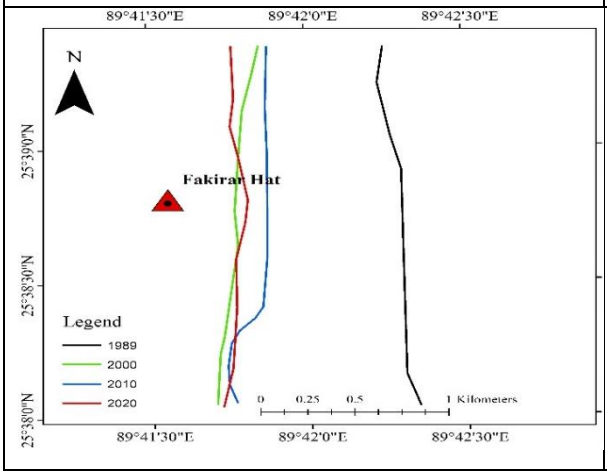

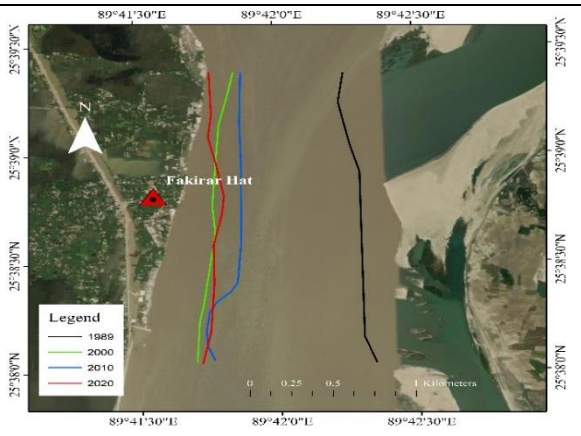

Market-80: Hatia Vobesh in Lalmonirhat sadar Upzila of Lalmonirhat District

- Flood Risk: The market is located in a **Moderate** flood risk area, considering the inundation patterns of all major floods in recent times.
- Bank Erosion Risk: Based on planform analysis using historical satellite images, the market is located in the **High** bank erosion risk area.

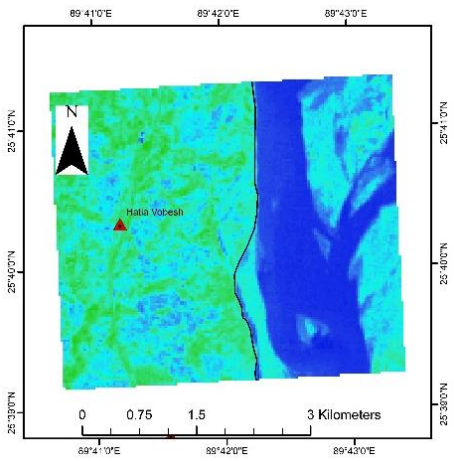

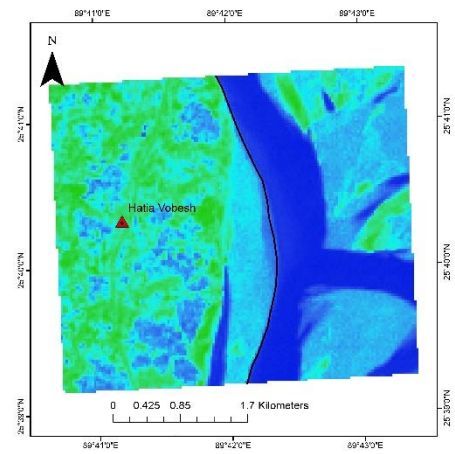

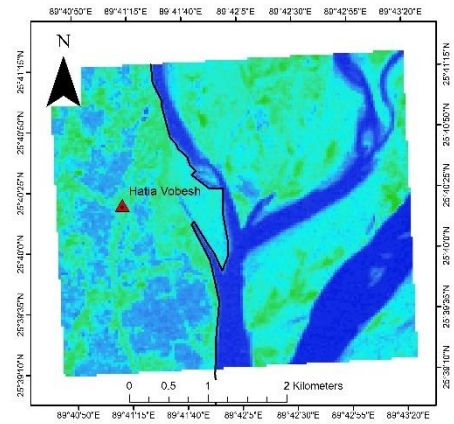

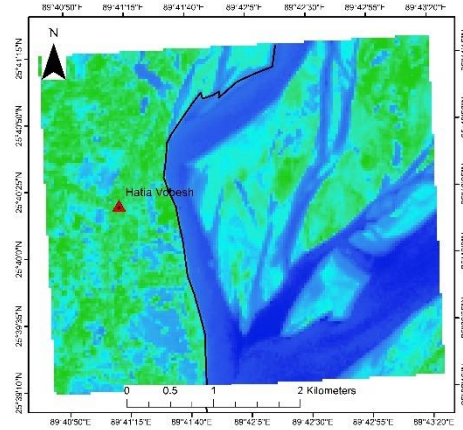

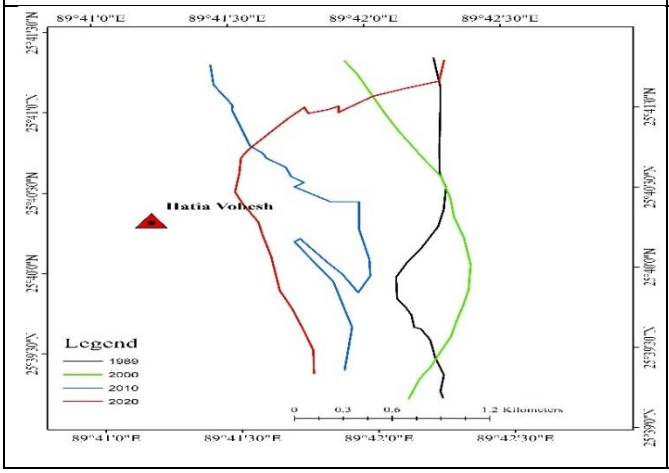

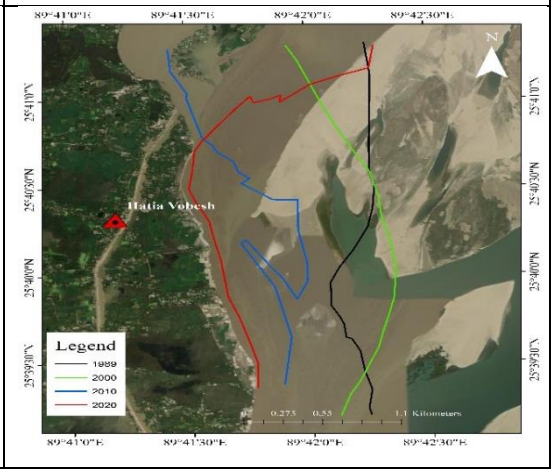

Market-81: Mollar Hat in Ulipur Upzila of Kurigram District

- Flood Risk: The market is located in a **Low** flood-risk area, considering the inundation patterns of all major floods in recent times.
- Bank Erosion Risk: Based on planform analysis using historical satellite images, the Market is located in the **High** bank erosion risk area.

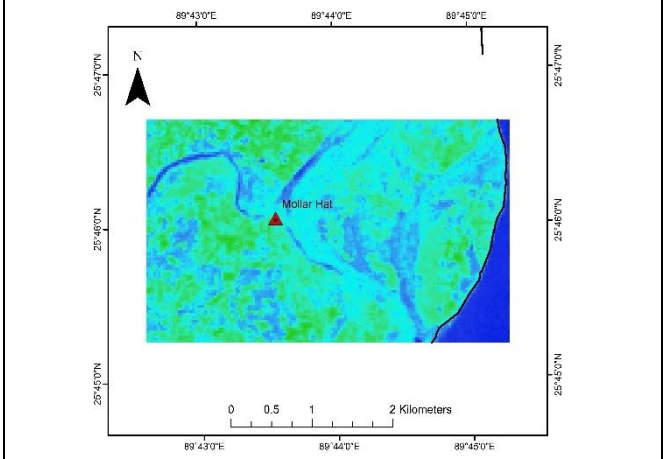

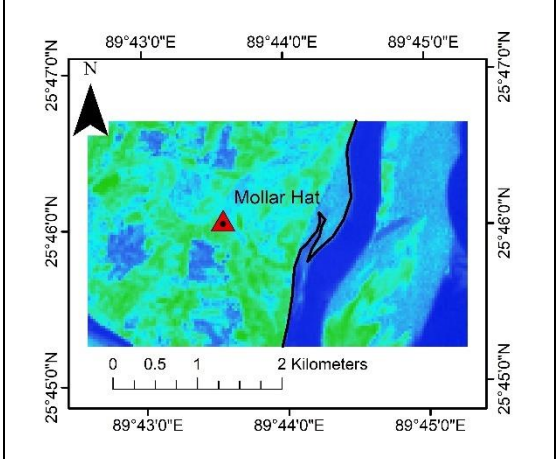

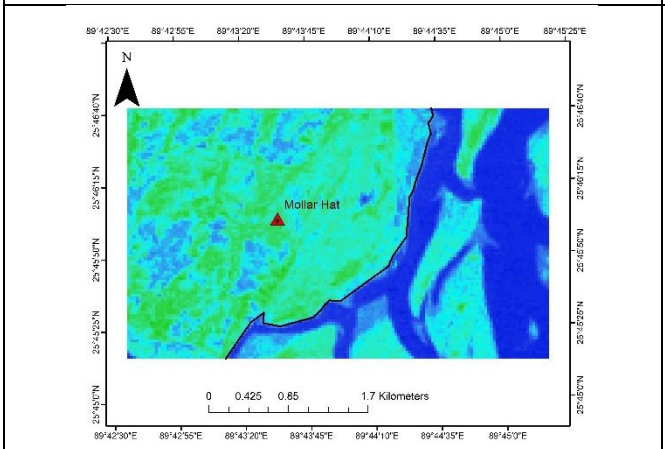

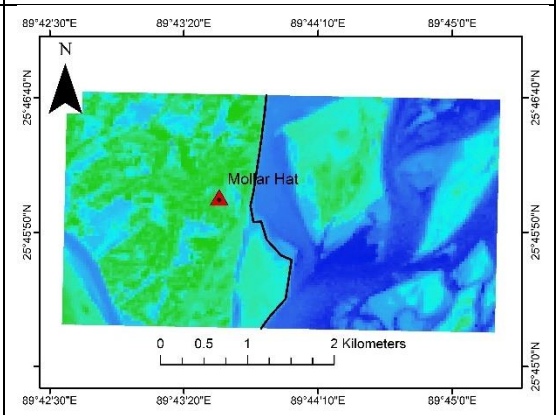

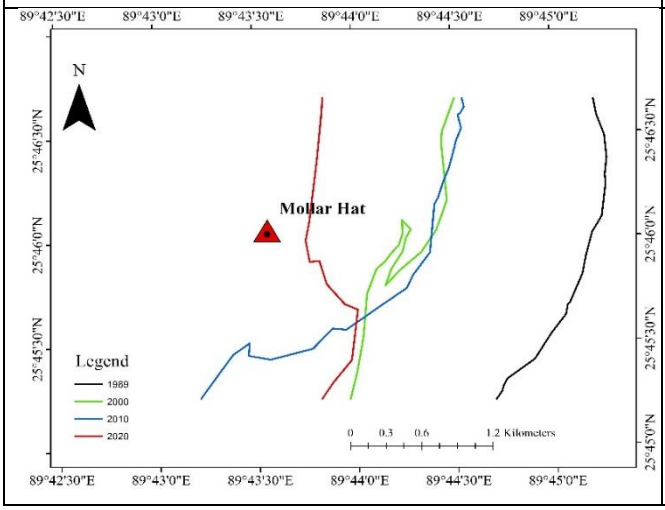

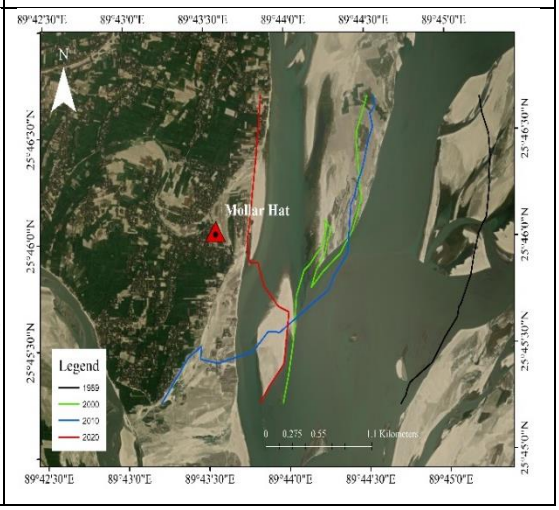

Market-82: Jatiner Hat in Ulipur Upzila of Kurigram District

- Flood Risk: The market is located in a **Low** flood-risk area, considering the inundation patterns of all major floods in recent times.
- Bank Erosion Risk: Based on planform analysis using historical satellite images, the market is located in the **Low** bank erosion risk area.

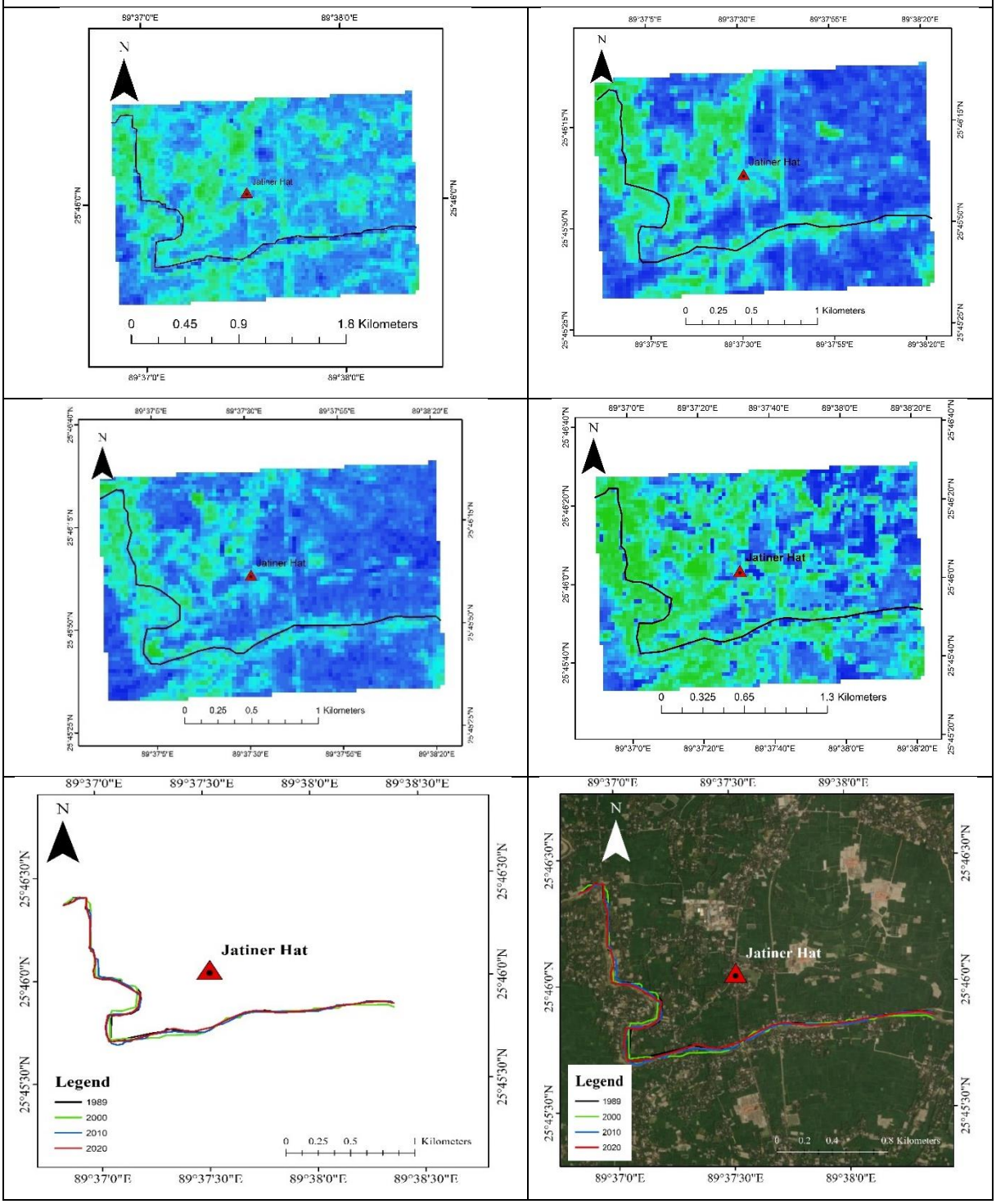

Market-83: Panchgachi Bazar in Kurigram Sadar Upzila of Kurigram District

- Flood Risk: The market is located in a **Low** flood-risk area, considering the inundation patterns of all major floods in recent times.
- Bank Erosion Risk: Based on planform analysis using historical satellite images, the Market is located in the **Low** bank erosion risk area.

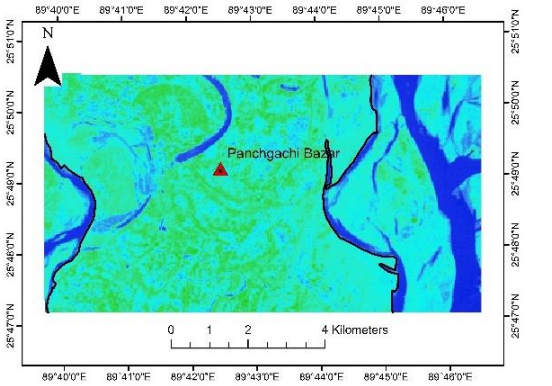

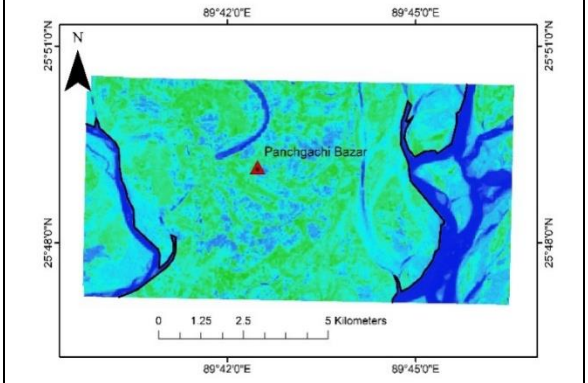

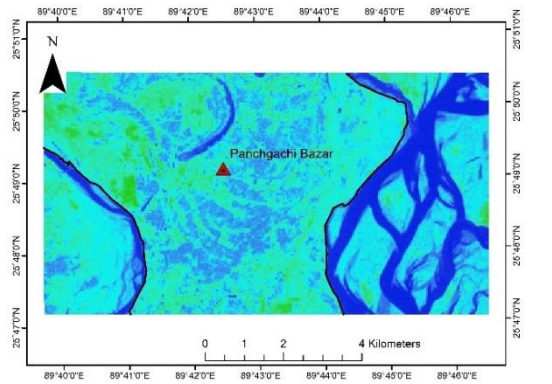

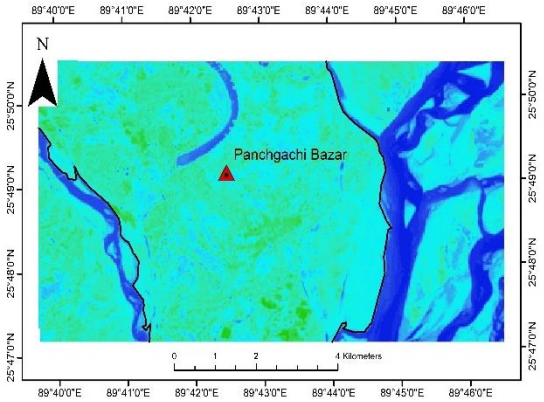

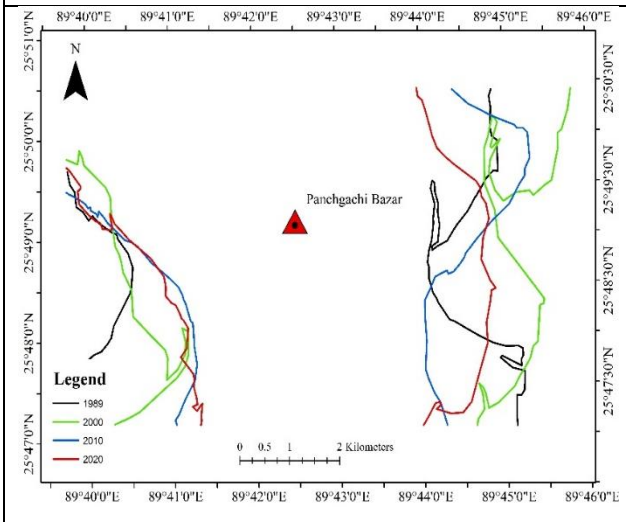

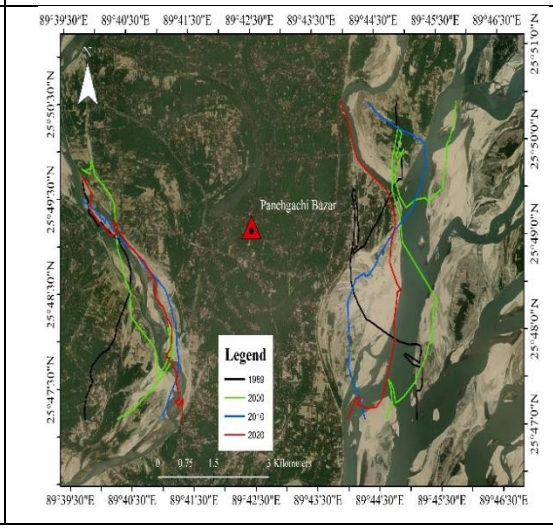

Market-84: Rajmallir Hat in Kurigram sadar Upzila of Kurigram District

- Flood Risk: The market is located in a **Moderate** flood risk area, considering the inundation patterns of all major floods in recent times. However, the surrounding area is at severe flood risk.
- Bank Erosion Risk: Based on planform analysis using historical satellite images, the Market is located in the **High** bank erosion risk area.

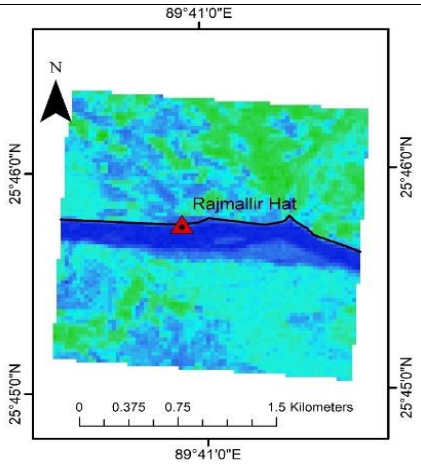

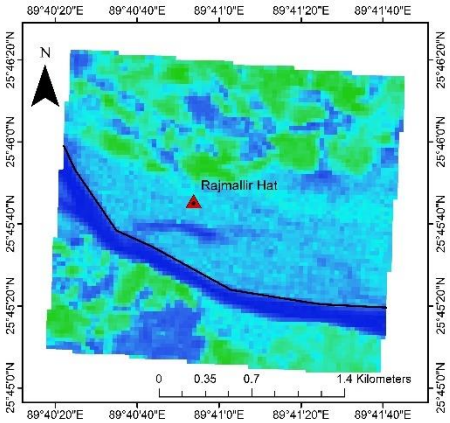

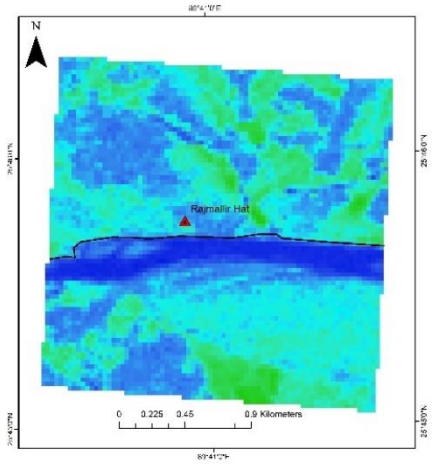

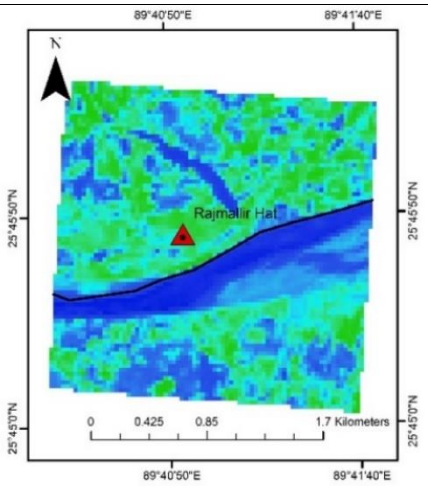

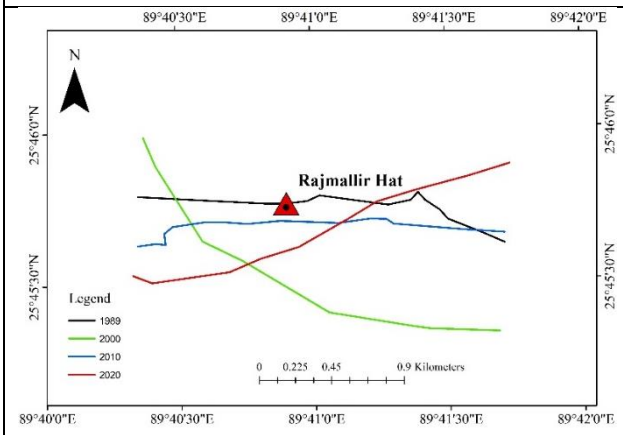

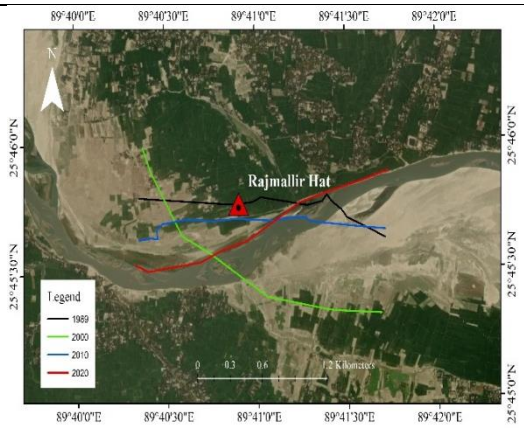

Market-85: Rajarhat Bazar in Kurigram sadar Upzila of Kurigram District

- Flood Risk: The market is located in a **Moderate** flood risk area, considering the inundation patterns of all major floods in recent times.
- Bank Erosion Risk: Based on planform analysis using historical satellite images, the Market is located in the **Low** bank erosion risk area.

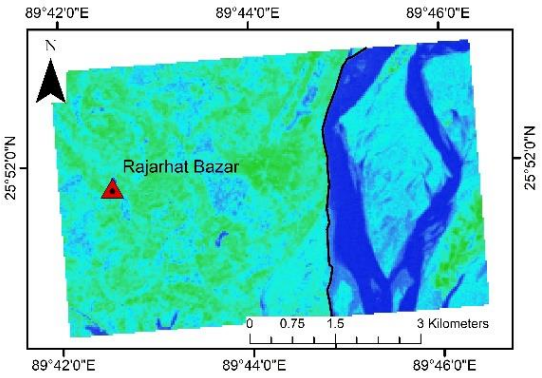

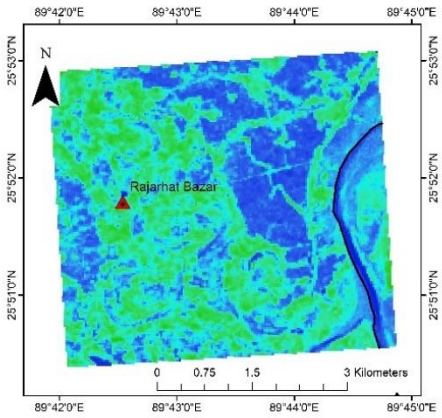

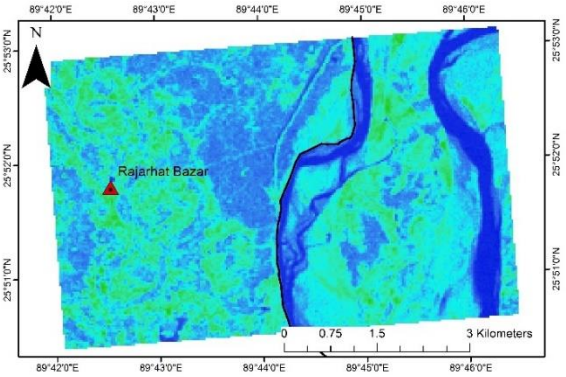

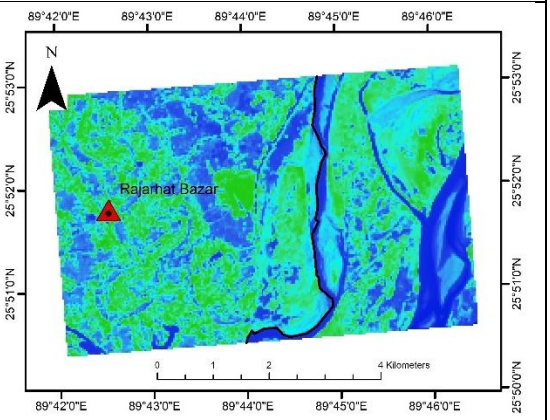

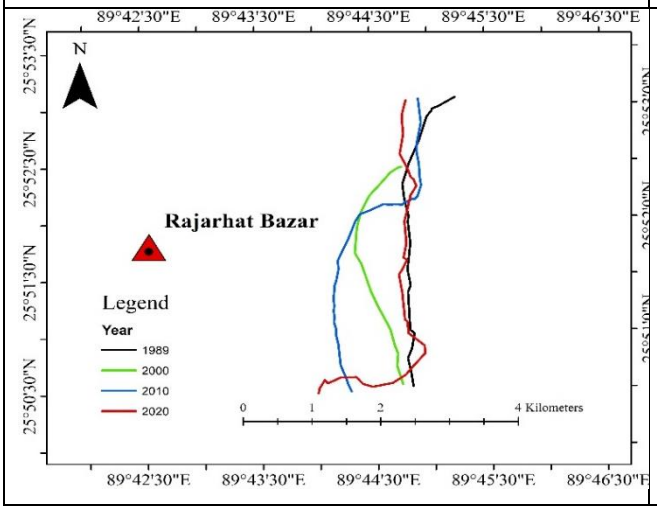

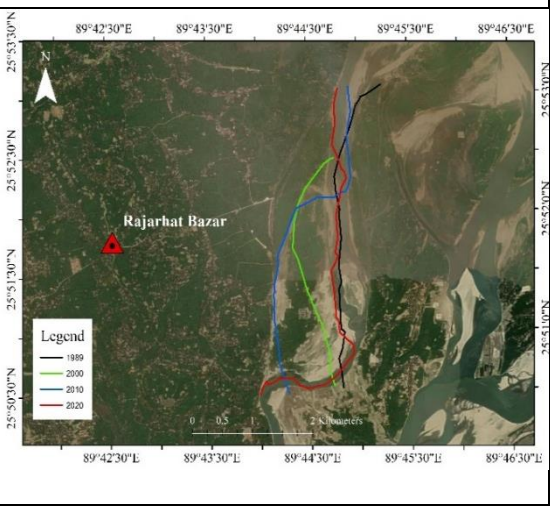

Market-86: Masterer Hat in Kurigram Upzila of Kurigram District

- Flood Risk: The market is located in a **Low** flood-risk area, considering the inundation patterns of all major floods in recent times.
- Bank Erosion Risk: Based on planform analysis using historical satellite images, the Market is located in the **Low** bank erosion risk area.

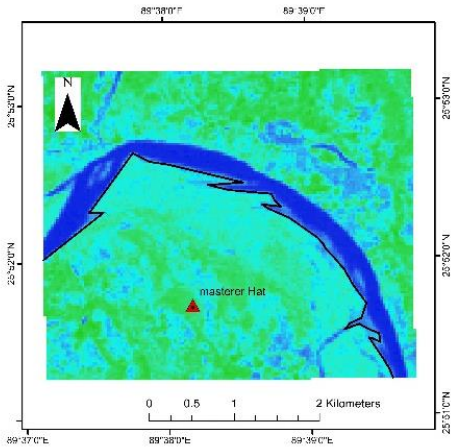

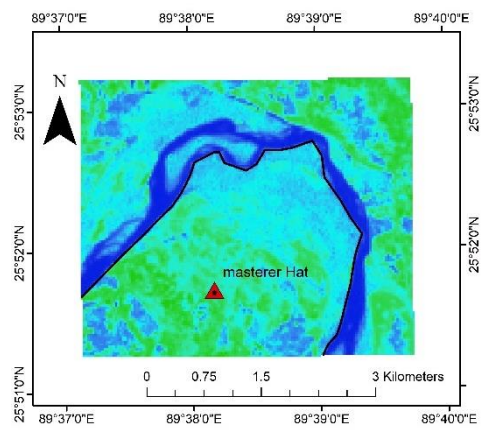

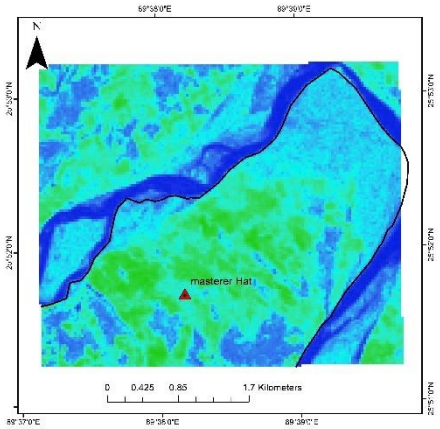

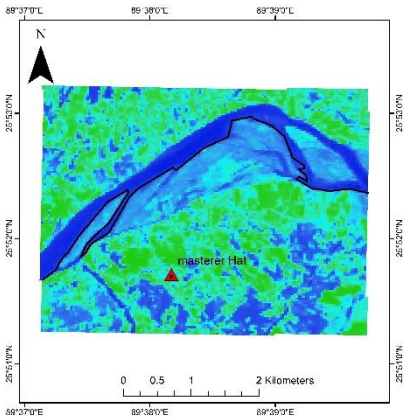

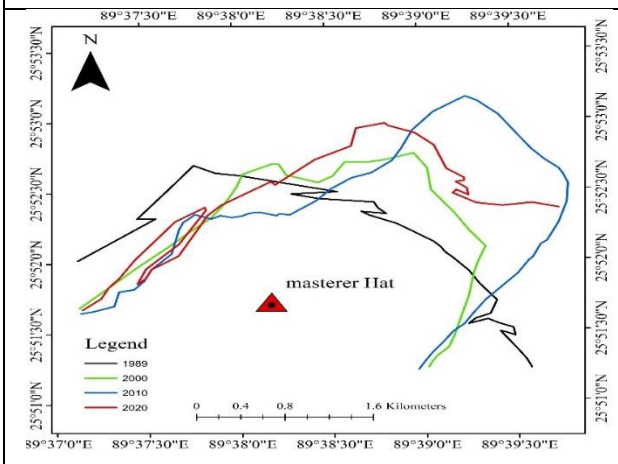

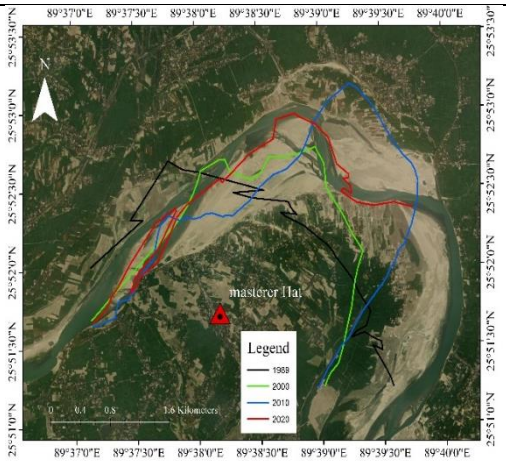

Market-87: Baraikandhi Hat in Raumari Upzila of Kurigram District

- Flood Risk: The market is located in a **Low** flood-risk area, considering the inundation patterns of all major floods in recent times
- Bank Erosion Risk: Based on planform analysis using historical satellite images, the market is located in the **Low** bank erosion risk area.

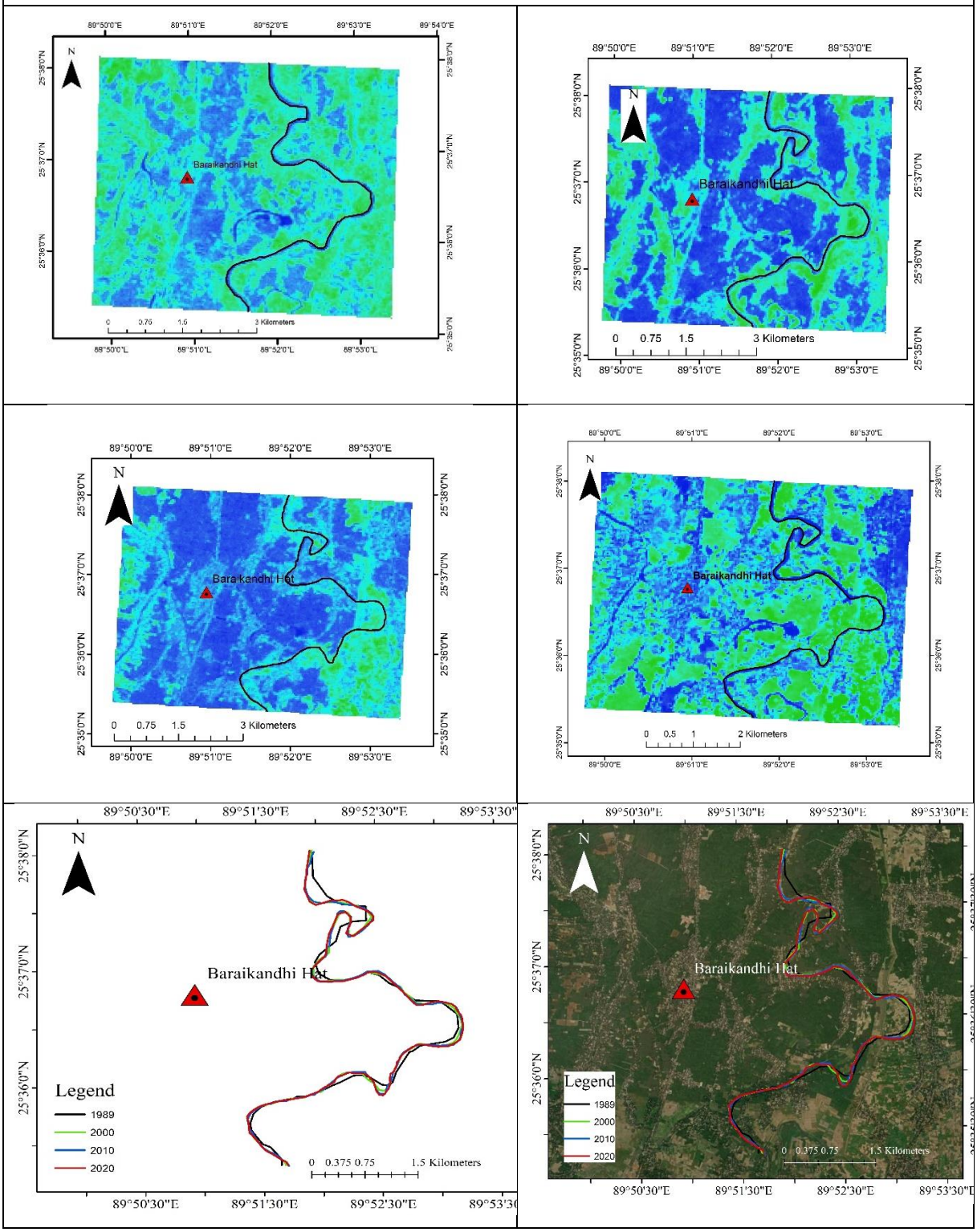

Market-88: Saydabad Bazar in Raumari Upzila of Kurigram District

- Flood Risk: The market is located in a **Moderate** flood risk area, considering the inundation patterns of all major floods in recent times.
- Bank Erosion Risk: Based on planform analysis using historical satellite images, the Market is located in the **Moderate** bank erosion risk area.

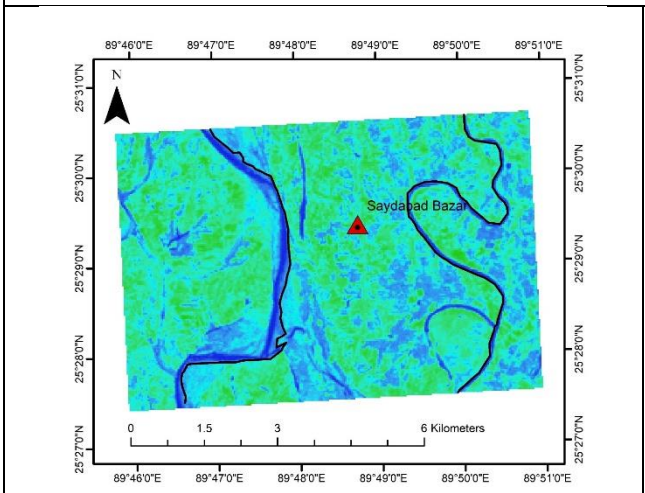

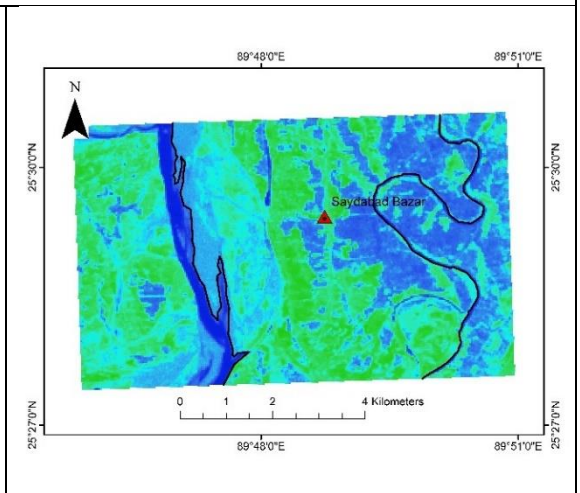

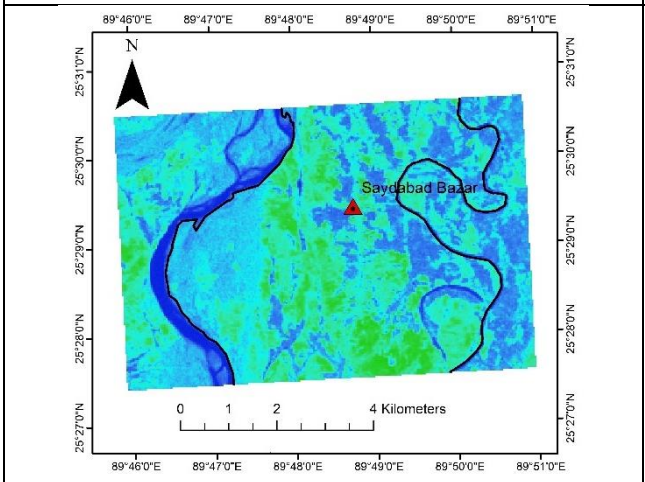

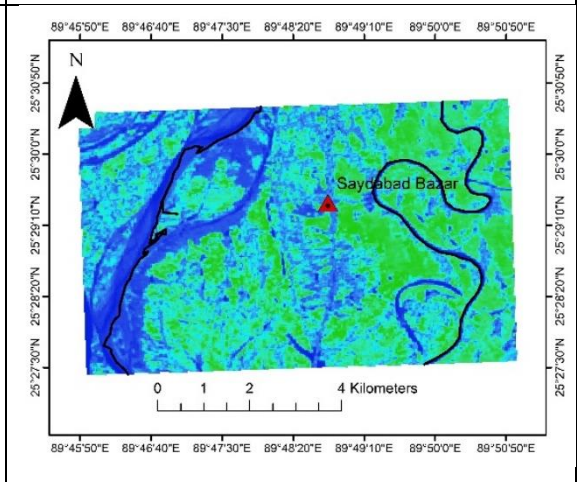

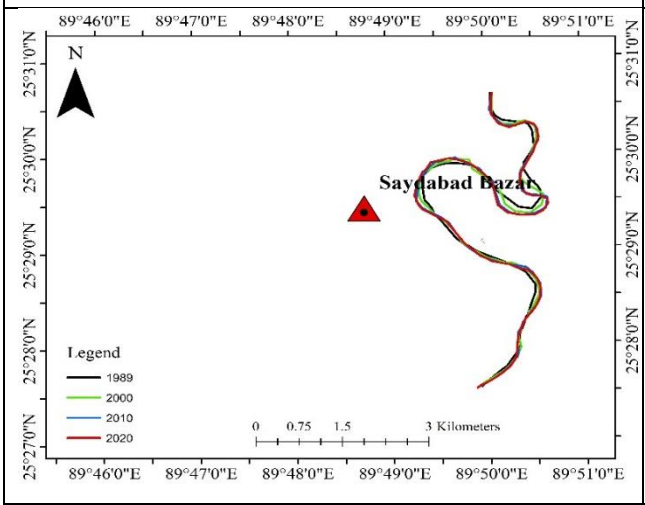

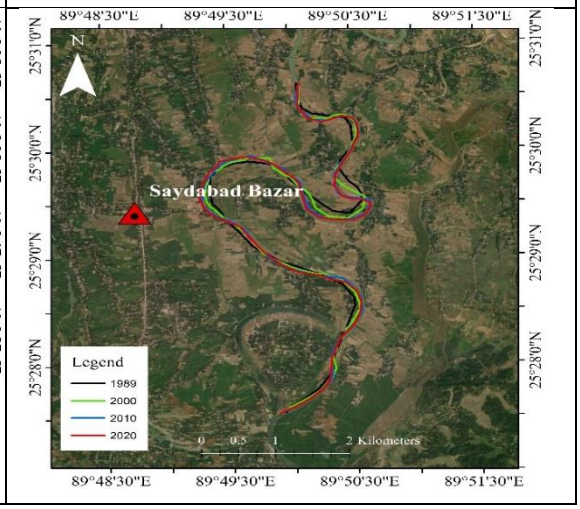

Market-89: Rajibpur GC Bazar in Char Rajibpur Upzila of Kurigram District

- Flood Risk: The market is located in a **Low** flood-risk area, considering the inundation patterns of all major floods in recent times.
- Bank Erosion Risk: Based on planform analysis using historical satellite images, the Market is located in the **High** bank erosion risk area.

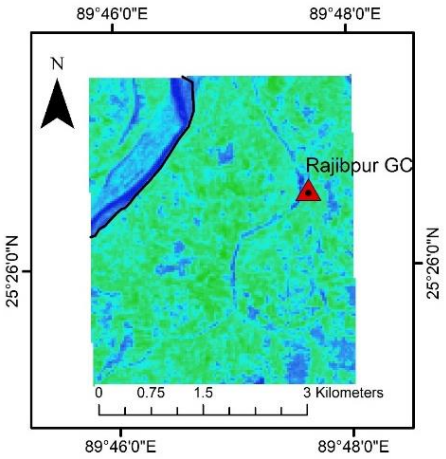

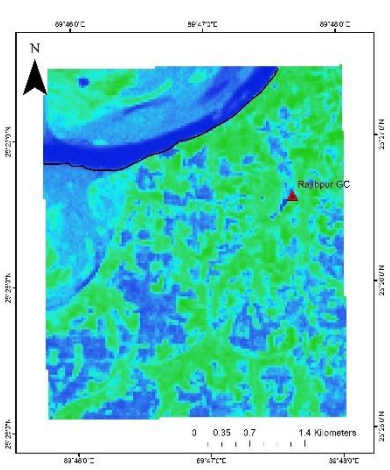

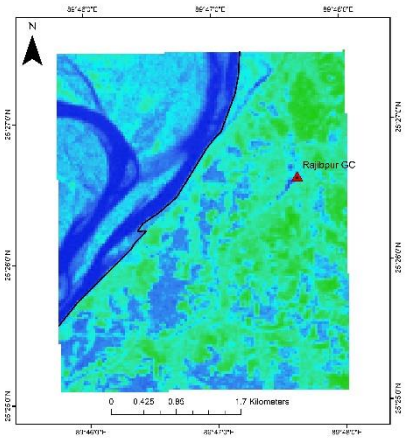

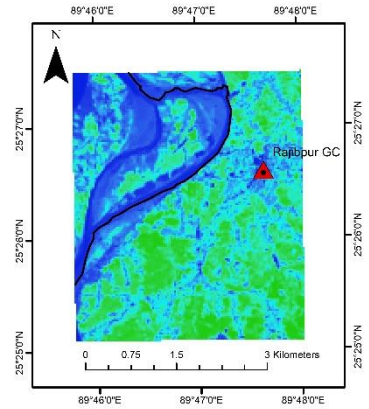

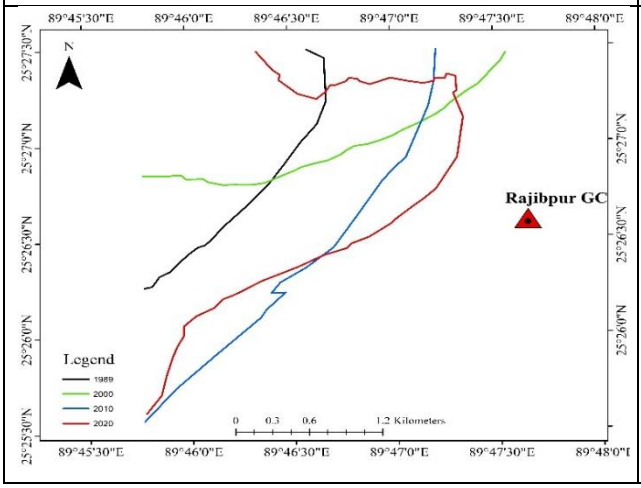

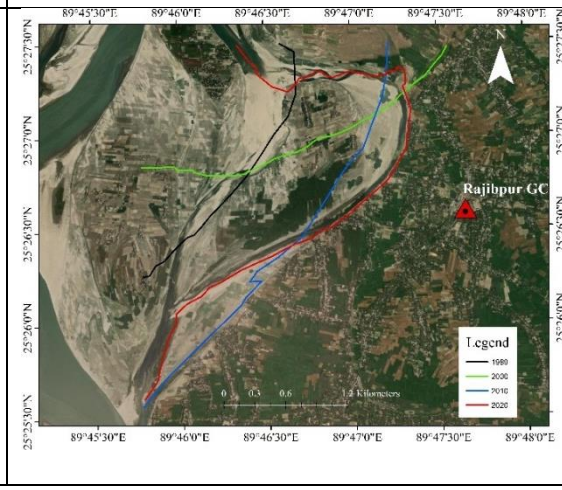

Market-90: Balagram Bazar in Jaldhaka Upazila of Nilphamari District

- Flood Risk: The market is located in a **Low** flood-risk area, considering the inundation patterns of all major floods in recent times.
- Bank Erosion Risk: Based on planform analysis using historical satellite images, the market is located in the **Low** bank erosion risk area.

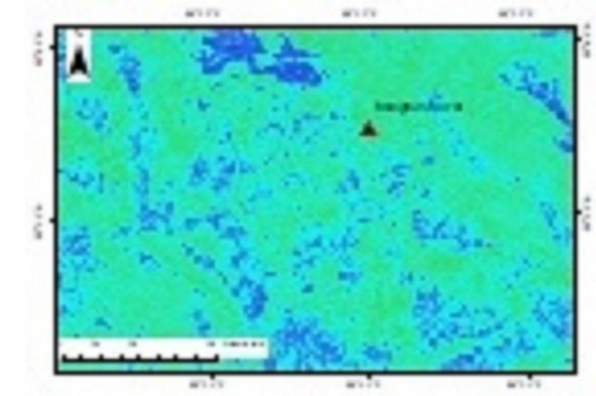

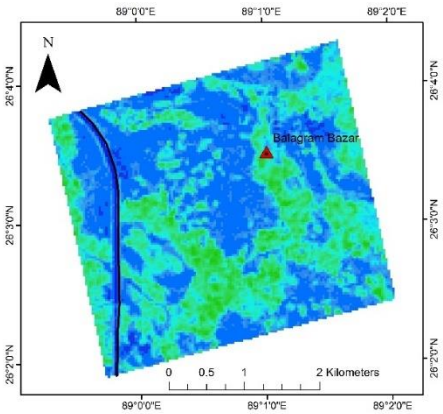

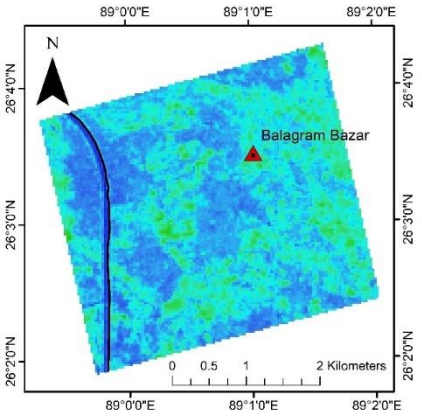

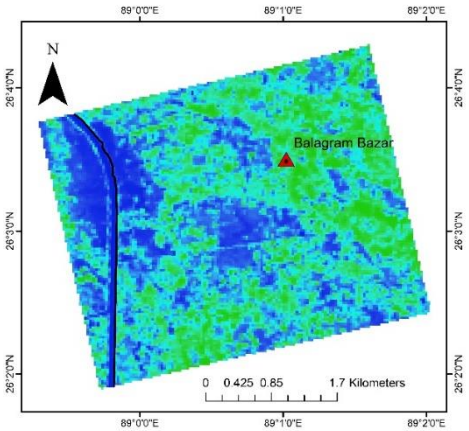

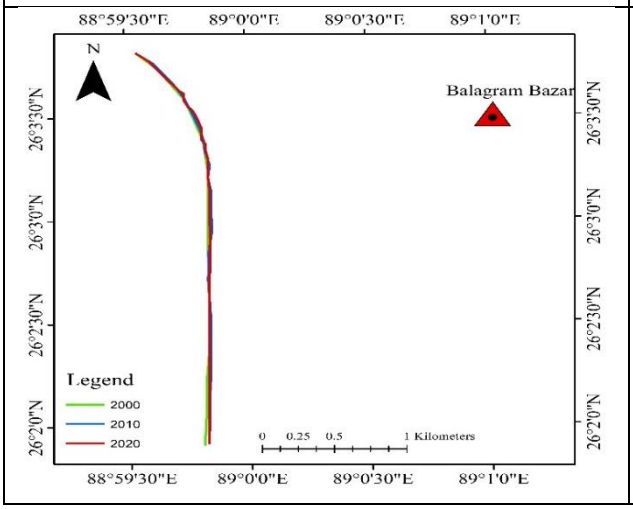

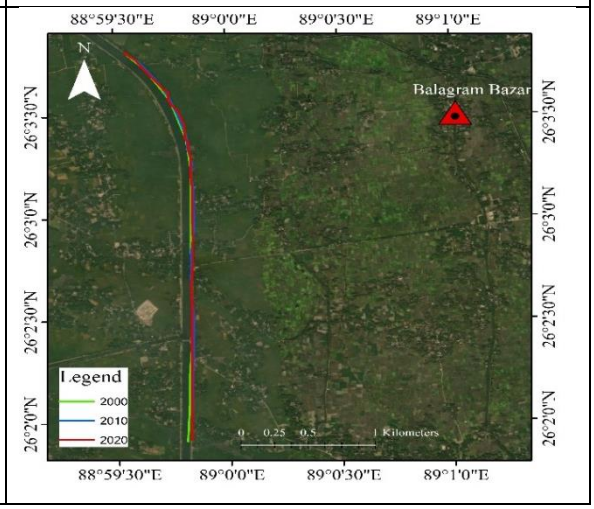

Market-91: Bhabonchur Bazar in Jaldhaka Upazila of Nilphamari District

- Flood Risk: The market is located in a **Low** flood-risk area, considering the inundation patterns of all major floods in recent times.
- Bank Erosion Risk: Based on planform analysis using historical satellite images, the market is located in the **Moderate** bank erosion risk area.

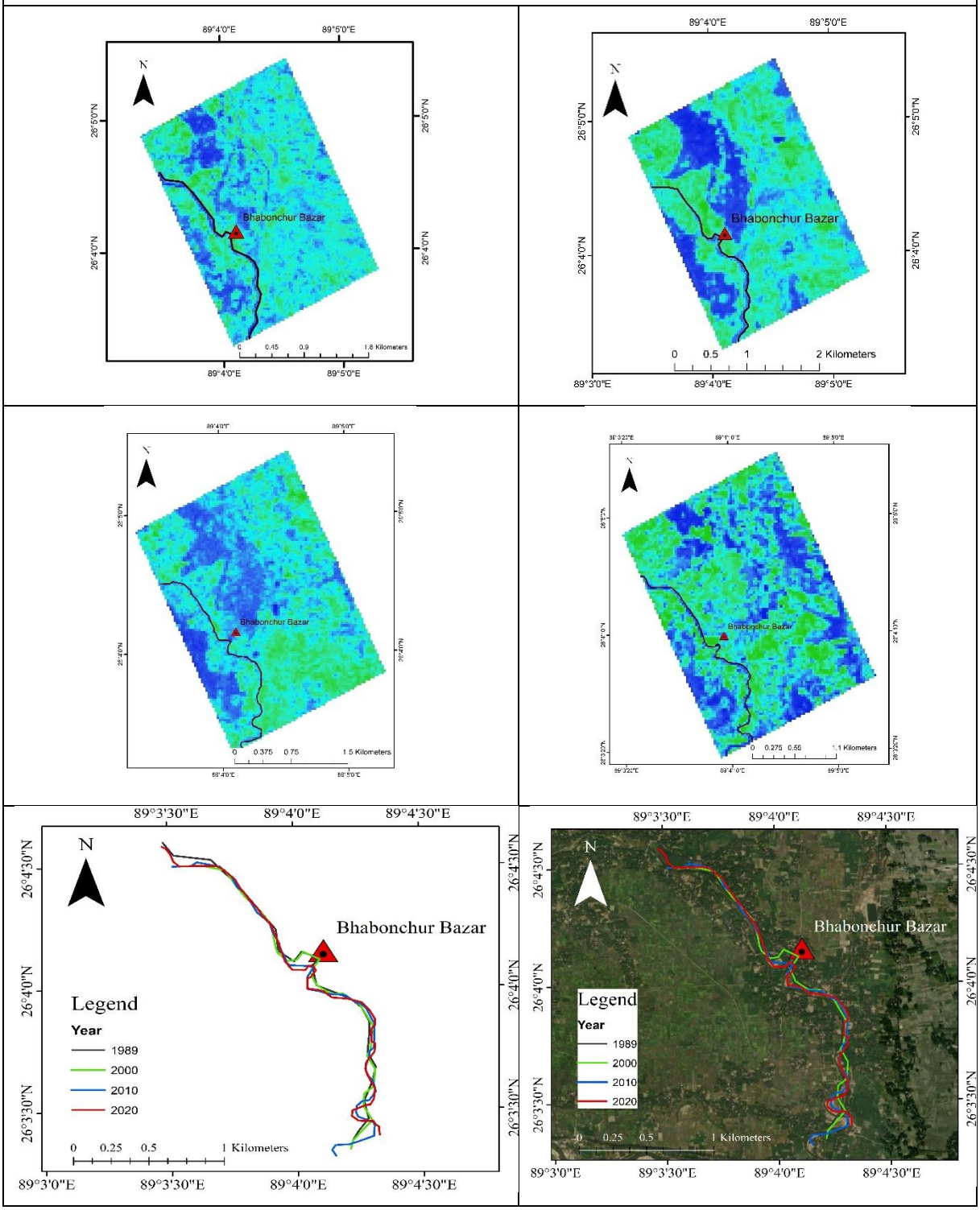

Market-92: Dakligonj Hat Bazar in Jaldhaka Upazila of Nilphamari District

- Flood Risk: The market is located in a **Low** flood-risk area, considering the inundation patterns of all major floods in recent times.
- Bank Erosion Risk: Based on planform analysis using historical satellite images, the market is located in the **High** bank erosion risk area.

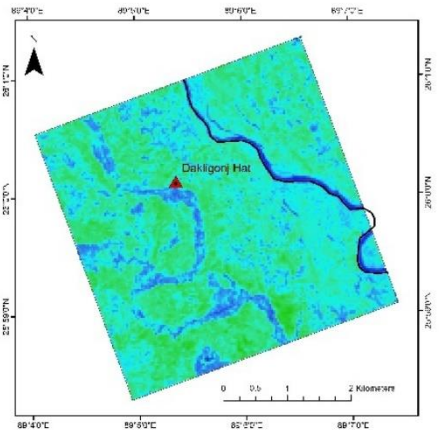

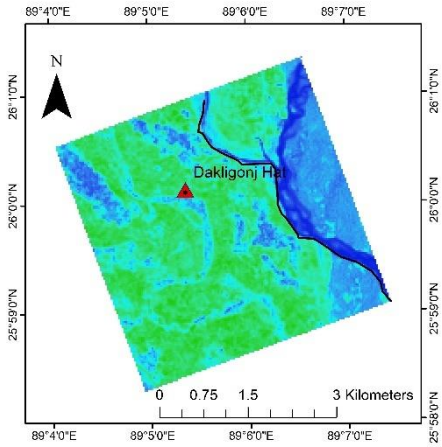

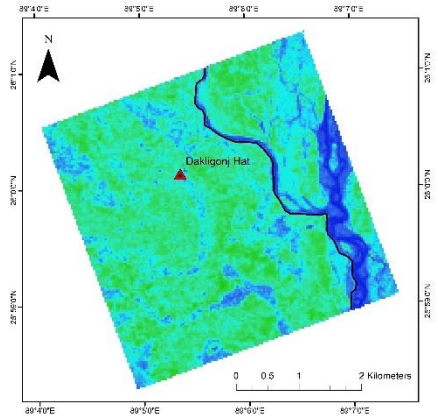

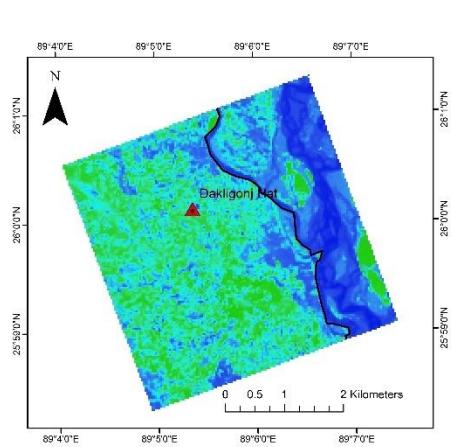

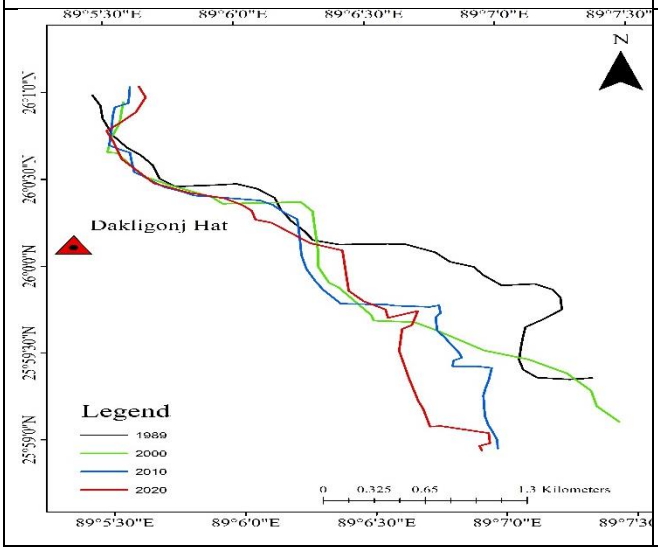

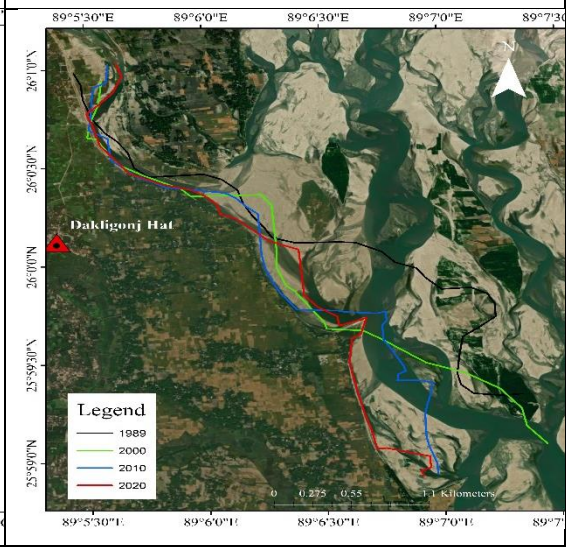

Market-93: Goulmunda Bazar in Jaldakha Upzila of Nilphamari District

- Flood Risk: The market is located in a **Low** flood-risk area, considering the inundation patterns of all major floods in recent times.
- Bank Erosion Risk: Based on planform analysis using historical satellite images, the market is located in the **High** bank erosion risk area.

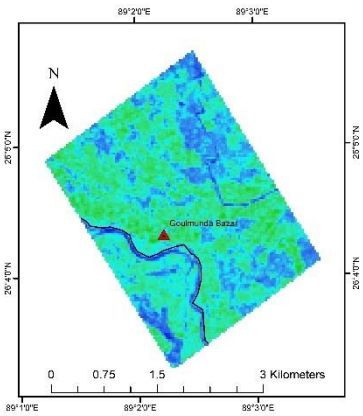

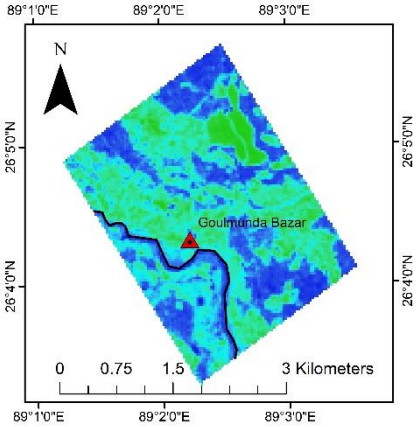

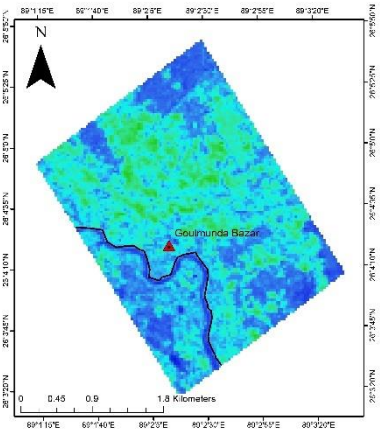

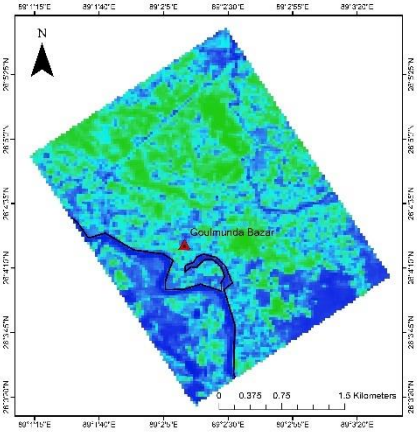

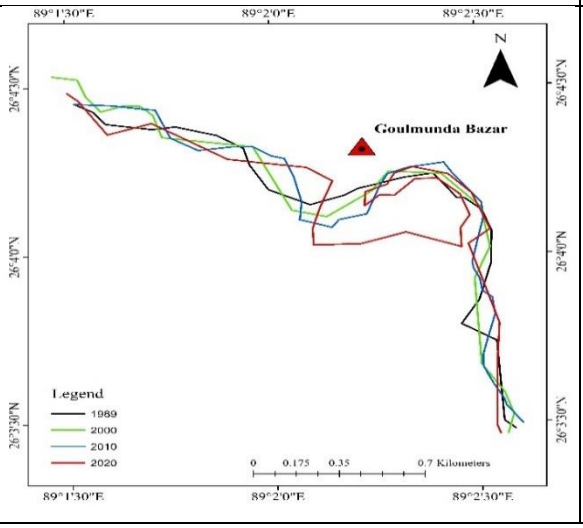

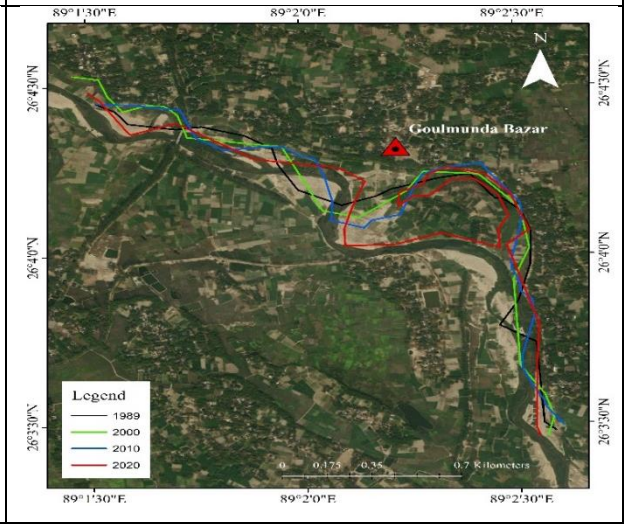

Market-94: Kaligonj Bangha Bandhu Bazar in Jaldakha Upzila of Nilphamari District

- Flood Risk: The market is located in a **Low** flood-risk area, considering the inundation patterns of all major floods in recent times.
- Bank Erosion Risk: Based on planform analysis using historical satellite images, the market is located in the **Low** bank erosion risk area.

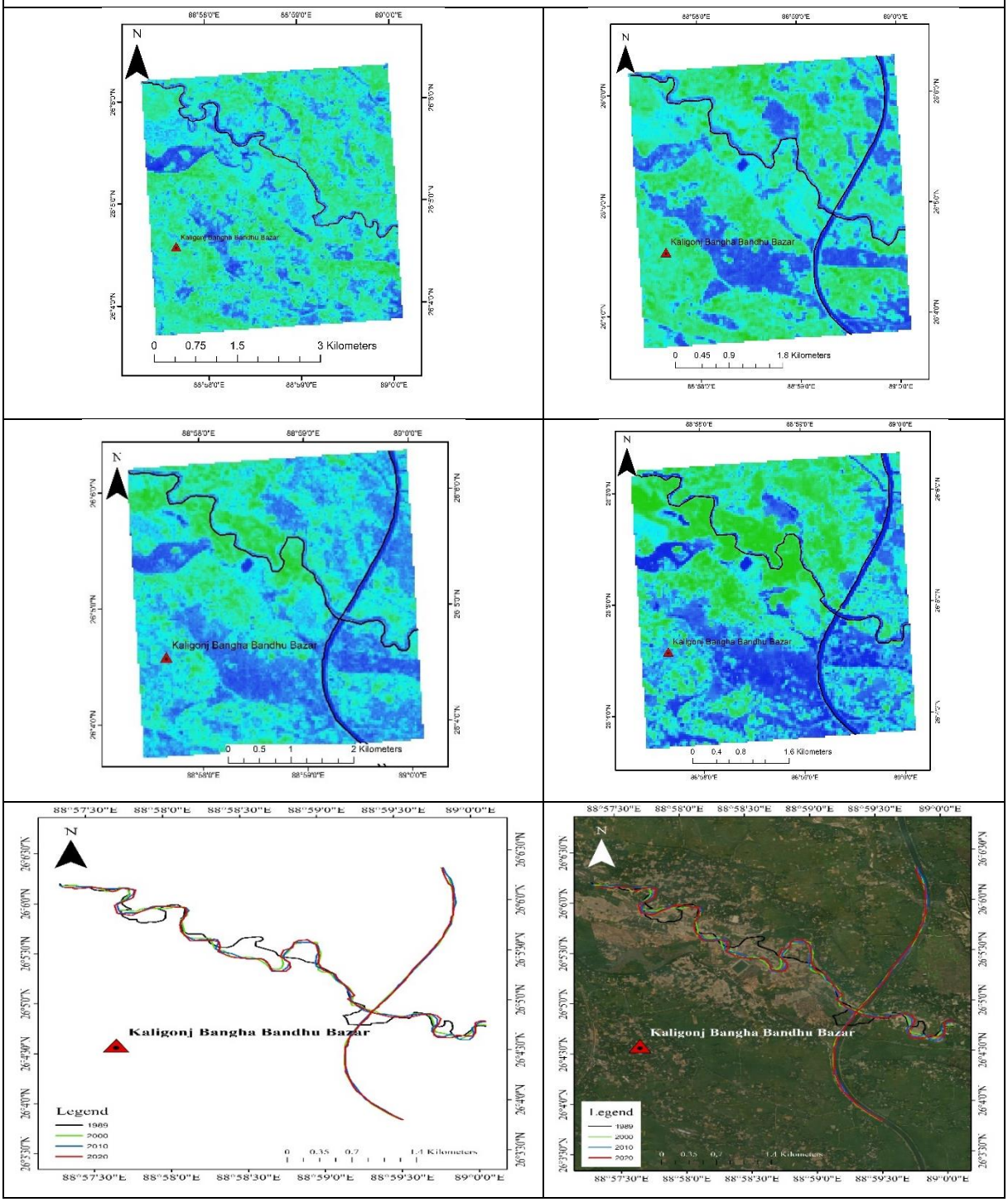

Market-95: Kathali Nayer Hat in Jaldhaka Upazila of Nilphamari District

- Flood Risk: The market is located in a **Low** flood-risk area, considering the inundation patterns of all major floods in recent times.
- Bank Erosion Risk: Based on planform analysis using historical satellite images, the market is located in the **Low** bank erosion risk area.

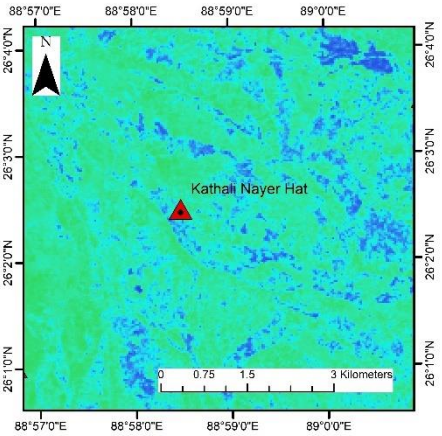

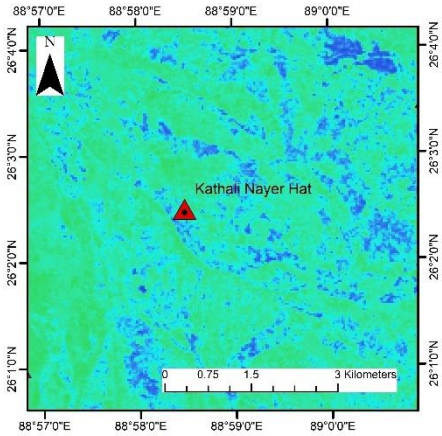

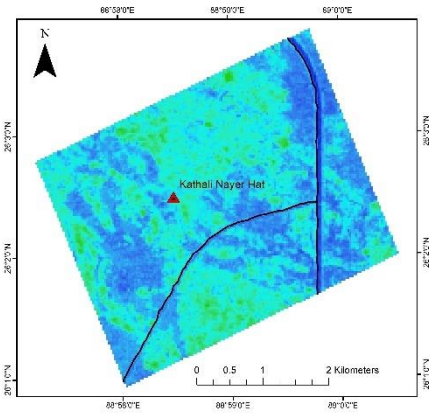

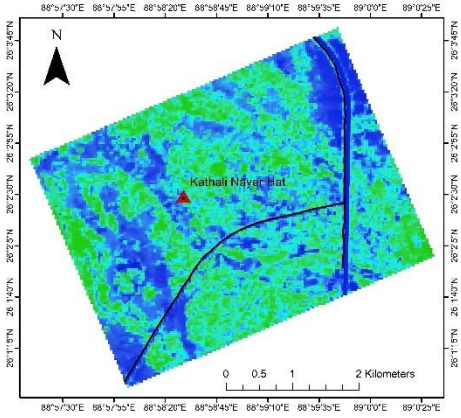

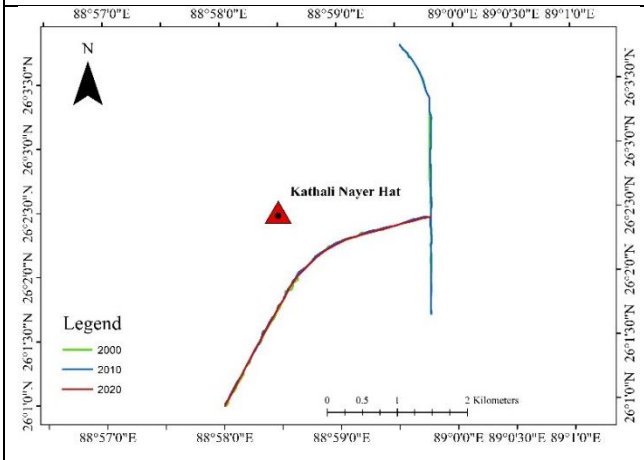

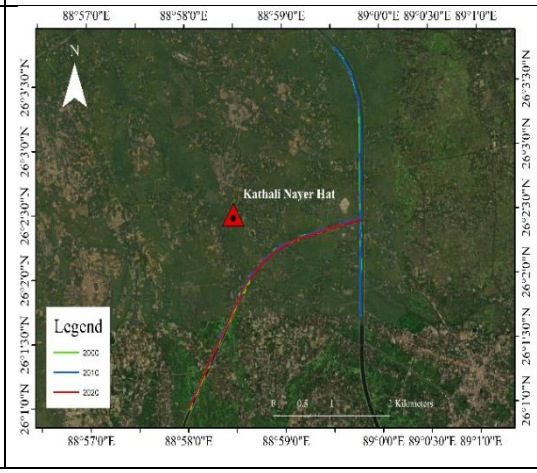

Market-96: Pathanpara Hat in Jaldhaka Upazila of Nilphamari District

- Flood Risk: The market is located in a **Low** flood-risk area, considering the inundation patterns of all major floods in recent times.
- Bank Erosion Risk: Based on planform analysis using historical satellite images, the Market is located in the **Low** bank erosion risk area.

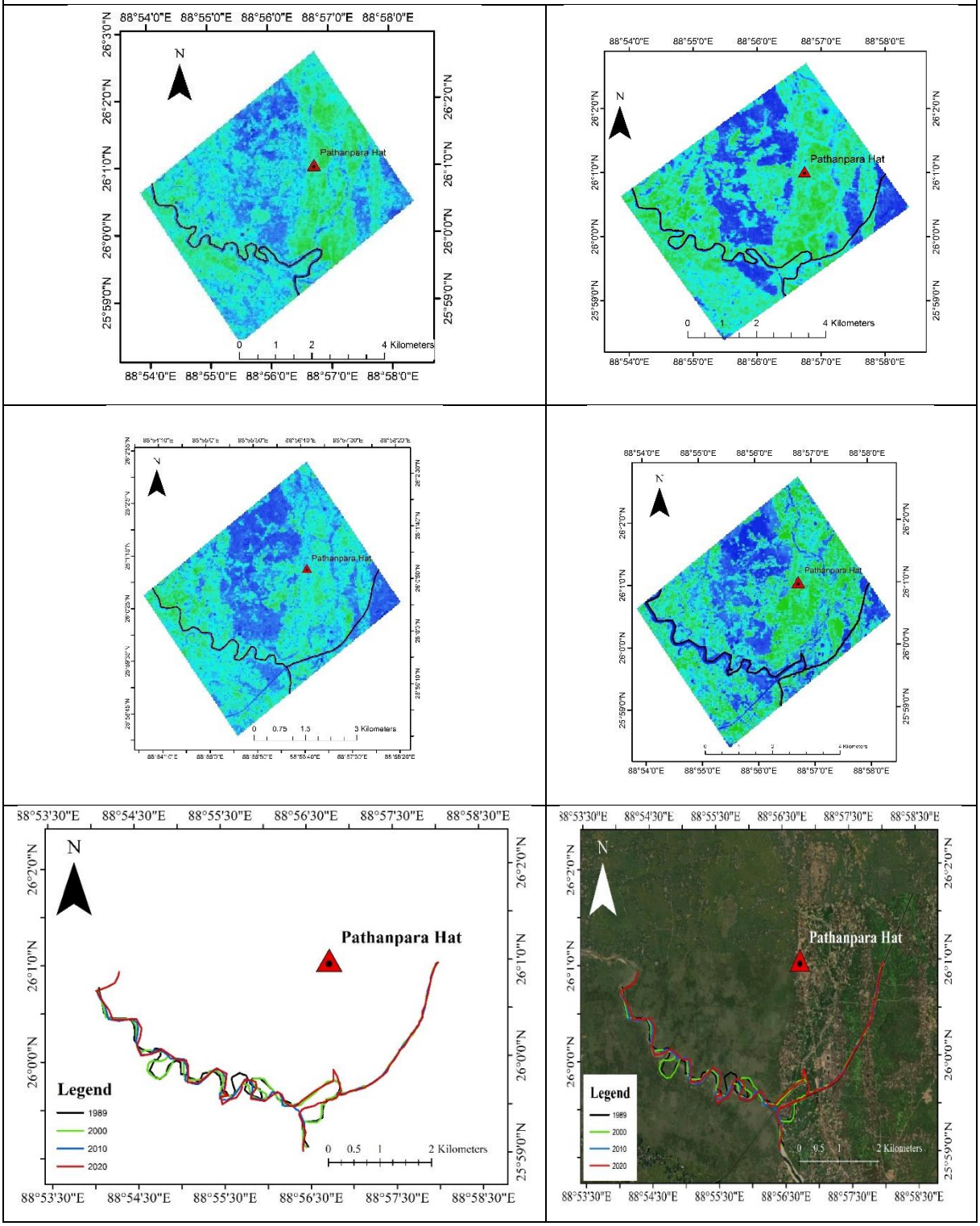

Market-97: Shibur Hat in Jaldhaka Upazila of Nilphamari District

- Flood Risk: The market is located in a **Low** flood-risk area, considering the inundation patterns of all major floods in recent times.
- Bank Erosion Risk: Based on planform analysis using historical satellite images, the Market is located in the **Low** bank erosion risk area.

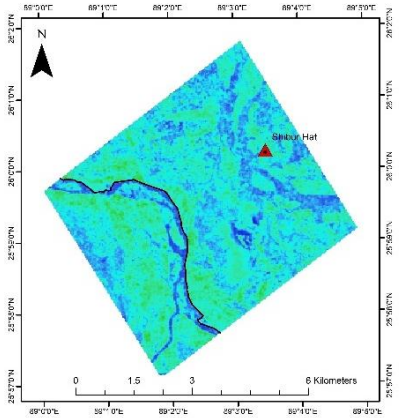

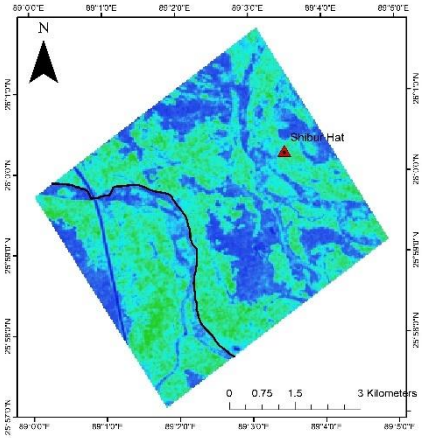

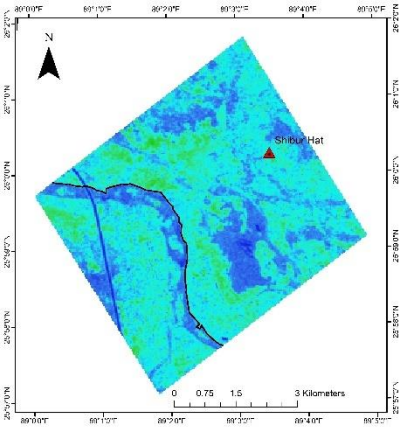

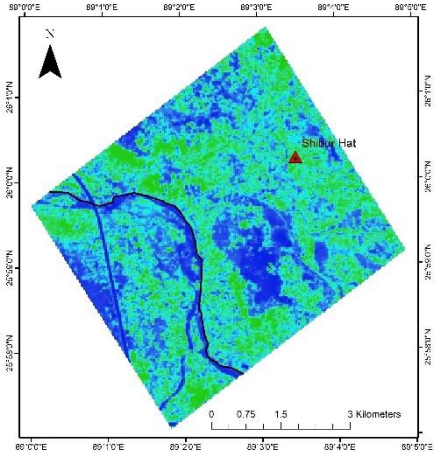

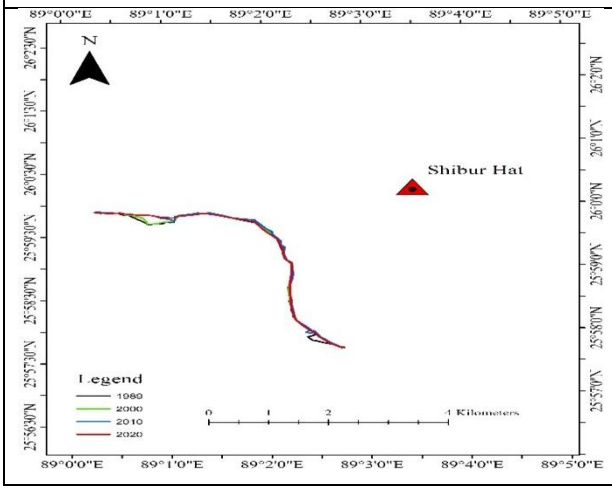

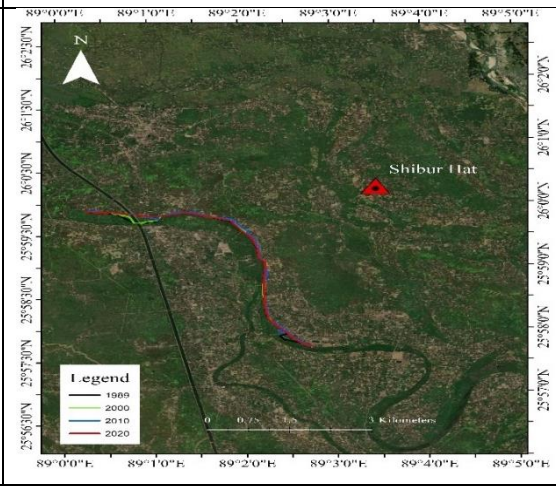

Market-98: Tunirhat in Dimla Upzila of Nilphamari District

- Flood Risk: The market is located in a **Low** flood-risk area, considering the inundation patterns of all major floods in recent times.
- Bank Erosion Risk: Based on planform analysis using historical satellite images, the Market is located in the **Low** bank erosion risk area.

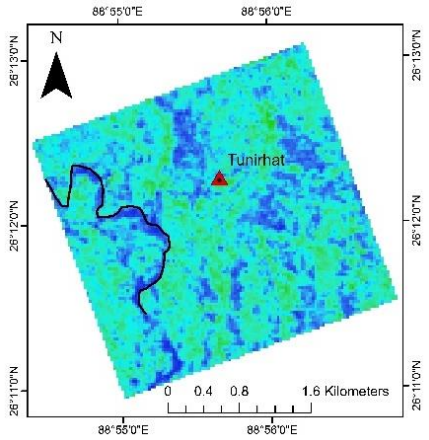

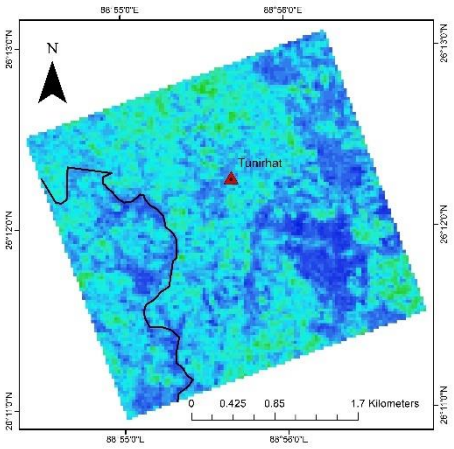

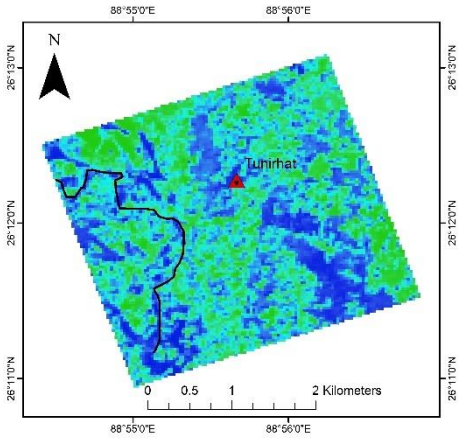

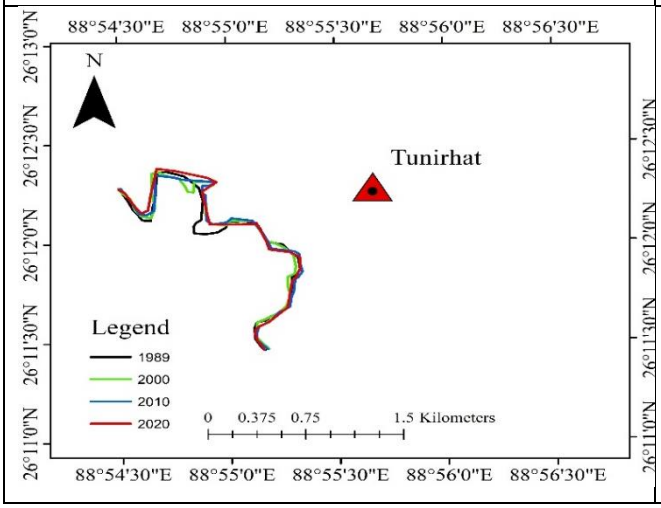

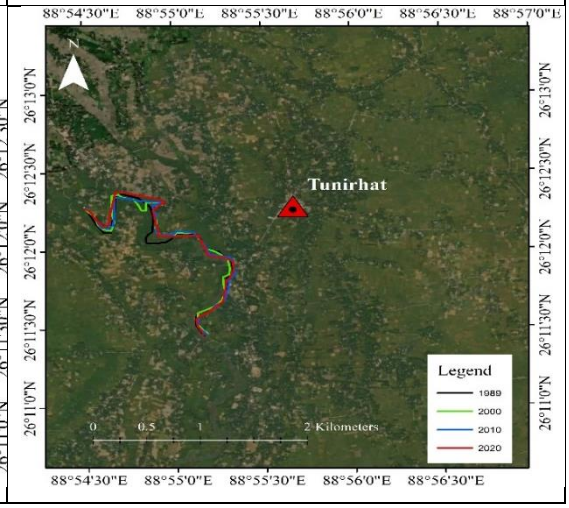

CHAPTER SIX
FLOOD FREQUENCY ANALYSIS

6.1 Introduction

Flood frequency analysis plays a vital role in the estimation of the recurrence of floods which can be applied in various planning activities regarding flood adaptation techniques, flood-resilient communities, and flood mitigation. Flood frequency analysis is used to relate the magnitude of extreme hydrologic events to their frequency of occurrence through the use of probability distribution functions. Historical records provide essential information to predict the recurrence interval of hydrological extremes. In this study, flood frequency analysis of water level data was conducted at 17 river stations which have been mentioned in the following section. Later it was used to generate design water levels corresponding to different return periods.

Using annual maximum water level data of a particular river station which has been available for a number of years, various types of flood frequency analysis are operated to compute statistical information for producing frequency distribution graphs. After choosing the probability distribution that best fits the annual maxima data, flood frequency curves are plotted. These graphs are then used to estimate the hydrologic design values for specific return periods, which can be used for hydrologic planning purposes. A few assumptions are made, which are - provided data are space and time-independent, identically distributed, and uninfluenced by natural or human activities that might have impacts on the existing hydrological system (Rao and Hamed, 2000). This analysis estimates the recurrence interval of extreme events by extrapolating beyond the length of the record. Obviously, the longer the available data, the more accurate the estimations are.

Overall, flood frequency estimates are a very important tool while working on designing various infrastructures under this project. Proper estimation of flood frequency assists in designing safe flood-resilient infrastructures as well as in reducing economic losses due to the maintenance of structures.

6.2 Flood Frequency Analysis

6.2.1 Selected Stations for Frequency Analysis

Flood frequency analysis has been conducted in 17 stations of 8 rivers which are mentioned below and shown in Figure 6.1.

1. Jamuna River: Noonkhawa (SW45), Chilmari (SW45.5), Bahadurabad (SW46.9L), Sirajganj (SW49)
2. Teesta River: Kaliganj (SW293), Kaunia (SW294), Haripur (SW294.5)
3. Dudhkumar River: Pateswari (SW81)
4. Dharala River: Taluk-Simulbari (SW76), Kurigram (SW77)
5. Ghaghat River: Jafarganj (SW96A), Gaibandha (SW97)
6. Bangali River: Mohimganj (SW155), Simulbari (SW10)
7. Old Brahmaputra River: Jamalpur (SW255)
8. Jhenai River: Offtake Jhenai (SW134B), Baushi Bridge (SW134A)

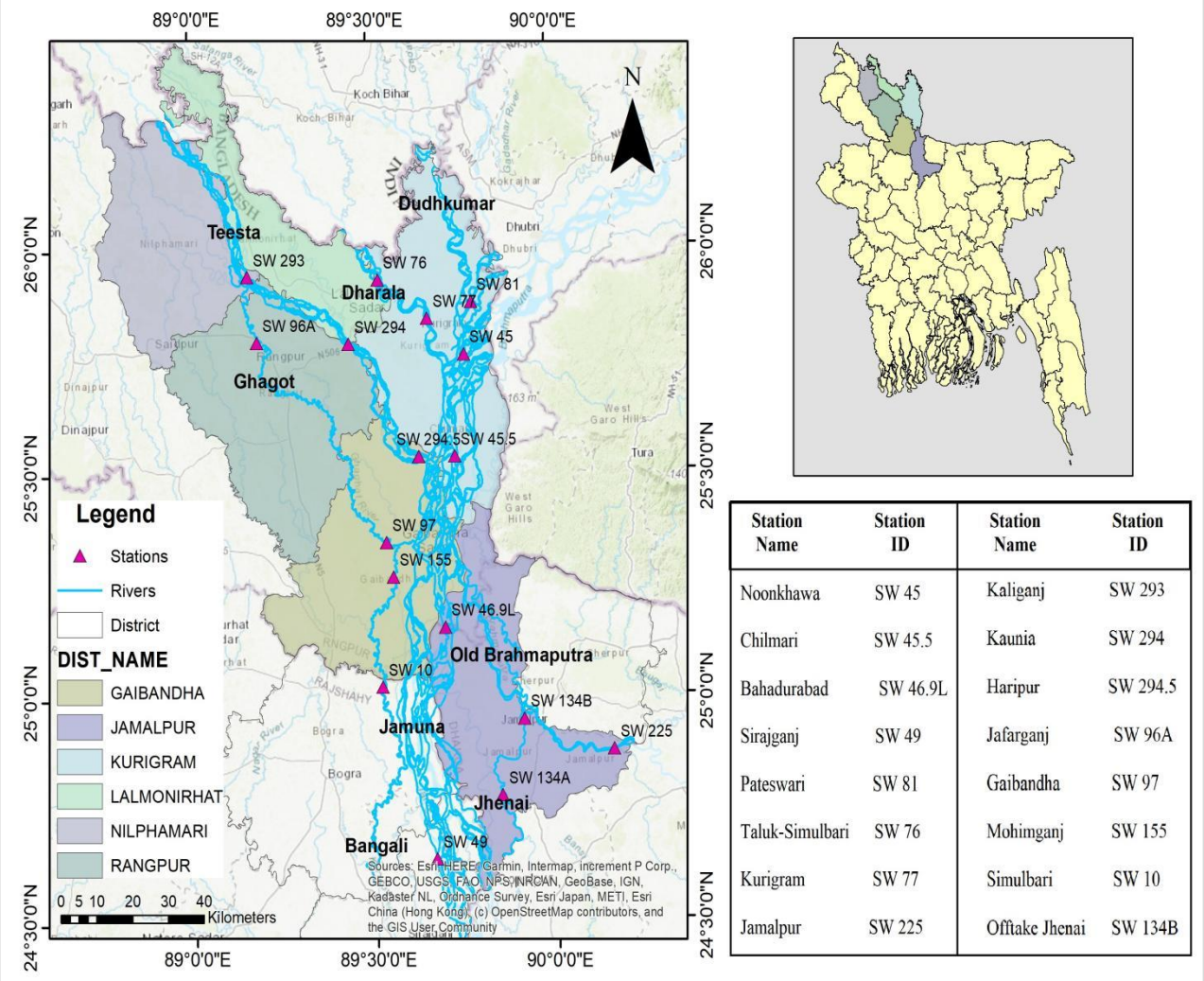

Station Name	Station ID	Station Name	Station ID
Noonkhawa	SW 45	Kaliganj	SW 293
Chilmari	SW 45.5	Kaunia	SW 294
Bahadurabad	SW 46.9L	Haripur	SW 294.5
Sirajganj	SW 49	Jafarganj	SW 96A
Pateswari	SW 81	Gaibandha	SW 97
Taluk-Simulbari	SW 76	Mohimganj	SW 155
Kurigram	SW 77	Simulbari	SW 10
Jamalpur	SW 225	Offtake Jhenai	SW 134B

Figure 6.1: Selected stations for Frequency analysis.

6.2.2 Methods of Frequency Analysis

Frequency analysis of a hydrologic event refers to the probability of a similar type (equaled or exceeded) of an event occurring in any year, which is also known as exceedance probability, P(F), and the reciprocal value of P(F) is the return period T in years.

Usually, frequency analysis is performed in two ways: one is the analytical approach, and the other is the graphical approach. The basis of Analytical frequency analysis fits the probability distributions with provided data. Several distributions are available to "fit" the plotted data from existing river gauge data (Linsley et al., 1988). In this study, six widely used methods have been selected for conducting the frequency analysis for the given data of previously mentioned river stations. The methods which have been applied are the following:

1. 2-Parameter Log-Normal (LN2)
2. 3-Parameter Log-Normal (LN3)
3. Pearson Type III (P3)
4. Log Pearson Type III (LP3)
5. Gumbel Distribution (Gumbel)
6. Generalized Extreme Value (GEV)

Table 6.1: Brief descriptions of Frequency analysis

Distribution Name	Brief Description	Equations
2-Parameter Log-Normal (LN2)	- This distribution is based on 2parameters. - The log transformation of the variable produces normal distribution. - Maximum likelihood is applied for best fitting (Stedinger, 1980).	$Y = \ln X$ $\bar{Y} = \frac{1}{n}\sum_{i=1}^{n} Y_i$ $S_y = \frac{1}{n}\sum_{i=1}^{n}(Y_i - \bar{Y})^2$ $Z_t = \frac{(1-\frac{1}{T})^{0.135} - (\frac{1}{T})^{0.135}}{0.1975}$
3-Parameter Log-Normal (LN2)	- One additional parameter, the lower bound parameter, is introduced compared to LN2. - Lower bound parameter and log transformation are used for producing normal distribution.	$d = \frac{x_{\max} x_{\min} - x^2_{med}}{x_{\max} + x_{\min} - 2x_{med}}$ $Y = \ln(X - d)$
Pearson Type III (P3)	- This distribution is fitted by using the product moment of data (Pilgrim, 1987).	$\bar{X} = \frac{1}{n}\sum_{i=1}^{n} X_i$

Distribution Name	Brief Description	Equations
	- Based on 3 parameters. Skewness is considered in this distribution. - Estimation of flood magnitude is done using frequency factor (K_t)	$S_x = \frac{1}{n}\sum_{i=1}^{n}(X_i - \bar{X})^2$ $C_s = \frac{n}{(n-1)(n-2)}\sum_{i=1}^{n}\frac{(X_i - \bar{X})^3}{S^3{}_x}$
Log Pearson Type III (LP3)	- Similar to P3 distribution only difference is it's applied in the logarithmic version.	(similar equations as P3 but using logarithmic version)
Gumbel Distribution (Gumbel)	- Based on cumulative distribution function, which consists of 2 parameters mainly (Greenwood 1979). - This distribution is most widely used worldwide.	$a = \frac{2b_1 - b_o}{\ln 2}$ $d = b_0 - \in$ $u_t = -\ln[-\ln(1-\frac{1}{T})]$
Generalized Extreme Value (GEV)	- This distribution incorporates EV1, EV2, and EV3 distributions for maxima. - Consist of location parameter (b_0), scale parameter (b_1), shape parameter(b_2).	$k = 0.859C + 2.955C^2$ $c = \frac{2b_1 - b_0}{2b_1 - b_0}\frac{\ln 2}{\ln 3}$ $d = b_0 + \frac{a[\sqrt{(1+k)} - 1]}{k}$ $a = \frac{(2b_1 - b_0)k}{\Gamma(1+k)(1-2^k)}$

6.2.3 Selection of Suitable Method

In order to select the optimum design water level to prevent overestimating or underestimating, it is mandatory to use statistical tools to conduct goodness of fit analysis. With the help of goodness of fit, the best suitable frequency distribution is selected from the existing statistical distributions such as Gumbel, LN2, LN3, P3, LP3, and GEV.

The goodness of fit refers to the process of describing how well the statistical model can estimate values compared to observed data sets. The goodness of fit was conducted using three statistical parameters, and finally, a combined ranking system was developed where the values of each statistical parameter were arranged in either ascending or descending order according to their properties. The statistical parameters that have been used are the following:

1. Probability Plot Correlation Coefficient (PPCC)
2. Root Mean Square Deviation (RMSD)

3. Chi-square test (χ^2)

Table 6.2: Statistical parameters used for goodness of fit of the PDFs.

Statistical Parameter	**Equation**	**Remarks**
Probability Plot Correlation Coefficient (PPCC)	$\frac{\sum_{i=1}^{n}(X_i - X_{avg})(Y_i - Y_{avg})}{\sqrt{(\sum_{i=1}^{n}(X_i - X_{avg})^2 \sum_{i=1}^{n}(Y_i - Y_{avg})^2)}}$	The ranking has been done in descending order.
Root Mean Square Deviation (RMSD)	$\sqrt{\sum_{i=1}^{n}\frac{(X_i - X_{obs})^2}{n}}$	The ranking has been done in ascending order.
Chi-square test (χ^2)	$\sum_{i=1}^{n}\frac{(X_{obs} - X_i)^2}{X_i}$	The ranking has been done in ascending order.

** Here, X_i = Estimated value, X_{obs} = Observed value, X_{avg} = Average value of observed data, n = Sample size.

6.3 Design Flood Frequency

The hydrologic analysis involves frequency analysis with different probability distribution functions for the selected design return period where historical annual peak water level and discharge data at appropriate locations are available. Six probability distribution functions (PDFs) viz. 2-Parameter Log-Normal (LN2), 3-Parameter Log-Normal (LN3), Pearson Type III (P3), Log Pearson Type III (LP3), Gumbel (EV1), and General Extreme Value (GEV) were used for frequency analysis. The PDFs were tested based on probability plot correlation coefficient (PPCC) (Filliben, 1975), Chi-square test, Root-mean-square-Deviation (RMSD) & goodness-of-fit study based on these parameters (Stedinger et al., 1993). Finally, a combined ranking system was developed, and the least total ranking was chosen as the best-fitted PDFs.

6.3.1 Flood Frequency analysis for Jamuna River

Water level data of 4 stations (SW 45, SW 45.5, SW 46.9L, SW 49) were selected in the Jamuna River for frequency analysis. The best-fitted PDFs for each station have been determined by developing a combined ranking system using the values of RMSD, PPCC, and Chi-square, which have been shown in Table 6.3 - 6.5, and the corresponding distributions have been shown in Figure 6.2.

Table 6.3: Fitted PDFs and the corresponding values of PPCC, RMSD, and Chi-square for the maximum water level of Jamuna River at Noonkhawa.

	PPCC	Ranking	RMSD	Ranking	Chi-square	Ranking	Remarks
LN2	0.994235997	4	0.004566082	4	0.006500305	4	**P3 selected**
LN3	0.994903868	3	0.004138425	3	0.005895079	3	
P3	**0.995223484**	**1**	**0.003931455**	**1**	**0.00559973**	**1**	
LP3	0.995175157	2	0.003959379	2	0.005640198	2	
Gumbel	0.965621846	5	0.02527676	5	0.035737857	5	
GEV	0.911269881	6	0.363924988	6	0.501313964	6	

Table 6.4: Fitted PDFs and the corresponding values of PPCC, RMSD, and Chi-square for the maximum water level of Jamuna River at Chilmari.

	PPCC	Ranking	RMSD	Ranking	Chi-square	Ranking	Remarks
LN2	0.942694319	6	0.049769675	5	0.076576458	5	**Gumbel selected**
LN3	0.965499567	3	0.03032598	2	0.04614953	2	
P3	0.962015768	5	0.033307824	4	0.051473013	4	
LP3	0.963912359	4	0.03168122	3	0.048787323	3	
Gumbel	**0.966111866**	**1**	**0.029774452**	**1**	**0.045315827**	**1**	
GEV	0.965603753	2	0.318998421	6	0.501788008	6	

Table 6.5: Fitted PDFs and the corresponding values of PPCC, RMSD, and Chi-square for the maximum water level of Jamuna River at Bahadurabad.

	PPCC	Ranking	RMSD	Ranking	Chi-square	Ranking	Remarks
LN2	0.996321348	4	0.00221319	4	0.004363329	4	**LP3 selected**
LN3	0.996376948	2	0.002175167	3	0.004304793	3	
P3	0.99637483	3	0.002156248	2	0.004285576	2	
LP3	**0.996394851**	**1**	**0.0021493**	**1**	**0.004271877**	**1**	
Gumbel	0.981332444	5	0.010082322	5	0.020105425	5	
GEV	0.93379355	6	0.239959886	6	0.455976987	6	

Table 6.6: Fitted PDFs and the corresponding values of PPCC, RMSD, and Chi-square for the maximum water level of Jamuna River at Sirajganj.

	PPCC	Ranking	RMSD	Ranking	Chi-square	Ranking	Remarks
LN2	0.996863104	4	0.002175646	4	0.006121676	4	**P3 selected**
LN3	0.997308234	3	0.001954989	3	0.005396078	3	
P3	**0.99744212**	**1**	**0.001886225**	**1**	**0.005278993**	**1**	
LP3	0.99738058	2	0.00191589	2	0.00537204	2	
Gumbel	0.973056566	5	0.016533318	5	0.045990107	5	
GEV	0.863443818	6	0.308849539	6	0.806661437	6	

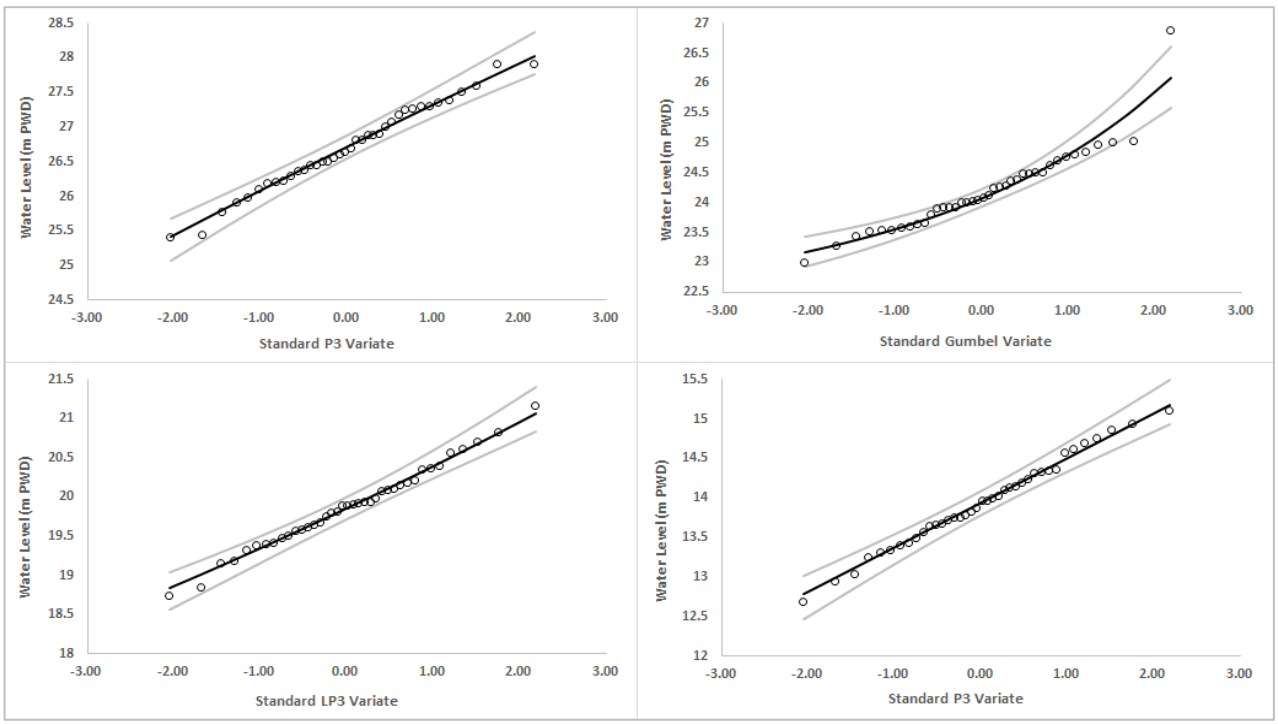

Figure 6.2. Probability plot along with 90% confidence interval of the P3, Gumbel, LP3, and P3 distribution fitted to the annual maximum water level data of the Jamuna River at Noonkhawa, Chilmari, Bahadurabad, and Sirajganj.

6.3.2 Flood Frequency analysis for Dudhkumar River

Water level data of 1 station (SW 81) were selected in the Dudhkumar River for frequency. The best-fitted PDFs for each station have been determined by developing a combined ranking system using the values of RMSD, PPCC, and Chi-square, which have been shown in Table 6.7, and the corresponding distributions have been shown in Figure 6.3.

Table 6.7: Fitted PDFs and the corresponding values of PPCC, RMSD, and Chi-square for the maximum water level of Dudhkumar River at Pateswari.

	PPCC	Ranking	RMSD	Ranking	Chi-square	Ranking	Remarks
LN2	0.992392311	4	0.004882558	4	0.006358008	4	**LN3 selected**
LN3	**0.993171851**	**1**	**0.004473573**	**1**	**0.005816337**	**1**	
P3	0.993126661	2	0.00450054	2	0.005854404	2	
LP3	0.993109764	3	0.004508568	3	0.00586556	3	
Gumbel	0.965591189	5	0.020942079	5	0.026949311	5	
GEV	0.927232745	6	0.291258377	6	0.365786498	6	

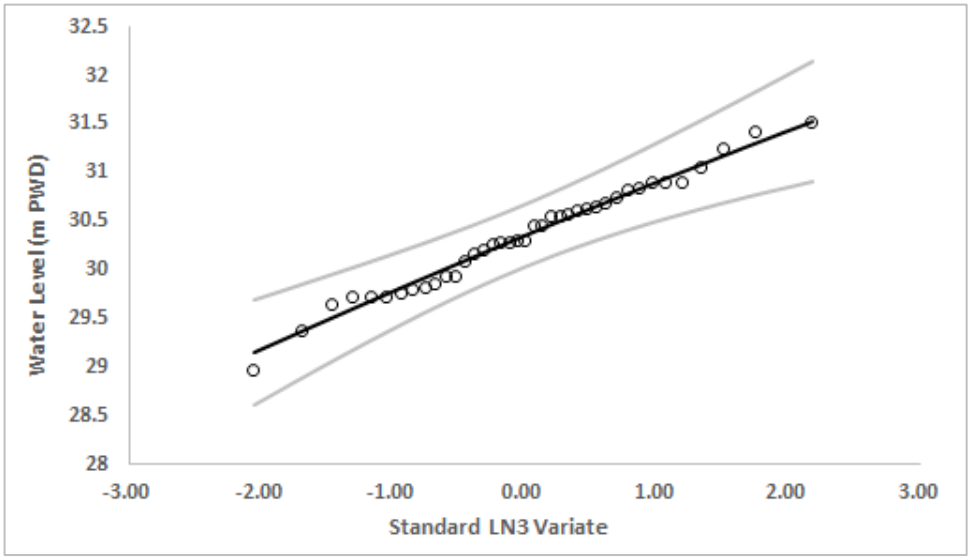

Figure 6.3: Probability plot along with 90% confidence interval of the LP3 distribution fitted to the annual maximum water level data of the Dudhkumar River at Pateswari.

6.3.3 Flood Frequency analysis for Dharala River

Water level data of 2 stations (SW 76, SW 77) were selected in the Dharala River for frequency analysis. The best-fitted PDFs for each station have been determined by developing a combined ranking system using the values of RMSD, PPCC, and Chi-square, which have been shown in Table 6.8 - 6.9, and the corresponding distributions have been shown in Figure 6.4.

Table 6.8: Fitted PDFs and the corresponding values of PPCC, RMSD, and Chi-square for the maximum water level of the Dharala River at Taluk-Simulbari.

	PPCC	Ranking	RMSD	Ranking	Chi-square	Ranking	Remarks
LN2	0.976680938	4	0.007917486	4	0.009733102	4	**P3 selected**
LN3	0.986631581	3	0.004859773	3	0.005991916	3	
P3	**0.989710804**	**1**	**0.003784218**	**1**	**0.004649612**	**1**	
LP3	0.989630502	2	0.003805381	2	0.004674913	2	
Gumbel	0.928133011	5	0.023837811	5	0.02914773	5	
GEV	0.897013257	6	0.16511151	6	0.198167245	6	

Table 6.9: Fitted PDFs and the corresponding values of PPCC, RMSD, and Chi-square for the maximum water level of the Dharala River at Kurigram.

	PPCC	Ranking	RMSD	Ranking	Chi-square	Ranking	Remarks
LN2	0.973802643	4	0.017952315	4	0.02588117	4	**LN3 selected**
LN3	**0.992512437**	**1**	**0.005689895**	**1**	**0.008306381**	**1**	
P3	0.991400527	2	0.006498251	2	0.009474412	2	
LP3	0.991306302	3	0.006529827	3	0.009521185	3	
Gumbel	0.916165008	5	0.056161711	5	0.080687836	5	
GEV	0.845206347	6	0.37899522	6	0.531504519	6	

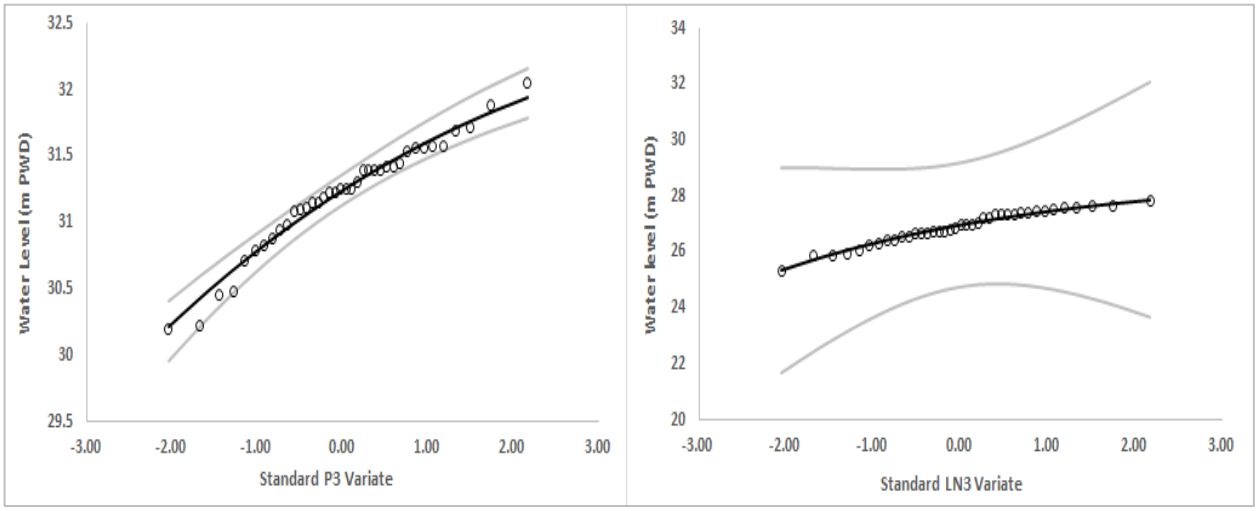

Figure 6.4: Probability plot along with 90% confidence interval of the P3, LN3 distribution fitted to the annual maximum water level data of the Dharala River at Taluk-Simulbari and Kurigram.

6.3.4 Flood Frequency analysis for Teesta River

Water level data of 3 stations (SW 293, SW 294, SW 294.5) were selected in the Teesta River for frequency analysis. The best-fitted PDFs for each station have been determined by developing a combined ranking system using the values of RMSD, PPCC, and Chi-square, which have been shown in Table 6.10 - 6.12, and the corresponding distributions have been shown in Figure 6.5.

Table 6.10: Fitted PDFs and the corresponding values of PPCC, RMSD, and Chi-square for the maximum water level of Teesta River at Kaliganj.

	PPCC	Ranking	RMSD	Ranking	Chi-square	Ranking	Remarks
LN2	0.922938239	4	0.05216281	4	0.044160504	4	**P3 selected**
LN3	0.984844491	3	0.01430873	3	0.012334514	3	
P3	**0.985383836**	**1**	**0.012062778**	**1**	**0.010382195**	**1**	
LP3	0.985199483	2	0.01209853	2	0.010410997	2	
Gumbel	0.84298606	5	0.103915576	5	0.087504324	5	
GEV	0.798811429	6	0.36514634	6	0.302383862	6	

Table 6.11: Fitted PDFs and the corresponding values of PPCC, RMSD, and Chi-square for the maximum water level of Teesta River at Kaunia.

	PPCC	Ranking	RMSD	Ranking	Chi-square	Ranking	Remarks
LN2	0.987028316	4	0.006816729	4	0.008914919	4	**LN3 selected**
LN3	**0.995477434**	**1**	**0.002618419**	**1**	**0.003462632**	**1**	
P3	0.99500334	2	0.002965789	2	0.00389947	2	
LP3	0.99490708	3	0.003000693	3	0.003944254	3	
Gumbel	0.939935097	5	0.030464056	5	0.039809737	5	
GEV	0.891377367	6	0.268510618	6	0.344971841	6	

Table 6.12: Fitted PDFs and the corresponding values of PPCC, RMSD, and Chi-square for the maximum water level of Teesta River at Haripur.

	PPCC	Ranking	RMSD	Ranking	Chi-square	Ranking	Remarks
LN2	0.875032774	3	0.448889154	4	0.416081687	4	**LN3 selected**
LN3	**0.875843621**	**1**	**0.442880289**	**1**	**0.408982375**	**1**	
P3	0.875367998	2	0.444725148	2	0.411689746	3	
LP3	0.874122945	4	0.44707575	3	0.410029382	2	
Gumbel	0.86761614	5	0.466422585	5	0.439899143	5	
GEV	0.84011286	6	1.301892589	6	1.182922386	6	

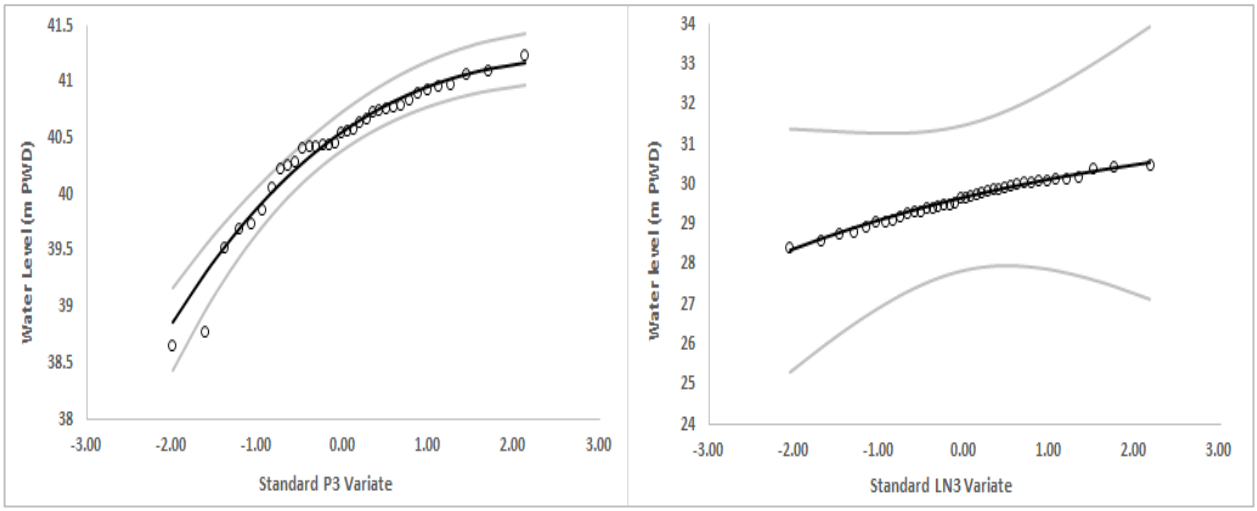

Figure 6.5: Probability plot along with 90% confidence interval of the P3, LN3 distribution fitted to the annual maximum water level data of the Teesta River at Kaliganj and Kaunia.

6.3.5 Flood Frequency analysis for Ghaghat River

Water level data of 2 stations (SW 96A, SW 97) were selected in the Ghaghat River for frequency analysis. The best-fitted PDFs for each station have been determined by developing a combined ranking system using the values of RMSD, PPCC, and Chi-square, which have been shown in Table 6.13 - 6.14, and the corresponding distributions have been shown in Figure 6.6.

Table 6.13: Fitted PDFs and the corresponding values of PPCC, RMSD, and Chi-square for the maximum water level of Ghaghat River at Jafarganj.

	PPCC	Ranking	RMSD	Ranking	Chi-square	Ranking	Remarks
LN2	0.973036249	4	0.043396489	4	0.042458618	4	**LN3 selected**
LN3	**0.976115204**	**1**	**0.038429215**	**1**	**0.038172515**	**1**	
P3	0.975523305	3	0.039286877	3	0.038996798	3	
LP3	0.97585573	2	0.038787652	2	0.038423814	2	
Gumbel	0.972807609	5	0.04385559	5	0.044267753	5	
GEV	0.950010304	6	0.643134175	6	0.627498462	6	

Table 6.14: Fitted PDFs and the corresponding values of PPCC, RMSD, and Chi-square for the maximum water level of the Ghaghat River at Gaibandha.

	PPCC	Ranking	RMSD	Ranking	Chi-square	Ranking	Remarks
LN2	0.978776917	4	0.012434522	4	0.021618858	4	**P3 selected**
LN3	0.988786243	3	0.006714339	3	0.011778581	3	
P3	**0.98946376**	**1**	**0.006564049**	**1**	**0.011539165**	**1**	
LP3	0.989426141	2	0.006568731	2	0.011552471	2	
Gumbel	0.930893526	5	0.039531255	5	0.068095734	5	
GEV	0.855436156	6	0.315969927	6	0.528213148	6	

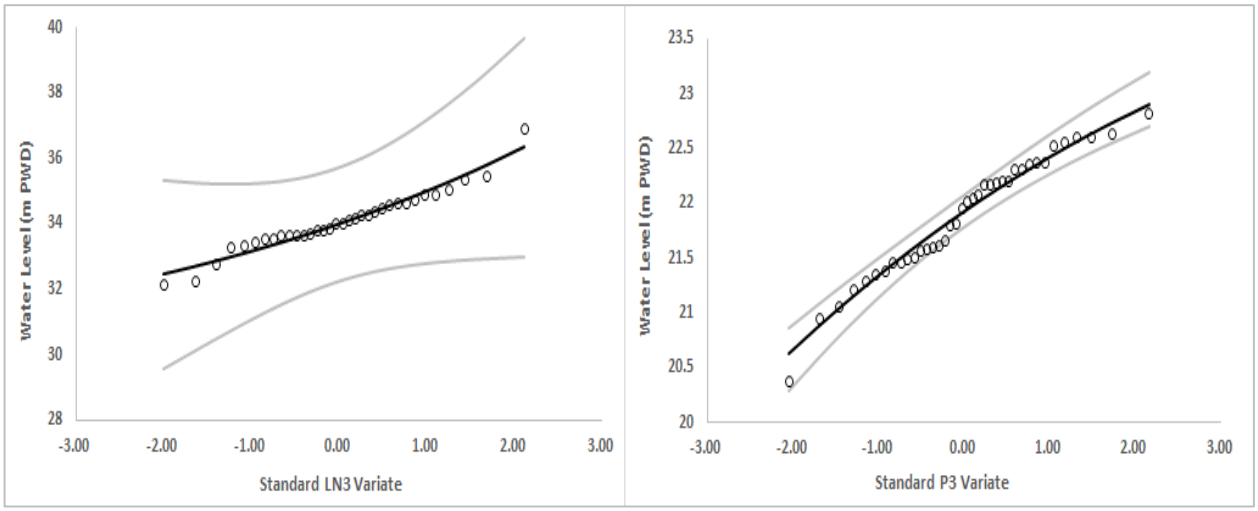

Figure 6.6: Probability plot along with 90% confidence interval of the LN3, P3 distribution fitted to the annual maximum water level data of the Ghaghat River at Jafarganj and Gaibandha.

6.3.6 Flood Frequency analysis for Old Brahmaputra

Water level data of 1 station (SW 225) were selected in the Old Brahmaputra River for frequency analysis. The best-fitted PDFs for each station have been determined by developing a combined ranking system using the values of RMSD, PPCC, and Chi-square, which have been shown in Table 6.15, and the corresponding distributions have been shown in Figure 6.7.

Table 6.15: Fitted PDFs and the corresponding values of PPCC, RMSD, and Chi-square for the maximum water level of the Old Brahmaputra River at Jamalpur.

	PPCC	Ranking	RMSD	Ranking	Chi-square	Ranking	Remarks
LN2	0.970629612	4	0.035902103	4	0.084316921	4	**LN3 selected**
LN3	**0.99362243**	**1**	**0.009549513**	**1**	0.023542709	2	
P3	0.993172124	2	0.009567068	2	**0.023517344**	1	
LP3	0.992978307	3	0.009645827	3	0.023698715	3	
Gumbel	0.915993643	5	0.100082427	5	0.233892899	5	
GEV	0.7362733	6	0.737641524	6	1.589948769	6	

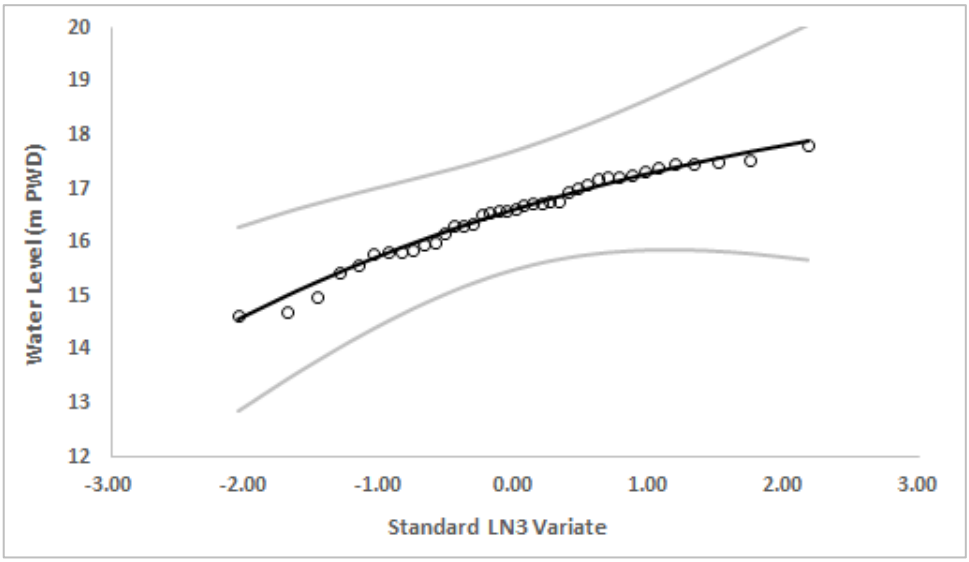

Figure 6.7: Probability plot along with 90% confidence interval of the LN3 distribution fitted to the annual maximum water level data of the Old Brahmaputra River at Jamalpur.

6.3.7 Flood Frequency analysis for Jhenai River

Water level data of 2 stations (SW 134A, SW134B) were selected in the Jhenai River for frequency analysis. The best-fitted PDFs for each station have been determined by developing a combined ranking system using the values of RMSD, PPCC, and Chi-square, which have been shown in Table 6.16 - 6.17, and the corresponding distributions have been shown in Figure 6.8.

Table 6.16: Fitted PDFs and the corresponding values of PPCC, RMSD, and Chi-square for the maximum water level of Jhenai River at Baushi Bridge.

	PPCC	Ranking	RMSD	Ranking	Chi-square	Ranking	Remarks
LN2	0.942605961	5	0.170530798	4	0.393741231	4	**P3 selected**
LN3	0.966593855	2	0.096729123	2	0.232388362	2	
P3	**0.968758544**	**1**	**0.091873498**	**1**	**0.212909759**	**1**	
LP3	0.963269911	3	0.10763111	3	0.241721689	3	
Gumbel	0.904172138	5	0.266425218	5	0.602826899	5	
GEV	0.68687911	6	1.241149489	6	2.442864044	6	

Table 6.17: Fitted PDFs and the corresponding values of PPCC, RMSD, and Chi-square for the maximum water level of Jhenai River at Offtake Jhenai.

	PPCC	Ranking	RMSD	Ranking	Chi-square	Ranking	Remarks
LN2	0.884720701	4	0.519099292	4	1.035682224	4	**P3 selected**
LN3	0.978461353	2	0.108321202	2	0.258047758	3	
P3	**0.980251392**	**1**	**0.101481336**	**1**	**0.235228466**	**1**	
LP3	0.977018273	3	0.111370179	3	0.250031808	2	
Gumbel	0.822765585	5	0.697803706	5	1.395777211	5	
GEV	0.530420889	6	2.063268533	6	3.679218921	6	

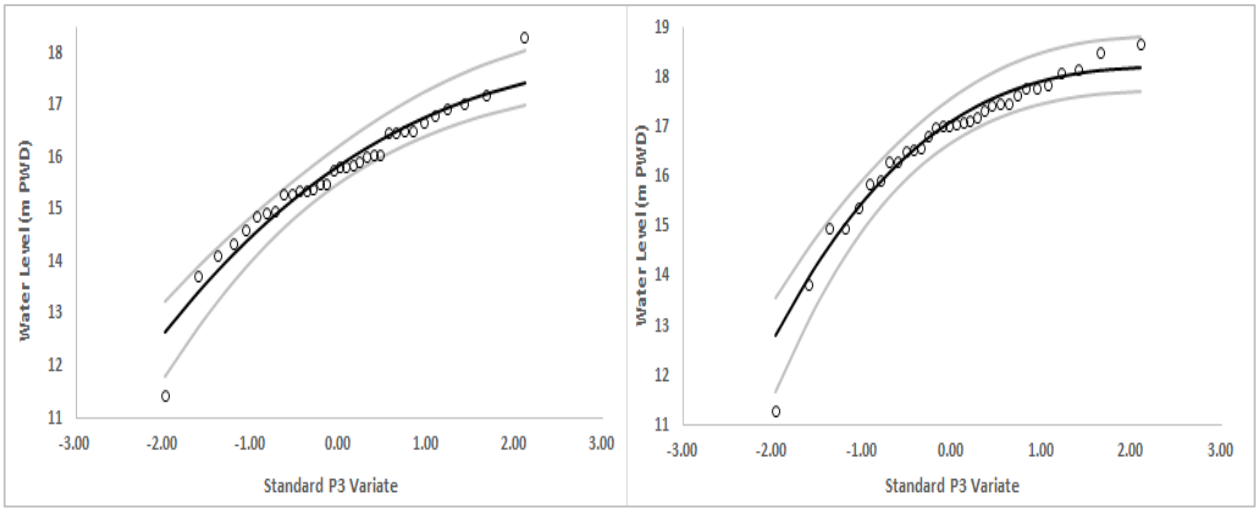

Figure 6.8: Probability plot along with 90% confidence interval of the P3 distribution fitted to the annual maximum water level data of the Jhenai River at Baushi Bridge and Offtake Jhenai.

6.3.8 Flood Frequency analysis for Bangali River

Water level data of 4 stations (SW 155, SW 10) were selected in the Bangali River for frequency analysis. The best-fitted PDFs for each station have been determined by developing a combined ranking system using the values of RMSD, PPCC, and Chi-square, which have been shown in Table 6.18 - 6.19, and the corresponding distributions have been shown in Figure 6.9.

Table 6.18: Fitted PDFs and the corresponding values of PPCC, RMSD, and Chi-square for the maximum water level of the Bangali River at Mohimganj.

	PPCC	Ranking	RMSD	Ranking	Chi-square	Ranking	Remarks
LN2	0.953853051	3	0.035591055	4	0.077980476	4	**P3 selected**
LN3	0.97266245	4	0.02146702	3	0.04701153	3	
P3	**0.976174654**	**1**	**0.018880099**	**1**	**0.040672682**	**1**	
LP3	0.975513834	2	0.019383118	2	0.041629923	2	
Gumbel	0.906726906	5	0.070244405	5	0.152856223	5	
GEV	0.823976608	6	0.387154099	6	0.793121953	6	

Table 6.19: Fitted PDFs and the corresponding values of PPCC, RMSD, and Chi-square for the maximum water level of Bangali River at Simulbari.

	PPCC	Ranking	RMSD	Ranking	Chi-square	Ranking	Remarks
LN2	0.959370256	4	0.03504707	4	0.08010243	5	**P3 selected**
LN3	0.980130978	3	0.017748274	3	0.041079084	3	
P3	**0.981531923**	**1**	**0.016732427**	**1**	**0.038104473**	**1**	
LP3	0.980551638	2	0.017583847	2	0.039800283	2	
Gumbel	0.955688085	5	0.03525805	5	0.07406565	4	
GEV	0.813275631	6	0.444948229	6	0.929955868	6	

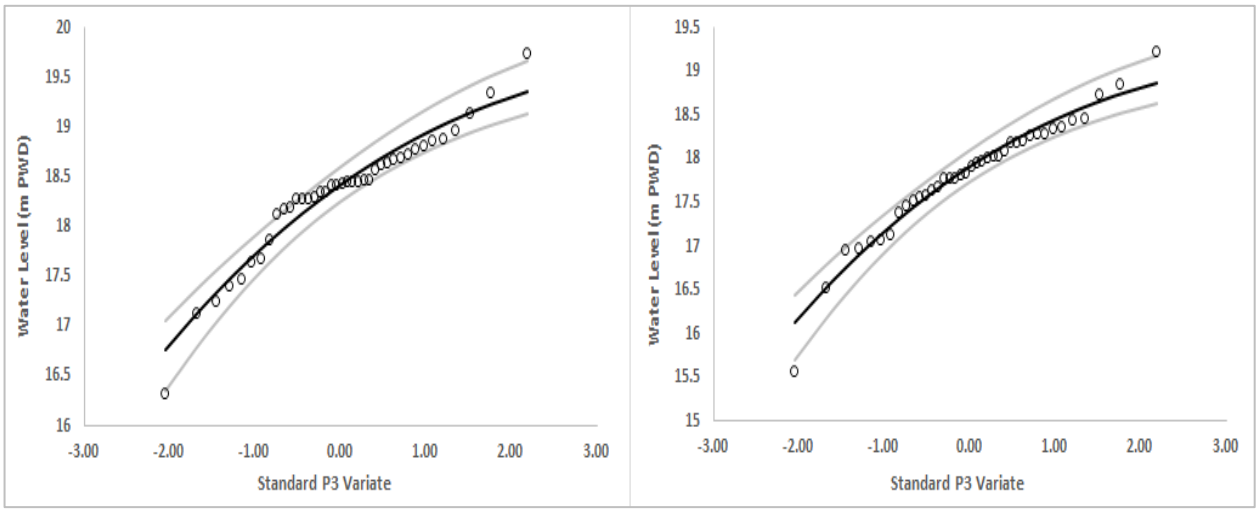

Figure 6.9: Probability plot along with 90% confidence interval of the P3 distribution fitted to the annual maximum water level data of the Bangali River at Mohimganj and Simulbari.

6.4 Design Water-level for Various Return Periods

In this section, the design water level has been computed using the selected PDF, which was best fitted for each station. The design water level has been generated for 2.33, 10, 25, 50, and 100-year return periods, which has been provided in Table 6.20. The design water level corresponding to various return periods of all the stations has been presented in Figure 6.10-6.17.

Table 6.20: Design Water-level for 2. 33, 10, 20, 50, 100-year Return Period.

River Name	Station Name	Station ID	Selected PDF	Historical Highest WL	Return Period					Difference (m)	Difference (m)
					2.33	10	20	50	100	100 & 10	100 & 20
Jamuna	Noonkhawa	SW 45	P3	27.92	26.83	27.50	27.72	27.96	28.12	0.62	0.40
Jamuna	Chilmari	SW 45.5	Gumbel	25.91	24.20	25.08	25.46	25.95	26.32	1.24	0.86
Jamuna	Bahadurabad	SW 46.9L	LP3	21.16	19.96	20.56	20.76	21.00	21.16	0.60	0.40
Jamuna	Sirajganj	SW 49	P3	15.11	14.04	14.67	14.88	15.11	15.26	0.59	0.38
Dudhkumar	Pateswari	SW 81	LP3	31.52	30.46	31.06	31.26	31.47	31.61	0.55	0.35
Dharala	Taluk-Simulbari	SW 76	P3	32.05	31.32	31.71	31.81	31.92	31.99	0.28	0.18
Dharala	Kurigram	SW 77	LN3	27.82	27.08	27.58	27.71	27.84	27.92	0.34	0.21
Teesta	Dalia	SW291.5R	LN3	53.30	52.53	52.88	53.01	53.14	53.23	0.35	0.22
Teesta	Kaliganj	SW 293	P3	41.24	40.66	41.04	41.11	41.17	41.19	0.15	0.08
Teesta	Kaunia	SW 294	LN3	30.49	29.76	30.23	30.37	30.50	30.59	0.36	0.22
Ghagat	Jafarganj	SW 96A	LN3	35.43	34.15	35.3	35.74	36.26	36.64	1.34	0.90
Ghagat	Gaibandha	SW 97	P3	22.81	22.02	22.55	22.7	22.87	22.97	0.42	0.27
Old Brahmaputra	Jamalpur	SW 225	LN3	17.81	16.75	17.44	17.63	17.83	17.95	0.51	0.32
Jhenai	Offtake Jhenai	SW 134B	P3	18.67	17.33	18.05	18.14	18.20	18.25	0.20	0.11
Jhenai	Baushi Bridge	SW 134A	P3	18.30	16.07	17.01	17.23	17.51	17.68	0.67	0.45
Bangali	Mohimganj	SW 155	P3	19.74	18.54	19.07	19.2	19.33	19.41	0.34	0.21
Bangali	Simulbari	SW 10	P3	19.22	18.04	18.58	18.72	18.84	18.91	0.33	0.19

Historical highest water level information is available at the site of the infrastructure. In case the historical highest flood level information is not available, the highest water level of the recent severe floods in 2019 can be considered the historical highest flood level for practical purposes.

(a)

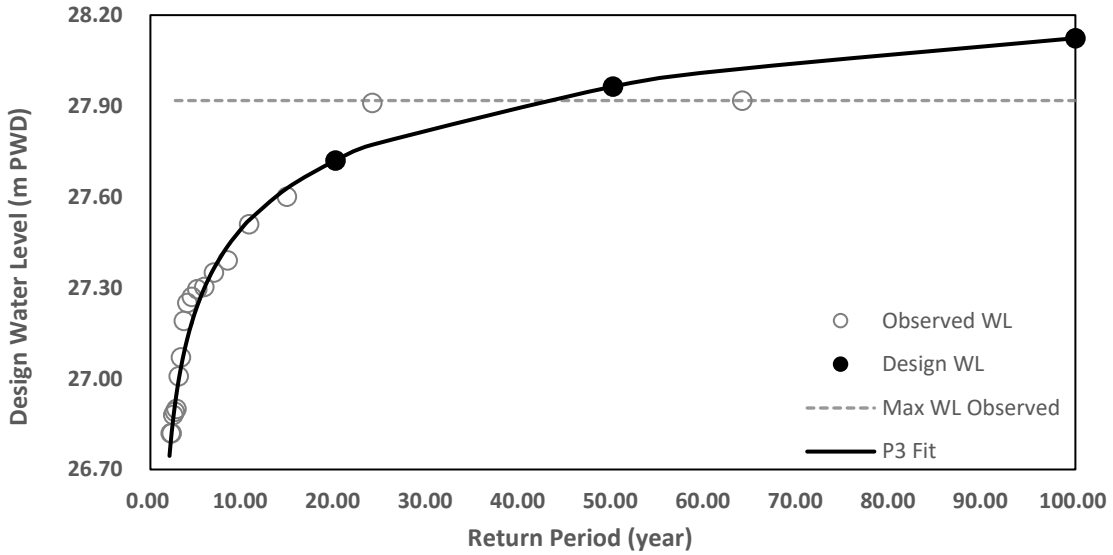
28.20
27.90
27.60
27.30
27.00
26.70
Design Water Level (m PWD)
0.00
10.00
20.00
30.00
40.00
50.00
60.00
70.00
80.00
90.00
100.00
Return Period (year)
Observed WL
Design WL
Max WL Observed
P3 Fit

(b)

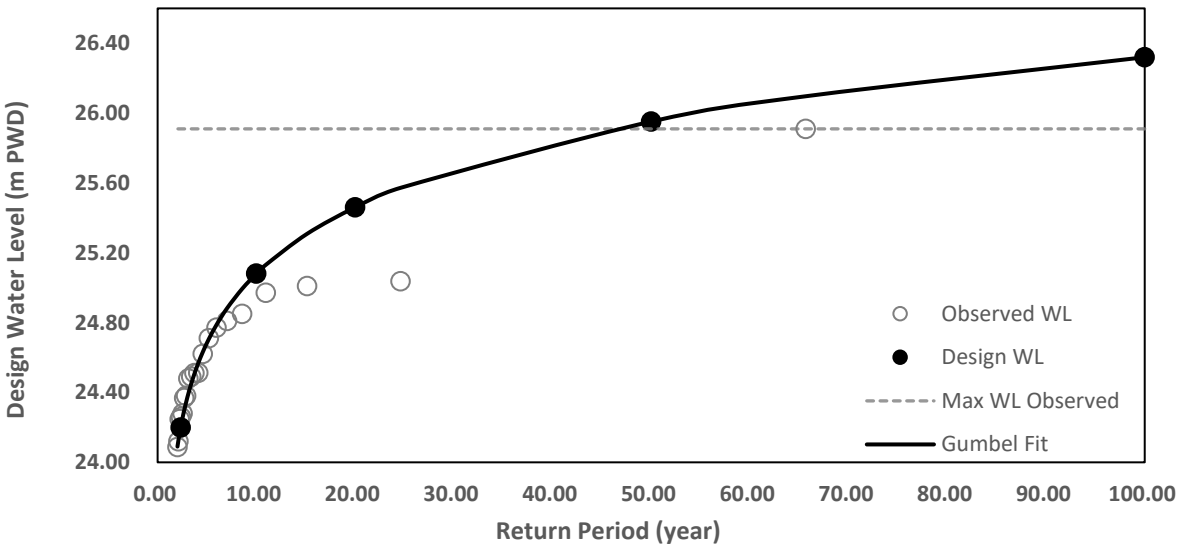
26.40
26.00
25.60
25.20
24.80
24.40
24.00
Design Water Level (m PWD)
0.00
10.00
20.00
30.00
40.00
50.00
60.00
70.00
80.00
90.00
100.00
Return Period (year)
Observed WL
Design WL
Max WL Observed
Gumbel Fit

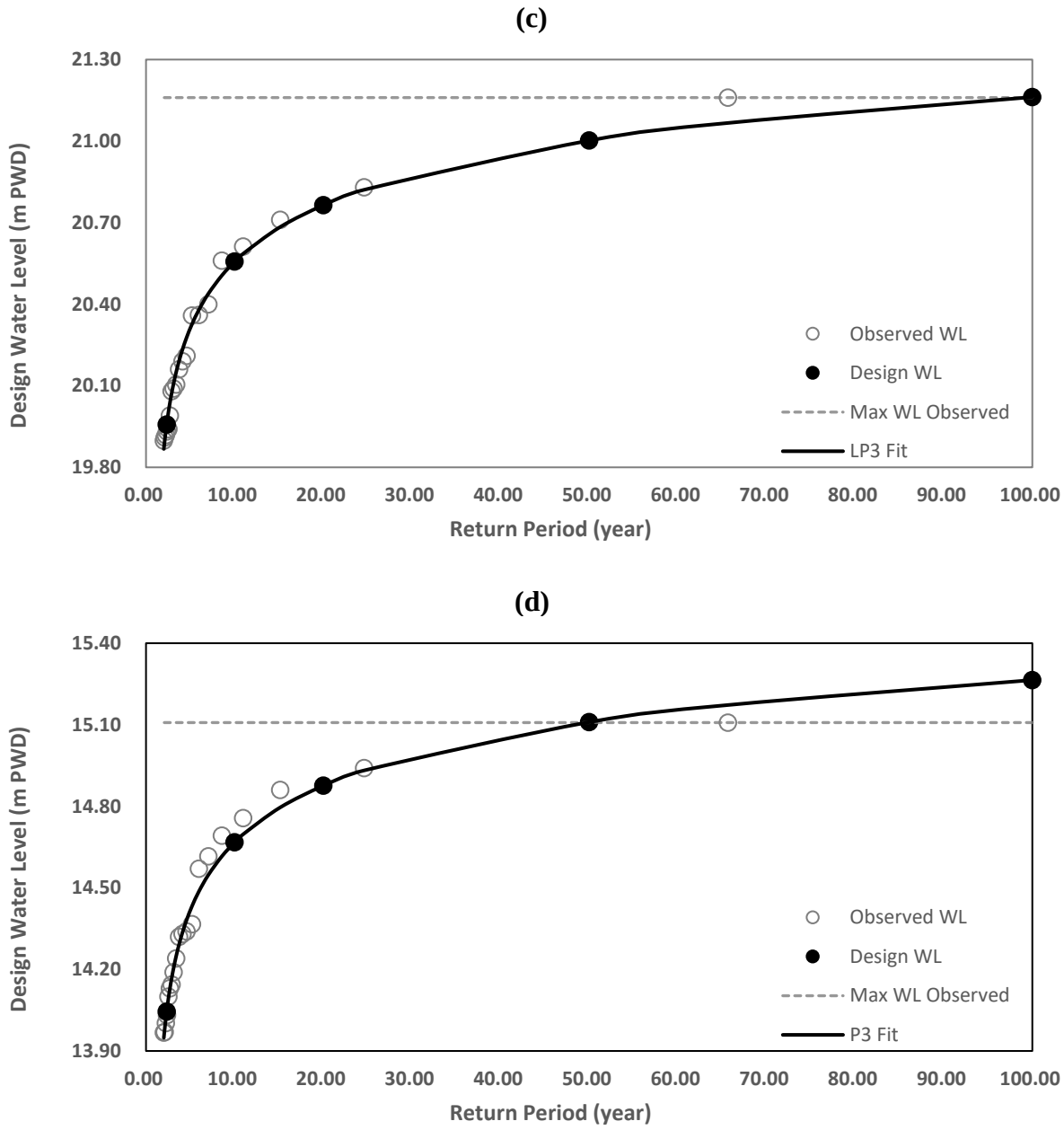

Figure 6.10: Design Water-level for a corresponding return period of the Jamuna River at a) Noonkhawa, b) Chilmari, c) Bahadurabad, d) Sirajganj.

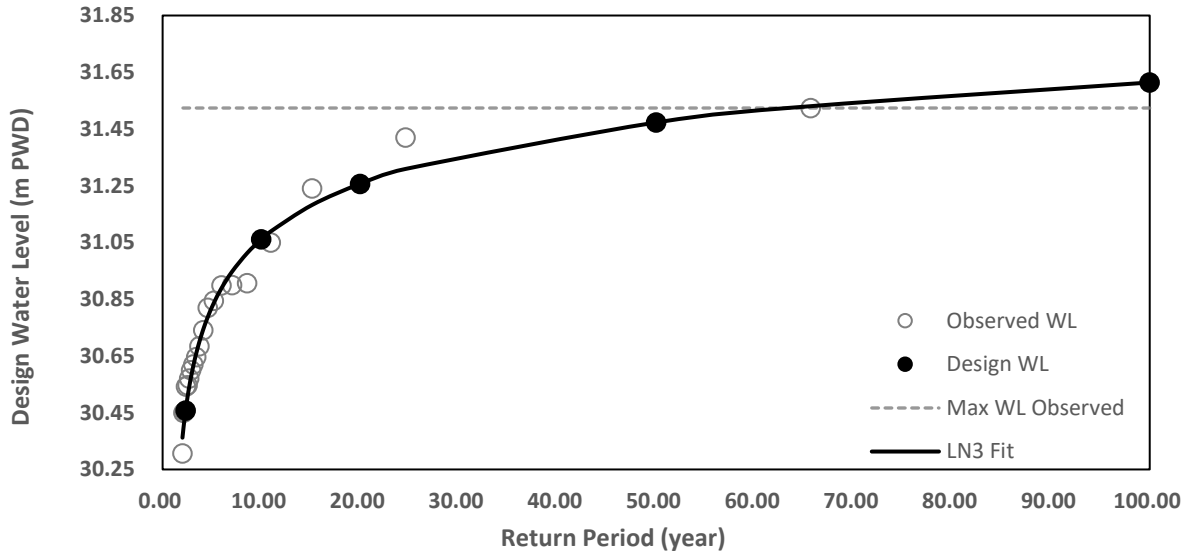

Figure 6.11: Design Water-level for a corresponding return period of the Dudhkumar River at Pateswari.

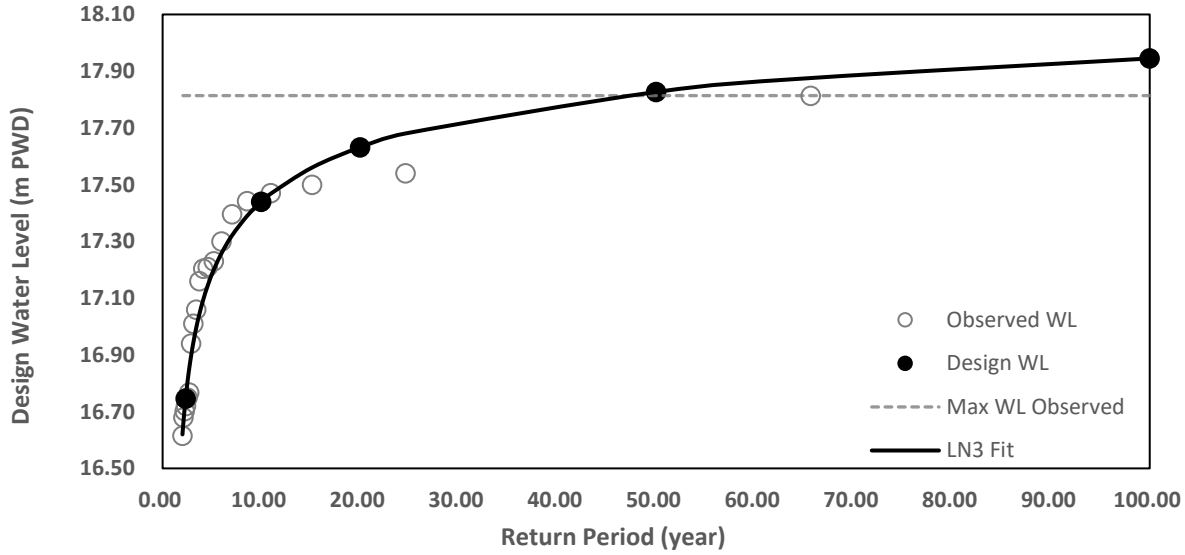

Figure 6.12: Design Water-level for the corresponding return period of the Old Brahmaputra at Jamalpur.

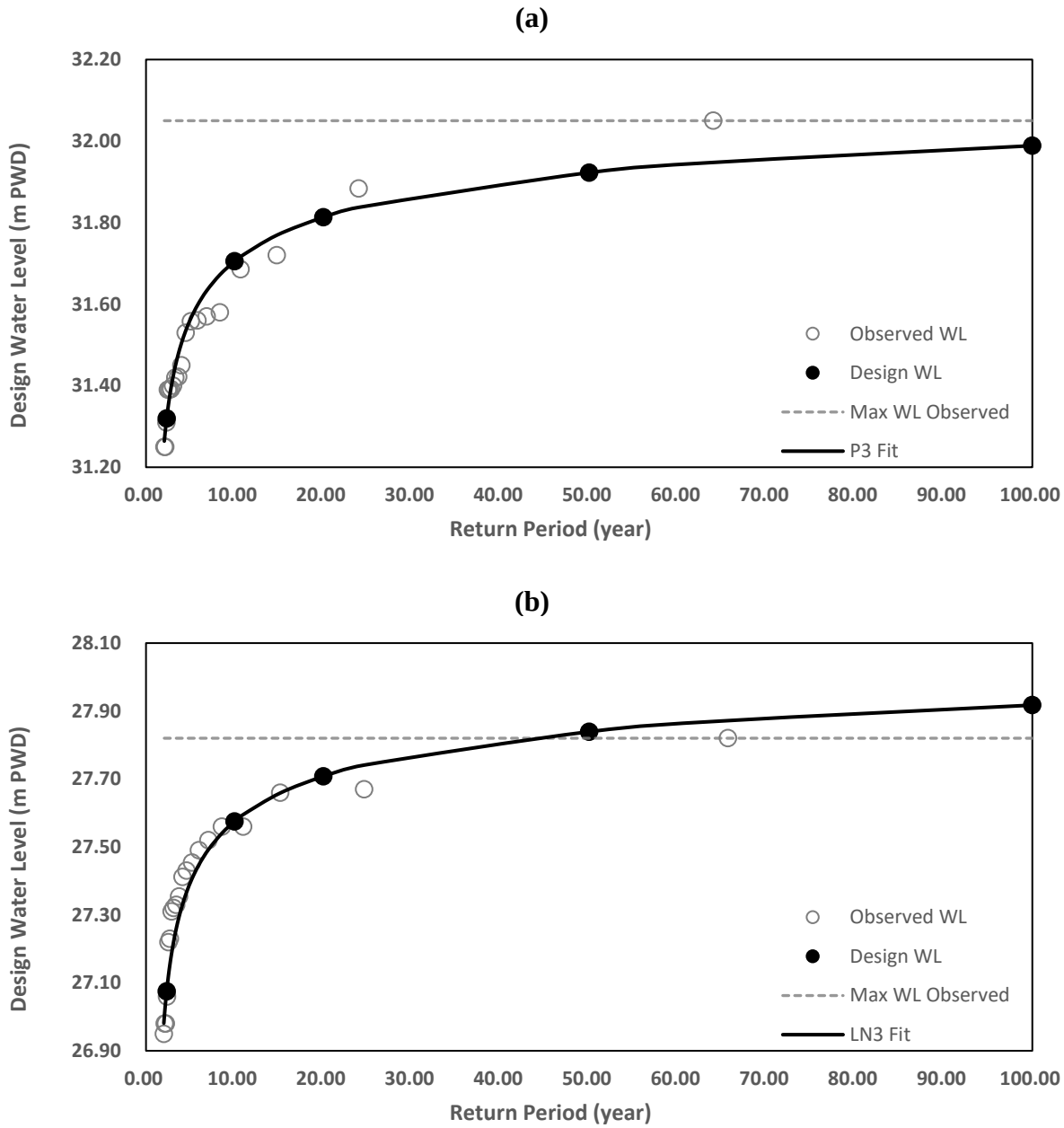

Figure 6.13: Design Water-level for the corresponding return period of the Dharala River at a) Taluk-Simulbari, b) Kurigram.

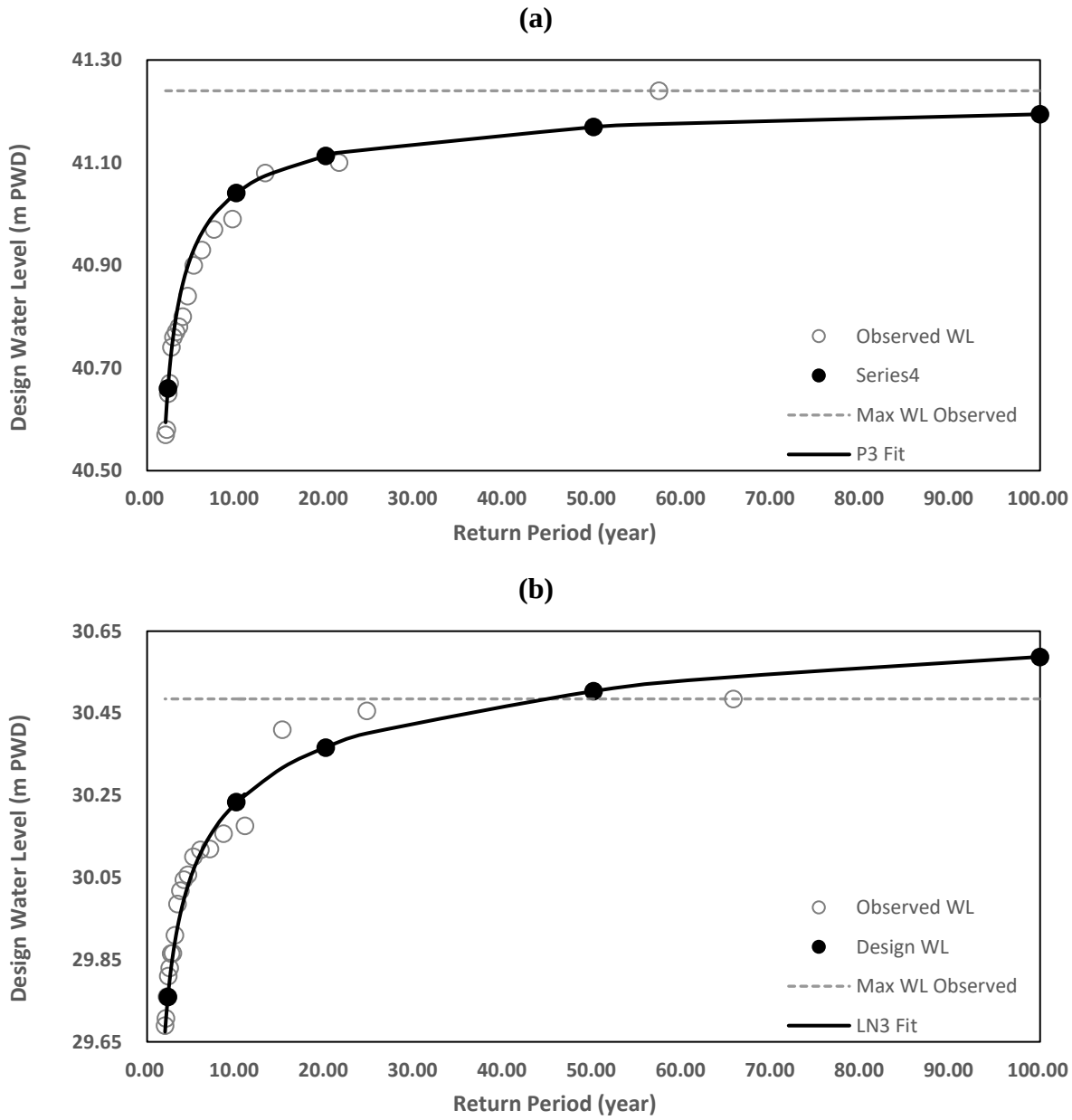

Figure 6.14: Design Water-level for the corresponding return period of the Teesta River at a) Kaliganj, b) Kaunia.

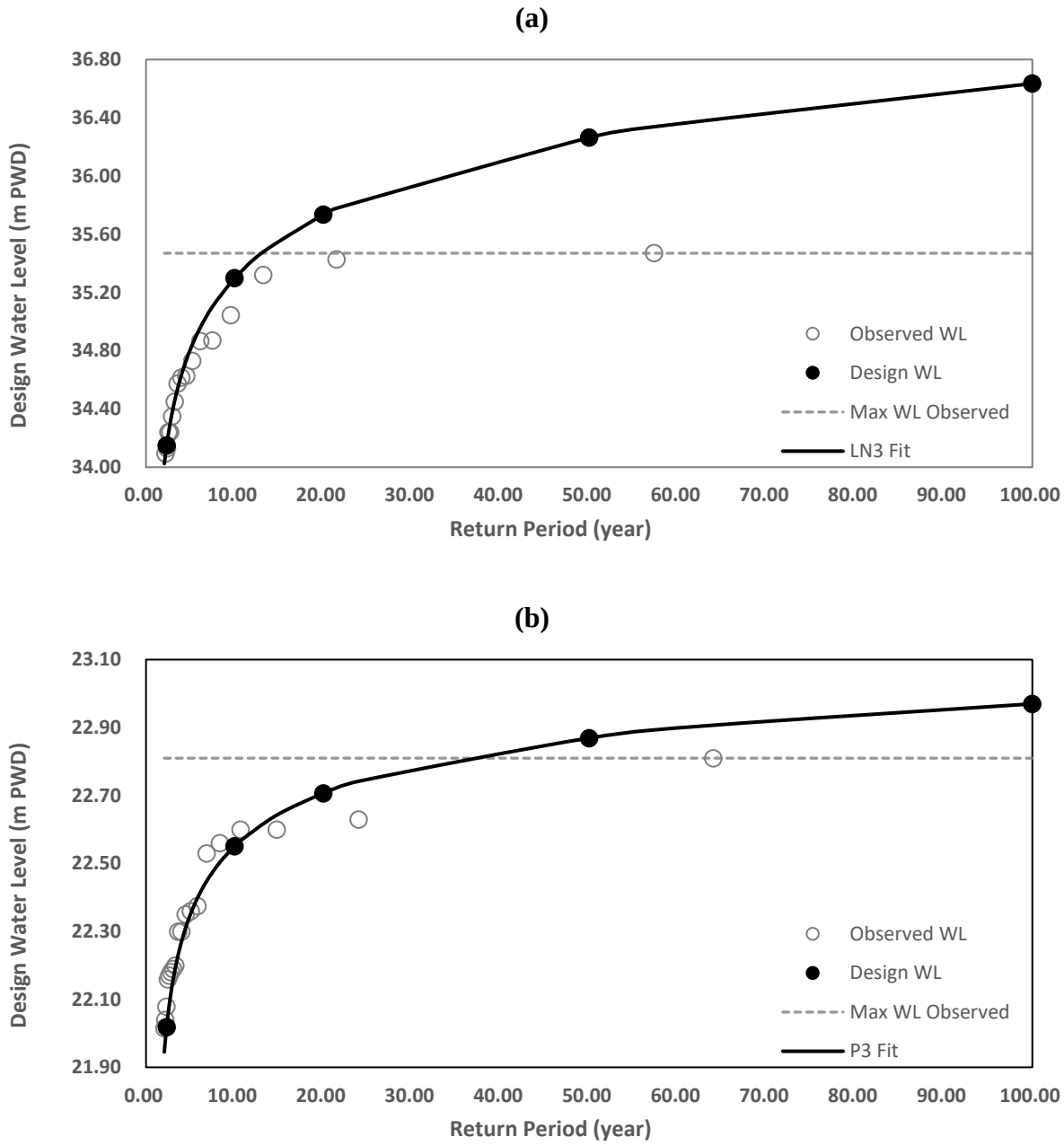

Figure 6.15: Design Water-level for the corresponding return period of the Ghaghat River at a) Jafarganj, b) Gaibandha.

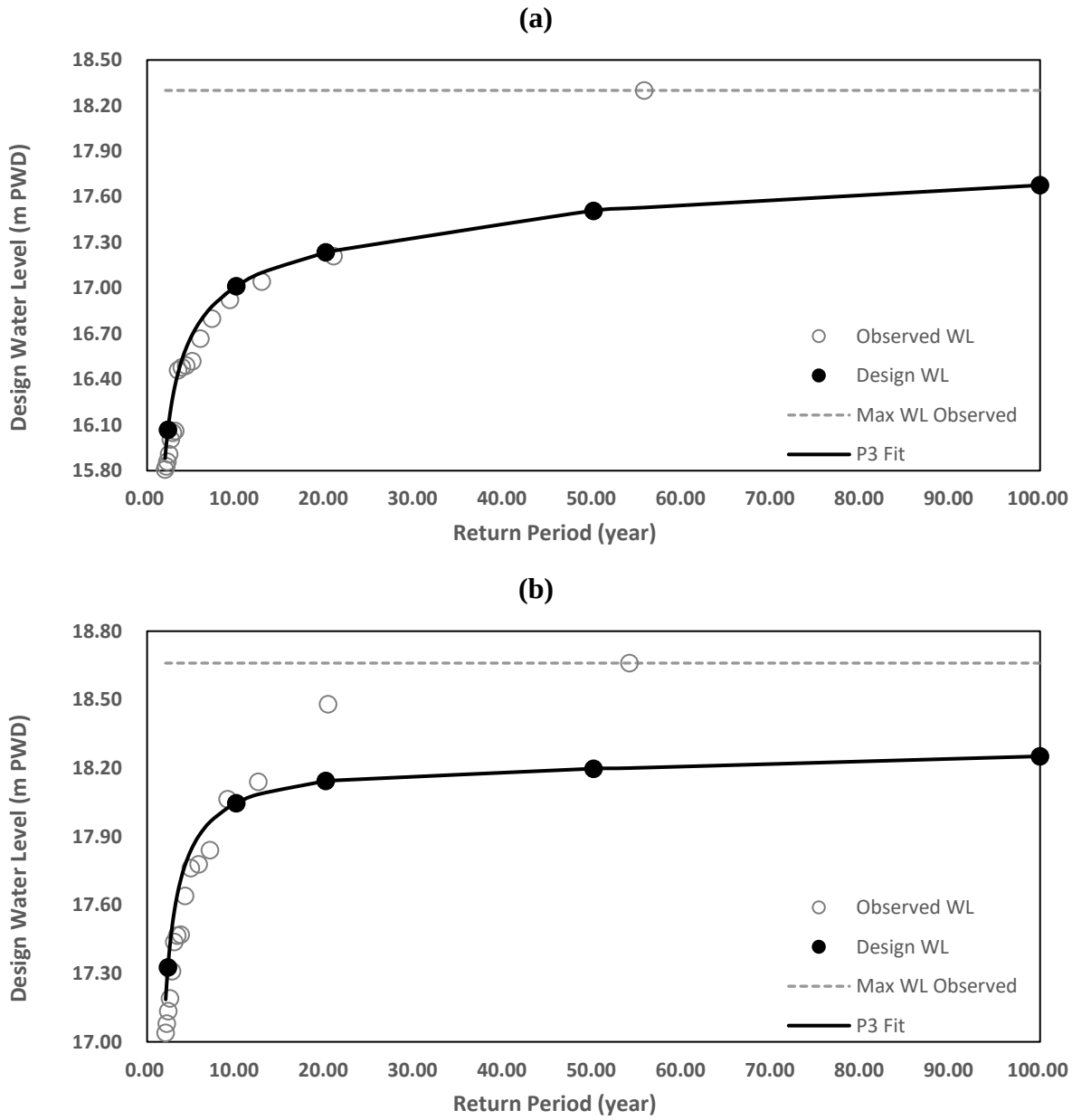

Figure 6.16: Design Water-level for the corresponding return period of the Jhenai River at a) Baushi Bridge, b) Offtake Jhenai.

(a)

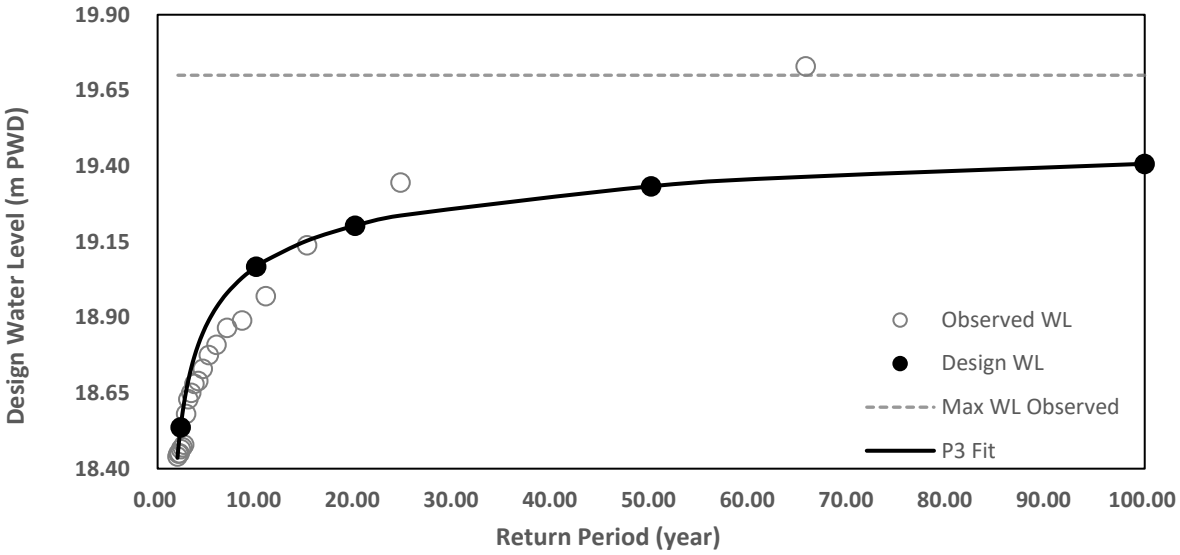

(b)

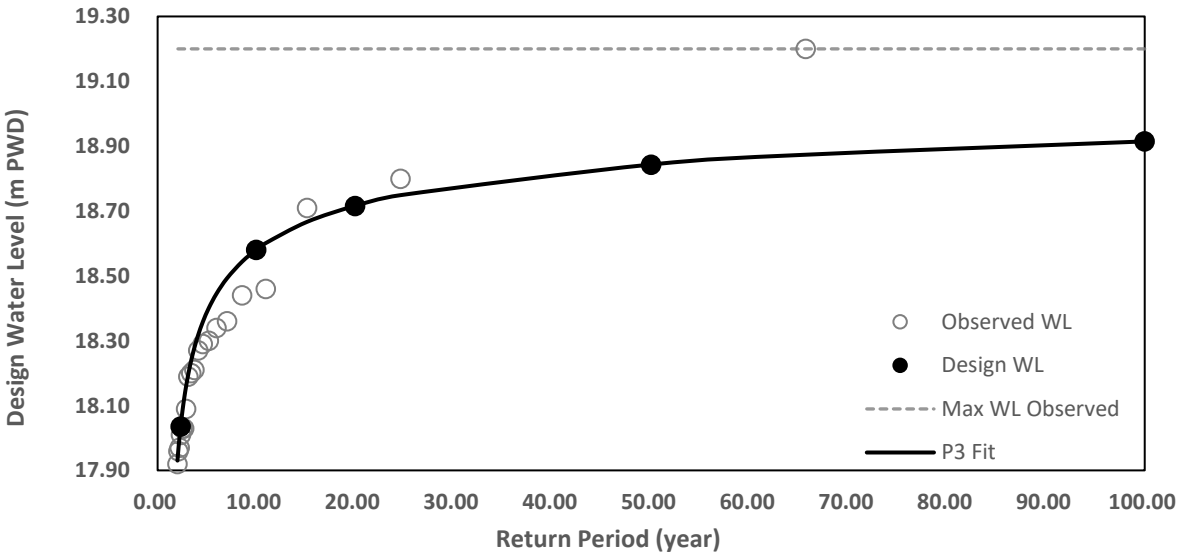

Figure 6.17: Design Water-level for the corresponding return period of the Bangali River at (a) Mohimganj, (b) Simulbari.

6.5 Changes in Flood Frequency Considering Climate Change

Frequency analysis has been carried out for 2.33, 10, 25, 50- and 100-year return periods for major rivers of the study area using HEC-RAS hydrodynamic model simulated yearly maximum water level for near future (2025-2054) and far future (2071-2100) with respect to the baseline period (1985-2014). The boundary flows of the HEC-RAS model are provided from the SWAT hydrological model over the Brahmaputra-Teesta river basins. The SWAT model was derived by CMIP6 projected rainfall under SSP2-4.5 and SSP5-8.6 experiments.

Dharala River at Kurigram (SW77)

Frequency analysis of the Dharala River at Kurigram (SW77) using mean ensemble climate projections for the near and far future is presented in Table 6.21. It has been found that differences in water level for 10 year return period are 60 cm and 80 cm for the near future under SSP2-4.5 and SSP5-8.5, respectively. A plot of the frequency of maximum water level of Dharala River at Kurigram (SW77) using climate projections for the near future (2025-2054) and far future (2071-2100) with respect to the baseline period (1985-2014) is shown in Figure 6.18. The shaded areas denoted ensemble spreads and the 95% confidence interval of CMIP6 SSP2-4.5 and CMIP6 SSP5-8.5 experiments with nine climate models. The dark solid line represents the ensemble mean value of the spreads under different climate scenarios.

Table 6.21: Frequency analysis of Dharala River at Kurigram (SW77) using mean ensemble climate projections for the near and far future.

Return Period	Obs	SSP2-45_near	SSP2-45_far	SSP5-85_near	SSP5-85_far
2.33	27.08	27.36	27.43	27.63	27.79
10	27.58	27.88	27.95	28.13	28.30
25	27.74	28.05	28.13	28.28	28.47
50	27.84	28.16	28.24	28.38	28.57
100	27.92	28.25	28.33	28.46	28.66

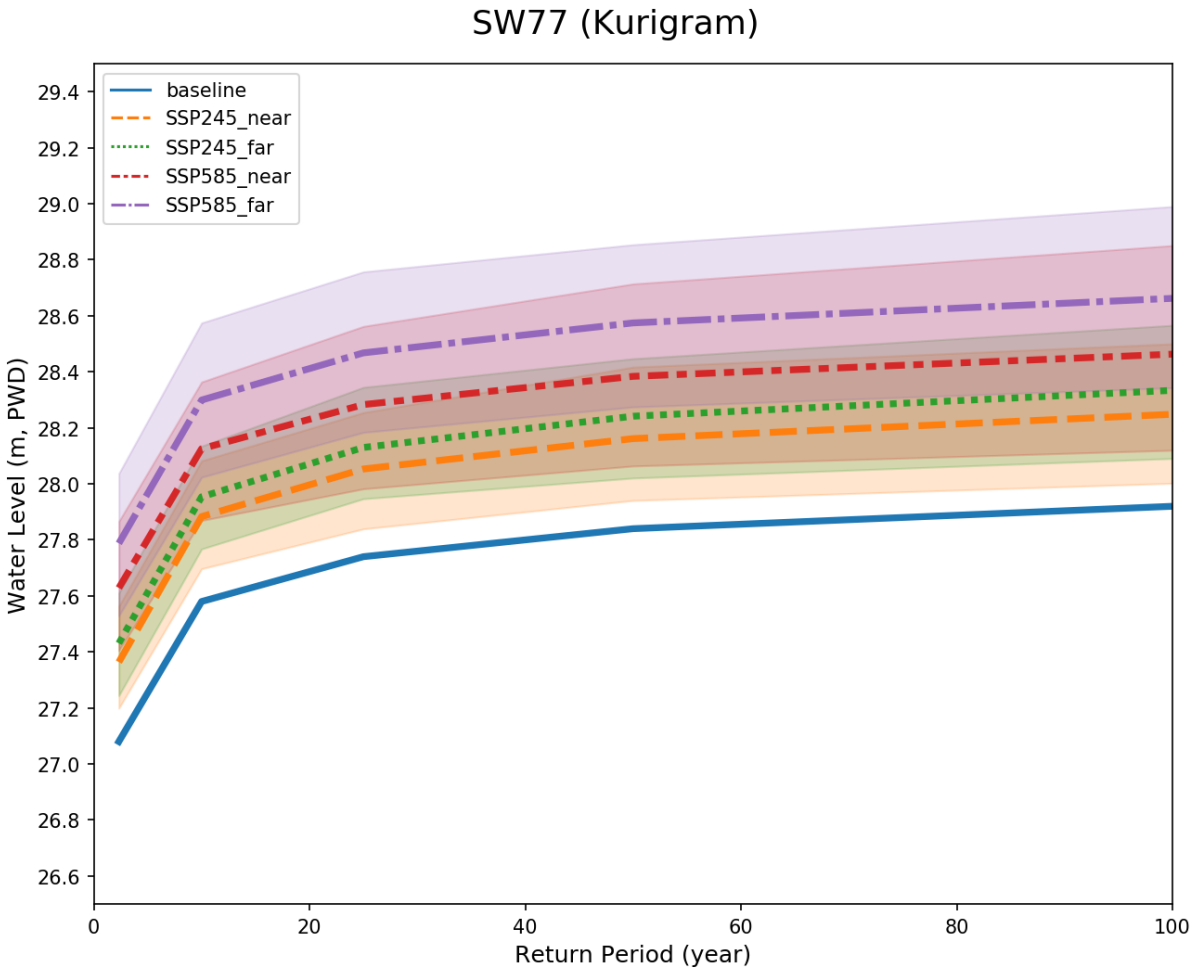

Figure 6.18: Frequency of maximum water level (m, PWD) of Dharala River at Kurigram (SW77) using climate projections for the near future (2025-2054) and far future (2071-2100) with respect to the baseline period (1985-2014).

Dudhkumar River at Pateswari (SW81)

Frequency analysis of Dudhkumar River at Pateswari (SW81) using mean ensemble climate projections for the near and far future is presented in Table 6.22. It has been found that differences in water level for 10 year return period are 70 cm and 130 cm for the near future under SSP2-4.5 and SSP5-8.5, respectively. A plot of the frequency of maximum water level of Dudhkumar River at Pateswari (SW81) using climate projections for the near future (2025-2054) and far future (2071-2100) with respect to the baseline period (1985-2014) is shown in Figure 6.19. The shaded areas denoted ensemble spreads and the 95% confidence interval of CMIP6 SSP2-4.5 and CMIP6 SSP5-8.5 experiments with nine climate models. The dark solid line represents the ensemble mean value of the spreads under different climate scenarios.

Table 6.22: Frequency analysis of Dudhkumar River at Pateswari (SW81) using mean ensemble climate projections for the near and far future.

Return Period	Obs	SSP2-45_near	SSP2-45_far	SSP5-85_near	SSP5-85_far
2.33	30.46	30.73	30.80	31.01	31.19
10	31.06	31.37	31.45	31.63	31.83
25	31.31	31.64	31.73	31.89	32.11
50	31.47	31.81	31.91	32.05	32.29
100	31.61	31.97	32.07	32.20	32.45

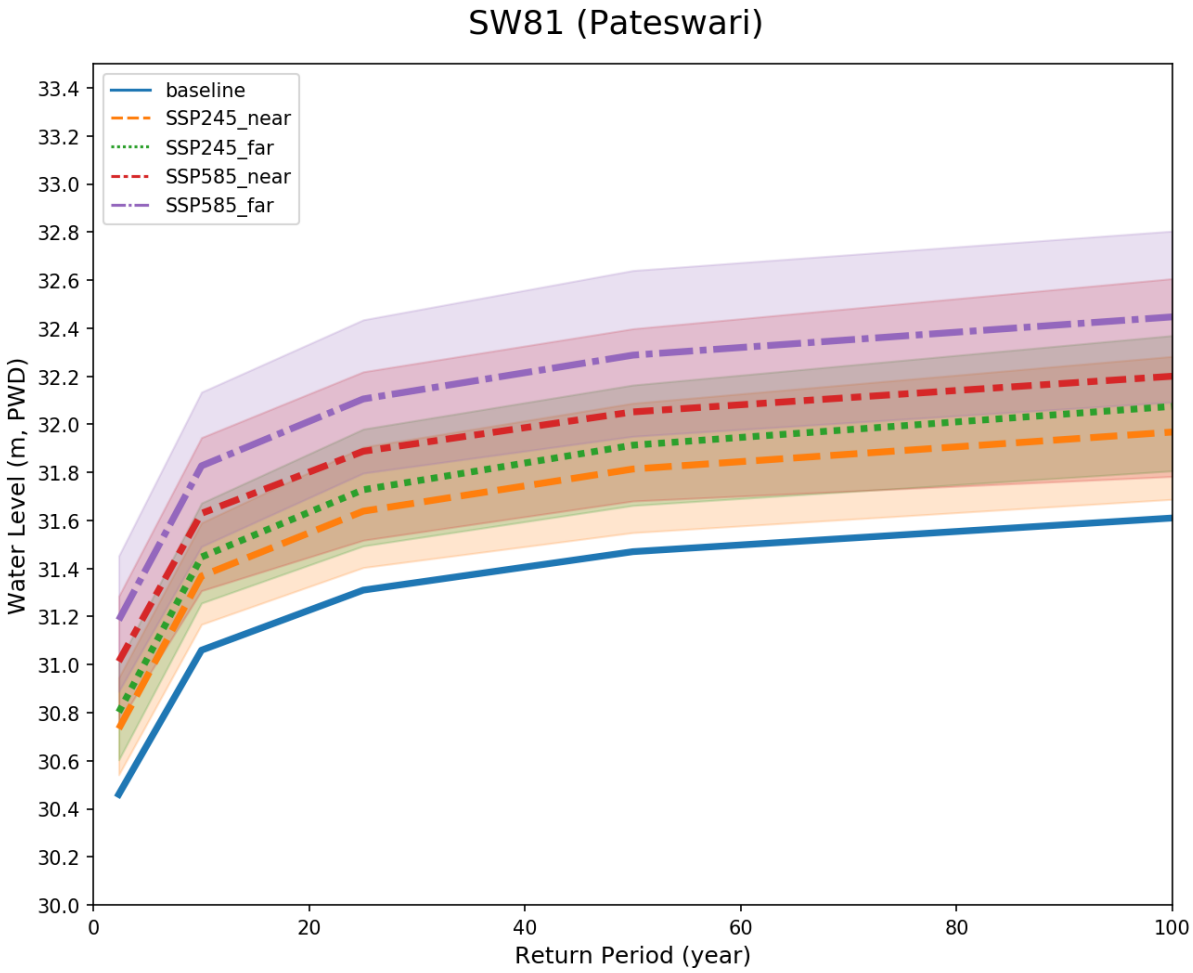

Figure 6.19: Frequency of maximum water level (m, PWD) of Dudhkumar River at Pateswari (SW81) using climate projections for the near future (2025-2054) and far future (2071-2100) with respect to the baseline period (1985-2014).

Brahmputra River at Chilmari (SW45.5)

Frequency analysis of Brahmputra River at Chilmari (SW45.5) using mean ensemble climate projections for the near and far future is presented in Table 6.23. It has been found that differences in water level for 10 year return period are 23 cm and 70 cm for the near future under SSP2-4.5 and SSP5-8.5, respectively. A plot of the frequency of maximum water level of Brahmputra River at Chilmari (SW45.5) using climate projections for the near future (2025-

2054) and far future (2071-2100) with respect to the baseline period (1985-2014) is shown in Figure 6.20. The shaded areas denoted ensemble spreads and the 95% confidence interval of CMIP6 SSP2-4.5 and CMIP6 SSP5-8.5 experiments with nine climate models. The dark solid line represents the ensemble mean value of the spreads under different climate scenarios.

Table 6.23: Frequency analysis of Brahmputra River at Chilmari (SW45.5) using mean ensemble climate projections for the near and far future.

Return Period	Obs	SSP2-45_near	SSP2-45_far	SSP5-85_near	SSP5-85_far
2.33	24.2	24.43	24.48	24.64	24.75
10	25.08	25.31	25.37	25.51	25.66
25	25.58	25.82	25.89	26.01	26.18
50	25.95	26.20	26.27	26.38	26.57
100	26.32	26.57	26.65	26.76	26.95

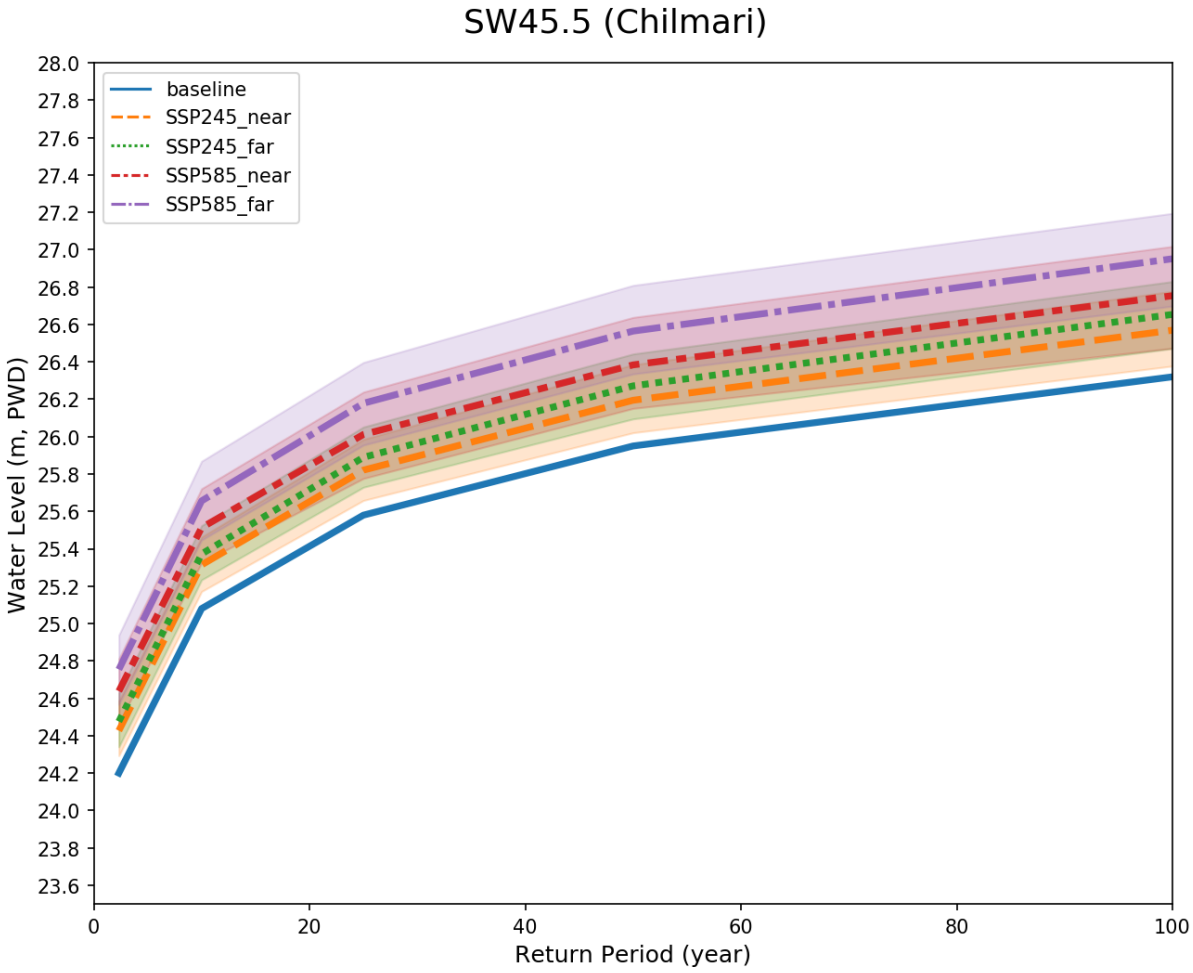

Figure 6.20: Frequency of maximum water level (m, PWD) of Brahmputra River at Chilmari (SW45.5) using climate projections for the near future (2025-2054) and far future (2071-2100) with respect to the baseline period (1985-2014).

Jamuna River at Bahadurabad (SW46.9L)

Frequency analysis of Jamuna River at Bahadurabad (SW46.9L) using mean ensemble climate projections for the near and far future is presented in Table 6.24. It has been found that differences in water level for 10 year return period are 100 cm and 170 cm for the near future under SSP2-4.5 and SSP5-8.5, respectively. A plot of the frequency of maximum water level of Jamuna River at Bahadurabad (SW46.9L) using climate projections for the near future (2025-2054) and far future (2071-2100) with respect to the baseline period (1985-2014) is shown in Figure 6.21. The shaded areas denoted ensemble spreads and the 95% confidence interval of CMIP6 SSP2-4.5 and CMIP6 SSP5-8.5 experiments with nine climate models. The dark solid line represents the ensemble mean value of the spreads under different climate scenarios.

Table 6.24: Frequency analysis of Jamuna River at Bahadurabad (SW46.9L) using mean ensemble climate projections for the near and far future.

Return Period	Obs	SSP2-45_near	SSP2-45_far	SSP5-85_near	SSP5-85_far
2.33	19.96	20.32	20.43	20.68	20.87
10	20.56	20.92	21.03	21.25	21.42
25	20.83	21.20	21.31	21.51	21.67
50	21.00	21.38	21.48	21.67	21.84
100	21.16	21.54	21.65	21.82	21.99

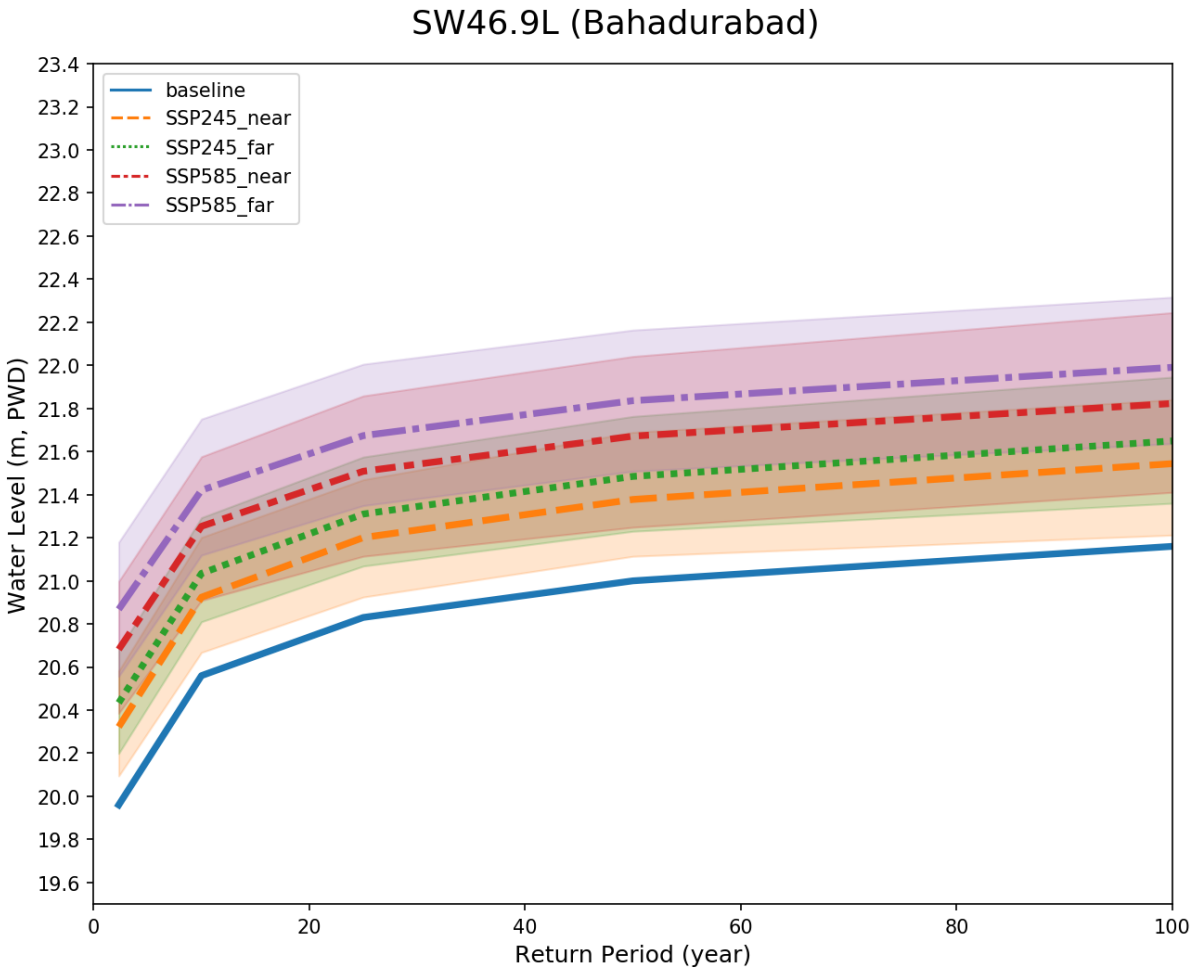

Figure 6.21: Frequency of maximum water level (m, PWD) of Jamuna River at Bahadurabad (SW46.9L) using climate projections for the near future (2025-2054) and far future (2071-2100) with respect to the baseline period (1985-2014).

Teesta River at Dalia (SW291.5R)

Frequency analysis of Teesta River at Dalia (SW291.5R) using mean ensemble climate projections for the near and far future is presented in Table 6.25. It has been found that differences in water level for 10 year return period are 10 cm and 40 cm for the near future under SSP2-4.5 and SSP5-8.5, respectively. A plot of the frequency of maximum water level of Teesta River at Dalia (SW291.5R) using climate projections for the near future (2025-2054) and far future (2071-2100) with respect to the baseline period (1985-2014) is shown in Figure 6.22. The shaded areas denoted ensemble spreads and the 95% confidence interval of CMIP6 SSP2-4.5 and CMIP6 SSP5-8.5 experiments with nine climate models. The dark solid line represents the ensemble mean value of the spreads under different climate scenarios.

Table 6.25: Frequency analysis of Teesta River at Dalia (SW291.5R) using mean ensemble climate projections for the near and far future.

Return Period	Obs	SSP2-45_near	SSP2-45_far	SSP5-85_near	SSP5-85_far
2.33	52.53	52.65	52.69	52.74	52.81
10	52.88	52.99	53.01	53.07	53.13
25	53.04	53.14	53.15	53.22	53.29
50	53.14	53.23	53.25	53.32	53.40
100	53.23	53.32	53.33	53.40	53.50

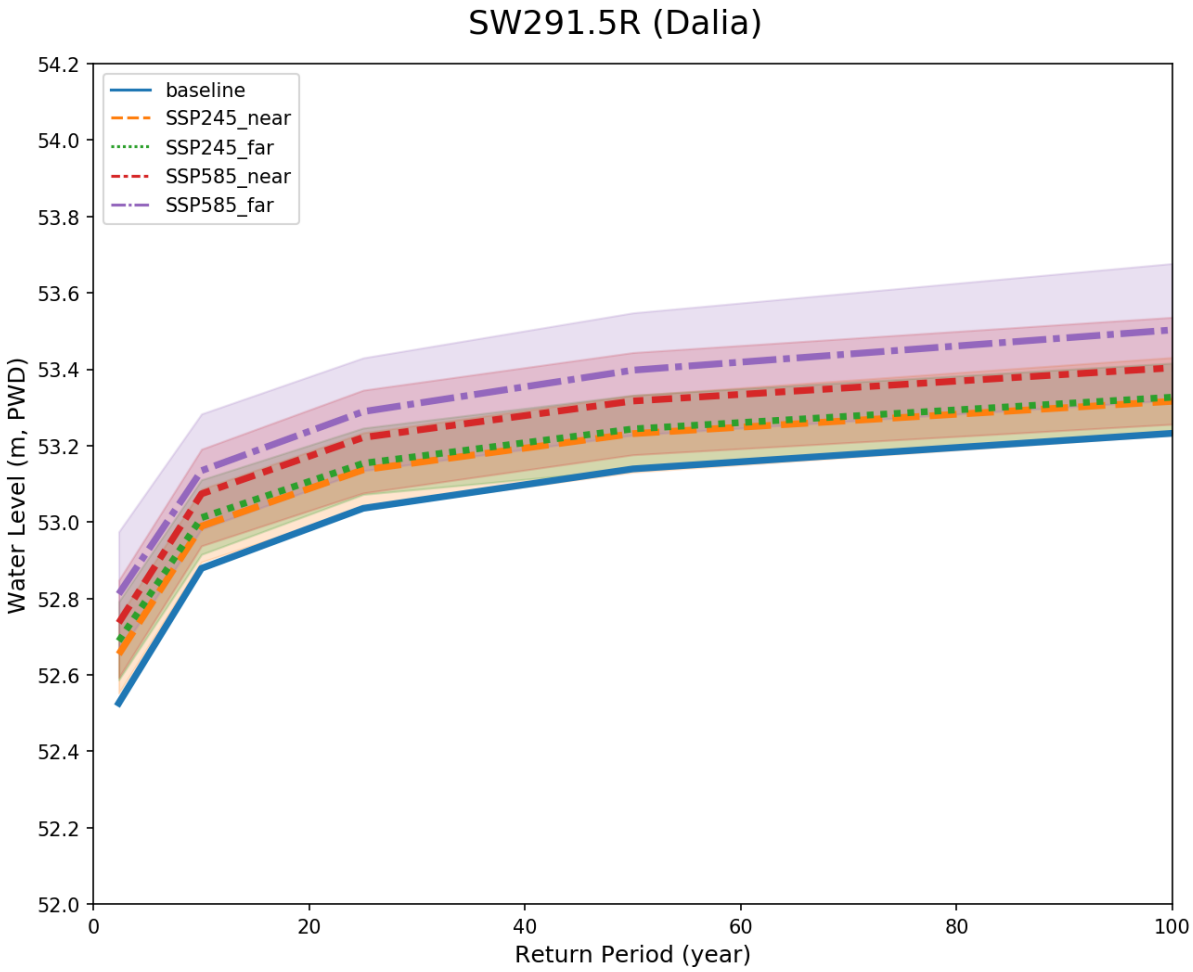

Figure 6.22: Frequency of maximum water level (m, PWD) of Teesta River at Dalia (SW291.5R) using climate projections for the near future (2025-2054) and far future (2071-2100) with respect to the baseline period (1985-2014).

Teesta River at Kaunia (SW294)

Frequency analysis of Teesta River at Kaunia (SW294) using mean ensemble climate projections for the near and far future is presented in Table 6.26. It has been found that differences in water level for 10 year return period are 20 cm and 50 cm for the near future under SSP2-4.5 and SSP5-8.5, respectively. A plot of the frequency of the maximum water level of Teesta River at Kaunia (SW294) using climate projections for the near future (2025-2054) and far future (2071-2100) with respect to the baseline period (1985-2014) is shown in

Figure 6.23. The shaded areas denoted ensemble spreads and the 95% confidence interval of CMIP6 SSP2-4.5 and CMIP6 SSP5-8.5 experiments with nine climate models. The dark solid line represents the ensemble mean value of the spreads under different climate scenarios.

Table 6.26: Frequency analysis of Teesta River at Kaunia (SW294) using mean ensemble climate projections for the near and far future.

Return Period	Obs	SSP2-45_near	SSP2-45_far	SSP5-85_near	SSP5-85_far
2.33	29.76	29.96	30.03	30.10	30.21
10	30.23	30.44	30.46	30.55	30.63
25	30.4	30.63	30.61	30.70	30.78
50	30.5	30.74	30.69	30.79	30.88
100	30.59	30.85	30.77	30.87	30.97

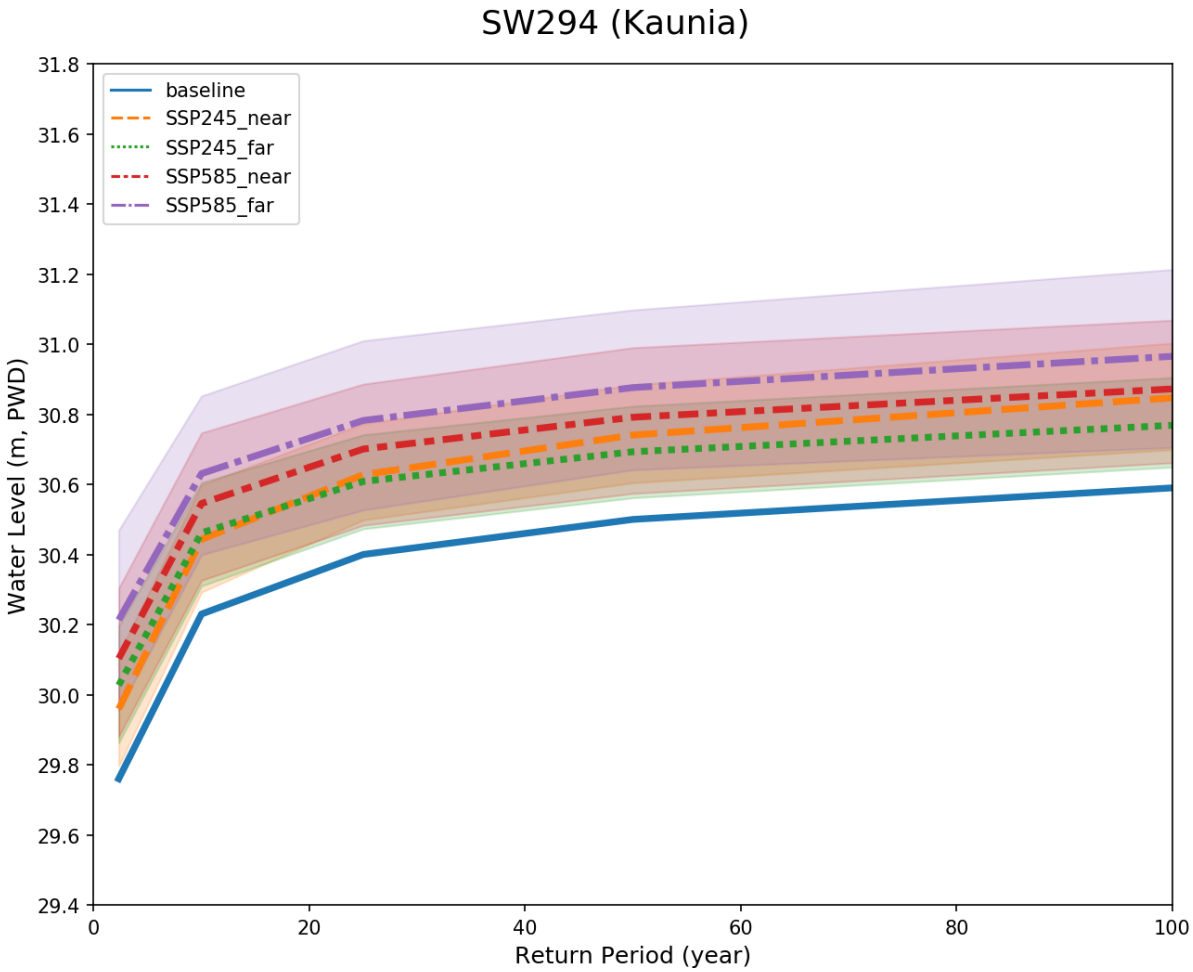

Figure 6.23: Frequency of maximum water level (m, PWD) of Teesta River at Kaunia (SW294) using climate projections for the near future (2025-2054) and far future (2071-2100) with respect to the baseline period (1985-2014).

Old Brahmaputra River at Jamalpur (SW225)

Frequency analysis of the Old Brahmaputra River at Jamalpur (SW225) using mean ensemble climate projections for the near and far future is presented in Table 6.27. It has been found that differences in water level for 10 year return period are 90 cm and 160 cm for the near future under SSP2-4.5 and SSP5-8.5, respectively. A plot of the frequency of maximum water level of Old Brahmaputra River at Jamalpur (SW225) using climate projections for the near future (2025-2054) and far future (2071-2100) with respect to the baseline period (1985-2014) is shown in Figure 6.24. The shaded areas denoted ensemble spreads and the 95% confidence interval of CMIP6 SSP2-4.5 and CMIP6 SSP5-8.5 experiments with nine climate models. The dark solid line represents the ensemble mean value of the spreads under different climate scenarios.

Table 6.27: Frequency analysis of Old Brahmaputra River at Jamalpur (SW225) using mean ensemble climate projections for the near and far future.

Return Period	Obs	SSP2-45_near	SSP2-45_far	SSP5-85_near	SSP5-85_far
2.33	16.75	17.15	17.27	17.54	17.75
10	17.44	17.82	17.90	18.17	18.35
25	17.68	18.07	18.13	18.39	18.57
50	17.83	18.22	18.26	18.52	18.72
100	17.95	18.34	18.38	18.63	18.85

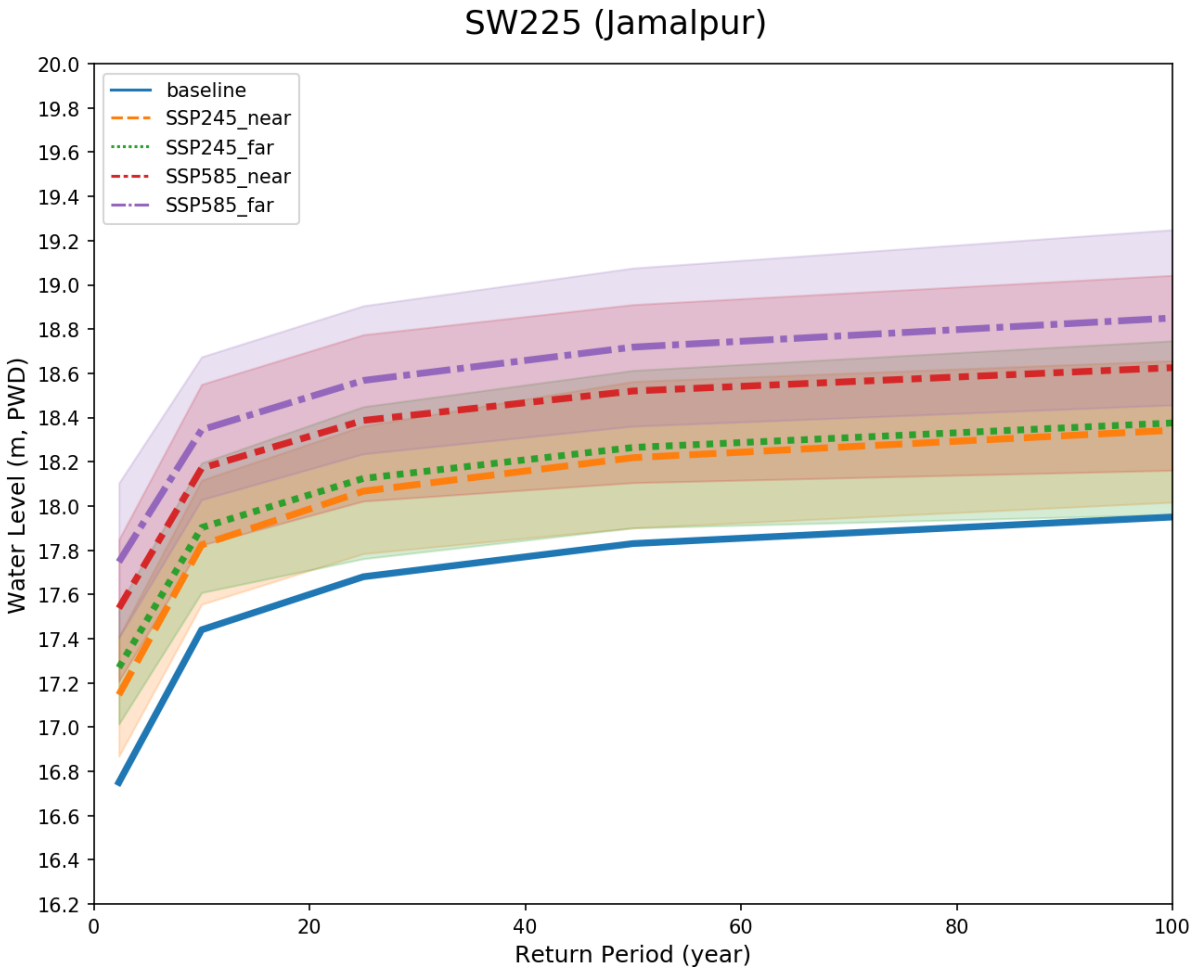

Figure 6.24: Frequency of maximum water level (m, PWD) of Old Brahmaputra River at Jamalpur (SW255) using climate projections for the near future (2025-2054) and far future (2071-2100) with respect to the baseline period (1985-2014).

6.6 Increase of crest height of Village, Union and Upazila Roads, markets and school cum flood shelters

Projected changes in the frequency of the maximum water level of seven major rivers have been calculated for the near future (2025-2054) and far future (2071-2100) with respect to the baseline period (1985-2014). As the design period of the village, union and Upazila roads of LGED is 10 years, projected changes in maximum water level in the near future will be considered. Although all climate scenarios are equally possible, SSP2-4.5 is recommended, which is the balance between high and low-emission scenarios. A summary of the maximum water level for the 10-year return period under SSP2-4.5 scenarios is presented in Table 6.28. Due to the uncertainty of future changes in water levels (varies from 11 cm to 38 cm), an increase of 30 cm (0.3 meters) of the crest level of the roads is recommended. A summary of the maximum water level for the 100-year return period under SSP2-4.5 scenarios is presented

in Table 6.29. Due to the uncertainty of future changes in water levels (varies from 10 cm to 49 cm), an increase of 50 cm (0.5 meter) of the crest level of the markets and flood shelters is recommended.

Table 6.28: Increase of crest height of village, union and Upazila roads of LGED for 10-year return period design flood considering climate change.

River	Station Name	Station ID	10-year Return Period			Recommendations for an increase of Crest height of LGED roads considering climate change (cm)
			Observed WL (m, PWD)	Near future WL (m, PWD)	Crest height increase (cm)	
Brahmaputra-Jamuna	Chilmari	SW 45.5	25.08	25.31	23	30
Brahmaputra-Jamuna	Bahadurabad	SW 46.9L	20.56	20.92	36	
Dudhkumar	Pateswari	SW 81	31.06	31.37	31	
Dharala	Kurigram	SW 77	27.58	27.88	30	
Teesta	Dalia	SW291.5R	52.88	52.99	11	
Teesta	Kaunia	SW 294	30.23	30.44	21	
Old Brahmaputra	Jamalpur	SW 225	17.44	17.82	38	

Table 6.29: Increase of crest height of market and flood shelters of LGED for 100-year return period design flood considering climate change.

River	Station Name	Station ID	100-year Return Period			Recommendations for an increase of Crest height of flood shelters considering climate change (cm)
			Observed WL (m, PWD)	Fur future WL (m, PWD)	Crest height increase (cm)	
Brahmaputra-Jamuna	Chilmari	SW 45.5	26.32	26.65	33	50
Brahmaputra-Jamuna	Bahadurabad	SW 46.9L	21.16	21.65	49	
Dudhkumar	Pateswari	SW 81	31.61	32.07	46	
Dharala	Kurigram	SW 77	27.92	28.33	41	
Teesta	Dalia	SW291.5R	53.23	53.33	10	
Teesta	Kaunia	SW 294	30.59	30.77	18	
Old Brahmaputra	Jamalpur	SW 225	17.95	18.38	43	

CHAPTER SEVEN
CLIMATE-RESILIENT INFRASTRUCTURES DESIGN

7.1 Review of the existing guidelines

There are two guidelines for the design of rural roads. One guideline was prepared by the Planning Commission of the Government of Bangladesh entitled "Road design Standards, Standard Designs and Costing of Zila, Upazila and Union Roads, Bridges and Culverts" (Planning Commission, 2004). The report did not mention anything about the hydro-morphological investigation before constructing any new roads. However, the report asserts that some of the roads built under the "Food For Work" program were built without proper pavement and drainage structures. As a result, adequate gaps were not provided, which resulted in water logging and flooding (Planning Commission, 2004). This statement indicates the importance of carrying out hydro-morphological investigations for the proper design of roads and culverts, especially in flood-vulnerable areas. The crest level of roads and culverts would be dictated by the hydrologic analysis. The alignment of roads along a riverbank should be dictated by the shifting characteristics of the river. Usually, culverts are provided for drainage purposes. The size of the culverts should be designed by hydraulic analysis of the incoming flows. If adequate drainage structures are not provided along the roads, the roads, as well as the drainage structure, may fail due to the hydraulic forces. According to the guideline prepared by the planning commission (Planning Commission, 2004), the following guidelines are practiced for the construction of new roads (Table 7.1). As can be seen in the Table, the slope, height, and size of the roads, bridges, and culverts are selected based on predefined values for three different areas, namely, plane, hilly and swampy haor. Actually, the slope, height, and size of the roads, bridges, and culverts should be designed based on estimates based on the hydro-morphological investigation. There are numerous examples of the failure of such a structure during flood flows. The culverts mainly fail due to faulty design with inadequate opening. In most cases, the culvers are constructed based on a typed design that does not take care of the actual hydraulic loads, which should decide the dimension of the culverts. Photo 7.1-7.3 shows some of the culvers which were failed due to inadequate opening. The report concluded that in order to avoid water-logging and flooding, adequate gaps should be provided for drainage, and no road should be built by any agency without the proper design of such structures (Planning Commission, 2004).

Table 7.1: Dimension of road embankment, bridges, and culvers (Planning Commission, 2004).

Type Area	**Slope Protection**	**Embankment Height**	**Bridges (per km)**	**Culverts (per km)**
Plane	Turfing only	3 m	5 m – 7 m	1 m – 3 m
Hilly	Concrete retaining wall (lower slope), and slope protection on the upper slope	1 m	4 m – 7 m	3 m – 8 m
Swampy and Haor	Brick block and geotextile	4 m	8 m – 11 m	2 m – 4 m

According to LGED (2005), the gap requirements for drainage by type of road are shown in Table 7.2.

Photo 7.1: Failure of abutment of a bridge constructed by constricting the width of the Darbhanga River in Islampur Upazila of Jamalpur.

Photo 7.2: Failure of a culvert built in the floodplain of the Jamuna River in Jamalpur.

Photo 7.3: Failure of a culvert built in the floodplain of the Jamuna River in Jamalpur.

Another guideline was prepared by the Local Government and Engineering Department (LGED) and Japan International Cooperation Agency (JICA) entitled “Road Design Standards: Rural Roads” (LGED, 2005). The report provides typical gaps by type of road per kilometer.

Table 7.2: Typical gaps by type of road, meters per kilometer

New Class	Road design type	Geographical location			
Upazila and Union	Type 6, 5, 4 Type 8,7	Swampy	Hilly	Haor	Plane
		10-15	7-15	10-15	6-10

The report provides options for road embankment protection at Haor or waterlogged areas where tremendous wave results from erosion on the embankment due to storm and high-speed wind. According to the design standard, if the char land remains above normal flood water level, the embankment of the road shall be lined with clayey soil (0.30 m thick), PI value range of 8 20%. The guideline also suggests turfing or seeding with 'Durba' grass over the lining of the side embankment. The guideline provides four typical sections for slope protection with gynny bagged rip-rap and geotextile (Figure 7.1); cc blocks and geotextile (Figure 7.2); brick blocks and geotextile (Figure 7.3); and brickbats mattress and geotextile (Figure 7.4). The guideline suggests that any method specified above may be used where it is most appropriate, as can be seen from the figures that nothing is mentioned about the crest level of the road embankment and slope, which are two important dimensions for climate-resilient design. The guideline does not provide any specific size of the gunny bags as well as CC blocks.

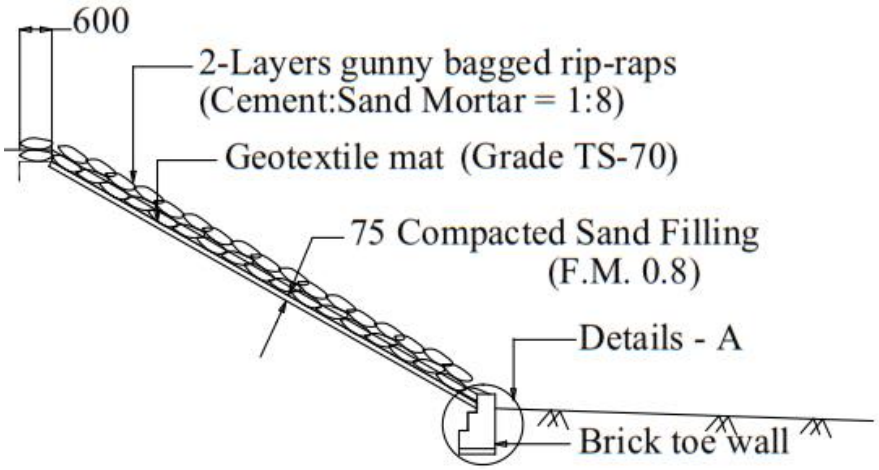

Figure 7.1: Slope protection work with gunny bagged Rip-Rap and Geotextile.

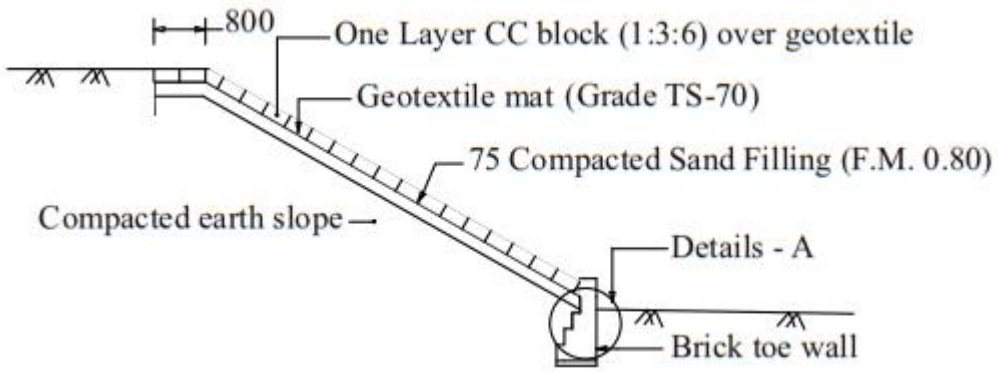

Figure 7.2: Slope protection work with CC block and geotextile.

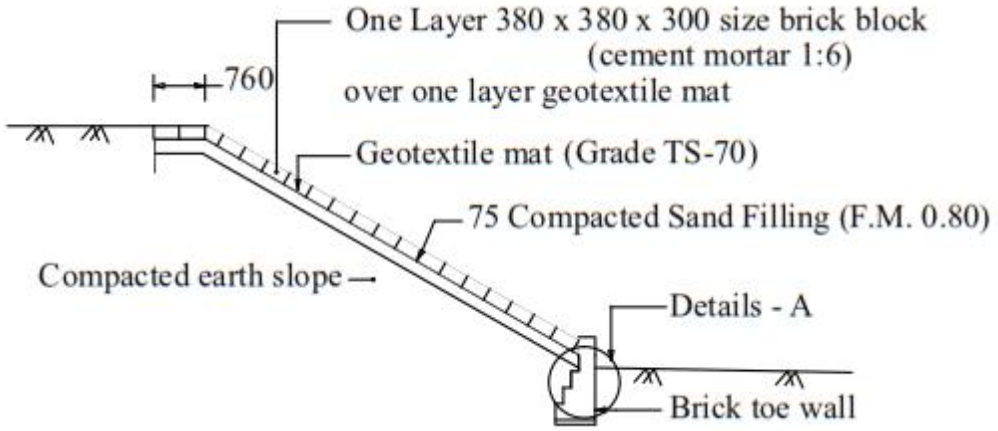

Figure 7.3: Slope protection work with brick block and geotextile.

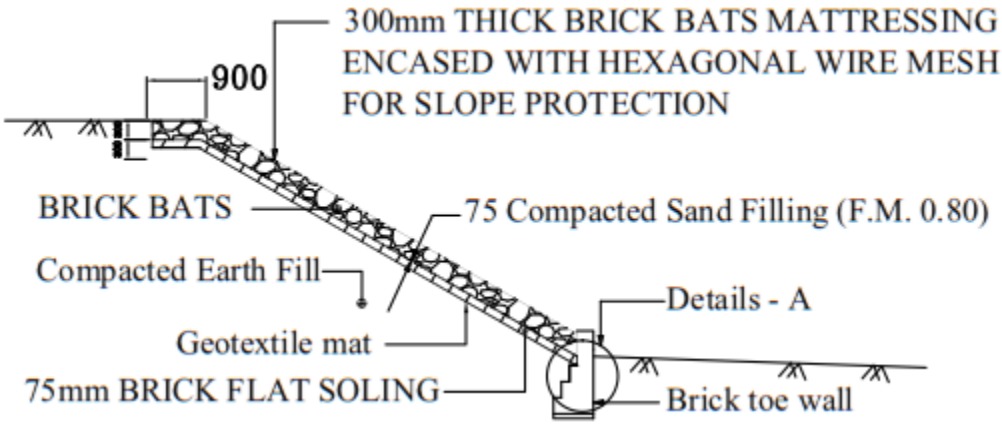

Figure 7.4: Slope protection work with brickbat mattressing and geotextile.

As per the BWDB guideline for the design of flood embankment, the design water level (DWL) is fixed based on the annual maximum flood level corresponding to a 100-year return period. The design crest level (DCL) is fixed by adding a freeboard of 1.2 m with the DWL. The crest

width is set at 6.0 m, along with 1:3 side slopes (IWFM, 2019). A typical cross-section of an embankment is shown in Figure 7.5.

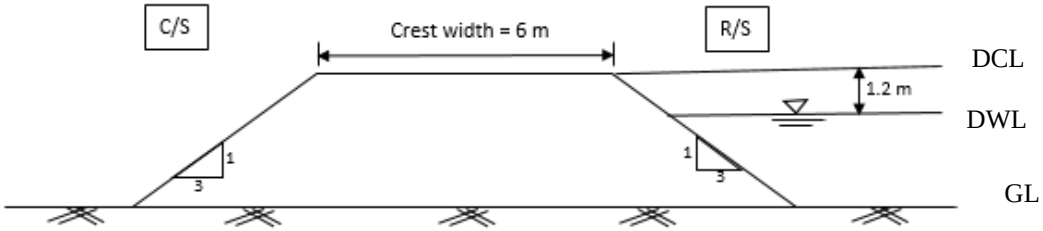

Figure 7.5: A typical cross-section of an embankment as per the guideline of BWDB.

The PROVATi[3] project has provided the following design sections for village and union roads (Figures 7.6, 7.7, and 7.8). According to the design, the side slope is suggested to be 1:1.50. In the case of sandy soil, the side slope is 1:2.0. The suggested measure for slope protection is vetiver grass. The crest width for village and union roads are 4.50 m and 4.90 m, respectively. The design, however, does not specify the crest level.

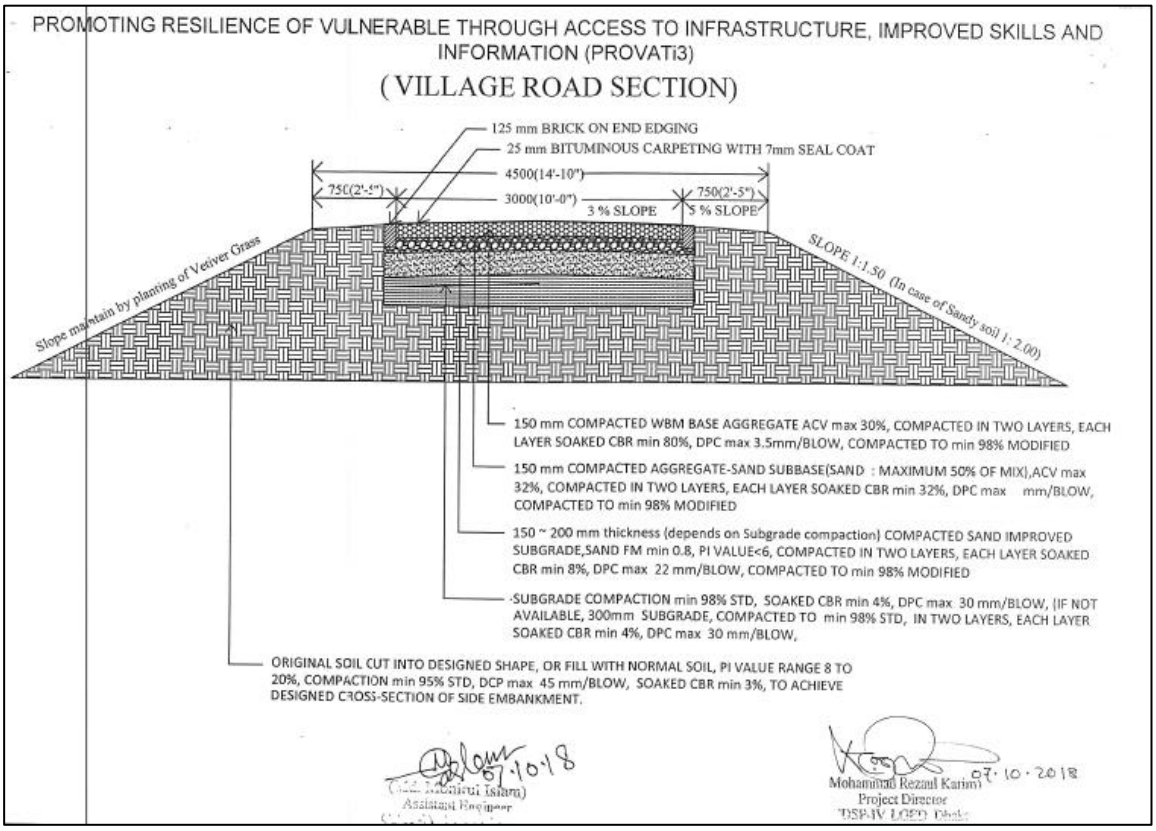

Figure 7.6: Typical village road section.

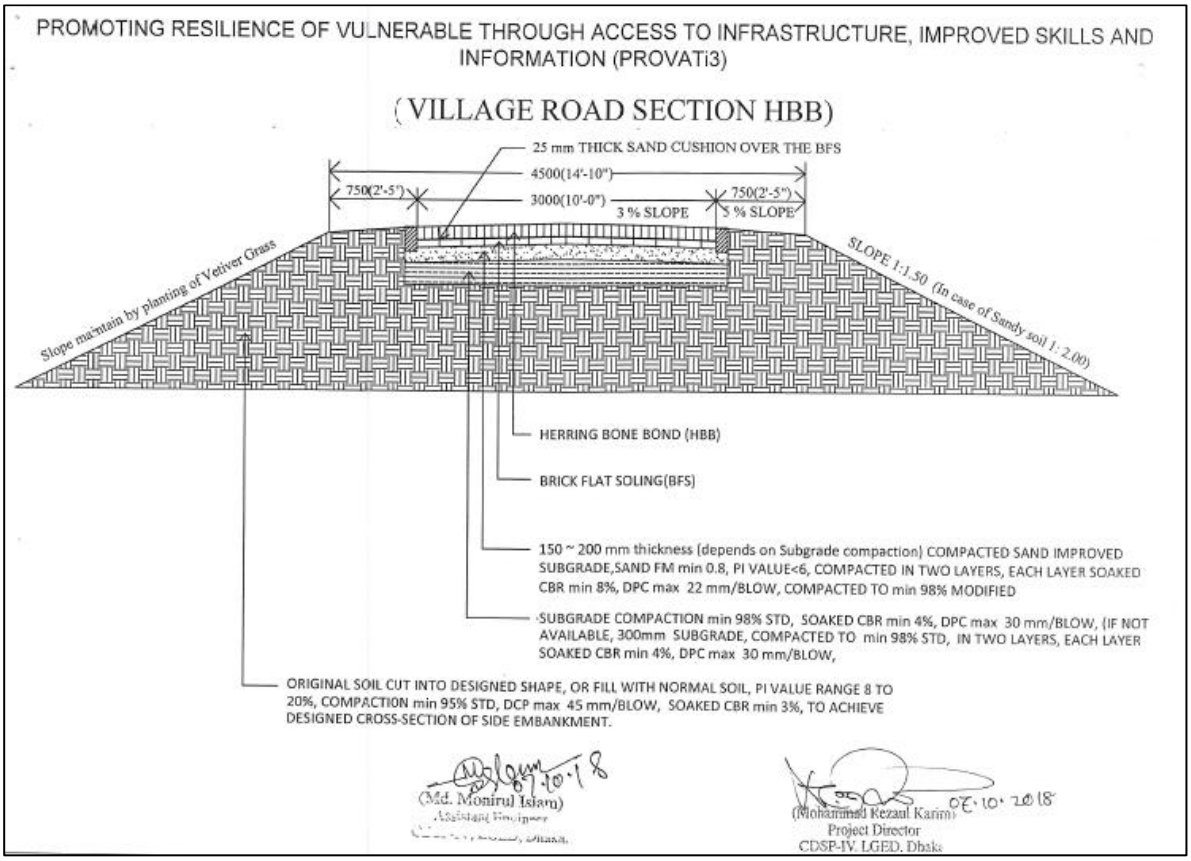

Figure 7.7: Village road section (HBB).

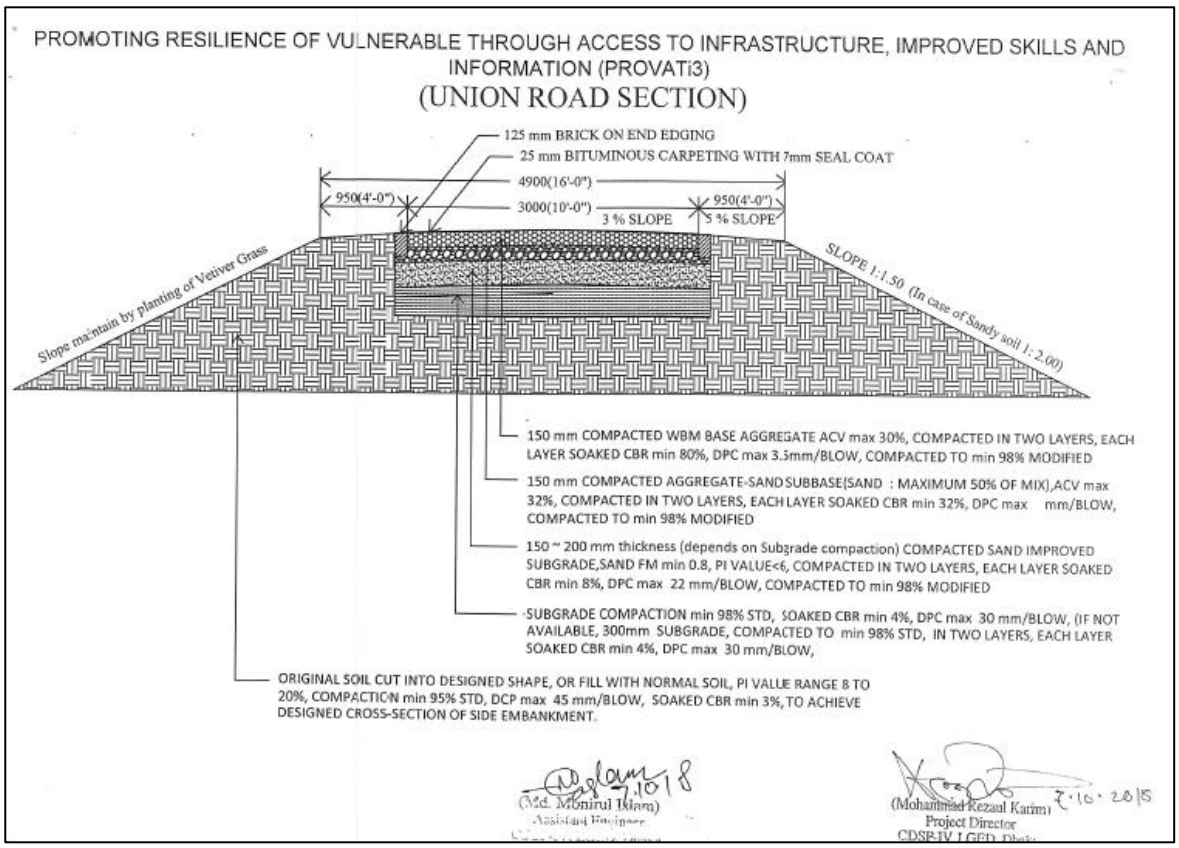

Figure 7.8: Typical union road section.

7.2 Design of Climate Resilient Growth Centers/Markets

The socio-economic development of Bangladesh is closely linked to the improvement of rural infrastructure. Bangladesh is one of the most vulnerable countries to climate variability and change because of its geographic location, low deltaic floodplain, and hydro-meteorological influence of erratic monsoon rainfall and other extreme climate events.

In Bangladesh, rural markets are considered growth centers (LGED, 1995). The growth center performs as the center of economic, social, and cultural activities in rural areas. In Bangladesh, agriculture accounts for about 50% of the Gross Domestic Product and employs around 60% of the labor force (LGED Manual). It is of utmost importance that the agricultural products reach the buyers through an efficient marketing system, and at the same time, inputs of agriculture, like seeds, fertilizers, pesticides, and other necessities, are made available on time for delivery. A growth center is a focal point with a specific level of facilities (ESCAP, 1979). It's a 'growing point' included with its vicinity and its effects as the spread of development. The growth center makes a great contribution in the areas of trade volume and turnover, employment opportunities and economic upliftment, social services improvement, infrastructure development, recreational activities, the place to exchange knowledge on production and marketing, and the place of social gathering.

As is emphasized in the Rural Road Master Plan (2005), the development of rural roads that connect growth centers with Upazila headquarters and villages with growth centers is critical to poverty reduction, and the development of rural markets and other facilities in a comprehensive manner is recognized as an effective approach. This study explores the existing situation and problems of growth center development and the effect of growth centers in rural development due to climate change-induced hazards and vulnerabilities. Guidelines for developing resilient climate infrastructure will be developed for those different kinds of infrastructures, as mentioned above.

In the study area, climate change will aggravate flooding scenarios. In order to plan and design climate-resilient infrastructures, it is vital to assess how much the flood level will increase in the future due to climate change. The National Water Policy of the Government of Bangladesh (GoB, 1999) states that:

“Designate flood risk zones and take appropriate measures to provide desired levels of protection for life, property, vital infrastructure, agriculture, and wetlands. In this regard, the following principles will guide future action:

i. Regions of economic importance, such as metropolitan areas, sea and airports, and export processing zones, will be fully protected against floods as a matter of first priority. Other critical areas such as district and Upazila towns, important commercial centers, and places of historical importance will be gradually provided with a reasonable degree of protection against floods. In the remaining rural areas, with the exception of those already covered by existing flood control infrastructure, the people will be motivated to develop different floodproofing measures such as raising platforms for homesteads, marketplaces, educational institutions, community centers, etc., and adjusting the cropping pattern to suit the flood regime.

ii. In the future, all national and regional highways, railway tracks, and public buildings and facilities will be constructed above the highest ever-recorded level of flood in the country. This principle will also apply in cases of reconstruction of existing structures of this nature.”

As the Upazila growth centers (Bazar) are important commercial centers, a reasonable degree of protection should be provided against floods. In this context, the plinth level of the growth centers should be raised to a level such that they can withstand the flood having a return period of 50 years. This implies that the centers do not get inundated in flood, having a 50-year return period. The growth centers located in a floodplain or in close proximity to an alluvial river should also be protected from flow velocity and wave-induced erosion. The slope protection guideline is described in detail in the climate-resilient rural roads section.

7.3 Design of Climate-Resilient Roads and Culverts

The crest level of roads and culverts would be dictated by the hydrologic analysis. As per the guidance of the water polity, the crest level of the roads and plinth level of the commercial center (Bazar), flood shelter, and other infrastructures need to be raised. As the rural roads (especially village and union roads) do not fall under the preview of the national and regional highways, a lower degree of protection from flood risk would be appropriate. In this context, the crest level of the village and union roads can be designed to protect from floods having a 20-year return period. In the deeply flooded region with prolonged inundation, submersible roads (Photo 7.4) and causeways (Photo 7.5) are recommended.

Photo 7.4: A submersible road in Islampur Upazila of Jamalpur.

Photo 7.5: A causeway in Islampur Upazila of Jamalpur.

The magnitude of flood level corresponding to different return periods can be obtained by flood frequency analysis. It can be noted that there is an upward trend in the annual maximum flood level of the Brahmaputra River. This implies that the flood magnitude is more for a particular return period if the length of the data increases. If the flood level data are partitioned into several groups, such as 1949-1984, 1949-1988, 1949-1998, 1949-2016, 1949-2017, 1949-2019, and 1984-2020 for flood frequency analysis, it is observed that the flood magnitudes are getting increased with the addition of the latest flood data (Figure 7.9). The increase in flood level for

the 100-year return period is 65 cm. If the flood level data are partitioned into two groups, such as 1949-1998 and 1999-2020, for flood frequency analysis, it is observed that the flood magnitude is increased as well for the latest data series (Figure 7.10). The increase in flood level from 1949-1998 to 1999-2020 for a 100-year return period is 88 cm. Thus, while carrying out frequency analysis with flood level data in the project area, it is suggested to consider the latest data series to accommodate the increase in flood level.

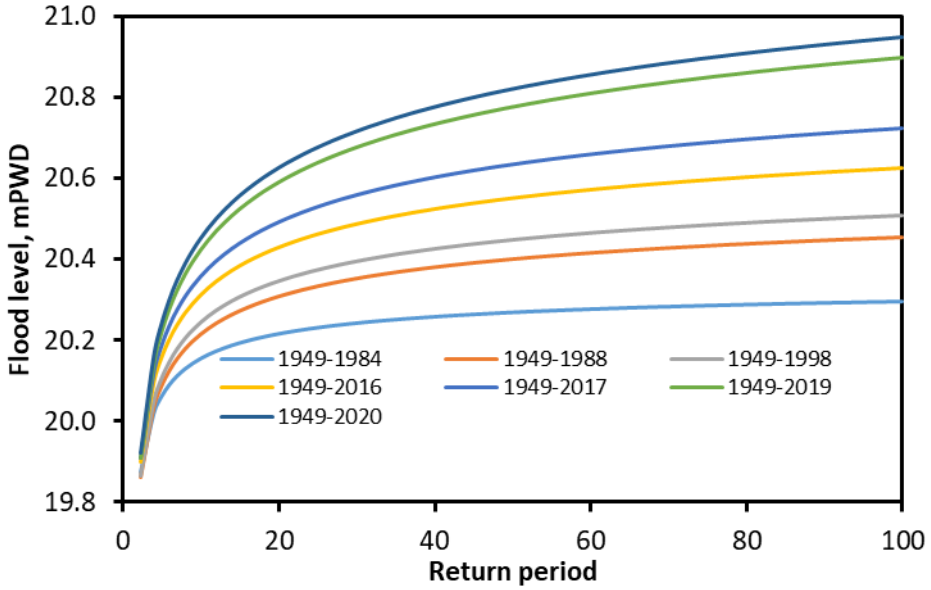

Figure 7.9: Change in the magnitude of the flood level for a particular return period in the Brahmaputra River at Bahadurabad.

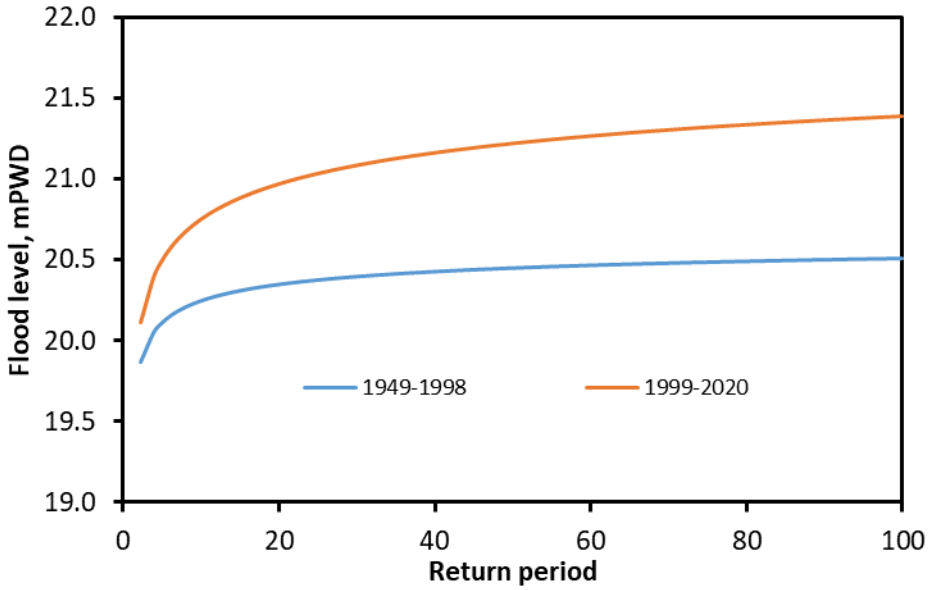

Figure 7.10: Change in the magnitude of the flood level (1949-1998 and 1999-2020) for a particular return period in the Brahmaputra River at Bahadurabad.

One of the major causes of the failures of roads and drainage structures associated with the roads is their inadequate size. This also causes drainage congestion. If adequate drainage structures are not provided along the roads, the roads, as well as the drainage structures, may fail due to the hydraulic forces. In order to design the size of the drainage structures, especially bridges and culverts, a hydro-morphological investigation should be conducted. In fact, the hydro-morphological analysis should guide the design of the roads and drainage structures. Otherwise, they may be over-designed or under-designed, which is not desirable. The alignment of roads along a riverbank should be guided by the shifting characteristics of the river. The shifting characteristic can be assessed by plan form analysis of the river reach under consideration.

The side slopes of the roads should be constructed with adequate drainage so that pore water pressure cannot be developed. In Bangladesh, sometimes roads are constructed without the proper design of the stability of the side slope. If the side slope of the road is more than the angle of repose of the soil, then the slope would be unstable and highly susceptible to failure. As such, the stability of the side slope must be ensured by testing the soil characteristics, especially the angle of repose.

In the context of Bangladesh, the roads which are constructed along the river bank are most vulnerable due to riverbank erosion. In recent times, it has been observed that in many places, riverbank erosion is caused by unplanned dredging, which alters the morphological behavior of the river and adversely affects morphological stability. The unplanned sand mining and dredging subsequently may cause the failure of the existing bank protection works and roads along the banks. Hence the dredging works must be based on the morphological assessment of the river by gathering the data through hydrographic survey and planform analysis of satellite images.

The slope protection works of roads and embankments with geotextile have proved to be effective and cheaper alternatives to concrete blocks. Large-scale application of geotextile bags or geo-bags as slope protection has provided encouraging results and, in some places, has indicated superior behavior compared with more conventional materials, especially concrete blocks (Knut and Hossain, 2010). Such types of low-cost measures can be considered for slope protection works in roads and embankments along the river banks in the study area.

Bioengineering in the form of vetiver grass has been successful in checking vulnerable river banks, especially in minor rivers. It has also been successful in slope protection of embankments and roads from wave erosion in the Haor region. Islam et al. (2013) found that the vetiver application is about 8 times cheaper than the masonry wall protection and about 5 times cheaper than the revetment stone slope protection system. They suggested that the vetiver grass plantation for slope protection could be a sustainable, green, and cheaper bio-engineering solution. As such, vetiver grass can be considered a low-cost bio-engineering intervention where there is a favorable condition to apply such protective nature-friendly measures. As a general rule of thumb, banks with slopes steeper than 2:1 cannot be stabilized just with vegetation.

The roads which run parallel and close in proximity to a riverbank should be protected with CC block revetments. A revetment normally comprises the different layers of a protection system, which covers a natural slope (subsoil) or an artificial embankment (core material). The cover layers must persist the assumed design impacts (mainly current and wave), whereas the intermediate layers between the cover and core material are required for drainage and filtering to allow for a stable foundation of the overall system. In certain cases, a cushion layer is required to protect the geotextile and base layer, which is used to level the existing subsoil and core material. A revetment structure also includes toe protection and a crest layout. The design of different parts of the revetment structure is employed based on the prevailing hydraulic and morphological parameters. A typical multi-layer design of a revetment system is shown in Figure 7.11 below.

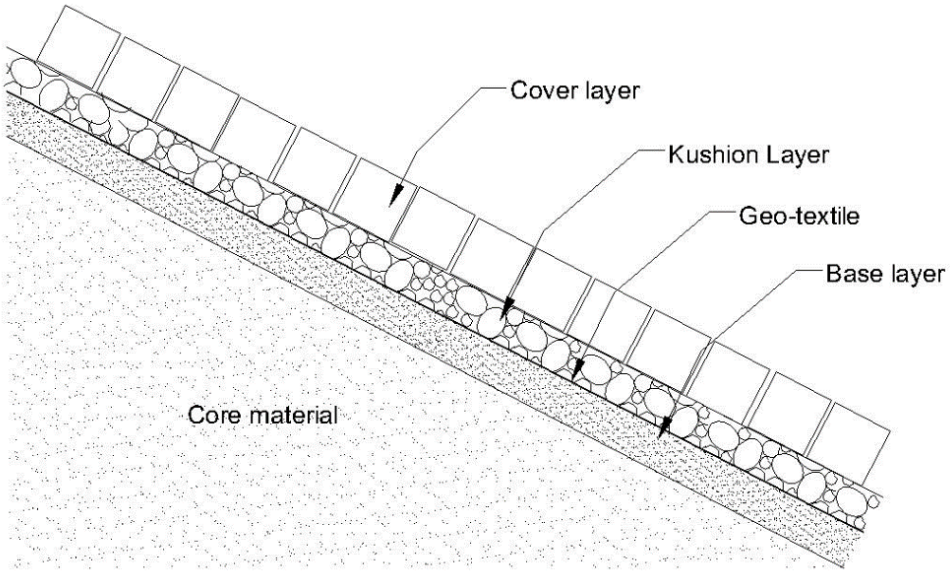

Figure 7.11: Typical multi-layer revetment system.

The cover layer must provide protection against erosive forces of currents, wave action, and other external effects. Various elements and materials are used for cover layers, including loose boulders and blocks, as well as mattress systems, asphalt layers, etc. For cover layers of standardized revetments, concrete cubes (CC-blocks) would be recommended, which are resistant to various impacts and have the advantage of uncomplicated manufacturing, possible prefabrication, and being applicable for different structural components. The dimension of the CC block would be determined based on two hydraulic loads, such as current attack and wave attack.

Intermediate layers between the cover and core material would be suggested for drainage and filtering to allow for a stable foundation of the overall system. The properties of granular filters depend significantly on particle size. The filter criterion relates the grading of the filter to that of the subsoil. The main design parameters for geotextile filters are the retention criterion and the permeability criterion, which define the capability of the material to retain the existent sub-soil without clogging and to allow unhindered water transport through the membrane.

The toe protection would be provided by a falling apron. The falling apron is toe protection of granular material, such as concrete blocks or boulders, placed directly on the existing subsoil or river bed. The extent of the protection depends on the local scour at the revetment structure. The design of revetment structures, including the cover layer, filter material, and falling apron, would be based on guidelines and the design manual for standardized bank protection structures (FAP 2001).

The dimension of the CC-block is determined based on two hydraulic loads, such as current attack and wave attack. The design of protective layers based on the current attack and wave attack is described below.

FAP 21 (2001) recommends the Pilarczyk (1990) method to estimate the size of the revetment cover layer as it includes the turbulence intensity by an empirical coefficient. The general formula for the design against current loads is given by Eq. (7.1).

$$D_n \geq \frac{0.035 \cdot \bar{u}^2}{\Delta_m \cdot 2g} \cdot \frac{\phi_{sc} \cdot K_t \cdot K_h}{K_s \cdot \psi_{cr}} \qquad \text{(Eq. 7.1)}$$

where,

D_n= characteristics size of the revetment cover layer material (m)

$\bar{u}$= depth averaged flow velocity (m/s), if replaced by u_b = 0.6 $\bar{u}$ (theoretical bottom flow velocity for a logarithmic velocity profile) a value of K_h = 1 must be applied.

Δ_m= relative density of submerged material = $(\rho_s - \rho_w)/\rho_w$

g = acceleration due to gravity (m^2/s)

ϕ_{sc}= stability factor for current

ψ_{cr}= critical shear stress parameter

K_t= turbulence factor

K_h= depth factor, dependent on the assumed velocity profile and the water depth to equivalent roughness height ratio:

$K_h = \left(1 + \frac{h}{K_r}\right)^{-0.2}$ for non-developed velocity profile with k_r= D_n for relatively smooth material where k_r is the bed roughness.

K_s= bank normal slope factor = $\sqrt{1 - \left(\frac{sin\alpha}{sin\epsilon_s}\right)^2}$

α = bank slope angle with horizontal (^{o})

ϵ_s= angle of repose considering the material-specific internal friction (^{o})

ρ_s= density of khoa agreement (kg/m^3)

ρ_w= density of water (kg/m^3)

The minimum dimensions for the stability of the cover material under wave attack can be determined by Eq. (7.2) as follows (Pilarczyk, 1990):

$$D_n \geq \frac{H_s \cdot \xi_z^b}{\Delta_m \cdot \psi_u \cdot \phi_{sw} \cdot cos\alpha} \qquad \text{(Eq. 7.2)}$$

where,

D_n= characteristics size of the revetment cover layer material (m)

H_s= significant wave height (m)

Δ_m= relative density of submerged material = $(\rho_s - \rho_w)/\rho_w$

ψ_u= system-specific stability upgrading factor

ϕ_{sw}= stability factor for wave loads

α = bank normal angle (^{o})

ξ_z =wave similarity parameter = $tan\alpha . \frac{1.25.T_m}{\sqrt{H_s}}$

T_m= mean wave period (s)

b =wave-structure interaction coefficient, mainly dependent on roughness and porosity of protective material

The stability of the cover layer strongly depends on the type and composition of the filter and other intermediate layers (Figure 7.11). The most important functions of a filter are: to prevent the migration of subsoil out of the bank line (filtering), to prevent the sinking of cover layer units into the core material (separation) and to allow water exchange between core and surface in order to prevent from excessive pore pressure during wave run-down and in case of rapidly decreasing water levels.

A granular filter is formed by layers of grain of different sizes according to the filter criteria. The properties of granular filters depend significantly on particle size. The filter criterion relates the grading of the filter to that of the subsoil. Pilarczyk (1990) defined the following criteria regarding the relationship between the characteristics of grain size of the subsoil D_s and the filter D_f.

$D_{15f} < (4\ to\ 5).D_{85s}$ (stability criteria)

$D_{15f} > (4\ to\ 5).D_{15s}$ (permeability criteria)

$D_{50f} > (20\ to\ 25).D_{50s}$ (segregation criteria)

$C_u = \frac{D_{50}}{D_{10}} < 10$ (no migration)

$C_u = \frac{D_{50}}{D_{10}} > 20$ (susceptible to migration)

where $C_u$is the coefficient of uniformity and D_{50}(mm) in diameter according to x % undersize by mass taken from grain size distribution. The minimum overall thickness of the granular filter should be 150 mm, as suggested by FAP 21 (2001). Wherever practicable, the granular material must be carefully compacted to minimize settlements.

The main design parameters for geotextile filters are the retention criterion and the permeability criterion, which define the capability of the material to retain the existent sub-soil without

clogging and to allow unhindered water transport through the membrane. Minimum standards of geotextile fabrics, as suggested by FAP 21 (2001), are given below.

Protective layers of uniformly sized concrete blocks (placed in parallel rows) of more than 50 kg single weight or stone mattresses of 2.5 cm to 40 cm thickness require filter fabrics (non-woven needle-punched geotextile) of the following specification as shown in Table 7.3:

Table 7.3: Specification of filter fabrics used as revetment filter layer (non-woven needle-punched geotextile).

Geotextile parameters	**Specifications**
Material	preferably 100% Polyester (PES), or 50 % Polypropylene (PP) and 50 % PES
Maximum effective opening size, EOS/AOS	0.075 mm
Thickness	≥ 3.0 mm
Area mass	≥ 350 g/m^3
Minimum tensile strength longitudinal transversal	 > 15 KN/m > 15 KN/m
Minimum elongation longitudinal transversal	 ≥ 80 % ≥ 50 %
Puncture resistance (CBR)	> 600 Nm
Mechanical filtering capacity maximum quantity of soil passage maximum quantity of soil passage in the last test phase	 300 grams 30 grams

The specification of geotextile material for manufacturing of geo-bag or geo-sand containers is shown in Table 7.4 (FAP, 2001).

Table 7.4: Specification of geotextile material for manufacturing of geo-sand containers.

Geotextile parameters	**Unit**	**Value**
Effective opening size O90	mm	< 0.09
Area mass	g/m2	≥ 400
Thickness	mm	≥ 3.5
Minimum tensile strength as per DIN 538557 longitudinal transversal	 N/10 cm N/10 cm	 ≥ 1700 ≥ 2700
Minimum elongation longitudinal transversal	 % %	 ≥ 50 ≥ 50
Coefficient of permeability at a load of 2 km/m^2	m/s	1×10-7
Materials	-	PP/PES

The design of toe protection should be based on guidelines and a design manual for standardized bank protection structures (FAP 2001).

7.4 Design of Climate-Resilient Flood Shelters

The plinth level of the flood shelter should be designed in such a way that it can withstand the highest ever recorded flood level or 100-year return period flood level, which is larger. In the recent past, many flood shelters were damaged due to riverbank erosion. As such, flood shelters should be located away from vulnerable river banks. The flood shelters located in a floodplain should also be protected from flow velocity and wave-induced erosion. The slope protection guideline is described in detail in the climate-resilient rural roads section.

7.5 Monitoring and maintenance of roads and other infrastructures

The roads and other infrastructures should be periodically checked and maintained. Road deterioration due to lack of maintenance has become a growing issue in a number of developing countries. The problem has been discussed at length, and the results of a lack of maintenance have been well-defined and quantified. It is important that maintenance is performed on a timely and regular basis. Consequently, it is a recurrent activity and needs to be financed as such.

Unfortunately, road maintenance is often viewed as a set of projects to be carried out on roads that, because of lack of maintenance, have deteriorated to a state where they need reconstruction (ILO, 2007). If the roads are not maintained on a regular basis, they cannot function properly when a flood event occurs, even with a lesser magnitude for which the roads were originally designed. In the context of Bangladesh, the failure of roads during a flood event in the form of breaching is attributed to the fact that they were not properly maintained. A regular inspection, monitoring, and maintenance program of all the protection works shall be made mandatory.

7.6 Socializing and Engendering Design of Infrastructures of PROVATi^3 Project

Any civil structure is to bring benefits to the society leading to the development of the country. How to maximize the benefits is an important question hovering over the mind of all people related to the project. It is a very vital question now to go for any structure befriending all stakeholders in a society, ensuring the well-being of each citizen, and making it acceptable to all.

Huge infrastructural developmental works are going on in Bangladesh to turn the country into an economically vibrant one, socially acceptable and environmentally sustainable. PROVATi^3 is also one of them. PROVATi^3 denotes 'Promoting Resilience of Vulnerable Through Access to Infrastructure, Improved Skills, and Information.' The title of the project announces a lot explaining the trajectory of its philosophical setting. PROVATi^3 is to be community friendly, gender-sensitive, resilient to vulnerability providing access to the infrastructure, and ensuring improved skills and information. So, the core value of the project is based on humanitarian well-being focusing on integrated concepts where resilience is to be enhanced in the bottom layers of the country. A brief discussion is made in this section to describe how it would be achieved through various pro-poor activities in the project.

7.6.1 Socializing and PROVATi^3 Project

The road sector has come out as the dominant mode of transport in Bangladesh. The country has developed an enormous network of urban and rural roads across the country. Since its independence, the developmental activities of the country have been focused on poverty reduction in the poor community considering pro-poor approaches as much as possible and providing people access to basic social services. But it was not so easy to ensure those services

like livelihood opportunities, education, health care, and economic enhancement in rural areas, where the larger part of the total population lives. Short funding and the absence of integrated and coherent planning were the barriers. It gradually came to be clear that larger participation of local communities via labor-intensive and community-based construction and maintenance of rural feeder roads is vital. Now the Government, together with the Development Partners, realized the overarching importance of the inclusion of all sectors of the economy and society in infrastructure to improve their overall functionality, especially the transport system. Such inclusion is to enhance private sector growth, foster agricultural production, reduce poverty, vibrate investment and human development, and increase the capacity to deliver social services, etc. Such integrated activities and strategies in pre, during, and post-construction of infrastructure are critical to ensure the participation of the rural poor leading to a resilient society.

Infrastructure projects should not only improve transportation and the related infrastructure but also enhance multiple necessities of social life like trade, public health, education, social, economic, and gender equity, etc. Knowledge sharing and inclusion of good practices in road projects create opportunities on many levels out of the box of the defined transport sector. IFAD has given ample attention to the design of the PROVATi^3 project providing many spaces for the inclusion of gender-responsive activities in various stages of the project, which ultimately would lead to the socialization of the rural road infrastructures.

To make pro-poor infrastructures in rural Bangladesh, attention and efforts were given on the part of planners and donors. Bangladesh has a long history of the inclusion of poor sections of society in the developmental activities of infrastructures, especially in the rural road infrastructures.

The PROVATi^3 Project is aimed at six poverty-driven districts - Gaibandha, Jamalpur, Kurigram, Lalmonirhat, Nilphamari, and Rangpur. Among them, the worst poverty-stricken districts are Gaibandha, Jamalpur, and Kurigram. The main causes of poverty are the flood-prone of these districts to the proximity of the mighty Brahmaputra and the Teesta Rivers.

7.6.2 Socializing Approaches in PROVATi^3 Project

PROVATi^3 vision aligns with the GoB Vision 2021, the 7th Five Year Plan, and the commitments to achieving the SDGs and becoming a middle-income country. PROVATi³ will

be focused on ending extreme poverty, gender equality, women's empowerment and on the realization of the youth's potential. Activities and outputs are targeted especially at the poor, women, and youth.

PROVATi^3 focuses on highly prevalent poverty and vulnerability areas: the six districts of Kurigram, Gaibandha, Jamalpur, Rangpur, Nilphamari, Lalmonirhat; 25 Upazilas and 90 Unions. The project covers about 303,000 households, approximately 45 percent of the total population targeting poor women and men, marginal and small farmers, traders and shop owners in markets, micro-entrepreneurs, and other local private and government institutions. The infrastructure and flood information system will benefit the overall population of the project areas.

The development focuses on increasing the resilience of communities incorporating two main components with three mutually reinforcing pathways. The first component carries improvement of the design of infrastructure and builds, rehabilitates, and upgrades infrastructure, enhancing connectivity, reducing production costs, and creating access to services and markets.

The second component strengthens vocational and income-generating skills in order to create on- and off-farm employment to increase and diversify the incomes of poor households. It enhances local people-centric flood warning and dissemination systems for improved preparedness, planning, and emergency response.

Thus, improved infrastructure, increased skills for employment, and access to information for preparedness form the three thrusts driving the project toward its objective.

Specific target groups will include 15,000 ultra-poor and poor HHs for LCS work and livelihood capacity building and 30,000 youth from poor-near to poor households for vocational training.

PROVATi^3 will work targeting to eliminate all forms of poverty and to ensure that none is left behind in the development processes it engenders. For each project activity, measures, selection criteria, and processes have been defined in the Gender and Social Inclusion Action Plan. A

Gender and Social Inclusion Officer is part of the PROVATi[3] team and is to ensure continued efforts at optimized targeting.

The project directly targets 10,500 women and 4,500 men in LCS and 9,000 young women and 21,000 young men in vocational training and skills development. PROVATi[3] will engage 21,000 young men and 9,000 young women in skills development for employment in construction and other sectors, such as garments, embroidery, block-batik, computer operation, etc.

To ensure that targeting is a continuous concern and process throughout the duration of PROVATi[3]. The project will ensure that the LGED Gender and Development Platform is informed of and involved in all poverty, gender, and youth targeting efforts in order to ensure mainstreaming and advocacy.

Implementing partners are provided guidance and technical support and are supervised to deliver and report on agreed objectives and targets.

The effectiveness of targeting is to be regularly reviewed and reported upon in the progress reports. Proposals for enhanced targeting are to be raised with the supervision missions.

Component 2 includes resilient communities through employment and early flood warning. The outcome of this component is “Increased adaptive capacity of vulnerable communities through diversified incomes and access to precise location-specific and early flood information in project Upazilas.”

Subcomponent 2.1 of the project focuses on women and men working under ‘cash for work’ schemes through LCSs in project construction and maintenance and receiving training in IGAs, as well as general support in managing their livelihoods, including water, sanitation and hygiene, nutrition aspects and financial literacy. Subcomponent 2.2 focuses on providing a solid skills base for youth in the project area. Vocational training paired with apprenticeships will lead to hands-on skills that will allow youth to enter on- and off-farm remunerative activities. This contributes to diversified incomes for local households.

Subcomponent 2.3 scales up a proven community-focused flood information/warning system. A combination of local data generation, advanced hydrological modeling/analysis, and information dissemination through SMS and local volunteers will increase preparedness and informed decision-making by the affected population. Subcomponent 2.4 focuses on practical policy and regulatory reviews and includes a partnership with the World Food Programme (WFP) in the area of detailed poverty and nutritional status mapping.

Staff capacity building targets the capacity building of project staff through several internal training courses and workshops. Hands-on training will help project staff members to internalize project activities and procedures and help maintain quality and timeliness. Training courses include organization and engagement of Labour Contracting Societies (LCS); Involvement of Local Government Institutions (LGI); Market and School Management Committees in infrastructure development and management; Livelihood improvement activities for LCSs; and organization of skill development for youth employment.

Staff training will include the formation of LCS groups, selection criteria, training on construction and social issues, use of protective gear and construction tools, LCS construction work management including payment system, supervision, and monitoring works as per the LGED operation manual. Those training will target 2 participants from the LGED Gender and Development Platform, 2 participants from PMU (Gender and Livelihoods Officers), and 6 participants from NGO-MFIs recruited for LCS empowerment.

All staff of the project will undergo training on poverty, gender, and youth issues in year one as part of the orientation meetings at the district level. A follow-up training will be planned before mid-term to ensure continued focus on the special target groups. The training will focus on why poverty and gender awareness make a difference in project execution, how poverty targeting and gender mainstreaming make development projects more successful, and what tools are available to involve these special target categories.

Capacity building of LCS members on livelihood development is to build the capacity of about 15,000 men and women from poor households (70% female heads of households) engaged in LCS work to gradually and sustainably move 75% of the project-supported LCS members out of extreme poverty. PROVATi[3] will target this component at the beneficiaries of LCS work

financed by PROVATi[3], as well as beneficiaries of LCS work in the project area, which is financed otherwise.

Two models for capacity building of LCS are to be taken up by PROVATi[3]. One model integrates the Gender Action Learning System-methodology (GALS) in the training curriculum for the LCSs. The methodology aims at empowering LCS members to develop skills for business, leadership, and financial management, as well as mindsets and behavioral changes that address structural causes of poverty and gender inequality. This model targets 7,000 LCS members (45% of the total target). Another model replicates the practices applied by LGED in other projects. The training curriculum integrates training on income-generating activities (IGA) and social issues. The replication model will target 8,000 LCS members (55% of the total target).

7.6.3 Experiences of Bangladesh in Socializing Infrastructures

Bangladesh has good experiences in socializing infrastructures through the integration of gender in road and transport projects. General approaches taken in various rural road projects in Bangladesh are discussed in the following paragraphs.

The general goals of rural road improvement projects were to achieve improved infrastructure to reduce rural poverty through economic growth and rural development, creating economic opportunities for the rural poor. Participatory and sustainable rural infrastructure, social and gender development, and improved local governance in the project area were the philosophy. Women are to be encouraged to participate in all aspects of the development process, and short- and long-term employment opportunities are to be created. Thus, the inclusion of social elements together with other road improvement components is to ensure greater community benefits in society.

Such poor friendly actions have resulted in healthy life aspects of rural Bangladesh in many ways. Usually, the undertaken projects focused upon five components like improvement of rural roads; improvement of rural infrastructure, such as GCMs, boat landings, ferries, and union Parishad complexes (UPCs); improvement of infrastructure maintenance; strengthening of

LGED capacity and improvement of local governance; and support to LGED in project management.

The Improvement of Rural Infrastructure by LGED could address the construction of community-friendly structures like Growth Centre Markets and boat landings. GCMs, include sections for women. The election of management committees was done through public meetings to ensure the proper management of GCMs. Small ferries were procured for small river locations. Management committees for boat landings and ferries were formed through public discussions. Union Parishad Centres were constructed to improve local governance.

Local governance was improved through training focusing on local government issues, planning, financial management, administration, and participatory methodologies to Union Parishad Members to ensure their efficient and effective local governance. The management committees of GCMs, boat landings and ferries, and market traders' associations were trained to operate and maintain the infrastructure. Upazila and UPs were given training for managing and maintaining village roads, boat landings, and ferries. Third, through Piloting, training was done for Ups to generate funds from market leases and retain for local union operations and maintenance for enhancing the sense of ownership and sustainability.

Tree planting on Upazila and Union roads was achieved by employing labor contracting societies (LCS). LCS also performed off-pavement road maintenance.

Infrastructure maintenance of Upazila and union roads is carried out by LGED, while the UPs maintain minor rural roads. Such works are carried out by rural disadvantaged women through LCS under intensive supervision.

The development of growth center markets was one of the main jobs through improved GCMs. Common public facilities like pavement and drainage in the market area, internal roads, multipurpose sheds, fish sheds, meat sheds, tube wells, sanitary latrines, garbage pits, market offices, and a women's market section (WMS) were established for each GCM. LCSs were employed in the construction activities.

Construction of boat landings and paved areas was done to facilitate the safe mooring of boats and easy access for passengers and goods to GCMs.

Construction of Union Parishad Complexes, cyclone shelter buildings constructed in cyclone-prone areas, is a continuous process. These activities are to support government efforts to pass on authority to UPs and to encourage community participation in local government to smoothen union-level services.

Thus, social inclusion and gender were targeted through various activities designed in the projects. Various techniques were employed to incorporate social and gender perspectives in the design and implementation arrangements of physical infrastructure projects.

7.6.4 Suggestions for socializing infrastructure

Flood-sensitive design of infrastructures with adequate flood information is a good technique to enhance socialization and poverty reduction. Construction of any infrastructure mitigates socials, can enhance awareness through programs on the risks and might be carried out at construction sites and for the surrounding communities. Transport projects can include programs to support health awareness campaigns, access to health services, and other activities. Risks of human trafficking can be focused and equal pay for equal work and facilities for workers and safe working conditions, and prohibiting the use of child labor, etc., can be promoted.

A few new initiatives which can be included in the infrastructures project are mentioned for achieving better socialization and engendering design of infrastructures:

i. *Provision and Marking of historical flood events in important structures, locations, GCMs, etc.*

Flood is a common phenomenon in Bangladesh. It turns out very serious during a big flood event. Flood information becomes very important for our day-to-day activities. But we cannot find anywhere any flood information marked at our market, road structure, or school premise to get some idea about the flood magnitude. The only news about the flood in the media is forecasted or broadcasted, informing the community but almost unaware of its magnitude as it is quite impossible to have some clear idea about flood magnitude, which is very necessary for rural people to know when the flood is rising or falling.

Big flood events marked by the water level in public premises like a bridge, culverts, roads, schools, growth centers, etc., could come out as very useful information providers for the

common people. Such an engineering design with flood information would be very useful in socializing an infrastructure as well as making it popular among society.

ii. Making infrastructures community-friendly

Infrastructures need to be socially acceptable, considering community-friendly components in the design as far as possible. It is a matter of concern that mostly our design, planning, construction, operation and maintenance, and monitoring - are left with traditional designs. No remarkable components are considered for fulfilling the needs of the community, like some sitting arrangements with additional recreational facilities if the structure is located nearby a rural setting. Local people very often get together around a structure during the evening time. Any new structure attracts the community, especially the young generation turning the place into an evening festival.

We need to recognize this public sentiment and incorporate design components as it best fits their aspirations. Thus we can socialize our infrastructures by attracting sympathy and love from the community.

iii. Removing gender biases

Our infrastructures are mostly gender blind, indicating that the needs and requirements of disadvantaged, elderly, and pregnant women groups are ignored. This can be addressed wherever possible, keeping some space for them.

iv. Poverty analysis for influence zone of rural road infrastructures for conforming poverty incidence and ranking

v. Poverty analysis and its distribution and poverty profile of a project area;
vi. Social/ Gender Analyses along the influence zone of a project;
vii. Comprehensive poverty, social, and gender Analyses;
viii. Connection of rural areas with community-based initiatives;
ix. Employing good practices in addressing social and gender at home and abroad; and
x. *Provision and Providing Innovative Options.*

CHAPTER EIGHT
OBSERVATIONS FROM FIELD VISITS

8.1 Field visit to the Jamalpur flood vulnerable Area

A field visit was made by BUET and LGED Project Design Team during 17-19 March 2021 in the Bakshiganj, Islampur, and Madarganj Upazila of Jamalpur District. The primary objective was to visit the proposed Flood Shelters, Roads, and Markets. The team includes Prof A.K.M. Saiful Islam and Prof. G.M. Tarekul Islam from IWFM, BUET, and Eng. Saiful Islam and Engr. Md. Khalid from LGED. This visit was made after the severe and prolonged floods in 2020. The study team found many roads were damaged due to the flood water standing for a long period (more than 1.5 months) in 2020. Our observations from the field visits on the existing roads, bridges, and markets constructed by LGED and also proposed Flood Shelters under this project are presented in photos 8.1 to 8.10. A summary of the key issues of the failure or damage, or resilience of different infrastructures observed during the field visit is presented in Table 8.1.

Table 8.1: A summary of the major observations from field visits.

Infrastructure type	**Remarks**	**Reference**
Village Road	Vulnerable as no slope protection	Photo 8.1
Single span bridge	Failure due to inadequate opening	Photo 8.2
Union Road	Slope failure from seepage pressure	Photo 8.3
Union Road	Slope failure	Photo 8.4
Village Road	Damage from overflowing	Photo 8.5
Village Road	Flood Shelter plinth level	Photo 8.6
Cattle Shelter	Flood proofing example	Photo 8.7
Village Road	Flood Resilient RCC road example	Photo 8.8
Union Road	Steep side slopes vulnerable to flood	Photo 8.9
Flood Shelter	Poorly designed existing flood shelter	Photo 8.10

Photo 8.1: There is no slope protection on this newly constructed village road. The slope of the road is highly vulnerable during floods. CC-block type of protection should be used as the road extends right from the abutment of a bridge in Kamalbarti Bazar, Bakshiganj, Jamalpur. But it was learned during the field visit that the slope of the road would be protected by vetiver grass which may not be suitable along the bank of a river during flood flows.

Photo 8.2: Damage of a bridge in Bakshiganj Upazila in Jamalpur. The damage appears to be due to the inadequate opening of the one-span bridge. As the area is located in the floodplain of the mighty Jamuna and the Dashani rivers, the waterway width of the river/canal should never be reduced while constructing a bridge.

Photo 8.3: Damage to the approach road of a bridge is probably due to seepage pressure developed during flood flow from the other side of the road. The slope should have been constructed with adequate filter material so that the seepage pressure can no longer develop and undermine the slope as well as the road itself.

Photo 8.4: Damage of a road due to slope failure in Bankishang Upazila, Jamalpur.

Photo 8.5: Damage of a village road due to overflowing. This road would connect a flood shelter in Chinar Char in Bakshiganj, Jamalpur. While renovating the road, the sufficient opening should be ensured by providing a culver of adequate size so that the flood flow can safely pass beneath the culvert without damaging the curve itself and the road.

Photo 8.6: Chinar Char Uttarpara Primary School. A new flood shelter-cum-primary school would be constructed on these premises. The corrugated sheet of the school clearly marks the flood of 2019 and 2020. The plinth level of the flood shelter should be set above the highest flood level or the 100-year flood level with an appropriate freeboard.

Photo 8.7: A flood-proofing straw pile in the Shapdhori Union of Islampur Upazila of Jamalpur district. The straw piles will not be inundated even during the flood.

Photo 8.8: A village road constructed with rigid pavement (RCC) in Madarganj Upazila, Jamalpur. This type of road is more climate-resilient, especially during floods. The village roads in areas vulnerable due to floods should be constructed with RCC with appropriate side slopes so that the damage is minimum even during overtopping during extreme flood events.

Photo 8.9: The side slope of the road, located in Madarganj Upazila, is almost vertical, thus making it utterly vulnerable during flood flow.

Photo 8.10: A poorly designed primary school in Shukh Nagari village of Madarganj Upazila. The two buildings have two different plinth levels. The plinth of the school gets inundated even during the moderate flood. A new flood shelter would be constructed on these premises. The plinth should be set at a 100-year flood level with an appropriate freeboard.

CHAPTER NINE
CONCLUSIONS AND RECOMMENDATIONS

9.1 Conclusions

In this study, a detailed hydrological, hydraulic, and morphological analysis of the watersheds in determining suitable design criteria for the proposed flood-vulnerable areas in order to build climate-resilient infrastructures. To achieve this goal, this study has been designed to assess the impact of climate change on the Teesta-Brahmaputra river system; assess erosion and accretion of land/char due to meandering of rivers; determine flood risk zones by combining both model results with ground-based and satellite image analysis of historic floods and potential impact of climate change on river flows of each project Upazila, and prepare a guideline for designing the climate-resilient infrastructures. The results indicated the necessary modifications in design on roads, culverts/bridges, markets, slope protection, etc., and might lead to updates in design standards at LGED.

To carry out this study, baseline data, including socio-economic setting, climate, land use characteristics, river system and morphology, hydrological characteristics, and the infrastructures and communication network, have been collected. Hydrological modeling of the Brahmaputra-Teesta river basins has been conducted using SWAT modeling. The model showed a very good agreement between the observed and simulated discharges. The NSE values are 0.75 and 0.71, the coefficient of determination values (R2) values are 0.76 and 0.73, and the PBIAS values are 4.2 and 3.0 for the calibration and validation stage. After calibration, the hydrological model is forced by CMIP6 climate projections over the basin under balanced SSP2-4.5 and high-end SSP5-85 scenarios. Changes in future peak water level height are determined by simulating a 1-D hydraulic model, HEC-RAS, for the major rivers of the study area. Most of the stations provided very good results in terms of R^2 (>0.8) except Simulbari (SW 10) station in the Bangali river and Gaibandha (SW 97) station in the Ghaghat river.

The flood frequency analysis has been conducted at the gauge stations of the rivers nearby the study area for present and future conditions. The design water level for the various return periods is calculated for present and future conditions. Due to the uncertainty of future changes in water levels (varies from 11 cm to 38 cm), an increase of 30 cm (0.3 meter) of the crest level

of the roads is recommended, while an increase of 50 cm (0.5 meter) of the crest level of the markets and flood shelters are recommended.

Flood risks are assessed from flood inundation mapping using high-resolution satellite images, whereas bank erosion risks are assessed from the changes in the river planform through historical satellite image analysis. Based on planform analysis using historical satellite images, bank erosion risks are identified for the proposed markets and flood shelters in the above-selected locations on a scale of low, moderate and high. Finally, combined flood and bank erosion risks on the above infrastructures are presented in Table 5.28 and Table 5.29. All of these composite flood vulnerability maps are prepared in an open source-based Google KML format which can be easily visualized and shared across many applications.

9.2 Recommendations

A summary of the key recommendations for climate-resilient infrastructure under this project is presented in the following table (Table 9.1).

Table 9.1: Recommendations for Climate Resilient Infrastructures under this PROVATi[3] project.

Infrastructure	Parameters	Recommendations	References
Village/Union Road	Design Crest Level	10-year return period and freeboard of 0.3m	Table 6.20
		Additional increment of 0.3 m considering climate change	Table 6.28
	Side Slope	• The minimum slope is 1:1.5 • The minimum slope is 1:2.0 (Sandy Soil) • The actual side slope should be determined by slope stability analysis	Figures 7.1-7.3
	Slope protection	• vetiver grass (*Chrysopogon zizanioides*) • Clay Blanket and vetiver grass (Sandy Soil) • CC Block (Riverside)	
	Road Surface	• BC (Not Frequently Inundated Areas) • RCC (Frequently Inundated Areas)	Figure 5.9-5.12
	Culverts	Hydraulic Analysis is recommended for designing the size and number of culverts	Table 7.1
	Bridges	Waterway opening should be adequate to pass the flow of the river	
	O&M	Periodic monitoring and maintenance are essential to make the road climate resilient	
Flood Shelter	Design Plinth Level	100-year return period and freeboard of 0.5 m	Table 6.20
		Additional increment of 0.5 m considering climate change	Table 6.29

	Erosion vulnerability	Planform analysis of nearby river banks should be carried out	Figure 5.18-5.21 Table 5.10-5.13
	O&M	Periodic monitoring and maintenance are essential to make the flood shelter climate resilient	
Markets	Design Plinth Level	100-year return period and freeboard of 0.5m	Table 6.20
		Additional increment of 0.5m considering climate change	Table 6.29
	Erosion vulnerability	Planform analysis of nearby river banks should be carried out	Figure 5.14-5.17 Table 5.4-5.9
	O&M	Periodic monitoring and maintenance are essential to make the market climate resilient	

A few new initiatives which can be included in the infrastructures project for achieving better socialization and engendering design of infrastructures are also recommended, such as-

- Provision and Marking of historical flood events in important structures, locations, GCMs, etc.
- Making infrastructures community-friendly
- Removing gender biases
- Poverty analysis for influence zone of rural road infrastructures for conforming poverty incidence and ranking
- Poverty analysis and its distribution and poverty profile of a project area
- Social/ Gender Analyses along the influence zone of a project
- Comprehensive poverty, social, and gender Analyses
- Connection of rural areas with community-based initiatives
- Employing good practices in addressing social and gender at home and abroad; and
- Provision and Providing Innovative Options.

REFERENCES

Abbaspour, K. (2007). User manual for SWAT-CUP, SWAT calibration and uncertainty analysis programs. Eawag: Swiss Federal Institute of Aquatic Science and Technology, Duebendorf, Switzerland.

Abbaspour, K. C., Vejdani, M., Haghighat, S., & Yang, J. (2007). SWAT-CUP calibration and uncertainty programs for SWAT. In MODSIM 2007 International Congress on Modeling and Simulation, Modeling and Simulation Society of Australia and New Zealand, pp. 1596-1602.

Abbaspour, K., Johnson, C. and Van Genuchten, M.T. (2004). Estimating uncertain flow and transport parameters using a sequential uncertainty fitting procedure. Vadose Zone Journal, 3(4), 1340-1352.

Abbaspour, K.C., Faramarzi, M., Ghasemi, S.S. and Yang, H. (2009). Assessing the impact of climate change on water resources in Iran. Water Resources Research, 45(10), W10434.

Alfieri, L., Feyen, L., Dottori, F., & Bianchi, A. (2015). Ensemble flood risk assessment in Europe under high end climate scenarios. Global Environmental Change, 35, 199-212.

Andersen, T. K., & Marshall Shepherd, J. (2013). Floods in a changing climate. Geography Compass, 7(2), 95-115.

Arnell, N. W. (1999). Climate change and global water resources. Global environmental change, 9, S31-S49.

Arnold, J.G., Srinivasan, R., Muttiah, R.S. and Williams, J.R. (1998). Large area hydrologic modeling and assessment Part I: Model development. J. Am. Water Resour. Assoc., 34(1), 73-89.

Bharati, L., Gurung, P., Maharjan, L. and Bhattarai, U. (2016). Past and future variability in the hydrological regime of the Koshi Basin, Nepal. Hydrol. Sci. J., 61(1), 79-93.

Priestley, C.H.B. and Taylor, R. J. (1972). On the Assessment of Surface Heat Flux and Evaporation Using Large-Scale Parameters. Division of Atmospheric Physics, Commonwealth Scientific and Industrial Research Organization, Aspendale, Victoria, Australia.

Casagli, N., Frodella, W., Morelli, S., Tofani, V., Ciampalini, A., Intrieri, E., ... & Lu, P. (2017). Spaceborne, UAV and ground-based remote sensing techniques for landslide mapping, monitoring and early warning. Geoenvironmental Disasters, 4(1), 9.

Chalov SR, Jarsjö J, Kasimov N, Romanchenko A, Pietron J, Thorslund J, Belozerova E. (2015). Spatio-temporal variation of sediment transport in the Selenga river basin,

Mongolia and Russia. Environ Earth Sci 73(2):663–680. Doi: 10.1007/s12665-014-3106-z.

Eyring, V., Bony, S., Meehl, G. A., Senior, C. A., Stevens, B., Stouffer, R. J., and Taylor, K. E. (2016). Overview of the Coupled Model Intercomparison Project Phase 6 (CMIP6) experimental design and organization, Geosci. Model Dev., 9, 1937–1958, https://doi.org/10.5194/gmd-9-1937-2016.

FAP 21 (2001): Guidelines and Design Manual for Standardized Bank Protection Structures, Bank Protection Pilot Project, Flood Action Plan 21 (FAP 21), Water Resources Planning Organization, Ministry of Water Resources, Government of Bangladesh.

Forzieri, G., Feyen, L., Russo, S., Vousdoukas, M., Alfieri, L., Outten, S., ... & Cid, A. (2016). Multi-hazard assessment in Europe under climate change. Climatic Change, 137(1-2), 105-119.

George H. Hargreaves, Zohrab A. Samani. (1985). Reference crop evapotranspiration from temperature. Applied Engineering in Agriculture. 1(2): 96-99. (doi: 10.13031/2013.26773).

GoB (1999): National Water Policy, Ministry of Water Resources, Government of the People's Republic Bangladesh.

Gosain, A. K., Rao, S., & Mani, A. 2011, Hydrological modeling: a case study of the Kosi Himalayan basin using SWAT, CABI Publishing, Wallingford.

Gupta, N., Atkinson, P. M., & Carling, P. A., 2013. Decadal length changes in the fluvial planform of the River Ganga: bringing a mega-river to life with Landsat archives. Remote Sensing Letters, 4(1), 1-9.

Hossain, M. A., Gan, T. Y., & Baki, A. B. M. 2013. Assessing morphological changes of the Ganges River using satellite images. Quaternary International, 304, 142-155.

Immerzeel, W. (2008). Historical trends and future predictions of climate variability in the Brahmaputra basin. International Journal of Climatology, 28(2), 243-254.

Imran S., L. N. Bukhari. and Gul S. (2018). Water Quality Assessment Report: Mingora City District Swat Khyber Pakhtunkhwa 2018. Pakistan Council of Research in Water Resources (PCRWR), pp. 40.

Islam, M.K., Dustegir, M.M., Rahman, M.M. and Rahman, M. (2018). Changes in Planform and Meander bends of Rivers in Southern Estuarine Region of Bangladesh and Its Implications on Development Project. Changes, 6(1).

IWFM (2019): Feasibility Study for Flood Control, Drainage and Irrigation System at Gowainghat in Sylhet District, prepared for Bangladesh Water Development Board by the Institute of Water and

Jha, M., Arnold, J. G., Gassman, P. W., Giorgi, F., & Gu, R. R. (2006). Climate change sensitivity assessment on upper Mississippi river basin stream flows using SWAT. JAWRA Journal of the American Water Resources Association, 42(4): 997-1015.

Ritchie, J.T. (1972). Model for predicting evaporation from a row crop with incomplete cover. Water resources research, - Wiley Online Library.

Kumarl N. and Kumar S. (2017). Investigation of impacts of land use/land cover change on water availability of Tons River Basin, Madhya Pradesh, India. Springer International Publishing AG, part of Springer Nature.

Lange, Stefan (2019): WFDE5 over land merged with ERA5 over the ocean (W5E5). V. 1.0. GFZ Data Services. https://doi.org/10.5880/pik.2019.023

LGED (2005) Road Design Standards: Rural Road. Local Govt. Engineering Department.

Liu, C. C., Shieh, M. C., Ke, M. S., & Wang, K. H. (2018). Flood prevention and emergency response system powered by google earth engine. *Remote sensing*, *10*(8), 1283.

Lobo, F. D. L., Souza-Filho, P. W. M., Novo, E. M. L. D. M., Carlos, F. M., & Barbosa, C. C. F. (2018). Mapping mining areas in the Brazilian amazon using msi/Sentinel-2 imagery (2017). *Remote Sensing*, *10*(8), 1178.

Markert, K. N., Schmidt, C. M., Griffin, R. E., Flores, A. I., Poortinga, A., Saah, D. S., ... & Ganz, D. J. (2018). Historical and operational monitoring of surface sediments in the lower Mekong basin using Landsat and google earth engine cloud computing. *Remote Sensing*, *10*(6), 909.

Martinis, S. (2010). Automatic near real-time flood detection in high resolution X-band synthetic aperture radar satellite data using context-based classification on irregular graphs (Doctoral dissertation).

Mateo-García, G., Gómez-Chova, L., Amorós-López, J., Muñoz-Marí, J., & Camps-Valls, G. (2018). Multitemporal cloud masking in the Google Earth Engine. *Remote Sensing*, *10*(7), 1079.

Mirza, M. Q. and Dixit A. (1997). Climate Change and Water Management in The GBM Basins; Journal of water resources development. ISSN, 1027-0345.

Mishra, V., Bhatia, U. & Tiwari, A.D. (2020). Bias-corrected climate projections for South Asia from Coupled Model Intercomparison Project-6. Sci Data 7, 338. https://doi.org/10.1038/s41597-020-00681-1.

Mohammed, K., Islam, A.S., Islam, G.M.T., Alferi, L., Bala, S.K. and Khan, M.J.U. (2018). Future floods in Bangladesh under 1.5°C, 2°C and 4°C global warming scenarios, Journal of Hydrological Engineering,.23(12): 04018050-13.

Monteith, J. L. (1965). Evaporation and environment. Symposia of the Society for Experimental Biology. 19, pp. 205-234.

Moriasi, D. N., Arnold, J. G., Van Liew, M. W., Bingner, R. L., Harmel, R. D. and Veith, T. L. (2007). Model Evaluation Guidelines for Systematic Quantification of Accuracy in Watershed Simulations.

Narsimlu, B., Gosain, A.K., Chahar, B.R., Singh, S.K. and Srivastava, P.K. (2015). SWAT model calibration and uncertainty analysis for streamflow prediction in the Kunwari River basin, India, using Sequential Uncertainty Fitting. Environ. Proc., 2, 79–95.

Nasirzadehdizaji, R., Akyuz, D. E., & Cakir, Z. (2019). Flood mapping and permanent water bodies change detection using Sentinel SAR data. The International Archives of Photogrammetry, Remote Sensing and Spatial Information Sciences, 42, 797-801.

Neitsch, S. L., Arnold, J. G., Kiniry, J. R., & Williams, J. R. (2011). Soil and water assessment tool theoretical documentation version 2009. Texas Water Resources Institute.

Neitsch, S.L., J.G. Arnold; J.R. Kiniry, J.R. and K.W. King. (2002). Soil and Water Assessment Tool Theoretical Documentation, Version 2000. Grassland, Soil and Water Research Laboratory, Temple, TX and Blackland Research Center, Temple, TX.

Oki, T., & Kanae, S. (2006). Global hydrological cycles and world water resources. Science, 313(5790), 1068-1072.

Pal, R. and Pani, P., 2016. Seasonality, barrage (Farakka) regulated hydrology and flood scenarios of the Ganga River: a study based on MNDWI and simple Gumbel model. Modeling Earth Systems and Environment, 2(2), p.57.

Pal, R. and Pani, P., 2018. Remote sensing and GIS-based analysis of evolving planform morphology of the middle-lower part of the Ganga River, India. The Egyptian Journal of Remote Sensing and Space Science.

Patrick G. Sloan, Ian D. Moore. (1984). Modeling subsurface stormflow on steeply sloping forested watersheds. https://doi.org/10.1029/WR020i012p01815.

Planning Commission (2004) Road Design Standards: Standard Designs and Costing for Zila, Upazila and Union Roads, Bridges and Culverts. Planning Commission. Govt. of the Peoples Republic of Bangladesh.

Psomiadis, E. (2016, October). Flash flood area mapping utilising SENTINEL-1 radar data. In Earth Resources and Environmental Remote Sensing/GIS Applications VII (Vol. 10005, p. 100051G). International Society for Optics and Photonics.

Reliefweb (2021). Monsoon Floods in Bangladesh. Available at: https://reliefweb.int/sites/reliefweb.int/files/resources/SitRep_2_Bangladesh%20Flood_16%20August%202017.pdf (Last Accessed 25 March 2021).

Richard G. Allen, Marvin E. Jensen, James L. Wright, Robert D. Burman. (1989). Operational Estimates of Reference Evapotranspiration.

Salehin M., Chowdhury, J.U., and Islam, A.K.M.S. (2011). Development of a water resources model as a decision support tool for national water management, Tech. The report, Institute of water and flood management, BUET.

Sazib, N., Mladenova, I., & Bolten, J. (2018). Leveraging the google earth engine for drought assessment using global soil moisture data. *Remote sensing*, *10*(8), 1265.

Sinha, R., & Ghosh, S. (2012). Understanding the dynamics of large rivers aided by satellite remote sensing: a case study from Lower Ganga plains, India. Geocarto International, 27(3), 207-219.

Sinha, R., Tandon, S. K., & Gibling, M. R. (2010). Shallow sub-surface stratigraphy of the Ganga basin, Himalayan foreland: Present status and future perspectives. Quaternary International, 227(2), 81-86.

Sproles, E. A., Crumley, R. L., Nolin, A. W., Mar, E., & Lopez Moreno, J. I. (2018). SnowCloudHydro—A New Framework for Forecasting Streamflow in Snowy, Data-Scarce Regions. *Remote Sensing*, *10*(8), 1276.

Syeda Zehan Farzana, Md. Abu Zafor, Jabed Al Shahariar. (2019). Application of SWAT Model for Assessing Water Availability in Surma River Basin. https://doi.org/10.22146/jcef.39191.

Tavus, B., Kocaman, S., Gokceoglu, C., & Nefeslioglu, H. A. (2018). Considerations on the use of Sentinel-1 data in flood mapping in urban areas: Ankara (Turkey) 2018 floods. International Archives of the Photogrammetry, Remote Sensing & Spatial Information Sciences.

Thakur, P. K., Laha, C., & Aggarwal, S. P. (2012). River bank erosion hazard study of river Ganga, upstream of Farakka barrage using remote sensing and GIS. Natural Hazards, 61(3), 967-987.

Townsend, P. A. (2002). Relationships between forest structure and the detection of flood inundation in forested wetlands using C-band SAR. International Journal of Remote Sensing, 23(3), 443-460.

Uhe, P. Mitchell, D., Bates, P., Sampson, C., Smith, A., Islam, A.S. (2019) Enhanced flood risk with 1.5C global warming in the Ganges-Brahmaputra-Meghna basin. Environmental Research Letter, 14(7), doi: 10.1088/1748-9326/ab10ee.

Uniyal, B., Jha, M. K., & Verma, A. K. (2015). Assessing climate change impact on water balance components of a river basin using SWAT model. Water resources management, 29(13), 4767-4785.

UNRCO (2020) Bangladesh: Monsoon Floods Update (01) from UNRCO in Bangladesh. Retrieved from https://www.humanitarianresponse.info/en/operations/bangladesh/document/bangladesh-monsoon-floods-update-unrco-bangladesh-22-july-2019 (Last Access on 22 February 20200.

Vilches, J. P. (2013, March). Detection of areas affected by flooding rivers using SAR images. In Seminar: Master in Space Applications for Emergency Early Warning and Response (Vol. 40).

Xu, D., Bai, Y., Ma, J., & Tan, Y. (2011). Numerical investigation of long-term planform dynamics and stability of river meandering on fluvial floodplains. Geomorphology, 132(3-4), 195-207.

Appendix A:

Hydrological and Morphological Data Collected from BWDB

Appendix A1: Daily time-series water level data to be collected from BWDB

River Name	Station Number	Station Name	Station Type	Year
Jamuna/Brahmaputra	SW_45	Noonkhawa	Water Level	1981-2019
Jamuna/Brahmaputra	SW_45.5	Chilmari	Water Level	1981-2014
Jamuna/Brahmaputra	SW_46.9L	Bahadurabad	Water Level	1981-2019
	SW_48	Jaganathganj	Water Level	1981-2019
Jamuna/Brahmaputra	SW_49	Sirajganj	Water Level	1981-2019
	SW_49A	Kazipur	Water Level	1981-2019
	SW_293	Kaliganj	Water Level	1981-2015
	SW_294	Kaunia	Water Level	1981-2019
	SW_294.5	Haripur	Water Level	1981-2019
	SW_77.5	Gujimari	Water Level	1987-2019
	SW_77	Kurigram	Water Level	1981-2019
	SW_96.5	Mirjapur	Water Level	1981-2012
	W_96A	Jafarganj_Rd_Crossing	Water Level	1981-2014
	SW_97	Gaibandha	Water Level	1981-2019
	SW_134B	Offtake_jhenai	Water Level	1981-2014
	SW_134A	Baushi Bridge	Water Level	1981-2014
	SW_228	Mymensing	Water Level	1981-2019
	SW_155	Mohimganj	Water Level	1981-2019
	SW_10	Simulbari	Water Level	1981-2019
	SW_11	Khanpur	Water Level	1981-2019

Appendix A2: Discharge data to be collected from BWDB.

Station Number	Station Name	Station Type	Year
SW_46.9L	Bahadurabad	Discharge	1995-2019
SW291.5R	Dalia	Discharge	1997-2019
SW81	Pateswari	Discharge	1998-2019
SW76	Taluk_Simulbari	Discharge	1990-2019

Appendix A3: River x-section data to be collected from BWDB.

River Name	Required cross-section	Year
Jamuna/Brahmaputra	J7-J17	2015-2019
Old Brahmaputra	OB01-OB13	2015-2019
Dudhkumar	DK01-DK05	2015-2019
Dharala	DL01-DL10	2015-2019
Teesta	T01-T20	2015-2019
Ghaghot	GHT01-GHT12	2015-2019
Bangali	BNG01-BNG19	2013-2014
Jhenai	JHE01-JHE10	2013-2014

Appendix B:

Cross-sectional Profiles of Brahmaputra-Teesta River Systems

Appendix B1. X-section of the Dudhkumar River

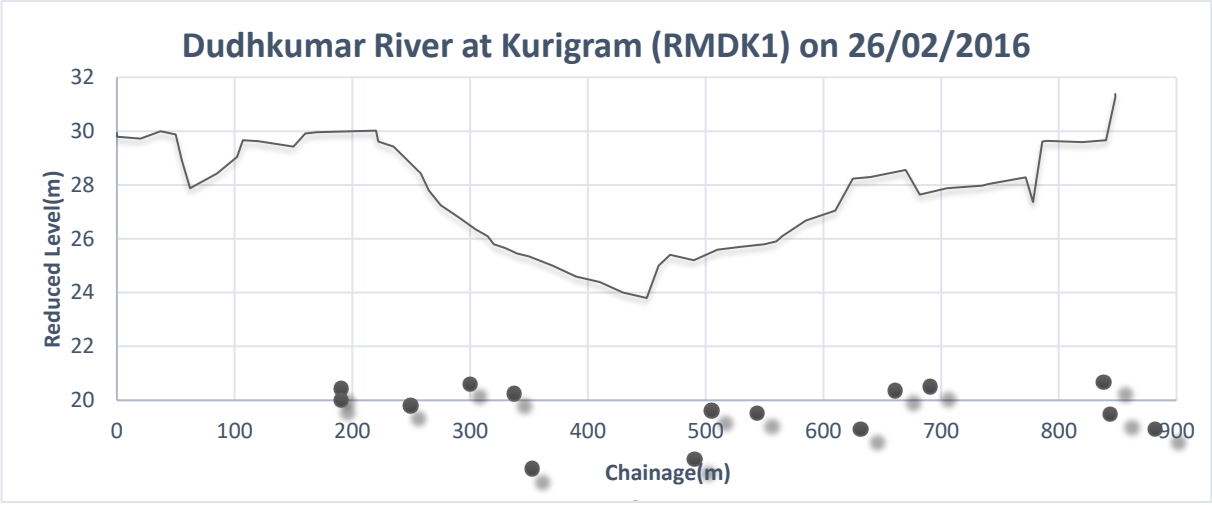

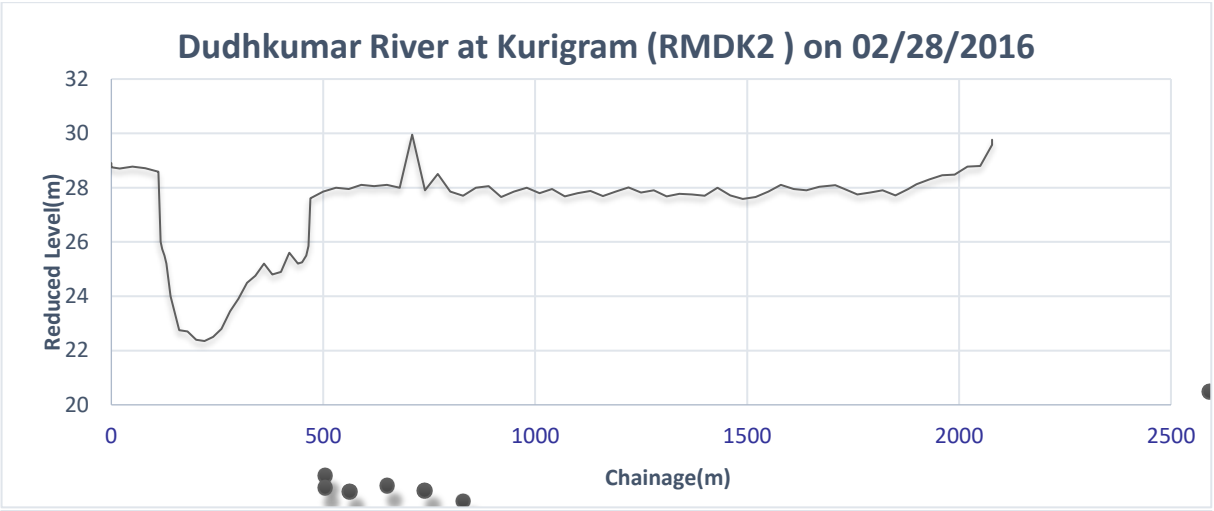

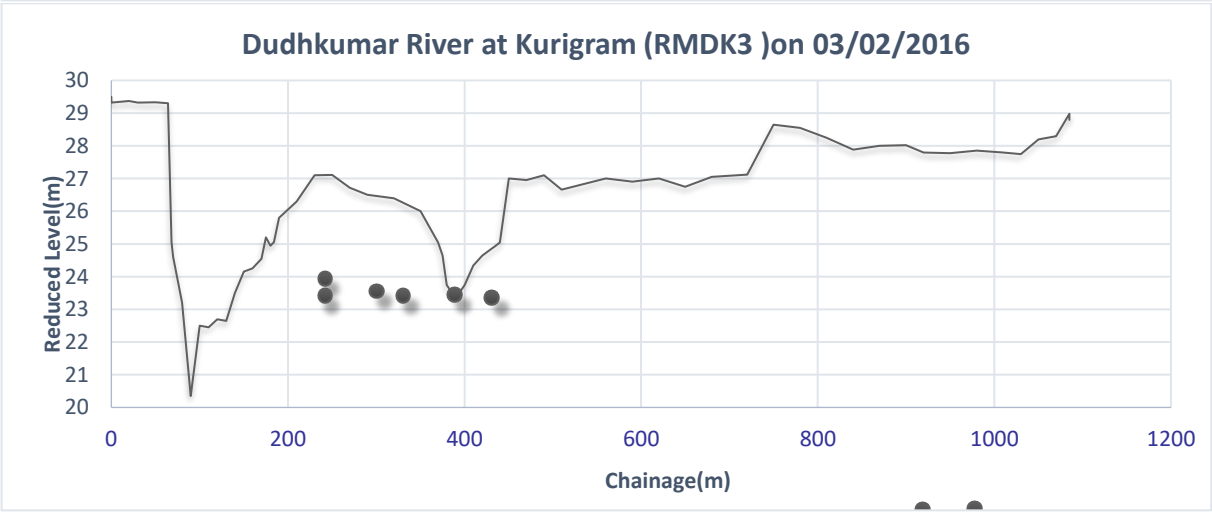

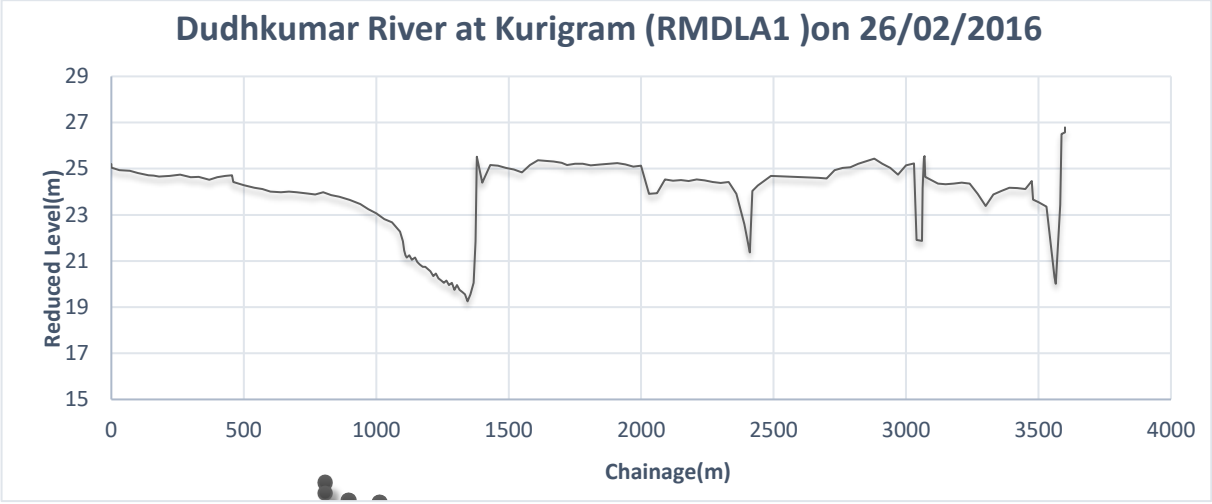
Dudhkumar River at Kurigram (RMDLA1)on 26/02/2016
Reduced Level(m)
29
27
25
23
21
19
17
15
0
500
1000
1500
2000
2500
3000
3500
4000
Chainage(m)

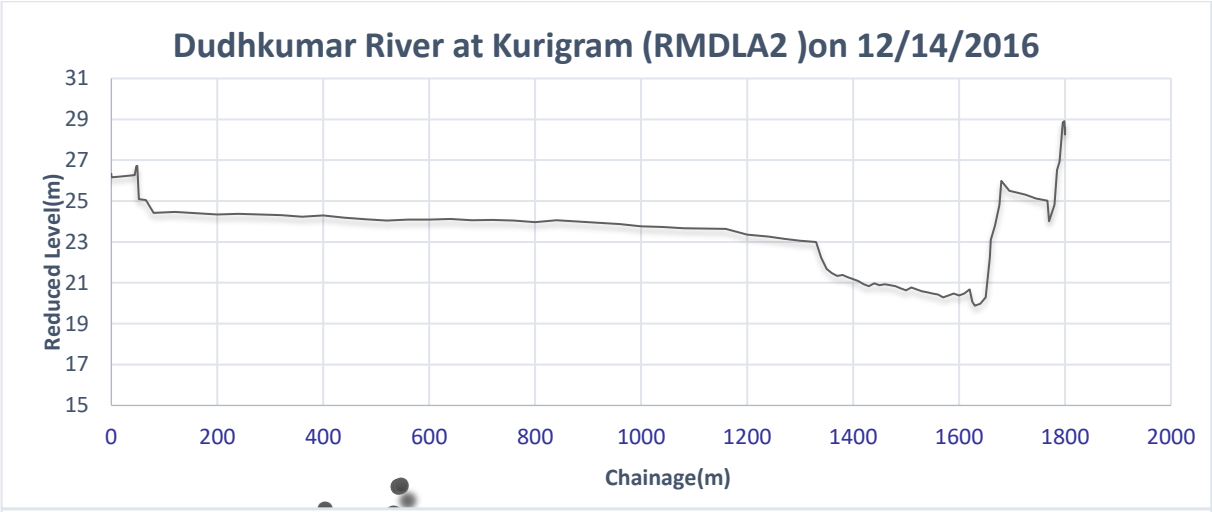
Dudhkumar River at Kurigram (RMDLA2)on 12/14/2016
Reduced Level(m)
31
29
27
25
23
21
19
17
15
0
200
400
600
800
1000
1200
1400
1600
1800
2000
Chainage(m)

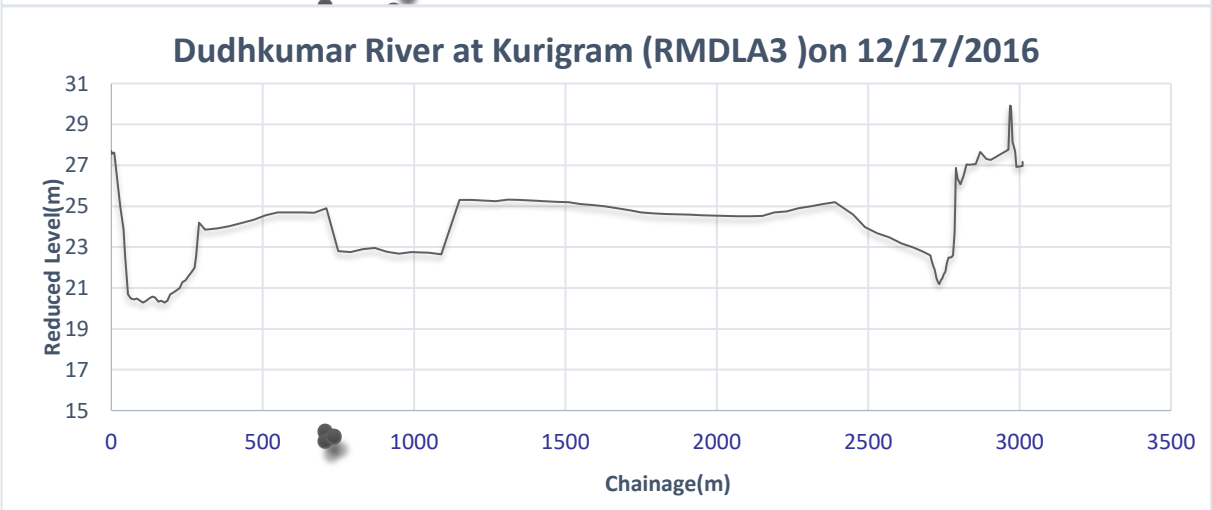
Dudhkumar River at Kurigram (RMDLA3)on 12/17/2016
Reduced Level(m)
31
29
27
25
23
21
19
17
15
0
500
1000
1500
2000
2500
3000
3500
Chainage(m)

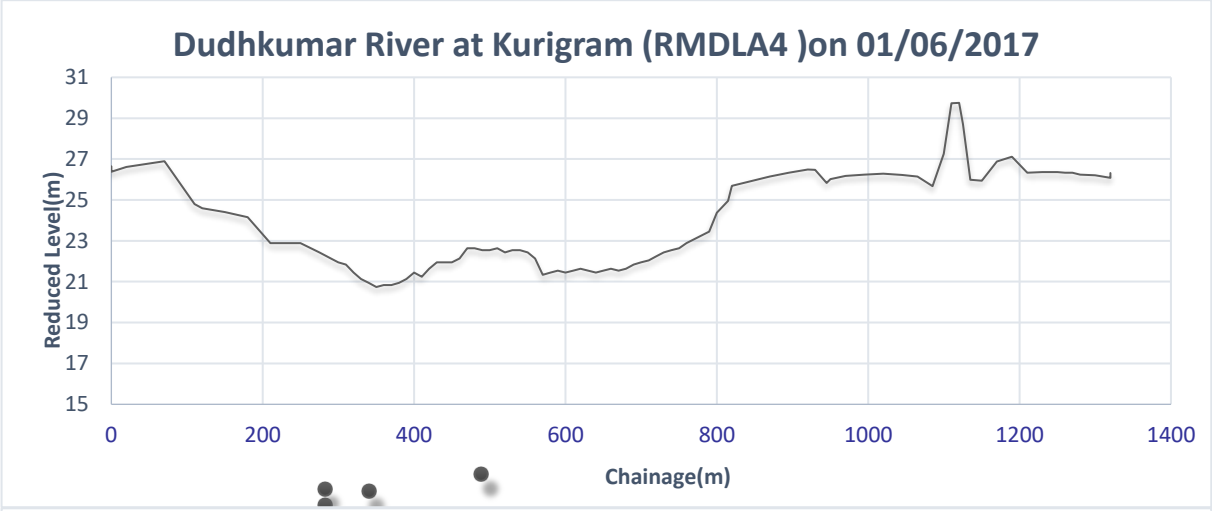
Dudhkumar River at Kurigram (RMDLA4)on 01/06/2017
Reduced Level(m)
31
29
27
25
23
21
19
17
15
0
200
400
600
800
1000
1200
1400
Chainage(m)

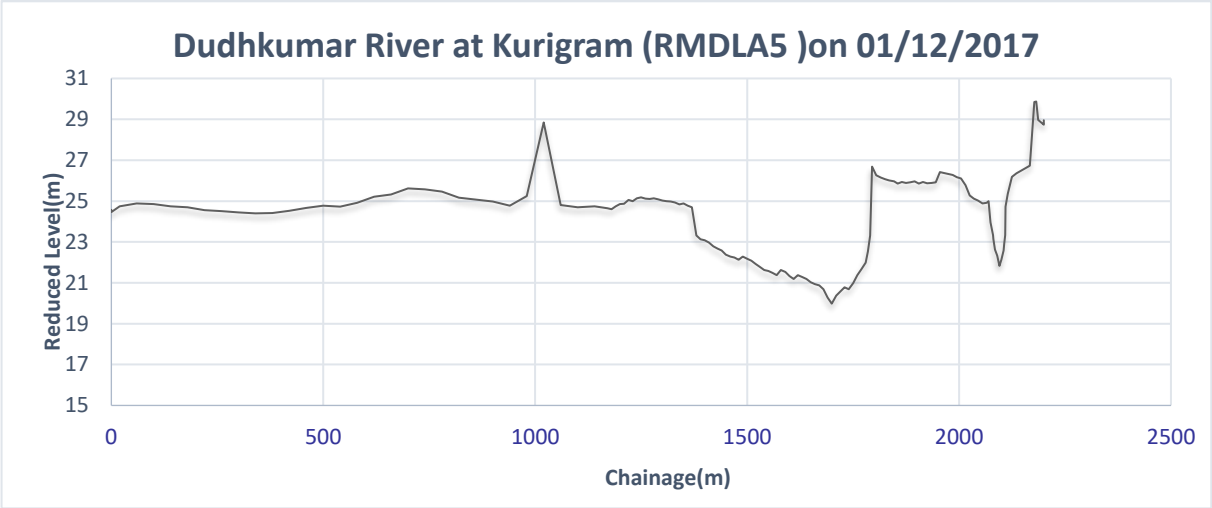
Dudhkumar River at Kurigram (RMDLA5)on 01/12/2017
Reduced Level(m)
31
29
27
25
23
21
19
17
15
0
500
1000
1500
2000
2500
Chainage(m)

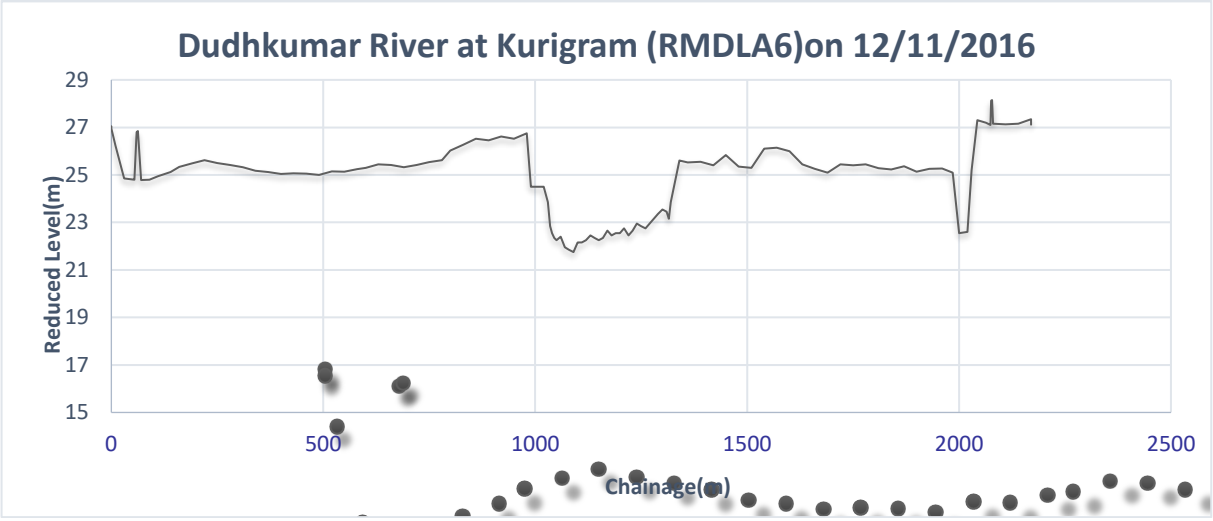
Dudhkumar River at Kurigram (RMDLA6)on 12/11/2016
Reduced Level(m)
29
27
25
23
21
19
17
15
0
500
1000
1500
2000
2500
Chainage(m)

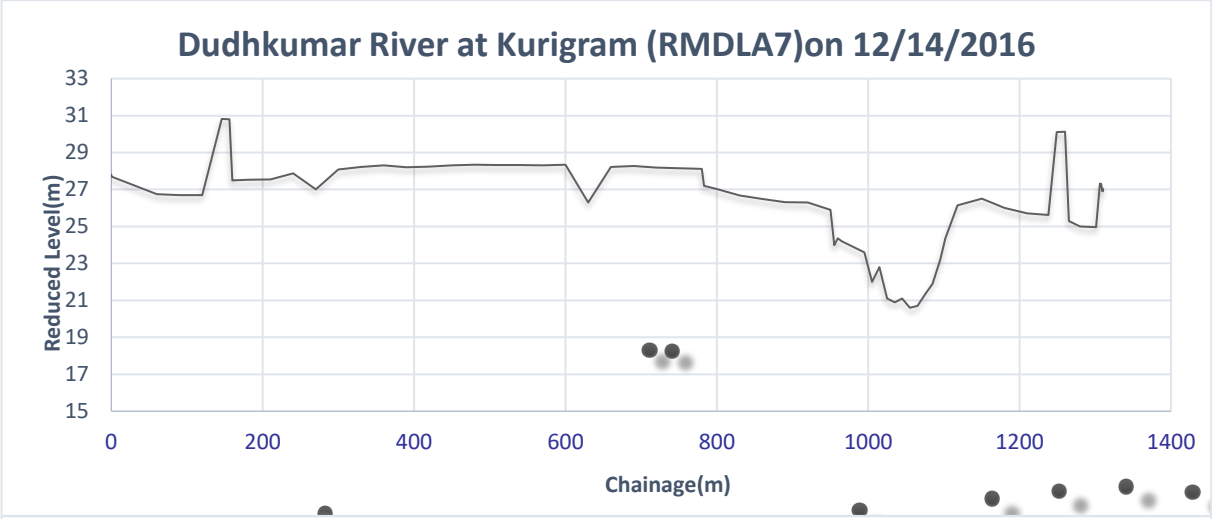
Dudhkumar River at Kurigram (RMDLA7)on 12/14/2016
Reduced Level(m)
33
31
29
27
25
23
21
19
17
15
0
200
400
600
800
1000
1200
1400
Chainage(m)

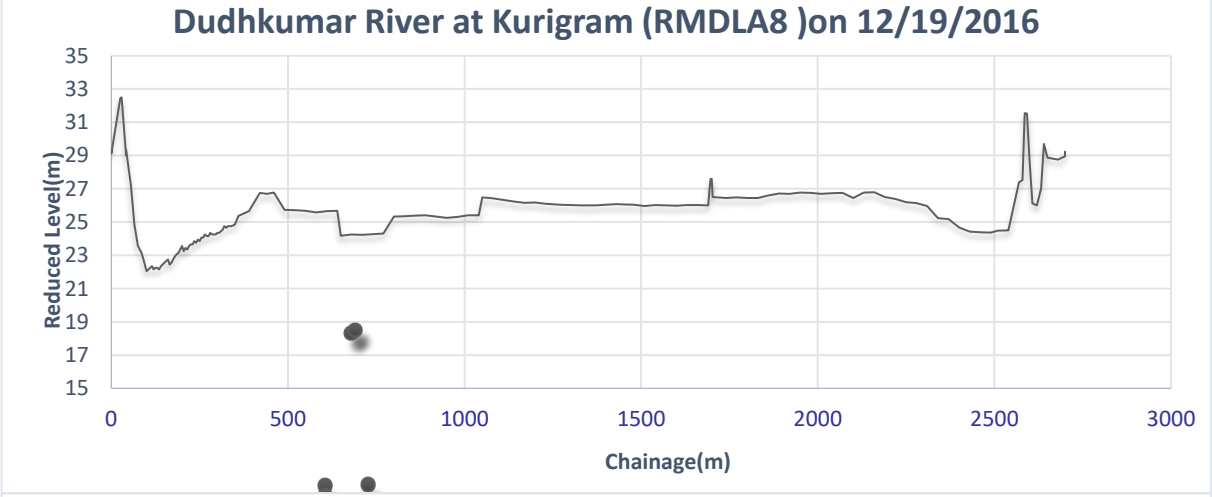
Dudhkumar River at Kurigram (RMDLA8)on 12/19/2016
Reduced Level(m)
35
33
31
29
27
25
23
21
19
17
15
0
500
1000
1500
2000
2500
3000
Chainage(m)

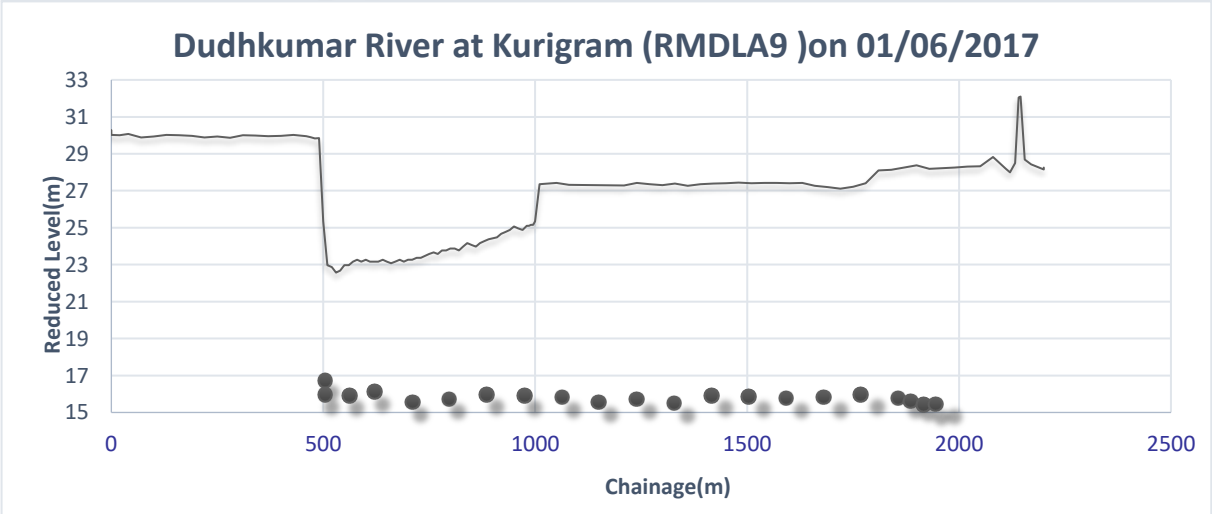
Dudhkumar River at Kurigram (RMDLA9)on 01/06/2017
Reduced Level(m)
33
31
29
27
25
23
21
19
17
15
0
500
1000
1500
2000
2500
Chainage(m)

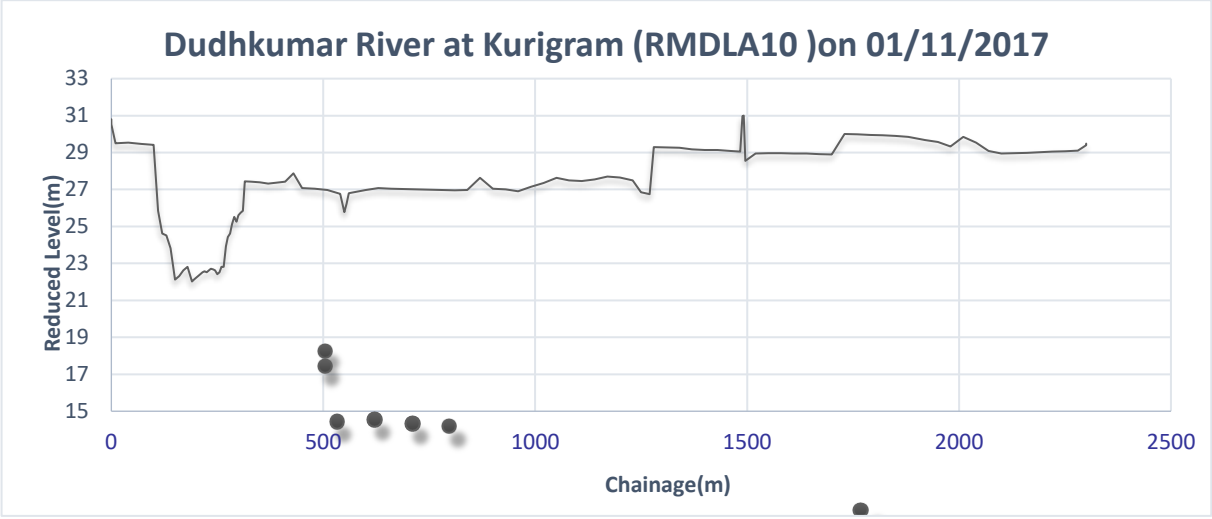
Dudhkumar River at Kurigram (RMDLA10)on 01/11/2017
Reduced Level(m)
33
31
29
27
25
23
21
19
17
15
0
500
1000
1500
2000
2500
Chainage(m)

Appendix B2. X-section of the Teesta River

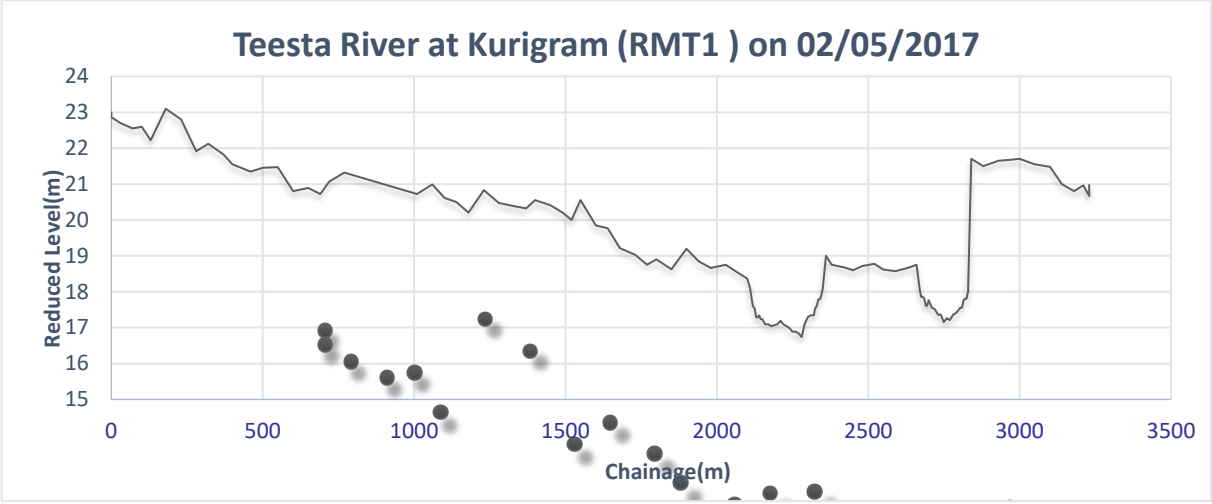

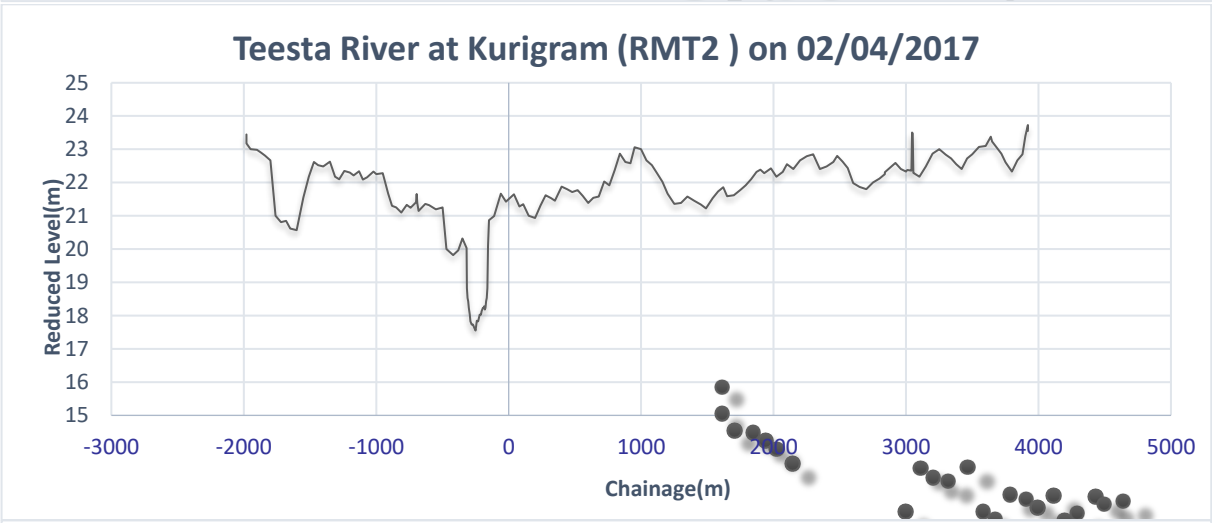

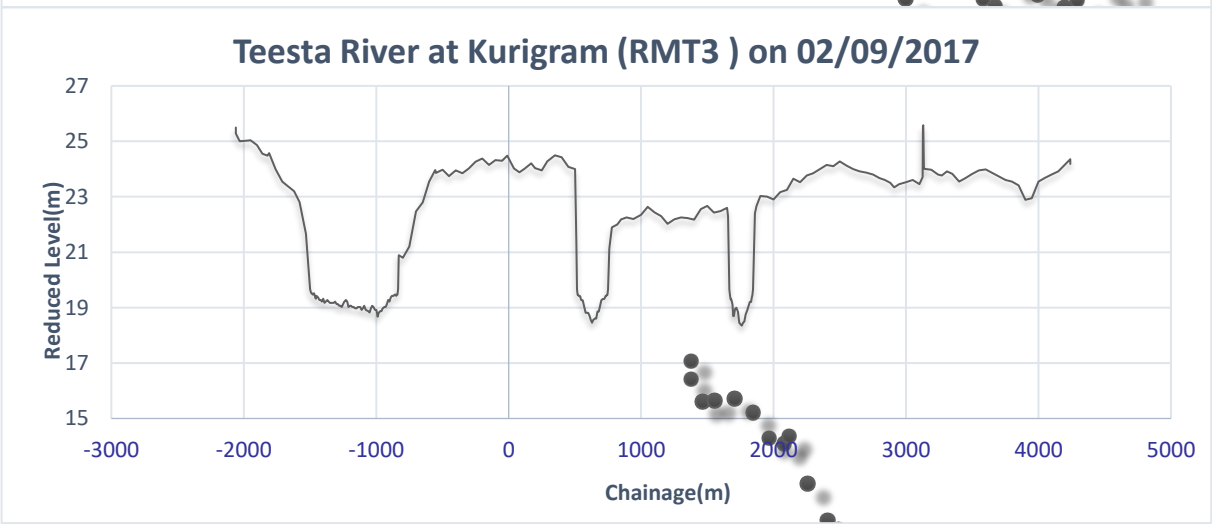

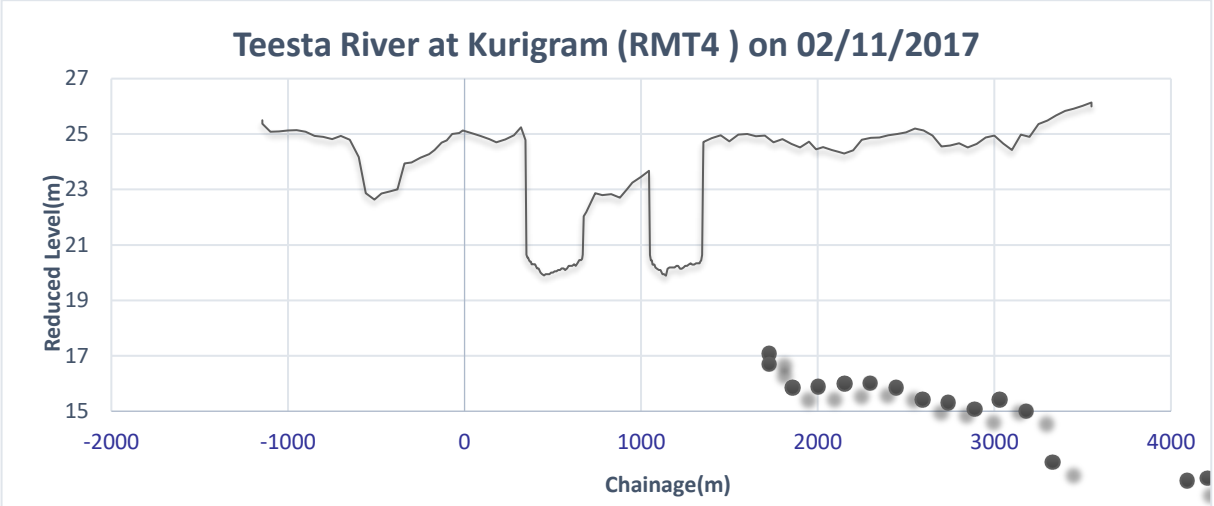
Teesta River at Kurigram (RMT4) on 02/11/2017
Reduced Level(m)
27
25
23
21
19
17
15
-2000
-1000
0
1000
2000
3000
4000
Chainage(m)

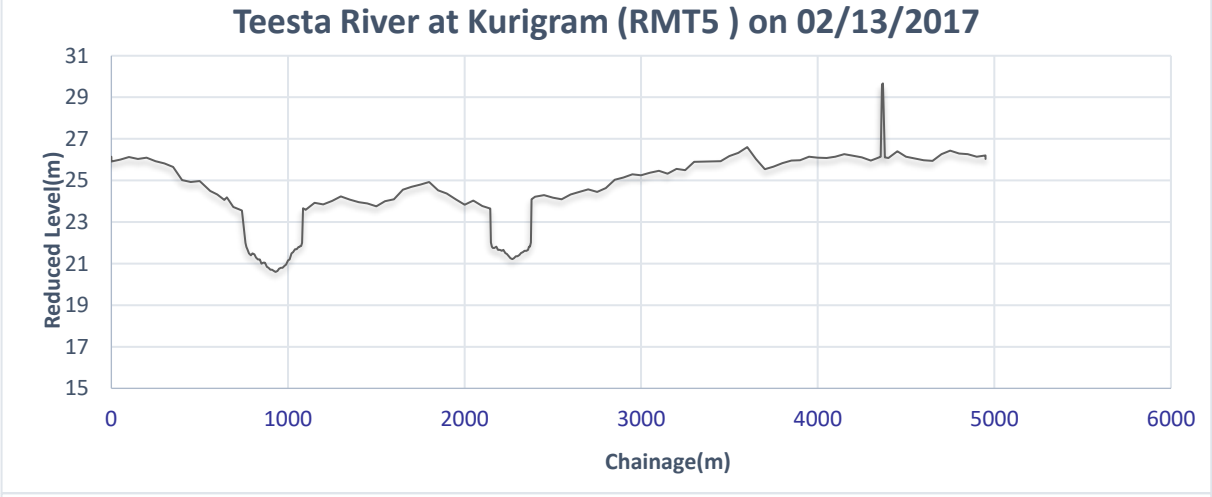
Teesta River at Kurigram (RMT5) on 02/13/2017
Reduced Level(m)
31
29
27
25
23
21
19
17
15
0
1000
2000
3000
4000
5000
6000
Chainage(m)

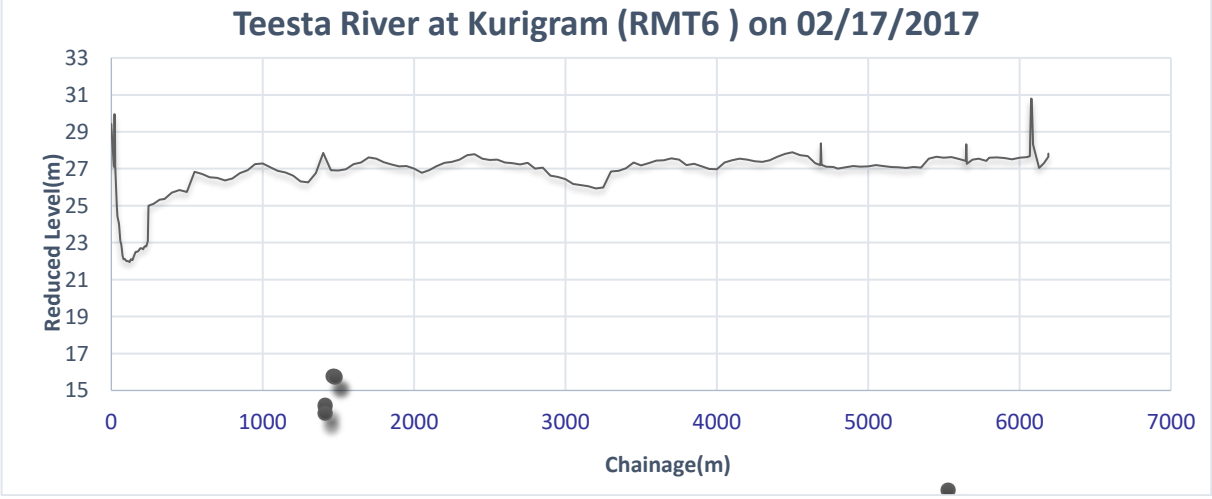
Teesta River at Kurigram (RMT6) on 02/17/2017
Reduced Level(m)
33
31
29
27
25
23
21
19
17
15
0
1000
2000
3000
4000
5000
6000
7000
Chainage(m)

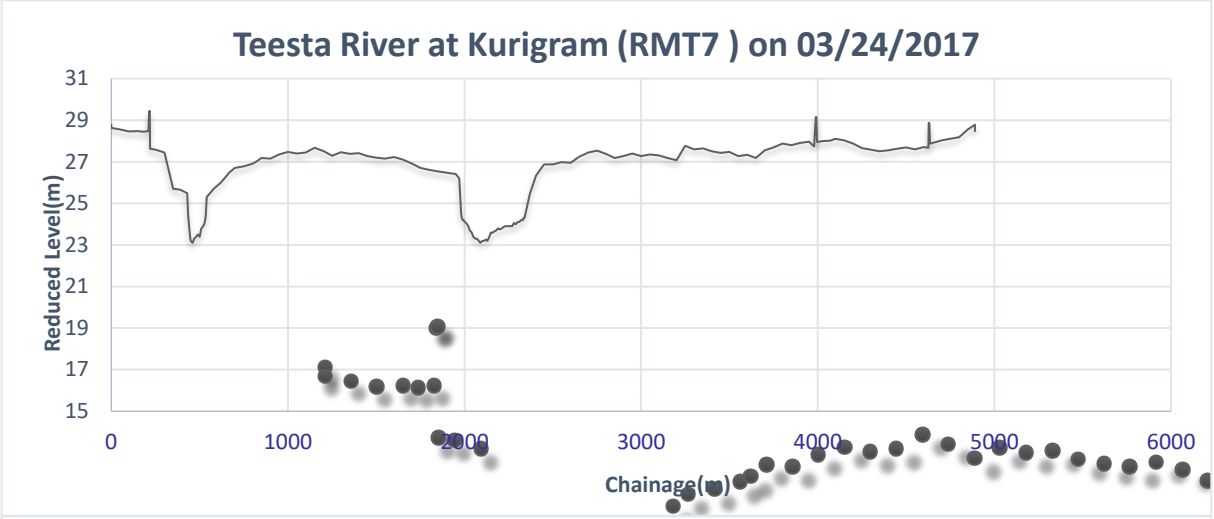
Teesta River at Kurigram (RMT7) on 03/24/2017
Reduced Level(m)
31
29
27
25
23
21
19
17
15
0
1000
2000
3000
4000
5000
6000
Chainage(m)

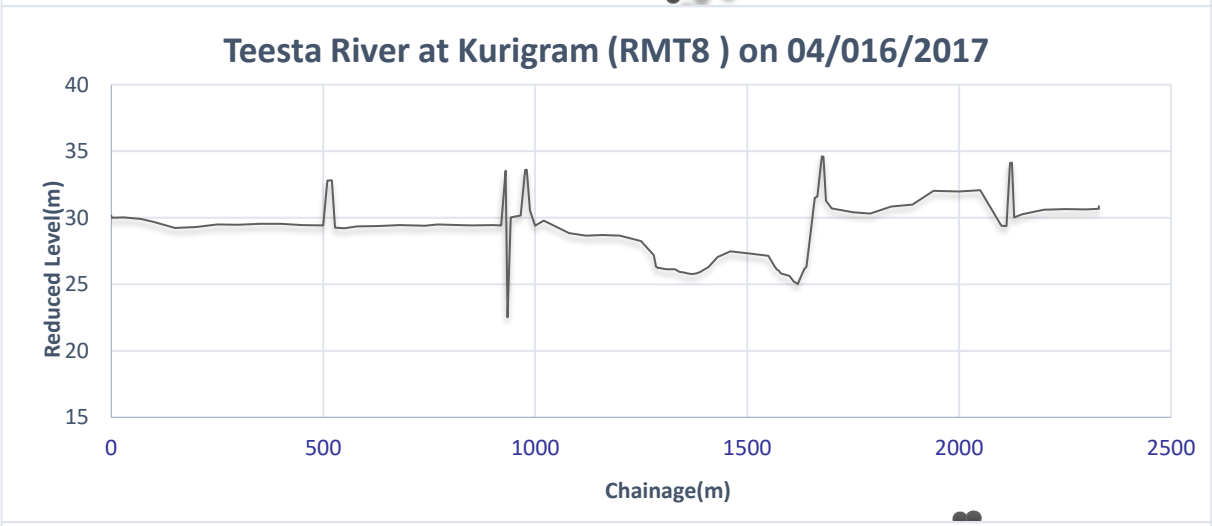
Teesta River at Kurigram (RMT8) on 04/016/2017
Reduced Level(m)
40
35
30
25
20
15
0
500
1000
1500
2000
2500
Chainage(m)

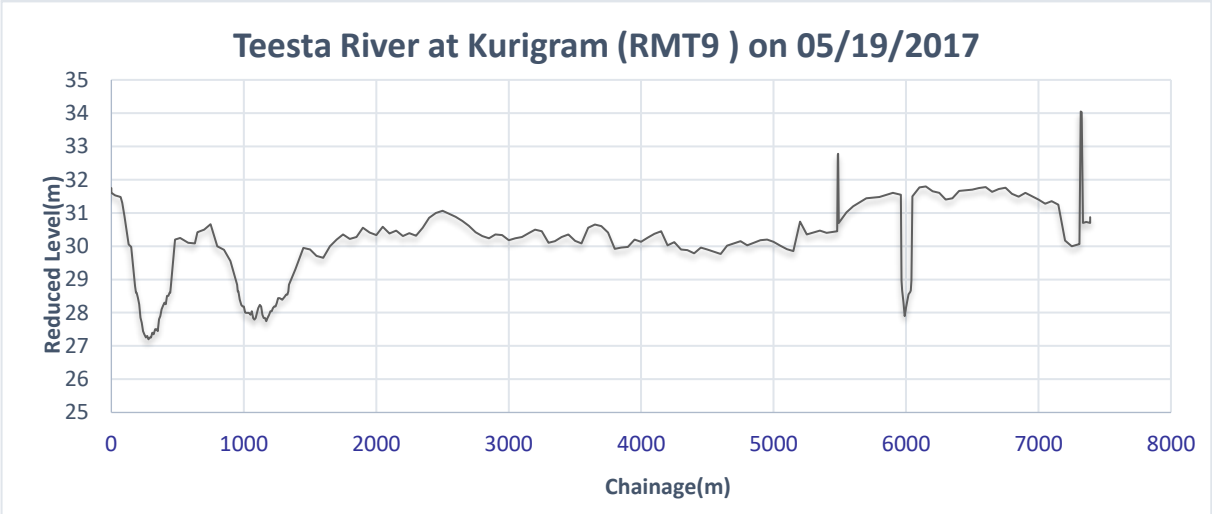
Teesta River at Kurigram (RMT9) on 05/19/2017
Reduced Level(m)
35
34
33
32
31
30
29
28
27
26
25
0
1000
2000
3000
4000
5000
6000
7000
8000
Chainage(m)

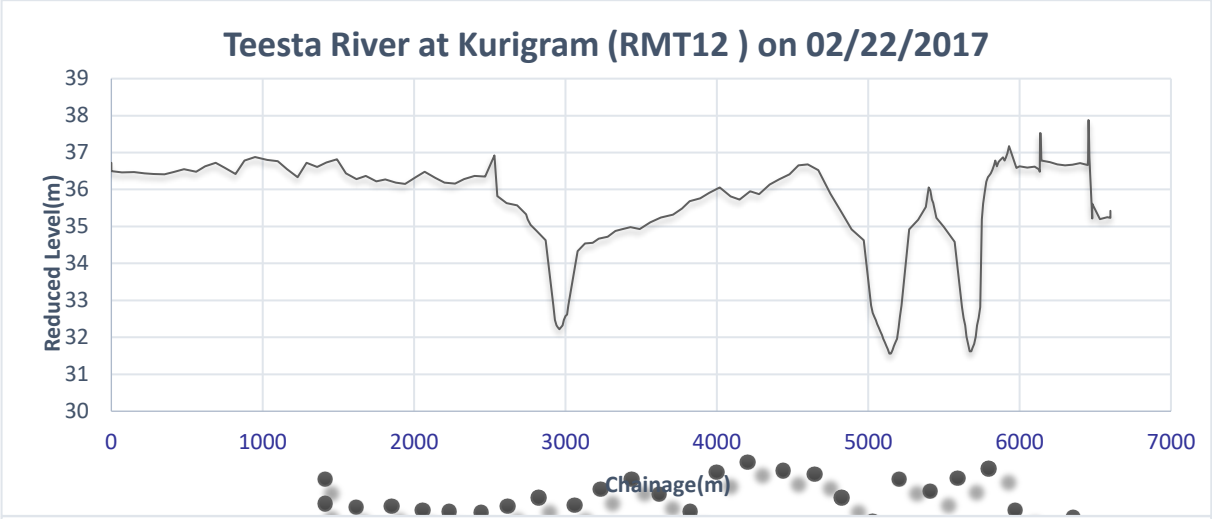
Teesta River at Kurigram (RMT12) on 02/22/2017
Reduced Level(m)
39
38
37
36
35
34
33
32
31
30
0
1000
2000
3000
4000
5000
6000
7000
Chainage(m)

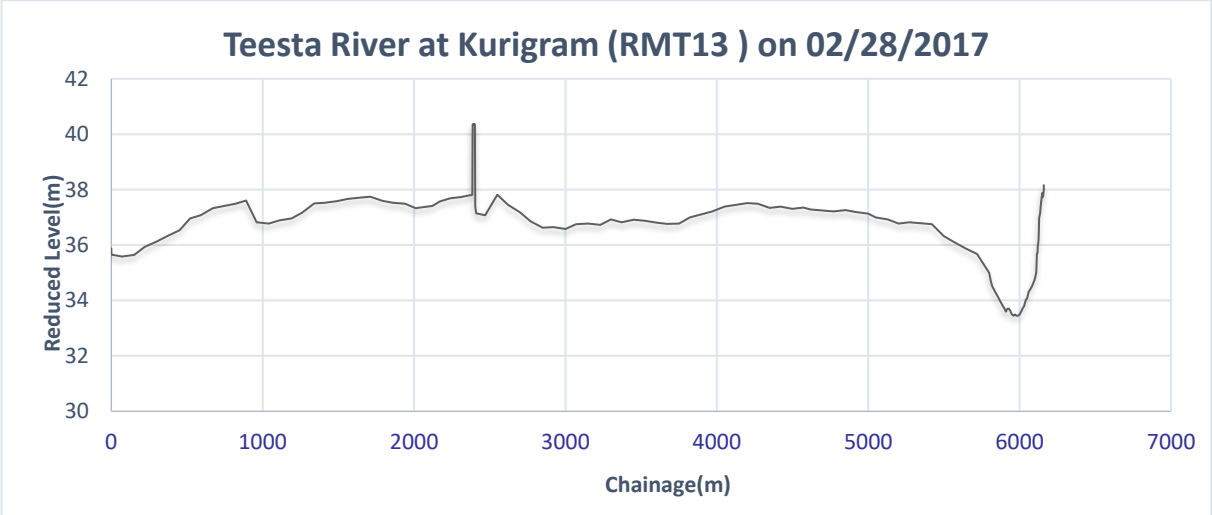
Teesta River at Kurigram (RMT13) on 02/28/2017
Reduced Level(m)
42
40
38
36
34
32
30
0
1000
2000
3000
4000
5000
6000
7000
Chainage(m)

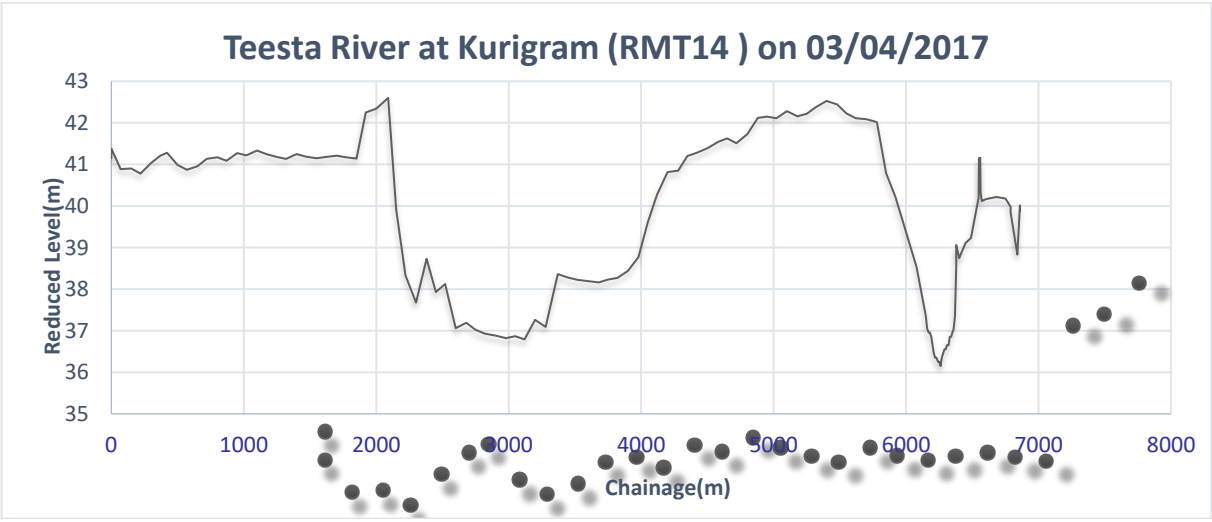
Teesta River at Kurigram (RMT14) on 03/04/2017
Reduced Level(m)
43
42
41
40
39
38
37
36
35
0
1000
2000
3000
4000
5000
6000
7000
8000
Chainage(m)

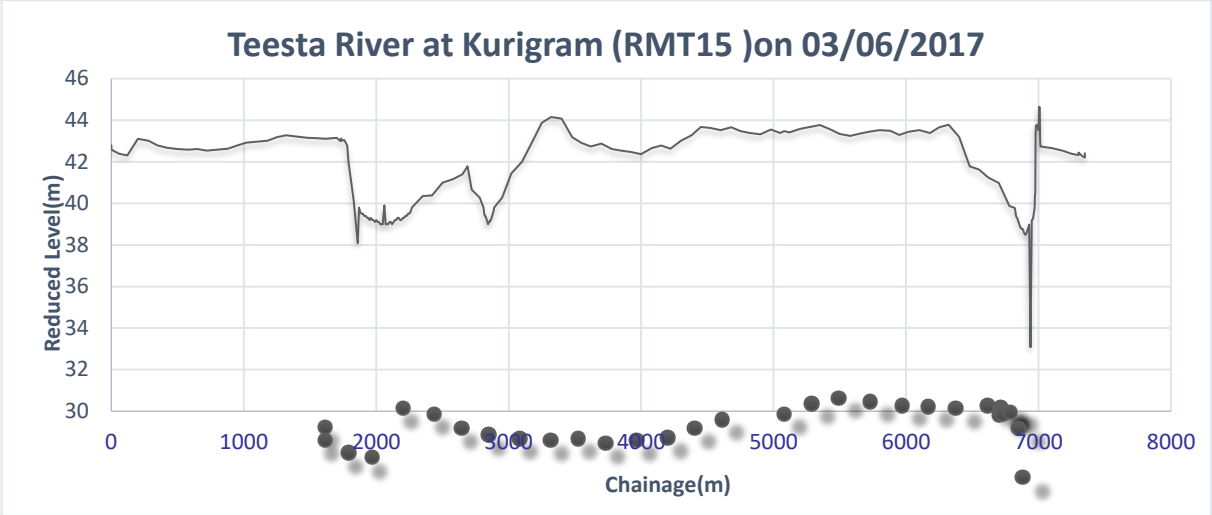
Teesta River at Kurigram (RMT15)on 03/06/2017
Reduced Level(m)
46
44
42
40
38
36
34
32
30
0
1000
2000
3000
4000
5000
6000
7000
8000
Chainage(m)

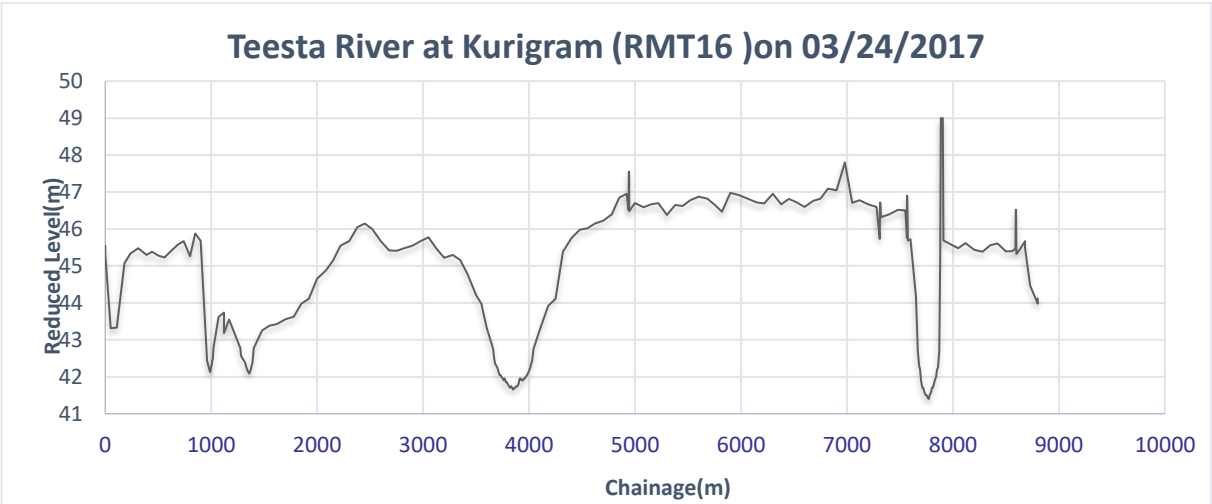
Teesta River at Kurigram (RMT16)on 03/24/2017
Reduced Level(m)
50
49
48
47
46
45
44
43
42
41
0
1000
2000
3000
4000
5000
6000
7000
8000
9000
10000
Chainage(m)

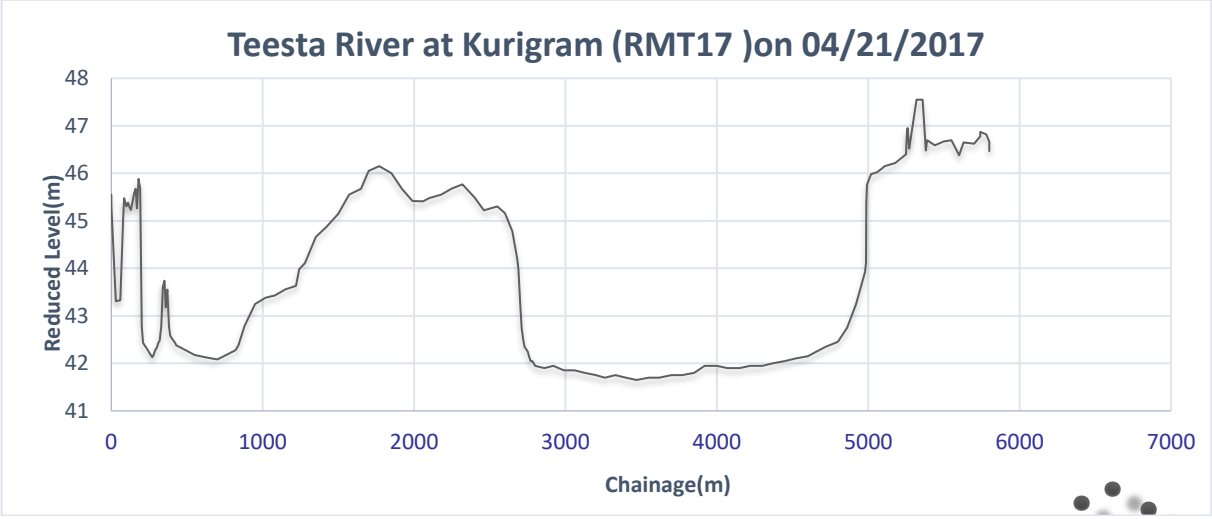
Teesta River at Kurigram (RMT17)on 04/21/2017
Reduced Level(m)
48
47
46
45
44
43
42
41
0
1000
2000
3000
4000
5000
6000
7000
Chainage(m)

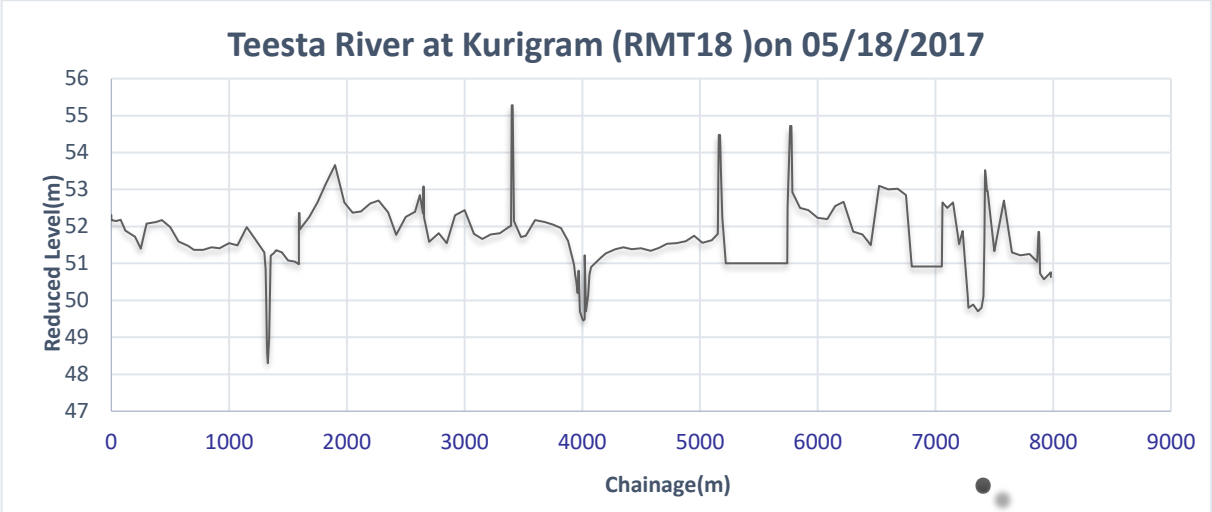
Teesta River at Kurigram (RMT18)on 05/18/2017
Reduced Level(m)
56
55
54
53
52
51
50
49
48
47
0
1000
2000
3000
4000
5000
6000
7000
8000
9000
Chainage(m)

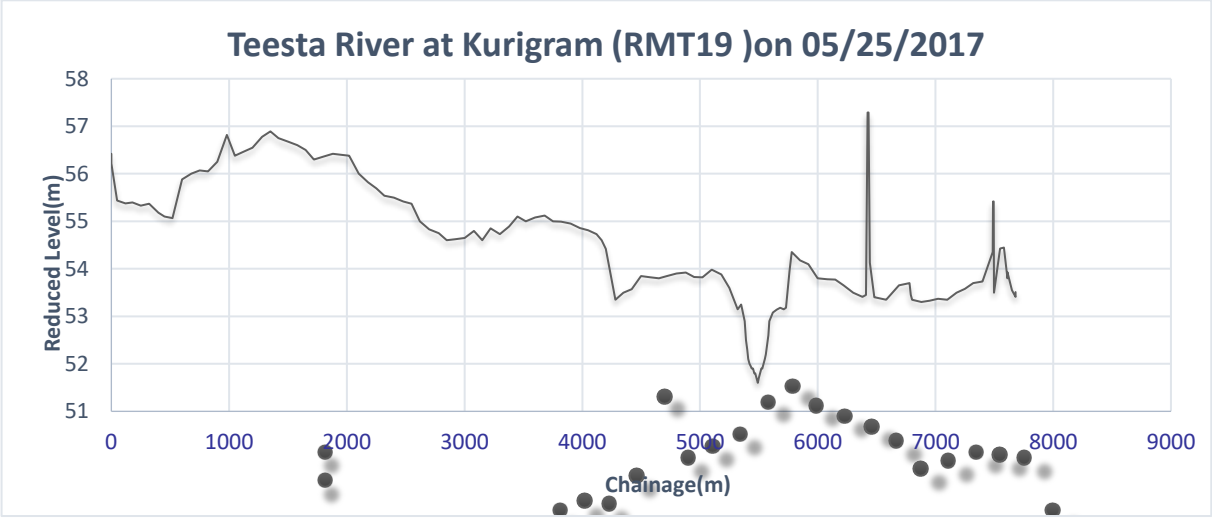
Teesta River at Kurigram (RMT19)on 05/25/2017
Reduced Level(m)
58
57
56
55
54
53
52
51
0
1000
2000
3000
4000
5000
6000
7000
8000
9000
Chainage(m)

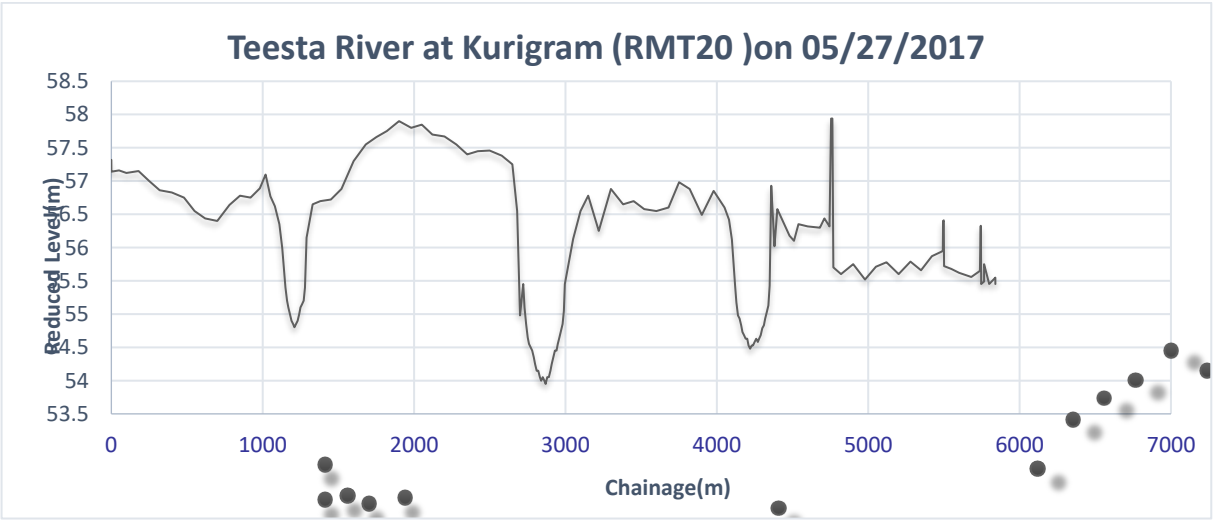
Teesta River at Kurigram (RMT20)on 05/27/2017
Reduced Level(m)
58.5
58
57.5
57
56.5
56
55.5
55
54.5
54
53.5
0
1000
2000
3000
4000
5000
6000
7000
Chainage(m)

Appendix B3. X-section of the Brahmaputra-Jamuna River

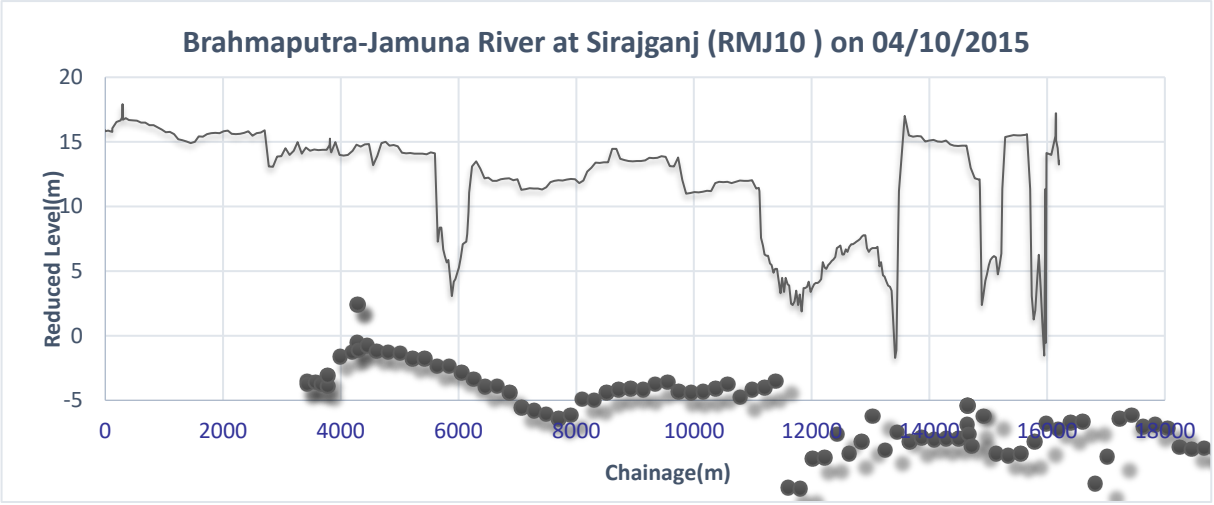

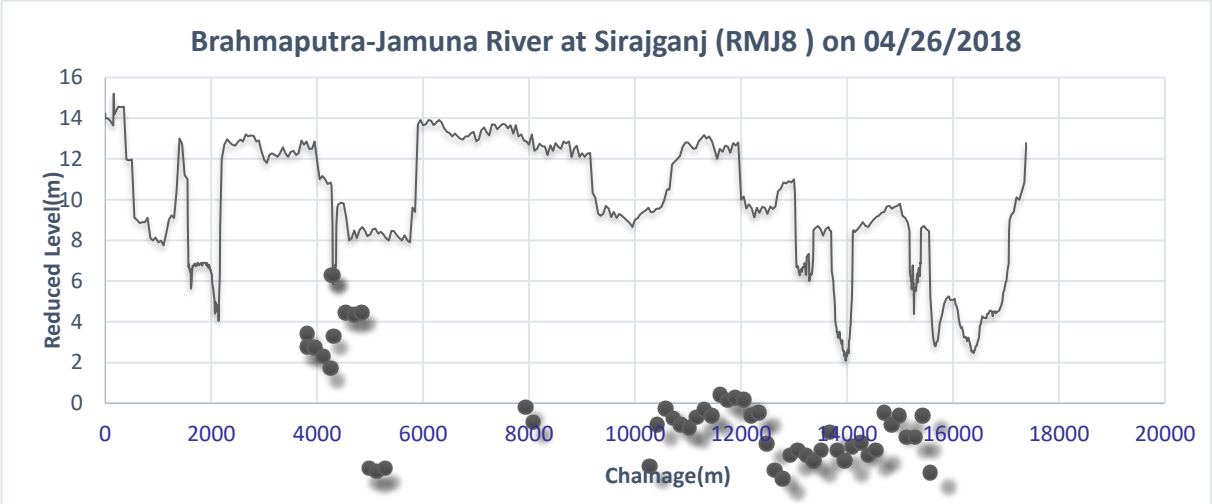

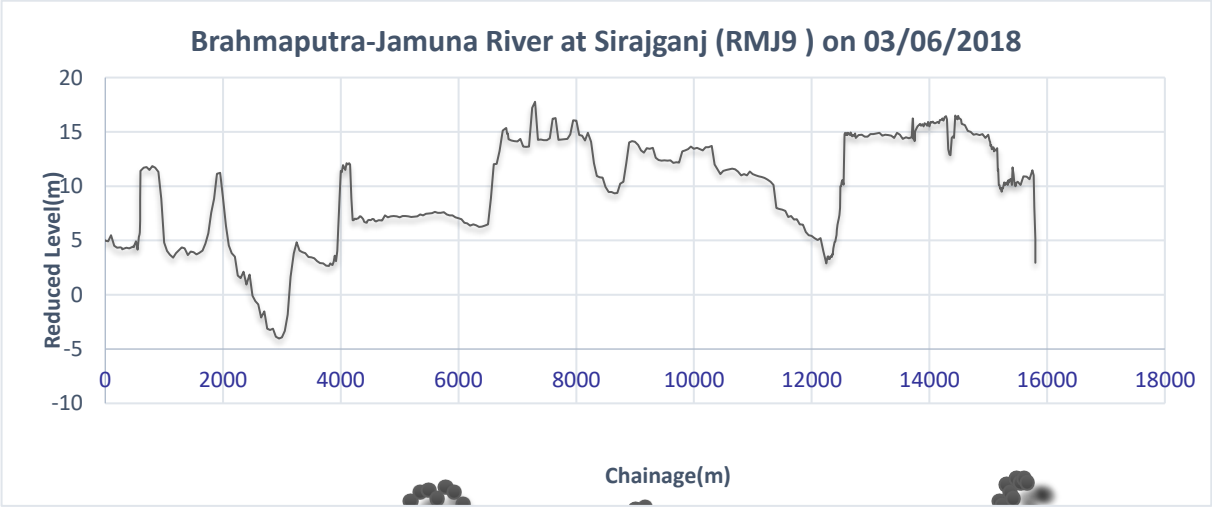

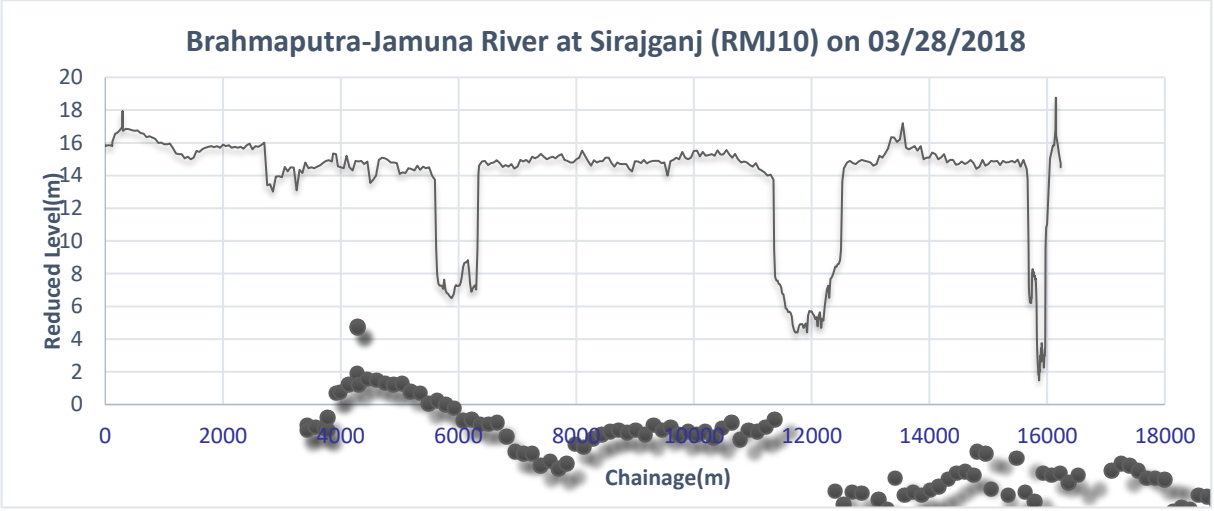
Brahmaputra-Jamuna River at Sirajganj (RMJ10) on 03/28/2018
Reduced Level(m)
20
18
16
14
12
10
8
6
4
2
0
0
2000
4000
6000
8000
10000
12000
14000
16000
18000
Chainage(m)

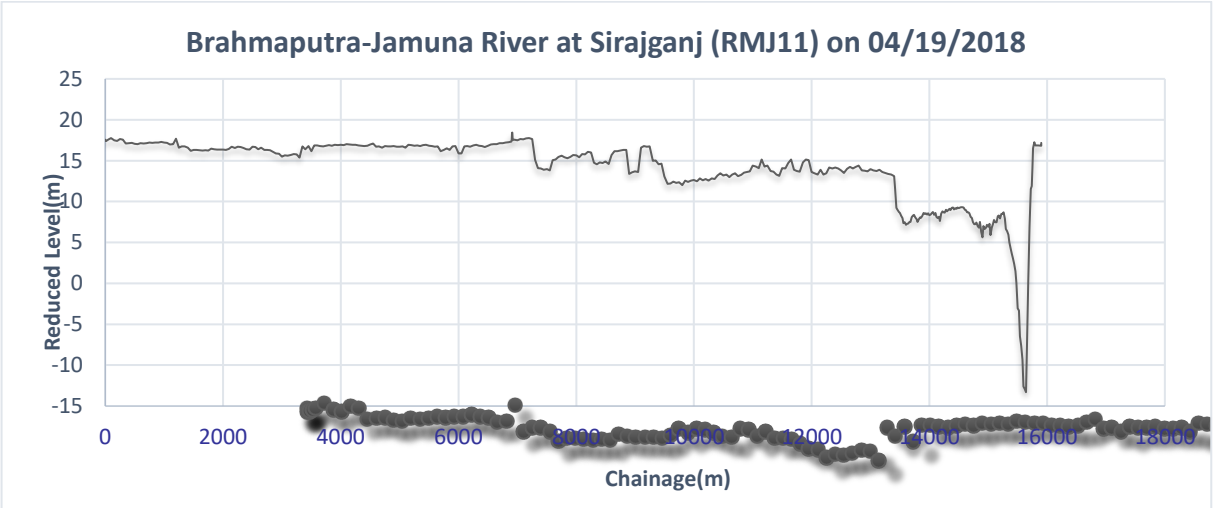
Brahmaputra-Jamuna River at Sirajganj (RMJ11) on 04/19/2018
Reduced Level(m)
25
20
15
10
5
0
-5
-10
-15
0
2000
4000
6000
8000
10000
12000
14000
16000
18000
Chainage(m)

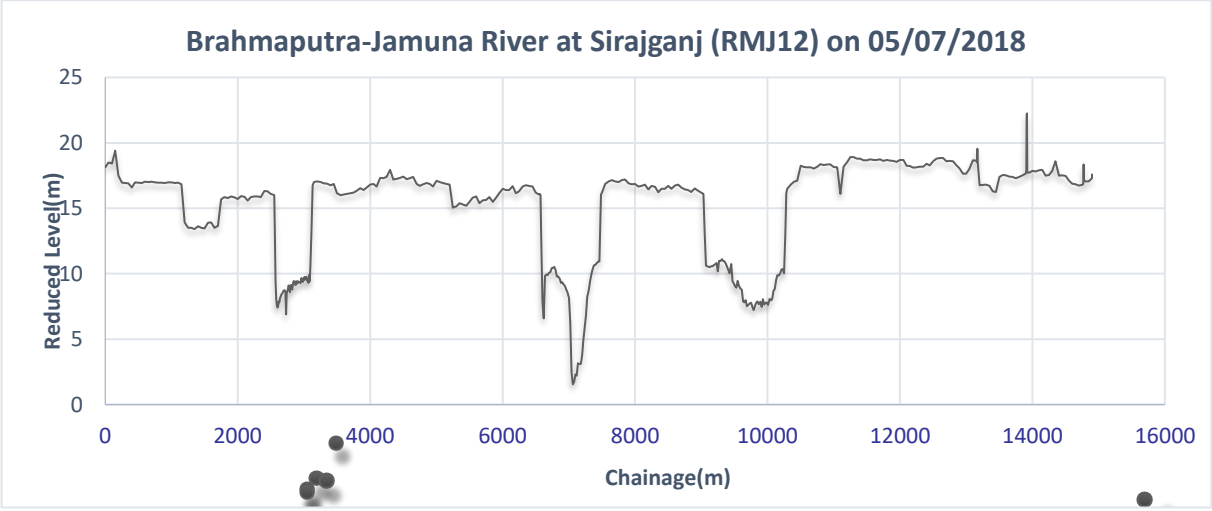
Brahmaputra-Jamuna River at Sirajganj (RMJ12) on 05/07/2018
Reduced Level(m)
25
20
15
10
5
0
0
2000
4000
6000
8000
10000
12000
14000
16000
Chainage(m)

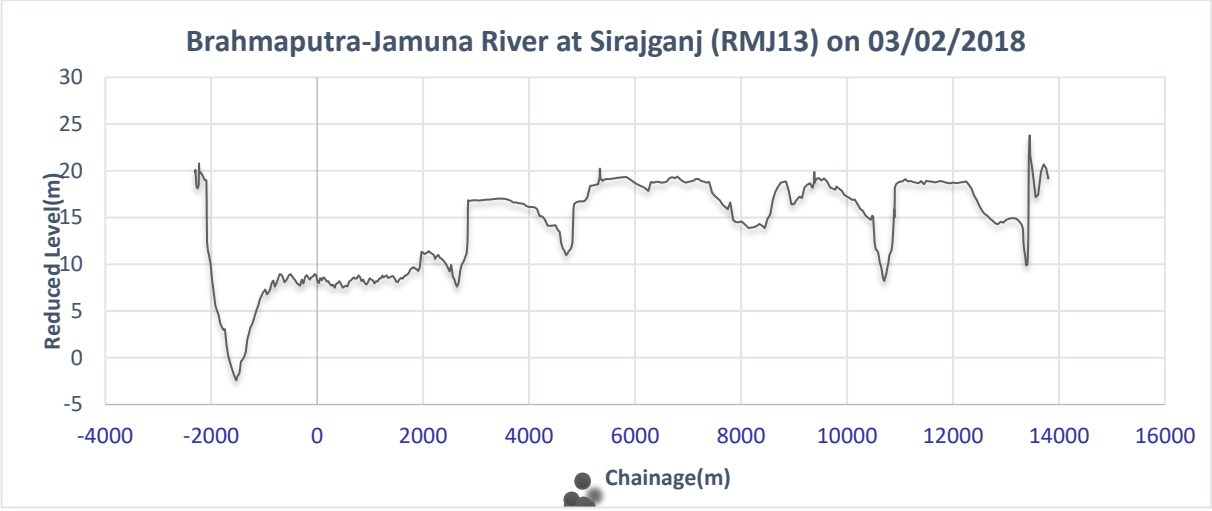
Brahmaputra-Jamuna River at Sirajganj (RMJ13) on 03/02/2018
Reduced Level(m)
30
25
20
15
10
5
0
-5
-4000
-2000
0
2000
4000
6000
8000
10000
12000
14000
16000
Chainage(m)

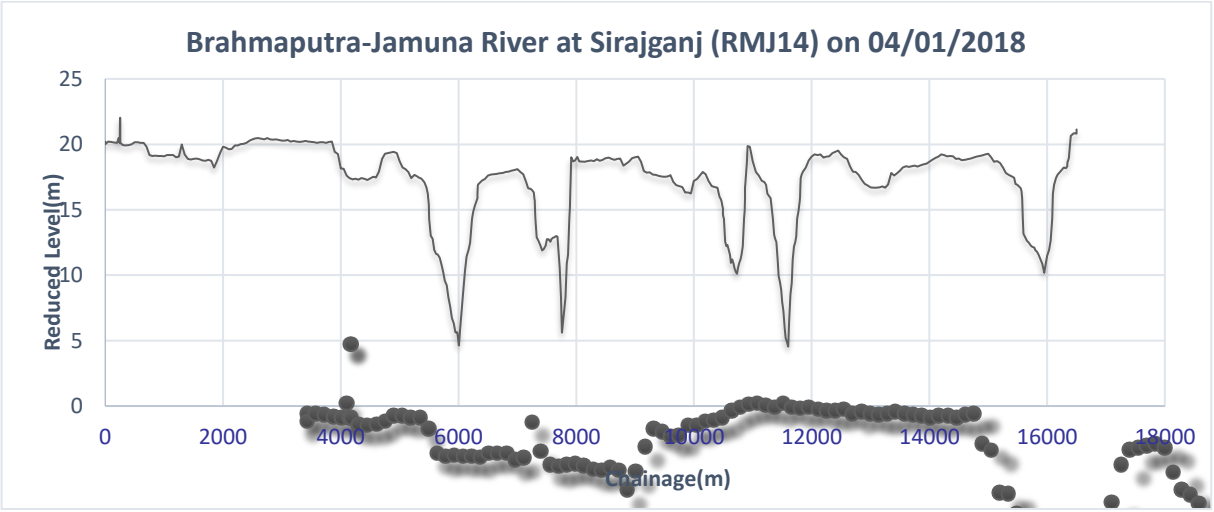
Brahmaputra-Jamuna River at Sirajganj (RMJ14) on 04/01/2018
Reduced Level(m)
25
20
15
10
5
0
0
2000
4000
6000
8000
10000
12000
14000
16000
18000
Chainage(m)

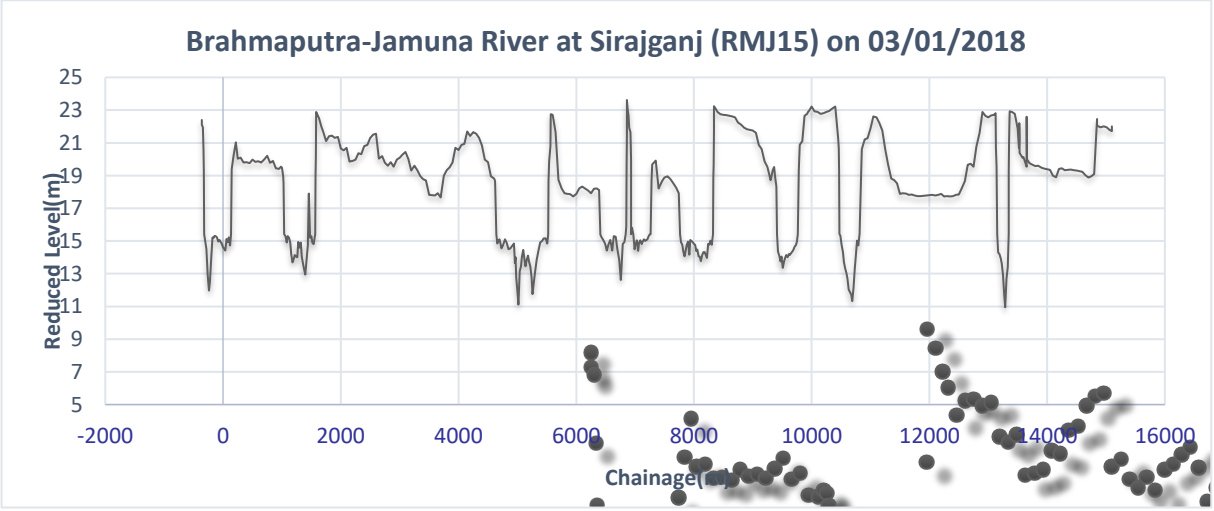
Brahmaputra-Jamuna River at Sirajganj (RMJ15) on 03/01/2018
Reduced Level(m)
25
23
21
19
17
15
13
11
9
7
5
-2000
0
2000
4000
6000
8000
10000
12000
14000
16000
Chainage(m)

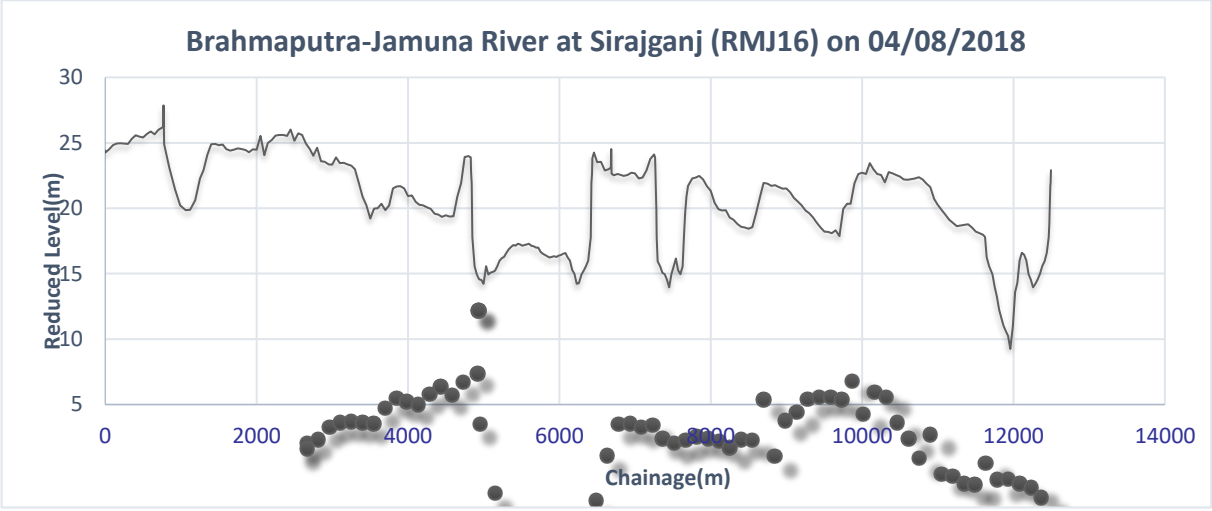
Brahmaputra-Jamuna River at Sirajganj (RMJ16) on 04/08/2018
Reduced Level(m)
30
25
20
15
10
5
0
2000
4000
6000
8000
10000
12000
14000
Chainage(m)

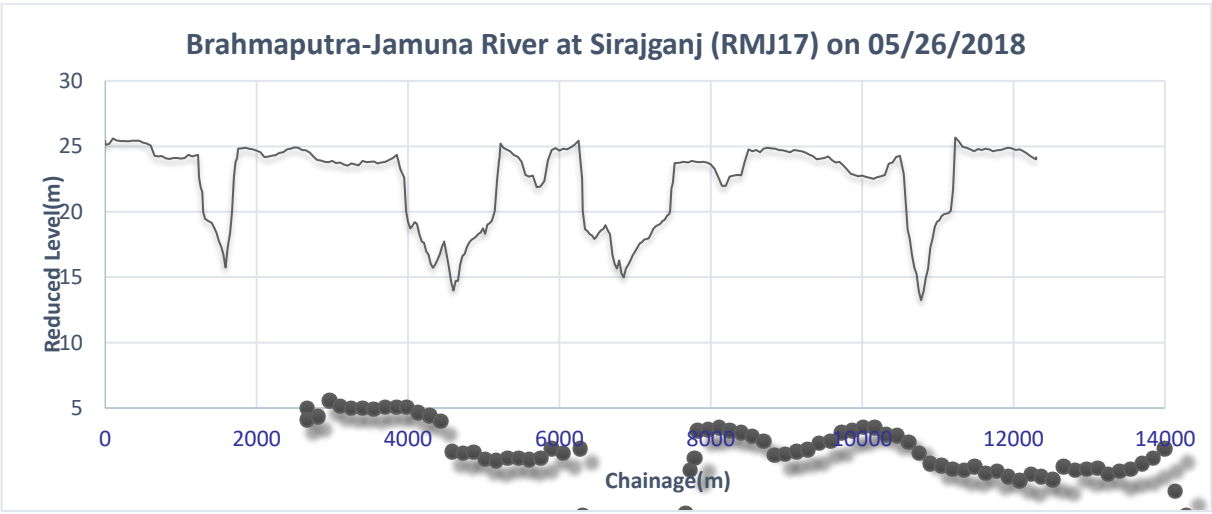
Brahmaputra-Jamuna River at Sirajganj (RMJ17) on 05/26/2018
Reduced Level(m)
30
25
20
15
10
5
0
2000
4000
6000
8000
10000
12000
14000
Chainage(m)

Appendix B4. X-section of the Old Brahmaputra River

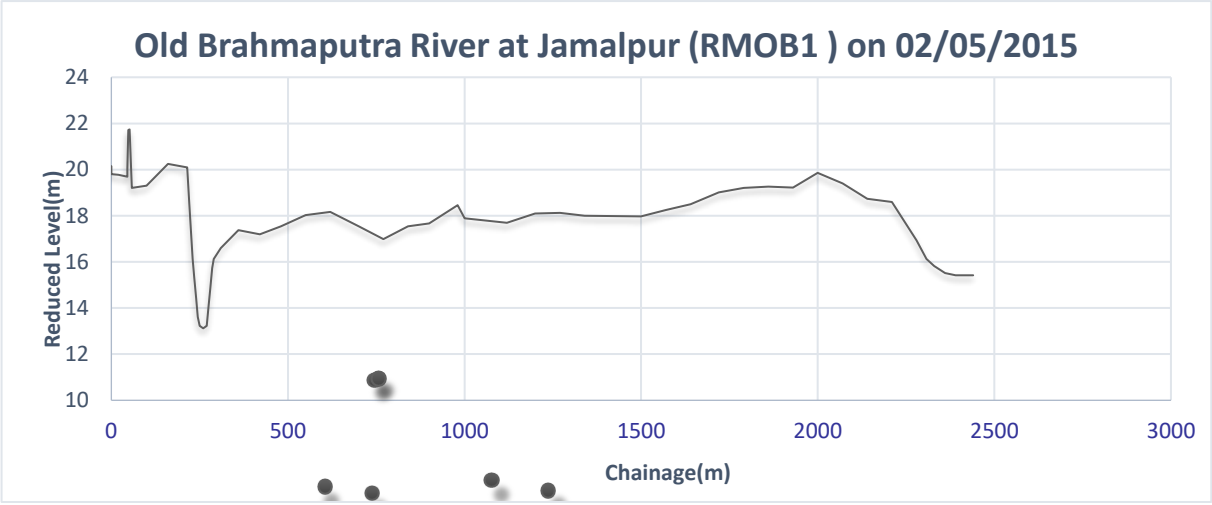

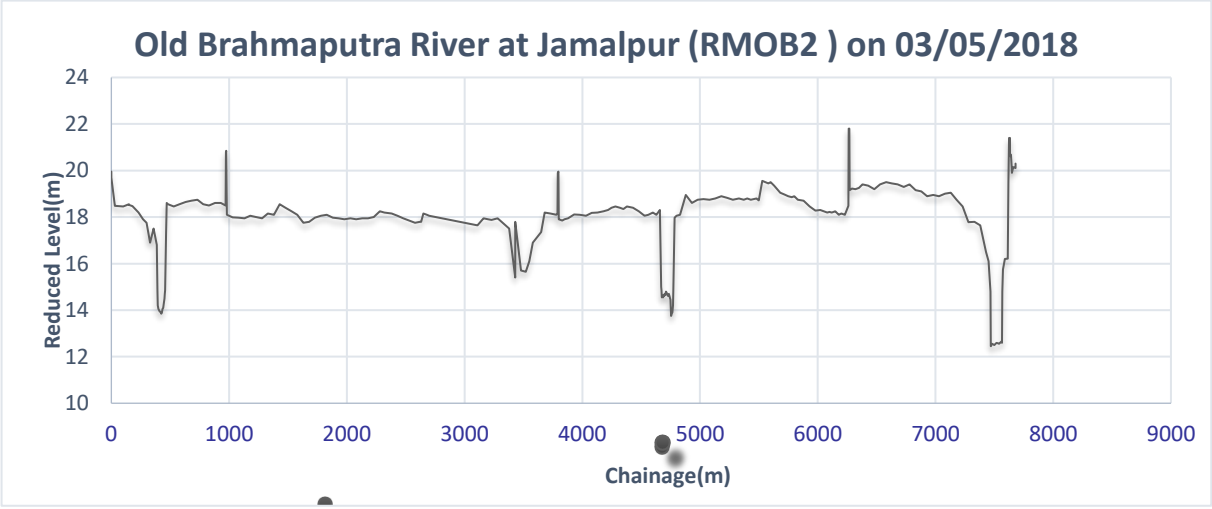

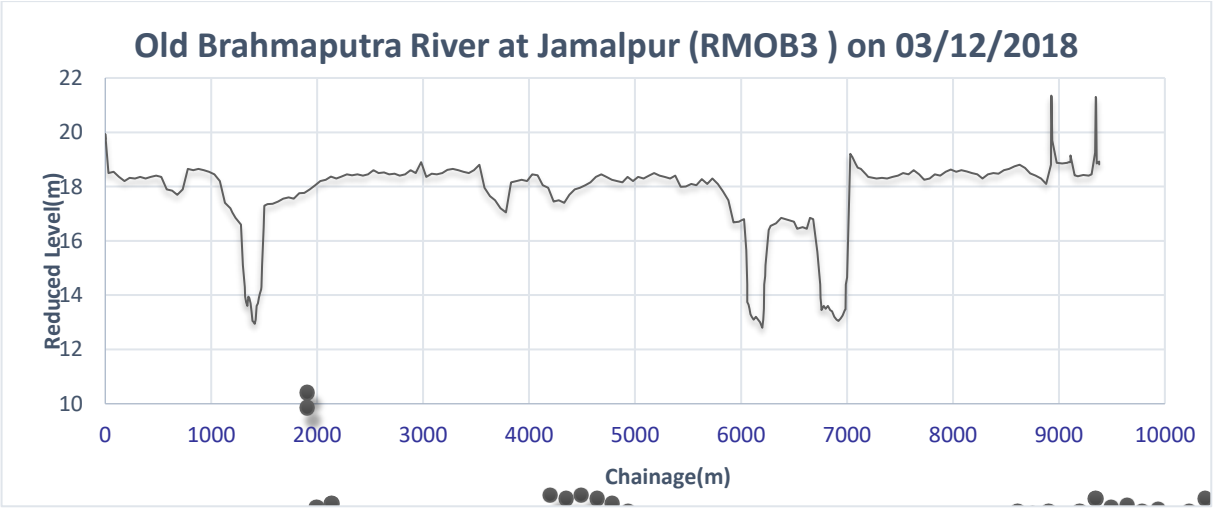

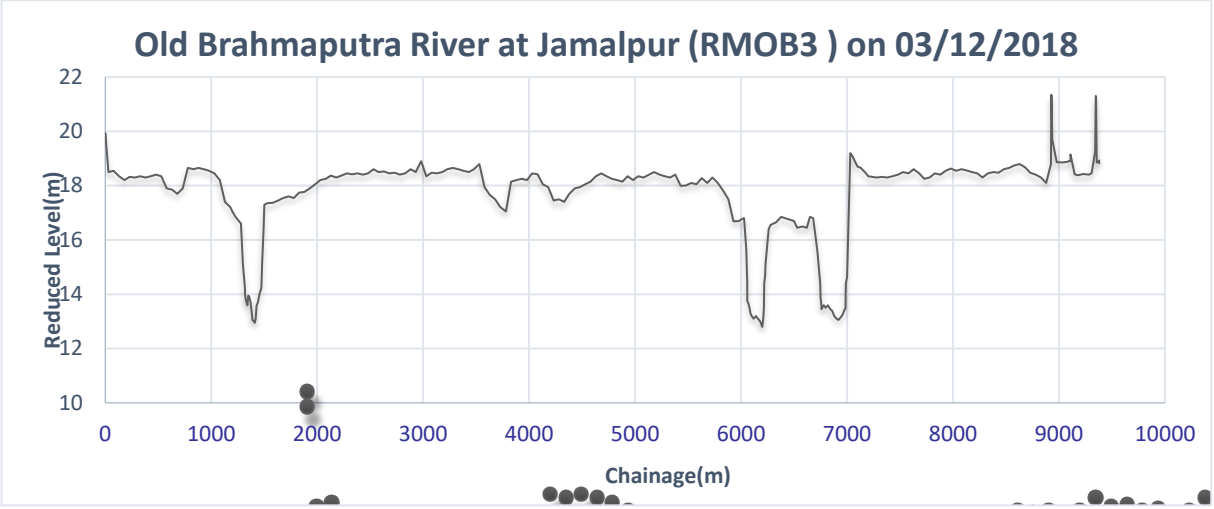
Old Brahmaputra River at Jamalpur (RMOB3) on 03/12/2018
Reduced Level(m)
22
20
18
16
14
12
10
0
1000
2000
3000
4000
5000
6000
7000
8000
9000
10000
Chainage(m)

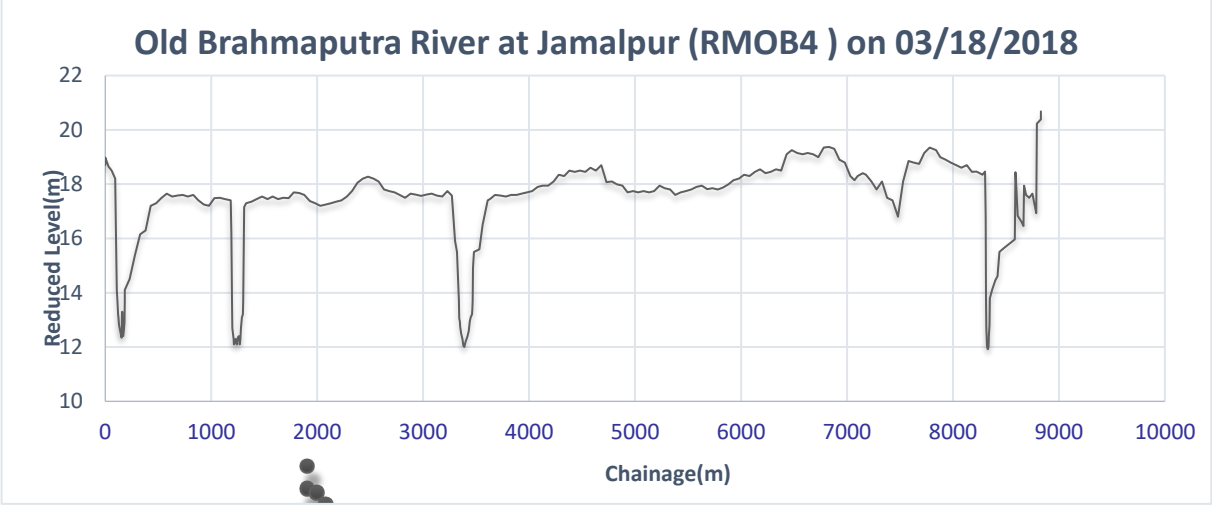
Old Brahmaputra River at Jamalpur (RMOB4) on 03/18/2018
Reduced Level(m)
22
20
18
16
14
12
10
0
1000
2000
3000
4000
5000
6000
7000
8000
9000
10000
Chainage(m)

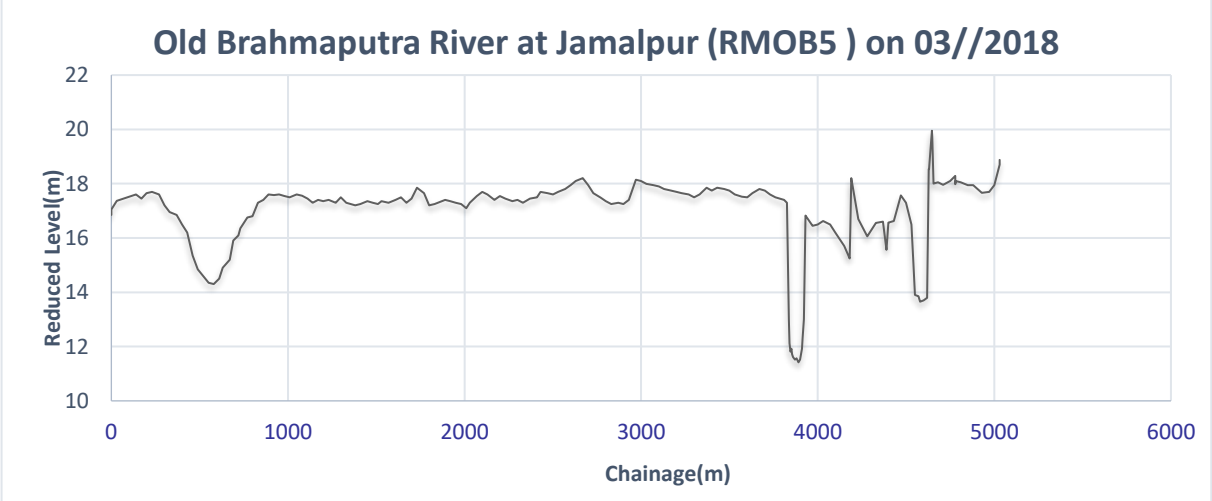
Old Brahmaputra River at Jamalpur (RMOB5) on 03//2018
Reduced Level(m)
22
20
18
16
14
12
10
0
1000
2000
3000
4000
5000
6000
Chainage(m)

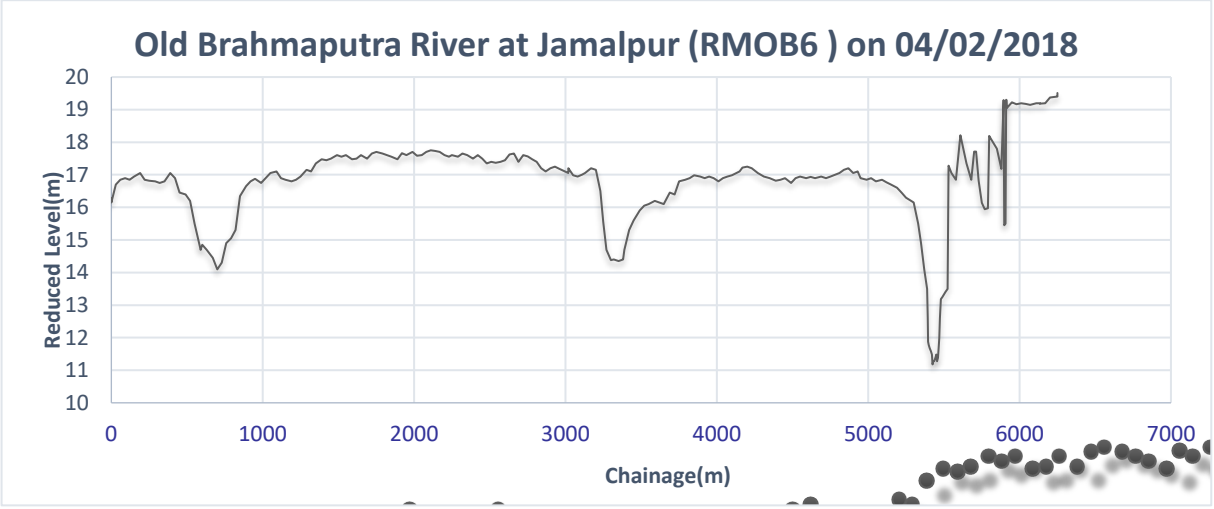
Old Brahmaputra River at Jamalpur (RMOB6) on 04/02/2018
Reduced Level(m)
20
19
18
17
16
15
14
13
12
11
10
0
1000
2000
3000
4000
5000
6000
7000
Chainage(m)

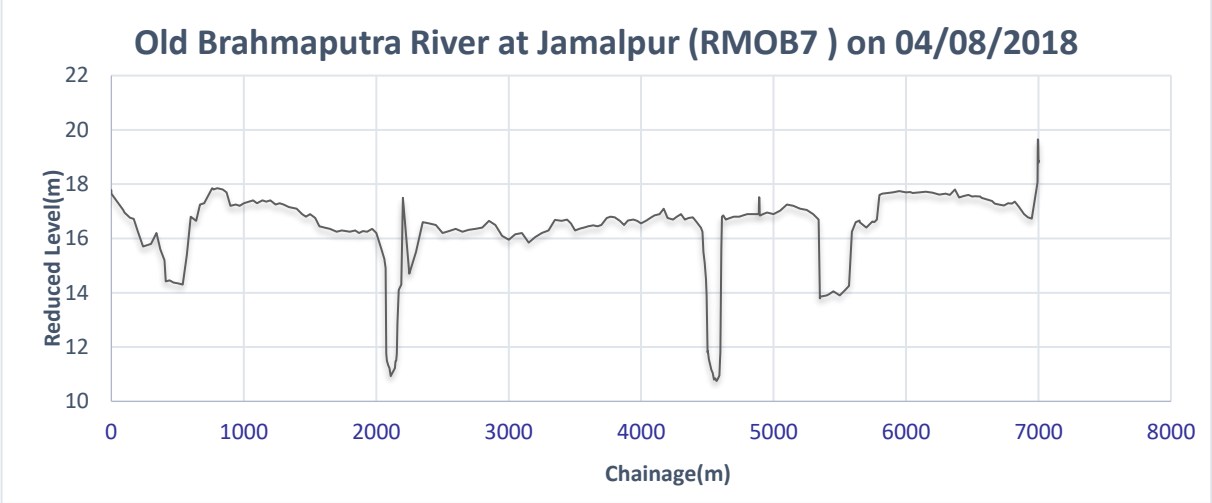
Old Brahmaputra River at Jamalpur (RMOB7) on 04/08/2018
Reduced Level(m)
22
20
18
16
14
12
10
0
1000
2000
3000
4000
5000
6000
7000
8000
Chainage(m)

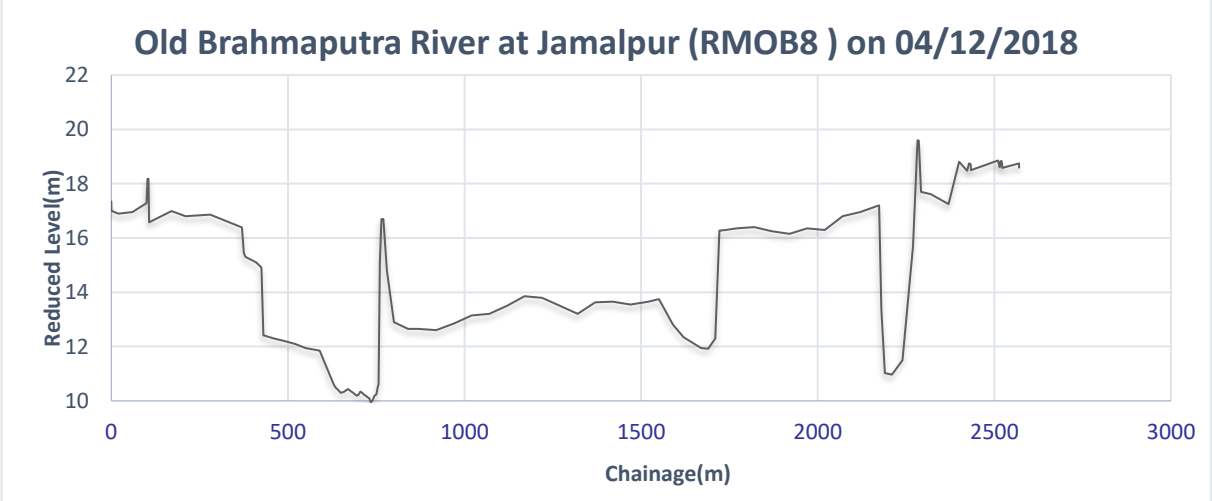
Old Brahmaputra River at Jamalpur (RMOB8) on 04/12/2018
Reduced Level(m)
22
20
18
16
14
12
10
0
500
1000
1500
2000
2500
3000
Chainage(m)

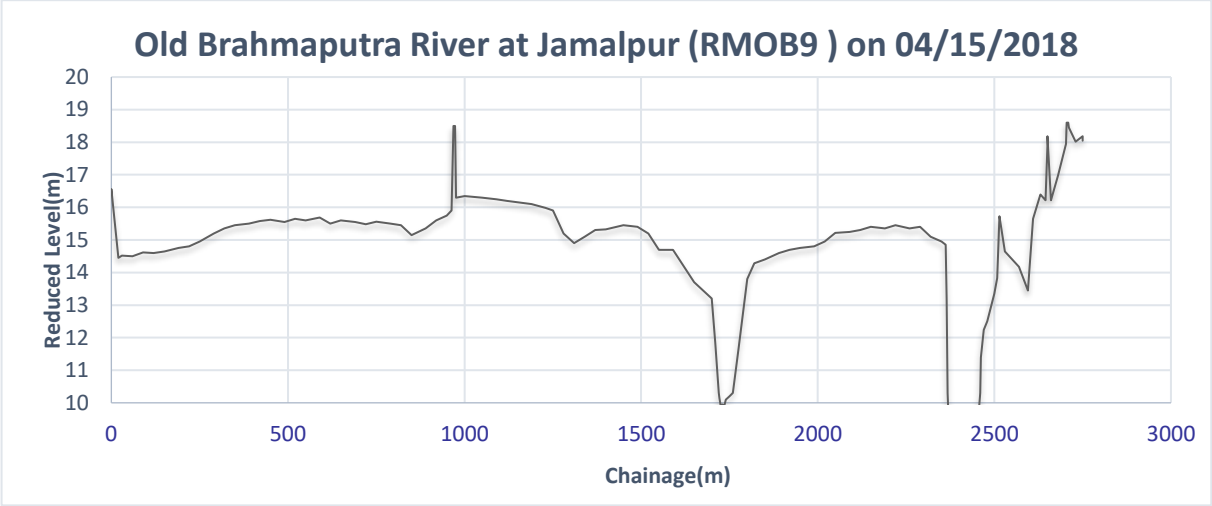
Old Brahmaputra River at Jamalpur (RMOB9) on 04/15/2018
Reduced Level(m)
20
19
18
17
16
15
14
13
12
11
10
0
500
1000
1500
2000
2500
3000
Chainage(m)

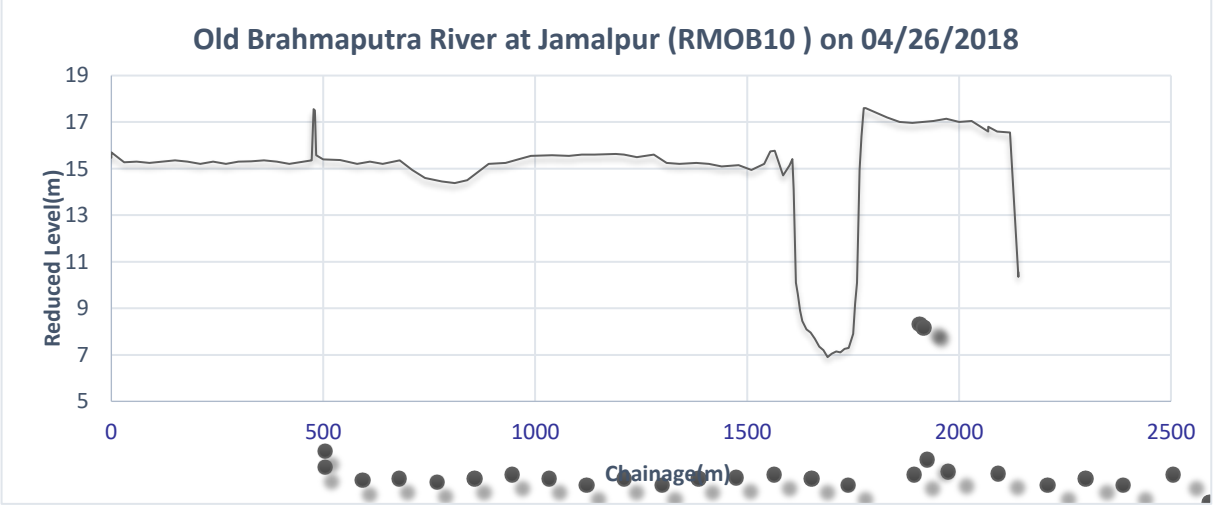
Old Brahmaputra River at Jamalpur (RMOB10) on 04/26/2018
Reduced Level(m)
19
17
15
13
11
9
7
5
0
500
1000
1500
2000
2500
Chainage(m)

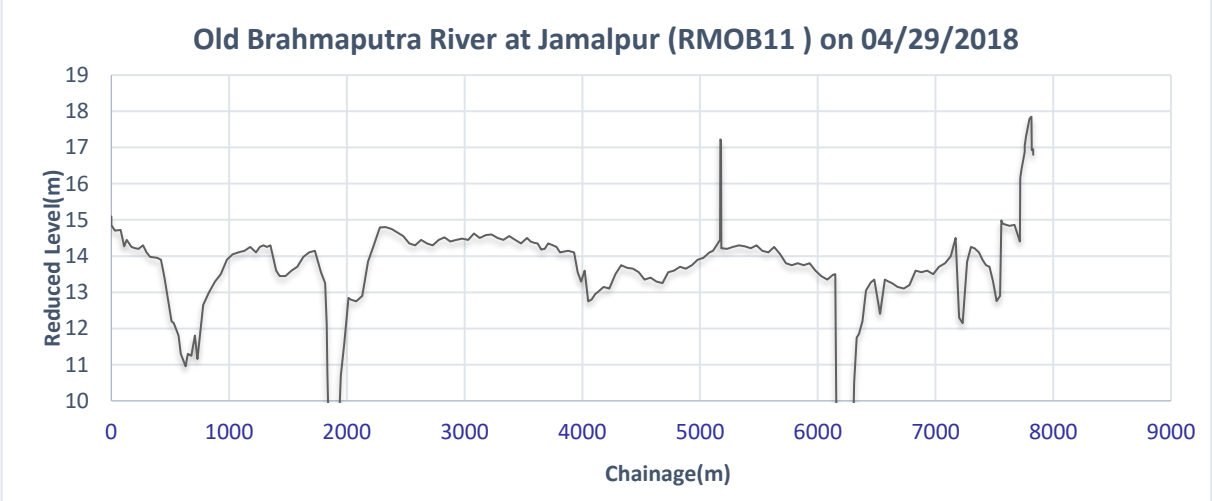
Old Brahmaputra River at Jamalpur (RMOB11) on 04/29/2018
Reduced Level(m)
19
18
17
16
15
14
13
12
11
10
0
1000
2000
3000
4000
5000
6000
7000
8000
9000
Chainage(m)

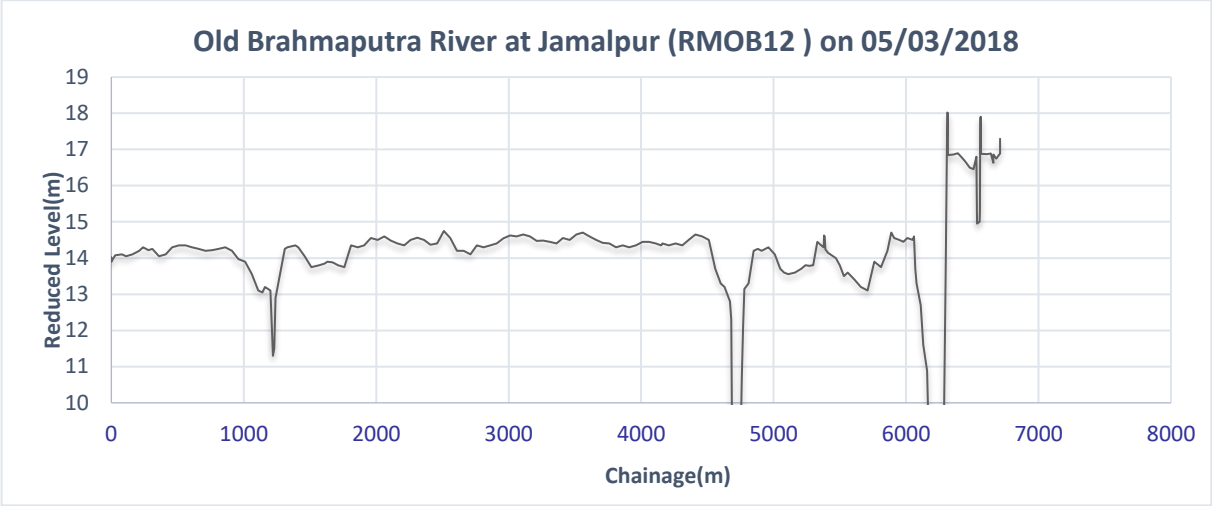
Old Brahmaputra River at Jamalpur (RMOB12) on 05/03/2018
Reduced Level(m)
19
18
17
16
15
14
13
12
11
10
0
1000
2000
3000
4000
5000
6000
7000
8000
Chainage(m)

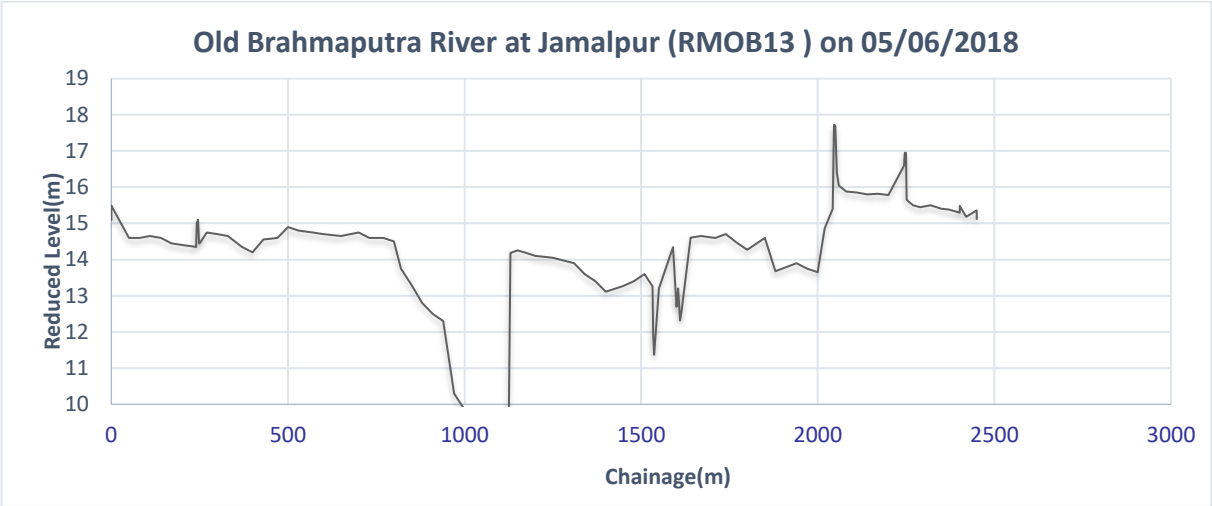
Old Brahmaputra River at Jamalpur (RMOB13) on 05/06/2018
Reduced Level(m)
19
18
17
16
15
14
13
12
11
10
0
500
1000
1500
2000
2500
3000
Chainage(m)

Appendix B5. X-section of the Ghaghat River

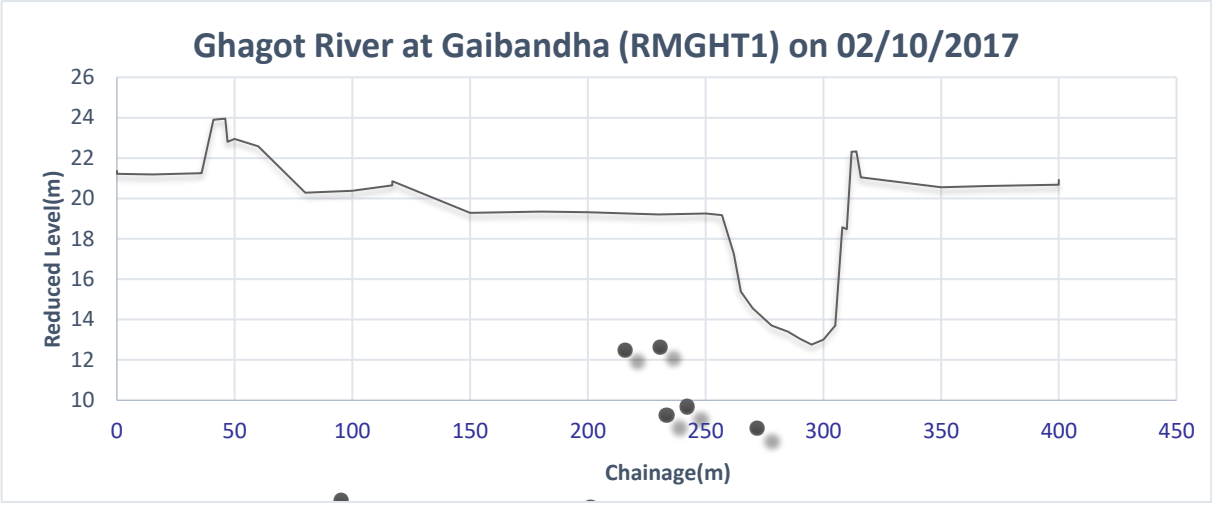

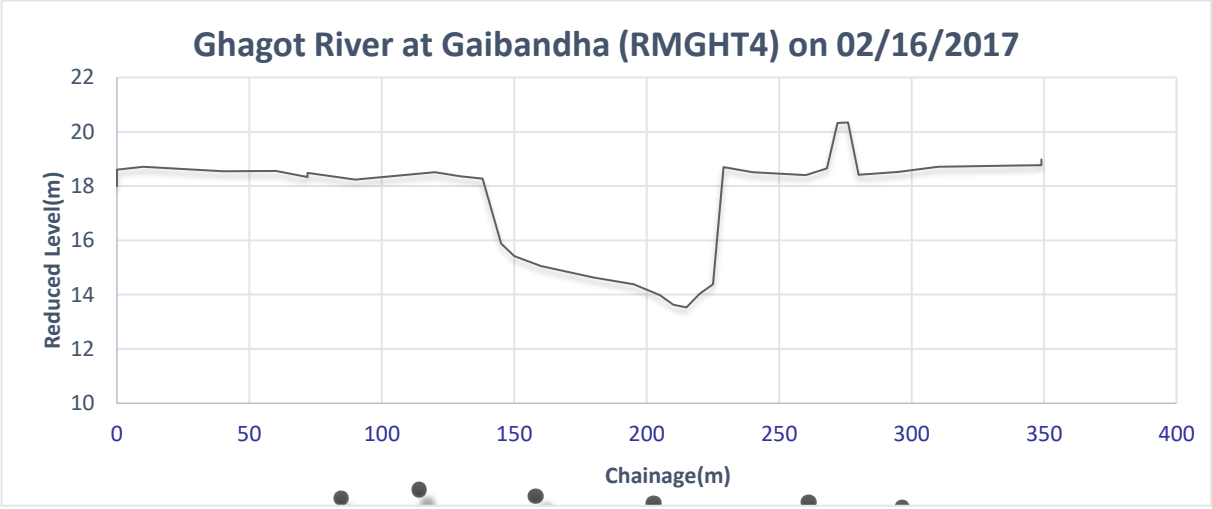

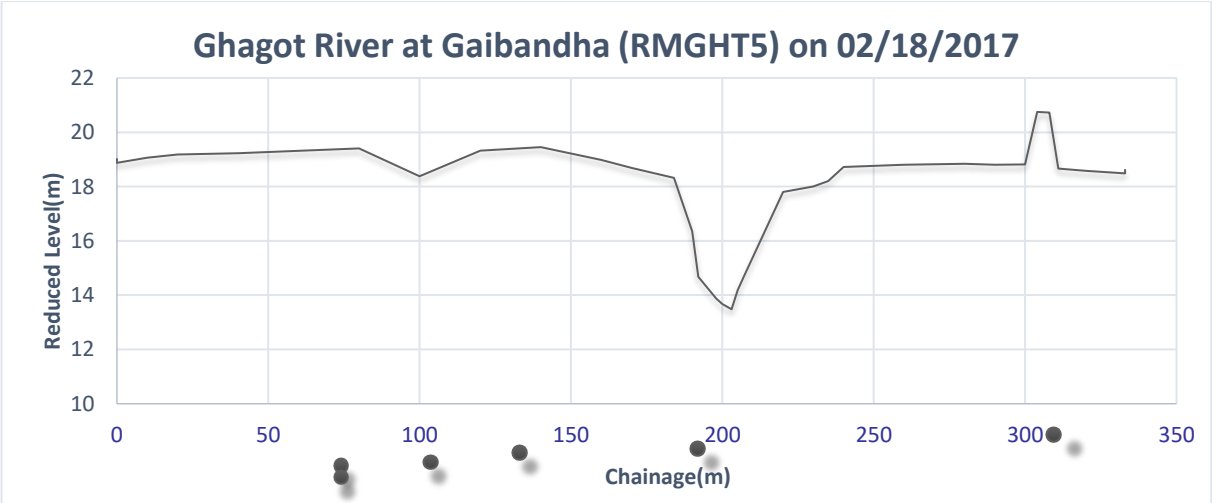

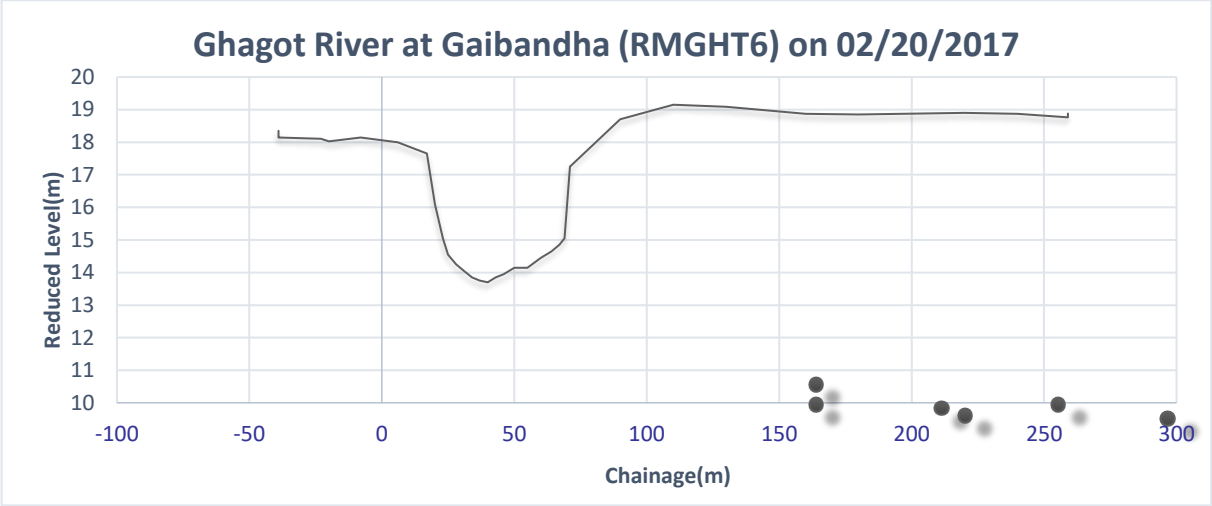
Ghagot River at Gaibandha (RMGHT6) on 02/20/2017
Reduced Level(m)
20
19
18
17
16
15
14
13
12
11
10
-100
-50
0
50
100
150
200
250
300
Chainage(m)

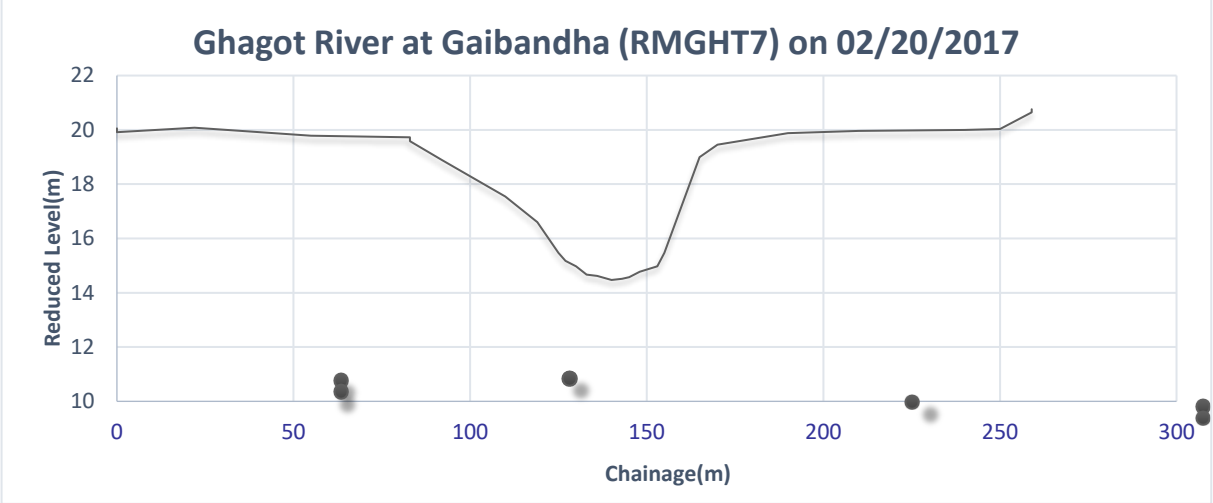
Ghagot River at Gaibandha (RMGHT7) on 02/20/2017
Reduced Level(m)
22
20
18
16
14
12
10
0
50
100
150
200
250
300
Chainage(m)

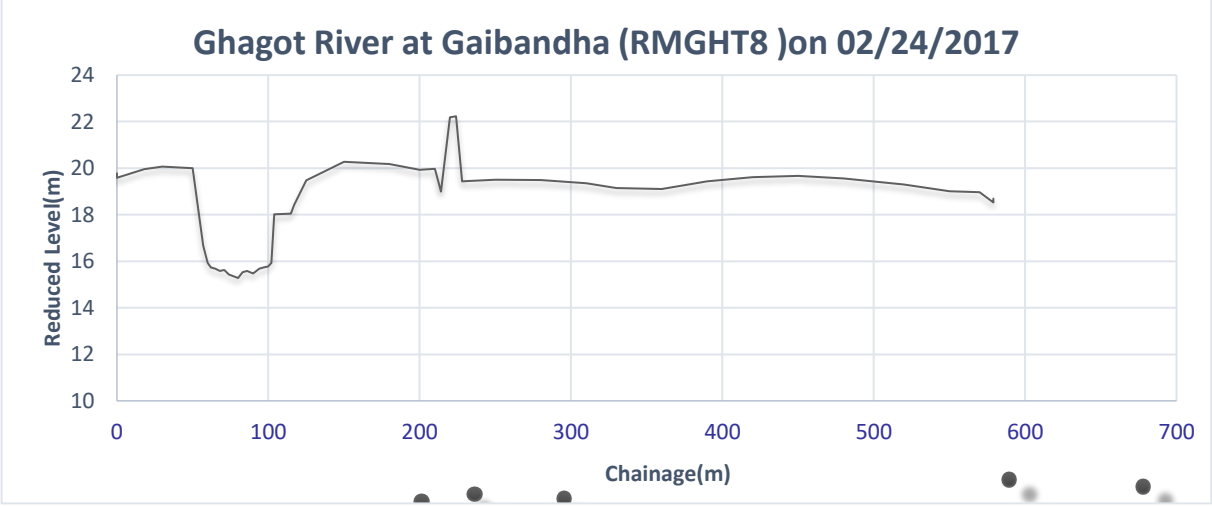
Ghagot River at Gaibandha (RMGHT8)on 02/24/2017
Reduced Level(m)
24
22
20
18
16
14
12
10
0
100
200
300
400
500
600
700
Chainage(m)

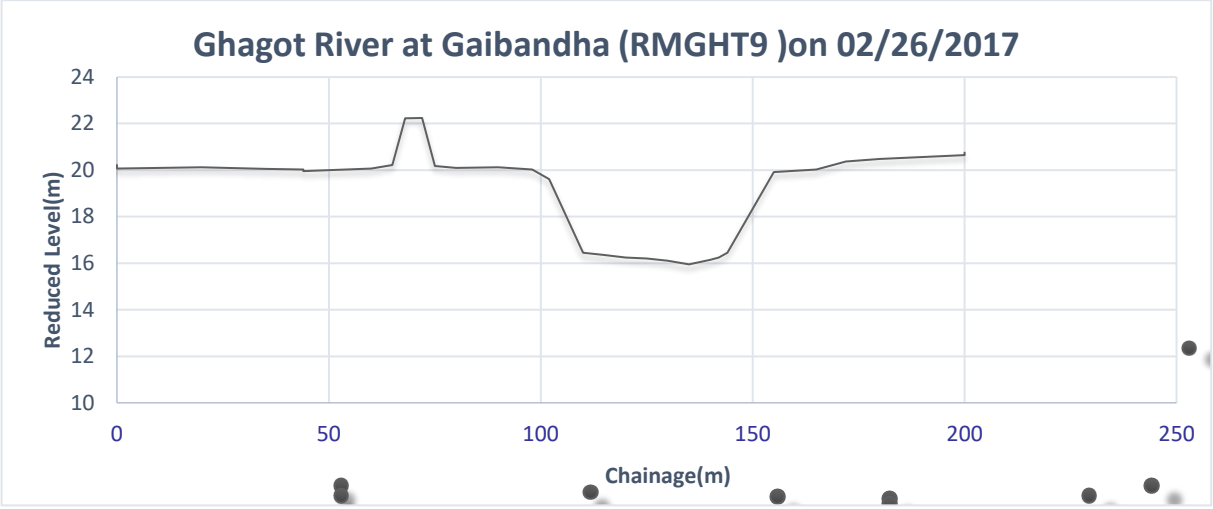
Ghagot River at Gaibandha (RMGHT9)on 02/26/2017
Reduced Level(m)
24
22
20
18
16
14
12
10
0
50
100
150
200
250
Chainage(m)

Appendix B6. X-section of the Bangali River

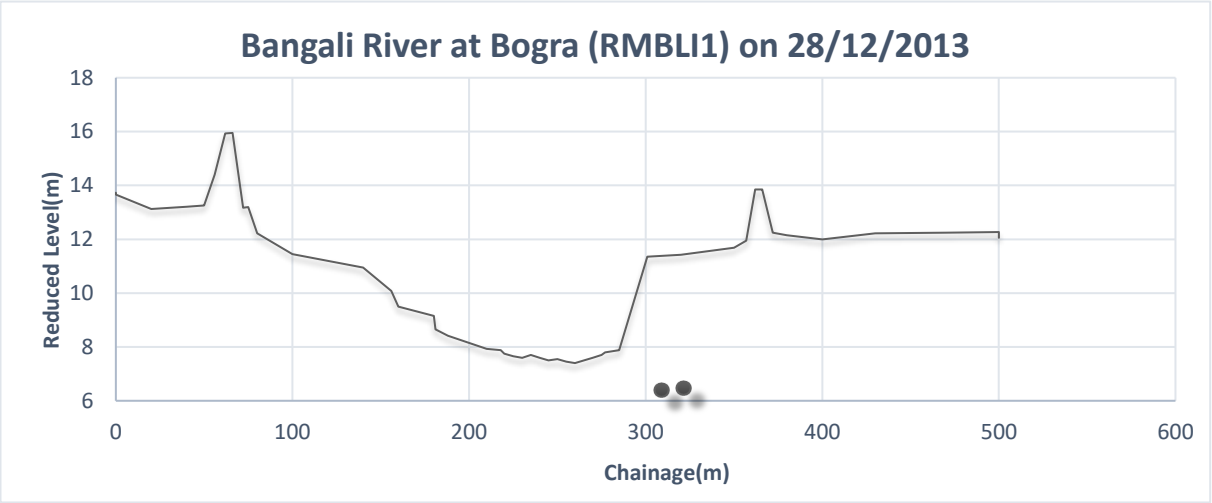

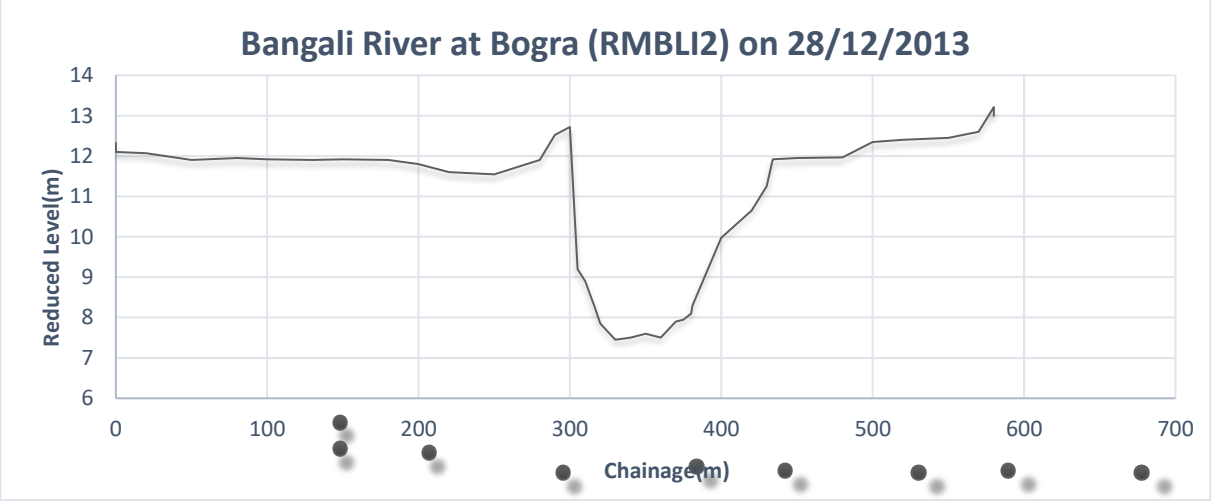

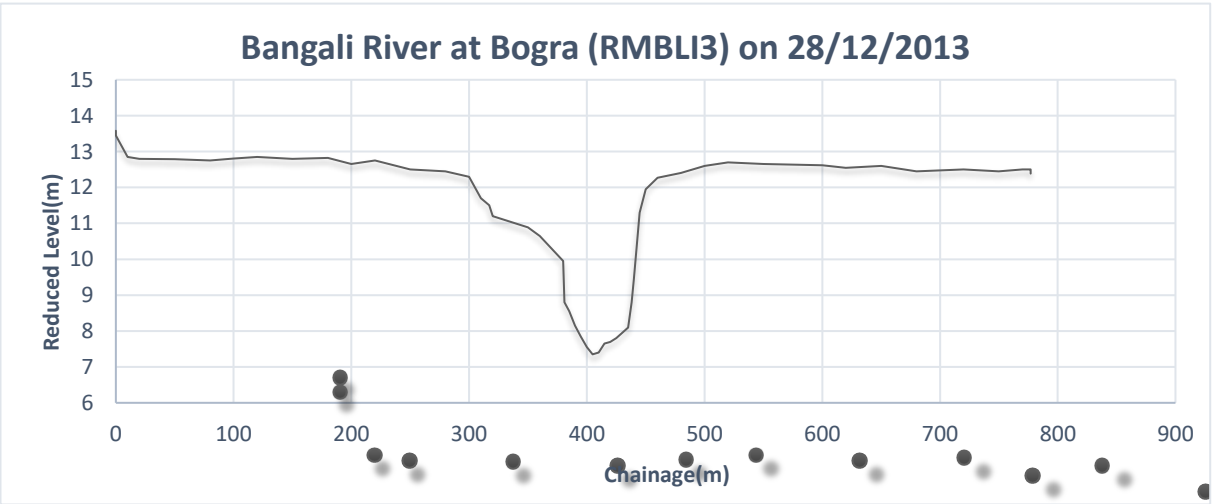

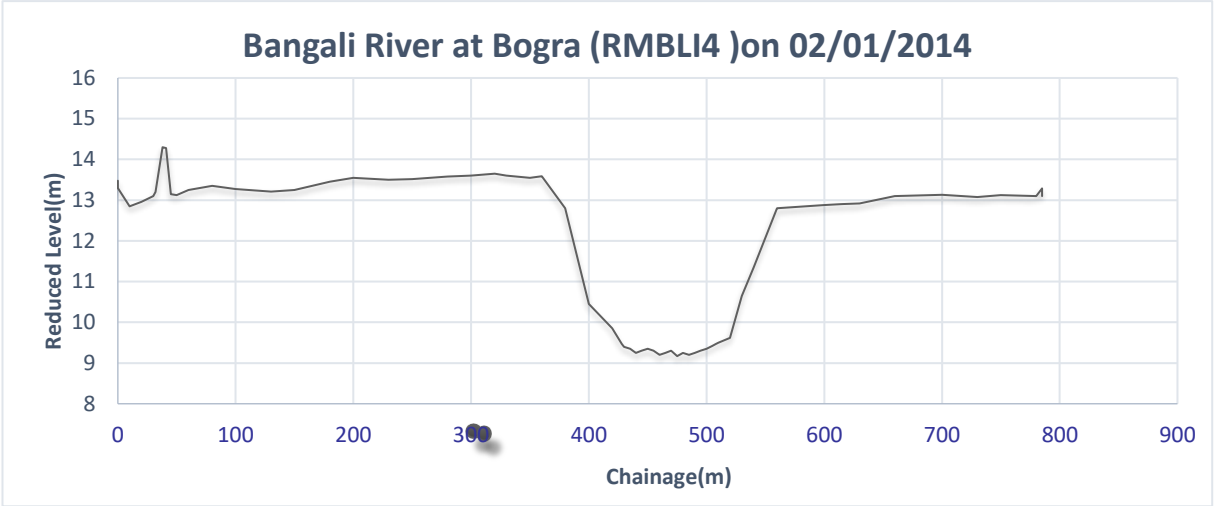
Bangali River at Bogra (RMBLI4)on 02/01/2014
Reduced Level(m)
16
15
14
13
12
11
10
9
8
0
100
200
300
400
500
600
700
800
900
Chainage(m)

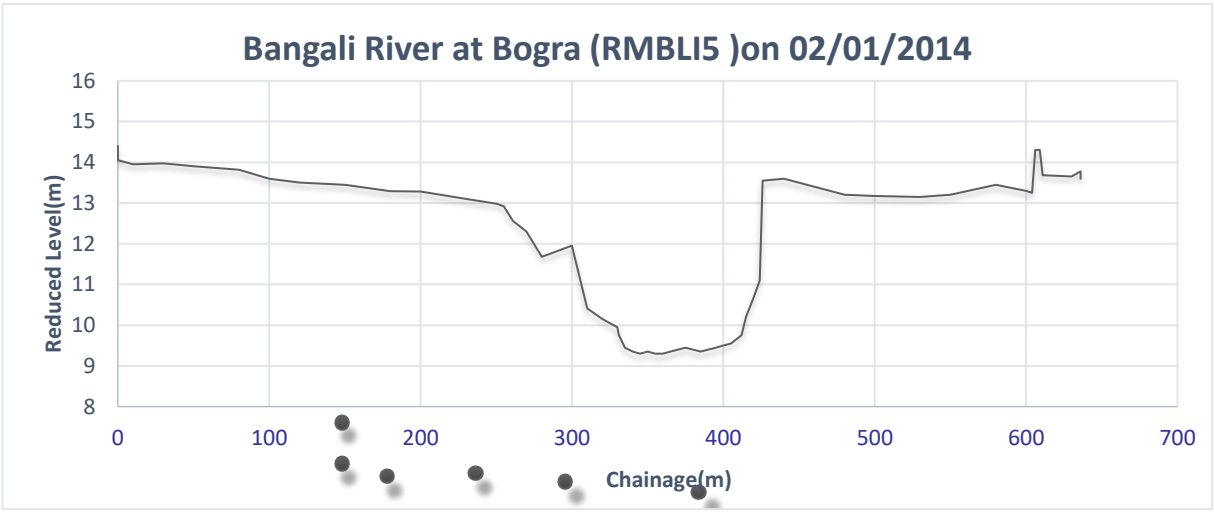
Bangali River at Bogra (RMBLI5)on 02/01/2014
Reduced Level(m)
16
15
14
13
12
11
10
9
8
0
100
200
300
400
500
600
700
Chainage(m)

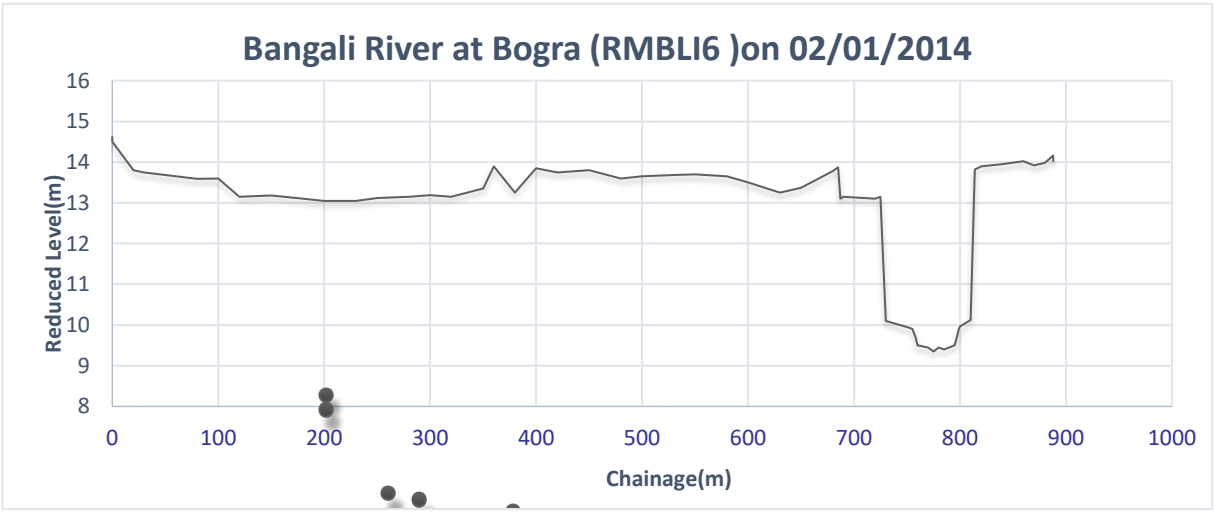
Bangali River at Bogra (RMBLI6)on 02/01/2014
Reduced Level(m)
16
15
14
13
12
11
10
9
8
0
100
200
300
400
500
600
700
800
900
1000
Chainage(m)

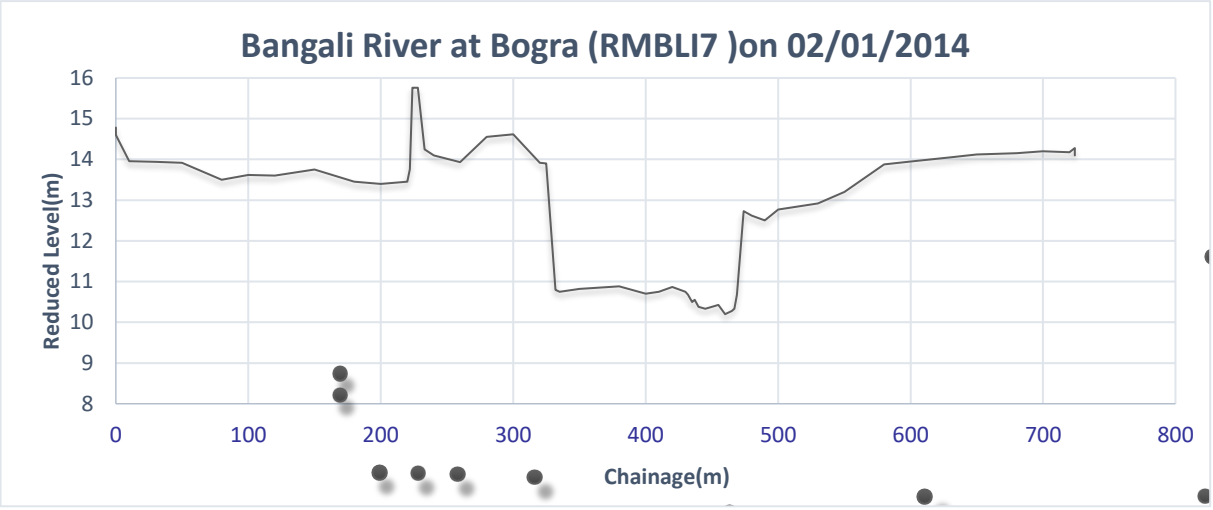
Bangali River at Bogra (RMBLI7)on 02/01/2014
Reduced Level(m)
16
15
14
13
12
11
10
9
8
0
100
200
300
400
500
600
700
800
Chainage(m)

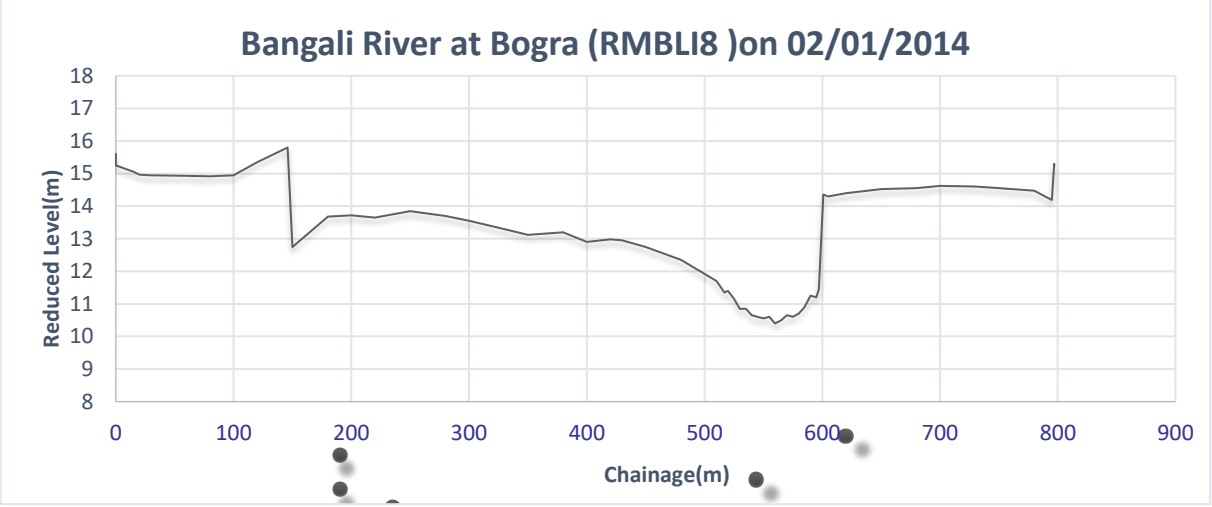
Bangali River at Bogra (RMBLI8)on 02/01/2014
Reduced Level(m)
18
17
16
15
14
13
12
11
10
9
8
0
100
200
300
400
500
600
700
800
900
Chainage(m)

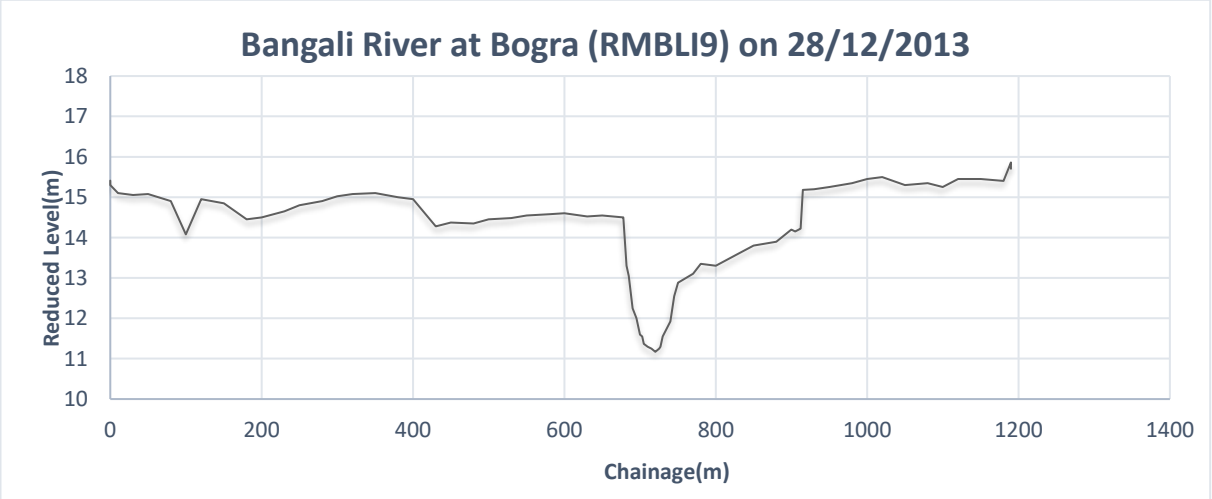
Bangali River at Bogra (RMBLI9) on 28/12/2013
Reduced Level(m)
18
17
16
15
14
13
12
11
10
0
200
400
600
800
1000
1200
1400
Chainage(m)

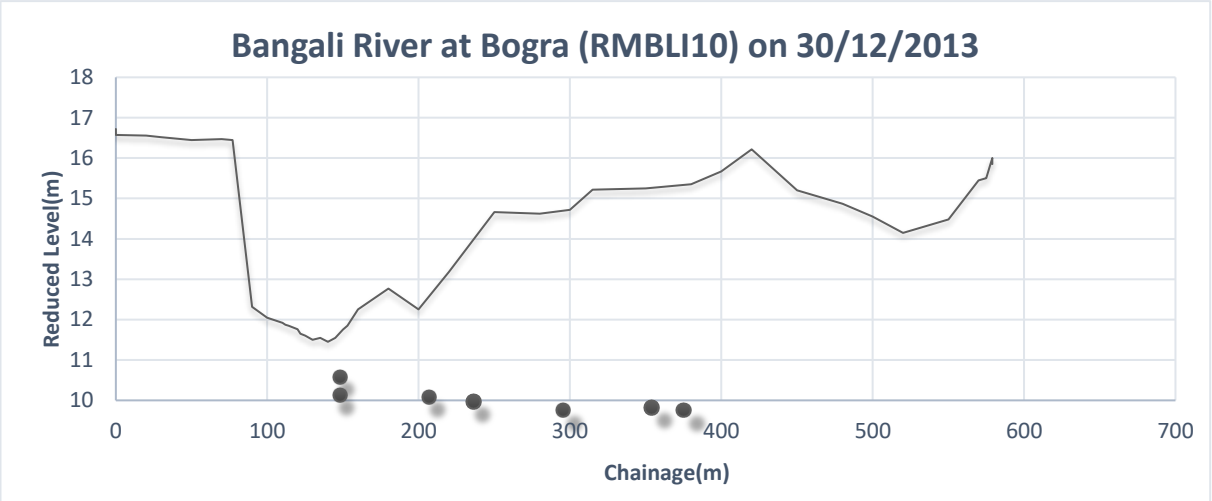
Bangali River at Bogra (RMBLI10) on 30/12/2013
Reduced Level(m)
18
17
16
15
14
13
12
11
10
0
100
200
300
400
500
600
700
Chainage(m)

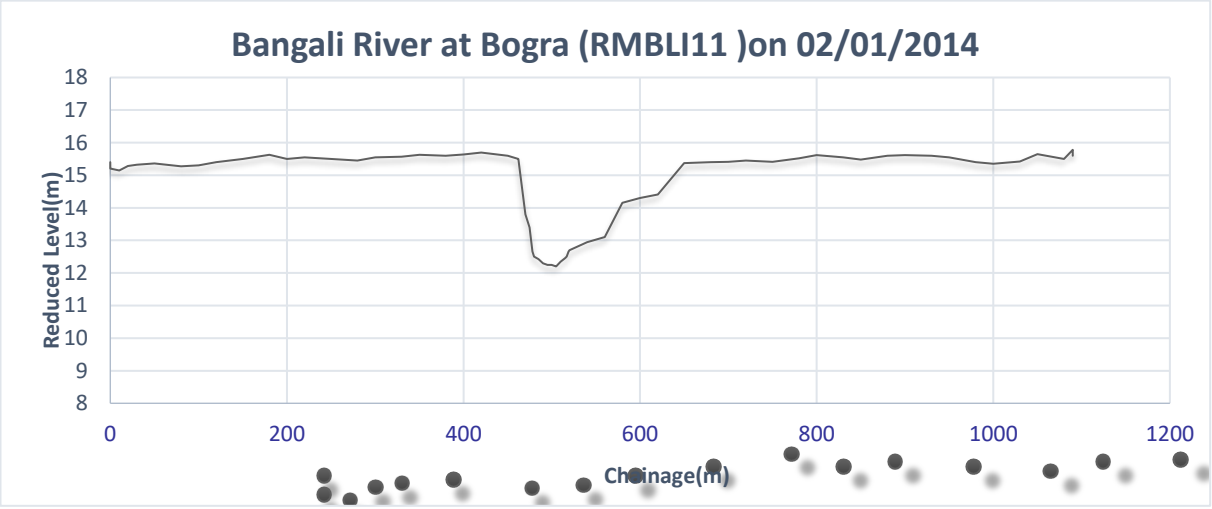
Bangali River at Bogra (RMBLI11)on 02/01/2014
Reduced Level(m)
18
17
16
15
14
13
12
11
10
9
8
0
200
400
600
800
1000
1200
Chainage(m)

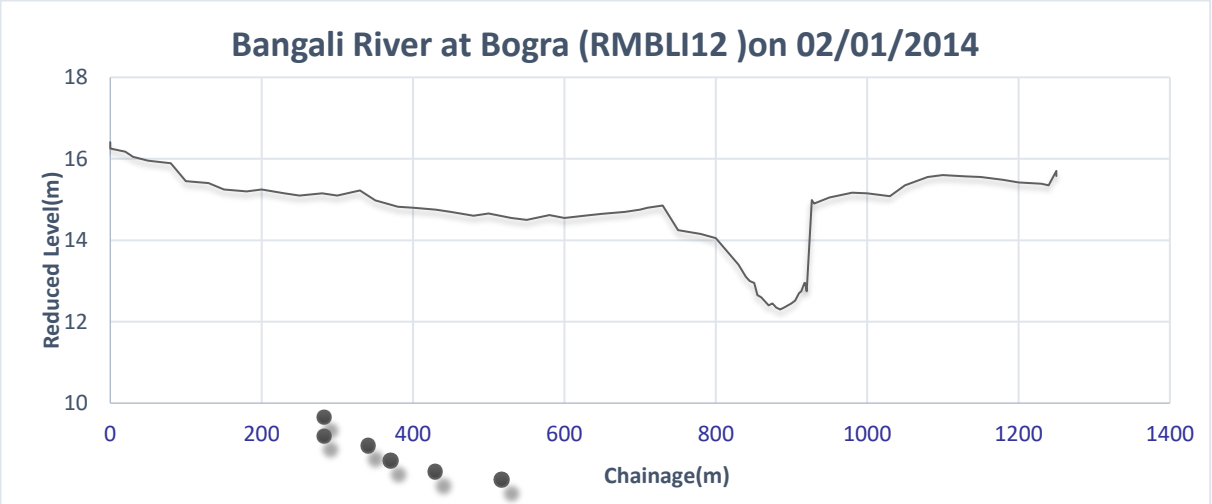
Bangali River at Bogra (RMBLI12)on 02/01/2014
Reduced Level(m)
18
16
14
12
10
0
200
400
600
800
1000
1200
1400
Chainage(m)

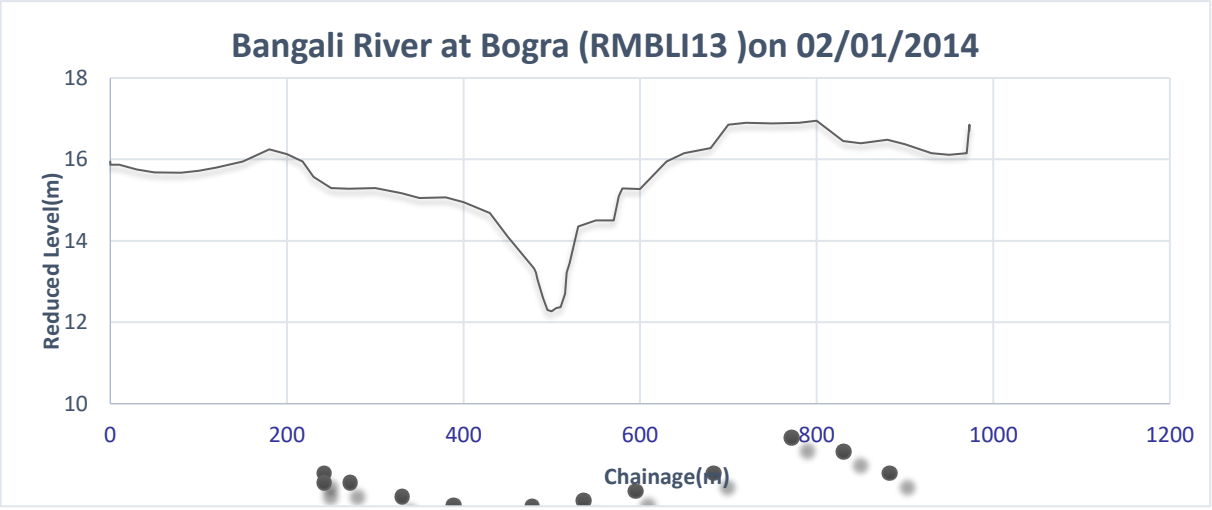
Bangali River at Bogra (RMBLI13)on 02/01/2014
Reduced Level(m)
18
16
14
12
10
0
200
400
600
800
1000
1200
Chainage(m)

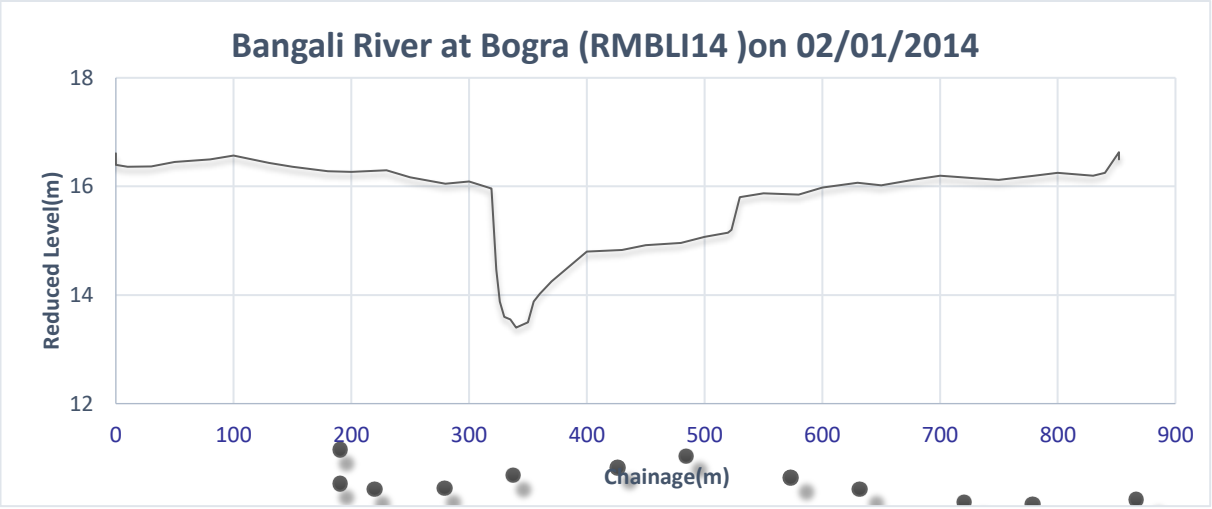
Bangali River at Bogra (RMBLI14)on 02/01/2014
Reduced Level(m)
18
16
14
12
0
100
200
300
400
500
600
700
800
900
Chainage(m)

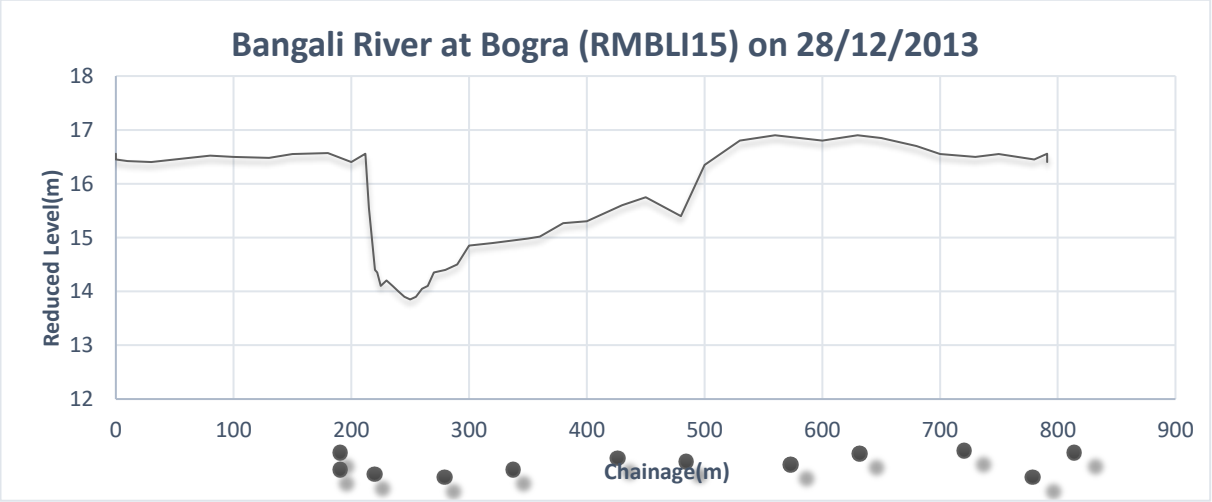
Bangali River at Bogra (RMBLI15) on 28/12/2013
Reduced Level(m)
18
17
16
15
14
13
12
0
100
200
300
400
500
600
700
800
900
Chainage(m)

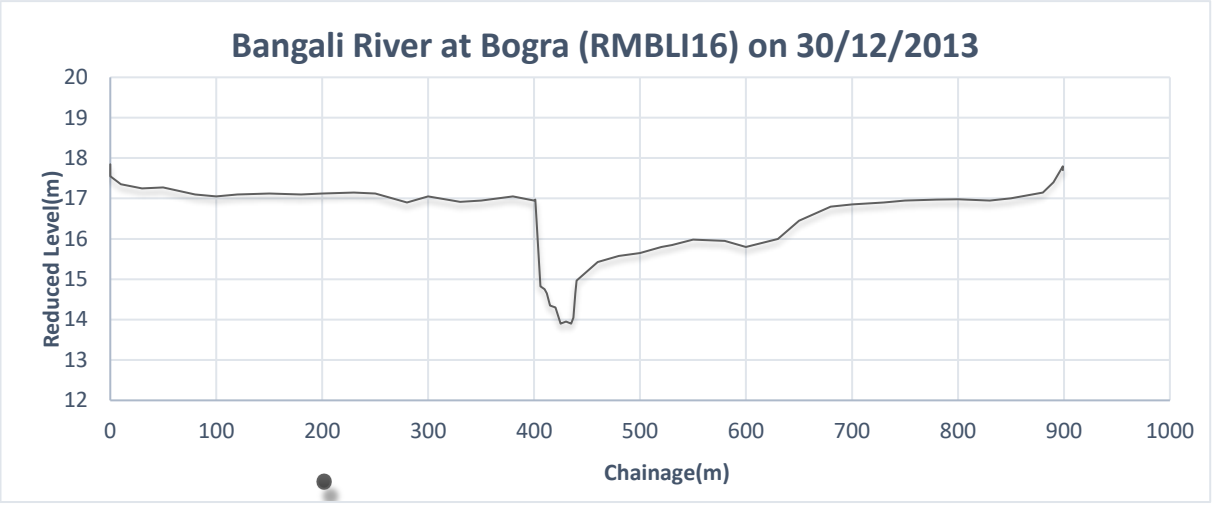
Bangali River at Bogra (RMBLI16) on 30/12/2013
Reduced Level(m)
20
19
18
17
16
15
14
13
12
0
100
200
300
400
500
600
700
800
900
1000
Chainage(m)

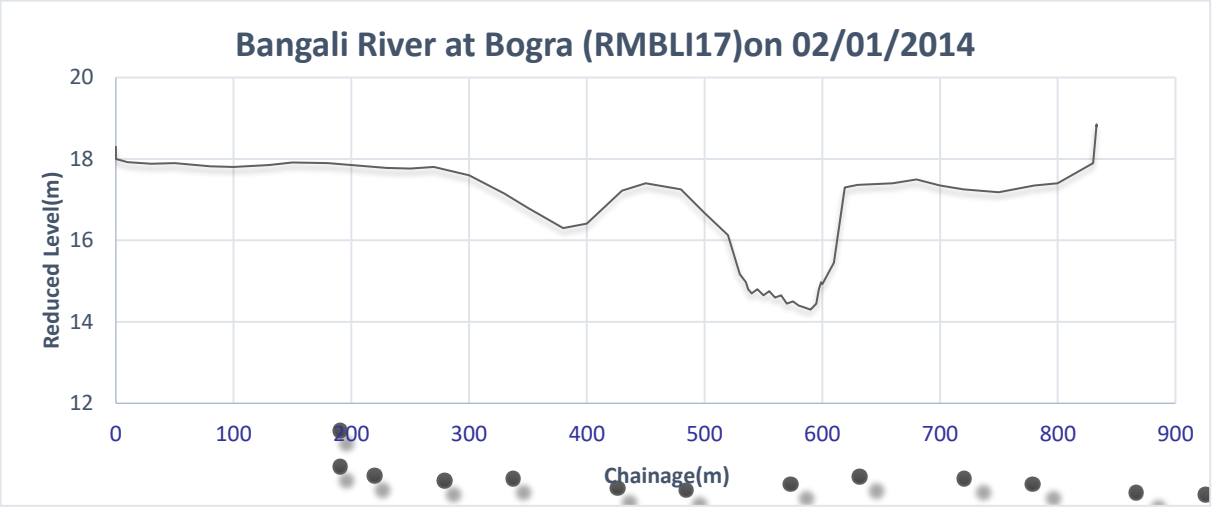
Bangali River at Bogra (RMBLI17)on 02/01/2014
Reduced Level(m)
20
18
16
14
12
0
100
200
300
400
500
600
700
800
900
Chainage(m)

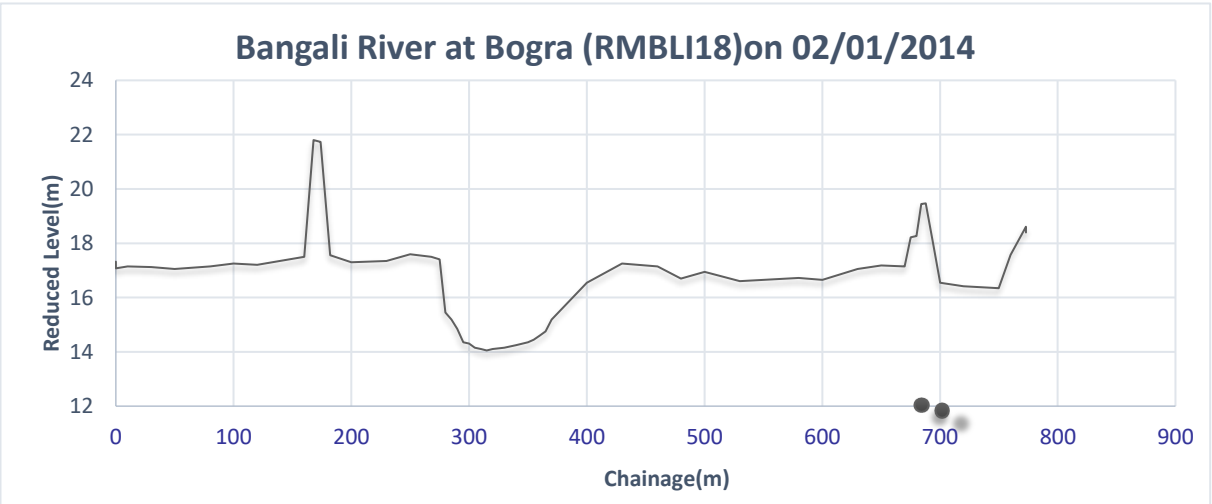
Bangali River at Bogra (RMBLI18)on 02/01/2014
Reduced Level(m)
24
22
20
18
16
14
12
0
100
200
300
400
500
600
700
800
900
Chainage(m)

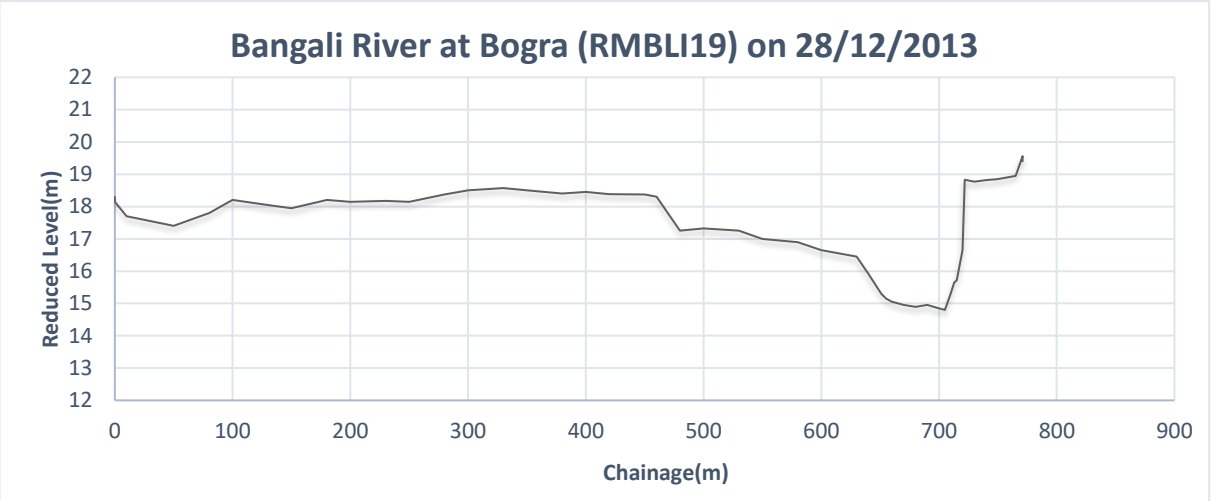
Bangali River at Bogra (RMBLI19) on 28/12/2013
Reduced Level(m)
22
21
20
19
18
17
16
15
14
13
12
0
100
200
300
400
500
600
700
800
900
Chainage(m)

Appendix B7. X-section of the Jhenai River

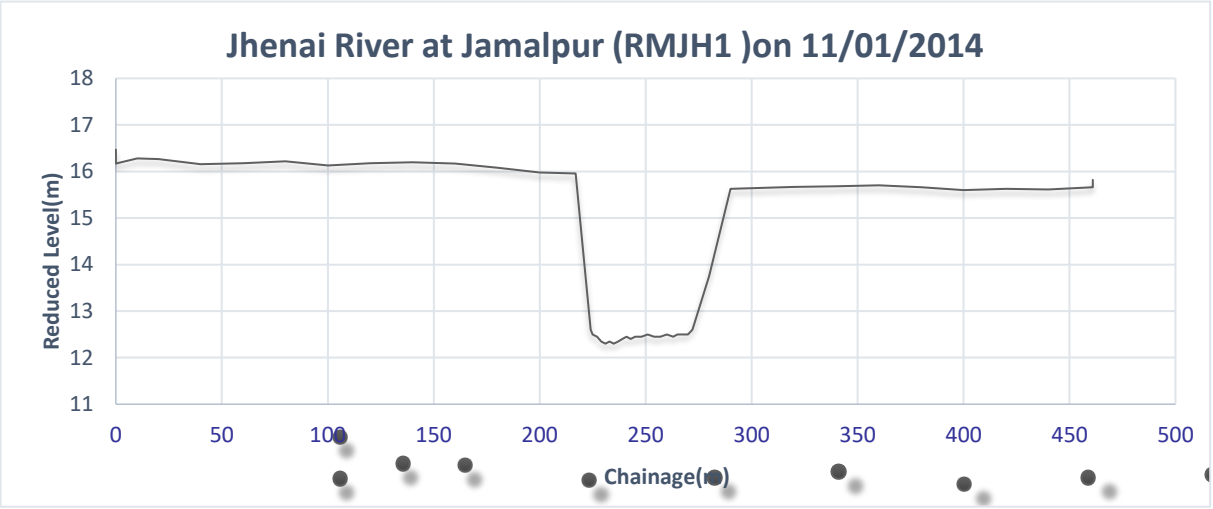

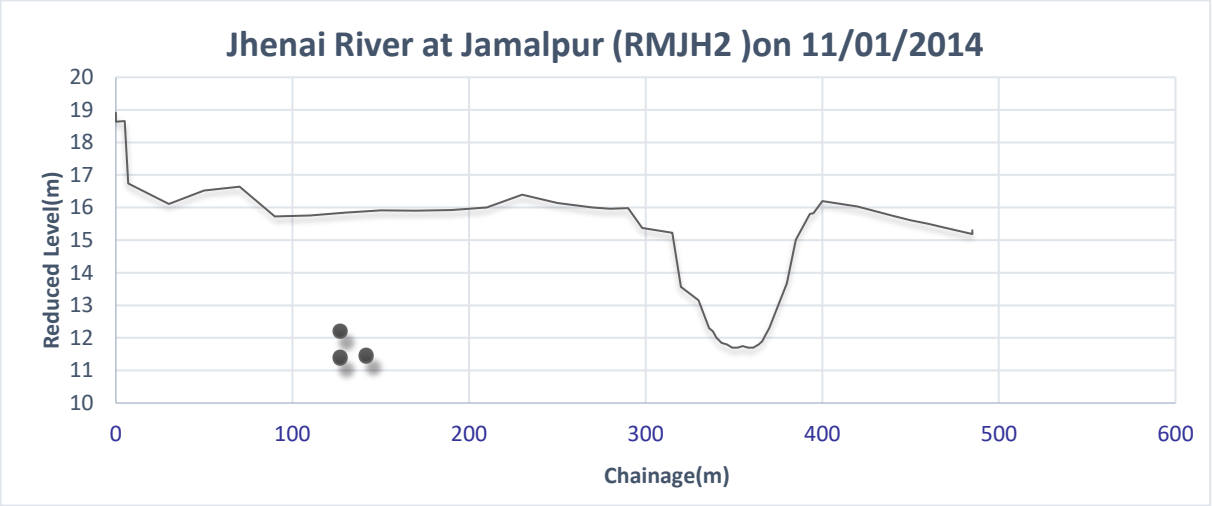

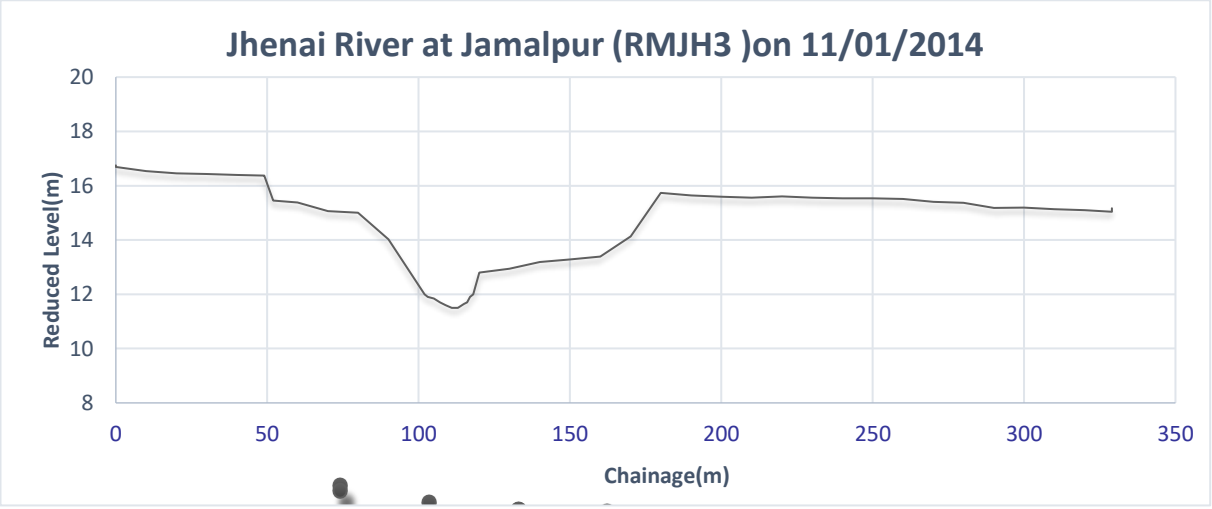

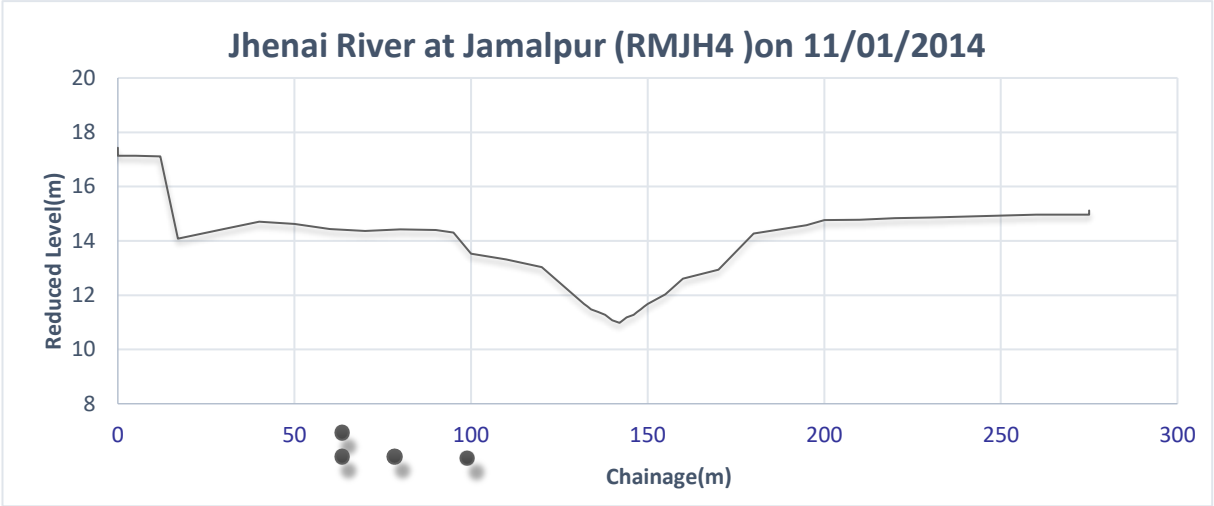
Jhenai River at Jamalpur (RMJH4)on 11/01/2014
Reduced Level(m)
20
18
16
14
12
10
8
0
50
100
150
200
250
300
Chainage(m)

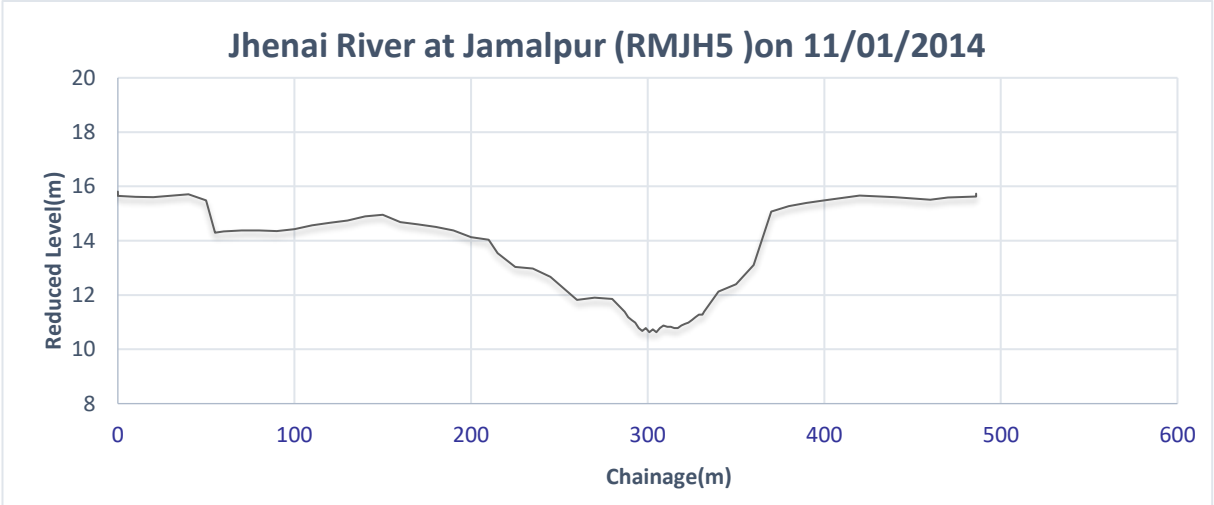
Jhenai River at Jamalpur (RMJH5)on 11/01/2014
Reduced Level(m)
20
18
16
14
12
10
8
0
100
200
300
400
500
600
Chainage(m)

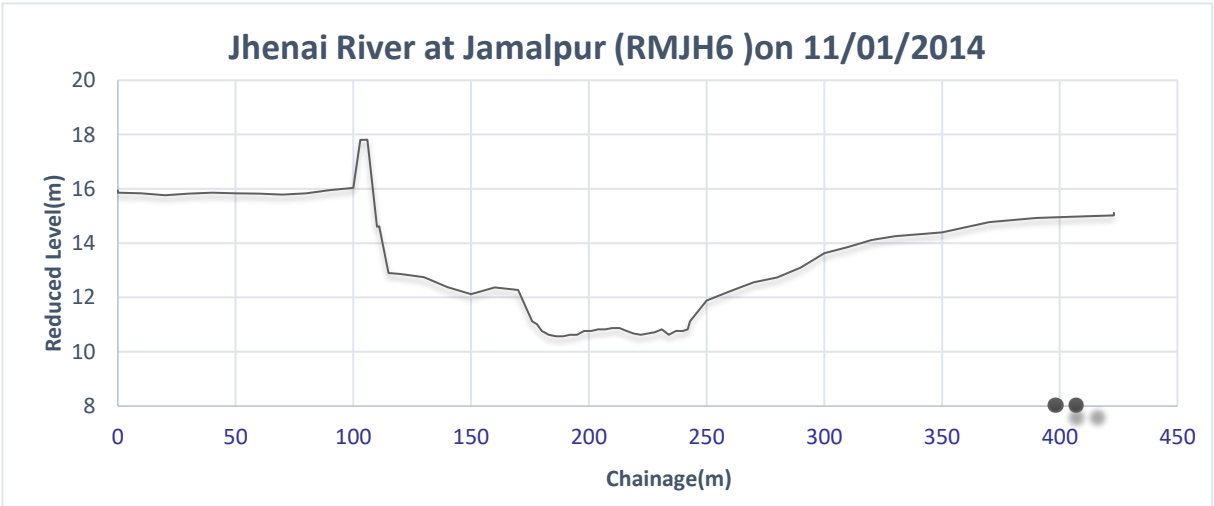
Jhenai River at Jamalpur (RMJH6)on 11/01/2014
Reduced Level(m)
20
18
16
14
12
10
8
0
50
100
150
200
250
300
350
400
450
Chainage(m)

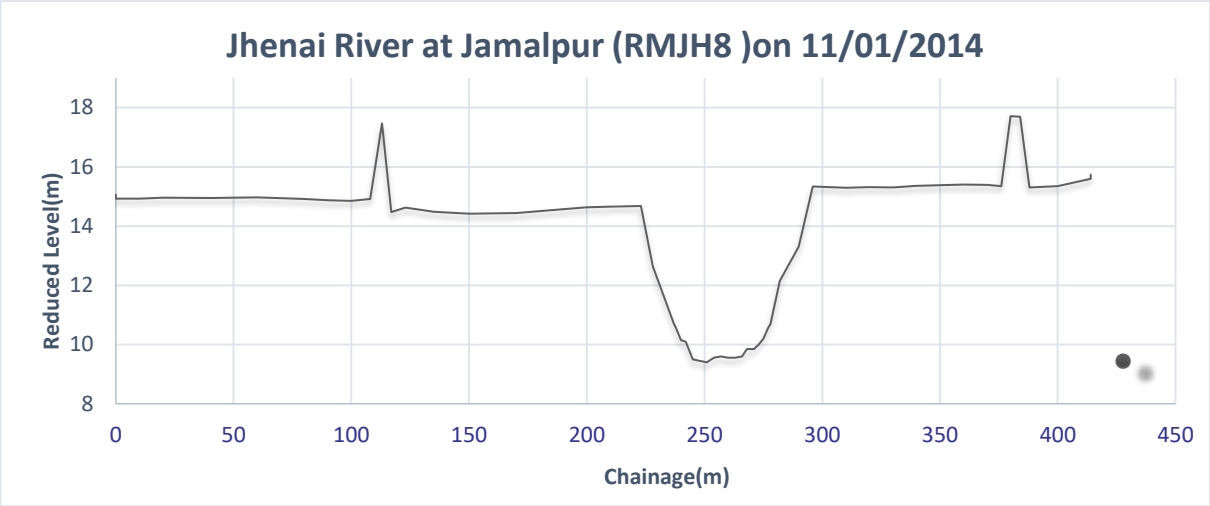
Jhenai River at Jamalpur (RMJH8)on 11/01/2014
Reduced Level(m)
18
16
14
12
10
8
0
50
100
150
200
250
300
350
400
450
Chainage(m)

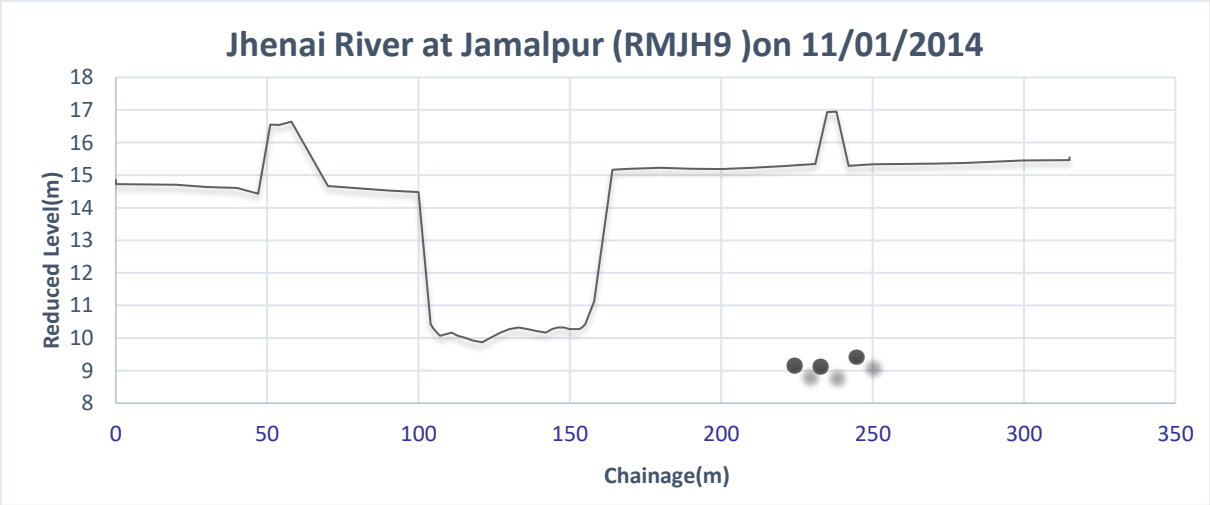
Jhenai River at Jamalpur (RMJH9)on 11/01/2014
Reduced Level(m)
18
17
16
15
14
13
12
11
10
9
8
0
50
100
150
200
250
300
350
Chainage(m)